

**This PDF was created from the British Library's microfilm copy of the original thesis. As such the images are greyscale and no colour was captured.**

**Due to the scanning process, an area greater than the page area is recorded and extraneous details can be captured.**

**This is the best available copy**

**DX79 249**

**VOL I**



THE BRITISH LIBRARY DOCUMENT SUPPLY CENTRE

**TITLE** THE FOYERS GRANITIC COMPLEX AND ITS AUREOLE.  
.....

**AUTHOR** Philip Thomas Hood.  
.....

UNIVERSITY City of London Polytechnic.  
1990

Attention is drawn to the fact that the copyright of this thesis rests with its author.

This copy of the thesis has been supplied on condition that anyone who consults it is understood to recognise that its copyright rests with its author and that no information derived from it may be published without the author's prior written consent.

1	2	3	4	5	6
cms.					

THE BRITISH LIBRARY  
DOCUMENT SUPPLY CENTRE  
Boston Spa, Wetherby  
West Yorkshire  
United Kingdom

REDUCTION X .....

12

MEMA. 7

THE FOYERS GRANITIC COMPLEX AND ITS AUREOLE.

Volume 1. Text and Appendices.

Philip Thomas Hood.

August 1990.

Degree of Doctor of Philosophy.

City of London Polytechnic.

This thesis is submitted to the Council for National Academic Awards in partial fulfilment of the requirements for the degree of Doctor of Philosophy.

**THE BRITISH LIBRARY DOCUMENT SUPPLY CENTRE**

# **BRITISH THESES NOTICE**

The quality of this reproduction is heavily dependent upon the quality of the original thesis submitted for microfilming. Every effort has been made to ensure the highest quality of reproduction possible.

If pages are missing, contact the university which granted the degree.

Some pages may have indistinct print, especially if the original pages were poorly produced or if the university sent us an inferior copy.

Previously copyrighted materials (journal articles, published texts, etc.) are not filmed.

Reproduction of this thesis, other than as permitted under the United Kingdom Copyright Designs and Patents Act 1988, or under specific agreement with the copyright holder, is prohibited.

**THIS THESIS HAS BEEN MICROFILMED EXACTLY AS RECEIVED**

**THE BRITISH LIBRARY  
DOCUMENT SUPPLY CENTRE  
Boston Spa, Wetherby  
West Yorkshire, LS23 7BQ  
United Kingdom**

**MAPS/CHARTS  
RELATING TO THIS THESIS  
HAVE NOT BEEN FILMED**

**PLEASE APPLY DIRECT  
TO ISSUING UNIVERSITY**

**A**

## CONTENTS.

### VOLUME 1.

ABSTRACT.	Pg.1
ACKNOWLEDGEMENTS.	Pg.2
CHAPTER 1.HISTORY OF GEOLOGICAL RESEARCH IN THE FOYERS AREA.	
1.1 Aims Of Project.	Pg.4
1.2 Previous Work On The Foyers Complex.	Pg.6
1.3 Geological Affinities Of The Rocks In The Monadhliath Mountains.	Pg.12
1.4 Stratigraphy Of The Foyers Area.	Pg.16
1.5 Caledonian Magmatism.	Pg.18
CHAPTER 2. PETROGRAPHY AND FIELD RELATIONSHIPS OF IGNEOUS UNITS IN THE FOYERS COMPLEX.	
2.1 Introduction.	Pg.23
2.2 Errogie Quartz Diorite.	Pg.26
2.2.1 Petrography.	Pg.26
2.2.2 Field relationships.	Pg.27
2.3 Chliabhain Quartz Monzodiorite.	Pg.28
2.3.1 Petrography.	Pg.28
2.3.2 Field relationships.	Pg.29
2.4 Dalcrag Granodiorite.	Pg.30
2.4.1 Petrography.	Pg.30
2.4.2 Field relationships.	Pg.31
2.4.3 Loch Kemp Marginal Granodiorite Facies.	Pg.33
2.5 Meall a' Bhuaile Granodiorite.	Pg.34
2.6 Dun Garbh Granodiorite.	Pg.35
2.7 Aberchalder Adamellite.	Pg.36
2.7.1 Petrography.	Pg.36
2.7.2 Field relationships.	Pg.37
2.7.3 Granitic porphyries.	Pg.39
2.7.4 Emplacement of adamellite and porphyries.	Pg.40
2.8 Carn Bhreabaig Adamellite.	Pg.41
2.9 Microdiorite Enclaves.	Pg.44
2.9.1 Petrography.	Pg.44
2.9.2 Field relationships.	Pg.45

2.10 Microdiorite Dykes.	Pg.46
2.10.1 Introduction.	Pg.46
2.10.2 Petrography.	Pg.47
2.10.3 Field relationships.	Pg.50
2.11 Appinitic Diorites.	Pg.52
2.11.1 Petrography.	Pg.52
2.11.2 Field relationships.	Pg.53
2.12 Minor Acid Sheets.	Pg.54
2.12.1 Felsites.	Pg.54
2.12.2 Pegmatites.	Pg.55
2.12.3 Aplites.	Pg.55
2.13 Geochemistry Of The Major Units.	Pg.56

### CHAPTER 3. GRANITOID VEINING AND STOPING IN THE FOYERS COMPLEX.

3.1 Veining.	Pg.59
3.1.1 Veining as part of the Foyers Complex.	Pg.60
3.1.2 Controls on veining.	Pg.60
3.1.3 Vein dilation and replacement.	Pg.62
3.1.4 Propagation of the veins.	Pg.64
3.2. Relationships Between Veining And Stopping.	Pg.65
3.2.1 Lithological control of stopping.	Pg.66
3.3 Conclusions.	Pg.68
3.4 Veins On Beinn Sgurrach.	Pg.69
3.4.1 Gneissose granite dykes.	Pg.71

### CHAPTER 4. FABRICS AND FOLIATIONS IN THE FOYERS GRANITIC COMPLEX.

4.1 Introduction.	Pg.73
4.2 Field Descriptions Of The Foliation And Other Igneous Structures.	Pg.73
4.2.1 Encalves.	Pg.75
4.2.2 Xenoliths.	Pg.76
4.2.3 Appinitic diorites.	Pg.77
4.2.4 Schlieren.	Pg.78
4.2.5 Internal contacts.	Pg.78
4.3 Microscopic Investigation Of The Mineral Fabric.	Pg.79
4.3.1 Foliation.	Pg.79
4.3.2 Mineral textures.	Pg.80
4.4 Relationship Between Granitoid Fabric And Deformed Envelope.	Pg.83

4.5 Origin Of The Fabric In The Foyers Complex.	Pg.84
4.5.1 Introduction.	Pg.84
4.5.2 Microscopic evidence.	Pg.85
4.5.3 Enclaves.	Pg.88
4.5.4 Xenoliths.	Pg.91
4.5.5 Appinitic diorites.	Pg.92
4.5.6 Internal contacts.	Pg.94
4.5.7 Marginal stocks and veins.	Pg.95
4.5.8 Conclusions.	Pg.96
4.6 Foliations In The Dalcrag Granodiorite North East Of Loch Kemp; A Special Case?.	Pg.98
4.6.1 Fabric descriptions.	Pg.100
4.6.2 Influence of metasedimentary rafts.	Pg.103
4.6.3 A model for the Loch Kemp area.	Pg.105
4.7 Deformation Of Microdiorite Enclaves.	Pg.106
4.7.1 Introduction.	Pg.106
4.7.2 Enclaves in the Foyers Complex.	Pg.107
4.7.3 Measurement of the enclaves.	Pg.108
4.7.4 Analysis.	Pg.109
4.7.5 Conclusion.	Pg.115
CHAPTER 5. THE MAOL CHNOC COMPLEX.	
5.1 Introduction.	Pg.117
5.2 Field Relationships Of Igneous Units In The Maol Chnoc Complex.	Pg.117
5.3 Petrography Of The Maol Chnoc Complex.	Pg.119
5.3.1 Granodiorite.	Pg.120
5.3.2 Adamellite.	Pg.121
5.3.3 Diorite.	Pg.122
5.3.4 Aplites.	Pg.123
5.4 Structure Of The Maol Chnoc Complex.	Pg.124
5.5 Field Descriptions Of Mineral Fabrics.	Pg.125
5.5.1 Changes shown by rock fabric as deformation increases.	Pg.126
5.5.2 Rocks dominated by flow fabrics.	Pg.127
5.5.3 Rocks showing solid state deformation.	Pg.127
5.5.4 Rocks showing strong solid state deformation.	Pg.128
5.5.5 Gross strain distribution within the Maol Chnoc Complex.	Pg.129
5.6 Microscopic Fabrics.	Pg.129
5.6.1 Microscopic fabrics in weakly foliated rocks.	Pg.130
5.6.2 Microscopic fabrics in rocks showing moderately strong foliations.	Pg.130
5.6.3 Microscopic fabrics in strongly deformed rocks.	Pg.131
5.6.4 Discussion.	Pg.131



5.7 Relationships Between The Maol Chnoc  
And Foyers Complexes. Pg.133

5.8 Conclusions. Pg.136

#### CHAPTER 6. INNER AUREOLE PSAMMITE MOBILISATION IN THE ENVELOPE OF THE FOYERS COMPLEX.

6.1 Introduction. Pg.138

6.2 Timing Of The Mobilisation. Pg.139

6.3 Description Of The Mobilised Areas. Pg.139

6.4 Mobilisation On Cairn Gairbthinn. Pg.142

6.5 Discussion. Pg.144

#### CHAPTER 7. RELATIONSHIPS BETWEEN THE FOYERS COMPLEX AND THE REGIONAL STRUCTURE.

7.1 Introduction. Pg.150

7.2 Stratigraphic Setting. Pg.151

7.3 Field Descriptions Of Psammite Units. Pg.153

7.3.1 Pebbly Psammite. Pg.153

7.3.2 Micaceous Psammite. Pg.155

7.3.3 Migmatitic Semi-Pelite. Pg.156

7.4 External Structure Of The Foyers Complex. Pg.156

7.5 Regional Structures. Pg.158

7.5.1 First deformation. Pg.158

7.5.2 Second deformation. Pg.159

7.5.3 Third deformation. Pg.160

7.5.4 Gross regional structure. Pg.160

7.6 Effects Of Foyers Emplacement On  
Regional Minor Structures. Pg.161

7.6.1 Bedding and D1 foliation. Pg.161

7.6.2 D2 deformation- minor asymmetrical folds. Pg.163

7.6.3 D3 deformation- crenulations. Pg.164

7.7 Minor Structures Formed In The  
Country Rocks By Granitoid Emplacement. Pg.165

7.7.1 Boudinage. Pg.165

7.7.2 Relationship of granitoid  
veining and boudinage. Pg.168

7.7.3 Late open folds. Pg.169

7.7.4 Shear structures. Pg.171

7.7.5 Strain markers. Pg.172

7.7.6 D2 Caledonian folds. Pg.173

7.7.7 Pre-Foyers granitoids: Maol Chnoc. Pg.174



7.8 Faulting.	Pg.174
7.8.1 Nature of the fault zones.	Pg.176
7.8.2 Gleann Liath Fault.	Pg.177
7.9 Discussion.	Pg.179

## CHAPTER 8. PETROLOGY AND CONTACT METAMORPHISM OF THE FOYERS ENVELOPE ROCKS.

8.1 Introduction.	Pg.183
8.2 Petrography.	Pg.184
8.2.1 Micaceous Psammite.	Pg.185
8.2.2 Pebbly Psammite.	Pg.189
8.2.3 Retrogressive Muscovite.	Pg.191
8.3 Mineral Textures And Interpretation Of Mineral Assemblages.	Pg.192
8.3.1 Andalusite/sillimanite.	Pg.194
8.4 Mineral Geochemistry.	Pg.197
8.4.1 Garnet.	Pg.198
8.4.2 Biotite.	Pg.199
8.4.3 Cordierite.	Pg.199
8.4.4 Plagioclase.	Pg.199
8.4.5 Ilmenite.	Pg.200
8.4.6 Geothermometry and Geobarometry.	Pg.200
8.5 The Relationship Of Aureole Deformation To Metamorphic Fabrics.	Pg.201

## CHAPTER 9. EFFECTS OF DENSITY ON THE EMPLACEMENT OF THE FOYERS COMPLEX.

9.1 Introduction.	Pg.205
9.2 Determination Of Rock Densities At 15C.	Pg.205
9.3 Densities Of Pluton And Aureole Rocks At Emplacement Temperatures And Pressures.	Pg.206
9.4 Density Evolution Of A Crystallising Magma.	Pg.209
9.5 Density Of Dalcrag Granodiorite.	Pg.211
9.6 Effects Of Density On Emplacement Models.	Pg.212
9.7 The Effect Of Density On Stoping.	Pg.215
9.7.1 Density contrasts between rafts and magma.	Pg.216

CHAPTER 10. THE INTRUSION OF THE FOYERS COMPLEX; SUMMARY AND CONCLUSIONS.

10.1 Summary Of The Preceeding Chapters.	Pg.220
10.2 Comparisons Between The Intrusion Of The Foyers Complex And Other Granitoids.	Pg.226
10.2.1 Comparison of the Foyers Complex with the ideal characteristics of diapiric intrusion.	Pg.228.
10.2.2 Comparison of the Foyers Complex with the ideal characteristics displayed by a granitoid emplaced by stoping.	Pg.231
10.3 An Emplacement Model For The Foyers Complex.	Pg.233
10.4 The Viability Of Magmatic Ballooning In The Foyers Granitic Complex.	Pg.235
10.5 The Foyers-Strontian Correlation.	Pg.238

APPENDICES.

Pg.I

APPENDIX A. PETROGRAPHY AND FIELD DESCRIPTIONS.

Pg.II

A1 Errogie Quartz Diorite.	Pg.II
A1.1 Field description.	Pg.II
A1.2 Petrography.	Pg.II
A2 Chliabhain Quartz Monzodiorite.	Pg.VI
A2.1 Field description.	Pg.VI
A2.2 Petrography.	Pg.VII
A3 Dalcrag Granodiorite.	Pg.IX
A3.1 Field description.	Pg.IX
A3.2 Petrography.	Pg.IX
A4 Meall A' Bhuailt Granite.	Pg.XI
A5 Aberchalder Adamellite.	Pg.XI
A5.1 Field description.	Pg.XI
A5.2 Petrography.	Pg.XII
A5.3 Granitic Porphyries	Pg.XIII
A6 Mafic Microdiorite Enclaves	Pg.XV
A7 Microdiorite Dykes.	Pg.XVI
A7.1 Field Description	Pg.XVI
A7.2 Petrography	Pg.XVII
A8 Appinitic Diorites.	Pg.XXII
A8.1 Field Description.	Pg.XXII
A8.2 Petrography.	Pg.XXII

A9 Acid Veins.	Pg.XXIV
A9.1 Aplites	Pg.XXIV
A9.2 Alkali Granite Veins.	Pg.XXV
 APPENDIX B. GEOCHEMISTRY.	 Pg.XXVII
B1 Sample Preparation For Major Element Analysis.	Pg.XXVII
B2 Sample Preparation For Trace Element Analysis.	P.XXVIII
B3 I.C.P.S Operating Conditions.	P.XXVIII
Tables showing granitoid geochemical analyses.	Pg.XXX
APPENDIX C. ESTIMATION OF DILATIONAL AND REPLACIVE COMPONENTS INVOLVED IN GRANITOID VEINING.	Pg.XXXII
APPENDIX D. USE OF MARKERS IN ESTIMATION OF STRAIN IN THE FOYERS COMPLEX ENVELOPE.	P.XXXIII
D1 Boudin Extensions.	P.XXXIII
D2 Metamorphic Spots.	P.XXXIII
APPENDIX E. MICROPROBE ANALYSIS OF MINERALS IN THE FOYERS ENVELOPE.	Pg.XXXV
Tables showing mineral compositions.	Pg.XXXVI
APPENDIX F. TABLE SHOWING THE POSITIONS OF FIELD LOCALITIES REFERENCED IN THE TEXT AND FIGURES OF THIS THESIS.	Pg.LII

#### REFERENCES

VOLUME 2 Figures, Plates and Enclosures to accompany the text in Volume 1.

ABSTRACT.

~~GRANITIC~~  
THE FOYERS COMPLEX AND ITS AUREOLE.

PHILIP T. HOOD, CITY OF LONDON POLYTECHNIC.

THESIS FOR DOCTOR OF PHILOSOPHY DEGREE.

The field mapping of the Foyers Granitic Complex and its psammite envelope provided data to study the emplacement of the complex, and produce part of British Geological Survey Sheet 73E.

The complex contains quartz diorite cut by quartz monzodiorite in the north, granodiorite in the south, and cross cutting adamellite stocks throughout the pluton. These units are the products of a differentiating magma body at depth. A north easterly trending suite of microdiorite dykes cross cuts the complex. The complex was emplaced into Grampian Group psammites, after the cessation of Caledonian orogenesis, and developed an extensive thermal aureole, with minor anatexis occurring in the inner aureole.

Granitoid fabrics, enclaves, xenoliths and internal contacts imply emplacement whilst in a magmatic state. The adamellite was emplaced into a solid pluton. Boudinage and shearing in envelope psammites, and intense solid state fabrics in pre-Foyers granitoids, indicate the envelope shortened perpendicular to the complex margin.

Major and minor D1, D2 and D3 regional structures are not rotated by granitoid emplacement. The orientations of the contact parallel psammite units are controlled by regional structures. Contact relationships between envelope and complex imply stoping was the major intrusion mechanism, with siliceous lithologies more readily stoped than others.

Low density contrasts between granitoid and envelope necessitate stoping occurred whilst the pluton was very fluid, extra bouyancy perhaps derived from connection with a magma source at depth.

The Foyers Complex was emplaced as a series of stocks stoping into the crust. Regional structures controlled the morphology of the magma chamber because certain stratigraphic units either facilitated or hindered stoping. The positions of these units are controlled by regional structure. Ballooning of the magma chamber occurred whilst the entire complex was fluid, and deformed the envelope.

#### ACKNOWLEDGEMENTS.

During the completion of this study, I gratefully received assistance and support from many sources, too numerous to name all individually.

Primarily I thank my supervisors, Dr. Paula Haselock and Dr. Ian Platten for the time and commitment they gave in discussion, supervision and criticism of my work.

I am grateful to the staff of Thames Polytechnic School of Earth Science (Ex-City Of London Polytechnic Geology Department), for their assistance with the many disciplines employed in this thesis. Permission to use the facilities at City Of London and Thames, Polytechnics was granted by Professor Ray Skelhorn and Dr. Alistair Baxter respectively.

During field work, land access was kindly allowed by the Forestry Commission, Economic Forestry, the estates of Farraline, Wester Aberchalder, Easter Aberchalder, Corriegarth, Dell, Dunmaglass, Garragie, and the farms, Mains of Gorthleck, Carnoch and Croftdhu. Pleasant living quarters were provided by Mrs MackIntosh of Inverfarigaig.

I also thank Miss Kerry Weedon for her field assistance; measuring enclaves and undertaking tedious Fry's analyses of orthoclase phenocrysts.

I thank my parents for their support, and Mr Batty and Mr Craig for their assistance in the final production of this thesis.

I gratefully received the financial assistance of a N.E.R.C. grant.

CHAPTER 1. GEOLOGICAL RESEARCH IN THE FOYERS AREA.

## CHAPTER 1. GEOLOGICAL RESEARCH IN THE FOYERS AREA.

### 1.1 AIMS OF PROJECT.

The project on the Foyers Granitic Complex and its envelope had two major objectives. The first an analysis of the evolution and structural development of the complex, the second to provide the field and laboratory data to assist in the production of British Geological Survey, 1:50,000 Sheet, 73 E.(Foyers), M.E.R.C. contract No:F60/G2/23 and the accompanying memoir. The contract work involved mapping the Foyers Complex, envelope rocks, and the rocks between the Foyers Complex and the Great Glen (excluding the Old Red Sandstone). An area of 110km<sup>2</sup> was mapped on a scale of 1:10,000, and the data compiled with data collected by other B.G.S. contract workers to produce Sheet 73 E.

### RESEARCH AIMS.

In addition to the contract mapping, the research aims included:

1. Production of a solid geology map of the lithologies and structures in the Foyers Complex and its envelope.
2. Description of the petrology and field relationships of the igneous units in the complex.



3. Description of the structure, petrology and origin of the igneous veins and plutonic bodies that lie in the aureole of the Foyers Complex.

4. Description, analysis and interpretation of the igneous structures and fabrics in the body of the Foyers Complex.

5. Description, analysis and interpretation of the regional and contact structures in the envelope of the complex.

6. Evaluation of the structural evolution of the Foyers Complex, paying particular attention to the structural relationships between the complex and regional structures.

7. Definition of a contact metamorphic aureole around the Foyers Complex, and an estimation of the P.T. conditions in the inner aureole.

8. Analysis of the time and structural relationships between faulting and the development of the Foyers Complex.

Previous workers who have studied the Foyers Complex include; Mould (1946), Marston (1971) and Highton (1986). All these workers focused strongly on the petrology, geochemistry and field relationships of the complex. The authors above, presented only brief structural histories of the Foyers Complex, and all three agreed the emplacement of the Foyers Complex caused strong reorientations of the regional strike into parallelism with the complex margin. Thus the main aim of this thesis is to study the emplacement mechanisms and structural evolution of the complex, paying close attention to any controls exerted by the envelope and the effects of granitoid emplacement on regional structures.



The interpretations of earlier workers were limited by the lack of comprehensive regional structural data in the Foyers area. Recently, December 1989/January 1990 Haselock has completed the mapping of the regional geology within the confines of B.G.S. sheet 73E. and a relatively reliable structural framework has been developed for the region into which the Foyers Complex is intruded, (Haselock and Leslie pers.comm.).

This now permits a study of the relationships between regional structures and the emplacement of the Foyers Complex.

#### 1.2 PREVIOUS WORK ON THE FOYERS COMPLEX.

Resulting from a rapid survey of the Foyers Granitic Complex, (in order to compare compare it to the Strontian Granite, mapped earlier by the Geological Survey,) Kennedy (1946), produced a simple map illustrating a granite of broadly triangular outline, containing a Central Psammite Septum. He showed the granite was a vertical stock of three members: an outer tonalite, an inner porphyritic granodiorite and a cross cutting biotite granite.

On the basis of their similar lithology and structure, Kennedy (1946), stated that the Strontian and Foyers Granites were originally a single granitoid mass emplaced across the Great Glen Fault, which then sinistrally displaced the two sides of the pluton by sixty five miles.

The first systematic survey of the Foyers area was

undertaken by D.M Mould (1946). She mapped a ten-mile wide strip of ground south-east of Loch Ness between Fort Augustus and Loch Duntelchaig concentrating on the Gleann Liath series and the Foyers Granitic Complex.(Fig.1.1)

Mould described Moine schists, ranging from siliceous psammities to semi-pelites, with occasional calc-silicates and amphibolites in the envelope of the Foyers pluton. She recognized the Foyers pluton as a tonalite, granodiorite, and granite (Aberchalder granite) complex, intruded in that order. She produced petrological descriptions of all the major units, accompanied by simple major oxide geochemistry and stated the intrusions between Loch Kemp and Loch Knockie were satellite bodies of Foyers, although their lithologies were slightly dissimilar.

Mould (1946) attributed the parallelism between the complex margin and the foliation in the envelope schists, to a regional strike swing resulting from the forceful emplacement of the granite.

Marston (1966, unpublished Ph.D. thesis and 1971), concentrated his study on the Foyers Complex and aureole. In the envelope rocks Marston (1966) described porphyroblastic quartz, plagioclase and orthoclase which he regarded as regrouping of minerals and feldspathization due to contact metamorphism. Marston (op cit.) conducted a study of the complex's petrology which he stated was a crudely zoned pluton of tonalite and granodiorite, cross cut by adamellite (Fig.1.2). Marston (op cit.) linked the Foyers Complex with those at Loch Knockie. He described aplites, pegmatites, porphyries and lamprophyres post-dating the emplacement of

the plutonic units, the latter intruded into north easterly trending tension joints.

Marston (1971), studying mineral textures showed the complex crystallised in accordance with Bowen's reaction series, with minor potassium autometasomatism due to fluids from the adamellite, pervading the complex.

Major element analyses showed a systematic chemical variation in all the major units excluding the appinites. Marston (1971), placed the chemical compositions of the Foyers granitoids in synthetic systems, and compared the predicted results to textures seen in thin section. This convinced Marston (1971) the anisotropy of the Foyers Complex was a result of magmatic differentiation. Any anomalies were explained by late potassium metasomatism.

Marston (1971) noted the presence of a margin parallel foliation in the tonalite and granodiorite defined by inequidimensional minerals and ellipsoidal microdiorite xenoliths. He concluded that the fabric was imparted by "non hydrostatic distention" during late stages of pluton crystallisation.

Marston (1971) assigned the regional swing in the strike of the country rock to the forceful emplacement of the pluton. A structural model showed firstly the tonalite was emplaced upwardly into its present position followed by the granodiorite, prior to tonalite solidification. Late, minor upward movement was accomplished by stoping, and then the adamellite was emplaced into a brittle pluton.

The presence of andalusite/sillimanite pairs and thermal muscovite porphyroblasts suggested a temperature between

500°C and 600°C and a pressure of less than 2.5 Kb.

Marston compared the Foyers and Strontian plutons. In 1967, he concluded that the two plutons were not originally the same body due to structural differences, but in 1971 he claimed that these differences could be explained by exposure of the Strontian complex at deeper crustal levels, and that the two complexes were possibly derived from a single original pluton.

Ahmad (1967), produced different magnetic anomalies for the two plutons.

Brown et al. (1968) dated the Foyers Complex using potassium/argon isotope data. They analysed biotite from the tonalite and granodiorite, at G.R.NH/556176 and G.R.NH/557167 respectively. The "tonalite" gave an age of 406±8 Ma. and the "granodiorite" an age of 397±8 Ma, dates significantly younger than those of the Strontian Complex. The dated "tonalite" was in fact Chliabhain Quartz Monzodiorite, corresponding to Marston's granodiorite.

Pigeon and Aftalion (1978), dated a sample of Foyers "granodiorite" from NH/54802040 at 385 Ma. They preferred the date of Brown et al. (1968) because they thought Foyers zircons had suffered late isotopic disturbance. Concordia plots showed the Foyers zircon population contained a significant proportion of inherited old zircon. Zircons in the Strontian Complex are all primary, implying a different magma source, and thus no Strontian-Foyers correlation.

Tyler and Ashworth (1983), produced pressure, temperature, and water activity estimates for the northern envelope of the Foyers Complex using the exchange equilibria reactions

of biotite, garnet and cordierite using samples from the north of the Foyers Complex.

They defined a regional assemblage of muscovite, biotite, plagioclase, and quartz, with or without sillimanite, garnet, ilmenite, and graphite. They identified an inner and outer aureole, the outer aureole beginning 3-4km from the pluton, and the inner aureole extending only several 100m from the contact. The outer aureole is characterised by the loss of muscovite and regional garnet and the development of new sillimanite, biotite, garnet and orthoclase. The inner aureole is characterised by presence of cordierite

Tyler and Ashworth arrived at a temperature of  $678^{\circ}\text{C}$  for the inner aureole, using exchange equilibria of iron and magnesium in garnet and biotite in conjunction with Thompson's empirical calibration. Using garnet and cordierite, they derived a temperature of  $654^{\circ}\text{C}$ . The Holdaway-Lees method for garnet and cordierite matrix yielded a pressure of 3.9 Kb and a water activity of 0.15.

Garson et al. (1984), suggested that beneath the Great Glen Fault are a suite of carbonatites, emplaced at 390 Ma. which form shock zone fenites, breccia dykes, albitites, and carbonitic veins adjacent to Loch Ness. These authors show the carbonatites fenitised the Foyers Complex, with minor microbreccia veins in the granite acting as channels for fenitizing fluids, depositing epidote and fibrous blue amphiboles.

Highton, (1986) (unpubl.Ph.D. thesis), studied the northern margin of the Foyers Complex, and the Grampian Group/Central Highland Division immediately to the north of

the Foyers Complex.

He described the stratigraphy, structure, petrology, and the effects of regional metamorphism in the rocks north east of the Foyers Complex. He defined two tectonostratigraphic successions, one of migmatites and gneisses, which he included within the Central Highland Division (Piasecki 1980), and the other of psammitic granulites which he placed within the Grampian Group (Harris 1978). He states that the gneisses contain one more deformation phase than the granulites. The junction between the 'cover' and 'basement' is formed by a ductile thrust of early Caledonian age. The attitude of the stratigraphical units are controlled by upright, steeply plunging, N.N.E. trending folds.

Highton (op. cit) concentrated his work on the igneous rocks within the northern part of the Foyers Complex, and the smaller bodies intruded into the country rocks to the north east. He describes the petrology, field relationships, structure, and particularly the geochemistry of all the igneous rocks. Highton (op. cit) identified the deformed Maol Chnoc complex and the vein complexes lying to the north of Foyers, stating that deformation in the Maol Chnoc complex was caused by the forceful emplacement of the nearby Foyers Complex. He stated that the Foyers Complex was a continuously zoned pluton, with an outer zone of quartz diorite grading into an inner granodiorite, with a late adamellite cross cutting this zoning, and representing a pulse of magma fractionated below the present level of exposure.

He describes the petrology, distribution, and geochemistry

of a suite of microdiorite dykes which cut the Foyers Complex and envelope, and suggests that the dykes were formed from magma derived from the differentiation of the Foyers magma. Highton (1986) studied the northern metamorphic aureole of the Foyers Complex, describing the petrology and mineral chemistry. He presented P.T. estimates of 3.9Kb and 650C. The structural model Highton developed to explain the intrusion of the Foyers Complex, included forceful emplacement producing a "strong re-orientation of regional deformation structures".

### 1.3 GEOLOGICAL AFFINITIES OF THE ROCKS IN THE MONADHLIATH MOUNTAINS.

The geology and structure of the Monadhliaths- the region containing the Foyers Complex, need to be understood if the emplacement and evolution of the Foyers Complex are to be studied successfully.

The Foyers Complex is intruded into a series of migmatites, micaceous psammities, and psammities which have had a contentious relationship with the remainder of Highland geology.

Hinxman et al., (1915) published a memoir to sheet 71. This work was to the east of Foyers and placed the regional granulites within the Moine Series.

Anderson (1956), conducted the first regional study of the Monadhliath Mountains close to the Foyers Complex. He classed the rocks as the Eilde Flags, lying on the north



west limb of the north easterly trending, Corrieyairack syncline. He correlated the Eilde Flags with the Central Highland Psammite Group of the Moine.

Johnstone (1966), placed the Moine-Dalradian boundary at the top of the Eilde Flags with the Lochaber Transition Group, containing the Monadliath Schists, forming the base of the Dalradian, thus confirming the Moinian age of the rocks close to the Foyers Complex.

Johnstone (1975), argued that the only criterion for differentiating Moine from Dalradian in the Grampian Highlands is that the Moine is lithologically homogenous, and the Dalradian heterogenous. He named the Central Highland Granulites which form the regional geology around the Foyers Complex "Young" Moine, because they lack pre-Caledonian metamorphic and structural events. He suggested the "Young" Moine was deposited on an "Old" Moine basement.

As the transition between the Central Highland Granulites and the Lochaber subgroup is sedimentary, Harris et.al. (1978), proposed that the Central Highland Granulites be named the Grampian Group, and are included within the Dalradian Supergroup.

Piasecki (1975 and 1976 amendment) described an area north west of the river Findhorn, rocks he believed to be "Young" Moine and defined three major folding events. The early F2 folds follow the Caledonian trend and dominate the outcrop pattern, forming major folds such as the Corrieyairack syncline. The F3 folds are limited to minor upright, open folds with a north westerly striking axial surface and a



plunge to the south east. The tight F4 folds are upright structures with fold axes with two azimuths, one at 010 and the other at 035. The F4 axial surfaces are defined by a strain slip cleavage and occasionally a weak biotite schistosity. Piasecki (1975) recorded a series of metamorphic events. The first, progressive and most major metamorphic event reached garnet grade, was synchronous with the D2 deformation, and produced migmatitic banding which is parallel to the lithological layering. Piasecki (1975), correlated the deformation in the Upper Findhorn with the deformation events in the Iltay nappe, although metamorphism was more intense in the Findhorn area.

Piasecki (1980), stated that the Central Highland Granulites could be divided into two units; the Central Highland Division and the Grampian Division, the Central Highland Division characterised by high grade migmatites and gneisses, forming a basement to the Grampian Division "cover" of finer grained, more weakly metamorphosed granulites. The contact between the two divisions is formed by the Grampian Slide. In the Central Highland Division, Piasecki (1980), recognised three fold phases absent from the Grampian Division. He correlated the Central Highland Division with migmatites in the Glenfinnan and Loch Eil Divisions of the Moine. A minor granite gneiss in the Central Highland Division gives a date of c950 Ma, a Grenvillian age, so Piasecki tentatively correlated the Central Highland Division with the Grenvillian Moine north west of the Great Glen. In the Grampian Division Piasecki (1980), recognised two Moravian deformation events and three

later Caledonian events. Deformed granitic pegmatites in the Grampian Slide Zone formed syntectonically with the D2 deformation and give Morarian isotopic dates between 573 and 718 Ma.

Piasecki (1980), stated that the oldest Grampian Division rocks were older than the Grampian slide and younger than the Grenvillian basement, and were deposited onto Grenvillian basement in the interval between the Grenvillian and Morarian events.

Harris et al. (1983), cast doubt on the correlation of Piasecki et al. (1980 & 1983), between the basement/cover relationships in the Grampian Highlands and the basement/cover relationships of the Glenfinnan and Loch Eil Divisions, along the Loch Quoich Line.

Lindsay et al. (1989), present a paper on the relationships between the Grampian Group (Harris 1978), and the Central Highland Division (Piasecki, 1980). They trace structures in the Atholl Nappe into the Central Highland Division, where these structures are the earliest seen. They recognise no structures <sup>which</sup> can be attributed to the Grenvillian event. All structures in the Central Highland Division may be traced into the Corrieyairack region. The structural similarity, of the three deformation phases, between the Central Highland Division and the Grampian Group, suggests to these authors that the former group of rocks are a high grade portion of the Grampian Group, and thus part of the Dalradian Supergroup. They thus place all the Foyers envelope rocks in the Grampian Group. (Fig. 1.3)

#### 1.4 STRATIGRAPHY OF THE FOYERS AREA.

Haselock et al. (1981 & 1982) studied the rocks to the south of the Foyers Complex, and developed a detailed understanding of the structure and stratigraphy in the southern Monadhliaths. The authors placed the base of the Dalradian below the Leven Schist, so the "Moine like" succession beneath including the Foyers envelope becomes a part of the Grampian Division. Haselock et al. (1982 & 1984) developed a detailed stratigraphy of the southern Monadhliaths, showing the Grampian Division divided into two Successions, the Corrieyairack and Glenshirra Successions, separated by the Gairbeinn slide. The top of the Corrieyairack succession forms the base of the Leven Schist in the Dalradian.

These authors recognised three deformation phases which correlate with the structures in the Lochaber district. The D1 deformation produced a bedding subparallel foliation which is axial planar to minor isoclinal folds. The movement along the Gairbeinn slide is associated with D1. The D2 event dominates the structure of the area, producing large folds with fold axial traces trending north east-south west e.g. the Corrieyairack syncline. Near Loch Killin the syncline and the D1 foliation swing from a north easterly to easterly trend. The authors thought this was due to folding around a D3 structure. Minor D3 structures include open folds with an axial planar crenulation that plunge to the south south east.

Haselock (pers. com.) has revised the Monadhliath stratigraphy (1982), as shown in (1.4), with both successions now included within the Dalradian Grampian Group and not the 'Moine' Grampian Division. As a result of field mapping for British Geological Survey, Sheet 73E., Haselock has extended the Grampian Group stratigraphy, defined in the southern Monadhliaths, to the north east, to include the rocks around the Foyers Complex, and those defined by Piasecki (1980), as the Central Highland Division. Haselock (pers com.) states that a number of units within the Grampian Group may be traced northwards into the Central Highland Division, although in the north they are at a considerably higher grade of metamorphism.

The Foyers Complex is intruded into rocks of the upper Glenshirra Subgroup and the lower Corrieyairack Subgroup. The pebbly psammites and quartzites in the Foyers envelope are part of the Gairbeinn Pebbly Psammite Formation, whilst the micaceous psammites form a part of the Glen Doe Micaceous Psammite Formation. The northerly envelope of the Foyers Complex contains the boundary between Central Highland Division migmatitic gneisses (Piasecki, 1980) and the granulitic psammites of the Grampian Group. Haselock (pers. comm.) suggests that these gneisses are stratigraphically below the Glen Doe Micaceous Psammite, and there is a conformable relationship between the two.

### 1.5 CALEDONIAN MAGMATISM.

The Foyers Complex is one of the "Newer Granite" suite of rocks emplaced into the Scottish Highlands (Fig.1.5), between 423 and 408 Ma (Thirwall, 1988). The last major Caledonian deformation event was synchronous with the peak metamorphism dated at 490-440Ma (Fettes et al., 1985) and thus this suite of rocks are post-tectonic. The Grampian Highlands also contain pre- or syn-tectonic granitoids, for example the Ben Vuirich granite dated by Rogers et al. (1989) at 590Ma, but these early granitoids are very minor compared to the voluminous Newer Granite suite.

Read (1961), separated this suite of undeformed granitoid rocks into two groups; the Forceful Newer Granites, those emplaced by veining and envelope deformation, and the later Permitted Granites, emplaced by cauldron subsidence and the formation of ring complexes. Pankhurst (1979), and Pitcher (1982) state that the difference in style between the Forceful and Permitted granites is due to the level of emplacement, rather than age differences. The Foyers Complex has been classed as a Forceful Newer granite (Read, 1961).

The igneous intrusions within the British Caledonides are dominantly calc-alkaline, ranging from gabbroic, for example Glen Tilt, to biotite granites, for example Monadhliath, (Harrison et al., 1987). Many of the plutons in the Newer Granite suite are petrologically very heterogenous, and may be compositionally zoned, for example, the Strontian granite (Sabine, 1963).

The Newer Granites show many similarities with I-type granitoids (Chappell and White, 1974), but also show some S-type characteristics. Pitcher (1982) suggests that the Caledonian Newer Granites are I-S intermediates, derived from partial melting of a gneissose basement.

Stephens and Halliday (1984), divided the Newer Granite plutons in Scotland into three suites, the Cairngorm, South of Scotland and Argyll suites. The Argyll suite, which contains the Foyers Complex, is petrologically heterogeneous, containing hornblende bearing diorites, granodiorites and adamellites. It is calc-alkaline, has high Ba and Sr values and was intruded at 410-415 Ma. Halliday and Stephens (1984) and Halliday (1984), state that the Argyll and South of Scotland suite of granitoids in the Grampian Highlands, may be separated from each other by the mid-Grampian line, marking the abrupt change between low Nd, north of the line and high Nd south of the line. (Fig.1.5)

The source of these granitoids is still disputed by many workers. U-Pb analyses of zircons by Pigeon et al. (1974 & 1978), and Halliday et. al (1979), show that zircons recovered from many of the plutons in the Grampian Highlands record pre-magmatic events, suggesting the granitoids are derived from the melting of crustal rocks. Stephens and Halliday (1984), state that the three suites they identified all have differing melt sources. Although the Argyll suite contains inherited zircons, it has a very high Ba and Sr content, which the authors state are elements incompatible to the upper mantle, and would partition strongly into melts generated in the upper mantle. They state the Argyll suite

was derived from melting the upper mantle and lower crust, which is possibly Lewisian. The South of Scotland suite contains no inherited zircon, and has primitive geochemical and isotopic characteristics indicative of a mantle derived melt. Halliday (1984), suggests north of the mid-Grampian line old basement is one source of granitoid magma, whilst south of the line magma is generated by the partial melting of young arc and oceanic crust.

The tectonic mechanisms which caused partial melting in the crust/mantle are open to debate. Originally Phillips et al. (1976), produced a two plate, east-west convergence of Laurentia and Europe the final closure of the Iapetus ocean occurring early in the Silurian, far too early to be responsible for the emplacement of the Newer Granite suite in the Lower Devonian. To overcome this timing problem, summarised by Watson (1984), many authors have suggested methods of magma generation not involving subduction. Pitcher (1982) and Simpson et al. (1979) suggested the lower crust in the root of the Caledonide chain melted during decompression associated with rapid post orogenic uplift on major Highland faults. Tackling the same problem, Soper (1986) produced a three plate collision model. This envisaged the east-west closure and collision of Laurentia and Baltica during the Silurian, followed by the northwards accretion of a number of microplates onto the Laurentian shield in the lower Devonian. A magmatic arc associated with the Laurentia/Baltica closure generated the early members of the Cairngorm suite whilst the early subduction along the Solway line generated the Argyll Suite.



Thirlwall (1988), states the closure of the Iapetus ocean finally occurred in the Devonian between 410-398Ma. As plutonism occurred between 423 and 408Ma, plutonism was synchronous with northerly directed subduction, and the relationship between timing and plutonism is not a problem. He demonstrated that Devonian volcanics show spatial chemical relationships, similar to those seen in present day magmatic arcs above descending plates. Thirlwall states that the S-type plutons in the southern uplands are not related to subduction in the Solway Firth area, as the trench-arc gap is far too narrow.



CHAPTER 2. PETROGRAPHY AND FIELD RELATIONSHIPS OF  
IGNEOUS UNITS IN THE FOYERS COMPLEX.

## CHAPTER 2- PETROGRAPHY AND FIELD RELATIONSHIPS OF IGNEOUS UNITS IN THE FOYERS COMPLEX.

### 2.1 INTRODUCTION.

This chapter presents lithological descriptions and classifications of the igneous rocks in the Foyers Complex, and their relationships to each other. Emphasis is placed upon field relationships as these are important in determining the structural evolution of the Foyers Complex. More detailed petrographical descriptions are presented in Appendix A. Petrological features related to structure and fabric are highlighted in Chapter 4.

The Foyers Complex contains four major lithological units: the Errogie Quartz Diorite, the Chliabhain Quartz Monzodiorite, the Dalcrag Granodiorite and the Aberchalder Adamellite. The Meall a' Bhuailt Granodiorite is a minor plutonic intrusion. Later minor intrusions include microdiorite dykes, felsites, pegmatites and aplites. The distribution of the lithologies is shown in Enclosure 1.

Marston (1971) named the major plutonic units using the classification of Williams et al. (1958), classing Errogie Quartz Diorite as tonalite, Chliabhain Quartz Monzodiorite and Dalcrag Granodiorite as granodiorite, and Aberchalder Adamellite as adamellite. In this thesis lithologies are classified after Streckeisen (1976), prefixed by geographical type locality names. The term adamellite, defined by Hatch

et al. (1983) is used in addition, as the granite field in the Streckeisen (1976) classification is compositionally rather broad and the term adamellite gives a better appreciation of the lithology.

Modal analyses of rocks from one recognisable lithological unit may fall into a number of Streckeisen (1976), classification fields, but do form a distinctive cluster when plotted on a Streckeisen Q.A.P. triangle, showing that the major rock units are mineralogically distinguishable, (Fig.2.1). The field where most rocks from one unit plot, gives that unit its name. The Q.A.P. plot shows a punctuated increase in alkali feldspar and quartz, and a decrease in plagioclase between the rock units intruded early in the pluton's history and those intruded later, indicating the Foyers Complex has differentiated through time. The rocks exposed in the complex represent only stages of this differentiation rather than the whole spectrum.

Mineral modes plotted on a Mafics A.P. triangle (Fig.2.2) also form distinctive fields and a clear differentiation trend is seen. The Chliabhain Quartz Monzodiorite is slightly anomalous as it contains too few mafics to lie exactly on the differentiation pathway defined by the other rock units. A Mafics Q.P. plot (Fig.2.3) produces distinct clusters although again the Chliabhain Quartz Monzodiorite, due to reduced mafic minerals, lies off the differentiation pathway defined by the other rock units. A Mafics Q.A. plot (Fig.2.4) shows the Chliabhain Quartz Monzodiorite is a little too rich in alkali feldspar to fall comfortably on the differentiation pathway.

The Errogie Quartz Diorite/Chliabhain Quartz Monzodiorite intermediate unit shows a mineralogical overlap between the Errogie Quartz Diorite and the Chliabhain Quartz Monzodiorite, which mirrors the intermediate nature of the rock established in the field.

The contacts between the major units reveal little information on the relative ages of the igneous units. There are no chilled contacts, new mineral growth, or mineral fabrics associated with the contacts. Mapping on a large scale indicates that the igneous units were emplaced in the order;

- 1- Errogie Quartz Diorite.
- 2- Chliabhain Quartz Monzodiorite.
- 3- Dalcrag Granodiorite.
- 4- Aberchalder Adamellite.
- 5- Pegmatites/aplites/felsites.
- 6- Microdiorite dykes.

It is unlikely the intrusions are large xenoliths in the Errogie Quartz Diorite on account of their large size and gradational contacts.

The Dalcrag Granodiorite and Chliabhain Quartz Monzodiorite do not form contacts with each other but the more basic nature of the Chliabhain Quartz Monzodiorite implies it pre-dates the Dalcrag Granodiorite.

The Aberchalder Adamellite was the last major unit to be intruded as it cuts contacts between all other units and contains xenoliths of the other granitoids.

The acid sheets and microdiorite dykes cut sharply through all the plutonic units with the microdiorites post dating the acid sheets.

## 2.2 ERROGIE QUARTZ DIORITE.

### 2.2.1 Petrography.

The northern part of the Foyers Complex is dominated by Errogie Quartz Diorite forming topographically low, flat to rounded outcrop, (Enclosure 1).

The Errogie Quartz Diorite contains two lithologies, a coarse grained pale grey Quartz Diorite and a pale grey, fine grained leucocratic diorite. The latter lithology is volumetrically subordinate.

The Errogie Quartz Diorite is equigranular to sub-porphyritic with a weak foliation of parallel mafics and plagioclase laths (Plate 2.1). The grainsize is 0.2-5mm, but sparsely distributed plagioclase phenocrysts are 10mm long.

Plagioclase, biotite and hornblende dominate the mineralogy, (Table 2.1), quartz and orthoclase are minor phases and accessories include abundant sphene and magnetite, with less numerous apatite and zircon. Plagioclase shows normal zoning with andesine cores and oligoclase rims. Green/brown biotite forms large ragged plates and small grains, and dominates over subhedral green hornblende. Quartz is interstitial and orthoclase forms large enclosing grains which may partially replace

plagioclase (Plate 2.2).

#### 2.2.2 Field Relationships.

Small, <50m bodies, of medium grained leucocratic diorite within the Errogie Quartz Diorite, occur dominantly to the north west of Errogie. The medium grained leucocratic diorite forms sharp but very irregular contacts with the enclosing coarse Errogie Quartz Diorite. Fingers <10m in length, of medium grained leucocratic diorite extend from the contact into the Errogie Quartz Diorite. (Fig.2.5) The tips of these fingers break down in the plane of foliation giving large irregular, and small elliptical enclaves. The X and Y axes of the small ellipses are within the granitoid fabric. There are numerous isolated enclaves of medium grained leucocratic diorite separated by 100m's from their parent body.

It is not clear <sup>h</sup> whether the relationship of the medium grained leucocratic diorite to the coarse Quartz Diorite is xenolithic or intrusive. If xenolithic, the shape of the medium grained leucocratic diorite bodies have been highly modified by processes in the enclosing host, forming an irregular fingered margin. It is more feasible that the finer grained Quartz Diorite was intruded as a magma into a magmatic host, in a similar manner to the melanocratic microdiorites (see section 2.9.2). Flow within the magma chamber then disrupted these bodies, shaping the margins and transporting and deforming magma globules to form

ellipsoidal enclaves.

The main, coarse member of Errogie Quartz Diorite forms a number of contacts with the envelope rocks, mainly from Tom Mor to Creag a' Chliabhain on the northern margin and along the Beinn Bhuraich ridge on the southern margin. Clear contacts between envelope and granitoid body are rare, but the limited exposure shows there is no major change in mineralogy or texture as the margin is approached. Contacts are dominantly parallel to bedding, but locally cross cut bedding. The envelope is sheeted and veined by the Errogie Quartz Diorite.

## 2.3 CHLIABHAIN QUARTZ MONZODIORITE.

### 2.3.1 Petrography.

The Chliabhain Quartz Monzodiorite forms low, flat to rounded outcrop, and occupies 13% of the exposed pluton. It is distinguished in the field from the Errogie Quartz Diorite by the presence of subhedral pink orthoclase phenocrysts (<1.5cm long) forming 5-15% of the rock surface, by its coarser groundmass (0.5-8mm), and fewer mafics.

The Chliabhain Quartz Monzodiorite is coarse grained, porphyritic and weakly foliated. The mineralogy is dominated by plagioclase, biotite and orthoclase (Table 2.2). Hornblende and quartz are readily seen in section (Plate 2.3).

Plagioclase shows normal or oscillatory zoning (Plate 2.4), with andesine cores and oligoclase rims. Green/brown biotite



is common forming large irregular plates. Hornblende forms small subhedral green/yellow grains and equigranular glomerophytic clusters. Perthitic orthoclase forms phenocrysts which often enclose other mineral phases and may partially replace plagioclase, (Plate 2.5). Quartz is interstitial but may develop larger aggregates.

#### 2.3.2 Field Relationships.

Chliabhain Quartz Monzodiorite forms irregular bodies within the Errogie Quartz Diorite, ranging in size from 10's m to several Km<sup>2</sup>. The contacts between the Chliabhain Quartz Monzodiorites and the enclosing Errogie Quartz Diorites are irregular, patchy, and gradational over distances up to 30m (Fig.2.6). Many contact zones are inferred due to poor exposure.

The gradational contacts imply that the Chliabhain Quartz Monzodiorites were magmatic when emplaced into magmatic Errogie Quartz Diorite, the magmatic nature of both the units probably allowing chemical and physical mixing across the contacts.

The Chliabhain Quartz Monzodiorite generally forms contacts with the envelope parallel to bedding, although is locally cross cutting. Clear envelope contacts are seen on the summit of Creag a' Chliabhain, and within the north western wall of Conagleann, although here the contact is difficult to trace due to the large numbers of bedding parallel sheets in the envelope. There is no change in the mineralogy or

texture of the granitoid as the contact is approached. The Chliabhain Quartz Monzodiorite veins and sheets the psammitic envelope parallel to bedding.

The Quartz Monzodiorite/Quartz Diorite intermediate lithology occurs within the Errogie Quartz Diorite, a good example occurring near Farraline at G.R.55602120. This lithology forms very irregular diffuse, indistinct boundaries, and contains a greatly fluctuating concentration of anhedral orthoclase phenocrysts (<5%). It is possible that the Quartz Monzodiorite/Quartz Diorite intermediates represent small magmatic pulses of magma which were slightly more differentiated than the Errogie Quartz Diorite. A high proportion of melt in the Errogie Quartz Diorite and in the intermediate pulse would allow substantial chemical and physical mixing, thus forming very gradational contacts. The intermediate rocks may be the collection points for late potassic fluids, which migrated during late solid state deformation of the Errogie Quartz Diorite, (Hibbard, 1987).

## 2.4 DALCRAG GRANODIORITE.

### 2.4.1 Petrography.

The Dalcrag Granodiorite is distinguished by the presence of numerous orthoclase phenocrysts, (10-15% of rock surface) and visible quartz.(Plate 2.6). Occasional minor units of granodiorite are equigranular or semi-porphyritic. Sometimes

present are abundant, irregular patches of medium grained leucocratic diorite, <1.5cm in diameter, with a mineralogy of plagioclase, hornblende and biotite. Unlike the microdiorite enclaves they have irregular shapes and orientations, and form an intrinsic part of the igneous fabric and are difficult to distinguish from the granodiorite.

The Dalcrag Granodiorite is coarse grained, (0.5-6mm) and weakly foliated. Plagioclase is the dominant mineral phase but orthoclase, quartz, biotite and hornblende are also abundant (Table 2.3). Accessory minerals sphene, zircon, magnetite and apatite are present in small numbers.

Plagioclase is oligoclase, which shows normal or oscillatory zoning. Green/brown biotite forms ragged subhedral plates and dominates over sub-euhedral green hornblende. Orthoclase forms subhedral phenocrysts which may partially replace adjacent plagioclase. Quartz forms interstitial fillings and larger aggregates, (Plate 2.7).

#### 2.4.2 Field Relationships.

Dalcrag Granodiorite forms a large body in the south west of the complex. This body is separated from the Errogie Quartz Diorite and the Chliabhain Quartz Monzodiorite by several hundred meters of the Carn Dubh to Carn Choire Riabaich Central Psammite Septum. (Enclosure 1). North east of this septum are two granodiorite bodies within the Errogie Quartz Diorite which when mapped at a scale of

1:10,000, show irregular outlines, and cover several square kilometers. Perhaps minor amounts of Dalcrag Granodiorite from south west of the Psammite Septum "underspilled" the Central Psammite Septum and entered the main Errogie Quartz Diorite body, (Fig.2.7). Contacts between Errogie Quartz Diorite and Dalcrag Granodiorite are gradational but are <5m wide. The contacts are defined by an increase in quartz, a decrease in mafics, and the appearance of orthoclase phenocrysts on entering the granodiorite (Fig.2.6). These gradational contacts imply the Errogie Quartz Diorite still contained abundant melt at the time of Dalcrag Granodiorite intrusion.

Within the porphyritic Dalcrag Granodiorite are occasional, more acidic, finer grained, equigranular granodiorites with sharp, well defined contacts. Reasonably intense contact parallel foliations, mafic banding and schlieren are developed close (<50cm) to the contact, in the finer grained granodiorite. Such a contact occurs in the B852 Foyers road cut (G.R.49951940). These individual, minor, finer grained granodiorites may represent later, more acid magma intruded into rigid Dalcrag Granodiorite.

The Dalcrag Granodiorite forms numerous contacts with the psammite envelope (Enclosure 1). The contacts are dominantly parallel to bedding, but locally cross cut, as seen between the River E. and Beinn Mheadhoin. Bedding parallel granodiorite veining in the envelope is intense. The envelope is heavily intruded by granodiorite, particularly between Cairn Gairbthinn and Whitebridge. Towards Whitebridge the psammite envelope breaks down forming

xenolithic granodiorite. This heavily veined area is interpreted as the stoped roof of the Dalcrag Granodiorite. Generally there is no strong change of mineralogy or texture in the granodiorite as the margin is approached.

#### 2.4.3 Loch Kemp Marginal Granodiorite Facies.

Approaching the south west margin of the Foyers Complex, close to Loch Kemp, the porphyritic Dalcrag Granodiorite develops a distinct marginal facies, (the Loch Kemp Marginal Granodiorite Facies) (Enclosure 2).

Coarse Dalcrag Granodiorite grades into the marginal facies by a reduction in grain size, becoming medium grained, accompanied by a reduction in the size, and number of orthoclase phenocrysts. The gradation occurs over a distance of 200m. Close to Loch Kemp the Marginal Facies Zone is 500m wide, but close to the River Foyers the zone reaches a width of 1.5km, the zone extending from north of Dell Lodge G.R.48561628 to the summit of Tom Rathail G.R.48111517.

The Loch Kemp Granodiorite Facies intensely veins and sheets the psammite envelope. Within the veined envelope are a number of coarse grained granodiorite stocks of irregular outline. The outer contacts of the stocks cross cut the bedding in the envelope. At G.R.46901555 a continuous (not occurring as veins) outcrop of fine grained granodiorite is sharply but irregularly cut by coarse grained granodiorite. The stocks have a lithology similar to this coarse grained granodiorite, suggesting the stocks may post date the

marginal veining. However, clear contacts where stock margins cross cut the veins are not seen. Veins are never seen cross cutting the stocks. Platten (pers.com.) suggests these stocks may be continuous with the Loch Knockie granitoid exposed in the Drummond plantation, mapped by Mould (1946) and Parsons (1982). Although no clear contact with the Foyers Complex is seen, these stocks probably post date the intrusion of the Dalcrag Granodiorite, because they cut the Loch Kemp Marginal Facies. However, different emplacement times do not preclude the stocks and granitoid bodies in the Drummond plantation from being part of the Dalcrag Granodiorite. Both Marston (1971) and Mould (1946) thought the Knockie granitoid and the envelope stocks, formed a roof zone to the Dalcrag Granodiorite. The Marginal Granodiorite Facies and veins at Loch Kemp may be a chill against country rocks. The coarse grained granodiorite stocks and the Loch Knockie granitoid may represent small stocks rising into the roof envelope which was already heated by buried Foyers Granite and veins of the Loch Kemp Granodiorite Facies.

#### 2.5 MEALL A' BHUAILT GRANODIORITE.

The Meall a' Bhuaile Granodiorite only occurs on the northern slopes of Meall a' Bhuaile (G.R.58601700). It is an equigranular, pale cream, coarse grained rock, containing abundant creamy plagioclase, and quartz aggregates, with lesser amounts of alkali feldspar. Mafics are moderately

abundant, with biotite more common than hornblende. There are minor pegmatite patches, <10cm in diameter, and are rich in alkali feldspar and euhedral hornblende.

The Meall a' Bhuaillt Granodiorite intrudes both Chliabhain Quartz Monzodiorite and Errrogie Quartz Diorite, forming irregularly shaped contacts which are gradational on a centimeter scale and is cut by adamellite. This body is an acid granodiorite falling very close to the adamellite field on a Q.A.P. plot, (Marston 1971), which on a Foyers' differentiation pathway falls between the granodiorite and the adamellite. It was probably intruded into an almost solidified pluton.

## 2.6 DUN GARBH GRANODIORITE.

The Dun Garbh Granodiorite occurs on the north western side of the Gleann Liath Fault, and is unconformably overlain by the Old Red Sandstone conglomerates (Enclosure 1). It intrudes a series of migmatites which have been interpreted as Lewisian (Mould, 1946), Dalradian, (Marston, 1971) and Albynian, (Rock et al. 1984 & 1986). It is difficult to say whether this granitoid mass was ever part of the Foyers Complex. Here it is treated separately from the Foyers Complex as it is only in fault contact with the Foyers Complex.

Petrographically it is similar to the Dalcrag Granodiorite, but contains approximately 10% more quartz. Harker plots of major and trace elements show that compositionally the Dun



Garbh Granodiorite lies close to the differentiation trends shown by elements within the Dalcrag Granodiorite. (Fig. 2.14)

The contact between the granodiorite and the migmatites is sharp, with no veining into the migmatites, and it cross cuts the migmatitic banding. Marston (1971), thought the Dun Garbh Granodiorite was a slice of Dalcrag Granodiorite carried north eastwards along the Gleann Liath Fault from the south west margin of the Foyers Complex. However the south west margin of the Foyers Complex is concordant with the psammite foliations, and is intensely veined. The distinctive fine grained marginal facies of the Dalcrag Granodiorite is absent in the Dun Garbh Granodiorite. Although these factors seem to indicate the Dun Garbh Granodiorite did not originate from the south west margin of the Foyers Complex, affinities with the Dalcrag Granodiorite cannot be discounted. If the Dun Garbh Granodiorite did originate in the south west of the Foyers Complex it would require dextral movement on the Gleann Liath Fault, whilst most post-Foyers Complex fault movements are thought to be normal and sinistral. (Chapter 7.)

## 2.7 ABERCHALDER ADAMELLITE.

### 2.7.1 Petrography.

The grey/pink Aberchalder Adamellite is equigranular and medium grained (1-4mm), although irregular finer grained patches frequently occur (Plates 2.8 & 2.9). The adamellite is dominated by plagioclase, quartz and alkali feldspar in

approximately equal amounts, accompanied by minor biotite and accessories. (Table 2.4) Most mineral phases are granular and form an-subhedral grains.

Plagioclase shows weak normal zoning, from oligoclase cores to rims occasionally as sodic as albite. Alkali feldspar is dominated by perthitic, subhedral orthoclase, although small grains of microcline are common. Quartz forms large interlocking aggregates. Biotite occurs as small chloritised plates and hornblende forms sparse anhedral crystals, (Plate 2.10). Minor accessories are sphene, zircon, apatite and magnetite, and often form irregular glomerocrysts.

#### 2.7.2 Field Relationships.

The Aberchalder Adamellite cuts all the other major units in the Foyers Complex and forms discrete stocks within the envelope, e.g. the Carn Bhreabaig stock at G.R.50401585. The majority of the Aberchalder Adamellite occurs south east of Loch Mhor, as highly irregular bodies (Enclosure 1). In areas of good exposure it is possible to see some of the margins "budding out" to produce rounded stocks connected to the main mass by a neck, exemplified by Meall Donn G.R.57602115 and Carn Liath G.R.55401860. The major areas of Aberchalder Adamellite occur in a large belt just north of the Psammite Septum, in the Carn Liath-Aberchalder Burn areas and south west of Creag a' Chliabhain. Whether all these intrusions are linked is difficult to determine due to drift cover.

The contacts, where seen, are always sharp with no marginal alteration in mineralogy or texture.(Fig.2.6), and have very steep attitudes. Crystals interlock across contacts between adamellite and host indicating the presence of interstitial liquid in the host, (Hibbard and Watters 1985).

Around some adamellite masses, particularly the mass south of Wester Aberchalder, there are broad zones of adamellite veins and small stocks, cutting earlier units of the Foyers Complex, but showing no particular trend. The veins have irregular to parallel sided morphologies, and are variable in width. The narrow veins show parallel sides whilst the wider veins are irregular. Occasional stocks are irregularly elongate, and are <100m wide. The large adamellite mass south, east of Migovie G.R.53901880, contains many xenoliths of Errogie Quartz Diorite and Chliabhain Quartz Monzodiorite, many >20m in diameter. The xenoliths show no assimilation by, or gradation into the Aberchalder Adamellite. There are also a few large bodies of Errogie Quartz Diorite and Chliabhain Quartz Monzodiorite, many hundreds of meters in diameter, within the adamellite (G.R.56901805). Whether these represent large xenoliths or plutonic roof pendants is not clear.

Contacts between Aberchalder Adamellite and the envelope psammites are always sharp and there are no veins of adamellite in the psammite envelope. An adamellite at Coire Bhuide shows vertical contacts in the eastern wall of the hanging valley leading into Conagleann. The occasional stock of Aberchalder Adamellite cross cuts the Maol Chnoc Complex,(Chapter 5).

### 2.7.3 Granitic Porphyries.

Within the Aberchalder Adamellite and Chliabhain Quartz Monzodiorite on Carn Liath (G.R.55401850) are both granitic porphyries and rocks texturally intermediate between the porphyries and Aberchalder Adamellite. The porphyries are characterised by phenocrysts (<6mm) in a very fine pink matrix (<0.1mm) (Plates 2.11 & 2.12). Phenocrysts are single crystals or monomineralic aggregates of biotite, plagioclase, orthoclase and quartz. The groundmass contains all mineral phases in similar proportions to those of the phenocryst phase.

Contacts developed between the adamellite and the porphyries are irregular and vary between sharp and gradational. Gradational contacts are rather patchy and not continuously gradational. Occasionally the porphyry occurs as horizontal, thick (<3m), planar sheets, cutting sharply through the adamellite.

The Aberchalder Adamellite/granitic porphyry intermediate grades texturally into both the porphyry and adamellite. The porphyries develop small areas of coarser groundmass minerals which become coarser, larger, and more abundant until a texture typical of the adamellite is developed.

#### 2.7.4 Emplacement Of Adamellite And Porphyries.

Field evidence suggests that the adamellite stocks are now exposed at crustal levels illustrating different degrees of structural development.

The adamellite was intruded into rigid rock units, containing minor amounts of melt. The presence of adamellite veins in the host granitoid and, granitoid xenoliths in the adamellite suggests that a veining and stoping intrusion mechanism was involved. The rather rounded nature of some of the stocks suggests some form of insitu expansion of the stocks. Coward, (1981) and Bateman, (1985) state that a rounded, external granitoid morphology is indicative of insitu ballooning or diapirism.

The vein complexes possibly lie above adamellite root zones, which are connected to the small stocks and veins. The small adamellite bodies within the vein complexes may represent the early sites of stoping.

The most feasible method of emplacement is illustrated in (Fig.2.8). Here the adamellite rises as a fluid magma by veining and stoping it's granitoid host. Where the host has been stoped, the adamellite is able to establish a more coherent magma chamber. The transition between veining and a large intrusive body is marked by the development of small stocks adjacent to the chamber, the stocks probably nucleating on adamellite veins, which had a greater than

average input of magma.

The granite porphyries are locally derived, textural variations, or late differentiates of the Aberchalder Adamellite. As some porphyries sharply cross cut the adamellite, they must post date the adamellite becoming rigid enough to sustain brittle fractures. Some porphyries show irregular gradational contacts with the adamellite implying that the adamellite was still melt rich. There is also a complete suite of rocks which mark the lithological changes between the adamellite and porphyry. This suggests that the porphyry was derived from the adamellite as a late differentiate. Thus the adamellite had cooled enough to allow the formation of brittle fractures, whilst in adjacent areas granite porphyry magma was still being generated from adamellite containing enough melt to allow lithological gradation into the porphyry.

## 2.8 CARN BHREABAIG ADAMELLITE.

An adamellite stock, 400m by 200m, intruding quartzites and pebbly psammities, is exposed on the south western slopes of Carn Bhreabaig. The adamellite is very pale, brownish-pink and equigranular. At outcrop it contains visible plagioclase, biotite, quartz and orthoclase. On two horizontal surfaces the granite develops lithological banding, (Plate 2.13).

The banding is a rhythmically repeated layering, defined by both changes in the rock grain size and the relative

proportions of all the major mineral species. Layers range from 7cm to 50cm thick, and are orientated at 100/60/S in one locality and 080 in the other. The gross mineralogy of the bands is similar to the remainder of adamellitic stock.

15 lithological bands are seen, but are volumetrically minor compared to unbanded adamellite. The widely spaced layers quickly fade into unbanded adamellite in a direction perpendicular to banding strike. The repeated layering extends over 10m along strike before disappearing under peat patches. As layering is limited to occasional outcrops it is assumed the layers also fade into unbanded adamellite along strike. The layers are not parallel to the walls of the stock and it is not clear whether the layers are in the same orientation as when they formed.

Each unit shows reverse mineral density grading and normal size grading when related to their present orientation (Fig.2.9). The contact between each layer is defined by a sharp lithological break between the fine grained biotite rich portion of each band and the coarse grained orthoclase rich portion, (Plate 2.14). In their present orientation the top portion of each cycle is dominated by plagioclase and biotite. The top of the cycle is finer grained than the non-banded adamellite. Moving down the cycle the biotite and plagioclase become scarcer, with quartz and orthoclase becoming more abundant. The bottom portion of the layer is coarser grained than the unbanded adamellite. The mineralogical banding is reflected by the weathering profile on horizontal surfaces. A relief of <5mm is developed to give a series of asymmetrical "ripples". The trough is



formed by the micaceous portion of the layer and the crest by the orthoclase rich portion. The gradation in the layer forms the 'stoss slope' and the break between the cycles forms the 'lee slope'.

Barriere (1981), states this form of grading is accomplished by size sorting, which controls the mineralogical grading. The fine fraction contains small minerals, often mafics and plagioclase. The coarse fraction contains larger minerals, often quartz and orthoclase. Barriere (1981), concludes that the fine (mafic) layer starts each cycle, indicating that the cycles in the Carn Bhreabaig adamellite young downwards. Inspection of the grading shows that it is defined by mineral size sorting with minerals of similar size but differing densities i.e. biotite and quartz, occupying the same horizon. This indicates the layering did not form by gravity settling.

Barriere (1981), states that granitic layering in the Ploumanac'h granite (Brittany) formed by magmatic flow, capable of size sorting crystals. The Bagnold effect is the main mechanism capable of inducing crystal size sorting during flow. The crystals are driven away from the high velocity flow zones adjacent to the chamber walls, and the larger crystals move further from the wall.

In the Carn Bhreabhaig Adamellite stock there are many layers, indicating a repeated layer-forming process. The most probable mechanism is magma convection, circulating magma past solidified magma walls, allowing the Bagnold effect to operate. As the banding is localised, the convection and/or layer forming mechanisms were also

localised. As the fine grained layer is structurally at the top, and stratigraphically at the bottom, of each cycle, then assuming no tectonic overturning, the layering may have formed on the roof of the magma chamber or perhaps the banding is a piece of solidified granitic wall rock which has been removed, transported and repositioned by magma currents. It is possible solid state deformation as the stock expands could tilt layers forming parallel to the pluton walls.

## 2.9 MICRODIORITE ENCLAVES.

### 2.9.1 Petrography.

Elliptical, dark grey, medium grained (0.2mm-1mm) microdiorite enclaves, often <30cm long, occur throughout Foyers Complex with the exception of the Aberchalder Adamellite (Plate 2.15). They are most abundant, as swarms, between Loch an Ordain (G.R.55402400) and Errogie (G.R.56402260), illustrated admirably on the shores of Loch Mhor' (G.R.55652213).

The enclaves are equigranular (Plate 2.16) to sub-porphyritic and are dominated by plagioclase, biotite and hornblende, (Fig.2.10) Orthoclase and quartz are minor phases whilst sphene, magnetite and rutile form the accessories (Table 2.5). The plagioclase is andesine and is weakly, normally zoned. Green/brown biotite and green hornblende form subhedral grains, often partially enclosing

plagioclase laths. Quartz and alkali feldspar are uncommon, forming interstitial grains.

Highton (1986) places the microdiorite enclaves in the same suite as the microdiorite dykes, which he states were derived from the differentiation of the Foyers Complex.

#### 2.9.2 Field Relationships.

The enclaves show no chill against their host and there is strong interlocking of crystals across the contact. Frequently phenocrysts of plagioclase are seen to straddle the enclave/host boundary. There is no mineralogical change from core to margin of the enclave. Occasionally, two or more microdiorite enclaves are joined by thin microdiorite necks, (Plate 2.17). Host granitoids, adjacent to the enclaves, do not differ in mineralogy or texture from more distant granitoid. Hibbard & Watters (1985), conclude interlocking of crystals across enclave/host contacts indicates both enclave and host were partially molten as the enclaves entered the host. The fine grained nature of the enclaves is possibly due to hot dioritic magma cooling more quickly in a more acid and crystallised host. (Blake 1981).

The field evidence appears to confirm the well documented ideas (Blake et al. 1965, Walker and Skelhorn 1966, Blake 1981, Vernon 1983 & 1989, Hibbard and Watters 1985) that microdiorite enclaves are a result of the mixing of both mafic and felsic melts. Both the single and the swarms of enclaves are derived from small magmatic microdiorite bodies

intruded into a magmatic host. The microdiorite body then broke up into blebs. The enclave swarms may represent bodies intruded into the pluton relatively late. Such microdiorites would only be subjected to a little mixing by magmatic currents with many of the enclaves remaining together. The isolated microdiorite enclaves represent earlier intrusions emplaced into a more mobile pluton where strong magmatic currents could separate the enclaves. Blake (1981), showed that felsic host adjacent to microdiorite swarms may become superheated during intrusion of the basic magma leading to re-mobilisation of the crystallised host. However the geochemical similarity of the enclaves and host in the Foyers Complex would limit superheating in the host.

In the bed of the River Gourag (G.R.51001770) there is an intense swarm of enclaves aligned with the igneous foliation, within generally enclave poor granodiorite, (Plate 2.18). About 80% of the swarm is microdiorite whilst the remainder is composed of psammite and appinite xenoliths. Magma currents may have concentrated a large number of differing xenoliths and enclaves. It is unclear whether the local intrusion of a microdiorite body aided the concentration of xenoliths.

## 2.10 MICRODIORITE DYKES.

### 2.10.1 Introduction.

Swarms of basic dykes are common throughout the Northern, Western and Central Highlands of Scotland. Pre-tectonic

dykes form the amphibolite suite, and those emplaced towards the end or after the Caledonian orogeny form the microdiorite suite, (Smith,1979).

Hinxman and Anderton (1915), classed mafic dykes in the upper Strathspey as lamprophyres. Marston (1971), thought the dykes at Foyers were part of the late Devonian lamprophyre suite on the basis of similar mineralogy and petrology. Dearnley (1966), associated the microdiorite suite with the intrusion of the Newer Granites.

On the basis of similar geochemistries and petrologies between the Foyers Complex and the microdiorite dykes, Highton (1986), concluded that, the dykes are the early differentiation products of the Foyers Complex.

#### 2.10.2 Petrography.

All the dykes are dominated by plagioclase and mafics but three types of microdiorite dyke can be petrographically distinguished.

##### 1 Melanocratic microdiorite.

This is a dark grey, fine/medium grained rock with visible plagioclase and hornblende. The grainsize is 0.1-0.4mm, although elongate hornblende laths may be 2mm long and define a well parallel mineral fabric, which is strongest near the dyke margin, (Plate 2.19). The fabric bifurcates

around glomerophyric mafic clots, and any quartz present is not strained. Both these criteria indicate the fabric was formed by magmatic flow. (Paterson et al. 1989).

Plagioclase is strongly zoned, with andesine cores and oligoclase rims. Hornblende is elongate or skeletal (Plates 2.20 & 2.21). Biotite forms small ragged chloritised plates which may pseudomorph hornblende. Orthoclase and quartz form small irregular grains, as do the accessories sphene, magnetite and zircon, (Table 2.6)

## 2 Fine grained, quartz xenocrystic microdiorite.

These dykes are buff grey with a very fine grained groundmass (<0.05mm) containing numerous large, rounded quartz xenocrysts and pink plagioclase phenocrysts, (Plate 2.22).

The groundmass is composed of narrow plagioclase laths, hornblende needles, chloritised plates of biotite and quartz and alkali feldspar only revealed in thin section by staining. Quartz xenocrysts are <1cm in diameter showing corroded and embayed margins, rimmed by actinolite, (Plates 2.23 & 2.24). The plagioclase phenocrysts are <2cm long and show sericitisation.

### 3 Mesocratic plagioclase porphyry.

These dykes have a pale brown weathering surface with prominent white plagioclase phenocrysts, <2cm in length. The groundmass is composed of grains <0.3mm in diameter, containing quartz, orthoclase, microcline, plagioclase and biotite, (Plate 2.25). The plagioclase phenocrysts are either single or form synneusis clusters. They often show three distinct compositional zones, the outer zone enclosing the whole of the synneusis cluster (Plate 2.26).

Although placed within the microdiorite suite, the dykes are not actually microdiorites (Streckeisen, 1976). The melanocratic dykes have a large compositional range and plot as micro quartz monzodiorites and micro tonalites. The plagioclase porphyries plot close to the granodiorite/quartz monzodiorite boundary, (Fig.2.11). The quartz xenocryst, bearing microdiorites are too fine to point count. As an estimate the latter dyke would fall compositionally between the other two members of the microdiorite suite.

The gradation from melanocratic dykes to plagioclase porphyries is marked by an increase in alkali feldspar, a decrease in mafics and an increase in the biotite:hornblende ratio.



### 2.10.3 Field Relationships.

All three lithologies occur as north east-south west trending dykes, 1-3m thick, steeply dipping (50-85) to the north west. They occur sparsely throughout the pluton, but are relatively abundant north east of Trinloist G.R.52212078, (Fig.2.12) Chilled margins only occur in dykes distal to the pluton. The sharpness of the dyke margin indicates intrusion into a brittle environment. Where exposure is good, it is common to see small irregular veinlets of microdiorite extending from the dykes into the plutonic host and these are finer grained than their parent dyke, (Plate 2.27).

On the summit of Tom a' Chliabhain (G.R.46601505) a mesocratic plagioclase porphyry dyke shows good chilled margins against its host, a granodiorite stock. The chill shows a strong trimodal grain size distribution. The large plagioclase phenocrysts in the chill show the same number of zones as plagioclase phenocrysts from unchilled dykes, including an outer zone rich in melt inclusions, suggesting the large phenocrysts were transported into the chill zone from their place of growth. The plagioclase phenocrysts become smaller towards the margins of the dyke, but retain the outer growth zone, indicating that the size decrease towards the margins may be due to hydrodynamic sorting by magma flowing parallel to the wall, rather than different

growth rates, (Barriere, 1981). The Bagnold and the Magnus effects, cause large particles to move away from the high velocity wall zone to the lower velocity centre of the dyke, thus forming a size gradient of plagioclase phenocrysts. Thus the large phenocrysts were carried into the dyke, and magma flow created a size gradient with smaller phenocrysts towards the margin.

The medium grained, flow aligned minerals, probably grew distal to the chill zone but were caught up in the fine grained matrix as it rapidly crystallised on the dyke wall.

It thus appears that distal to the Foyers Complex, the country rocks were cool enough to chill the dykes, whereas, at the time of pluton emplacement, the regional temperatures were too high to chill the plutonic complex. The rapid cooling of the crust between pluton and microgranodiorite dyke emplacement may be explained by large amounts of post pluton emplacement regional uplift.

The north westerly dip of dykes and their north easterly trend implies that the dykes were intruded along fractures associated with the Great Glen Fault. Normal faulting would be conducive to magma emplacement and Mykura (1983), states that the Devonian sediments were affected by normal faulting, with a downthrow to the north west. However, at Garthbeg (G.R.51791689) a quartz xenocrystic, melanocratic, microdiorite trends east-west.

Due to the paucity of exposure and general parallelism of the dykes, no cross cutting relationships have been recognised between the different microdiorite lithologies, (Fig.2.12). Melanocratic microdiorite dykes cut the Errogie

Quartz Diorite, Dalcrag Granodiorite and Aberchalder Adamellite, the quartz xenocryst bearing microdiorite cuts Dalcrag Granodiorite and Aberchalder Adamellite and the leucocratic microdiorite cuts the Dalcrag Granodiorite. All dyke lithologies cut the envelope rocks.

The dykes also cut Foyers pegmatites, and may use the same intrusion plane. Plate 2.28 shows a large euhedral orthoclase crystal enclosed by microdiorite, which forms a flow fabric around the crystal, indicating the orthoclase predates the microdiorite. The pegmatite and microdiorite form a composite dyke, 70cm thick, coating a low Errogie Quartz Diorite cliff.

The most basic dykes cross cut the Aberchalder Adamellite in a brittle fashion, so it is evident that the microdiorite suite was emplaced after solidification of the Foyers Complex. This casts doubt on the dykes being derived from the early differentiation products of the Foyers Complex magma, suggested by Highton (1986).

## 2.11, APPINITIC DIORITES.

### 2.11.1 Petrography.

Appinitic diorite bodies were mapped in the body and envelope of the Foyers Complex. There are melanocratic and leucocratic appinites identified in the field, although both have colour indices of 50-60. The leucocratic nature of some appinites is a result of the clustering of leucocratic

minerals. The appinitic diorites are dominated by sub-euhedral hornblende and plagioclase, but have very variable mineralogies, even within the same body. Other phases include biotite, augite, alkali feldspar, quartz, sphene and apatite, (Table 2.7), (Plates 2.29 & 2.30). The grain size of the appinites from 1mm to 1.5cm, with apatite and sphene often quite coarse. Leucocratic appinites contain abundant quartz but little alkali feldspar, whilst melanocratic appinites contain abundant alkali feldspar and little quartz. (Fig.2.13). Large prismatic hornblendes are common, (Plate 2.31), but many samples are dominated by stubby hornblende (Plate 2.32). It appears that the appinite diorite suite contains both appinites (ss.) and diorites, (French 1966).

The appinite diorite bodies are often cut by veins and patches of quartz-orthoclase pegmatite, with a grainsize of 5mm-1.5cm. These pegmatites do not extend into the host around the appinite body. They are 1cm-20cm thick, forming irregular networks where veins coalesce or feed into patches. Many veins are blind ended, and the patches isolated. The pegmatite forms an interlocking crystal fabric with the appinite.

#### 2.11.2 Field Relationships.

The appinites occur in the envelope and all the units of the pluton except the Aberchalder Adamellite. They form irregular to sub-rounded bodies 10m to 100m in diameter.

Contacts between the appinites and their plutonic host rocks are seldom seen, and yield little information about their relative ages. The Dalcrag Granodiorite close to a large appinite body, north east of Corriegarth (G.R.51301735) contains occasional, small appinitic xenoliths, possibly indicating the large appinite body is a large xenolith. An external contact of the large appinite body is seen in a very small outcrop, but the actual contact between appinite and granitoid is obscured by a narrow (<2m) septum of psammite.

On the south west margin of the complex, close to the northern shores of Loch Kemp are angular undeformed dioritic/appinitic bodies 5cm-2m in diameter, which are obviously xenoliths. With the evidence gathered it is only possible to say that some appinites have a xenolithic relationship to the plutonic rocks. It is possible that some of the appinites were intruded into the pluton and therefore the appinite suite may have a pre-plutonic to post-plutonic history.

## 2.12. MINOR ACID SHEETS.

### 2.12.1 Felsites.

Felsites are light pink to yellowish white in colour and are composed of saccroidal, very fine grained (<0.02mm) alkali feldspar and quartz. They occur only rarely as cross cutting dykes, <1m wide. They are more common in the

envelope, particularly in the roof zone south west of Loch Kemp, where felsite forms irregular bodies <7m in diameter, and cross cut the bedding. In the Central Psammite Septum a parallel sided, subvertical dyke 1m thick, cross cuts the psammite bedding.

#### 2.12.2 Pegmatites.

Most pegmatites form thin, <5cm, coatings along planar joint surfaces within all the granitoid units in the Foyers Complex. Pegmatites also occur as sparse, thin veins between 20cm and commonly 2cm thick. This type of pegmatite is found in areas close to the large Aberchalder Adamellite stocks. No pegmatites cut the envelope psammites. The pegmatites contain coarse grained orthoclase, (often with symplectic quartz intergrowths) and quartz.

It appears that the pegmatites simply represent the water rich phase remaining after adamellite crystallisation, moving out along cooling joints in the pluton, or close to the adamellite stocks where they fill fractures.

#### 2.12.3 Aplites.

Again these are sparsely developed as thin, <20cm veins which cross cut all the plutonic rocks. They are a very pale, ash grey in colour, with a saccharoidal texture composed of grains 0.02-0.3mm diameter (Plate 2.33). The aplites are dominated by quartz, (40-50%), with alkali feldspar forming 15-40%. Plagioclase content is very variable, more basic



aplites containing >15% plagioclase, and acidic aplites containing <10% plagioclase. Other mineral species are a very minor component, but are dominated by biotite and muscovite mica. Aplites form parallel sided veins <20cm wide with sharp contacts. The aplites are commonest close to the Aberchalder Adamellite and are the late, water saturated, silicate melt fraction.

### 2.13 GEOCHEMISTRY OF THE MAJOR UNITS.

Highton (1986), presents a detailed geochemical analysis and evolution of the Foyers Complex, and analyses presented here are for comparative purposes only.

24 whole rock samples of Errogie Quartz Diorite, Chliabhain Quartz Monzodiorite, Errogie Quartz Diorite/Chliabhain Quartz Monzodiorite intermediate, Dalcrag Granodiorite, Dun Garbh Granodiorite and Aberchalder Adamellite were analysed for major and trace elements using an Inductively Coupled Plasma Spectrometer, (I.C.P.S.) (Appendix B).

When plotted on Harker diagrams the majority of major and trace elements all show good differentiation trends indicative of a calc-alkaline magma, (Fig.2.14). This calc alkaline trend is also seen on an A.F.M. plot (Fig.2.15). The most important aspect of the Harker plots is that the major units within the Foyers Complex defined on the basis of mineralogy and field appearance, can also be defined by their geochemistry. The Harker plots show that the differentiation trend displayed by the rocks in the Foyers



Complex is not continuous, with each major unit forming a distinctive cluster of points. The Chliabhain Quartz Monzodiorite/Errogie Quartz Diorite intermediate forms a continuous trend between Errogie Quartz Diorite and Chliabhain Quartz Monzodiorite but in the potassium, barium, phosphorus and scandium plots the trend is discontinuous. The Chliabhain Quartz Monzodiorites show an unusually high enrichment of potassium and barium, (reflecting the unusually high modal proportion of orthoclase) so that the composition does not lie on the differentiation trend. Iron, magnesium, titanium, manganese, copper, nickel and vanadium in the Chliabhain Quartz Diorite are strongly depleted compared to the Errogie Quartz Diorite, but are at a similar concentration to the Dalcrag Granodiorite. This reflects the rather low modal mafic mineral content of the Chliabhain Quartz Monzodiorite, considering the basic nature of this rock defined by the Q.A.P. plot.

The geochemical analyses are similar to those presented by both Highton (1986) and Marston (1971), which strengthens the validity of the data.

CHAPTER 3. GRANITOID VEINING AND STOPING IN THE  
FOYERS COMPLEX.

## CHAPTER 3. GRANITOID VEINING AND STOPING IN THE FOYERS COMPLEX.

### 3.1 VEINING.

The psammite envelope around the Foyers Complex is heavily veined by granitoid material. There are three suites of veins.

- 1- Abundant veins, lithologically similar to units within the Foyers Complex.
- 2- Veins related to the Maol Chnoc Complex.
- 3- Granitoid veins, lithologically dissimilar to either major plutonic body, and vein the envelope on Beinn Sgurrach.

The veins of group 1 occur all around the Foyers Complex. Veins in group 2 are located adjacent to the Maol Chnoc Complex, especially on the Beinn Dubcharaidh ridge and in the Torr Shelly quarry-Croftdhu-Tom Mor areas. The Maol Chnoc veins are described by Highton (1986) and are discussed in Chapter 5. Group 3 veins are limited to the Beinn Sgurrach ridge and will be discussed at the end of this chapter.

The veins associated with the Foyers Complex are volumetrically the most important, and yield most information about the emplacement mechanisms of the Foyers Complex.

### 3.1.1 Veining As Part Of The Foyers Complex.

There are 3 major vein lithologies within this group of veins: quartz diorite, quartz monzodiorite and granodiorite. These are lithologically correlated with the Errogie Quartz Diorite, Chliabhain Quartz Monzodiorite and Dalcrag Granodiorite respectively, although on Meall Donn and Carn Gairbthinn some quartz diorite veins are more tonalitic than plutonic Errogie Quartz Diorite.

The lithology of the envelope veins reflects the igneous unit present in the adjacent pluton. Where the pluton is composed of a number of units (excluding the Aberchalder Adamellite), veins of all the lithologies in the adjacent pluton are found (Fig.3.1).

The presence of veins directly sourced by magmas from the main pluton implies that the Foyers granite was quite fluid. Emerman and Morret (1990), state that sheet like igneous bodies only form from low viscosity magmas. High viscosity magmas form stocks. The lack of Aberchalder Adamellite veins may imply this lithology was too viscous to form veins.

### 3.1.2 Controls On Veining.

The intensity of veining in the envelope is very variable. In many localities the veins form <10% of the outcrop, but in others, veins may account for 30-60% of the outcrop. Areas of high veining include; Cairn Gairbthinn, parts of

the Central Psammite Septum, areas proximal to Loch Kemp and the ground close to Meall Donn-Creag a' Chliabhain.

These areas often contain small dominantly bedding sub-parallel, granitoid stocks up to 800m in length and 300m in width, the geometry suggesting envelope psammites are roofing larger granitoid masses.

Structural anisotropies in the envelope rocks have a strong control on veining. The dominant control is bedding foliation, where the granitoid veins run parallel to bedding. Veins are seldom continuous over distances >75m, most are limited to <10m in length and <1m in width, and have an irregular lenticular morphology.(Fig.3.2). More isotropic rock types, like the migmatitic semi-pelite, contain far fewer veins. This is exemplified between Creag a' Chliabhain and Maol Chnoc where units of micaceous psammite, pebbly psammite, quartzite and migmatites crop out. The migmatites, which lack bedding planes, contain few granitoid veins whilst the other units contain up to 75% granitoid veins. Small shears in the envelope, developed during aureole deformation, also act as veining sites,(Plate 3.1). Areas of psammite mobilisation are cut by large numbers of granitoid veins. Here the veins are small, irregular and reticulose, due to the lack of wall control provided by the bedding foliations (Plate 3.2).

The pre-Foyers, Maol Chnoc Complex, contains no obvious Foyers veins even though adjacent psammites are intensely veined. The Beinn Dubhcharaidh ridge is intensely veined by Maol Chnoc diorite but is free of veins from the Foyers Complex. On the south easterly flanks of the ridge above

Coire Buidhe G.R.58701950 there are no diorite veins, but veining by Chliabhain Quartz Monzodiorite is intense. The structural isotropy of the Maol Chnoc Complex may prohibit vein formation. On Beinn Dubhcharaidh it is possible that a large diorite sheet extends along the ridge feeding the diorite veins. This body prevents the intrusion of quartz monzodiorite veins. The south westerly margin of this diorite body is marked by the absence of diorite veins, and southwest of this margin quartz monzodiorite magma is able to vein along the bedding foliation.

Granitoid veins show a weak mineral fabric defined by biotite flakes and plagioclase laths, lying parallel to the vein walls and are interpreted as a magmatic fabric, although, in thin veins, vein networks and lenticular bodies the fabric is absent. Where planar granitoid veins occasionally cross cut the bedding foliation the igneous fabric may lie obliquely to the vein walls, suggesting a solid state component in the fabric. Approximately 10% of the quartz diorite veins in the Central Septum show slightly stronger fabrics than those in the granodiorite veins, suggesting that occasional quartz diorite veins were solid during granodiorite veining. In a small number of veins, a good biotite schlieren fabric develops parallel to the vein wall, (Plate 3.3).

### 3.1.3 Vein Dilation And Replacement.

There are few criteria indicative of vein dilation, as a result of the bedding parallel orientation of the veins.

However, adjacent beds diverge around the tapered ends of granitoid veins, forming the walls of the veins, implying vein dilation. (Fig.3.2). Veins with minor lenticular thickening (<20% of average vein width) are accommodated within the same bedding plane by dilatational mechanisms, but greater lenticular thickening involves replacive mechanisms, as beds are seen striking into the granitoid lenses, where they are truncated by granitoid material.

A qualitative measurement of the amounts of replacement and dilation associated with veining was made, (Appendix C). Table 3.1 indicates that in the Central Psammite Septum, veining occurred by dilation and replacement in the proportions of 40% and 60% respectively. The dilation is probably confined to narrow veins, whilst the replacement occurs within the lenticular bodies. The replacement mechanism is probably stopping, as evidence of assimilation is absent.

(Plate 3.4) illustrates a large granodiorite vein terminating against a body of xenolithic mobilised psammite, both enclosed between walls of unmobilised psammite. If the granodiorite occupies an area once occupied by mobilised psammite, it is possible to envisage the granodiorite flushing out an essentially fluid xenolithic body, with the psammite xenoliths either sinking through, or being carried up, by the flowing magma.

Veining is permitted and controlled by structures in the envelope, whether regional structures or structures produced during pluton emplacement. Veins are initiated by dilation, but this mechanism is superceded by replacement in the form



of stoping, which forms wider and more irregular bodies.

#### 3.1.4. Propagation Of The Veins.

Shaw and Spera, (1980), present papers on the fracture mechanisms of magma transport. Both authors state that it is the effective differential stress between lithostatic and magmatic pressures that is responsible for the fracturing in the envelope of a magmatic body. These fractures remain open due to magma injection. Aki, (1978) shows that a magmatic pressure in excess of lithostatic pressure may form tensile cracks, which become filled by magma. Once this has occurred the magma is very effective at propagating the cracks further, resulting in the effective transport of magma. Spera (op.cit.) states that where maximum stress is vertical, as seen in the roof zone of a bouyant pluton, crack generation in a isotropic rock results in vertical cracks. This agrees with the early work of Anderson (1936), who stated cone sheets and ring dykes are developed in response to magma pressure greater than, and less than, lithostatic pressure respectively.

The generation of brittle fractures by magmatic processes relies upon the Griffiths Theory of brittle failure. This theory states inherent tiny cracks (Griffiths Cracks) in solid materials, lying in the correct orientation begin to grow when stress is applied giving crack failure.

In brittle isotropic rocks, regular fracture patterns may be identified. The structure around the Foyers envelope is

anisotropic, and at the emplacement depths of 14km, (Tyler & Ashworth, 1983) the rocks were possibly slightly plastic. This has resulted in granitoid veining controlled by the structural grain of the envelope rather than by vertical fracture patterns associated with the intrusion stress field. The bedding surfaces represent a very well developed set of Griffiths cracks approximately in the correct sub-vertical orientation, and it is along these planes that fracturing occurred.

### 3.2 RELATIONSHIPS BETWEEN VEINING AND STOPING.

It is probable that sheeting and veining are precursors of stoping; a mechanism involved in the overall emplacement of the Foyers Complex. Evidence for stoping includes the presence of a number of psammite rafts in the body of the Foyers Complex, and the ghost stratigraphy that these rafts may outline (Chapter 4). On the north west wall of Conagleann, Highton (1986) describes a small quartz diorite stock fingering upwards into a psammite roof, this stock shows the transition between veining and stoping.

The evidence discussed earlier indicates that once a vein is established by dilation, replacement mechanisms begin to operate by spalling off psammite sheets from the vein wall. This stoping is aided by the veining process, which isolates psammite sheets, which are then effectively suspended from above and along strike. To completely detach a psammite sheet three sets of fractures need to form. As the bedding

in the Foyers envelope is steeply inclined, the cracks will lie in a sub-vertical and sub-horizontal attitudes, both perpendicular to the bedding plane. The downward pull of a large psammite block suspended in granitoid magma would form such cracks (Fig.3.3).

Marsh (1982), states that the thermal stresses in the envelope of a magmatic body are greater than effective stresses created between magmatic and lithostatic pressures. It is possible that thermal stresses are concentrated at heterogeneities like bedding planes and this greatly aids the development of cracking. Failure of psammite sheets across the bedding planes may be assisted by early chocolate block boudinage, which created two fracture sets, both parallel to the fracture sets that may develop by the downward pull of a suspended psammite sheet.

### 3.2.1 Lithological Control Of Stoping.

#### Micaceous Psammites.

The units of micaceous psammite are intensely veined, but large granitoid stocks are rare. The largest stocks of granitoid in the Micaceous Psammite are seen in the Central Psammite Septum; they are greater than 50m in diameter, and are elongated in the direction of bedding. The stoping mechanisms,

described earlier, are envisaged in the formation of these stocks, with sheets of psammite breaking free and sinking

through the magma. The presence of large elongate, micaceous psammite rafts within the main body of the pluton, supports the idea that large micaceous psammite septa were removed by stoping. The lack of deformation in these rafts implies stoping occurred prior to pluton expansion. This contrasts with stoping seen within the roof zones which is associated with late veining.

#### Quartzite And Pebbly Psammite.

These units are lithologically more isotropic than the micaceous psammites, with less well developed bedding planes. Bedding parallel veining is well developed but a proportion, (<15%) of the veins are cross cutting, such fractures developing in response to stresses created by magmatic pressure or thermal expansion. The fractures develop due to the more brittle nature and the lack of well developed bedding planes in the pebbly psammites. In the micaceous psammite the well developed bedding planes are able to absorb the stresses generated during intrusion. Quartzite and pebbly psammite rafts are more equant (Table 3.2) than micaceous psammite rafts supporting the idea of abundant cross fractures (Fig.3.4). The relative ease of stoping in the pebbly psammites is illustrated on the southern margin of the Foyers Complex. On the southern margin there are units of both pebbly and micaceous psammite. Adjacent to Loch Kemp, the micaceous psammite is veined but continuous, whilst the pebbly psammite is intruded by a number of large granodiorite stocks. A north

westerly trending strip of ground, <450km wide, between Tor Pataig and Tom Rathail is composed of continuous micaceous psammite bounded to the north east and south west by granodiorite. This granodiorite contains up to 10% psammite blocks dominated by quartzite and pebbly psammite. This indicates that these two lithologies were stoped, whilst the micaceous psammite was veined, but remained cohesive. At the north westerly foot of the Beinn Sgurrach ridge there is a junction (faulted?) between weakly veined micaceous psammite and granodiorite, with numerous pebbly psammite blocks (Enclosure 3), again implying quartzite and pebbly psammite are more readily stoped than micaceous psammite.

### 3.3 CONCLUSIONS.

If stoping played a major part in introducing the Foyers granitoids into the crust then, as previously discussed, it is probable that the envelope lithologies influenced where that stoping took place. It has been established that variations in lithology affect the style and amount of veining in the envelope, and this in turn controls how easily a particular lithology is removed by stoping. It is probable that the position of the pebbly psammites and micaceous psammites controlled the intrusion of the Foyers granitoids by presenting areas of crust that were relatively difficult or easy to stope into. Structures which control the position of the units in the crust therefore influence the site of intrusion and the final morphology of the Foyers

Complex.

The external morphology of the Foyers Complex forms a rather unusual "triangular" outline. Many granitoids fall into a limited number of external morphologies. Granitoids emplaced as diapirs, for example Ardara (Holder, 1979), have circular to oval outlines, as do granitoids emplaced by cauldron subsidence, for example the Rosses Ring Complex, (Pitcher and Berger, 1972). Most stope granitoids have irregular outlines, for example the Cairn Gorm Granite, (Harrison, 1986), whilst granitoids emplaced along major crustal lineaments are elongated parallel to that lineament, for example the Main Donegal Granite (Hutton 1982). The extraordinary outline of the Foyers Complex is influenced by regional structures, and the susceptibility of different psammite units to stoping, provides the link between regional structure and granitoid emplacement.

#### 3.4 VEINS ON BEINN SGURRACH.

These veins occur on the north eastern flank of Beinn Sgurrach, 1700m from the Foyers Complex. They differ in style and lithology from adjacent Foyers veins. The veining is very localised and occurs as granitic (ss), and granodioritic veins.

The granitic veins are the most common, are pale in colour, medium grained, and contain primary muscovite and magmatic garnets, all features absent in the Aberchalder Adamellite. Veining is parallel to the bedding fabric in the micaceous

psammite host, although cross cutting veins are common. The veins are limited to one specific area 400mx100m, elongated in the direction of the bedding foliation. The granite veins often contain abundant tabular to equant micaceous psammite xenoliths showing a preferred orientation parallel to the vein walls. In some cases blocks are seen in the process of being prised off the vein walls by a rotational movement, indicating subhorizontal magma movement.(Plate 3.5). The flow of magma through these veins appears to have actively ripped psammite from the walls, which contrasts with the Foyers veins where magma flow appears more passive with little evidence vein wall disruption.

The granodiorite veins are located in one small area, 200mx50m, just to the north east of the summit of Beinn Sgurrach. The granodiorite differs from the Dalcrag granodiorite as it weathers to an ash grey colour, is buff on a fresh surface, has a fine grained quartzo-feldspathic matrix, and contains abundant biotite. The rock has a strong fabric defined by the parallel orientation of biotite flakes.

The granite and granodiorite veining is associated with areas of intense boudinage in the micaceous psammite, where the igneous material forms >70% of the outcrop. The micaceous psammite is included in the granodiorite veins as abundant xenoliths. Away from the veining the micaceous psammite is relatively undeformed.



#### 3.4.1 Gneissose Granite Dykes.

Gneissose granite veins occur in two localities on Beinn Sgurrach at G.R.49801468 and G.R.50251463. The granite veins are pale in colour and strongly porphyritic. The fine grained matrix is quartzo-feldspathic, the phenocrysts are plagioclase. They are adamellitic, the groundmass dominated by quartz and alkali feldspar of a grainsize  $<0.75\text{mm}$ . The quartz may show a hornfelsic texture. Biotite shows a strong parallel alignment as single flakes and ribbons. The gneissose granite dykes trend in north east-south west direction, are  $<2\text{m}$  wide, and are broken into a series of very large lenticular boudins along their length. These steeply dipping dykes sharply cross cut the easterly striking bedding foliation. The granite contains a strong fabric defined by biotite and deformed phenocrysts. This fabric can be traced across the dyke contact into the micaceous psammite, where it forms the early bedding parallel fabric, which in this area is slightly oblique bedding, (Plate 3.6). As this fabric is associated with the first regional deformational event the intrusion of these dykes was prior to Grampian deformation.

CHAPTER 4. FABRICS AND FOLIATIONS IN THE FOYERS GRANITIC  
COMPLEX.

## CHAPTER 4. FABRICS AND FOLIATIONS IN THE FOYERS GRANITIC COMPLEX.

### 4.1 INTRODUCTION.

For many years there has been a debate over whether foliations in granitoid rocks result from magmatic flow or tectonic processes. "There is considerable controversy regarding the origin of certain crystalline fabrics that occur in plutonic rocks. Such controversy is centred on the origin, whether fluidal or deformational, of these fabrics." (Castro, 1987).

Early workers (Balk, 1937 and Mayo 1941) argued that magmatic flow formed the foliations, but Berger and Pitcher (1970), thought granitoid foliations developed during deformation of solid rock. Recent work by Paterson et al. (1989), favours the idea that the majority of foliations in granitoid rocks develop during magmatic flow.

It is with this controversy in mind that the foliations in the Foyers granitic complex are studied.

### 4.2 FIELD DESCRIPTIONS OF THE FOLIATIONS AND OTHER IGNEOUS STRUCTURES.

At outcrop, all the major units in the Foyers Complex, except the Aberchalder Adamellite, show a distinctive

fabric, formed by the preferred orientation of hornblende, biotite and larger plagioclase crystals, (Plate 4.1). The preferred orientation of minerals is dominantly a foliation. Although difficult to distinguish in the field, some of the minerals, especially hornblende, form a lineation, pitching within the foliation plane 15-30 towards the east.

The fabric within any one unit shows a patchy variation in intensity. In the field, the fabrics in the Chliabhair Quartz Monzodiorite and the Dalcrag Granodiorite appear slightly less intense than in the Errogie Quartz Diorite.

Throughout most of the pluton the foliation is parallel to the strike of the pluton margin, and dips towards the centre of the pluton at over 75°. (Enclosure 4)<sup>+4A</sup>. The attitude of the foliation probably reflects the attitude of the pluton/envelope contact. At certain localities, Errogie Quartz Diorite contains horizontal foliations as seen at G.R.55102038. These localities are found adjacent to areas dominated by steeply dipping fabrics. The horizontal and steeply dipping igneous foliations show very similar intensities and styles. The change of foliation attitude is brought about by a strong curving of the foliation plane over a distance of 10-30m (G.R.55022033). There is no fabric over printing or development of new fabrics. Field evidence suggests that the same process produced the horizontal and sub-vertical fabrics.

Where a margin parallel foliation is well developed it is not possible to detect the lineation. The foliation is weaker in the north west portion of the pluton and the lineation is more easily recognised with an azimuth parallel

to the pluton margin.

#### 4.2.1 Enclaves.

Microdiorite enclaves occur within the pluton in moderate numbers and are interpreted as globules of diorite magma intruded into the fluid magma of the pluton, (Chapter 2). The majority of enclaves show an oblate form with their X and Y axes parallel to, and the Z axis normal to, the igneous foliation, which passes through the enclaves and remains parallel to the fabric in the host. In most cases the enclaves develop a slightly stronger foliation than their host, (Plate 4.2), but frequently enclaves with a very weak or no foliation are seen, (Plate 4.3).

An intense swarm of microdiorite enclaves, showing a wide shape and size range, is exposed on the shore of Loch Mhor (G.R.55702215). They are rounded, elliptical or tabular and may show angularity. This swarm is a disrupted but poorly dispersed microdiorite intrusion (Chapter 2). The X Y planes of the enclaves are horizontal within a host with a poorly developed mineral foliation, (Plate 4.4), although the closest outcrop, 400m to the south west, shows a steeply inclined fabric. A weak fabric defined by plagioclase laths within some enclaves, is steeply inclined at a very high angle to the long axes of the enclaves, indicating that the orientation and shape of the enclaves are controlled by a different process to that which formed the fabric within the enclaves, (Plate 4.5).

#### 4.2.2 Xenoliths.

Within the Errogie Quartz Diorite and the Chliabhain Quartz Monzodiorite metasedimentary xenoliths are rather rare and mainly occur as large rafts, often greater than 100m in length. Infrequent, small xenoliths align their long axes parallel to the igneous foliation in the surrounding granitoid but show no obvious deformation. The long axes of the larger elongate rafts are also aligned with the fabric in the pluton and show a bedding foliation, parallel to the margins of the raft and the plutonic foliation. The large rafts, particularly those of pebbly psammite, show well defined bedding and oblique, spaced, D2 fabrics. Rafts <5m in diameter have less distinct bedding and mineral foliations due to the development of a strong hornfelsic texture. The rafts seldom develop the boudinage, mobilisation and shearing seen in the psammite envelope. Where the rafts are equant, they show no preferred orientation, but the bedding foliation within the rafts remains parallel to the foliation in the pluton. The igneous foliation is not deflected around the rafts, although poor exposure may hide subtle deflections.

Within the Dalcrag Granodiorite, the abundance of the large rafts increases north east of Loch Kemp (Enclosure 1). Here the foliation patterns are more complex and will be discussed later. However, where the rafts are elongate, the long axis of the raft and the bedding foliations are parallel to the foliations in the pluton. Irregular or equant rafts show bedding foliations that remain parallel to

the foliation in the pluton. The exposure is reasonable in this area and there is no deflection of the fabric in the Dalcrag Granodiorite around the large metasedimentary rafts.

#### 4.2.3. Appinitic Diorites.

Appinitic diorites occur in the body and aureole of the Foyers Complex. Within the pluton they are poorly exposed and their origin, whether xenoliths or intrusions, is not always clear, (Chapter 2). These appinites show good appinitic textures with no evidence of the preferred mineral orientation seen in the host.

Within the Central Psammite Septum an appinite is intruded into micaceous psammite (G.R.53951710). The appinite is elongated in the direction of the surrounding bedding foliation which runs parallel to the nearby pluton margin. The appinite shows a very strong mineral foliation sub-parallel to that in the Foyers Complex. In thin section the fabric is a strong compositional layering with the hornblende and biotite producing ribbon-like aggregates. The hornblende shows grain size reduction, (Plates, 4.6 & 4.7), typical of solid state deformation. Running through the appinite and cross cutting the fabric are numerous undeformed felsic veins and clots.



#### 4.2.4 Schlieren.

There are few schlieren structures in the main complex, although the occasional Dalcrag Granodiorite vein within the Central Psammite Septum may show biotite, wall parallel schlieren.

#### 4.2.5 Internal Contacts.

There are many gradational internal contacts within the Complex. The contacts between the Errogie Quartz Diorite, Chliabhain Quartz Monzodiorite, and the Dalcrag Granodiorite are very irregular and show no preferred orientation. The foliation in the pluton cuts through these internal contacts.

There is no increase in fabric intensity at the Chliabhain Quartz Monzodiorite and Errogie Quartz Diorite boundary in either of the units, for example (G.R.54602370). However, at the boundary between the Errogie Quartz Diorite and the Dalcrag Granodiorite, west of Gorthleck House, G.R.54302082 an increase in the fabric strength is seen in both units. Here the boundary runs parallel to the main plutonic foliation. In the road cut above the River Foyers (G.R.49951946), a minor unit of acidic granodiorite cuts the Dalcrag Granodiorite. Mafic banding and schlieren mark the boundary, perhaps formed by convectional currents accreting

coarser mafic minerals onto a wall (Barriere, 1981), (Plate 4.8). This banding, and the host rock onto which it is accreted, shows a good fabric, parallel to the banding, the contact and the general plutonic fabric.

#### 4.3 MICROSCOPIC INVESTIGATION OF THE FABRIC.

##### 4.3.1 Foliations.

Foliations are unclear under the petrological microscope due to the coarseness of the rock. On a 'Shadow Master' with X10 magnification, whole thin sections are viewed, and fabrics present become clearer. As in outcrop, the fabric varies in intensity. The fabric is most readily picked out by the parallel alignment of albite twinned plagioclase laths, the twins and laths lying parallel to the general fabric direction. There are however numerous minerals, especially plagioclase, which cut the foliation at a high angle. The samples were not ideal for quantitative analysis of fabric strength because the slides were cut randomly with reference to the fabric. However, a large proportion of the slides show that the plagioclase laths have a reasonably strong preferred orientation. The plagioclase laths in some microdiorite enclaves show a very strong preferred orientation, indicating either greater deformation in the enclave, or differences in plagioclase lath shape between enclave and host.

#### 4.3.2 Mineral Textures.

Paterson et al. (1989) and Bateman et al. (1988) list a set of microscopic textural criteria that may be used to distinguish between different fabric forming processes. These criteria are summarised as follows;

##### Magmatic flow.

1. Preferred orientation of igneous minerals with no plastic deformation in or around the rotated mineral.

(Bateman et al. (1988) do not state whether high temperature solid state deformation can occur without leaving evidence of plastic deformation in the matrix.)

2. Aligned crystals surrounded by undeformed quartz aggregates.

3. Imbrication of crystals.

##### Solid state deformation at medium temperatures (sub 400°C).

1. Minerals show plastic deformation.

2. Recrystallisation of grains to finer aggregates.

3. The ribbon like foliation of aggregates, producing a lenticular banding.

4. Boudinage of strong minerals.

5. Inversion of orthoclase to microcline.

Solid state deformation at sub-solidus to low amphibolite grade temperatures.

1. Slip parallel to quartz C-axes, creating basal subgrains.
2. Recrystallisation of feldspars.
3. Homogenous deformation with the rapid movement of grain boundaries.

The study of microstructures in the Foyers pluton has thus been focused on textural features that have been used as evidence to support the various mechanisms of fabric formation.

#### Quartz.

In the Errogie Quartz Diorite and the Chliabhain Quartz Monzodiorite the quartz occurs as interstitial infills between plagioclase laths. It often shows undulose extinction and, very occasionally, subgrain formation. The Dalcrag Granodiorite contains larger aggregates of interstitial quartz, which also show undulose extinction, (Plate 4.9).

#### Plagioclase.

Plagioclase is the major foliation defining mineral, as euohedral, elongate laths with length parallel albite twinning, (Plate 4.10). The laths often show oscillatory and

normal zoning, (Plate 4.11). Plagioclase laths form contacts with each other ranging from; two fabric parallel laths contacting down their long axes, to the less frequent situation of two laths with normal long axes, one lath within and the other normal to the foliation plane. Where the contact takes place between long axes there is no evidence of deformation in the form of recrystallisation, solution, or bending of the albite twins. However, on rare occasions, some plagioclase laths show undulatory extinction, (Plate 4.12), and where a high angle contact occurs between two plagioclase laths there may be a slight bending of the albite twins within the impinged lath, (Plate 4.13), (Fig. 4.1) Very occasionally there is crystal dislocation (Fig. 4.1) in the bodies of fabric parallel laths where they contact with other laths lying at high angles to the fabric, (Plate 4.14).

#### Mafics.

Biotite and hornblende normally occur as single grains, often aligned with the igneous fabric. The biotite flakes define the foliation, whereas the hornblendes form a linear fabric. Frequent equant monomineralic or polymineralic glomerophyric aggregates of the mafic minerals, with an internal granular texture, show no evidence of deformation.

### Orthoclase.

Orthoclase occurs in all the major units of the Foyers Complex. The equant nature of the orthoclase phenocrysts in the Errogie Quartz Diorite and Chliabhain Quartz Monzodiorite prevents its use as a fabric marker, but in the Dalcrag Granodiorite, the orthoclase is tabular and is possibly weakly aligned with the granitoid fabric.

Very closely associated with the orthoclase is myrmekite. It occurs mainly as narrow patches at plagioclase orthoclase boundaries, and is undeformed.

### 4.4 RELATIONSHIP BETWEEN GRANITOID FABRIC AND DEFORMED ENVELOPE.

As described in Chapter 7 the envelope of the Foyers Complex contains deformational structures which are attributed to the shortening of the envelope perpendicular to the complex margin as a result of pluton expansion. The intensity of this deformation varies around the pluton, particularly on the northern margin, where the envelope between Tom Mor and Loch Mhor is weakly deformed, but the envelope between Creag a' Chliabhain and Beinn Dubhcharaidh shows intense deformation. The mineral fabrics in the pluton adjacent to these two areas are parallel to the contact, and show very similar intensities and styles. Where deformation

in the envelope is most intense, a solid state fabric in the adjacent granitoid should also be intense. It is difficult to envisage strong deformation in the envelope not reflected by the adjacent granitoid. As the strength of the igneous fabric does not increase with increasing envelope deformation, it is probably a magmatic fabric and the pluton is deforming its envelope whilst in a magmatic state.

#### 4.5 ORIGIN OF THE FABRIC IN THE FOYERS COMPLEX.

##### 4.5.1 Introduction.

The Foyers Complex shows foliations typical of numerous plutons throughout the world, and it is over the origin of this fabric that many workers disagree. It is necessary to understand the processes which produced the fabric, in order to give an indication of the pluton's crystallinity during intrusion and fabric formation. Structural data may only be interpreted accurately if the crystallinity of the pluton at the time of fabric formation is known.

The term "solid" is used when there are enough crystals in the granitoid body to form an interlocking framework and allows the melt/crystal mixture to behave mechanically as a true solid, with rheologies representative of solids, (Arzi 1978, Van der Molen & Paterson 1979.). The term liquid represents crystal/melt system where there are too few crystals to form a framework, in addition to a crystal free melt. Such systems have viscosities typical of fluid



silicates. Arzi (1978), and Van der Molen & Paterson (1979), show that the viscosity increase, representing a change from melt to solid rheologies, occurs rapidly around 20 to 30 melt volume percent. However, the physical state of the magma may change the percentage of crystals needed to reach the critical melt percentage of Arzi (1978). For example, if the melt is flowing and tabular minerals are aligned then the magma will be able to support more crystals than Arzi suggests and still remain fluid, as defined by Arzi (1978). The critical melt percentage varies between granitoids, depending upon mineral phases in the magma, mineral textures and flow of magma.

Paterson et al. (1989) define magmatic flow as "deformation by displacement of melt with rigid body rotations of crystals without sufficient interference to cause plastic deformation." and only occurs in plutons acting as fluids. Solid state deformation in granites (although not defined by these authors) probably occurs when there are enough crystals present to allow stress transmission, (Fig.4.2).

#### 4.5.2 Microscopic Evidence.

It is possible to compare textural, structural and mineralogical features seen in the Foyers Complex with those described by other authors, who use these features to indicate the physical state of the pluton during fabric formation. The Foyers granitoids show very little evidence of high or low temperature solid state deformation, apart

from undulatory extinction in interstitial quartz, and very rare plagioclase lath deformation. Paterson et al.(1989) regard this lack of evidence for solid state deformation as indicative of magmatic flow, particularly as plagioclase laths show delicate, undeformed, igneous textures for example oscillatory zoning, and mafics show undeformed glomerophyric textures. If plastic deformation has occurred then plagioclase laths normal to the foliation, impinging upon plagioclases parallel to the foliation, should show deformational or recrystallisation features at their contacts. Paterson et al.(1989), state that solid state deformation create intense undulatory extinction, kinking, ribbon aggregates and grain size reduction. Although undulatory extinction and occasionally subgrain reduction is seen in quartz this may be a result of other processes such as the stresses imposed by crystallisation. If solid state deformation occurred at high temperatures, recrystallisation of the plagioclases should be seen (Bateman et al. 1988). The mafic minerals in the Foyers Complex align as single grains rather than ribbon aggregates which Paterson et al.(1989), state are formed by solid state processes. Therefore using the criteria of Paterson et al (1989), the foliation in the Foyers pluton is a flow fabric. However field evidence, discussed later in this chapter, suggests solid state processes may also control fabric formation.

As a granitoid crystallises, magmatic processes may be superceded by solid state processes. This should occur at around 70 to 80 percent crystal volume (Arzi 1978). Many authors have suggested that magmatic flow may pass

continuously into solid state processes, (Holder, 1979 and Bateman, 1985).

Paterson et al.(1989), identified a series of features indicating solid state deformation whilst the rock still contained melt. Their most conclusive criteria is the presence of late magmatic minerals in pressure shadow positions, from Hibbard (1987).

The Foyers Complex shows minor myrmekite. Hibbard (1979) states myrmekite is magmatic and not replacive, as suggested by Phillips (1974), with the myrmekite crystallising from the last water saturated melt fraction. The remaining melt must represent less than the last 10 volume percent of the system because water bearing granites do not become saturated until the melt fraction is reduced to below 10%. Often associated with myrmekite are irregular phenocrysts of orthoclase feldspar, which Hibbard (1987), interprets as forming from late pools of alkali rich melt. Within the Errogie Quartz Diorite it is common to find areas of outcrop which contain irregularly spaced and shaped, pale orthoclase phenocrysts, (G.R.55632115). In thin section the phenocrysts are often associated with myrmekite and enclose and sometimes partially replace plagioclase laths. Hibbard (1987), suggests that both the myrmekite and orthoclase crystallise from aqueous melt expelled from the interstices of the crystal framework during deformation. Ideally the myrmekite should collect in mineral pressure shadows, for example adjacent to the 001 faces of plagioclase. In the Foyers Complex the myrmekite does not appear to occupy pressure shadow positions.

The mineral fabrics and textures in the major units of the Foyers Complex are formed by magmatic flow, although there is some evidence to suggest that very minor solid state deformation did occur.

#### 4.5.3 Enclaves.

The extensive dispersal of the microdiorite enclaves indicates magmatic flow occurred in the granitoid host, but this does not imply that the fabric within the enclaves is also magmatic.

In purely magmatic flow, enclaves show no internal foliation (Bateman 1983), and the foliation in the host granitoid passes around the enclave. Under conditions of solid state deformation the fabric in the host granitoid passes through the enclave. In the Foyers Complex the fabric is often well developed in the enclaves and lies parallel to the enclave's long axes and the igneous foliation, implying solid state deformation. However the microstructure of the enclaves shows none of the features associated with plastic deformation, described by Paterson et al. (1989). The enclave fabric is very similar to, or slightly stronger than that of the enclosing host, probably a result of the larger number of biotite flakes in the enclaves. Flow in the pluton may have imparted a flow fabric within fluid blobs of microdiorite magma, because the whole pluton, if highly liquid, would behave mechanically as one mass, thus explaining why igneous foliations pass through the enclaves.

Bateman et al.(1983) use the idea that differential rates of flow in the magma mould and orientate the enclaves so they lie parallel to the flow direction, and the enclave morphology mimics the morphology of the flow regime. Vernon et al.(1988) show that purely magmatic flow can shape and deform microdiorite enclaves. If applied to the Foyers Complex the igneous fabric indicates magma flow was parallel to the pluton walls forming wall parallel, oblate enclaves.

Ramsay (1967) modelled the movement of ellipsoids in a fluid matrix undergoing simple shear. He showed, using the work of Jeffery (1923), that an ellipsoidal particle carried in a simple shear fluid flow is subjected to two couples,(Fig.4.3i) one causing the particle to adopt the same rotation as the fluid and the other tending to set the ellipsoid so that its axes move towards the shear direction in the fluid (Fig.4.3ii). Prolate and oblate ellipsoids behave differently in laminar fluid flow. Prolate ellipsoids produce a linear fabric because their long axes rotate into parallelism with the shear plane direction (a) (Fig.4.3iii), and remain in that orientation. Oblate ellipsoids lie with their short unique axis at a high angle to the shear plane direction (a) and this produces a planar fabric.(Fig.4.3iv)

If the shear strain rate is high then according to Jeffery (1923), prolate particles will lie with the long axis parallel to the (b) direction of the shear plane and the particle rotates about this axis (Fig.4.3v). With an oblate ellipsoid one of the long equatorial axes lies parallel to the (b) direction and the disc rotates with variable angular velocity (Fig.4.3vi). Ramsay (1967), states that fluid flow

within a granitoid rock may create shear strain rates high enough for the latter conditions to develop.

If magma flow in the Foyers Complex was wall parallel and vertical, with high shear strain rates, oblate microdiorite enclaves would lie parallel to the walls, as should platy minerals. There would also be a good lineation developed by the acicular minerals running horizontally, parallel to the walls. (Fig.4.4.a) In the Foyers Complex the foliation and enclaves show this orientation and the lineation tends to be sub-horizontal but is poorly developed. If the shear strain rate during magmatic flow was low, then with vertical wall parallel flow, the oblate microdiorite enclaves and the planar fabric would be parallel to the walls but the lineation should be vertical, (Fig.4.4.b) and this is not the case in the Foyers pluton because the lineations are not vertical.

Ramsay (1989) indicates that upward magma flow, against fixed walls should not form oblate ellipsoids but ellipsoids in accord with simple shear ( $X > Y > Z$ ), with long axes plunging towards the pluton centre at a lower inclination than the dip of the walls. (Fig.4.4.c). As the enclaves in the Foyers Complex are oblate, with their long axes parallel to the wall of the pluton, the criterion of Ramsay (1989), indicates that the enclaves were not shaped by magmatic flow.

The work of Ramsay (1967), shows how the crystalline fabric in the pluton developed as a result of flow. However, Ramsay (1987 & 1989) treats the enclaves as solid particles. It is probable that during magmatic flow in the pluton the

enclaves were also fluid as the liquidus of both diorite and quartz diorite are close. Thus the shapes and orientations of enclaves in the Foyers Complex cannot be compared with certainty to the experimental shapes and orientations that Ramsay (op. cit.) predicted would occur during fluid flow.

#### 4.5.4 Xenoliths.

Large metasedimentary xenoliths or rafts within a magmatic flow should align their long axes with the igneous fabric (Ramsay 1967), which should deflect around the raft. A fabric formed by solid state deformation should pass through the raft. In the Foyers Complex, the rafts are aligned with a mineral fabric which is not deflected around the rafts, so the rafts indicate that both solid state and magmatic mechanisms operating in the surrounding host. The occasional equant raft is seen, and although they show no external shape alignment, the bedding foliation within the raft is parallel to the igneous fabric. This may indicate that the outcrop pattern of the raft is an equant section of a larger tabular raft which has been eroded or is buried, and that the magmatic alignment of the unseen raft controls the orientation of the bedding in the exposed section. The bedding foliation controls the fracturing that shapes the tabular rafts, and thus the bedding is always parallel to the elongation of the raft. Equant rafts with bedding parallel to the igneous fabric may also imply the bedding is in its pre-emplacement orientation, implying very little rotation of the rafts by flow in the pluton, and that the



bedding orientation controls flow in the granite. This latter idea negates the need for magmatic flow in a fluid granite to produce raft alignment. Magmatic flow and/or solid state deformation occurring parallel to the margin, which is parallel to the bedding foliation in the country rocks, may have helped to maintain the bedding in the rafts in its original orientation.

The metasedimentary rafts within the Foyers Complex show none of the contact deformation seen in the envelope of the complex. If solid state deformation was an important factor in the structural evolution of the Foyers Complex then rafts close to the pluton contact (G.R.57901900) should have been frozen into solid magma relatively early. If this was the case, the rafts should show some deformation. As the rafts are undeformed they were probably included into the pluton prior to envelope deformation. This suggests the complex was emplaced by stoping followed by dilation and as the pluton expanded and deformed its envelope it was not rigid enough to deform the rafts it contained. Thus the Foyers Complex was deforming its envelope whilst still in a magmatic state.

#### 4.5.5 Appinitic Diorites.

The intensity of the solid state fabric within the appinite in the Central Psammite Septum indicates that this appinite was solid during the deformation of the envelope, and that the deformation was recorded as a solid state fabric. The

cross cutting, undeformed pegmatitic veins and patches indicate that during deformation the minor acidic fraction of the appinite remained fluid, perhaps due to the high heat flow from the main mass of granite which surrounds, and intimately veins the micaceous psammite around the appinite. As the heat from a granitic body remains after deformation has ceased, the felsic material probably crystallised after deformation had stopped, thus producing cross cutting undeformed felsic veins.

This appinitic diorite existed in a rigid environment, where the micaceous psammite transferred the stresses from the expanding pluton to the solid appinite. The appinites within the pluton show no parallel mineral fabric implying that the deformation in the aureole was not transferred to them. Appinites, internal and external to the pluton, record magmatic and solid state fabrics respectively. The appinite body in the Central Septum was deformed due to the high rigidity of the surrounding medium; indicating that internal appinites were surrounded by a magmatic host as the Foyers Complex expanded. Stretching and deformation of the Foyers' envelope thus occurred whilst the main body of the pluton remained fluid. The deformation seen in the envelope appinite is an example of a fabric that formed under solid state conditions in a body subjected to deformation from the expanding Foyers Complex. If the fabric in the Complex records solid state deformation, it should show a similar style of fabric to that in the appinite. However, the plutonic fabric is much weaker, perhaps because it is magmatic, or perhaps because the pluton only became

solid during the late stages of deformation.

#### 4.5.6 Internal Contacts.

Berger & Pitcher (1970), favoured a solid state origin for many of the fabrics in granitoid rocks. They state that many microgranitoid enclaves, having a minor viscosity contrast with their hosts, mirror the local deformational ellipsoid, assuming the enclaves developed their shape whilst solid. Pitcher & Berger (1972) showed that mineral alignments cut across internal contacts within the Thorr, Fanad and Ardara plutons of Donegal. They stated mineral alignments must postdate the formation of the contact, as no internal contact could remain regular if the materials were in a fluid state during the deformation.

In the Foyers Complex the fabric passes through internal contacts indicating it is a solid state fabric, especially if Paterson et al. (1989) are correct in suggesting magmatic flow fabrics should run parallel to internal contacts. However, the contacts in the complex are gradational indicating that both the intruding and intruded members of the complex were fluid. For laminar fluid flow to develop parallel to the contact, the host should be solid, providing a wall capable of controlling the orientation of flow in the intruding magma. In the Foyers Complex, contact parallel magmatic foliations would not develop due to the fluid nature of the host. Although the Foyers Complex contains a number of igneous units, it is possible that the whole

pluton (excluding the Aberchalder Adamellite) was capable of flow without extensive disruption of the fluid contacts, with the walls of the pluton providing the control over the direction of flow. Unlike many classically zoned plutons, i.e. the Criffel Granodiorite (Courrioux 1987), the Foyers internal contacts are quite irregular and it may be possible that fluid flow in the pluton has weakly reorientated internal contacts. If the fabric is solid state, one might expect internal contacts to show a preferred orientation, especially the small bodies. If the fabric forms by the flow of melt, orientating crystals, then there is no need to intensely deform the internal contacts.

If the granitoid rocks adjacent to the outer wall of the Foyers Complex begin to form a solid framework soon after intrusion then one might expect internal contacts close to the pluton margin to be sharper than those in the centre. However the width of the contact zones between the Chliabhain Quartz Monzodiorite and the Errogie Quartz Diorite are variable throughout the complex, and show no systematic decrease in width towards the margin. Thus it appears that each unit of Chliabhain Quartz Monzodiorite was emplaced into a host that, in all areas, had a similar crystal fraction.

#### 4.5.7 Marginal Stocks And Veins.

The marginal intrusions may yield information about the origin of the fabric in the complex because the fabrics they contain have the same style and orientation as the fabric in

the main complex, and so probably formed in a similar manner.

If the fabric is magmatic then it should form by magma flowing parallel to the vein wall. If the fabric is solid state, and is formed by expansion of the adjacent complex, then the fabric should develop parallel to the complex margin.

Veins are of limited value because they lie parallel to the pluton walls and thus the fabric in the veins would have the same orientation whether formed by solid state processes or wall parallel flow.

Stocks are more informative because they have walls at all angles to the pluton margin. The foliations are parallel to the pluton margin and cannot be traced parallel to the stock walls. This implies the fabric in the stocks is a solid state foliation, although minerals lose their preferred orientations adjacent to the contacts.

If the stocks develop from areas of exceptionally intense bedding parallel sheeting, it is possible that magma flow in the stocks would be parallel to the complex margin, thus forming a foliation parallel to the complex margin.

#### 4.5.8 Conclusions.

If Paterson et al. (1989), are correct the texture of the igneous fabric within the Foyers Complex indicates it formed by magmatic flow with minimal plastic deformation.

Microdiorite enclave shape indicates solid state deformation (Berger & Pitcher 1970), but the same shapes

may be caused by magmatic flow (Bateman et al., 1983 and Vernon et al., 1988). The nature of the metasedimentary rafts does not distinguish between the fabric forming processes, but does show that the pluton was capable of magmatic flow for part of its history. Internal igneous contacts are cut by the mineral fabric, which according to Berger & Pitcher (1970) is indicative of solid state deformation. However magmatic flow could possibly form a fabric which cross cuts internal contacts if the internal contacts formed when the intruding and intruded granitoids were both magmatic. Finally the presence of stocks and veins indicate that the magma within the pluton was fluid, but the fabric patterns in the stocks may indicate the mineral fabric has a solid state component.

Most of the criteria discussed suggest that during the majority of its structural development, the Foyers Complex was capable of magmatic flow. These criteria however fail to exclusively link the fabric within the complex to flow in the complex. The field evidence suggests that both solid state and magmatic processes could have formed structures within the pluton, and that even the origin of a single form of structure is debatable.

The igneous fabrics show features that many workers agree form by flowing melt, rotating suspended or non interferring crystals. The fabric also provides evidence of minor solid state deformation.

If solid state deformation is important in the formation of the fabric in the Foyers Complex, then the claim by Paterson et al. (1989), that solid state deformation forms a



distinctive microscopic texture is not substantiated.

It is probable that an early magmatic fabric was overprinted by a co-planar solid state fabric. It is difficult to estimate the relative importance of the two processes, some structures in the field may indicate solid state deformation was relatively important, whilst microfabrics suggest solid state deformation was very weak. If solid state deformation was co-planar to an early magmatic fabric then mineral rotation and thus deformation of crystals will be limited.

The Foyers Complex appears to have existed for most of its emplacement history as a fluid body, that is, contained more melt than the rheological critical melt percentage, (Arzi, 1978). The fabric records late solid state deformation overprinting a co-planar magmatic fabric.

#### 4.6 FOLIATIONS IN THE DALCRAG GRANODIORITE, NORTH EAST OF LOCH KEMP; A SPECIAL CASE?.

The structure of the igneous foliations within the Dalcrag Granodiorite, north east of Loch Kemp, (G.R.470164) differs from the other igneous structure found in the remainder of the pluton (Enclosure 2). North east of Loch Kemp the igneous foliations are parallel to the pluton margin, but moving away from the margin the fabric undergoes a strong strike swing, a feature not seen in the remainder of the complex.

The pluton boundary, close to Loch Kemp, is parallel to the bedding in the envelope. The envelope is highly veined, and



the Dalcrag Granodiorite forms a number of stocks and thick bedding parallel sheets. The Foyers Complex north east of Loch Kemp is entirely Dalcrag Granodiorite, and the strong swing in the igneous foliation is not related to an observable internal igneous contact or the development of the marginal chill, (Chapter 2), composed of the Fine Grained Granodiorite Facies, (Enclosure 2).

Between Loch Kemp and Whitebridge, the foliation in the Dalcrag Granodiorite is parallel to bedding and the pluton margin, as is the foliation in the igneous veins, sheets, and stocks within the envelope. However, approximately 500m north east of Loch Kemp (Enclosure 2) the margin parallel fabric swings abruptly through  $60-70^{\circ}$  to lie on a north easterly trend. In the vicinity of the River Foyers downstream from Dell Lodge, the north easterly trending fabric swings over a distance of 1km to lie on an east south easterly trend, parallel to the fabric in the large mass of Dalcrag Granodiorite lying to the east of the River Foyers.

The area close to Loch Kemp provides a unique situation, where petrologically similar and spatially related rocks show mineral foliations that are almost perpendicular to each other. It is possible that the two fabric strikes formed by different mechanisms, and thus fabric characteristics which are indicative of plastic or magmatic flow may be compared. Having established these characteristics in one area, this may help in determining the nature of mineral fabrics in the main Foyers Complex.

#### 4.6.1 Fabric Descriptions.

The south easterly trending igneous fabric is parallel to the pluton margin and defines a foliation that dips at 60-75 to the north east, (Enclosure 2). The fabric is formed by the parallel alignment of single minerals. In the chill zone these are dominantly biotite because the plagioclase laths are rather equant. Although, in the coarser granodiorite, plagioclase laths also define the foliation. Mesoscopically, the style and intensity of this fabric is similar to that seen throughout the main body of the pluton.

Very close to the pluton margin, in the area bordering Loch Kemp, there are a number of enclaves or xenoliths composed of diorite, appinitic diorite and quartz diorite. They are <5m in diameter, and where visible have angular outlines. They show no chill against the granodiorite, and are probably true xenoliths rather than syn-magmatic enclaves. Some xenoliths lack any fabric whilst others have intense fabrics with random trends, implying a pre-Dalcrag Granodiorite fabric forming event. Only one enclave has a strong fabric that lies parallel to the fabric in the surrounding granodiorite. This is probably a locally developed zone of blocks, which rising magma has ripped up from the wall zone and randomly relocated.

Small microdiorite enclaves are quite scarce especially in the outer chill zone, and are too few in number to sensibly use in quantitative strain analyses, (Ramsay 1989). The enclaves show a number of features indicative of both magmatic flow and solid state deformation in the host

granodiorite. Some are elliptical and have a long axis and an internal fabric, parallel to the fabric in the granodiorite. Others are elliptical but show no internal fabric. Occasionally, elliptical enclaves have a long axis at a high angle to the host fabric. Most enclaves however, show no fabric and are irregular.

The sheets and stocks of granodiorite which lie within the metasedimentary envelope, to the south west of Loch Kemp, contain a fabric very similar to the margin parallel fabric north of Loch Kemp. The fabric in these satellite bodies is parallel to the bedding in the envelope, and the margin of the main pluton. It is not, however, parallel to the walls of the stocks where they cut across the bedding in the envelope. The fabric in these satellite bodies becomes less intense at distances of >2km from the Foyers Complex margin.

The sub-vertical, north easterly trending igneous foliation in the Dalcrag Granodiorite is very similar to the margin parallel fabric in both style and intensity. It contains no schlieren structures, and the enclaves tend to be rather irregular, although some enclaves are oblate with long axes parallel to the fabric. There are a large number of metasedimentary rafts through which the fabric passes, within the north easterly foliated granodiorite.

Thin sections of rock samples taken from either side of the fabric strike swing shows mineralogically indistinguishable rocks which have the same fabric structure; both showing very scarce, weak quartz granulisation; a product of solid state deformation (Paterson et al. 1989). Parallel plagioclase laths show no internal deformation, and the

biotite shows no ribboning. The deformation of the quartz may be due to very weak solid state deformation.

The mesoscopic and microscopic structures suggest that the igneous fabric formed dominantly by magma flow, perhaps with late, weak solid state deformation, which only deformed the susceptible quartz. Evidence provided by enclaves and xenoliths suggests magmatic flow, but there are features, including foliations within some enclaves, and a fabric which does not bifurcate around the psammite xenoliths that are indicative of a solid state fabric (Paterson et al, 1989).

The fabric strike swing is marked by an area <20m wide and over 2km in length (Enclosure 2). North east of the boundary the fabric strikes north easterly, whilst south west of the boundary the fabric strikes south easterly, with an average strike swing of  $70^{\circ}$  between the two areas. Areas of clear outcrop containing the strike swing are limited in number, although at G.R.47781665 and G.R.47901696 the strike swing is well exposed. The actual 20m wide zone marking the change in strike is composed of granodiorite which lacks any preferred mineral orientation. There is no evidence of one fabric overprinting another, or of a strong but continuous swing in strike. Fabric reworking would indicate two fabric forming mechanisms were involved in the formation of the two fabric orientations. Thus the same mechanism is envisaged for both fabric trends, that mechanism probably being magmatic flow.

#### 4.6.2 Influence Of Metasedimentary Rafts.

Some factor must control the development of both fabric orientations and the strike swing. It is possible that external structures may influence the orientations of igneous fabrics, and thus explain the presence of the fabric boundary. The most likely structures are regional structures developed in the metasediments, which may have influenced the intrusion of the Dalcrag Granodiorite

Within the granodiorite north of Loch Kemp are found numerous large rafts, one over 700m in length (Enclosure 2). The rafts are composed of pebbly psammite and micaceous psammite. The two lithologies have a structurally ordered distribution through the raft swarm, perhaps reflecting the ghost stratigraphy of a regional structure, or a regional structure that has been modified during granodiorite emplacement.

The orientation of the rafts is always parallel to the igneous foliation in the adjacent granodiorite. One large raft at G.R.47901680 straddles the strike swing, where it bends to maintain parallelism with the igneous fabric. However the fabric boundary may occur away from the immediate control of the rafts perhaps indicating the rafts are orientated by the granodiorite rather than the rafts controlling the formation of the fabric boundary. It is possible that an early major structure established the igneous fabric pattern, and then the structure was partially

removed by granodiorite stoping leaving only the rafts to reflect part of the original structure.

A stereographic projection of the bedding foliations within the rafts defines a fold structure plunging at 64/035, (Fig.4.5) which is similar to the plunge of the 'D3' folds described in Chapter 7.

A detailed study of the igneous fabric orientation around the large folded raft in (Fig.4.6) shows there is a marked step in the position of the fabric boundary. This step can be explained if the raft is exerting a local influence on igneous fabric development, and the fabrics are magmatic. In area (A) the north easterly trending raft allows granodiorite magma flowing parallel to a north easterly direction to reach further to the south west. Where the raft forms a margin parallel screen, dipping at 70 to the north east the granodiorite flows parallel to this screen. This screen also acts as a 'margin' and the granodiorite flowing parallel to a north easterly direction is prevented from reaching area (B) in the lee of the screen. Thus the strike swing develops further to the north east. To allow the step in the strike swing to form it is necessary for the regional structure to be removed by stoping, leaving only the psammite rafts, at the time when the preserved igneous fabric was forming in the area adjacent to the raft.

#### 4.6.3 A Model For The Loch Kemp Area.

The most reasonable model involves only one pulse of granodiorite emplaced into the region to the north east of Loch Kemp. The fabrics exhibited by the granodiorite were dominantly created by magmatic flow. The flow of the granodiorite close to the pluton margin was controlled by this margin, whose attitude was defined by the south easterly trending foliations in the envelope, a very similar situation to that in the remainder of the Foyers Complex. The swing of the igneous foliation into a north easterly trend is caused by granodiorite veining and stoping along north east trending bedding. The bedding north of Loch Kemp has these different attitudes due to the presence of a large D3 fold.

The lack of a preferred alignment along the strike swing may be due to the meeting of vertically flowing magma. North east of the strike swing, magma flows upwards along north easterly striking planes, and southwest of the strike swing magma flows upwards along easterly trending planes. These plane orientations are imparted on the granodiorite magma by the regional structure. Any parallel fabrics formed at the fabric boundary will be destroyed at the interface of two opposing flows. The field and microscopic evidence suggest that the mineral fabrics in the Loch Kemp area are flow fabrics. As these fabrics are continuous with the fabrics



within the main body of the Dalcrag Granodiorite to the east of the River Foyers then the fabrics within the whole of the Dalcrag Granodiorite are probably flow fabrics. The granitoid fabrics close to Loch Kemp have the same intensity and style a fabrics seen in the remainder of the Foyers Complex, (except the Aberchalder Adamellite), suggesting the majority of the parallel mineral fabrics in the Foyers Complex are magmatic.

#### 4.7 DEFORMATION OF MICRODIORITE ENCLAVES.

##### 4.7.1 Introduction.

Microdiorite enclaves have been used to determine the distribution of solid state strain within plutons by authors which include Holder (1979), Hutton (1988), Ramsay (1989).

Initially spherical, solid enclaves of microdiorite become enclosed by solid granite as the granite crystallises through the rheological critical melt percentage (Arzi, 1978). Once the enclave is frozen in position any further deformation in the host granite will be recorded by a change in the shape of the enclave. As the competence contrast between the enclave and host is small, the deformation recorded by the enclave should closely resemble that within the host. Holder (1979), Hutton (1988), Ramsay (1989).

Strong evidence has been presented in this chapter to imply that magmatic flow occurred for much of the Foyers Complex's structural development, and this produced a flow fabric co-planar with a later minor solid state fabric. This

produces the strong possibility that the enclaves, which were initially magma globules, were shaped by both magmatic and solid state processes.

Holder (1979), Hutton (1988), and Ramsay (1989) show the enclaves used in their studies had an initially spherical shape and deformation was entirely due to solid state deformation. The criteria the authors use to indicate solid state deformation include, the presence of rounded enclaves where the granitoid fabric is weak, a correlation between increasing fabric strength and increasing X/Z ratio, and the inability of magmatic flow to produce the ellipsoidal disc morphology that enclaves often display. However Bateman (1983), Vernon (1988), and Paterson (1989) state that microdiorite enclaves are strongly deformed by magmatic flow, flattening the enclaves against the pluton wall, producing enclave shapes indicative of 60% solid state shortening.

#### 4.7.2 Enclaves In The Foyers Complex.

The internal fabric and ellipse long axes of the microdiorite enclaves are usually parallel to the fabric in the surrounding granitoid. The enclaves show oblate ellipsoidal shapes. South of Loch an Ordain where enclaves are common, there is a little three dimensional control of enclave morphology giving a  $X=Y>Z$  form of 2.65:2.5:1. X and Z are sub-horizontal axes respectively parallel and perpendicular to the granitoid foliation, and Y is a

sub-vertical axis. This morphology probably indicates solid state deformation of the enclave, and would convince many granitoid workers that the shape of the enclaves results from solid state deformation. However, early magmatic process may also effect the final shape of the enclaves. This is exemplified in the microdiorite swarms north west of Errogie where the enclaves often form highly irregular, and elongate ribbons, their morphology apparently not controlled by solid state processes.

#### 4.7.3 Measurement Of The Enclaves.

The shapes of a number of enclaves were analysed to determine the amount and distribution of deformation in the Foyers Complex, and whether this deformation is caused by magmatic flow or solid state processes.

The amount of exposure available to study the enclaves was limited to rounded outcrops protruding through peat, often containing low numbers of enclaves which necessitated the combining of data from adjacent outcrops to provide a data base large enough for calculations. Ramsay (1989), recommends 30 measurements per outcrop. The X and Z axis lengths were measured on all available surfaces. The abundance of horizontal surfaces and the dearth of vertical surfaces perpendicular to the igneous fabric allowed the analysis of strain within the horizontal plane but prevented any serious attempt at three dimensional strain analysis.

Enclaves within the Errogie Quartz Diorite and the Dalrag

Granodiorite were studied in a series of traverses extending from the pluton margin towards its centre. Most of the data were collected from three traverses;

- 1- Loch an Ordain to the Pass of Inverfarigaig.
- 2- Farraline to Loch Mhor bridge.
- 3- Loch Bran to the junction between the Foyers and Gorthleck roads.

Enclaves within swarms were not studied as they show strongly irregular shapes, perhaps reflecting irregular pre-deformational shapes. Single, well spaced enclaves showed a more uniform shape. The wide enclave spacing may result from transport over large distances within an early magmatic environment, with the enclave becoming more rounded. This is analagous to the effect of the sedimentary cycle on conglomeratic pebbles used as strain markers.

#### 4.7.4 Analysis.

The enclave shape data was analysed using the methods described by Holder (1979), Hutton (1988) and Ramsay (1989).

The geometric mean of enclave ellipticities was calculated for each outcrop, employing the method used by Ramsay (1989).

#### Traverse 1.

This traverse within Errogie Quartz Diorite starts adjacent to the pluton contact and extends 1400m to the south west. The first 600m is through an area containing numerous swarms of enclaves, but the remainder of the traverse records more isolated enclaves. In (Fig.4.7) the X/Z ratio of the enclaves are plotted against distance from the pluton margin. The first 600m of the traverse shows quite irregular axial ratios with a mean of 2.65 and maximum and minimum of 3.3 and 1.9. The remainder of the traverse records much more constant axial ratios of 2.2. There appears to be no systematic increase in axial ratios as the margin is approached although the outer 600m of the pluton appears to contain enclaves with higher axial ratios. Figure 4.8 presents the enclave axial ratios in a map form.

Figure 4.9 shows the X/Z ratios of the microdiorites plotted against the area of the enclave observed on horizontal surfaces. The graph displays a trend which shows that larger enclaves have higher axial ratios. Hossack, (1968) cited original shape of marker, orientation of marker, competency contrast of marker and matrix, and volume change, effect the final shape of strain markers. No workers noted, cite the original size of markers as effecting the final ellipticity. Where competency contrast between host and matrix is high it is possible small markers, sheltering

in the pressure shadows of larger markers, may record less strain, for instance small clasts in a coarse conglomeratic schist. However the competency contrast between dioritic markers and the quartz diorite host is minimal so this mechanism cannot be used to explain the size/axial ratio distribution. When the size of enclaves from the other traverses are plotted against ellipticity the graph suggests that the two factors are independent of each other (Figs.4.10 & 4.11)

In Traverse 1, magmatic flow may have elongated large enclaves close to the enclave swarms. The enclave swarms are emplaced into the granitoid host as dioritic magmas which become disaggregated by magmatic flow in the host. The large enclaves may represent large blobs of magma which are elongated by magmatic flow, but fail to break down into small enclaves. The well distributed enclaves away from the swarms are formed by intense disaggregation during magmatic transport resulting in a more uniform size and shape.

The enclaves in Traverse 1 show a non systematic weak increase in ellipticity close to the pluton margin that many workers have associated with the flattening of a solidified skin around a ballooning granite. However in the Foyers Complex the increase in ellipticity coincides with enclave swarms where early magmatic processes elongated enclaves co-axially with the later solid state fabric, assuming magmatic flow was parallel to the pluton wall.

#### Traverse 2.

This traverse again was within the Errogie Quartz Diorite. It began 400m from the pluton margin and progressed in a south westerly direction to finish 2100m from the margin. The X/Z ratios of the enclaves were very constant throughout the traverse at 2.15:1 (Fig.4.12) which is lower than seen in the enclaves to the south of Loch an Ordain. There is no increase in ellipticity as the margin was approached. This is illustrated in (Fig.4.7).

#### Traverse 3.

This traverse was within Dalcrag Granodiorite between Loch Mhor/Loch Bran and the south west pluton margin.

The traverse covered a distance of 2100m in a NE-SW. direction. The enclaves show reasonably constant ellipticity of around X:Z= 3.15:1 which is higher than ellipticities in the Errogie Quartz Diorite, (Figs.4.13 & 4.14).

A summary map of the whole pluton (Fig.4.15), shows the ellipticities of the enclaves throughout the pluton, are rather homogenous. The Maol Chnoc Complex is the only location to show strongly deformed enclaves with X/Z ratios of 8.5:1.

Within the Foyers Complex envelope there are numerous structures resulting from granitoid emplacement and indicate flattening strains around the complex, typically associated



with an inflating pluton, (Bateman 1985), (Chapter 7). Many authors, including Ramsay (1989) and Holder (1979) show flattening deformation in the envelope is associated with a granitoid solid state fabric intensifying towards the pluton margins, mirrored by an increase in enclave ellipticity. The plutons studied by Ramsay (1989) and Holder (1979) show weaker enclave deformation within the lithologies intruded into the complex later. The Foyers Complex shows no well defined strain increase towards the margins, elliptical enclaves throughout the pluton and enclaves within the later granodiorite showing stronger ellipticities than enclaves within earlier quartz diorite. This suggests that the enclave ellipticity is not solely due to solid state deformation, but early magmatic processes were also involved.

Hutton, (1988) and Ramsay, (1989) assume that prior to solid state deformation the enclaves were spherical. Hutton (1982), realised that the study of xenoliths, (inclusions foreign to the igneous suite of the host- Vernon 1983), was difficult due to the large range of initial shapes in objects not subjected to processes causing a regularity in shape i.e. transport within the sedimentary cycle. He developed a method to calculate the initial shape of xenoliths by the use of range diagrams. In Figure 4.16 the range of  $\log.X/Z$  ratios for individual suites of enclaves are plotted against the mean  $\log.X/Z$  ratio of the same enclave suite. Hutton (op.cit.) states that if irrotational deformation that has occurred was co-planar to the initial  $X/Z$  plane of the enclave, the log minimum and log maximum

lines on the graph should intercept the X and Y axes respectively on the graph at the same value, have slopes of 1, and therefore be parallel to each other.

A range diagram of Foyers enclaves produces log maximum and minimum lines that are sub-parallel, have intercept angles of 40°, and intercept values of 0.27 and 0.23. The closeness of these figures with those described by Hutton (op cit.) probably indicates that irrotational strain has occurred. The small differences are possibly caused by initial shape variations within the enclaves. Best fit lines (log.max. and log.min.) for the grand means of all three enclave suites are drawn, and rotated to lie with a gradient of 1. This averaging process gives intercepts on the graph's axes of 0.305 and 0.295 giving an average intercept value of 0.3. This shows the enclaves had an initial axial ratio of 1.99:1, possibly caused by magmatic flow.

Thus the average initial axial ratios throughout the pluton have been increased by solid state deformation to produce enclaves which in different areas of the pluton have ellipticities of 2.15, 2.65, and 3.15. If the enclaves were initially spherical the solid state deformation would have produced enclaves with X/Z ratios of 1.16:1, 1.66:1, and 2.16:1, which is low strain. The values of strain calculated for each enclave suite may be inaccurate as the differences in ellipticity may be due to initial shape differences and not differences in strain. The method used to determine the initial enclave shape (Hutton, 1982), does not permit the calculation of the enclave shapes in individual suites or areas of the pluton.

#### 4.7.5 Conclusion.

Analysis of microdiorite enclaves within the Foyers Complex indicates that they have been shaped by both magmatic and solid state processes. The solid state strain was co-planar to the magmatic flow and was much weaker than the finite enclave shapes indicate.

The enclaves close to the pluton contact show a slightly stronger ellipticity but this is probably caused by inherited enclave shape heterogeneity formed by magmatic flow rather than higher solid state strains. Paterson et al. (1989) state that magmatic foliations will increase in intensity towards contacts, reflected by an increase in ellipticity within the microdiorite enclaves. Thus it appears that solid state strain was of similar intensity throughout the pluton. If the pluton was solidifying from the outside inwards, then expansion of the complex during emplacement of new magma should impart a solid state fabric upon the outer crystallised granitoids, with the outer granitoids showing the strongest fabrics. Envelope structures (Chapter 7) show that the Foyers Complex did expand. Perhaps the outer rocks retained too high a melt fraction throughout the evolution of the complex to record a solid state strain. Only very late strain was recorded after most of the magma was emplaced.

CHAPTER 5. THE MAOL CHNOC COMPLEX.

## CHAPTER 5. THE MAOL CHNOC COMPLEX.

### 5.1 INTRODUCTION.

The Maol Chnoc Complex is an elongate granitoid body lying parallel to the north eastern margin of the Foyers Complex. For most of its length it is separated from the Foyers Complex by 500m-1km of psammites and semi-pelites. Outcropping Maol Chnoc Complex strikes south east-north west from Maol Chnoc summit to the south eastern slopes of Beinn Dubhcharaidh. The complex is at least 3.5km long, and <1km wide. Highton (1986) includes a large area of veined psammites to the north east of the main body as part of the Maol Chnoc Complex. The main body is patchily exposed, with outcrop on the summits of Maol Chnoc (G.R.58082185), Meall an Tuir (G.R.58672232), and on the north eastern slopes of Beinn Dubhcharaidh (G.R.58901990) (Enclosure 1).

The most noteworthy feature of the Maol Chnoc Complex is the intense mineral fabric it contains.

### 5.2 FIELD RELATIONSHIPS OF IGNEOUS UNITS IN THE MAOL CHNOC COMPLEX.

The Maol Chnoc Complex is composed of granodiorite, adamellite, a large diorite body exposed in Conagleann, and a number of aplite veins. Clear contacts are developed

between these igneous units allowing the intrusion sequence to be defined as diorite, granodiorite, adamellite and aplite.

A large diorite body 200mx700m occurs on the south eastern wall of Conagleann, and occasional diorite xenoliths occur in the surrounding granodiorite, implying the diorite predates the intrusion of the granodiorite, (Enclosure 5). On the Beinn Dubcharaidh ridge, diorite veins are intruded along bedding planes in the micaceous psammite. It is possible that the diorite body extends to the south under the psammities of Beinn Dubhcharaidh, and the diorite veins its roof. The granodiorite forms 80% of the complex and is lithologically similar to Dalcrag Granodiorite. The granodiorite is cut by adamellite, which forms ramifying vein stockworks, sheets less than 2m thick, and irregular stocks often less than 50m in diameter. The veins and sheets trend in a south easterly direction with dips between 70 and 90 to the south west. The veins are irregular in size and form, often thickening out into stock like bodies or tapering to extinction. The stocks are irregular, but are elongated in a south easterly direction. The adamellites are either medium grained and equigranular, or porphyritic micro-adamellites. Aplites occur as irregular masses and planar dykes, cross cutting both adamellite and granodiorite. The aplite dykes are parallel to the planar mineral fabric within the Maol Chnoc Complex.

North east of the Loch Mhor Fault, at Tom Mor (G.R.560025000), Carnoch (G.R.56402350) and Torr Shelly quarry (G.R.57382357), are a number of large granitoid

sheets, stocks and veins (Enclosure 1). At Carnoch and Tom Mor the sheets and stocks are parallel to both bedding and the adjacent north east margin of the Foyers Complex. At Torr Shelly, a stockwork of bedding parallel diorite and granodiorite veins is exposed. The granodiorites at Tom Mor and Carnoch are cut by stockworks of porphyritic micro-adamellite; a relationship found in the main Maol Chnoc Complex. The granodiorite contains orthite which is common in Maol Chnoc Granodiorite but not in the Dalcrag Granodiorite. Such similarities suggest that these granodiorite sheets are part of the Maol Chnoc Complex. However, the veins lack the strong fabrics seen within the main Maol Chnoc Complex and Haselock (pers.com.) states these granitoids show magnetic signatures similar to the Foyers Complex, not the Maol Chnoc Complex. This casts doubt on the correlation between these sheets and the Maol Chnoc Complex.

### 5.3 PETROGRAPHY OF THE MAOL CHNOC COMPLEX.

Many Maol Chnoc granitoid thin sections show an excellent foliation of biotite and plagioclase laths, defining both solid state and flow fabrics. In all petrographic descriptions thin sections showing the least solid state deformation are used.



#### 5.3.1 Granodiorite.

This is a relatively coarse grained porphyritic rock with a groundmass grain size between 0.5mm and 5mm. The phenocrysts are orthoclase often exceeding 1cm in length. The groundmass is dominated by plagioclase, but contains abundant biotite and visible quartz.

The Maol Chnoc Granodiorite plots within the granodiorite field of the Streckeisen Q.A.P. classification (Fig.5.1). The modal proportions of the constituent minerals are displayed in Table 5.1.

Plagioclase is the most abundant mineral, forming euhedral laths up to 1cm in length. Weak normal zoning and occasional intense oscillatory zoning occurs in a few plagioclase laths. Unzoned plagioclase laths have an oligoclase composition of An 20.

Quartz is common as interstitial material and large irregular grains which mould around the faces of early phases. Consertal boundaries exist between quartz grains. Many of the grains show quite strong undulose extinction.

Orthoclase forms subhedral phenocrysts and small subhedral groundmass grains. The orthoclase phenocrysts often lie parallel to the rock fabric.

Biotite is the dominant mafic mineral and occurs as single grains and as poorly defined ribbon aggregates. The biotite shows strong preferred alignment and a pleochroic scheme of X= pale yellow, Y and Z= dark brown. The biotite may show weak chloritisation.

Hornblende is variable in abundance and occurs as small sub-euhedral grains, X= light yellow, Y= green Z= sea green.

Accessories include magnetite, rutile, sphene, zircon, apatite and relatively abundant orthite. Sphenes are small, sparse, and show a pleochroic halo in adjacent biotite. Orthite forms both irregular and euhedral grains with pleochroic haloes. Some orthites show a metamict texture, (Plate 5.1). Magnetite and rutile are sparsely developed as small grains.

Myrmekite is common where plagioclase and orthoclase are adjacent. It forms small irregular grains on the outer surface of plagioclase laths, and small patches within the orthoclase and occasionally quartz rods within the body of euhedral plagioclase laths.

#### 5.3.2 Adamellite.

The adamellites range from strongly porphyritic micro-adamellites to equigranular medium grained adamellites. In the porphyritic micro-adamellites the phenocrysts are biotite and plagioclase (2mm-1cm) and the granular groundmass (0.05mm), is quartz and orthoclase rich. The equigranular adamellites have a grain size of 2-4mm with visible quartz, plagioclase, biotite and orthoclase.

The Maol Chnoc adamellites, (Hatch et al.1983), plot in the granitic field (Streckeisen 1976), (Fig.5.1). The proportions of minerals are displayed in Table 5.1.

In the porphyritic micro-adamellites, plagioclase forms large euhedral phenocrysts and small, minor grains in the

granular groundmass, (Plate 5.2). Many of the plagioclase phenocrysts occur singularly, but some occur as synneusis clusters of 2-3 crystals contacted along the 010 faces, (Vance 1969). The plagioclase shows weak normal zoning and extensive sericitisation. The outer margins of the laths often enclose equant quartz grains from the groundmass indicating continued plagioclase growth during or after groundmass formation.

Biotite is the dominant mafic phase occurring as large phenocrysts and small flakes within the groundmass. Hornblende is absent.

The groundmass is dominated by granular, equant, quartz and slightly larger irregular orthoclase crystals which are interstitial to the quartz.

Large, 1mm-1.5mm, grains of irregular quartz and subhedral orthoclase do occur in the groundmass of porphyritic adamellites. This is the habit of all the quartz and orthoclase in the equigranular adamellites. Accessories are scarce, but include magnetite, sphene, and abundant large zircons within the biotite laths.

#### 5.3.3 Diorite.

The diorite is medium grained and equigranular. In the field its appearance is variable with some areas leucocratic and others more melanocratic. The two lithologies occur as two bands trending in a south east, with a gradational contact between the two.

The diorite is dominated by hornblende and plagioclase. The

hornblende forms irregular, glomerocrystic, granular aggregates and large irregular and subhedral grains. Many of the hornblende crystals have large cores of clinopyroxene, and are replaced by thin laths of biotite. Plagioclase (An45) forms euhedral elongate laths, which may be partially enclosed by the hornblende. Some plagioclase crystals occur in minor hornfelsic patches. Sphene, apatite, pyrite and magnetite form the accessories. The accessory phases are sparse, small and anhedral.

Although this diorite is not an appinite, petrographically it could be placed in the appinitic diorite suite described in the Foyers Complex and aureole.

#### 5.3.4 Aplites.

The cream coloured aplites are exceptionally fine grained. They have a granular texture and equant mineral phases. The main mineral phase is quartz, although slightly enclosing orthoclase is common. Sparse plagioclase forms euhedral grains. Biotite grains are very seldom seen. Zircon is rare.

#### 5.4 STRUCTURE OF THE MAOL CHNOC COMPLEX.

The Maol Chnoc Complex lies parallel to the bedding foliation in the micaceous psammities. Where clearly seen the granitoid/psammite contact grades over a distance of 10-150m from granitoid, to granitoid containing psammite septa, to psammite with bedding parallel granitoid veins into psammite. On the north western walls of Conagleann the granodiorite/envelope contact dips  $65^{\circ}$  to the south west. In this wall there are a number of Maol Chnoc Granodiorite sheets up to 30m wide, running parallel to the regional foliation and the Maol Chnoc margin. At a distance of 200m south west of the main contact these sheets are no longer found.

The exposure of the south western margin of the Maol Chnoc Complex in the south eastern wall of Conagleann is rather complex. The structurally deeper level of exposure provided by Conagleann, shows that at depth the Maol Chnoc Complex widens out considerably, and the psammities on the Beinn Dubhcharaidh ridge form a roof to the granitoids exposed in the lower valley wall (Enclosure 5). The psammite roof extends from the mapped contact on the north eastern slopes of Beinn Dubhcharaidh to the south westerly contact of the Maol Chnoc Complex exposed in the lower south eastern wall of Conagleann.

In Conagleann (south eastern wall) 200m north east of the Maol Chnoc Complex margin, continuous Maol Chnoc Granodiorite gives way to a series of granodiorite and

adamellite sheets, intruded parallel to wide bedding parallel psammite septa. These granitoids are lithologically distinct from the other Maol Chnoc granitoids, being paler in colour and having more patchy distributions of phenocrysts. The aplites and micro-adamellites are absent from this region and some of the granodiorites contain irregular enclaves of adamellite <1m in diameter.

South west of the complex margin the quartzites and psammites are veined by Chliabhain Quartz Monzodiorite from the Foyers Complex.

Towards the top of the south eastern wall of C. nagleann, the Maol Chnoc Granodiorite encloses large septa and pendants of psammite which coalesce upwards forming a continuous micaceous psammite roof. The roof contains numerous sheets and veins of granitoid material. Below the roof zone is the occasional psammite raft.

The presence of an irregular veined roof, and psammite rafts below the roof suggests that emplacement involved veining the roof then stoping large bedding parallel slabs of psammite. This leaves an irregular roof, caused by variation in rate of pendant removal during stoping.

#### 5.5 FIELD DESCRIPTIONS OF MINERAL FABRICS.

The Maol Complex is notable for the development of strong planar and linear mineral fabrics. Fabric intensity ranges from a strong magmatic flow fabric to a mylonitic solid state fabric.

Planar fabrics strike in a south easterly direction, parallel to the south western margin of the Maol Chnoc Complex. Dips are steep towards the north east and south west, but close to the pluton wall, dips are concordant to the contact. Where intense, the planar fabric cross cuts internal igneous contacts. The lineation is contained within the plane of the mineral foliations, and plunges at  $40^{\circ}$ - $50^{\circ}$  towards the south east. (see enclosure 4A).

#### 5.5.1 Changes Shown By Rock Fabrics As Deformation Increases.

In the field, changes from magmatic to solid state foliations are readily observed. Increase in solid state deformation is marked by a decrease in grain size and increase in linear fabric strength.

Very intense mylonitic deformation is limited to poorly defined zones <2m wide. These zones are parallel to the complex margin, and the mineral fabrics. Fabric intensity increases gradually towards the centre of the zone, although there is a fabric intensity jump at the margin of these zones between intensley deformed zones and strongly deformed granitoid. The zones may be situated at internal igneous boundaries, (Plate 5.3). Shear criteria have not been identified.



#### 5.5.2 Rocks Dominated By Flow Fabrics.

These rocks contain planar mineral fabrics. The flow fabric is defined by the parallel alignment of biotite and plagioclase laths. Good flow fabrics are only seen in the granodiorites. Aplites and adamellites lack tabular minerals capable of defining a flow. They also have compositions closer to the minimum melt, implying crystallisation of the whole rock fabric is rapid. The time provided for the coexistence of crystals and melt will be short. The presence of the former and movement of the latter is necessary for the formation of a flow fabric.

#### 5.5.3 Rocks Showing Solid State Deformation.

With an increase in solid state deformation the strength of linear fabrics increases. Plagioclase and orthoclase are undeformed, but biotite forms ribbons which partially wrap feldspars giving a weak anastomosing cleavage, (Plates 5.4 & 5.5). Biotite and quartz form linear aggregates within the plane of foliation. Quartz often forms aggregates in the strain shadows adjacent to orthoclase phenocrysts.

#### 5.5.4 Rocks Showing Strong Solid State Deformation.

Linear mineral fabrics dominate planar fabrics. Grainsize is greatly reduced with the complete loss of feldspar phenocrysts. Quartz feldspar aggregates form prolate augens wrapped by biotite with dimensions of  $X:Y:Z = 10:2.5:1.5$ . The strongest fabrics form augens with dimensions of  $X:Y:Z=10:1:1$ . These strongly deformed rocks are well developed mylonites. (Bell and Etheridge, 1973)

Field evidence strongly implies that solid state deformation mechanisms operated in the Maol Chnoc Complex. Augened phenocrysts, augens of recrystallised felsic material wrapped by biotite, mylonites, and biotite ribbons only form during deformation of a solid material. Occasional quartz veins cross cutting the Maol Chnoc Granodiorite act as a focus for intense fabric development in the adjacent granodiorite. The granodiorite must have been solid to allow the formation of quartz veins in brittle fractures.

Intense fabrics cut across the contacts between all the lithological units within the Maol Chnoc Complex, again indicating a solid state fabric, (Plate 5.6).

#### 5.5.5 Gross Strain Distribution Within The Maol Chnoc Complex.

The Maol Chnoc Complex contains a mineral fabric, which is very heterogenous in intensity, with some areas of the complex free of recorded solid state strain.

A field estimate of fabric strength shows that the strain north of Conagleann, increases towards the south western margin of the complex. Although, the fabric becomes more intense to the south west, intensity is variable, often occurring in wide, poorly defined, north west-south east trending shear belts.

There are few microdiorite enclaves in the Complex, although, a small swarm found close to the south west margin gives a X:Z ratio of 8:1 on a horizontal surface, (Plate 5.7).

The increase in fabric intensity towards the south west margin is not necessarily purely a result of solid state strain, as flow fabrics also become more intense on approaching pluton margins. (Patterson 1988).

#### 5.6 MICROSCOPIC FABRICS.

Field evidence shows conclusively that the strong fabrics in the Maol Chnoc Complex were dominantly formed by solid state processes.

The microfabrics should thus show features indicative of solid state, fabric forming processes.

#### 5.6.1 Microscopic Fabrics In Weakly Foliated Rocks.

Fabrics in rocks with weaker foliations are defined by the strong parallel alignment of plagioclase laths, biotite flakes and orthoclase phenocrysts. The alignment of plagioclase laths is only well developed in the granodiorite. The plagioclase laths show no internal or external deformation, and fine textures of oscillatory zoning and albite twinning are undeformed. Biotite occurs as single flakes and glomerophyric aggregates aligned with the rock fabric, (Plates 5.8 & 5.9). However the biotite does show weak ribboning and accommodation around the plagioclase framework, implying minor solid state strain. The quartz shows undulose extinction and irregular subgrain boundaries.

In porphyritic micro-adamellite the phenocrysts show a very weak parallel orientation and no internal deformation. The fine grained groundmass has a granular texture, but within this is a fabric defined by the parallel orientation of small single biotite flakes.

#### 5.6.2 Microscopic Fabrics Of Rocks Showing Moderately Strong Foliations.

Plagioclase laths show little deformation, although where two laths impinge at right angles, the lath in the plane of foliation shows internal deformation, (Plate 5.10). Biotite

forms well defined ribbons, producing a weak anastomosing cleavage, (Plate 5.11). Quartz grains show a 70% reduction in grain size implying recrystallisation has occurred. Some of these quartz aggregates show a polygonal arrangement, typical of quartz textures Bell and Etheridge (1973), attribute to recovery after strain.

#### 5.6.3 Microscopic Fabrics in Strongly Deformed Rocks.

The most highly deformed rocks have mylonitic textures. (Bell and Etheridge, 1973). The felsic grains are <0.1mm in diameter, implying recrystallisation of feldspar and quartz, although irregular protoclasts of orthoclase feldspar occur. There is little internal strain or preferred orientation in the felsic grains indicating crystallisation was very extensive. Biotite forms ribbons which wrap augened or parallel sided fine grained felsic lithons. The augens probably represent biotite free areas in the original igneous texture, (Plates 5.12, 5.13, 5.14 & 5.15).

#### 5.6.4 Discussion.

Microtextural criteria outlined by Paterson et al. (1989) are used to evaluate the origin of the Maol Chnoc fabric. However the author's experience indicates many of the microscopic criteria proposed by Paterson to determine fabric origins (especially solid state), are only detectable

when the fabric is strong enough to determine its origin by field observations alone. Paterson et al. (1989) states the alignment of plagioclase laths is the result of magmatic flow. To rotate random plagioclase laths into the same plane using only solid state mechanisms involves much more disruption in the surrounding minerals than seen in the Maol Chnoc granitoids. Large amounts of recrystallised aggregate should form around the laths, and where individual laths impinge on each other deformation should occur in the form of distorted and broken twinning and igneous microstructure. This latter feature is only seen in rocks where field observations indicate strong solid state deformation. Bateman et al. (1988) ascribe "brittle" features in plagioclase (fracturing of albite twins and boudinaged plagioclase laths), to solid state deformation at low temperatures. Such features are absent from the Maol Chnoc Complex implying deformation occurred at temperatures  $>400^{\circ}\text{C}$ . Alignment of single flakes is due to magmatic flow but to form ribbon aggregates a solid state process is invoked, (Paterson et al. 1989). In extremely well deformed rocks Paterson et al. (1989), state that recrystallisation of minerals, augening and streaky gneissosity is irrefutable evidence of solid state fabric formation.

Thus it appears the Maol Chnoc Complex developed a margin parallel magmatic foliation, and after solidification was subjected to further strain. Only in a limited number of places did the solid state strain become intense enough to dominate the magmatic microfabric.

Coaxial solid state strain removes the need for mineral

rotation through large angles in response to the stress so reduces the amount of microdeformation observed.

The microscopic fabric shows none of the criteria outlined in Chapter 4, (Paterson, 1989) indicating that magmatic fabrics are overprinted by solid state fabrics as the granitoid crystallises through the rheological critical melt percentage (Arzi, 1978). Thus the Maol Chnoc Complex was solid during imposition of the stress from an external source.

#### 5.7 RELATIONSHIPS BETWEEN THE MAOL CHNOC AND FOYERS COMPLEXES.

Highton (1986), who first described the Maol Chnoc Complex, thought it was separate from, and predated the Foyers Complex, because the Foyers Complex lacked the intense solid state deformation found within the Maol Chnoc Complex.

The deformation in the Maol Chnoc Complex is localised, with the deformation zone not extending into the Foyers Complex or north eastern parts of the Maol Chnoc Complex. Thus the absence of a strong fabric from the Foyers Complex does not necessarily imply the Foyers Complex post dates the intense fabric forming event.

The Maol Chnoc Complex contains granodiorite with a field lithology superficially similar to the Dalrag Granodiorite in the Foyers Complex. The Maol Chnoc Complex is cut by adamellites, as is the Foyers Complex. These similarities suggest a correlation between the two complexes. In the



south eastern wall of Conagleann, the two granitoid complexes are separated by <300m of quartzite and migmatitic semi-pelite, which are heavily veined, (<35%), by granodiorite and quartz monzonite, whose affinities are not certain (map 5). This lack of distinction between the two complexes may suggest they are both the same intrusion, with the southern wall of Conagleann containing the veined gradation between the Maol Chnoc and Foyers Complexes.

Cross cutting relationships are used to establish the relative ages of igneous intrusions. There is a notable lack of cross cutting relationships between the Maol Chnoc and Foyers Complexes which is suprising for two adjacent plutons with high numbers of marginal veins. As the granitoids from both complexes form sheets along the psammite bedding foliations it is possible that Maol Chnoc granitoids already emplaced and solidified in the envelope do not provide a medium allowing veining by later granitoids.

On the southern wall of Conagleann, small stocks of unfoliated Aberchalder-type adamellite cross cut weak solid state fabrics within Maol Chnoc Granodiorite. The igneous units within the Maol Chnoc Complex including the aplites, show strong solid state fabrics. Thus the solid state deformation of the Maol Chnoc Complex occurred after intrusion and solidification of the most acid Maol Chnoc differentiates prior to the intrusion of the Aberchalder Adamellite, implying the Maol Chnoc differentiation was temporally ahead of Foyers Complex differentiation. This supports the thesis that the Maol Chnoc Complex is older and therefore not a part of the Foyers Complex.

In addition to structural data, there are differences of composition and form between the igneous units from each pluton. The Maol Chnoc Granodiorite has a more acidic nature and contains relatively abundant orthite, which is absent from the Dalcrag Granodiorite. The Maol Chnoc Adamellite occurs as small, irregular vein stockworks, and also stocks in both the porphyritic and equigranular varieties, whereas the Aberchalder Adamellite is equigranular and forms large stocks. The Maol Chnoc Complex contains abundant aplitic material, which is absent in such abundance from the Foyers Complex.

Haselock (pers.comm.), states the Foyers Complex has a high positive magnetic susceptibility, whilst the Maol Chnoc Complex has a magnetic susceptibility only weakly discernable above background implying the complexes contain considerably different magnetite abundances.

It is probable that the solid state fabric within the Maol Chnoc Complex was generated by the stress associated with the intrusion of the nearby Foyers Complex. By the time the stocks of Aberchalder Adamellite were intruded the fabric forming event had ceased. The emplacement of the Errogie Quartz Diorite was probably the unit from the Foyers Complex responsible for the strain recorded in the Maol Chnoc Complex.

As the Maol Chnoc Complex contains strong solid state fabrics, but proximal Errogie Quartz Diorite shows no evidence of solid state fabrics, it is possible the Errogie Quartz Diorite was in a state unable to record strain, perhaps a magmatic state.

#### 5.8 CONCLUSIONS.

The Maol Chnoc Complex is separate from, and predates the intrusion of the Foyers Complex. It was intruded by mechanisms which involved, veining, sheeting and stoping into the micaceous psammities. The sheeting and thus the elongate morphology of the pluton was controlled by the north west-south east trending bedding foliations. Intrusion was by a dominantly magmatic granitoid, which developed a good flow fabric parallel to the margin of the complex and the bedding foliations in the micaceous psammite. Deformation of the envelope by expansion of the Maol Chnoc Complex is not evident, and it seems probable that the majority of the "space problem" was solved by stoping.

After emplacement all the units of the complex had solidified prior to intrusion of the Foyers Complex. The strain developed during the emplacement of Foyers formed a very strong fabric within the the Maol Chnoc Complex.

CHAPTER 6. INNER AUREOLE PSAMMITE MOBILISATION IN THE  
ENVELOPE OF THE FOYERS COMPLEX.

## CHAPTER 6. INNER AUREOLE PSAMMITE MOBILISATION IN THE ENVELOPE OF THE FOYERS COMPLEX.

### 6.1 INTRODUCTION.

Boudinage and pinch and swell structures are well developed throughout the envelope of the Foyers Complex, but within the Central Psammite Septum and on the southern margin, psammite bedding fabric breaks down, forming either a chaotic jumble of boudins within a fine grained hornfelsic matrix, or a very streaky, hornfelsic rock containing a few refractory boudins.

These areas are thought to represent partial psammite melting due to the high temperatures attained in the inner aureole of the Foyers Complex, forming anatectic migmatites of mobilised psammite. Mould (1946), described the mobilised psammites as intrusion breccias, recognising their association with the intrusion of the Foyers Complex. Pattison and Harte (1988) describe very similar "chaotic" anatectic migmatites on the western margin of the Ballachulish granite.

## 6.2 TIMINIG OF MOBILISATION.

Mobilisation is not a regional feature, but is associated with the intrusion of the Foyers Complex, as there is a strong correlation between the inner cordierite bearing aureole and the mobilisation. Outside the inner aureole the mobilisation does not occur.

The mobilisation post dates the formation of all the regional fabrics because the F3 crenulations are truncated by the boundary between the boudins and the enclosing matrix, and neither the D3 crenulations nor the F1 or F2 fabrics are seen within the matrix. The mobilisation post dates or is synchronous with the boudinage around the Foyers Complex because boudin trains lose their regular arrangement within the mobilised areas.

## 6.3 DESCRIPTION OF MOBILISED AREAS.

Within the Central Psammite Septum the mobilisation occurs in the micaceous psammite, but not the quartzite or pebbly psammite. The distribution of the mobilisation is shown in (Fig.6.1), although mobilisation rarely exceeds 20% of the psammite.

Patchy outcrop makes the true morphology of the mobilised bodies difficult to determine, but they appear to form discrete, irregular-planar, dyke-like bodies with lengths <70m, running sub-parallel to the bedding foliation. The

mobilised bodies have irregular walls grading across several beds, where successive beds are breached by mobilised material. The walls often show a sharply gradational contact <1m wide between mobilised psammite and strongly boudinaged wall rock, (Plate 6.1). Mobilised bodies range from 10m to 50cm in width.

Many mobilised areas are dominated by an agglomeration of randomly orientated angular to rounded psammite boudins or clasts, ranging from 2-50cm in length. The clasts are often tabular, due to the morphological control of the bedding. The clast lithology is the same as the host metasediment, ranging from siliceous psammite to semi-pelite, with a minor amount of distinctive calc-silicate. Boudin trails within unmobilised psammite may be traced over several meters, but in the highly mobilised "intrusion breccias" there is no possibility of matching the boudins, (Plate 6.2). In the intrusion breccias the clasts show a random orientation, with clasts of differing lithologies intimately mixing with each other, suggesting substantial transport. The amount of transport is difficult to assess but in highly mobilised breccias it is probably over several meters. Where the clast lithologies are rather homogenous, clasts with "exotic" compositions tend to show more rounding, perhaps indicating that the rounding was due to transport, (Plate 6.3). Highly mobilised areas show greater block rotation and heterogeneity of clast type than the weakly mobilised areas.

The clasts are always partially or totally surrounded by a fine-medium grained, granular, psammitic matrix which



contains slightly less, and finer grained biotite than the psammite boudins. The matrix is composed of granoblastic quartz, plagioclase and also biotite. In thin-section the granoblastic quartz and plagioclase show no preferred orientation, or lithological banding. The biotite may form a planar parallel fabric, defined by isolated laths of undeformed biotite, a fabric typical of flow fabrics, (Plate 6.4) (Paterson et al, 1989).

Where the matrix is more abundant than the boudins it has a rather streaky nature consisting of a discontinuous faint lithological banding and biotite shlieren, with a faint planar alignment of biotites which strike parallel to the walls of the mobilised body and the regional bedding fabric (Plate 6.5). Plate 6.6 shows a rather streaky matrix, enclosing thin calc-silicate boudins. One boudin is rotated by  $180^{\circ}$  so it lies parallel to the major stress direction of boudin formation. Rotation into this stress direction could only occur if the major stress was released and a shearing mechanism was capable of rotating the boudin.

Some clasts in the mobilised bodies contain strongly cross cutting quartz-feldspar rich veins which penetrate deep into the clast, (Plate 6.7). These veins may be traced into the matrix surrounding the clast and are formed by the injection of matrix into fractures within the clast. It is evident the matrix was actually a melt capable of flow in order to inject into the clasts. The rotation of a rather delicate boudin through  $180^{\circ}$  into a position parallel to the maximum stress direction is most easily envisaged if the enclosing matrix is a flowing fluid capable of rotating the boudin.

The faint alignment of biotites are flow fabrics and the faint lithological banding is a ghost of the lithological banding remaining after intensive partial melting. There are no solid state fabrics developed in the mobilised areas which may be related to deformation generated by the intrusion of the Foyers Complex.

Outside the mobilised zones, small, <2cm in diameter, irregular veins of material similar to the matrix from the mobilised areas, may be seen cross cutting the fabric of the envelope rocks, (Plate 6.8). These veins are often rooted in shear zones or the 'gaps' between boudins, where the vein dissipates into the mineral fabric of the rock and disappears. These veins suggest there was some melting in the inner aureole away from the zones of intense mobilisation. However this melting was not extensive enough to break down the rock fabric and then flow as seen in the mobilised bodies.

#### 6.4 MOBILISATION ON CARN GAIRBTHINN.

The Carn Gairbthinn ridge in the southern envelope of the Foyers Complex also contains abundant evidence of partial melting. The mobilisation is confined to a 400m wide belt adjacent to the pluton margin, extending from the summit of Carn Gairbthinn (G.R.51701540) to the archaeological field system (G.R.51701630) on the north eastern slopes of Carn Bhreabaig. The mobilisation occurs within the micaceous psammite, and to a minor extent in the pebbly psammite, but

is absent from the quartzites. The belt of mobilisation is not continuous, and contains numerous wide, bedding parallel septa of unmobilised psammite which form 65% of the outcrop. Adjacent to the belt of mobilisation a number of the intrusion breccias similar to those within the Central Septum are found. The mobilisation belt is very heavily veined by Dalcrag Granodiorite forming up to 50% of the outcrop, and running down its centre is a very large, margin parallel sheet of Dalcrag Granodiorite 1300m long and 250m wide. The whole area is interpreted as a roof stopped and veined into from below by Dalcrag Granodiorite. The mobilised rock has a medium grained granoblastic texture, very similar to that seen in the matrix of the intrusion breccias, with a composition of biotite, plagioclase and quartz. The mobilised psammites show a well defined ghost of their original lithological banding and small <3cm coarse grained schlieren of biotite restite. Xenoliths or boudins of the parent rock dominated by the more refractory lithologies, including semi pelite and calc-silicates occur infrequently.

This form of mobilisation has the same anatectic origin as the intrusion breccias in the Central Septum, although here the mobilisation is much more intense. The presence of isolated xenoliths indicates that the melt actually flowed but mechanically continuous ghost banding suggests the majority of flow did no more than streak out the ghost banding.

## 6.5 DISCUSSION.

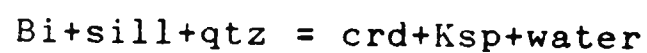
In the presence of P.T. conditions capable of generating cordierite and alkali feldspar in the inner aureole, Tyler and Ashworth (1983), indicated that melting should occur on the northern margin of the Foyers Complex. They state the absence of anatectic migmatisation is a result of a very low water activity, due to the initial scarcity of regional muscovite.

Muscovite free, micaceous psammites contain approximately 0.5% water. (Pattison and Harte, 1988). Using the work of Van der Molen and Paterson (1979), Pattison and Harte (1988) state that 1% water derived from a semi-pelite is insufficient to produce the amount of melting and mobilisation seen in the Ballachulish aureole at the temperatures experienced. They conclude, that to produce the extensive melting seen in the Ballachulish aureole, input of water from a water saturated pluton is needed. This method of inducing melting is not feasible in the Foyers envelope because the Foyers granitoids show no miarolitic texture which is indicative of water saturation, and the mobilised areas are intimately veined by Dalcrag Granodiorite, (Chapter 3), and evidence presented in Chapters 2 and 4 shows the Errogie Quartz Diorite contained substantial melt at the time of Dalcrag Granodiorite emplacement. Thus it is unlikely that a quartz diorite magma with a high melt content was water saturated. The conditions in the Foyers aureole were such that trondjhemitic rocks with a low water activity melted in limited areas, producing large quantities

of trondjhemitic melt.

Rafts of micaceous psammite found deep within the body of the Errogie Quartz Diorite, show no mobilisation. As they have similar compositions to, and may have reached higher temperatures than the envelope micaceous psammites, it is peculiar they show no mobilisation. Thus deformation, which occurred within the envelope but not in the rafts, is necessary for mobilisation to develop. The rafts melted to the same degree as the mobilised envelope rocks, but under static conditions the melt remained where it formed, and after cooling is indistinguishable from the granoblastic texture of unmelted grains. However, in the envelope deformation helped to disrupt the crystalline framework which released the melt to produce a crystal mush capable of flow. Alternatively the deformation may facilitate the movement of intercrystalline water or melt through the framework of the rock, using a filter pressing mechanism. The melt may then collect as larger bodies, or in the case of water, facilitate melting processes in particular areas.

The amount of melting in felsic beds depends upon the amount of free water, the rock composition and the actual P.T. conditions. Tyler and Ashworth (1983) show that water is generated in the inner aureole by the reaction;



This dehydration reaction will be prevalent in the unmobilised pelitic layers perhaps providing substantial quantities of water to facilitate melting within the more

felsic layers.

The composition of the plagioclase in the micaceous psammite was determined to be An 31 using electron microprobe data. The compositions of individual beds range from 20-30% plagioclase and 70-80% quartz discounting the biotite which throughout the whole micaceous psammite sequence accounts for 30% of the rock. The data of Johannes (1985) and Yoder (1968), for the An-Ab-Q system indicates that beds with 20% plagioclase have a liquidus of  $883^{\circ}\text{C}$  and a solidus of  $723^{\circ}\text{C}$ , whilst beds containing 30% plagioclase have a liquidus of  $802^{\circ}\text{C}$  and a solidus of  $723^{\circ}\text{C}$ . This data is for a system with excess water. Water saturated psammite with a 30% plagioclase content requires a temperature of  $763^{\circ}\text{C}$  to undergo 50% melting.

The envelope rocks in the Foyers aureole are probably not water saturated and without the migration of water from adjacent pelitic beds into the areas of anatexis, complete dehydration of biotite in a psammite would only provide 0.5% insitu water. Van der Molen & Paterson (1979), show that P.T. conditions similar to those in the Foyers aureole would only melt 7% of a granitic rock and thus an even lower percentage of a trondjhemitic rock would melt. This amount of melting is far too low to cause substantial mobilisation and matrix flow (Van der Molen & Paterson, 1979). It is thus likely that migration of water from dehydration reactions within the pelite layers facilitated anatexis. An additional 2.5% water which could be derived from pelitic layers would cause 42% melting (Winkler 1976), under Foyers aureole conditions, (Tyler and Ashworth, 1983). At higher aureole

temperatures less water is needed to form the same amount of melt. The amount of melt, free water from dehydration reactions, and initial composition of mobilised areas can only be crudely estimated in the Foyers Complex aureole.

A psammite containing 30% plagioclase, (An 31) and 70% quartz forms a 50% melt at  $673^{\circ}\text{C}$  in water saturated conditions. If an additional 2.5% migrated water was present at the site of melting, it would saturate 40% of the melt, and a temperature  $50^{\circ}\text{C}$  higher (Winkler 1976) would be needed to obtain the same proportion of melt. Thus a temperature of approximately  $815^{\circ}\text{C}$  was needed to cause mobilisation in the Foyers inner aureole. Generation of lower melt fractions needs lower temperatures.

It is possible to raise envelope temperature close to that of a pluton if the envelope rocks are in very close spatial contact to the magma and the magma flows past the walls. Convection in the pluton is necessary so that cooling magma close to the pluton/envelope boundary is replenished by hot magma from deep within the pluton body. It is only under these conditions that a high envelope temperature can be maintained. In Chapters 2, 4 and 9 evidence is presented showing that the Erroglie Quartz Diorite was emplaced as a melt with a crystal content of 17%. A quartz diorite with a crystal content of 20% has a temperature of  $850^{\circ}\text{C}$  (Chapter 8), high enough to raise the temperature of the inner envelope rocks to  $815^{\circ}\text{C}$ . It is thus possible to achieve temperatures in the Foyers inner aureole to achieve psammite melting.

As mobilisation is very localised, anatexis probably only



develops where conditions are optimised. Such areas may include a high plagioclase:quartz ratio, an elevated temperature due to intimate contact with the Foyers granitoids, an area well fluxed by water from dehydration reactions in local biotite rich beds and possibly deformation to facilitate the movement of fluids or to assist in the breakdown of rock fabric which will allow the melt-crystal mush to flow as a fluid at lower melt percentages.

CHAPTER 7. RELATIONSHIP BETWEEN THE FOYERS COMPLEX AND THE  
REGIONAL STRUCTURES.

## CHAPTER 7. RELATIONSHIPS BETWEEN THE FOYERS COMPLEX AND THE REGIONAL STRUCTURES.

### 7.1 INTRODUCTION.

To date the models developed for emplacement of the Foyers Complex have all involved intense forceful deformation of the psammite envelope. Highton (1986), Marston (1967) and Mould (1946) state the intrusion of the Foyers Complex was responsible for massive crustal reorientations in the region of the complex. Initially, north easterly striking bedding was rotated into parallelism with the southern and north easterly margins of the complex. This effectively forms a large fold hinge around the easterly "apex" of the Foyers Complex. This postulated fold is named the "Foyers fold" in this thesis. The granitoid complex occupies the core of the fold. Highton (1986), states that the fold axes of D3 folds are rotated into parallelism with the northern margin of the complex.

The effect of the intrusion upon regional structures may yield information about the structural mechanisms involved in the emplacement of the Foyers Complex. The orientations of regional structures indicate wether<sup>h</sup> granitoid emplacement is syn, pre, or post regional deformation, and wether<sup>h</sup> regional structures are reworked by intrusion.

Until the virtual completion of this thesis the regional structure of the Foyers area was incomplete. Highton (1986), describes four recognisable regional deformation events in

the rocks to the north, but is unsure <sup>h</sup> whether all four events are seen within both the Central Highland Division and the Grampian Division (Piasecki 1980). Recently, Haselock, as part of a B.G.S. mapping contract for sheet 73E (Foyers), has re-mapped regional structures around the Foyers Complex. The lack of exposure hampered the identification of major structures, and therefore placing these major structures within a tectonic time sequence was very difficult. Thus the regional structural synthesis in the Foyers area was always unsatisfactory, and structural solutions had a very transient nature, although the presence of a large fold around the eastern apex of the complex was always present. Haselock and Leslie, between May and November 1989, conducted a major geomagnetic survey of the unexposed ground. Data from this survey allowed the tracing of the Garbeinn Pebbly Psammite Formation across unexposed ground producing a more accurate and less problematical structural synthesis. (Enclosure 6)

## 7.2 STRATIGRAPHIC SETTING.

The Foyers Complex is intruded into a series of micaceous psammites, quartzites, pebbly psammites and semi pelites. The micaceous psammites are a part of the Glen Doe Formation of the Corrieyairack Subgroup, whilst the quartzites and pebbly psammites are a part of the Gairbeinn Pebbly Psammite Formation of the Glenshirra Subgroup, (Haselock et al.1982). Piasecki (1980), and Highton, (1986) suggest that the

semi-pelitic migmatites are part of the Central Highland Division. Mapping for sheet 73E, (Haselock, pers com.) and (Lindsay et al. 1989) show that the migmatitic semi-pelites are above the Garbeinn Formation and thus all formations are within the Grampian Group of the Dalradian, (Fig.1.4).

The junction between the migmatitic Central Highland Division "basement" and Grampian Division "cover" (Piasecki, 1980), occurs at a number of localities on the northern margin between Carn a' Chliabhain and Maol Chnoc, (Highton 1986). No transition between unmigmatized micaceous psammite and migmatized semi pelites was seen within the area mapped, although the migmatites are interbedded with quartzites. Both micaceous psammite and pebbly psammite can be seen in contact with the migmatites. The contacts are parallel to bedding, and there is no increase in strain towards the boundary, implying the presence of a slide (Piasecki, 1980), or a meta-conglomerate which may imply a sedimentary transition over a crystalline basement. The regional deformation seen in both the Central Highland Division and Grampian Division are similar in both style and number of recognisable deformation events, implying the boundary in the Foyers area does not represent a basement/cover relationship.

The Gairbeinn slide zone identified by Haselock (1982) between the Corrieyairack and Gairbeinn Formations occurs within the Foyers envelope at a number of locations, where the micaceous psammite and pebbly psammite lie adjacent to each other. The junction between the pebbly psammites and micaceous psammites is parallel to bedding within the

adjacent formations. There is an increase in platiness towards the "slide", although this is often obscured by granitoid veins. The slide also removes several hundred meters of the regional stratigraphy, (Haselock 1982). The intense deformation of pebbles in the pebbly psammite, and development and deformation of quartz veins, which characterise the Gairbeinn slide 15km south of the Foyers Complex, where it was initially described by Haselock et al. (1982) are absent.

### 7.3 FIELD DESCRIPTIONS OF PSAMMITE UNITS.

The estimated field proportions of biotite, quartz and feldspar were used to differentiate between quartzite, psammite, micaceous psammite and semi pelite, based upon the petrological classification of Haselock et al. (1982), although the term micaceous psammite replaces semi psammite (Haselock et al. 1982). The term semi pelite is used to describe a unit of coarse, biotite rich migmatites.

#### 7.3.1 Pebbly Psammite.

The Gairbeinn Pebbly Psammite Formation, contains two units, pebbly psammite and less extensive quartzites. Haselock (1984), stated the pebbly psammite is a texturally and mineralogically immature arkosic sediment deposited in an alluvial/braided river system.

The pebbly psammite has a medium grained, pale grey, slightly pink psammitic matrix containing distinctive, large <1cm, clasts in variable abundance. The lithology of the clasts is dominated by pale pink-white orthoclase crystals, but quartz pebbles and quartz/alkali feldspar clasts also occur. Some clasts are flattened parallel to the main foliation within the rock, although orthoclase crystals appear to resist deformation. Marston (1966) stated that these clasts were formed by porphyroblastic growth of quartz and feldspar in the Foyers aureole, due to the regrouping of minerals and feldspathization. However these clasts are characteristic of the stratigraphical unit, and can be found many kilometers from the Foyers Complex. Bedding is often defined by magnetite rich layers, graded bedding and cross beds (Plate 7.1). Lensoid bodies of conglomeratic quartzite occur within the pebbly psammite. These are slightly discordant to the foliation, an inherited sedimentological feature, and are difficult to trace for more than 20m. The rounded clasts are composed of quartzite and occasionally vein quartz, have diameters up to 8cm, and are strongly flattened in the plane of the major foliation seen in the pebbly psammite.

Quartzites appear as planar to lensoid beds at the top of the pebbly psammite formation, often with thicknesses exceeding 50m. The pebbly psammites beneath grade into the quartzites by the loss of mica, feldspar and clasts. The quartzites are very flaggy and weather to a distinctive pink colour. Frequently the quartzites contain thin <5mm, seams of pure sillimanite or muscovite after sillimanite.



### 7.3.2 Micaceous Psammite.

The Glen Doe micaceous psammite is a grey brown, well bedded rock. The beds, around 10cm thick, are defined by the proportions of biotite, quartz and feldspar. Some beds are siliceous psammites whilst others are semi pelites. Occasional beds within the micaceous psammite have a richer mineralogy, of small <2mm red/brown garnets and prismatic sillimanite, which cross cuts planar mineral fabrics. The larger prisms of aluminosilicates may develop muscovite jackets. This is well developed in a micaceous psammite screen, (G.R.47351712), close to Loch Kemp, where andalusite prisms 7cm in length develop a thick muscovite jacket. Within the micaceous psammite are thin <6cm, bedding parallel calc-silicate ribs which weather proud from the surrounding psammite. They have a homogenous pale green colour, although some may have a reddish core. Highton (1986), states they have a mineralogy of plagioclase, calcite, garnet, zoisite and actinolite. Spatially associated with psammite rich in garnet, sillimanite, and calc-silicates are bedding parallel amphibolites. They occur infrequently as thick, <1m, lenticular bodies, but are normally confined to thin <20cm discontinuous beds. Their association with more diverse psammite mineralogies may imply the thin amphibolites are possibly of sedimentary origin, although they have previously been interpreted as pre-tectonic tholeiitic minor intrusions. (Haselock, 1982 &

Highton, 1986).

#### 7.3.3 Migmatitic Semi-Pelite.

These rocks have a very distinctive lithology of medium grey, coarse grained, trondhjemitic, stromatic migmatites showing a strong crenulation. Thin bands of quartzite <1m, frequently occur.

The migmatites show coarse grained leucosomes, up to 3cm thick, dominated by quartz and plagioclase, and thinner melanosomes dominated by biotite. In the more pelitic migmatites, fresh red garnets and sillimanite are seen. The sillimanite cuts all fabrics and the garnets are equally abundant in the melanosome and leucosome.

#### 7.4 EXTERNAL STRUCTURE OF THE FOYERS COMPLEX.

The Foyers Complex is broadly triangular in outline, the north eastern and southern margins of the complex are intrusion contacts, whilst the north western margin is a fault contact formed by the Gleann Liath Fault (Enclosure 1).

A large micaceous psammite septum running from Beinn Mheadhoin to Carn Dubh divides the complex into two separate bodies. The presence of the psammite septum in the areas of Lochgarthside and Drummussady is completely obscured by a deep till ridge, although Borehole data from Smith, B.G.S

Report No. HE70/R13 (Foyers Hydro scheme) and a ground geomagnetic survey (Haselock pers com.), show that the psammite exposed north east of Loch Bran continues to the shores of Loch Mhor.

The actual contact between the main pluton and the envelope rocks is seldom seen, although outcrop and topographical features allow the contact to be traced with reasonable accuracy. The envelope rocks form positive features, often ridges, with the contact generally lying within the slope rising up from the low lying granitoid interior of the pluton, (Haselock and Leslie pers. comm.).

The contact between the envelope and the main pluton is seen on the summit of Creag a' Chliabhain, and in the steep north western valley wall of Conagleann. Here the contact is difficult to trace, due to the steep valley sides and the bedding parallel veined nature of the contact, although it appears to dip steeply  $75^{\circ}$ - $85^{\circ}$  to the south west and is broadly concordant with the bedding.

Although locally cross cutting, the pluton contact is generally concordant with bedding in the envelope and the mineral fabric in the granitoid, (Enclosure 4.).<sup>+44</sup> The igneous fabric in the complex is often parallel to the strike of the margin and the bedding in the envelope.

On the southern margin between Cairn Gairbthinn and Whitebridge the envelope is intruded by large amounts of Dalrag granodiorite, to such an extent that close to Whitebridge the envelope becomes xenolithic granodiorite. In this area, the envelope is probably acting as a roof to the granodiorite. South of Loch Kemp the main Foyers Complex is

separated from a system of large stocks, which form the Loch Knockie granodiorite, by a 500m wide septum of dominantly micaceous psammite. The area of stocks probably forms a stoped roof zone with large masses of Dalcrag granodiorite extending under the psammite. The granodiorite is exposed as large bodies where stoping is the greatest.

## 7.5 REGIONAL STRUCTURES.

### 7.5.1 First Deformation.

The first deformation is marked by a bedding sub parallel foliation, defined by a penetrative planar fabric of biotite. Occasionally in pelitic units narrow <1.5mm, fabric parallel quartz-plagioclase segregations may occur. This is the dominant fabric within the country rocks and increases bedding definition, often giving the bedding a flaggy appearance. In the semi pelitic migmatites the S1 fabric is defined by the leucosome-melanosome migmatitic segregations. Within conglomeratic units of the pebbly psammite the quartzite pebbles are flattened parallel to the S1 fabric to form oblate ellipsoids.

On Beinn Sgurrach and on the north eastern envelope of the Foyers Complex close to Loch an Ordain the penetrative fabric is oblique by up to  $10^{\circ}$  to bedding.

Folding is limited to minor isoclinal intrafolial folds. They have wave lengths of <10cm, and are normally defined by thin biotite layers.

#### 7.5.2 Second Deformation.

Folds (F2), produced by the second deformation event form the dominant minor fold structures in the envelope of the Foyers Complex. They are most strongly developed within the micaceous psammite, due to the banded nature of the rock, (Plate 7.2). The more micaceous units act incompetently compared to the psammitic layers, producing layers in the folds with attenuated limbs and thickened hinges. Overall the folds range from 1B to 2 in the Ramsay fold classification, (Ramsay, 1967). The fold axial planes of the folds are parallel to the early S1/bedding foliation, except where the bedding is folded around the F2 fold hinges. The fold axes have a variable plunge to the south east. Interlimb angles are variable  $40^{\circ}$ - $120^{\circ}$ , and the folds are often asymmetrical. An axial planar crenulation cleavage, (Plate 7.3) is occasionally developed within the core of D2 folds in the more micaceous beds. S2 planar fabrics away from fold cores are not common. At some localities e.g.-Tom Mor, the S2 fabric is composed of a transposed S1 fabric which forms a coarse spaced fabric composed of biotite and quartz-feldspar segregations. This fabric is also well developed within the pebbly psammite where spaced lithons of biotite lie strongly oblique to bedding.

### 7.5.3 Third deformation.

The most prominent D3 structure is a small scale crenulation, well developed within the semi pelitic migmatites and the more pelitic units of the micaceous psammite. Few mesoscopic F3 folds are seen but these have a fold classification of class 1B-1C (Ramsay 1967), (Plate 7.4)

The crenulations have a wavelength of 0.5cm-3cm, and the deformation is normally not sufficiently intense to develop a crenulation cleavage in the fold limbs. The crenulations refold S1 and S2 fabrics, and F2 folds, (Plate 7.5). The axial planes of the folds strike north north east, and the fold axes often plunge steeply  $>60^{\circ}$  to the north. A spaced planar fabric only develops within the hinge zones of folds in the migmatites. Here D3 reworking transposes early S1 migmatitic banding into a S3 cleavage.

### 7.5.4 Gross Regional Structure.

The recent synthesis of major regional structures, developed by Haselock and Leslie (pers. com.) using data from an intensive geomagnetic survey is displayed in enclosure 6. The attitude of the bedding, D1 and D2 structures in the Foyers northern envelope are controlled by a large northerly trending D3 synform. The northern margin of the Foyers Complex is parallel to the south western limb of this fold. South of the Foyers Complex is a large easterly

trending D2 antiform, whose orientation is weakly modified by northerly trending D3 folds. This D2 fold controls the orientation of the bedding and the orientation of southern margin of the Foyers Complex.

#### 7.6 EFFECTS OF THE EMPLACEMENT OF THE FOYERS COMPLEX ON REGIONAL MINOR STRUCTURES.

The bedding foliation in the Corrieyairack region strikes north east, but as the Foyers Complex is approached from the south the bedding rotates into an easterly direction, (Haselock et al., 1982) This rotation begins in the ground between the River Fechlin and Glen Brein. The bedding strike south of the Foyers Complex is parallel to the complex margin, whilst north of the complex parallelism is retained as both bedding and complex margin strike in a south south easterly direction.

Both Marston (1967) and Highton (1986), thought this large deflection in bedding the result of a late structure, generated by granitoid emplacement. All earlier structures should therefore be rotated.

##### 7.6.1 Bedding And D1 Foliation.

Enclosure 4, <sup>+4A</sup> and the contoured equal area stereographic projections of poles to bedding (Figs. 7.1-7.6) from north of the Foyers Complex, the Central Psammite Septum, Cairn Gairbthinn to Beinn Bhuraich, the Beinn Sgurrach ridge, and



south west of Loch Kemp illustrate the orientations of bedding around the complex.

The bedding trace and stereonets imply that a large late structure may exist, the most feasible structure being a large fold hinge plunging at  $70^{\circ}/232^{\circ}$ , enclosing the eastern apex of the Foyers Complex. The abrupt easterly cessation of the Beinn Dubhcharaidh and Beinn Bhuraich ridges to form lower ground, may suggest the hinge is now replaced by granitoid material.

The Foyers contact sharply cross cuts bedding between the River E and the south western slopes of Beinn Mheadhoin, (G.R.55351625). Although the bedding lies at a high angle to the complex, there are no folds or boudinage structures developed on the north western slopes of Carn na Saobhaidhe, (G.R.55351425), the only locality so close to the pluton which shows no deformation. This suggests that the large lobe of granodiorite south of the central psammite septum did not flatten its south eastern margin, in turn, implying that expansion of the lobe towards the south east was by replacement rather than displacement. Bedding in the country rocks remains parallel to the margin up to 3.5km north east and 2km south of the pluton. Haselock et al.(1982), show that the beds start to lose parallelism with the complex margin 7-8 km south west of the complex.

Many authors state that plutons which create room by flattening their envelopes show strong granitoid fabrics, strong deformation in their aureoles and rotate beds into parallelism with their margins. Phillips (1956), shows that bedding begins to rotate into margin parallelism with the

Criffel granodiorite 2-3 km from the pluton. Pitcher & Berger\* (1972) state that rotation of bedding occurs up to 800m from the margin of the Ardara pluton, Brun & Pons (1981), show that intrusion of the Valencia and Brocales plutons rotates bedding into margin parallelism 1-2 km from the contact, and Paterson (1988) shows that the regional bedding strike begins to rotate into parallelism 2.5km from the contact.

If the regional strike of the bedding was rotated into parallelism with the margin of the Foyers Complex by stress associated with the emplacement of the complex, then rotation of the beds has occurred at an anomalously large distance from the complex (7-8km). It seems more probable that the beds are rotated from north easterly to easterly by a structure which pre dates the intrusion of the Foyers Complex.

#### 7.6.2 D2 Deformation- Minor Asymmetrical Folds.

The stereograms of D2 fold plunges in (Figs.7.7-7.11) show that between the northern and southern margins there is a difference of approximately  $30^{\circ}$ - $40^{\circ}$  in plunge direction. If these folds were developed as parasitic folds on the same major structure, then initially they should all have had a similar plunge direction. This implies there has been rotation of the axes by the same structure which rotated the bedding. It is a post D2 structure, perhaps the Foyers fold generated by the emplacement of the Foyers Complex.

### 7.6.3 D3 Deformation- Crenulations.

At all the localities around the Foyers Complex the fold axial planes of the crenulations have a northerly strike and dip steeply,  $70^{\circ}$ , to the east and west (Figs. 7.12-7.15). Only on the ground between Meall Donn and Carn Bad-Earbaig (C.R.58802430), do the crenulations deviate from their northerly trends, to strike between north east and east, dipping to the south east. Haselock (pers. comm.) suggests that this orientation may be a conjugate set of crenulations, occasionally seen in areas distant from the Foyers Complex.

The D3 crenulations have not been rotated by the structure which rotates the beds on either side of the Foyers Complex (Fig. 7.16), implying the structure rotating the D1 and D2 structures developed prior to or at the same time as the D3 crenulations were formed. Thus the structure which causes the bedding to swing around the Foyers Complex cannot be post Caledonian, and is not caused by the emplacement of the Foyers Complex.

Fig. 7.17 illustrates how the crenulations would lie on the northern and southern margins of the Foyers Complex when rotated around the fold axis of the Foyers fold. The amount of rotation applied is equal to the rotation required to deflect the bedding from its "original" north easterly strike into its present contact parallel attitude. This amount of rotation would cause the crenulation fold axial

planes on the northern margin to strike at  $110^{\circ}$  and dip very steeply to the north north east, whilst crenulations on the southern margin would lie at  $150^{\circ}$  and dip very steeply to the north east. Both these orientations are dissimilar to the actual orientations of the crenulations recorded.

#### 7.7 MINOR STRUCTURES FORMED IN THE COUNTRY ROCKS BY GRANITOID EMPLACEMENT.

There are no major structures attributable to the stresses generated by the emplacement of the Foyers Complex, but minor structures are abundant.

Minor structures include intense boudinage, minor shearing, late very open folds, deformation of metamorphic spots in amphibolites, and a strong L-S to S fabric within the Maol Chnoc Complex. There is no good evidence to indicate the development of a cleavage or lineation within the psammitic envelope. Folds within the psammities, indicative of compression by an expanding pluton are absent.

##### 7.7.1 Boudinage.

All around the Foyers Complex, the psammitic envelope rocks show boudinage of varying intensities. The development of boudinage is determined by; the actual stress applied to the envelope, the lithology of the rock, and the orientation of the structure (normally bedding) to be boudinaged. Of the

lithologies within the envelope, the micaceous psammite shows the greatest boudinage, (Plate 7.6). This is a result of its banded nature, where competent and incompetent layers are interbedded. The pebbly psammite shows some boudinage in thin quartzite layers, but the semi-pelitic migmatite appears unboudinaged. The quartzite also shows no boudinage apart from the occasional development of mica boudins, where thin micaceous layers are pulled apart.

The orientation of bedding is nearly always parallel or sub parallel to the pluton margin, and exhibits chocolate block boudins, implying flattening parallel to the bedding.

Infrequently, calc-silicate beds, perpendicular to the pluton margin, show weak boudinage although in most cases it is evident the calc-silicate boudins and the enclosing rocks are within small blocks (<20m diameter), rotated by post- or syn-boudinage shearing. However very occasionally shearing is absent and boudinage still occurs perpendicular to the margin. In this situation it is possible that plastic flow in the incompetent micaceous psammite caused slight vertical shear which fractured the brittle calc-silicates.

Beds lie at high angles to the pluton contact where they are in the vicinity of D2 and D3 Caledonian minor folds. These beds show no boudinage, and no folding attributable to the boudin forming deformation. Perhaps the deformation in these areas is taken up by the tightening, or opening of Caledonian minor folds.

In areas of micaceous psammite, free from other lithologies, the deformation is restricted to intense pinch and swell, with occasional boudins with tapered necks.

Increasing competency contrasts displayed by the semi-pelites, siliceous psammites and calc-silicates, are matched by a decrease in boudin tapering, defined by an increase in the internal angle between the long axis of the boudin and the tapering surface. The calc-silicates form "square ended" boudins with no evidence of tapering, indicating that deformation was entirely brittle, (Plate 7.6). Competent lithologies often show fractures, <3mm thick, filled with felsic material which lie perpendicular to the boudin sides. Boudin necks are most frequently filled by the infolding of less competent layers which run parallel to the long axis of the boudins, (Plate 7.7). Sometimes the necks are partially filled by a felsic fine grained granitic textured rock, similar to the matrix seen within the anatectic intrusion breccias.

Frequently the boudins within a train will lie en-echelon to each other and the fractures at the end of the boudins will be oblique to the boudin long axis, (Plate 7.8). This structure is developed when the deformed bed is not perpendicular to the principal stress direction. Under such circumstances the infilling material between the boudins shows minor shearing.

The deformation causing the boudinage, is associated with the emplacement of the Foyers Complex. This is evident because the maximum stress directions are always perpendicular to the pluton margin whatever the orientation of that margin, and the intensity of boudinage dies away from the pluton contact. Traverses on the north eastern and south western margins show that boudinage dies away



completely 1.5-2km from the pluton/envelope contact.

To see how the intensity of intrusion related strain varies in the envelope, the extension shown by calc-silicate boudins within the micaceous psammite as studied, (Table.7.1), (Appendix D), The micaceous psammite provides a lithology which occurs adjacent to the contact all round the pluton, and by its banded nature is also very sensitive to boudinage. Figure 7.18 displays the variation in amount of boudinage around the pluton, showing that maximum horizontal extension is parallel to the contact, and boudinage is most intense close to the pluton.

#### 7.7.2 Relationship Of Granitoid Veining And Boudinage.

The Foyers aureole is intensely veined by Errogie Quartz Diorite, Chliabhain Quartz Monzodiorite and Dalcrag Granodiorite veins which vary in width between 100m and 1cm, and these veins occur within areas of intense boudinage. There are no examples of granitoid veins or bodies showing pinch and swell or boudinage. As the veins virtually always follow the bedding foliations, veins are shaped by the morphology of the vein walls, (Fig.7.19). Granitoid veins often pseudomorph pinch and swell structures due to magma injection between the deformed walls of micaceous psammite, (Plate 7.9). In severe cases where the boudin necks become very stretched and thinned, the granitoid vein will lose continuity, forming a train of pseudomorphing granitoid boudins, separated by micaceous psammite necks. In areas of



brittle boudinage it is common to see thin, <5cm, undeformed granitoid veins running between the boudins and their hosts, frequently occupying the fractures between the boudins. If granitoid material is plentiful boudins in a train may be completely surrounded by granite. In the intrusion breccias, numerous irregular granitoid veins cut through the matrix and run between the clasts.

Field evidence shows that many granitoid veins postdate boudinage structures, with boudinage structures controlling granitoid vein intrusion. It is possible that boudinage structures developed during veining, but the granitoid veins acted as fluids and were unable to record the deformation.

#### 7.7.3 Late Open Folds.

These folds are spatially related to the Foyers Complex, only occurring close to the complex margin. They are only developed in areas which show strong boudinage or pinch and swell. The open folds (1E- Hudleston, 1973) are seen on Carn Chliabhain, the Central psammite septum, Beinn Bhuraich, Beinn Dubcharaidh and Carn Gairbthinn, of which the Central Psammite Septum shows the strongest fold development. The folds are sporadically developed, symmetrical, and have interlimb angles of  $150^{\circ}$  to  $170^{\circ}$ , (Plate 7.10). They plunge steeply to the north west or south east. The folds in the Central Septum plunge steeply to the south south east. The trace of the fold axial plane on horizontal outcrop surfaces

is frequently perpendicular or sub-perpendicular to the strike of bedding and complex margin. Any one set of folds is seldom composed of more than 2-3 complete wavelengths, and the amplitude of the folds dies rapidly away along the trace of the axial plane.

Boudin trains are often folded by these open folds. The boudins show no internal deformation, as either half wave development or boudin shortening due to simple shear and pure shear, (Sengupta 1983). Occasionally, calc-silicates develop a weak zig-zag pattern around the hinges of open folds, which Sengupta (1983), states is a feature developed by folding rigid boudin trains of high competency contrast to the enclosing rock, (Plate 7.11). Frequently boudins show no obvious rotation out of the plane of bedding on either limb of the open folds, and the fold morphology, defined by the boudins, is similar to, and controlled by, adjacent plastic beds of micaceous psammite. Although the boudin trains are folded around the open folds, suggesting folding after boudinage, angular deviation of the fold limbs from the general bedding strike is small enough to allow boudinage without distinctive boudin rotation.

The origin of these folds is problematical. The orientation of the fold axial plane trace suggests maximum compression is parallel to the strike of bedding and thus parallel to the strike of the Foyers Complex margin. Such a fold pattern could not be developed by simple pluton expansion. A horizontal shear mechanism could form folds in such an orientation, but such folds should be strongly asymmetrical.

The open folds show a strong similarity in both style and shape to the much smaller "folds" in the bedding which are necessarily developed when a bed shows pinch and swell structures. It is possible that the large open folds develop to accommodate large scale pinch and swell, where perhaps large blocks of beds are weakly stretched out, with the folds developing in the more plastic beds.

#### 7.7.4 Shear Structures.

The development of shear structures within the envelope of the Foyers Complex is minimal. Only a small number of localities showed shear structures which enabled the sense of shear to be determined. This may be because the bedding is parallel to the shear zones, which form parallel to the contact strike of the Foyers Complex. It is only where shear zones cross cut bedding lying at an angle to the pluton margin (close to the hinges of D2 asymmetrical folds) that bedding off sets develop, and a sense of shear can be determined. The actual shear zones often have a mobilised appearance, with a discontinuous and streaky reworked bedding fabric lying parallel to the walls of the shear zone, (Plates 7.12 & 7.13). Analysis of 4 shears on the northern margin indicate sinistral movement whilst analysis of 4 shears in the Central psammite septum indicate dextral movement, (Fig.7.20).

In mobilised areas, or where deformation is very intense there are boudins and blocks of coherent rock which show

bedding at a high angle to the bedding in adjacent areas. This degree of rotation,  $>60^{\circ}$ , is far in excess of the rotation associated with formation of en echelon boudin trains. The rotation of these blocks probably requires some form of shearing, which is accommodated within the less competent, often partially mobilised adjacent rocks, (Plate 7.14). There is often very little evidence to indicate which way the boudins or blocks have rotated, as their original position is not known. Where mobilisation is intense, rotation of individual boudins, to lie sub-perpendicular to nearby bedding is quite common, suggesting that shearing was caused by the flow of mobilised material.

#### 7.7.5 Strain Markers.

Within the micaceous psammites and the migmatitic semi-pelites are bedding parallel, amphibolite bodies containing rusty brown spherical garnets ranging from  $<0.5\text{cm}$  to  $>2\text{cm}$  in diameter.

Within the aureole of the Foyers Complex the amphibolites develop a hornfelsic texture and the garnets break down to form fine grained aggregates of plagioclase, biotite and amphibole. Where the garnets are large, replacement is incomplete and the fine grained "spots" contain ragged remnants of garnet. The aggregates pseudomorph the garnets to form spherical "spots". However on a number of occasions these spots form well defined ellipses with long axes running parallel to the bedding foliation and the pluton

margins, (Plate 7.15). As thermal metamorphism is responsible for the garnet break down, and the emplacement of the Foyers Complex is post regional deformation, it is probable the spherical aggregates were deformed into ellipses by deformation associated with granitoid intrusion. As the spots are abundant and have an originally spherical shape they may be used as strain markers to define the local strain ellipse, (Table 7.2), (Appendix D)

The results indicate the strain ellipse for the north east and southern margins of the complex, close to the nose of the fold, show a strongly prolate form, with the X-axis lying sub-parallel to the contact. The amphibolite spots within the central psammite septum have an oblate form with the Z-axis sub-perpendicular to the pluton contact, whilst spots in the envelope of the north eastern part of the complex show only very weak deformation (Fig.7.21).

#### 7.7.6 "D2" Caledonian Folds.

The fold axial planes of D2 folds are sub parallel to the Foyers Complex contact, thus lying in an orientation where the hinge of the folds should tighten up if the Foyers Complex compresses its envelope perpendicular to the contact. Soula (1982) describes how envelope folds tighten up as Pyrenean gneiss domes are approached, and thus define a strain gradient.

The interlimb angles of 90 "D2" folds or fold sets with the correct orientation were measured around the Foyers Complex

(Table 7.3). It is evident that some folds do show tightening, (Plate 7.16), although no clear systematic strain gradient is seen as the pluton is approached (Fig.7.22). It is unclear whether this is due to an actual lack of a strain gradient, or the inability of the folds to reflect strain. It is possible the data set used was not large enough to remove effects of the original interlimb angle heterogeneity.

#### 7.7.7 Pre-Foyers Granitoids- Maol Chnoc.

The minor structures developed in the Maol Chnoc Complex as a result of the emplacement of the Foyers Complex are well documented in Chapter 5.

#### 7.8 FAULTING.

The Foyers Complex is cut by a number of north easterly trending faults which are considered to be part of the late Caledonian suite of faults traversing the Grampian Highlands, (Johnstone, 1966).

The abundance of faults in the Foyers Complex may be due to the proximity of the Great Glen Fault Zone.

The faults displaying the largest displacements of regional psammite formations outside the Foyers Complex, (Highton 1986, and Haselock pers com.) form well defined fault valleys within the Foyers Complex, (Enclosure 1), (Plates

7.17 & 7.18). The major faults include the Gleann Liath Fault, Ault-na-Goire Fault, Loch Mhor Fault pair, and the Conagleann Fault. There are also smaller parallel faults which form less well defined topographical lineations.

Lack of exposure and the irregular nature of igneous contacts in the Foyers Complex prevent accurate determination of fault movements. However, the incomplete field evidence implies displacements of internal igneous boundaries and the external contact of the complex are minor, with displacement of contacts less than several hundred meters. Highton (1986) and Haselock (pers com.) record large displacements in these faults outside the Foyers Complex. Highton states the Loch Mhor Fault sinistrally displaces regional structures by 5km although Haselock states the faults are dominantly normal, with downthrows of several hundred meters to the north west. North east of the Foyers Complex the pre-Foyers Maol Chnoc Complex (described in Chapter 5), is cut by the Conagleann Fault. More of the complex is unroofed south east of the fault than north west of the fault, implying downthrow to the north west. Where the fault cuts the Foyers Complex, field evidence implies sinistral displacement of this contact by less than 150m. Thus the faults cutting the Foyers Complex were most active prior to Granitoid emplacement.



#### 7.8.1 Nature Of The Fault Zones.

Fault zones in the Foyers Complex are till filled, presenting little evidence of their nature. The presence of deep valleys suggests that they are broad shatter belts. The granitoids bordering the fault valleys often show brittle deformation features, which increase in frequency towards the faults. The most common features are reddened micro-cataclasite veins. Close to the faults the veins form rather intense irregular networks. The veins are <2cm in width. Distant from the fault valleys, the veins are more regular, striking east, and dipping steeply south. The veins show very little displacement, with large plagioclase laths remaining undisplaced on either side of the vein. Possibly the comminuted material in the veins formed by a series of elastic shocks rather than finite displacement. In section the veins are finely comminuted granitoid, with coarse epidote, opaques and calcite cross cutting the comminuted material. The veins often show hydrothermal alteration halos where biotite is altered to epidote (Plate 7.19). Granitoid outcrops adjacent to the fault valleys show a slight reddening, stronger sericitisation of the plagioclases, and epidotisation and chloritisation of the biotites. The fault zones and cataclasite veins act as channels for late hydrothermal fluids. The fluids react with plagioclase and biotite forming sericite (Newman, 1987) and chlorite. Excess calcium forms calcite and epidote when combining with iron from biotite. Winkler (1976), states epidote only develops

above 200°C. Garson et al. (1984) state veins containing blue amphiboles cross cut the cataclasite veins. These veins are associated with fenitisation related to the intrusion of a 390ma carbonatite body in the Great Glen area. The author of this thesis saw no evidence of the blue amphibole veins. There are however irregular open fractures close to fault zones which cross cut the cataclasite veins. These fractures show thin coatings of dusty red and specular haematite. Similar fractures and mineral coatings occur in the Old Red Sandstone. It is possible the haematite was deposited by oxidising waters flowing down from the Devonian land surface.

#### 7.8.2 Gleann Liath Fault.

The only fault causing major displacements of the Foyers Complex is the Gleann Liath Fault, (Enclosure 1). The fault forms the north west margin of the Foyers Complex, where the complex abuts against migmatites of uncertain affinity (Mould, 1946, Marston 1971, Eyles and MacGreggor 1972, and Rock et al. 1984 and 1986) and the Dun Garbh granodiorite (Chapter 2). The author feels the pre-Middle Old Red Sandstone rocks between the Gleann Liath fault and Loch Ness are part of a fault slice melange formed in the Great Glen Fault Zone.

The Gleann Liath Fault is not a pre-intrusion fault controlling emplacement of the Foyers Complex. The migmatites north west of the fault show no deformation or

veining typical of the Foyers envelope, the fault cuts internal igneous contacts, and granitoid mineral fabrics are not parallel to the contact.

North of the Gleann Liath Fault there are no large granitoids that may be correlated with the Foyers Complex, excluding the Strontian Granite (Chapter 10). It is improbable the Gleann Liath Fault displaced a large granitoid mass over great distances because 5km north east of the Foyers Complex, displacement along the fault becomes negligible, (Haselock pers com.) and immediately south of the complex evidence of fault displacement is difficult to determine. Although the Gleann Liath Fault does not control the emplacement of the Foyers Complex it is probable the Great Glen Fault Zone formed the north western emplacement margin of the complex, a small distance north west of the Gleann Liath Fault. Hutton (1988), suggests intracrustal strike slip faults act as pathways for granitoid emplacement.

Late movement on the Gleann Liath Fault then displaced the north western boundary of the Foyers Complex. The lack of displacement shown by the Gleann Liath Fault north and south of the complex discounts strike slip movement. Normal faulting with a downthrow to the north west could bring lithologies from well above the roof of the complex to lie adjacent to the complex. The downfaulted lithologies are part of the Great Glen tectonic melange created during large strike slip movements in the Great Glen Fault Zone.

## 7.9 DISCUSSION.

It is evident from the minor structures that the Foyers Complex deformed the rocks in its aureole..

Chocolate block boudinage is the major deformational feature, consistent with an expanding granitoid shortening an aureole containing margin parallel bedding. This form of deformation is described by a number of authors (Bateman, 1985, Barriere, 1977, Pitcher & Berger, 1972), who all attribute boudinage to flattening of the envelope rocks. Quantitative analysis of boudinage shows strain decreases away from the pluton margin, and increases towards the east of the complex.

Many authors show bedding deforms by minor folding to accommodate an expanding granitoid body. Bateman (1985) describes kinking in the aureole of the Cannibal Creek pluton, Soula (1982) describes folds generated by the intrusion of gneiss domes, Brun and Pons (1981) describe minor folds adjacent to plutons in southern Spain, Barriere (1977), describes minor folds adjacent to the Ploumanac'h complex, and Holder (1979) describes fold structures within the aureole of the Ardara pluton, Eire. Boudinage in the Foyers aureole shows shortening did occur but was perpendicular to bedding. This implies that the margins of the Foyers Complex developed parallel to regional bedding. Marston (1967), and Highton (1986) state north easterly trending bedding is rotated into contact parallelism by the intrusion of the Foyers Complex. If this was the case,

aureole shortening should have caused folding. It is probable that the easterly to south south easterly trend of the bedding is determined by a pre-intrusion regional structure, thus any expansion of the Foyers Complex would produce boudinage rather than folding. Alternatively, an early pulse of magma intruding sub horizontally towards the east could rotate the bedding without forming minor folds in the bedding, the beds would then lie in an orientation which could be boudinaged during later pluton expansion. However the lack of rotation displayed by the D3 crenulations precludes the second model.

One of the major lines of evidence for aureole flattening is the formation of a new cleavage or crenulation, produced during the intrusion and expansion of a granitoid pluton. Pitcher & Berger (1972), demonstrate in the Thorr, Ardara, and Main Donegal plutons of Eire a crenulation cleavage develops, overprinting the regional fabric. The fabric is parallel to the pluton margin, and increases in intensity towards the contact. Bateman (1985) describes similar structures around the Cannibal Creek pluton. Courrioux (1987), and Kafafy & Tarling (1982) describe a penetrative cleavage in the aureole of the Criffel granodiorite. In the aureole of the Foyers granitic complex there is no evidence of a mineral foliation related to the intrusion of the complex. This may indicate the deformation was not great enough for a cleavage to develop. Hobbs et al. (1976) state a cleavage develops at >30% tectonic shortening. If expansion of the Foyers Complex was perpendicular to the composite bedding/regional D1 foliation, then any margin

parallel foliation formed during the intrusion of the complex may be masked by the intensity of the coaxial D1 foliation.

The shear structures, prolate metamorphic spots, and the lineations within the Maol Chnoc complex all suggest there was strong sub-horizontal stretching of the margins within the eastern "nose" of the Foyers Complex. The small shear zones indicate the granitoids in the Foyers Complex moved towards the east.

Analysis of minor regional and contact structures in the Foyers aureole indicates the disposition of the minor regional structures is controlled by major regional structures, and the emplacement of the Foyers Complex did not re-orientate these structures. The external morphology of the Foyers Complex is influenced by the strike of the psammite units, and thus by the major regional structures. This conclusion is at odds to the models presented by Highton, (1986), Marston (1967) and Mould (1946), who argued that the forceful emplacement of the Foyers Complex caused large scale crustal rotations.

The regional structural synthesis (Haselock and Leslie (pers. com.) supports the thesis developed in this chapter, that the disposition of the bedding in the vicinity of the Foyers Complex is controlled by regional structures, and intrusion of the Complex did not re-orientate regional structures.

CHAPTER 8. PETROLOGY AND CONTACT METAMORPHISM OF THE  
ENVELOPE ROCKS.



## CHAPTER 8. PETROLOGY AND CONTACT METAMORPHISM OF THE ENVELOPE ROCKS.

### 8.1 INTRODUCTION.

It has proved difficult to map out distinct thermal metamorphic zones in the envelope of the Foyers Complex as a result of the psammitic nature of the rocks. However previous workers have reported the presence of cordierite, sillimanite and andalusite in the aureole, (Mould, 1946 and Marston, 1971).

Tyler and Ashworth (1983), identified an inner and outer aureole in the northern envelope of the complex. The inner aureole, several 100m wide, is characterised by the presence of cordierite, whilst the outer aureole 3-4km wide is characterised by loss of regional garnet and muscovite, and the growth of new sillimanite, biotite, garnet and orthoclase. These authors calculated temperatures of  $678^{\circ}\text{C}$  and  $654^{\circ}\text{C}$  for the inner aureole using Fe-Mg exchange equilibria in garnet and biotite, and garnet and cordierite respectively. Using the Holdaway and Lee (1977), method for garnet and cordierite they derived a lithostatic pressure of 3.9Kb and a water activity of 0.15. This compares with 1.5-2.0Kb estimated by Marston (1971) who used the andalusite-sillimanite inversion curve of Fyfe (1967), and Turner (1968). Highton (1986), also studying only the northern envelope recognised Foyer's contact metamorphism

overprinted an early thermal event associated with the intrusion of the Maol Chnoc Complex. He defined an outer sillimanite and alkali feldspar zone, and an inner alkali feldspar and cordierite zone, (Fig.8.1). He quotes pressure temperature conditions of 3.9 Kb and 650°C for the northern envelope of the Foyers Complex. The present study concentrates on conditions in the inner aureole, particularly the Central Psammite Septum, parts of the southern margin and psammite rafts in the granite where, unlike the northern margin, there is anatectic psammite mobilisation. These areas have the advantage of being well away from the influence of the Maol Chnoc Complex.

## 8.2 PETROGRAPHY.

Of the aureole rocks, the micaceous psammites shows the greatest diversity and abundance of index metamorphic minerals due to their heterogenous nature, although the development of metamorphic index minerals is limited to the more pelitic beds.

All the aureole rocks collected and analysed from the southern margin, the Central Psammite Septum and xenoliths fall within the cordierite and K-feldspar inner aureole, defined in the northern aureole by Tyler and Ashworth (1983), and Highton (1986). Authors including Haselock (1982), Tyler and Ashworth (1983), and Highton (1986), give detailed descriptions of the same rock formations outside the aureole, and the changes that occur as the inner aureole

is approached. The structure and lithology of the rock formations inside and outside the aureole are very similar, presenting no problems with correlation.

#### 8.2.1 Micaceous Psammite.

In the inner aureole the micaceous psammite retains its well defined bedding, S1, S2 and S3 fabrics, and shows no tendency at outcrop to become a massive or splintery.

Most micaceous psammite samples were collected from beds which showed either garnet or sillimanite. Samples not showing a rich metamorphic mineral assemblage in the field seldom showed metamorphic minerals in thin section.

All beds from the micaceous psammite have a mineralogy of plagioclase, quartz, biotite, ilmenite and zircon. The more pelitic beds may additionally contain sillimanite +- andalusite +- cordierite +- garnet +- K-feldspar +- tourmaline +- apatite and retrogressive muscovite.

Plagioclase is subidioblastic, forming grains 0.1-0.6mm in diameter. In most samples the plagioclase grains are equant, but in biotite poor samples, the plagioclase may form a very poorly developed polygonal granoblastic texture with quartz. Where the S1 regional fabric is strongly defined by biotite and quartz, the plagioclase may show a weak alignment parallel to this fabric.

Quartz occurs in a number of forms, the most frequent is a xenoblastic, granoblastic mosaic of crystals <0.3mm in diameter. Where biotite is scarce the quartz forms large,

<3mm, unstrained, xenoblastic grains, which enclose biotite and plagioclase, (Plate 8.1). This large scale loss of grain boundaries is suggestive of sustained high temperature annealing. The presence of parallel biotite boundaries in the more pelitic areas impedes the removal of the quartz grain boundaries, and the quartz grains remain small. Quartz infrequently displays a weak polygonal granoblastic textures.

Alkali feldspar is a minor phase, often revealed by the presence of myrmekite. It occurs in 60% of the micaceous psammite slides, particularly associated with layers rich in biotite, sillimanite and/or cordierite.

Fox-red to straw-yellow biotite is common, and contains numerous zircons. The biotite is concentrated in narrow, <2mm, pelitic domains, often with aluminosilicates, cordierite and ilmenite. These domains define the S1 fabric, (Plate 8.2) The biotite plates lie parallel to these domains, although the larger biotite plates may lie at high angles, suggesting crystallisation after the D1 deformation. Biotite defines S3 crenulations but is not deformed around their hinges, lying tangentially and suggesting that these are new aureole biotites whose position and orientation are controlled by the old regional biotite fabric.

Sillimanite is the most abundant contact metamorphic index mineral, and occurs as large, (<1cm) prisms, fibrolite, and small needles <2mm in length, the latter habit being most common. The sillimanite occurs preferentially in the pelitic domains, and in slides that contain K-feldspar. Sillimanite needles frequently lie parallel to the biotite laths, and

the strike of the pelitic domains, although sillimanite cross cuts the biotite fabric. The biotite and sillimanite are very closely associated, with sillimanite penetrating and perhaps replacing biotite flakes, (Plate 8.3). Where biotite shows no preferred alignment neither does the sillimanite, suggesting the orientation of the biotite controls the direction of sillimanite growth. This is particularly well developed where an S3 crenulation is seen, and an epitaxial relationship develops between 001 biotite faces and the z axis of sillimanite needles. At the crenulation hinge the sillimanite needles lie tangentially to the curve of the hinge, with needles on either limb cross cutting each other at the hinge, somewhat akin to a teepee. However many sillimanite needles may be seen cross cutting these S3 hinges, (Plate 8.4). Where sillimanite forms large fascicular aggregates it often encloses granular opaques within the needle meshwork, (Plate 8.5).

The abundant sillimanite is probably of contact, rather than regional origin. Winchester (1974, 1981), states minor regional sillimanite may be found north of Foyers, and south of Foyers the metamorphic zone index mineral is almandine garnet. Wells, (1979, 1981) states the regional aluminosilicate to the north and south of the Foyers Complex is kyanite, and that any minor sillimanite present formed as a result of either retrogression during rapid crustal uplift at the end of the Caledonian, or the high geothermal gradient associated with large volumes of Newer Granites intruded into the Central Highlands. Highton (1986), reports minor fibrolite to the north of the Foyers aureole, although

the dominant aluminosilicate is kyanite. Winchester and Whittles (1979), state that peak metamorphism in the Central Highlands pre dated D3 deformation.

As sillimanite cross cuts S1 and S3 fabrics in the Foyers aureole, the sillimanite must post date these fabrics and the regional aluminosilicate assemblage is kyanite or very minor sillimanite after kyanite it appears aureole sillimanite was generated during contact metamorphism.

Andalusite occurs in the inner aureole, within the pelitic domains containing K-feldspar. It occurs as relatively large <2mm grains, of idioblastic to sub-xenoblastic habit, indicative of rather slow sustained growth. In psammite screens close to Loch Kemp andalusite forms randomly orientated prisms several centimeters long.

Andalusite may show rose pink pleochroism, and is frequently partially or totally pseudomorphed by sillimanite having a common z axis, (Plate 8.6), suggesting andalusite is not in thermodynamic equilibrium, (Plate 8.7).

Cordierite occurs in the more pelitic rocks, and is intimately associated with biotite. Large anhedral aggregates of cordierite, develop very irregular contacts with biotite, the cordierite often embaying, and infrequently replacing the biotite, the biotite forming ragged scraps within the cordierite aggregate, (Plate 8.8). Frequently, fabric defining biotite ribbons show narrow cordierite rims, (Plate 8.9). This association of biotite with cordierite suggests biotite plays an important role in cordierite generation. Cordierite also forms discrete xenoblastic grains, often partially or completely enclosing

quartz grains, or as subidioblastic porphyroblasts. One slide shows cordierite growing within the interstices of a skeletal garnet, (Plate 8.10).

Pale mauve garnets are sparsely developed within more pelitic micaceous psammite, although they occur in equal numbers within the pelitic or felsic lithons of individual samples. Garnets have a skeletal xenoblastic to sub-xenoblastic habit with inclusions of biotite, quartz and plagioclase in proportions similar to the remainder of the slide, although some skeletal garnets may contain numerous opaque inclusions. Garnets lack rim reaction textures, and aureole garnets and biotite aggregates pseudomorph large early garnets implying the garnets present are new aureole garnets, not regional garnets, (Plate 8.11). Highton (1986), Tyler and Ashworth, (1983), and the data in section 8.4.1, (this thesis), show that garnets from the inner aureole show no geochemical evidence of a relict regional core, and are true new aureole garnets.

#### 8.2.2 Pebbly Psammites.

In the Foyers aureole, and in large rafts, the pebbly psammite retains its bedding, regional fabrics, and sedimentary structures. Only within small rafts <3m diameter does the pebbly psammite begin to lose its structure to form a grey, splintery and slightly "flinty" hornfels.

The pebbly psammites show few new minerals which may be used to indicate metamorphic conditions in the inner



aureole, and the mineralogy is constrained to approximately plagioclase (24%), quartz (45%), alkali feldspar (18%), biotite (10%), and (3%) magnetite, aluminosilicates, zircon, apatite, zircon and sphene, often concentrated in heavy mineral bands.

Plagioclase forms subidioblastic grains in the matrix fraction of the pebbly psammites. The matrix grain size ranges from 0.05-0.3mm.

Quartz occurs as both matrix and pebbles. Matrix quartz varies from a fine grained, well developed granoblastic polygonal texture, (Plate 8.12), sometimes capturing fine grained biotite within the polygonal framework, to large xenoblastic grains enclosing other minerals. Polygonal hornfelsic textures are only well developed within small rafts. Where biotite is abundant development of polygonal and xenoblastic quartz textures are inhibited by biotite grains interfering with the migration and loss of quartz grain boundaries.

K-feldspar occurs in the matrix and clast fractions, but dominantly as clasts. In the matrix K-feldspar forms small xenoblastic grains often revealed by the presence of myrmekite. The K-feldspar clasts are subidioblastic-xenoblastic. As there are rarely inclusions within the body of K-feldspar clasts, it suggests enclosure of matrix by K-feldspar did not occur, and the clast did not grow during porphyroblastesis, as mooted by Marston (1967).

Biotite defines a parallel fabric. It is a straw yellow-olive green colour, which Haselock (1984), states is a regional feature of the Glenshirra subgroup resulting from

the high oxidation state of iron in the biotites. Pebbly psammite biotites do not hold the numerous zircons present in micaceous psammite biotite. Biotite is often associated with heavy mineral concentrations, of which subidioblastic magnetite forms the major phase.

Aluminosilicates include sillimanite and andalusite, the latter frequently replacing the former. They occur in pelitic layers, although sillimanite seams may form in felsic areas, perhaps sites of sedimentary or diagenetic kaolinite.

Quartzites are common in the pebbly psammite formation, containing up to 90% quartz, and minor biotite, muscovite, K-feldspar and plagioclase. The quartz forms large xenoblastic unstrained grains, often enclosing biotite, plagioclase and K-feldspar grains.

#### 8.2.3 Retrogressive Muscovite.

Muscovite occurs in all the psammites, being particularly abundant in the pebbly psammites.

Regional muscovite is described as porphyroblastic by Ashworth and Tyler (1983), and this is removed by aureole reactions. The muscovite in the aureole occurs as laths, and as replacements of aluminosilicates.

As discrete grains the muscovite is found as euhedral flakes within the biotite rich layers, lying parallel to, or cross cutting the biotite fabric.

Muscovite may form jackets around sillimanite and

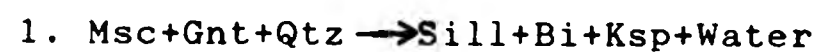
andalusite grains, (Plate 8.13) and in one slide partially pseudomorphs cordierite.

As muscovite replaces aluminosilicates and has a different habit to the regional muscovite it is probably retrogressive. The most intense development of muscovite comes from micaceous psammite screens within the Foyers Complex. This may be due to a sustained cooling period within the pluton, or localised metasomatic effects.

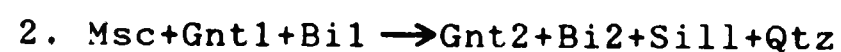
### 8.3 MINERAL TEXTURES AND INTERPRETATION OF THE MINERAL ASSEMBLAGES.

Tyler and Ashworth (1983) and Highton (1986) produced accounts of metamorphic reactions involved in the formation of a contact aureole around the Foyers Granitic Complex (Fig.1.1).

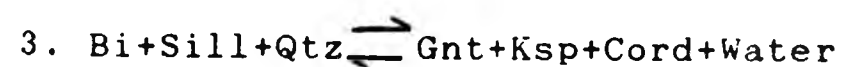
Outer aureole reactions are summarised below;



which includes the reaction,



The development of the inner aureole is summarised by the reaction;



Further to the general petrography there are a number of textures important for interpretation of the mineral assemblages, and for establishing the viability of the reactions presented above.

The mineral phases in the inner aureole are approximately equidimensional, suggesting the inner aureole reached textural equilibrium. Biotite does not bend around the F3 crenulation hinges, suggesting it is aureole rather than regional biotite. It is often intimately intergrown with sillimanite but it is not clear from the texture whether this is epitaxial growth of sillimanite on biotite, (Chinner, 1961), the co-formation of aureole biotite and sillimanite, or the replacement of biotite by sillimanite as suggested by Chinner (1966). Co-formation of sillimanite and biotite could result from reaction 1, whilst replacement of biotite results from reaction 2. Fascicular mats of sillimanite contain opaque ore granules which may be relicts of the complete replacement of biotite by sillimanite. Shelly, (1968), states biotite is broken down in the presence of excess quartz to form sillimanite, alkali feldspar, water and magnetite granules. Where sillimanite is aligned parallel to the biotite defining the F1 regional fabric it is possible the texture is derived from either reaction 1 or 2.

Garnet accompanied by biotite may pseudomorph regional garnet, a condition possibly generated by reaction 2. Cordierite often replaces biotite, as predicted by reaction 3. The association of cordierite with scraps of aureole

garnet in the pseudomorph of a regional garnet may be explained by reaction 2 generating aureole garnet and biotite from regional garnet, followed by reaction 3 generating cordierite from the biotite, thus giving an aureole garnet/cordierite pseudomorph.

It is evident that reactions, proposed by Tyler and Ashworth (op.cit.), are compatible with textures and mineralogy seen in the inner aureole. As all the samples are from the inner aureole, it is difficult to determine whether each texture is the result of a particular reaction. To determine which reaction is responsible for a particular texture it is necessary to trace one particular texture out through the aureole into lower temperature regimes, where changes in the relative abundance of the mineral phases involved in the texture would allow the identification of reactants and products. The lack of a suitable lithology, with a very similar bulk chemistry, occupying both the inner and outer Foyers aureole, prevented a study of texture development.

#### 8.3.1 Andalusite/Sillimanite.

The aureole of the Foyers Complex contains both andalusite and sillimanite. The andalusite forms porphyroblasts and the sillimanite shows a close association with biotite. Only in the inner aureole are andalusite porphyroblasts partially replaced by sillimanite needles (Fig.8.1). Highton (1986) observed andalusite and sillimanite in the outer Foyers aureole, but never as one replacing the other, which

suggests it requires higher thermal energy to reconstitute andalusite into sillimanite, than it does to generate new sillimanite.

The sillimanite and andalusite in the Foyers aureole may be created by different reactions at different stages in the evolution of the aureole, alternatively it is possible the inner aureole is on the boundary of the andalusite and sillimanite stability fields, implying, (using the stability fields proposed by Ehlers *et al.* (1980)- compiled from numerous data sources), that the PT estimates (Tyler and Ashworth 1983), and (Highton 1986), are erroneous. However anatectic migmatisation in the inner aureole needs a temperature of 680°C or above (Chapter 6) and the aureole pressure would have to be in the order of 1Kb to fall on the sillimanite/andalusite field boundary. This is much lower than the 3.9Kb determined by Tyler and Ashworth (1983).

It is more likely that andalusite is strongly metastable in the sillimanite field. Winkler (1976), accepts the metastability of aluminium silicate polymorphs, but states a polymorph can only be generated in its own stability field.

It appears that in the Foyers aureole, PT conditions were such that first andalusite and then sillimanite were the stable phases. This is not unusual because contact aureoles often prograde through the andalusite field to reach the sillimanite stability field. It is unusual that both minerals are preserved, because normally andalusite is totally replaced by sillimanite, or rapid aureole heating does not allow andalusite the time to crystallise.

The presence of andalusite porphyroblasts in the Foyers

aureole indicates either andalusite forming conditions were maintained in the aureole for an extended period of time or the andalusite grains are large because they are replacing a regional porphyroblastic mineral. Coarse sillimanite and the total equilibration of garnets (see later in chapter) suggest later sillimanite grade metamorphism also occurred over an extended time span.

Thus the coarse habit of both aluminosilicates suggest the Foyers aureole may have experienced prolonged metamorphism at andalusite grade which prograded to an extended period of metamorphism at sillimanite grade.

As the replacement of andalusite by sillimanite is seen all around the Foyers Complex, the aureole conditions which promoted andalusite and then sillimanite stability cannot be related to the intrusion of Errogie Quartz Diorite and then Dalcrag Granodiorite magma pulses, which have different geographical distributions.

Andalusite and sillimanite define an aureole of similar morphology and extent all around the complex, suggesting the Foyers Complex formed both aluminosilicates.

The extra heat needed to transform the Foyers aureole from the andalusite stability field to the conditions estimated by Tyler and Ashworth (1983) would require an increase in temperature of approximately 150°C. A change from a non convecting to a convecting granitoid would increase the heat flow into the envelope, but convection in magmas normally decreases after emplacement.

It would be more realistic to develop a model with only one phase of aureole heating where andalusite is metastable in



the sillimanite field. When the Foyers Complex is initially emplaced andalusite is formed, perhaps involving the conversion of regional muscovite porphyroblasts (Highton 1986) to andalusite porphyroblasts. As the envelope rocks continue to heat up the temperature conditions in the aureole move well within the sillimanite stability field, and sillimanite is generated by breakdown of regional biotite. In the outer aureole the temperature is too low to initiate the conversion of andalusite porphyroblasts to sillimanite. However in the inner aureole there is enough energy to partially break down the andalusite structure and reconstitute it as sillimanite. This produces a texture of sillimanite replacing andalusite.

#### 8.4 MINERAL GEOCHEMISTRY.

Minerals from three slides from the inner aureole of the Foyers Complex were analysed using the electron microprobe. Two slides 2210 and 2300 are of micaceous psammite from the Central Psammite Septum, whilst slide 2735 comes from a micaceous layer within the pebbly psammites to the southwest of Loch Kemp. The minerals biotite, garnet, cordierite, plagioclase and ilmenite were analysed. The complete analyses are displayed in Appendix E, although mean compositions are displayed in (Table 8.1).

The data supplements data from the northern margin provided by Highton (1986), and Tyler and Ashworth (1983).

#### 8.4.1 Garnet.

The garnets are within the almandine series (Deer et al., 1983) They were analysed as single random points, and as traverses from rim to core. The traverses reveal the garnets from slides 2210 and 2300 are unzoned and have no relict core, as reported by Tyler and Ashworth for garnets in the outer aureole, (Fig.8.2). Only in the very outer rim is there very minor loss of calcium and a slight increase in manganese, features possibly related to late retrogressive reactions. (Loomis 1975). Regional garnets are zoned and have a significantly higher calcium content and lower manganese content than those of the inner aureole (Highton, 1986 and Tyler and Ashworth, 1983). The inner aureole garnets are therefore either new garnets or regional garnets in total chemical equilibration with the conditions in the inner aureole. As the inner aureole garnets show textural equilibration with the matrix and Highton (1986), reports regional garnet breaking down to plagioclase and biotite in the outer aureole, it is more likely that the inner aureole garnets are new. The garnets from slide 2735 have a distinctly different chemistry to those in slides 2210 and 2300 (Fig.8.3). They have a reduced iron content, increased manganese content, and show up to twice the calcium content. As this slide is from within the pebbly psammite, a unit with a geochemistry greatly different to that of the micaceous psammite (Haselock, 1984), it is probably the original bulk chemistry of the rocks causing the geochemical

differences.

#### 8.4.2 Biotite.

Analyses of biotite (Table 8.1) show it lies between eastonite and siderophyllite. Plotted upon an AFM projection (Fig.8.4a) the points are strongly clustered suggesting little compositional variation. In contrast to Highton (1986) different populations of biotite could not be geochemically distinguished. Biotites from slide 2735 are very similar to those in the micaceous psammite slides, although do show weak depletions in titanium and aluminium and weak enrichment in manganese and magnesium.

#### 8.4.3 Cordierite.

Only fresh unpinnitised cordierite was analysed, which showed no compositional zoning and a limited compositional range as illustrated by the tight clustering of points on the AFM plot, (Fig.8.4a).

#### 8.4.4 Plagioclase.

The composition of plagioclase is displayed in Table 8.1, where a composition of An<sub>32</sub> (andesine) is indicated. Zoning in the plagioclase is minimal.

#### 8.4.5 Ilmenite.

All the opaques analysed were ilmenite, as shown in Table 8.1.

#### 8.4.6 Geothermometry And Geobarometry.

The biotite, cordierite and garnet analyses above were used to estimate the temperature and pressure of the Foyers aureole during emplacement. Previous estimates by Tyler and Ashworth (1983) and Highton (1986) placed inner aureole conditions in the northern envelope at 650-678°C and 3.9 Kb.

The mean compositions of biotite, cordierite and garnet cores from samples 2210 and 2300 were used to estimate the conditions in the Central psammite Septum. Temperature was estimated by the method of Thompson (1976), using the Fe-Mg exchange equilibria between garnet and biotite and garnet and cordierite. Pressure was estimated by the method of Holdaway and Lee (1977), using Fe-Mg exchange equilibria in garnet and cordierite.

The results are,

Garnet/Biotite 653°C (Thompson, 1976)

Garnet/Cordierite 660°C (Thompson, 1976)

Garnet/Cordierite 4.0 Kb (Holdaway and Lees, 1977).

These results show metamorphic conditions recorded by the Fe-Mg exchange equilibria in the Central Psammite Septum are very similar to the conditions on the northern margin, established by Highton (1986) and Tyler and Ashworth (1983).

As metamorphic conditions were no more intense in the Central Psammite Septum than on the northern margin, differing metamorphic conditions (recorded by Fe-Mg equilibria) do not explain why the Central Psammite Septum shows psammite mobilisation but the northern aureole does not.

#### 8.5 THE RELATIONSHIP OF AUREOLE DEFORMATION TO METAMORPHIC FABRICS.

The mineral fabrics in pluton aureoles are used by many authors to determine the relationships between new aureole mineral growth and contact aureole or regional deformation. Fabrics used include, deformed contact metamorphic minerals and the growth of new minerals producing new cleavages and lineations, for example (Pitcher & Berger 1972, Barriere 1977, Holder 1979, Coward, 1981, Bateman 1984, Castro, 1987). Most authors state aureole cleavages and lineations are developed within the aureoles of plutons emplaced as diapirs, for example, Coward (1981), Bateman (1984 & 1985), Castro (1986).

The development of margin parallel contact cleavages, lineations and the deformation of contact minerals requires

the granitoid to develop a thermal aureole during or before deformation of the envelope. Granitoid emplacement mechanisms such as dyking, stoping, cauldron subsidence or intrusion into spaces created by syn intrusion tectonism do not involve envelope deformation, and as such any new mineral growth should be random and undeformed, with no new cleavages or lineations.

As described in Chapter 7, there are no foliations or lineations visible in the field, that can be related to intrusion of the Foyers Complex and subsequent deformation of the envelope. This is also true in thin section where the biotite defines the S1 or S3 regional fabrics, and sillimanite has an epitaxial or a random orientation to the biotite. Cordierite and andalusite have random orientations or hold positions controlled by the orientations of regional fabrics.

None of the new aureole minerals in the Foyers envelope show any deformation, either as kinking, folding, boudinage or recrystallisation into a new orientation.

Many quartz grains in the envelope of the Foyers Complex are large, xenoblastic, unstrained, and enclose other mineral species, a feature not described by authors studying the regional rocks. Their enclosing nature suggests grain boundary loss during a lengthy period of annealing. The lack of deformation or preferred orientation shown by the contact minerals and quartz porphyroblasts implies the Foyers aureole was tectonically static during the growth of new aureole minerals and fabrics.

The lack of deformation is critical in discounting the

diapiric or ballooning mechanisms of granitoid emplacement, (Bateman, 1984). However field evidence in the form of boudinage, shearing, and deformation of metamorphic spots in amphibolites indicates envelope deformation did occur although probably the strain in the envelope was rather weak, and deformation was concentrated along bedding planes, thus giving rise to boudinage (Chapter 7). Strain was too weak to develop new penetrative fabrics that would define new aureole cleavages, lineations or show synkinematic metamorphic mineral growth.

If the majority of the Foyers Complex was emplaced within a short, time span it is possible envelope deformation was limited to early stages of granitoid intrusion. As the Foyers Complex was dominantly magmatic, at least during emplacement, it probably maintained a high temperature for an extended period of time, as suggested by the lack of a contact chill in the Foyers Complex. The large amount of heat transferred to the aureole as the complex crystallised from a magma, and the length of time this could take, would enable a static aureole to develop, overprinting any mineral fabrics associated with early envelope deformation. The development of andalusite and then sillimanite implies peak metamorphism did not occur during magma emplacement.

Thus petrofabrics in the Foyers envelope suggest the aureole was dominantly static and thus granitoid intrusion was not dominated by diapirism or ballooning. Some expansion of the granitoid did occur, either during early structural development of the Foyers granite, or was rather weak and restricted to heterogeneities in the envelope.



CHAPTER 9. THE EFFECTS OF DENSITY ON THE EMPLACEMENT OF THE  
FOYERS COMPLEX.

## CHAPTER 9. THE EFFECTS OF DENSITY ON THE EMPLACEMENT OF THE FOYERS COMPLEX.

### 9.1 INTRODUCTION.

Granite workers believe the major force causing granitoid magma ascent is gravity. The magma is less dense than its host, gravitational instability occurs, and the magma rises through the crust. (Dixon 1975, Ramberg 1981). If a magma body,, isolated from its source, becomes denser than the surrounding crust it will stop rising. However, the density contrast of a magma body still in connection with its source, includes the effects of the density contrast between the source and host. Rheological and structural factors may also arrest magma ascent.

Studying the density evolution of the Foyers Complex may indicate the rheological state of the complex when it became denser than the country rocks, and thus reached its emplacement position.

### 9.2 DETERMINATION OF ROCK DENSITIES AT 15°C.

The densities of different granitoid and envelope lithologies were calculated by weighing samples in air and water at 15°C. The density of an alpha quartz crystal was measured as a standard. All samples were fresh and clean.

The densities obtained for different lithologies are displayed in (Table 9.1). The results show the Errogie Quartz Diorite is considerably denser than envelope rocks at 15°C. Thus to be emplaced as an isolated granitoid body by gravitational forces, the Errogie Quartz Diorite must have had a lower density, indicating emplacement as a partial melt.

### 9.3 DENSITIES OF PLUTON AND AUREOLE ROCKS AT EMPLACEMENT TEMPERATURES AND PRESSURES.

The density of an entirely molten igneous rock can be calculated using the equation presented by Bottinga & Weill (1970).

$$\rho = \sum_i (X_i \cdot M_i / X_i \cdot \bar{V}_i)$$

where:

$M_i$  mole fraction of component.

$X_i$  gram formula weight of component.

$V_i$  partial molar volume of component

The mole fraction of each component was calculated using the geochemical composition of Errogie Quartz Diorite, (Appendix A).

The melt densities of three Errogie Quartz Diorite samples were calculated using the above equation, giving a mean magma density of 2.543g at 1000°C. 1000°C is the temperature

that quartz diorite will completely melt (Piwinski 1968). The effect of pressure is ignored because: i) liquids are only slightly compressible, ii) there are no data available for the compressibility of silicate melts in the region of 3.9 Kb, the lithostatic pressure at the time of Foyers emplacement. (Tyler & Ashworth 1983).

The calculated density of quartz diorite melt must be compared with the density of the country rocks within the inner aureole at a temperature of 654°C and 3.9Kb. (Tyler & Ashworth 1983). Densities were recalculated to aureole temperature and pressure for all the major rock types within the aureole, taking into account the effects thermal expansion and compressability will have on the density of minerals within each lithology. Data source Clarke Jr. (1966). Mineralogies of the country rocks are displayed in (Table 9.2).

The aureole densities of these rocks at 3.9Kb and 654°C are:

Quartzite	2.425g/cm <sup>3</sup>
Pebbly Psammite	2.606g/cm <sup>3</sup>
Micaceous Psammite	2.632g/cm <sup>3</sup>
Semi-pelite	2.720g/cm <sup>3</sup>

The lithological composition of the Foyers aureole is estimated at; 42% micaceous psammite, 32% pebbly psammite, 11% quartzite and 15% semi-pelite, giving a mean envelope density of 2.61g/cm<sup>3</sup> at aureole temperatures and pressures.

Totally molten Errogie Quartz Diorite (D=2.543 g/cm<sup>3</sup>) is theoretically capable of ascending through the crust

( $D=2.61\text{g/cm}^3$ ) by bouyancy. It is necessary to calculate the point in the magma's solidification history where it became denser than the country rocks.

The density of the Errogie Quartz Diorite when it first totally solidifies is calculated. Pwinski, (1973) showed quartz diorites solidify completely at  $680^\circ\text{C}$ , so the density of a totally solid quartz diorite was calculated at a temperature of  $680^\circ\text{C}$  and a pressure of 3.9Kb. A modal mineral composition of Errogie Quartz Diorite was calculated from 10 point counted thin sections giving a mean Errogie Quartz Diorite mineralogy. The thermal expansion, and the compressibility were calculated for each mineral species at  $680^\circ\text{C}$  and 3.9Kb. using data from Clarke Jr.(1967), showing that Errogie Quartz Diorite with a density of  $2.775\text{g/cm}^3$  at room temperature and pressure has a density of  $2.74\text{g/cm}^3$  as a solid at  $680^\circ\text{C}$  and 3.9Kb.

The densities of entirely molten Errogie Quartz Diorite, and solid Errogie Quartz Diorite at  $680^\circ\text{C}$  and 3.9Kb were plotted against temperature (Fig.9.1). The line between the two points represents the approximate increase in density as the magma cools and crystallises to a solid body, provided the solids remain in suspension. This graph ignores the effects fractional crystallisation would have on density evolution.

The constant gradient slope in (Fig.9.1) shows Errogie Quartz Diorite reached the same density as the crust, ( $2.609\text{g/cm}^3$ ), when it had cooled to a temperature of  $872^\circ\text{C}$ . At this temperature the pluton should stop rising.

#### 9.4 DENSITY EVOLUTION OF A CRYSTALLISING MAGMA.

A more accurate representation of density change in a cooling pluton would include the effects of fractional crystallisation. The difference between the constant gradient and curved slopes in (Fig.9.1) is controlled by the ratio of melt to solid in the magma, and the density increase in each mineral species as it changes from liquid to solid state. This density change is represented by the equation.

$$P_X = \text{No. mineral components} \cdot \left( \frac{\% \text{ solid in melt}}{100} \cdot \frac{\% \text{ increase mineral}}{100} \cdot P_Y \right) + P_Y$$

i = single mineral species,  $P_X$  = new melt density,  $P_Y$  = original melt density

To calculate the density of the pluton at a specific temperature it is necessary to know:

- i) The density of each mineral species in its molten and solid state.
- ii) The proportion of melt to solid for each mineral species.
- iii) The proportion of each mineral species in the pluton.

To calculate the proportion of solid to melt, a crystallisation history for the Errogie Quartz Diorite was developed using textural criteria seen in petrographical work, and textural data presented by Highton (1986) (Fig.9.2). In experimental melting of quartz diorite,

Pwinski (1973), showed that at 3.9Kb, hornblende, plagioclase, biotite and quartz begin to crystallise at specific temperatures. Combining the crystallisation history of the Errogie Quartz Diorite with the data of Pwinski, (1973) it was possible to estimate the crystal content (species and volume) of the Errogie Quartz Diorite at temperatures when a particular mineral species will first appear in the melt.(Table 9.3).

The equation of Bottinga & Weill (1970) allows calculation of the density of molten minerals at specific temperatures. The chemical compositions of each mineral species, which are applied to the equation, were taken from microprobe data presented by Highton (1986).

Density data for solid minerals at room temperature and pressure were taken from Deer et al. (1983), recalculated for the correct temperature and pressure using thermal expansion and compressibility data from Clarke (1967). The composition of each mineral species (Highton, 1986) was taken into account when selecting the densities from Deer et al.(1983)

The densities of the different mineral species are illustrated in (Table 9.4). Employing the equation presented above it is possible to calculate the new densities of the Errogie Quartz Diorite at differing temperatures.(Table 9.5). The temperatures used are those marking the appearance of a new mineral species in the melt, whichs marks a specific crystal content in the magma (Pwinski, 1973).

The new densities are plotted in (Fig.9.1) and form a



curve. The graph indicates the pluton reached the same density as the country rock when it had cooled to  $857^{\circ}\text{C}$ ,  $48^{\circ}\text{C}$  lower than indicated by the straight line slope. If the percentage of solids in the magma are plotted for the temperature when new mineral species begin to crystallise (Table 9.5), the pluton should reach a density equilibrium when the magma contained 18% solids.

#### 9.5 DENSITY OF DALCRAG GRANODIORITE.

The Dalcrag Granodiorite was treated to the same modelling processes as the Errogie Quartz Diorite.

Three Dalcrag Granodiorite samples were analysed, and using the equation of Bottinga and Weill (1970), the density of fully molten Dalcrag Granodiorite was calculated to be  $2.469\text{g/cm}^3$  at a temperature of  $900^{\circ}\text{C}$ . Pwinski (1967), states granodiorite will become solid at  $680^{\circ}\text{C}$  under a pressure of  $3.9\text{Kb}$ . Using the modal mineral proportions from point counted slides the density of solid Dalcrag Granodiorite under these conditions was calculated to be  $2.649\text{g/cm}^3$ .

The crystallisation state of the granodiorite at various temperatures was estimated by combining the melting experiments of Pwinski (1967) with the crystallisation history estimated from mineral textures and the data presented by Highton (1986), (Fig. 9.2). However, the textural criteria did not allow an accurate estimate of the proportions of each crystalline mineral species, present at the temperatures which Pwinski (1967) states a new mineral

species begin to crystallise. Because the composition (crystal:melt), of the magma is not accurately known at specific temperatures, the density changes along the fractionation pathway, shown in Figure 9.1 are probably inaccurate. The density change pathway chosen to represent nature, is one lying mid way between the curved slope influenced by differentiation, and the constant gradient slope connecting the density values when the granitoid is fully solid and fully liquid (Fig.9.1).

The solid content, (vol.%), of the magma was also calculated at different temperatures and plotted onto the graph (Fig.9.1), showing Dalcrag Granodiorite magma attained the same density as the crustal rocks at 725°C with a suspended crystal content of 50%.

Calculating the density evolution of the whole pluton, (the combined densities of the Erroglie Quartz Diorite and Dalcrag Granodiorite), is not viable because the Dalcrag Granodiorite and Erroglie Quartz Diorite were spatially and temporally intruded as separate units.

#### 9.6 EFFECTS OF DENSITY ON EMPLACEMENT MODELS.

From the previous calculations, it is apparent each lithology reached density equilibrium with the adjacent crust when they had a high melt content and thus the Foyers Complex was intruded in a fluid state.

In the envelope of the Foyers Complex there is evidence for deformation (Chapter 7), possibly caused by expansion of the

complex. The development of a ballooning pluton (Ramsay 1981), is dependent upon a density contrast between the pluton and country rock, producing a bouyancy effect. When the magma reaches a limiting height in the crust, the ascent of bouyant magma into the body of the pluton causes lateral spreading of the pluton and subsequent aureole deformation.

Castro, (1987) using the work of Marsh, (1982) states that a body with a density contrast of  $1\text{g/cm}^3$  is not sufficiently bouyant to deform its aureole. As the Errogie Quartz Diorite, when fully molten, has a density contrast of  $0.07\text{g/cm}^3$  it is doubtful that the Errogie Quartz Diorite would be bpuyant enough to deform its envelope and create room by dilational processes. However ballooning is thought to be a relatively minor, late emplacement mechanism in the Foyers Complex, with most of the granitoid material replacing the country rock via sheeting and stoping.

Ascent of magma from depth via fracture systems, as indicated by Shaw (1980), Bateman (1984) and Castro (1987) is the favoured mechanism. The fracturing related to the Great Glen Fault would provide the ideal medium for magma to rise through a dyke system. The magma (if isolated from source) should not rise once 18% crystallinity is reached. When the Errogie Quartz Diorite magma reached this density equilibrium, dyking and stoping by the magma ceased, and collection of the magma in an upper reservoir began.

If new magma enters the Foyers Complex via a vein system it must be connected with its source at deeper crustal levels. Although the magma may have a very weak density contrast with the crust at the level exposed today, the much higher

density contrasts found at depth between host and magma, (possibly lower crust/upper mantle, Stephens and Halliday, 1984), will provide extra bouyancy to magma higher in the dyke system (Ramberg 1981), and it could be this higher density contrast that promotes minor ballooning of a magma chamber established by veining and stoping (Chapter 7).

Fabric and structural studies in the Foyers Complex show it was magmatic during most of its emplacement history, and the aureole deformation associated with granitoid ballooning occurred whilst the pluton was fluid, driven by new magma entering the complex via a vein system. This mechanism does not explain the very minor, late solid state deformation in the granitoids which would occur when the Errozie Quartz Diorite and Dalcrag Granodiorite had negative bouyancies. For ballooning to continue, fluid magma would have to intrude solid granite. The Aberchalder Adamellite intrudes into a solid complex, but solid state deformational strain shows no spatial correlation with this event.

Castro (1987), shows that quartz diorites may be intruded into less dense host rocks due to syn-intrusive movement along shear zones. Although there is no evidence to support this idea, it is possible that deformation in the crust adjacent to the Great Glen compressed the Foyers Complex creating the late very minor solid state deformation within the pluton.

Castro (1987) doubts that the density contrast between any pluton and host will produce enough bouyancy to form stresses capable of causing aureole deformation seen around ballooning plutons. This idea is reinforced by the intrusion

models of Marsh (1982), who concluded that stress due to bouyancy is very weak. Castro (1987), states that to produce the stresses needed for aureole deformation it is necessary to constrict the lower part of the pluton, which will have the effect of ballooning the upper part of the pluton. He states two processes may cause this constriction. One is demonstrated in Dixon's diapir models (1975), where the inward flow of the lower walls of the pluton will develop a constrictive neck towards the pluton base. The major ballooning force, Castro (1987) believes to be compressional regional deformation. However seemingly minor, the deformation will act upon the intrusion and cause constriction of the lower intrusion, and swelling of the upper.

#### 9.7 THE EFFECT OF DENSITY ON STOPING.

As stated in Chapter 7, the Foyers Complex created a large space for itself in the crust by stoping. The Foyers Complex contains a number of large psammite rafts, mainly pebbly psammites, which were probably removed from the roof of the complex by a stoping mechanism. It is important to demonstrate that the contrasts between the densities of the Foyers magmas and the psammites in the envelope do not preclude the possibility of stoping.

#### 9.7.1 Density Contrasts Between Rafts And Magma.

The density contrast between totally molten Errogie Quartz Diorite at  $1000^{\circ}\text{C}$  and 3.9Kb and micaceous psammite and pebbly psammite, under the same PT conditions, is  $0.089\text{g/cm}^3$  and  $0.063\text{g/cm}^3$  respectively, as indicated in (Fig.9.1). When the Errogie Quartz Diorite has cooled to a crystal content of 26% the density contrast between it and micaceous psammite is reduced to zero, and when the Errogie Quartz Diorite reaches a crystal content of 16% it has the same density as the pebbly psammite. It is at these two points that both psammite lithologies will no longer sink.

The results of calculations of settling velocities for various sizes and lithology of raft in Errogie Quartz Diorite at  $1000^{\circ}\text{C}$  are presented in the text below.

The viscosity of Errogie Quartz Diorite melt at  $1000^{\circ}\text{C}$  was calculated using the data and method of Bottinga and Weill (1972). Stoke's law was used to calculate the settling velocities.

A pebbly psammite raft with a diameter of 100m sinks at 15.8 cm/s, whilst a pebbly psammite raft with a diameter of 10m sinks at 0.158cm/s. A micaceous psammite raft 100m in diameter sinks at 22.4cm/s, while a raft with a diameter of 10m sinks at a rate of 0.22cm/s. The effects of convection in the pluton are not accounted for, nor the shape of the rafts, although Marsh (1982) states xenolith shape has

little effect on the rate of descent in a magma.

It is possible to calculate how the settling rate of xenoliths decreases as the magma both cools and crystallises.

A study into how the cooling of Errogie Quartz Diorite affects the settling rate of micaceous psammite rafts with a diameter of 100m was undertaken. The density contrasts between micaceous psammite and magma at various temperatures were taken from the graph in (Fig.9.1), as were the changing crystal contents of the magma. The viscosity data had to be extrapolated from Bottinga and Weill (1972), because the temperatures involved are slightly lower than the data these authors present. The effect of solid suspensions on viscosity was calculated using an equation presented in Bottinga and Weill (1972), after Roscoe (1952).

The settling rates for a 100m diameter micaceous psammite raft in Errogie Quartz Diorite at different temperatures are displayed in (Table 9.6) and (Fig.9.3).

Only the behaviour of rafts in Errogie Quartz Diorite magma has been considered so far. As the Dalcrag Granodiorite is less dense than the Errogie Quartz Diorite it may provide a better medium for rafts to sink through, although the increased silica content will increase viscosity. A 100m diameter micaceous psammite block in totally molten Dalcrag Granodiorite will sink at a rate of 5.5cm/s. This is an estimate because the density of Dalcrag Granodiorite is only modelled up to a temperature of 900°C in (Fig.9.1), a temperature too low to accurately use the viscosity data of Bottinga and Weill (1972). The Dalcrag Granodiorite remains



less dense than the micaceous psammite until it has reached a crystallinity of 50-60%, thus extending the time period over which stoping can occur.

The major conclusions drawn from these calculations are that, although the density of totally molten Errogie Quartz Diorite is only slightly less than that of micaceous and pebbly psammite rafts, the difference was great enough to cause quite rapid settling of the rafts. However stoping could only occur when the Errogie Quartz Diorite had a low crystal content, and thus it is assumed that stoping was a feature that occurred early in the structural development of the complex. The early timing of stoping becomes more crucial because the velocity of raft settling, and thus the rate of stoping rapidly decreases as crystals begin to appear in the melt, (Fig.9.3).

CHAPTER 10. THE INTRUSION OF THE FOYERS COMPLEX;  
SUMMARY AND CONCLUSIONS.

CHAPTER 10. THE INTRUSION OF THE FOYERS COMPLEX;  
SUMMARY AND CONCLUSIONS.

10.1 SUMMARY OF THE PRECEEDING CHAPTERS.

The lithologies of the Foyers Complex form part of a differentiation series with a single, calc-alkaline, parent magma, although only a limited variety of granitoid lithologies were either generated or emplaced at the crustal level exposed today.

The restricted lithologies and geochemistries, show that differentiation did not occur within the exposed portion of the Foyers Complex, but within a magma body deeper in the crust. The products of differentiation were released spasmodically as magma pulses and ascended through the crust to be emplaced at the present level as the Foyers Complex.

There are four major igneous units, emplaced in the order; Errogie Quartz Diorite, Chliabhain Quartz Monzodiorite, Dalcrag Granodiorite and Aberchalder Adamellite.

There are no regular structural relationships developed between the units, as seen in ring complexes and zoned plutons, as later intrusions form irregular stocks within the earlier units.

The Errogie Quartz Diorite shows gradational contacts with the Chliabhain Quartz Monzodiorite and the Dalcrag Granodiorite, indicating the host quartz diorite and the intruding bodies were magmatic during contact formation.

Thus the whole complex remained in a magmatic state during the greater part of its formation.

The Aberchalder Adamellite sharply cross cuts all other major units indicating emplacement into rigid host granitoids. The development of adamellite veins of in the host granitoids adjacent to adamellite stocks indicates some of the adamellite was intruded as a magma.

Microdiorite enclaves show morphologies and distributions indicating they were intruded as magma into fluid Errogie Quartz Diorite, Chliabhain Quartz Monzodiorite and Dalcrag Granodiorite.

Veining by all the major igneous units, excluding the Aberchalder Adamellite, is very intense in the envelope of the Foyers Complex. Volumetrically, replacement is more important than dilation. The style and intensity of the veining is controlled by structural inhomogeneities in the envelope, of which the most important is bedding.

The two major envelope psammities show different veining styles. Veins in the micaceous psammities are largely limited to the bedding planes, whilst veining in the pebbly psammities is less regular, with veins cross cutting bedding and forming irregular "stocks".

Veining is possibly a precursor of stoping, and pebbly psammities close to the margin are strongly replaced by granitoids, whilst the micaceous psammities are veined but unstopped. It appears that the variations in metasedimentary lithologies had a strong influence on the extent of stoping.

This model provides a link between regional structure and morphology of the complex. Regional structure controls the

disposition of psammite units in the crust, and the psammite units influence where the granitoids are emplaced. This may explain the rather unusual "triangular" outline of the Foyers Complex.

Mineral fabrics in the complex indicate that the preferred mineral orientation was formed by fluid flow, superimposed by very weak, coaxial, solid state deformation. The study of microdiorite enclaves, appinite bodies, internal contacts and xenoliths presents conflicting evidence concerning the origin of the mineral fabrics in the host granitoids and the relative importance of solid state and fluidal processes in the pluton. However, the majority of the evidence implies that magmatic processes were dominant. The process forming this weak solid state fabric could not cause the strong deformation in the envelope. It appears <sup>that</sup> the Foyers Complex was in a magmatic state whilst the envelope was deforming. Minor areas of psammite mobilisation, in the inner Foyers aureole complex formed when psammites flowed during extensive local melting. Substantial melting occurs only when conditions are optimised by; an intimate association between complex and envelope, to raise temperatures above that of the average inner aureole, a bulk chemistry favorable for melting and a source of water from dehydration reactions in local pelitic beds. Aureole deformation facilitated the movement of melt/water, and helped break down the rock fabric thus promoting fluid flow at low melt concentrations.

Small blind patches of psammite melt in the remainder of the inner aureole imply there was minor melting in the inner

aureole. It is unlikely the presence of minor melt would substantially change the rheology of the envelope, (Arzi 1978).

To achieve inner aureole temperatures capable of melting trondjhemitic psammities, the Foyers Complex must have been at a temperature such that the magma was dominantly liquid.

Major and minor structures in the Foyers aureole show there were three phases of regional deformation, overprinted by boudinage and minor shearing resulting from the emplacement of the Foyers Complex.

The margins of the complex are grossly parallel to the regional D1/bedding foliation, although there are a number areas where the margin cross cuts bedding.

D1, D2, and D3 structures show little or no rotation by the emplacement of the Foyers Complex. The work of Haselock and Graham (pers.com.) indicates the margin parallel attitudes of envelope lithological units are controlled by regional structures.

Structures created by emplacement of the Foyers Complex, indicate maximum stress was approximately perpendicular to the pluton margin. Deformation intensity dies away from the contact with no coinciding loss of parallelism between granitoid contact and bedding foliation, and minor shearing in the inner aureole indicates there was sub horizontal movement of Errogie quartz diorite magma to the south east. The aureole deformation implies expansion of the Foyers Complex occurred, but major and minor regional structures show no rotation approaching the Foyers Complex, indicating the majority of the space now occupied by the Foyers Complex

was not created by shouldering aside the crust.

D1 and D2 structures are sub-parallel to the granitoid contact, and D3 structures are at a high angle to the contact so undetected minor structural rotations cannot be discounted.

Calculations of psammite and magma densities show intrusion of Errogie Quartz Diorite and Dalcrag Granodiorite, if isolated from a magmatic source, was only possible when the magmas had high liquid:solid ratios. If the magmas were connected to a source region much deeper in the crust, the extra bouyancy would allow the Foyers magmas to ascend when the density of the magma was above that of adjacent crust. The Foyers Complex could be connected to a source by a vein system utilising the fractures associated with the Great Glen Fault.

It is doubtful whether stresses created by the bouyancy of Foyers magma alone would be great enough to dilate the crust sufficiently to accommodate the whole of the complex. Aureole deformation was caused by new pulses of magma dilating the magma chamber established by stoping. The large density contrasts between magma and crust in the source region provided the bouyancy for aureole deformation.

Density contrasts between aureole lithologies and magmas indicate rapid and effective stoping occurs when the intruding magmas are highly fluid. The crustal space now occupied by the Foyers Complex was thus created by highly fluid magmas.

On the north east margin of the Foyers Complex is an elongate granitoid body, the Maol Chnoc Complex. It lies



sub-parallel to the margin of the Foyers Complex, although separated from the latter by 400m-1km of psammites. It contains adamellite, diorite, aplite and granodiorite, the latter forming the bulk of the complex. The complex was emplaced parallel to the regional strike of the psammites by sheeting and stoping, the bedding in the psammites dictating the morphology of the stoped blocks and therefore the final shape of the complex. A very strong flow fabric is developed parallel to the margins. This fabric is coaxially overprinted by an intense solid state fabric, often mylonitic, generated by the emplacement of the adjacent Foyers Complex. In Maol Chnoc granitoids distant from the Foyers Complex the solid state fabric is very weak.

The magmatic fabrics in the Foyers Complex adjacent to the Maol Chnoc complex suggests the rheology of the former was incapable of recording solid state strain. This implies the Foyers Complex was in a magmatic state whilst it deformed its envelope.

A 4km wide metamorphic aureole around the Foyers Complex contains extensive contact sillimanite. The inner aureole of the complex contains a distinctive assemblage of sillimanite, cordierite, alkali feldspar, and garnet. The P.T. estimates for the inner aureole are 658°C and 4.0 Kb. .

The metamorphic minerals developed over an extensive period of aureole heating, show a random orientation, and no deformation, implying the aureole was static, a characteristic of granitoids which did not dilate the crust during emplacement. The lack of mineral fabrics in the aureole psammites but strong mineral fabrics within the Maol

Chnoc Complex implies fabric formation was more readily achieved in the Maol Chnoc Complex, or metamorphism in the aureole peaked well after Foyers intrusion had occurred. This latter model requires that the Foyers Complex remained magmatic after intrusion and deformation.

#### 10.2 COMPARISONS BETWEEN THE INTRUSION OF THE FOYERS COMPLEX AND OTHER GRANITOIDS.

Most major bodies of granitoid magma create occupancy space in the crust by brittle, passive replacement of the crust or plastic forceful dilation. Passive intrusion involves either stoping or cauldron subsidence, whilst forceful emplacement is due to diapirism, either piercement or ballooning. The characteristics of the Foyers Complex suggest both forceful and permitted emplacement occurred, and stoping followed by diapirism were the mechanisms involved. Cauldron subsidence is ruled out because the complex lacks a central crustal block, and a flat roof zone. The Foyers Complex is a collection of small irregular stocks, a characteristic not seen in granitoids emplaced by cauldron subsidence. In short there is no evidence to support cauldron subsidence as a feasible emplacement mechanism.

Foyers emplacement involves both permitted intrusion (stoping) and forceful emplacement (ballooning diapirism) so it is necessary to assess the importance and validity of each mechanism.

Recently there has been considerable debate concerning the use of geological criteria to identify the mechanisms

(chiefly diapirism), involved in the emplacement of granitoids. The definition of diapirism used in this work is derived from discussions between Bateman (1984, 1986) and Van Den Eekhout et al. (1986), as;

The upwelling of mobile rock material through or into overlying rocks creating space by the ductile deformation of the mantling rocks.

A diapir which cuts structures in the mantling rocks is a piercement diapir, whilst a diapir which does not pierce the overlying crust is a ballooning diapir, (Ramsay 1975, 1971).

Criteria indicative of granitoid emplacement by diapirism are presented by numerous workers including, Stephansson (1977), Schwerdtner (1981), Bateman (1984), Van den Eekhout (1986), Courrioux (1987), and Castro (1987). Diapirism cannot be identified with certainty on the fulfillment of one criterion alone, (although the more criteria fulfilled the stronger the case for diapirism.)

The established criteria are summarised as:

1. Circular to ovoid plan.
2. Annular arrangement of igneous lithologies in the complex, the more acid members towards the centre.
3. On approaching the pluton, pre intrusion foliations, i.e. bedding become conformable with the pluton contact, although will never form completely closed trend lines around the granitoid.

4. New aureole foliations are most intense close to the conformable pluton contact, and are also parallel to foliations in the pluton. The foliations form closed trend lines around the pluton.

5. Foliations in the pluton form in the solid state and are parallel to the contact.

6. Deformation in the aureole is by bulk shortening perpendicular to the pluton contact around a ballooning diapir. Around a piercement diapir the aureole records rotational strain. Moving away from the contact the deformation becomes less intense.

7. Contact metamorphic porphyroblasts show synkinematic growth with regard to the new aureole foliations.

8. The pluton is less dense than the mantling rocks.

#### 10.2.1 Comparison Of The Foyers Complex With The Ideal Characteristics Of Diapiric Intrusion.

1. The Foyers Complex has a triangular rather than circular or ovoid plan. If the complex was intruded by shouldering aside the crust then the apices of the triangle would be mechanically unstable. It is possible diapirism was involved in the earlier stages of emplacement and later intrusion mechanisms formed the present day pluton plan.

2. The arrangement of the lithologies in the complex are dominantly asymmetrical with quartz diorite in the north and granodiorite in the south. Adamellite forms irregular stocks throughout the pluton. The Foyers Complex is not annular.

3. Bedding in the Foyers Complex shows strong parallelism to the pluton contact, a feature indicative of diapiric emplacement. However many kilometers from the pluton the bedding remains parallel to the contact and there are frequent examples of high angle relationships between bedding and contact. A parallel bedding/contact relationship would be developed if the pluton's magma chamber morphology was controlled by bedding strike, with the pluton walls developing parallel to bedding. Where the control of the bedding on pluton morphology breaks down, the contact cross cuts bedding. The attitude of contact parallel bedding is controlled by regional structures not the pluton.

4. The Foyers Complex does not develop a contact parallel aureole foliation within its psammite envelope. However the granitoid rocks of the Maol Chnoc Complex show a good solid state fabric which decreases in intensity away from the contact, indicating diapirism. The lack of an aureole fabric in the psammites may be because strain in the heterogeneous psammites was accommodated by boudinage. Also, any aureole fabric developed would be parallel to the intense D1 penetrative fabric, and could possibly be masked.

5. Mineral fabrics in the Foyers Complex are parallel to the contact, but they are magmatic fabrics, implying that if diapirism was involved it occurred when the pluton was in a magmatic, rather than solid state.

6. Chocolate block boudinage in the Foyers aureole shows that shortening was perpendicular to the pluton contact. Moving away from the contact the deformation becomes less intense, implying diapirism was involved.

7. The aureole porphyroblasts show no deformation. This may imply that the aureole was not substantially deformed by diapirism, or porphyroblasts did not begin to grow until after deformation had ceased, a function of slow heat conduction through the aureole.

8. The crust is less dense than the Foyers Complex. However intrusion of a crystal poor magma and connection with a magma source at depth could provide the necessary bouyancy to cause deformation.

Criteria 4, 6 and possibly 8, strongly suggest diapirism was involved in the emplacement of the Foyers Complex. Criteria 1, 3 and 5 imply that regional structure controls the morphology of the Foyers Complex, and emplacement of the complex was quite passive. Criteria 2 and 7 imply a passive mechanism was involved in the intrusion of the Complex.

Thus comparing the structural features of the Foyers Complex with published criteria, the model of passive

emplacement, influenced by regional fold structures, succeeded by later ballooning of the magma chamber, is tenable.

#### 10.2.2 Comparison Of The Foyers Complex With The Ideal Characteristics Displayed By A Granitoid Emplaced By Stoping.

Castro (1987), summarises the characteristics of plutons intruded by passive stoping mechanisms as:

1. Discordant to regional structures.
2. Irregular plan.
3. Sinuous contacts.
4. Contacts often interpenetrated with host rocks.
5. Lack of internal igneous structure. 6. No deformation of host near the contacts.
7. Minor stoping structures at the contact zone.

The Foyers Complex shows some, but not all these characteristics.

1 & 2. The Foyers Complex appears to be broadly concordant with the regional structures, and has a regular 'triangular' plan. This is not typical of stoped plutons, but control of stoping by regional structures would give a stoped pluton whose plan morphology is concordant with regional structures.



3. The contacts of the Foyers Complex are broadly straight, although there are many areas where the contact cross cuts bedding. This would occur where bedding does not control the stoping process.

4. Foyers granitoids interpenetrate the envelope all around the complex.

5. The Foyers Complex has a well defined wall parallel fabric but this is a flow fabric controlled by the orientation of the magma chamber walls.

6. There is strong deformation in the aureole of the Foyers Complex, not a feature typical of permissive emplacement.

7. Stopping features are abundant in some areas of the Foyers Complex.

Characteristics 1, 2, and 3 displayed by the Foyers Complex are not typical of intrusions emplaced by stoping, but regional structural control of the stoping could produce such structures. Characteristics 4, 5 and 7 are characteristic of emplacement by stoping. 6 is a feature associated with diapirism. Thus the combined stoping and then ballooning model still holds.

The major reservation is that regional structural control of pluton morphology is only applicable at the present level

of exposure. It is probable the regional structure influenced the shape of the magma chamber because there was a close 'fit' at the exposed crustal level between the size of the magma body and the position of lithologies difficult to stope. At greater crustal depths, where structural changes occur, it is highly probable that there is no close 'fit' between the magma body and correct lithology. In such a situation it is unlikely that lithology could control the shape of the magma body, and the pluton will replace crust regardless of the structure.

### 10.3 AN EMPLACEMENT MODEL FOR THE FOYERS COMPLEX.

A model which most accurately represents the emplacement of the Foyers Complex must explain the observations presented in this thesis and conclusions summarised in this chapter.

The morphology of the exposed Foyers Complex is controlled by large regional structures, and the lack of rotation shown by these and minor structures implies the Foyers Complex did not intrude by major crustal dilation. The major emplacement mechanism was stoping by very fluid magmas, creating a large magma chamber. The link between regional structure and morphology of the magma chamber is provided by the pre-intrusion position of psammite lithologies. The pebbly psammites are readily replaced by magma, whilst the micaceous psammite is more difficult to remove.

Further emplacement of magma caused the established magma

chamber to expand, resulting in the flattening and deformation of the envelope. Envelope deformation is strongest towards the eastern 'triangular apex' of the complex. The increased deformation in this region could be caused by subhorizontal movement of Errogie Quartz Diorite magma to the east, where magma has limited opportunities to create space by stoping so creates space by ballooning.

The Foyers Complex is connected at depth to a magma source by continuous column of magma within a vein system utilising fracturing associated with the Great Glen fault. The magma column creates the necessary bouyancy to deform the Foyers Complex envelope.

Intrusion of the Foyers Complex caused partial melting of the psammities in the inner aureole. The lack of mineral fabrics associated with granitoid intrusion implies the new aureole mineralogy developed in a static environment. Mineral foliations in the Maol Chnoc Complex, imply localised strong aureole deformation on the north east side of the complex, and development of the Foyers thermal aureole after deformation associated with granitoid intrusion. The Foyers Complex contained high temperature fluid magma after envelope deformation ceased.

#### 10.4 THE VIABILITY OF MAGMATIC BALLOONING IN THE FOYERS GRANITIC COMPLEX.

Intensive experimental laboratory work on diapiric models, (Ramberg 1967 and 1981, Berner et al. 1972, Dixon 1975, and Soula, 1982) shows diapirism occurs when the viscosity contrast between the diapir and mantling material is low. As most granitoid envelopes show little evidence of partial melting, and have rheologies of solids (Arzi, 1978), it is assumed granitoid diapirs are also solid. Soula (1982) stated diapiric granitoids in the Pyrenees were 1000 times stronger than the surrounding aureole at the time of emplacement. Marsh (1982) presents mechanical calculations showing deformation in the aureole of a pluton is only possible if the diapir has a similar rheology to the envelope. Ramberg (1981) presents a laboratory model where the magma is much less fluid than the host, which shows magma rises along brittle fractures rather than by plastic deformation.

There are numerous examples of workers showing granitoids had the mechanical strength of solids during the plastic deformation of their envelopes.

Barriere (1977), shows the Ploumanac'h complex was initially emplaced into the crust by brittle processes. As the complex crystallised and the aureole heated up, the viscosity contrast between granitoid and pluton decreased, and plastic deformation of the aureole began. Deformation in the aureole is accompanied by a strong solid state gneissose

and cataclastic fabric in the outer parts of the complex. Holder (1979), shows deformation in the aureole of the Ardara complex is accompanied by a strong gneissose fabric in the outer zone of the pluton. Bateman (1985), studying the Cannibal Creek granite describes plastic deformation in the aureole and gneissose fabrics in the granite close to the contact. Bateman (1985) states gneissose fabrics imply the granite was solid during the deformation of the aureole. Ramsay (1975, 1981 and 1989). describes strong solid state gneissose fabrics within the marginal granitoids of the Chindamora' batholith, a granitoid emplaced by ballooning.

In this and previous chapters it is established the Foyers Complex shows features indicating ballooning, but no features indicating the complex deformed whilst in a solid state. All the evidence points towards emplacement as a highly fluid magma, which mechanically behaved as a fluid during ballooning and aureole deformation. If the thesis that, ballooning only occurs where the aureole and pluton have similar viscosities, is correct, then it is necessary to reduce the viscosity of the Foyers aureole to that of a fluid, by substantial contact melting. Mobilised psammites indicative of high melt fractions do occur locally in the aureole, and it is possible that the unmobilised psammites also contained a proportion of melt. However the unmobilised psammites retain D1, D2 and D3 structures implying the melt fraction was too small to disrupt the mineral fabric of the psammites. Arzi, (1978) and Van der Molen et al. (1979) show melt contents below 20-30 vol.% have little effect on lowering the viscosity of solid rocks. The Foyers Complex

may have had a large crystal content at the time of deformation in the aureole, but rheologically it was acting as a fluid, (Arzi 1978). It thus appears the Foyers Complex, with the mechanical characteristics of a fluid, was capable of deforming its aureole which had the mechanical properties of a solid.

Examples of magmatic diapirs plastically deforming their envelopes are poorly documented. Recently, Paterson (1988), described the final emplacement of the Cannibal Creek granite as a diapir containing enough melt to behave as a fluid. Wikstrom (1987), shows granitoids in south east Sweden were emplaced as magmatic diapirs. He resolves the problem of viscosity contrasts by assuming the aureole rocks had the same viscosity as the fluid magma during emplacement, without presenting evidence to support the thesis that the aureole rocks had very low viscosities. Perhaps Wikstrom (1987) is actually describing magmatic diapirs deforming solid envelopes. Vernon et al. (1988), show magmatic flow may imprint solid state mineral fabrics in solid rocks.

The possibility of magmatic diapirs deforming solid envelopes is currently a topic of heated debate, (Paterson, 1989). The Foyers Complex appears to illustrate that igneous intrusions in a magmatic state can indeed plastically deform their solid envelopes during diapirism.

#### 10.5 THE FOYERS-STROUTIAN CORRELATION.

Many workers, for example, van Breemen et al. (1982), Piasecki (1983) and Winchester (1974), made correlations between lithostratigraphies on either side of the Great Glen fault. Markers capable of defining fault displacement may test whether correlations across the fault are accurate. The most recent correlation, (Lindsay et al., 1989), tentatively suggests the lithologies north of the Great Glen are a continuation of the Dalradian stratigraphy to the south, reducing the importance of the Great Glen on the structural continuity between the Northern and Central Highlands.

Kennedy (1946), first quantified Great Glen Fault movement, stating the Foyers and Stroutian complexes were initially the same body, separated by 65 miles of post emplacement sinistral displacement along the Great Glen Fault. His correlation was based upon the similarities of lithology and internal structure displayed by each pluton. He stated both complexes contained an outer tonalite (Erroglie Quartz Diorite), an inner granodiorite and a cross cutting biotite granite (Aberchalder Adamellite). The structural similarity of the biotite granites in both plutons (Fig.10.1) was the key to Kennedy's correlation. However recent mapping shows the Foyers Complex lacks the mass of biotite granite in the south, and biotite granite veins in the north, as proposed by Kennedy (1946).

Shand (1946), doubted the Great Glen was a major strike slip fault because it lacked abundant mylonite, and thus he



did not believe the Foyers and Strontian complexes were ever one body. Mould (1946), noted the presence of hornblende in the Aberchalder Adamellite, but not in the Strontian biotite granite, implying the two granites (ss) cannot be correlated.

Marston (1967), stated both complexes had differing geochemistries and structures, but further work lead Marston (1971), to proclaim that the geochemistries were too similar to discount a possible correlation, and structural differences could be explained by exposure of both plutons at different crustal levels.

Pigeon and Aftalion (1978), citing the work of Brown et. al (1968) show the Foyers Complex is approximately 20Ma years younger than the Strontian complex, and the zircon populations of both plutons indicate differing magma sources.

Pankhurst (1979), shows the Sr-Rb and the lead isotope systematics, and the trace and rare earth geochemistries of both complexes are different enough to rule out correlation.

Tyler and Ashworth (1983) showed the water activities and temperatures in the metamorphic aureole of the Strontian complex were higher than in the Foyers aureole, again casting doubt on a Foyers-Strontian correlation.

Hutton (1988), presents a model for the emplacement of the Strontian granite (Fig.10.2). He states the Strontian complex was emplaced as a subhorizontal sheet, with tonalite and granodiorite magma entering the space created between the foot and hanging wall ramps of an extensional listric fault. The emplacement of the biotite granite is associated

with dextral shearing, created by the extensional stresses which pull the hanging wall of the ramp/flat system to the south. This tensional regime is developed adjacent to a releasing bend on a dextral Great Glen fault. This model is vastly different to the emplacement model invoked for the Foyers Complex, where crustal space is created by stoping and minor ballooning, and the morphology of the complex is controlled by pre-faulting regional structures. The lack of similarity between the Foyers and Strontian emplacement mechanisms does not favour a correlation between the two.

APPENDICES.

## APPENDIX A. PETROGRAPHY AND FIELD DESCRIPTIONS.

### A1 ERROGIE QUARTZ DIORITE.

#### A1.1 Field Description.

At outcrop, medium grey, equigranular Errogie Quartz Diorite shows a foliation of variable intensity defined by the parallel orientation of mafics and plagioclase laths, (Plate 2.1).

Plagioclase dominates the mineralogy, with biotite more common than hornblende. Sphene is characteristically common, as waxy brown, euhedral sphenoids. Quartz is virtually absent and orthoclase is rare, forming very pale pink, anhedral phenocrysts often containing plagioclase inclusions.

A modal field estimate is plagioclase 75%, mafics 25%.

#### A1.2 Petrography.

The Errogie Quartz Diorite is dominated by plagioclase and biotite with very variable amounts of hornblende. Quartz and alkali feldspar are minor phases, and the accessories are dominated by sphene and magnetite. Apatite, zircon and occasionally rutile are also seen.

The rock has a weak sub-porphyritic to seriate texture with a grain size ranging between 0.2-10mm.

Plagioclase forms eu-subhedral laths of varying size, the larger plagioclases imparting a weak porphyritic texture on the rock. Plagioclases >7mm in length have aspect ratios of 3:1 whilst smaller plagioclases have aspect ratios of 2:1. Subhedral plagioclase may show compromise boundaries with other plagioclases, hornblende and to a minor extent biotite, although most plagioclase laths lie sub-parallel to each other and other mineral species.

Plagioclase laths show cores of andesine, (An 44), often sericitised and broadly rimmed by normally zoned feldspar down to oligoclase (An 25). The finer grained members of the Errogie Quartz Diorite contain a more calcic plagioclase with cores of labradorite (An 52), and outer rims of oligoclase (An 30). The composition of the plagioclase laths were calculated using the Michel-Levy optical determination.

Biotite, the dominant mafic component occurs as large, subhedral, ragged plates and smaller more euhedral grains. The pleochroic scheme is X=greenish brown, Y and Z=dark brown. The large plates contain numerous apatite rods, small plagioclase laths, magnetite and sparse zircons with poorly developed pleochroic haloes. The biotite is often chloritised, particularly along cleavage planes. Occasionally epidote accompanies the chlorite.

The amount of hornblende is very variable and occurs as stubby, sub-euhedral crystals up to 2.5mm long. Although the grains are bounded by crystal faces, compromise boundaries with plagioclase, biotite and accessories may occur. The larger crystals may contain inclusions of apatite, plagioclase and magnetite. The hornblende has a pleochroic

scheme of X=pale yellow, Y=olive green, Z=sea green.

Quartz is interstitial, occupying spaces bounded by plagioclase laths. Scarce concentrations of quartz may enclose chadocrysts of early euhedral hornblende and plagioclase. The quartz shows weak undulose extinction.

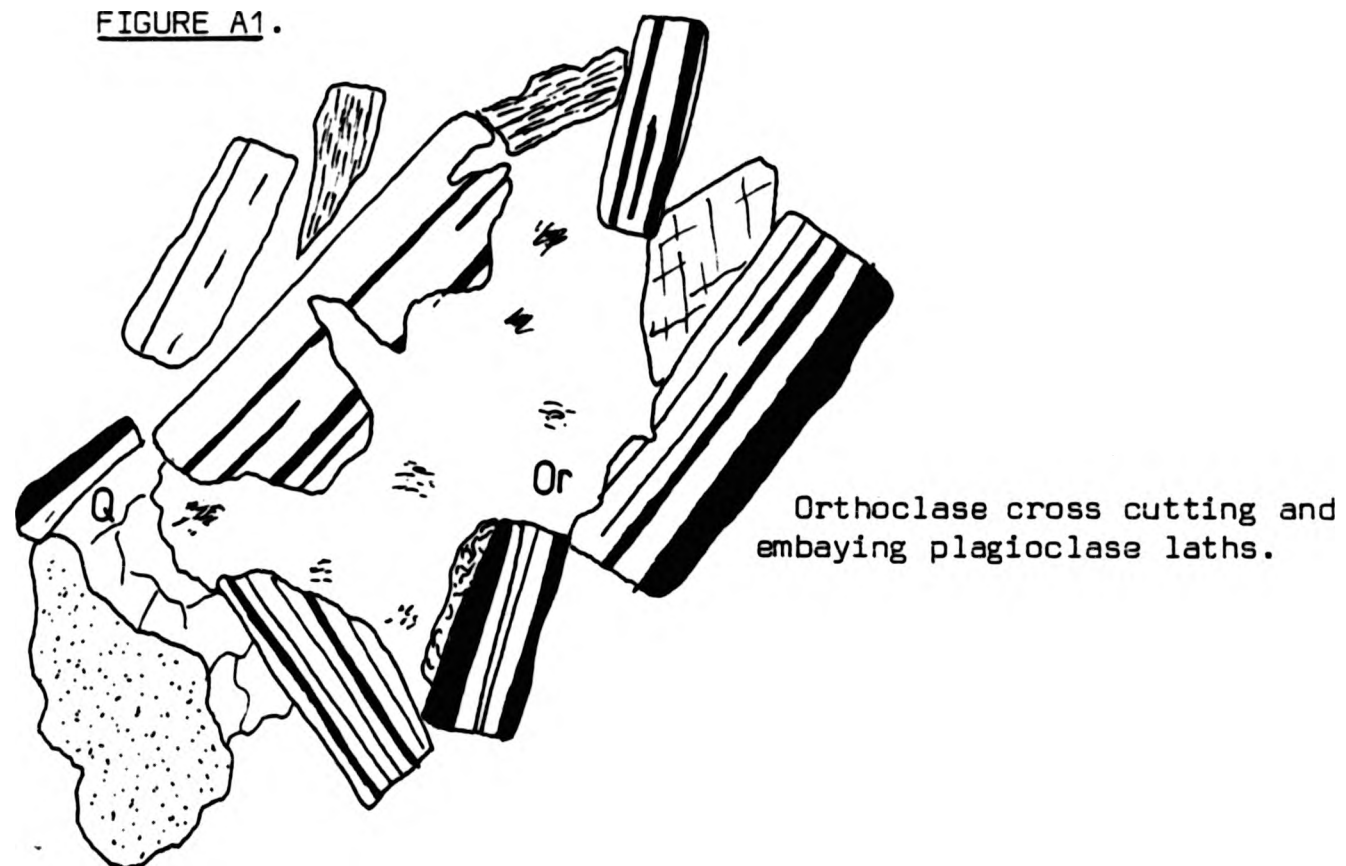
Orthoclase forms rare, large poikilitic phenocrysts which partially or totally enclose earlier chadocrysts, (Plate 2.2) Frequently the orthoclase partially replaces plagioclase. Textures which indicate replacement include orthoclase cutting irregularly across albite twins, embayments into plagioclase and irregular islands of plagioclase in the orthoclase, retaining optical continuity with each other, (Fig.A1). Although plagioclase is replaced by orthoclase this does not imply the orthoclase has a totally replacive origin as described by Stone & Austin (1961). The orthoclase is probably a late crystallising phase which may enclose and partially replace adjacent plagioclase laths. Myrmekite is developed when orthoclase is adjacent to plagioclase. The myrmekite forms irregular extensional rims to the plagioclase or seldomly embayments. Myrmekite is always external to the orthoclase and never develops at the contacts between islands of replaced plagioclase and orthoclase, perhaps indicating a magmatic rather than replacive origin for the myrmekite as it does not develop in areas isolated from late inter-granular magmatic fluids.

Sphene is the dominant accessory often forming large euhedral sphenoids <2mm long. Irregular clots of accessories do occur and sphene is often included in these where it is anhedral. Sphene is often cored by magnetite or it forms a

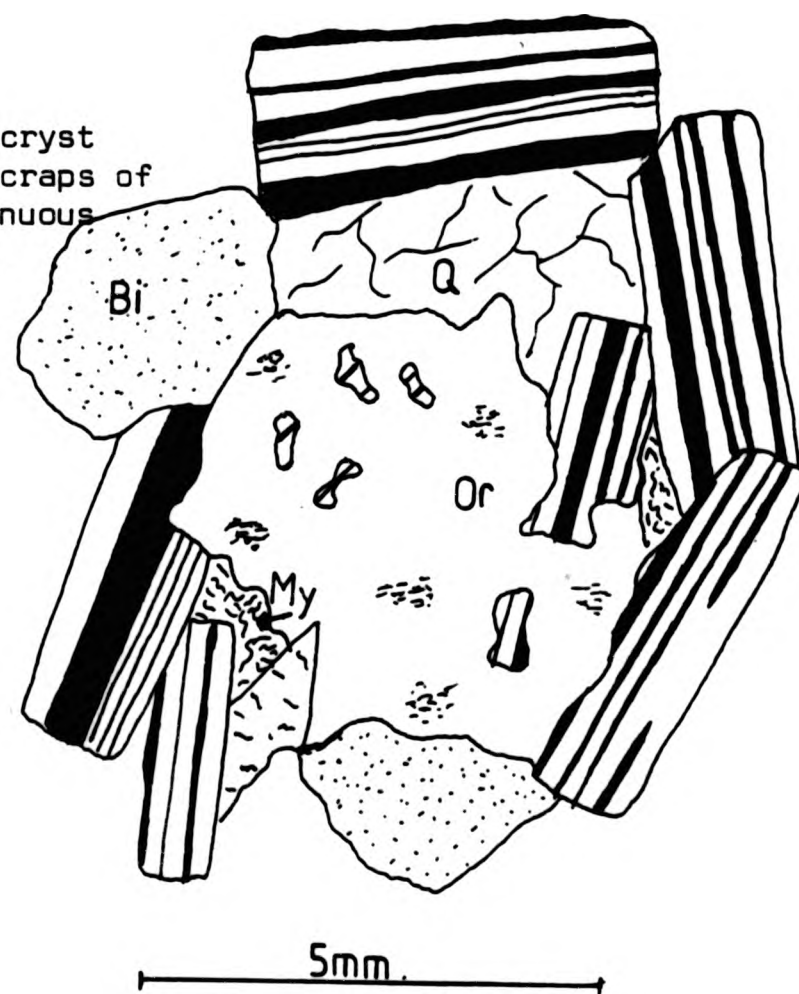


ILLUSTRATIONS OF ORTHOCLASE REPLACING PLAGIOCLASE IN  
ERROGIE QUARTZ DIORITE AND CHLIABHAIN QUARTZ MONZODIORITE.

FIGURE A1.



Orthoclase phenocryst  
enclosing small scraps of  
an earlier, continuous  
plagioclase lath.





thin rim around magnetite or rutile. Apatite is common as euhedral acicular prisms up to 2mm in length, within hornblende, biotite and plagioclase but is only readily seen in the mafic minerals. Zircon occurs as rounded anhedral grains or bipyramidal, euhedral crystals, <1mm in size.

## A2 CHLIABHAIN QUARTZ MONZODIORITE.

### A2.1 Field Description.

The Chliabhain Quartz Monzodiorite contains subhedral pink orthoclase phenocrysts, which form 5-10% of the rock. The groundmass is coarse, plagioclase and biotite are very common, hornblende occurs sparsely. Quartz is usually not visible and sphene occurs occasionally as small anhedral grains. A modal field estimate is, plagioclase 75%, mafics 15%, and orthoclase 10%.

The Errogie Quartz Diorite/Chliabhain Quartz Monzodiorite intermediate is similar to coarse grained Errogie Quartz Diorite units with the addition of anhedral, pale pink orthoclase phenocrysts. The number of phenocrysts on an outcrop surface is very variable, up to 5%, although often there are areas free of phenocrysts.

## A2.2 Petrography.

The Chliabhain Quartz Monzodiorites are dominated by plagioclase and mafics, although quartz and orthoclase are readily visible in section, (Plate 2.3)

The rock is porphyritic with orthoclase (<1.5cm), forming the phenocryst phase and the groundmass, (0.5mm-8mm.), containing the other mineral phases. Plagioclase may reach phenocryst dimensions.

Plagioclase shows a continuous size range within the grain size limits of the rock. The large laths have aspect ratios of >3:1 whilst smaller crystals have aspect ratios of <2:1. The plagioclase composition ranges from andesine (An 38) to oligoclase (An 25). Many of the laths are normally zoned, although crystals showing very fine multiple oscillatory zoning are common, (Plate 2.4). Laths are eu-subhedral occasionally showing compromise boundaries with each other, hornblende, and biotite. Large crystals are rich in inclusions of small euhedral biotite laths and small antiperthitic patches of orthoclase.

Biotite is the most common mafic phase with a size range of 0.2mm to 6mm. Large biotite plates are ragged and subhedral with a pleochroic scheme of X=greenish brown, Y and Z=dark brown. The small biotite fraction is more euhedral and may occur in polymineralic, glomerophytic clusters of <10 grains.

Hornblende occurs as sub-anhedral crystals, <3mm in diameter, and may form compromise boundaries with

plagioclase. The pleochroic scheme is X=pale yellow, Y=olive green and Z=sea green. The hornblende may occur within mafic clots. Occasionally hornblende is found in monomineralic glomerocrysts, where the hornblende is finer grained (0.3mm), equant and granular.

Perthitic orthoclase forms subhedral phenocrysts, with poikilitic or interstitial orthoclase being uncommon. The phenocrysts show features which indicate replacement of plagioclase, (Plate 2.5). Myrmekite is spatially associated with orthoclase, forming irregular rim extensions to plagioclase laths adjacent to orthoclase phenocrysts.

Quartz occurs as interstitial fillings and aggregates of anhedral grains, >2mm, with intra-aggregate boundaries forming a consertal texture.

Accessories include sphene, magnetite, apatite and zircon, often concentrated as mafic clots. Sphene is eu-subhedral and may form compromise boundaries with magnetite and hornblende. Frequently euhedral sphene is cored by a magnetite crystal, whilst anhedral sphene is often cored by numerous, anhedral, small magnetites, suggesting that some sphene crystals nucleate on magnetite.

Apatite is acicular whilst zircon is prismatic or rounded.

### A3 DALCRAG GRANODIORITE.

#### A3.1 Field Description.

The Dalcrag Granodiorite contains numerous, 10-15%, sub-euhedral pink orthoclase phenocrysts and also visible interstitial quartz, in addition to plagioclase and mafics, (Plate 2.6). Occasional minor units of Dalcrag granodiorite are equigranular or semi-porphyritic with small anhedral orthoclase phenocrysts.

Mafics in the Dalcrag Granodiorite are dominated by biotite although hornblende is abundant in some areas. Sphene is rarely seen. A mineral foliation of variable intensity is frequently developed. A field estimate of mineral proportions is; plagioclase 55%, orthoclase 15%, quartz 15%, mafics 15%.

#### A3.2 Petrography.

The Dalcrag Granodiorite is dominated by plagioclase, (Plate 2.7), but there are substantial amounts of quartz, alkali feldspar and mafics.

The Dalcrag Granodiorite is porphyritic, the orthoclase phenocrysts may exceed 2cm. The groundmass is coarse with crystal sizes ranging from 0.5 to 6mm, with the lower part of the size range occupied by the mafic components. Plagioclase is oligoclase with a composition between An 32

and An 18. Normal zoning is common in many crystals and fine oscillatory zoning is visible in large plagioclases. The plagioclase crystals unlike those in the Chliabhain Quartz Monzodiorite show few biotite inclusions. Sericitisation of the plagioclase cores is common. Plagioclase may form compromise boundaries with mafic phases and very occasionally with quartz, but laths normally lie sub-parallel to each other, and other mineral species. Perthitic orthoclase is most abundant as large, subhedral, often twinned phenocrysts. They show well formed faces and also compromise boundaries with plagioclase and quartz. Often plagioclase is replaced and embayed by adjacent orthoclase. Rims of myrmekite often extend out from euhedral plagioclase where the plagioclase is adjacent to orthoclase. The orthoclase may contain inclusions of opaques, mafics and corroded islands of plagioclase. Inclusions of quartz may occur as fissure fillings or as equant rounded blebs, the latter perhaps indicating the co-precipitation of both phases. The majority of the quartz occurs as large grains and interstitial material. Quartz grains meet to form a consertal texture and are often weakly strained.

The dominant mafic phase is biotite, forming ragged subhedral plates which are often chloritised. Hornblende forms sub-euhedral, often twinned crystals <2.5mm and also occurs as glomerocrysts <3mm, where it has a fine grained, equant and granular habit.

The accessories are dominated by sphene and magnetite, with apatite and zircon occurring in small amounts.

#### A4 MEALL A' BHUAILT GRANITE.

Meall a' Bhuailt is a very pale, equigranular, coarse grained rock. It contains abundant creamy plagioclase, abundant large aggregates of quartz with minor amounts of alkali feldspar. Mafics are moderately abundant with biotite dominating over hornblende. There are heterogenous patches <10cm in diameter, of slightly pegmatitic material. These pegmatitic patches contain less quartz and fewer mafics compared to the host rock, and euhedral hornblende dominates over biotite.

A field estimate of mineral abundance is, plagioclase 55%, quartz 20%, alkali feldspar 15%, mafics 10%.

#### A5 ABERCHALDER ADAMELLITE.

##### A5.1 Field Description.

The Aberchalder Adamellite contains abundant, grey, sometimes slightly reddened quartz grains, within a pink groundmass of equigranular plagioclase and orthoclase. Biotite is sparse and variable in abundance, (Plate 2.8). A field estimate is, quartz 34%, orthoclase 35%, plagioclase 27%, mafics 3%.

#### A5.2 Petrography.

The adamellite contains approximately equal proportions of quartz, plagioclase and orthoclase, with relatively minor mafics and scarce accessories. The adamellite is medium grained, 2-5mm, and equigranular, although some samples show minor irregular patches of finer, (0.2mm), equant or polygonal felsic material which occur within the coarser grained adamellite, (Plate 2.9).

Plagioclase forms eu-subhedral laths, often with highly sericitised cores, which may develop into secondary coarse white mica. The plagioclase may be antiperthitic and shows a weak compositional zoning. In fresh feldspars the cores range from An 30-25 and the margins An 20-12. Compromise boundaries occur between the plagioclase crystals especially where they occur as glomerocrysts.

Alkali feldspar occurs as perthitic orthoclase and microcline, the latter forming up to 25% of the alkali feldspar in some samples. The orthoclase forms large subhedral crystals whilst the microcline is finer grained. In some samples fine, equant grains of orthoclase form the minor fraction to quartz within the fine grained felsic patches described above. The large orthoclase grains often enclose, cross cut and embay plagioclase laths indicating partial replacement of plagioclase by orthoclase. Optically continuous islands of corroded plagioclase within enclosing orthoclase appear to indicate almost complete replacement of plagioclase crystals by orthoclase. Myrmekite is common



where orthoclase and plagioclase are adjacent but is not found where plagioclase crystals are enclosed by the orthoclase. The myrmekite normally occurs as rims growing out from the plagioclase margin, or as lobes extending into the orthoclase. Occasionally vermicules of quartz may cross cut albite twins which are continuous with twins within myrmekite free areas of the crystal.

Quartz occurs as large <3mm, anhedral interlocking grains with consertal boundaries, often developing into extensive aggregates. Occasionally quartz is seen cross cutting and replacing plagioclase and orthoclase. In most cases the quartz has a weak undulose extinction.

Biotite is the commonest mafic mineral and is frequently chloritised. It forms single, very ragged laths, (Plate 2.10). Hornblende is often present in small amounts forming small anhedral crystals. Euhedral sphene is infrequently seen as single grains or within mafic glomerocrysts which also contain magnetite, biotite, apatite and large zircon crystals. Very small crystals of tourmaline occur exceptionally sparsely.

### A5.3 Granitic Porphyries.

The porphyries are characterised by biotite and plagioclase phenocrysts (often revealed as euhedral weathering pits) within a pale pinky grey saccroidal groundmass of plagioclase and orthoclase.

The phenocrysts are <6mm in a fine groundmass with a size range between 0.1mm and 0.05mm, (Plate 2.11). The phenocrysts

are sub-euhedral plagioclase (often glomerocrysts), biotite, orthoclase and the infrequent cluster of several coarse interlocking quartz grains, (Plate 2.12). Zircon, sphene, magnetite and very seldomly orthite, form the accessories which often occur within mafic clusters. The plagioclase phenocrysts are normally zoned with andesine/oligoclase cores and oligoclase/albite rims.

The large euhedral orthoclase phenocrysts are often twinned and may show growth zoning picked out by perthite which occurs in the core region of the orthoclase. Rims of myrmekite may develop around the outer surface of these phenocrysts. Biotite is often euhedral with the pseudo-hexagonal form observed.

The groundmass consists of quartz, plagioclase, alkali feldspar, biotite and hornblende, with quartz the dominant phase. Groundmass quartz is equant or polygonal but may develop intricate consertal boundaries. Plagioclase forms small stubby laths, whilst orthoclase may partially enclose quartz and plagioclase groundmass minerals.

Aberchalder Adamellite/granitic porphyry intermediate rocks have a texture which represents a continuous textural gradation between the textures found in the adamellite and in the porphyries.

The intermediates show small irregular areas of coarser minerals in a fine grained groundmass. An increase in size, abundance, and grain size of these mineral patches marks the change from porphyry to adamellite.

#### A6 MAFIC MICRODIORITE ENCLAVES.

The grain size of the microdiorite enclaves varies between 0.2-0.8mm. The enclaves are dominated by plagioclase, but abundant biotite and hornblende produces a colour index between 30 and 40. Orthoclase and quartz form minor constituents whilst sphene, magnetite, rutile and apatite form the accessory phases.

The enclaves are equigranular, (Plate 2.16) although some samples show plagioclase phenocrysts and glomerophyric clusters.

Plagioclase forms subhedral laths which show interference boundaries between each other and some mafics, although most mafics, especially hornblende, produce a sub-ophitic texture. In the fine grained samples the plagioclase forms stubby laths, whilst coarser grained specimens hold more elongate laths. Plagioclase shows very weak normal zoning and sericitisation of varying intensity.

The mafic component is dominated by biotite and hornblende. Anhedral crystals of hornblende are penetrated by, or enclose, euhedral plagioclase laths to form a sub-ophitic texture. Hornblende has a pleochroic scheme of X=light brown, Y=olive green and Z=sea green.

Biotite, often weakly chloritised, is finer grained than the hornblende. It forms subhedral crystals which often show penetration by plagioclase laths. The biotite has a pleochroic scheme of X=light straw yellow, Y and Z=brown.

Sphene dominates the accessories and encloses or is

penetrated by euhedral plagioclase laths. Occasionally sphene forms the centres of plagioclase glomerocrysts where it forms an ophitic texture with the plagioclase laths whilst retaining a weak sphenoid morphology indicating that plagioclase precipitation was very early. The crystals in the glomerophyric clusters probably collect together by a synneusis mechanism operating early in the crystallisation history of the magma.

Quartz and orthoclase are rather minor. Quartz forms small interstitial grains with undulose extinction whilst orthoclase forms small equant grains or larger interstitial crystals which may partially enclose early phases.

#### A7 MICRODIORITE DYKES.

##### A7.1 Field Description.

In the field three types of microdiorite dyke are distinguished by their petrological characteristics.

##### 1 Melanocratic microdiorite.

This forms a dark grey, fine/medium grained rock with visible plagioclase and hornblende which may form elongate, or stubby prisms. An alignment of minerals is often seen running parallel to the dyke walls.

## 2 Fine grained, quartz xenocrystic microdiorite.

This is a very fine grained rock with unidentifiable groundmass minerals. The groundmass weathers to a distinctive rusty buff colour. These dykes also contain numerous large rounded quartz xenocrysts and pink plagioclase phenocrysts, (Plate 2.22).

## 3 Mesocratic plagioclase porphyry.

These dykes have a pale brown weathering surface dotted with prominent white plagioclase phenocrysts, <2cm in length. The groundmass is fine/medium grained with discernable quartz, orthoclase, biotite and hornblende.

## A7.2 Petrology.

### 1 Melanocratic microdiorite.

All the melanocratic microdiorites are dominated by plagioclase and mafics, but quartz and alkali feldspar are readily seen. The mafic component is dominated by hornblende with subsidiary biotite. Accessories include sphene, magnetite, rutile and very fine grained apatite needles. The grain size of the groundmass is 0.1-0.2mm, with phenocrysts of hornblende and plagioclase reaching 2mm in length.

The plagioclase laths define the planar fabric in the rock,

(Plate 2.19). The fabric may bifurcate around glomerophyric mafic clots, and any quartz present is unstrained.

Plagioclase is the dominant phase occurring as narrow laths (aspect ratio of 3:1), often with heavily sericitised cores leaving fresh rims. Unaltered cores have compositions of An 40 whilst rims, which often lack the Carlsbad twins of the core, have compositions of <An 20. (Kerr 1977).

Pale green hornblende dominantly occurs as an-subhedral crystals, (Plate 2.20). Many hornblendes are elongate and prismatic with hollow cores filled by plagioclase, and show well developed exsolution lamellae of dusty opaques, (Plate 2.21). Some hornblende occurs in monominerallic or polyminerallic glomerophyric clusters. Biotite occurs as small ragged, chloritised flakes. Fresh biotite has a pleochroic scheme of X= yellow, Y and Z= green. Biotite aggregates may pseudomorph hornblende.

Sphene and magnetite dominate the accessories, with sphene forming small anhedral grains, and magnetite subhedral grains.

Quartz occurs as small, irregular, very weakly strained grains, which may partially enclose plagioclase, biotite and hornblende.

Orthoclase is difficult to detect, but its presence is revealed by the presence of myrmekite, and staining with a combination of sodium cobaltinitrite, barium chloride and potassium rhodizonate, (Hutchinson, 1974). In coarser samples the orthoclase encloses plagioclase laths.

## 2 Quartz xenocrystic microdiorite.

This member of the microdiorite suite has a fine groundmass <0.05mm but containing distinctive quartz xenocrysts and large plagioclase phenocrysts with pink plagioclase rims, (Plate 2.22) The groundmass is dominated by plagioclase laths but staining reveals the presence of substantial orthoclase and thus probably quartz.

Plagioclase occurs in two forms; within the groundmass as tiny narrow unsericitised laths, and as large 0.5-2.0cm euhedral phenocrysts or collections of synneused phenocrysts (Vance 1969), which show weak to strong sericitisation throughout the crystal.

Pale green amphibole occurs as small acicular prisms within the groundmass and as glomerocrysts. The glomerocrysts are externally rounded, but are composed of radiating amphibole (possibly actinolite) sheaves. These glomerocrysts may be pseudomorphed by biotite or more often chlorite or epidote, and are often rimmed by concentrations of euhedral opaque minerals.

Biotite forms small, ragged, chloritised or epidotised plates in the groundmass.

The only quartz visible is that in the xenocrysts. The xenocrysts range in diameter from 1mm to 2cm, and are sub-spherical and rounded. Most xenocrysts are single unstrained crystals, but may be composed of several crystals. The xenocrysts are strongly embayed with fine grained microdiorite material extending deep into the quartz. The outer edge of the xenocrysts develops a thin



<0.07mm reaction rim of actinolite. The euhedral, prismatic actinolite crystals are rooted in the microdiorite, with the euhedral faces forming in the xenocryst, (Plate 2.24).

Accessories are dominated by very fine subhedral magnetite, and anhedral sphene.

### 3 Mesocratic plagioclase porphyry.

This member of the microdiorite suite is porphyritic, with a groundmass of <0.3mm and numerous plagioclase phenocrysts <2cm in length.

The groundmass is dominated by plagioclase laths, but it does contain substantial quartz, orthoclase (occasionally microcline) and biotite. Amphibole is rare or absent, (Plate 2.25).

Euhedral plagioclase laths have aspect ratios of >3:1 and highly sericitised cores, and define a moderately developed flow fabric. Many of the groundmass plagioclase crystals show a well developed normal or oscillatory zoning. The phenocrysts may be single or synneused collections of several phenocrysts. The plagioclases in the synneusis clusters tend to contact in Carlsbad or albite twin relationships. In clusters containing many crystals the relationships are more irregular. The phenocrysts often show three well developed compositional growth zones, excluding the extreme rim. The outer zone is the most distinctive and often contains large numbers of melt inclusions and strong sericitisation. In the synneusis clusters, this outer zone

encloses all the individual crystals in the cluster, indicating plagioclase growth after synneusis occurred, (Plate 2.26).

Biotite occurs within the groundmass as ragged plates, and finer euhedral crystals. Both have a pleochroic scheme of X=pale yellow, Y and Z=dark brown.

Quartz and alkali feldspar form the finer fraction of the groundmass as anhedral subrounded grains, interstitial fillings and poikilitic oikocrysts. No myrmekite is developed.

Accessories are dominated by magnetite and sphene.

1.25km from the Foyers Complex on the summit of Tom a' Chliabhain (G.R.46601505) the plagioclase porphyry dyke shows good chilled margins. The chill shows strong trimodal grain size distribution. The coarsest fraction is formed of large plagioclase phenocrysts <1.2cm. The medium grained fraction, <1.5mm, is composed of plagioclase laths and subordinate biotite flakes. The laths have sericitised cores and with the biotite define a strong flow fabric. The finest fraction, <0.02mm, forms a granular groundmass, containing quartz plagioclase and a little biotite.

The large phenocrysts in the chill show similar zoning to the phenocrysts from unchilled dyke, including the outer zone rich in melt inclusions. The large phenocrysts become smaller towards the margins of the dyke, but retain the outer growth zone.

## A8 APPINITIC DIORITES.

### A8.1 Field Description.

There are leucocratic and melanocratic appinitic diorites. Leucocratic appinites contain large <1cm stubby hornblendes which often occur as small clusters in a finer matrix of plagioclase, with relatively few single hornblendes. Melanocratic appinites are dominantly biotite and hornblende with only a little interstitial plagioclase visible. Mean grain size is <5mm, although individual hornblendes may be much greater in size. The distribution of mafics within the melanocratic appinite is very heterogenous with the development of both hornblende and biotite rich patches within the same outcrop.

### A8.2 Petrography.

In section, both leucocratic and melanocratic appinites show colour indices between 51 and 63. The leucocratic appinites appear lighter in the field as a result of a coarser grain size and clustering of felsic and mafic mineral phases.

Although all the samples do show large elongate prismatic hornblendes, some samples contain numerous stubby eu-subhedral hornblendes or equant hornblendes within glomerocrysts.

The mineralogy varies considerably but all appinites show

large modal proportions of hornblende, biotite and plagioclase. The amount of quartz and orthoclase is variable. If augite is present it forms a major component.

The rocks of the appinite suite are coarse grained with a grain size between 1 and 8mm, the hornblende and plagioclase dominating the coarse fraction.

Plagioclase occurs in two forms, as euhedral, highly sericitised laths and as anhedral oikocrysts enclosing mafics, (Plate 2.29), especially hornblende. In samples where sericitisation is weak the plagioclase laths are andesine, An44-An50.

Hornblende has a variety of forms, as coarse grained elongate prisms, medium grained eu-anhedral stubby crystals, (Plate 2.30), and as a component of granular glomerocrysts. It has a pleochroic scheme of X=pale yellow, Y=pale olive, Z=sea green. Hornblende may be highly altered to calcite along fractures and cleavage planes.

Augite if present, is pale green and forms euhedral prisms within the fine and medium grained fraction of the rock. Euhedral hornblendes may be cored by ragged crystals of augite, and augite prisms are often replaced, pseudomorphed or rimmed by hornblende, (Plate 2.28). Occasionally euhedral augite crystals are enclosed by hornblende perhaps indicating that augite acted as a site of hornblende nucleation, (Plate 2.27).

Perthitic orthoclase feldspar is common in some specimens, forming large crystals which often enclose euhedral mafic phases. Quartz if present, is interstitial or enclosing. Accessories include sphene, magnetite, apatite and

occasionally orthite. All the accessories are coarse grained, with sphene developing crystals <5mm, and apatite <3mm.

## A9 ACID VEINS.

### A9.1 Aplites.

Aplites are ash grey with a saccroidal texture. Grain size ranges from 0.02mm to 0.3mm, the fine grained samples develop a saccroidal<sup>ha</sup> texture, whilst the coarser samples have a more consertal texture.

The aplites are dominated by quartz, 40-50%, with alkali feldspar forming 15-40%. Plagioclase content is very variable, more basic aplites containing >15% plagioclase, and acidic aplites containing <10% plagioclase. Other mineral species form a very minor component, but are dominated by biotite and muscovite mica.

Quartz forms rounded to equant grains with very weak undulose extinctions. In fine samples the contacts between grains are straight line polygonal boundaries, whilst an increase in grain size is marked by the appearance of boundary intergrowths, (Plate 2.31).

Alkali feldspar occurs as perthitic orthoclase and microcline. The proportion of microcline may vary between 0% and 60% of the alkali feldspar. Orthoclase forms interstitial and sub-porphyrific grains, whilst microcline tends only to occur as interstitial equant grains, often

forming <sup>ha</sup>saccroidal masses in association with quartz.

Plagioclase (oligoclase) forms large, subhedral, unzoned crystals which may show weak sericitisation. Some plagioclase phenocrysts are studded with blebs of equant quartz indicating the co-precipitation of the two phases.

#### A9.2 Alkali Granite Veins.

These are medium grained, equigranular, and occur sparsely within the envelope rocks of Beinn Sgurrach.

Quartz dominates the mineralogy, forming irregular, weakly undulose grains with weakly intergrown boundaries. Alkali feldspar forms irregular grains of perthitic orthoclase feldspar, which may show minor myrmekite where it lies adjacent to plagioclase laths. When present, large irregular grains of perthitic orthoclase show a large euhedral core, the outer edge defined by a single layer of small plagioclase and biotite crystals, representing the nucleation of two mineral phases upon the free faces of an early euhedral orthoclase crystal. Later orthoclase overgrows the thin zone of crystal nucleation producing an irregular orthoclase phenocryst. There is abundant perthite in the core but very little in the irregular margin indicating the core is more sodic, and has exsolved perthite.

Biotite is the dominant mafic, containing abundant zircon grains with pleochroic haloes. Muscovite is also present in primary form. Euhedral magmatic garnets are also found in

these veins.



## APPENDIX B. GEOCHEMISTRY.

Whole rock granitoid samples from the Foyers Complex were analysed for both major and minor element oxides using an ARL 3510 Inductively Coupled Plasma Spectrometer, I.C.P.S at Thames Polytechnic .

All the samples weighed 2-3kg at collection, and were as fresh as outcrop allowed. Any weathering rinds on the samples were removed with a rock saw. Samples containing haematized fractures or enclaves were discarded. A rock splitter reduced the sample to fragments <5cm in diameter. The fragments were further reduced to <5mm in diameter using a steel jaw crusher, and then quartered to provide a 50-75cc sample which was ground in a Tema mill for 2 minutes. The sample was dried in a oven at 105°C for 24 hours.

### B1 Sample Preparation For Major Element Analysis.

The preparation of samples from the rock powders, for major element analysis on the I.C.P.S is adapted from the method of Thompson & Walsh (1983).

0.25g of sample powder was fused with 1.25g of lithium metaborate at 1050°C for 20 minutes. The molten bead was dissolved in 150ml 3.5% nitric acid, and the solution diluted to a dilution factor of x1000. Analysis using the I.C.P.S. was conducted within 24 hours, to minimize silica precipitation.

## B.2 Sample Preparation For Trace Element Analysis.

Again this method is adapted from Thompson and Walsh (1983).

A 0.5g rock powder sample is digested at 230°C in a mixture containing 10ml of 48% hydrofluoric acid and 8ml of 60% perchloric acid. This process is repeated twice, followed by a further digestion in perchloric acid.

The final salt was dissolved in 10ml of 50% hydrochloric acid and made up to a dilution factor of x100 with distilled water.

## B.3 I.C.P.S. Operating Conditions.

Calibration of the I.C.P.S used the published whole rock standards of NIM-S, NIM-N, NIM-P, NIM-G, BCR1 and GA, which were prepared with the rock samples. A number of blanks, (containing the sample preparatory reagents, but lacking the rock powders) were analysed to check the purity of the reagents. One rock standard was analysed repeatedly during the analysis of the rock samples to allow for later correction of machine drift.

The wavelengths listed below were those used by the spectrometer for element detection.

P=178.287nm,	Zn=213.856nm,	Si=251.611nm,	Mn=257.610nm,
Fe=259.940nm,	Cr=265.716nm,	Mg=279.080nm,	V= 290.880nm,
Al=308.215nm,	Ca=317.933nm,	Cu=324.754nm,	Ti=337.280nm,

Zr=343.823nm, Sc=361.384nm, Y=371.030nm, La=379.478nm,  
Sr=407.771nm, Ba=455.403nm, Na=589.592nm, K=766.491nm.

The results of analysis are presented in tables B1 and B2.

WHOLE ROCK ANALYSIS SHOWING MAJOR ELEMENTS IN VARIOUS FOYERS GRANITOIDS. TABLE B1

Locality & Sample No:	Oxide Weight Percentage:									
	Si	Al	Fe	Na	Ca	Mg	K	Ti	P	Total
Errogie Quartz Diorite:										
P1093	51.33	18.50	7.43	4.43	5.87	3.43	2.25	1.61	1.39	96.24
GP1612	52.50	20.9	5.87	5.06	5.18	2.53	0.53	1.23	2.59	96.39
P234	52.20	19.37	6.48	4.72	5.43	3.02	2.36	1.34	0.50	95.52
Errogie Qtz Diorite / Chliabhain Monzo-diorite Intermediate:										
GP1444A	53.57	17.53	5.37	4.80	4.07	2.22	2.79	1.12	0.42	91.89
GP1444B	53.57	18.89	5.39	5.07	4.52	2.17	0.43	1.22	2.49	95.74
GP1444E	55.89	18.32	5.33	5.08	4.41	2.25	2.37	1.10	0.38	95.13
Chliabhain Quartz Monzodiorite:										
GP654	55.50	19.11	5.73	5.47	4.65	2.22	2.56	1.21	0.43	96.88
GP592	53.20	20.90	5.27	5.37	5.02	2.11	2.29	1.24	0.42	95.82
GP640	57.40	18.49	4.60	4.69	3.69	1.96	3.26	0.91	0.34	95.33
GP648	58.17	18.71	5.04	5.00	4.17	1.88	3.23	0.93	0.33	97.46
GP107	54.5	18.85	5.90	4.97	4.25	2.38	3.46	1.14	0.44	95.89
P1574	57.44	20.26	4.55	5.16	3.86	1.97	3.57	0.89	0.35	98.05
Dalcrag Granodiorite:										
GP1680	62.17	17.74	4.57	4.35	4.15	3.34	3.34	0.99	0.31	100.90
GP1702	63.46	16.19	5.15	4.26	3.87	3.18	3.18	1.03	0.32	101.00
P1270	63.91	16.84	4.30	4.33	3.67	2.79	3.42	0.95	0.31	100.50
P1246	65.50	15.94	2.46	4.50	2.59	1.64	2.89	0.40	0.22	96.14
Dungarbh Granodiorite:										
GP414	64.64	16.99	3.62	4.33	1.93	2.09	3.43	0.69	0.22	97.94
GP416	65.57	14.62	2.93	4.51	2.29	1.72	2.67	0.60	0.21	95.22
Aberchalder Adamallite:										
P948	71.30	13.39	1.10	3.98	0.93	0.37	4.43	0.20	0.08	96.29
P780	76.10	12.83	1.58	3.61	0.60	0.47	4.43	0.27	0.08	99.97
P835	76.68	13.41	1.09	4.09	0.58	0.35	4.29	0.19	0.04	100.70
PX1	77.48	14.44	1.22	4.04	0.68	0.38	4.36	0.22	0.04	102.80
P945	75.22	14.31	1.79	4.17	1.13	0.56	4.43	0.38	0.08	101.50
P944	74.53	13.28	1.91	3.98	1.33	0.62	4.23	0.35	0.11	100.34

XXX

WHOLE ROCK ANALYSIS SHOWING TRACE ELEMENTS IN VARIOUS FOYERS GRANITOIDES. TABLE B2

Lithology & Sample No:	Trace Elements in Parts Per Million (Mn Weight %).												
	Ba	Sr	Mn	Zr	Cr	Cu	Ni	V	Zn	Sc	Y	La	
Errogie Quartz Diorite:	P1093	1549	1152	0.11	299.3	24.19	22.44	26.44	189.50	85.45	15.33	21.13	-
	GP1612	1961	1445	0.10	427.3	24.72	14.74	21.83	118.40	106.1	7.90	43.30	26.82
	P234	2051	1209	0.11	410.0	22.00	18.13	20.50	141.30	82.10	13.32	30.10	15.01
Errogie Qtz Diorite Chliabhain Monzo-diorite Intermediate:	GP1444A	2384	1144	0.10	370.6	16.99	11.55	11.98	94.10	80.90	9.30	16.90	17.31
	GP1444B	2381	1091	0.10	410.8	18.51	11.43	14.99	94.43	75.74	9.33	16.70	19.40
	GP1444E	2035	1024	0.10	362.1	39.00	12.85	24.08	88.70	76.72	8.77	16.27	14.79
Chliabhain Quartz Monzodioritie:	GP592	2407	1095	0.10	425.4	25.88	12.42	18.28	94.13	82.52	8.93	22.55	16.26
	GP654	2324	1087	0.11	406.5	31.46	11.18	16.28	97.10	139.4	9.16	15.79	22.90
	GP640	2886	1118	0.08	346.2	32.85	12.78	21.92	87.97	80.14	7.37	16.40	13.00
	GP648	3650	1181	0.08	386.0	22.24	10.91	19.10	83.64	75.27	7.00	32.82	22.79
	GP107	3045	1317	0.12	397.0	22.85	12.50	17.16	101.60	98.10	11.52	25.44	33.47
	P1574	2721	1009	0.10	352.7	29.30	11.04	21.17	80.76	95.62	7.96	27.79	19.68
Dalcrag Granodioritie:	GP1680	1813	792.3	0.09	259.0	28.62	11.43	25.97	90.39	67.79	10.05	22.89	28.38
	GP1702	1657	790.3	0.10	270.0	33.28	12.94	24.72	97.70	76.51	10.19	19.71	30.37
	P1270	1708	785.0	0.09	280.0	31.00	11.80	23.90	90.10	72.30	8.83	23.00	31.43
	P1246	2369	1099	0.06	221.0	38.28	6.29	29.13	46.90	45.80	5.88	5.28	-
Dungarbh Granodiorite:	GP414	1769	539.7	0.09	201.0	34.26	6.00	24.90	63.80	77.31	7.68	26.70	33.13
	GP416	1313	570.4	0.09	198.1	20.50	4.60	20.80	53.20	86.58	6.40	21.23	18.40
Aberchalder Adamalite:	P948	1091	334.7	0.03	90.8	14.42	2.36	9.60	17.08	18.00	2.37	4.83	-
	P780	606	167.0	0.03	155.6	15.00	3.11	9.20	20.42	34.32	4.81	9.5	5.50
	P835	974	247.0	0.03	63.0	10.05	4.15	7.05	13.41	22.20	2.63	4.40	-
	PX1	008	264.0	0.03	92.2	24.10	2.20	8.30	16.20	20.60	2.80	6.00	-
	P945	1091	334.0	0.05	143.0	14.41	2.36	9.60	17.80	33.81	5.00	19.80	-
	P944	955	322.0	0.06	197.2	19.90	4.10	12.20	28.23	42.80	5.26	19.53	12.97



APPENDIX C. ESTIMATION OF THE DILATIONAL AND REPLACIVE  
COMPONENTS INVOLVED IN GRANITOID VEINING.

The estimation of dilational and replacive components, (stoping), was conducted in the field at two localities in the Central Psammite Septum. At each locality two parallel and distinctive "marker" beds were traced from an area of few granitoid veins into an area of plentiful veins. The veins were parallel sided and also lenticular in nature. The distances between the marker beds inside and outside the veined areas were measured. The proportion of veins to psammite between the two marker beds, (the mean of four traverses between the markers beds), was also calculated within the intensely and sparsely veined areas. If veining was purely dilational, then when moving from the lightly to heavily veined areas, the distance between the marker beds should increase by an amount equal to the combined increase in thickness of the granitoid veins. If the increase in distance between the marker beds is less than the extra thickness of granitoid veins, stoping may be a component in the veining.

APPENDIX D. USE OF MARKERS IN ESTIMATION OF STRAIN IN THE  
FOYERS COMPLEX ENVELOPE.

D1 Boudin Extension.

At certain localities in the Foyers envelope, the total length and reconstructed pre-boudinage length of calc-silicate boudin trains were measured on horizontal surfaces. Calc-silicates were used, as they are the lithology showing the least plastic deformation prior to fracture, and thus provide the most accurate strain marker. Calc-silicates also form distinctive ribs that are easy to trace across the outcrop.

Calc-silicate boudin trains were measured at the following localities; the Beinn Dubhcharaidh ridge, Maol Chnoc and Croftdhu on the northern margin, Carn Gairbthinn and the Whitebridge plantation on the southern margin, and also a number of localities within the Central Septum. The boudin extension was calculated using  $e=(lf-1)/l$ .

D2 Metamorphic Spots.

Orientated samples of spotted amphibolite were removed from the field and sectioned perpendicular to the principal axes of the spots, revealing that the spots had spherical, oblate and prolate morphologies. In each sample a mean of 25 spots per section plane were measured and the orientation of the major axes noted. The amount of data collected was limited



by the number of amphibolites within the aureole, and of  
these, those that contain the mineral spots.

APPENDIX E. MICROPROBE ANALYSIS OF MINERALS WITHIN  
THE FOYERS ENVELOPE.

The minerals from three rock slides were analysed on an Electron microprobe at the University of Manchester, Department of Geology. Prior to analysis the rock slides were polished in four stages, using 6 micron, 3 micron, 1 micron and 0.25 micron aluminium oxide paste, and were then carbon coated.

The electron microprobe used was a CAMECA CAMEBAX, 15 Kv, with a LINK Analytical Energy Dispersive System. Software was the commercially available ZAF4 system.

The results of analysis are presented in tables E1.

## SLIDE 2210 - GARNET:

TABLE E1

Oxide Wt % Formula	Si	Ti	Al	Cr	Fe	Mn	Mg	Ca	Na	K	Total.
<hr/>											
Garnet A: Rim:	37.480 2.975	0.098 0.006	21.44 2.006	0.0 0.0	36.30 2.41	3.99 0.269	2.130 0.252	1.010 0.086	0.147 0.022	0.0 0.0	102.602 8.027
	37.910 2.993	0.065 0.004	21.75 2.024	0.065 0.004	36.098 2.380	3.390 0.227	2.044 0.240	0.912 0.077	0.474 0.092	0.0 0.0	102.712 8.051
	37.630 2.990	0.0 0.0	21.54 2.017	0.080 0.005	35.610 2.36	3.725 0.250	2.133 0.252	0.889 0.075	0.500 0.077	0.0 0.0	102.119 8.036
	37.968 2.979	0.049 0.003	21.835 2.020	0.003 0.0	36.159 2.373	3.768 0.250	2.403 0.281	1.016 0.085	0.186 0.028	0.0 0.0	103.380 8.021
Core:	37.980 2.980	0.044 0.002	21.848 2.021	0.025 0.004	36.571 2.401	3.610 0.240	2.220 0.260	0.912 0.076	0.160 0.024	0.0 0.0	103.438 8.015
	38.024 2.997	0.136 0.009	21.677 2.014	0.0 0.0	36.437 2.402	3.621 0.242	2.003 0.235	0.987 0.083	0.0 0.0	0.133 0.013	103.020 7.995
	37.984 2.99	0.102 0.006	21.528 1.998	0.093 0.006	36.481 2.402	3.752 0.250	2.040 0.239	0.920 0.077	0.423 0.064	0.0 0.0	103.323 8.034
	38.136 2.994	0.021 0.001	21.574 1.997	0.0 0.0	35.90 2.357	3.819 0.254	2.466 0.278	1.271 0.107	0.063 0.009	0.013 0.002	103.264 8.001
Rim:	37.405 2.996	0.0 0.0	21.363 2.017	0.0 0.005	35.713 2.392	3.727 0.253	1.765 0.210	1.072 0.092	0.318 0.049	0.049 0.005	101.501 8.020

XXXVI

SLIDE 2210 - GARNET: TABLE E1

Oxide Wt % Formula	Si	Ti	Al	Cr	Fe	Mn	Mg	Ca	Na	K	Total.
<hr/>											
Garnet B: Rim:											
	37.247	0.0	21.641	0.138	34.839	4.070	1.979	0.911	0.180	0.0	100.843
	2.911	0.0	2.048	0.009	2.339	0.277	0.235	0.078	0.003	0.0	7.982
	38.334	0.082	22.059	0.0	35.560	4.225	2.292	1.029	0.151	0.0	103.733
	2.922	0.005	2.029	0.0	2.321	0.259	0.267	0.086	0.023	0.0	8.000
	37.802	0.0	21.982	0.0	35.342	4.048	2.294	1.016	0.306	0.0	102.790
	2.979	0.0	2.042	0.0	2.329	0.270	0.239	0.086	0.047	0.0	8.023
	38.008	0.0	21.686	0.0	35.346	4.031	2.231	1.128	0.310	0.063	102.802
	2.996	0.0	2.016	0.0	2.330	0.269	0.262	0.095	0.048	0.007	8.023
Core:											
	38.029	0.084	21.323	0.0	35.027	4.205	1.985	0.994	0.427	0.077	102.151
	3.018	0.005	1.994	0.0	2.324	0.283	0.234	0.085	0.066	0.008	8.017
Garnet C:											
	37.280	0.0	21.278	0.0	35.367	4.027	1.568	1.046	0.048	0.0	100.615
	3.009	0.0	2.025	0.0	2.387	0.275	0.188	0.189	0.009	0.0	7.982
	37.676	0.0	21.368	0.025	36.124	3.857	1.879	1.127	0.158	0.038	102.252
	2.997	0.0	2.004	0.001	2.403	0.260	0.223	0.096	0.024	0.004	8.014
	37.969	0.151	21.609	0.010	35.843	3.719	2.186	0.913	0.107	0.049	102.556
	3.000	0.009	2.013	0.001	2.368	0.249	0.258	0.078	0.017	0.005	7.990
	37.701	0.0	21.805	0.002	35.800	3.390	2.360	0.927	0.142	0.0	102.127
	2.988	0.0	2.373	0.0	2.373	0.227	0.279	0.078	0.022	0.0	8.004

SLIDE 2210 - : BIOTITE

TABLE E1

Oxide Wt % Formula	Si	Ti	Al	Cr	Fe	Mn	Mg	Ca	Na	K	Total.
	35.269	4.051	20.063	0.183	22.125	0.191	5.545	0.0	0.499	9.414	97.414
	5.808	0.502	3.894	0.024	3.047	0.027	1.361	0.0	0.159	1.978	16.000
	34.599	4.346	20.194	0.0	22.519	0.372	5.688	0.063	0.713	9.255	97.749
	5.698	0.538	3.920	0.0	3.102	0.052	1.396	0.011	0.228	1.945	16.890
	34.976	3.990	20.013	0.247	23.210	0.0	5.904	0.115	0.470	9.469	98.469
	5.731	0.492	3.865	0.032	3.181	0.0	1.442	0.020	0.149	1.980	16.893
	33.970	3.691	19.617	0.0	22.918	0.151	5.925	0.0	0.444	8.814	95.579
	5.726	0.468	3.897	0.0	3.231	0.022	1.489	0.0	0.145	1.906	16.883
	34.994	4.796	20.151	0.103	21.403	0.069	6.453	0.059	0.104	9.237	97.370
	5.729	0.591	3.889	0.013	2.931	0.010	1.575	0.010	0.330	1.929	16.710
	35.146	3.866	19.966	0.192	22.851	0.0	5.536	0.0	0.212	9.342	97.111
	5.811	0.481	3.891	0.025	3.160	0.0	1.364	0.0	0.068	1.971	16.770
	34.255	3.683	19.730	0.117	23.452	0.0	5.559	0.104	0.181	8.832	95.914
	5.753	0.465	3.906	0.16	3.294	0.0	1.392	0.019	0.059	1.892	16.796
	34.308	3.857	19.747	0.005	22.338	0.211	5.548	0.0	0.445	9.123	95.583
	5.769	0.488	3.914	0.001	3.142	0.030	1.791	0.0	0.145	1.957	16.837
	34.711	3.942	20.436	0.0	22.729	0.119	5.940	0.069	0.729	9.313	97.987
	5.699	0.487	3.955	0.0	3.121	0.017	1.454	0.012	0.232	1.915	16.928
	34.984	3.533	20.135	0.199	22.743	0.025	5.446	0.140	0.0	9.056	96.260
	5.822	0.442	3.950	0.026	3.166	0.004	1.357	0.025	0.0	1.923	16.709
	34.869	4.007	20.711	0.074	22.048	0.182	6.020	0.182	0.335	9.453	97.881
	5.709	0.493	3.997	0.010	3.019	0.025	1.469	0.032	0.106	1.974	16.835



SLIDE 2210 - : BIOTITE continued:

TABLE E1

Oxide Wt % Formula	Si	Ti	Al	Cr	Fe	Mn	Mg	Cn	Na	K	Total.
	34.699 5.765	3.440 0.430	20.765 4.066	0.0 0.0	22.175 3.081	0.233 0.033	5.609 1.389	0.086 0.015	0.023 0.007	9.328 1.977	96.357 16.764
	35.083 5.795	3.643 0.453	20.338 3.959	0.0 0.0	22.574 3.118	0.0 0.0	5.574 1.372	0.0 0.0	0.584 0.187	9.324 1.965	97.120 16.847
	34.105 5.746	3.695 0.468	19.951 3.962	0.235 0.031	22.361 3.151	0.0 0.0	5.634 1.415	0.039 0.007	0.136 0.045	9.184 1.974	95.340 16.799
	35.079 5.802	4.068 0.506	19.891 3.878	0.023 0.003	22.541 3.118	0.093 0.013	5.508 1.358	0.063 0.011	0.410 0.132	9.435 1.991	97.112 16.812
	35.007 5.810	3.903 0.487	19.889 3.891	0.128 0.017	22.630 3.141	0.0 0.0	5.537 1.368	0.0 0.0	0.275 0.089	9.346 1.956	96.709 16.888
	34.840 5.722	3.969 0.490	20.504 3.909	0.0 0.0	22.262 3.058	0.288 0.040	5.881 1.440	0.0 0.0	0.669 0.213	9.336 1.956	97.748 16.888
	34.057 5.796	3.905 0.500	19.145 3.841	0.122 0.016	22.990 3.272	0.008 0.001	5.016 1.293	0.114 0.021	0.243 0.080	9.158 1.989	94.837 16.801
	34.378 5.724	4.053 0.507	20.088 3.940	0.191 0.025	22.776 3.170	0.130 0.018	5.533 1.373	0.021 0.004	0.348 0.112	9.124 1.937	96.661 16.811
	34.610 5.749	3.843 0.480	20.346 3.983	0.0 0.0	22.346 3.104	0.0 0.0	5.360 1.426	0.004 0.001	0.369 0.119	9.219 1.954	96.479 16.816
	33.469 5.737	3.737 0.482	19.833 4.007	0.026 0.003	21.518 3.085	0.153 0.022	5.452 1.393	0.200 0.037	0.611 0.203	8.318 1.819	93.318 16.787
	34.850 5.759	3.725 0.463	20.642 4.021	0.0 0.0	21.859 3.021	0.370 0.052	5.685 1.401	0.129 0.023	0.309 0.099	9.285 1.957	96.854 16.796

SLIDE 2210 - : CORDIERITE: TABLE E1

Oxide Wt % Formula	Si	Ti	Al	Cr	Fe	Mn	Mg	Cn	Na	K	Total.
	48.736	0.0	33.345	0.0	12.586	0.423	5.771	0.0	0.452	0.040	101.334
	4.974	0.0	4.011	0.0	1.072	0.036	0.878	0.0	0.158	0.005	11.06
	47.800	0.0	32.763	0.0	11.257	0.412	5.357	0.0	0.504	0.309	98.542
	4.938	0.0	4.039	0.0	0.984	0.036	0.834	0.0	0.114	0.041	11.054
	47.874	0.129	33.133	0.0	12.518	0.454	5.721	0.086	0.511	0.0	100.428
	4.938	0.009	4.029	0.0	1.08	0.039	0.879	0.009	0.102	0.0	11.088
	48.398	0.036	32.793	0.024	12.197	0.339	5.564	0.00	0.10	0.068	99.518
	5.013	0.003	4.003	0.002	1.056	0.03	0.858	0.00	0.02	0.009	10.995
	48.67	0.034	33.253	0.092	11.62	0.628	5.865	0.081	0.179	0.00	100.42
	4.99	0.002	4.019	0.007	0.996	0.054	0.897	0.009	0.035	0.00	11.012
	48.00	0.040	32.50	0.00	8.623	0.586	5.071	0.006	1.487	2.563	97.89
	5.07	0.003	4.047	0.00	0.762	0.025	0.663	0.00	0.304	0.345	11.22
	48.57	0.00	33.187	0.00	10.846	0.357	5.171	0.00	1.27	0.963	100.36
	5.00	0.00	4.029	0.00	0.934	0.032	0.794	0.00	0.253	0.126	11.172
	48.144	0.057	33.294	0.00	11.799	0.324	6.135	0.04	0.812	0.022	100.95
	4.94	0.004	4.028	0.00	1.01	0.028	0.939	0.004	0.161	0.003	11.121
	47.722	0.00	32.902	0.00	11.756	0.593	5.763	0.028	0.265	0.00	99.03
	4.97	0.00	4.02	0.00	1.023	0.052	0.894	0.003	0.053	0.00	11.037
	47.452	0.033	30.042	0.158	9.707	0.226	3.960	0.145	0.362	0.362	89.594
	4.94	0.003	4.123	0.014	0.945	0.022	0.687	0.018	0.081	0.081	11.22
	48.48	0.031	33.39	0.00	11.86	0.479	5.80	0.00	0.444	0.50	100.548
	4.973	0.002	4.037	0.00	1.809	0.041	0.886	0.00	0.088	0.006	11.05



SLIDE 2210 - : CORDIERITE Continued:

TABLE E1

Oxide Wt % Formula	Si	Ti	Al	Cr	Fe	Mn	Mg	Cn	Na	K	Total.
47.584 4.998	0.00 0.00	32.326 4.002	0.00 0.00	11.963 1.05	0.310 0.027	5.529 0.865	0.102 0.011	0.423 0.086	0.00 0.00	98.236 11.043	
48.88 5.00	0.088 0.006	33.211 4.005	0.036 0.003	12.175 1.041	0.399 0.0345	5.796 0.883	0.00 0.00	0.137 0.027	0.005 0.00	100.732 11.0	
48.484 4.97	0.00 0.00	33.410 4.037	0.050 0.00	12.047 1.032	0.507 0.044	5.670 0.866	0.001 0.00	0.54 0.107	0.00 0.00	100.709 11.062	
48.387 4.99	0.128 0.010	33.213 4.044	0.00 0.00	10.426 0.90	0.212 0.018	5.083 0.783	0.117 0.087	1.129 0.225	1.320 0.99	100.015 11.169	
48.326 4.988	0.00 0.00	33.164 4.035	0.009 0.00	12.138 1.047	0.202 0.018	5.647 0.869	0.071 0.007	0.271 0.054	0.00 0.00	99.828 11.02	
48.223 4.988	0.00 0.00	32.862 4.00	0.00 0.00	12.01 1.038	0.393 0.034	5.845 0.90	0.043 0.004	0.351 0.07	0.00 0.00	99.725 11.043	
48.442 4.947	0.00 0.00	33.34 4.038	0.00 0.00	12.108 1.041	0.450 0.069	5.776 0.885	0.00 0.00	0.189 0.037	0.00 0.00	100.304 11.029	
48.402 4.992	0.00 0.00	32.765 3.983	0.095 3.983	12.291 0.007	0.254 1.059	5.65 0.022	0.00 0.868	0.795 0.00	0.007 0.159	100.258 11.093	
47.213 5.01	0.00 0.00	32.127 4.018	0.00 0.00	11.744 1.043	0.415 0.037	5.186 0.82	0.002 0.00	0.345 0.07	0.231 0.031	97.263 11.031	
48.95 4.953	0.00 0.00	33.68 4.017	0.12 0.009	12.534 1.06	0.322 0.028	6.145 0.927	0.013 0.002	0.363 0.071	0.00 0.00	102.133 11.068	

SLIDE 2210 - : PLAGIOCLASE:

TABLE E1

Oxide Wt % Formula	Si	Ti	Al	Cr	Fe	Mn	Mg	Cn	Na	K	Total.
XII	57.547	0.027	24.06	0.00	1.48	0.194	0.00	6.511	6.676	0.215	96.713
	2.666	0.001	1.314	0.00	0.057	0.007	0.00	0.323	0.599	0.012	4.98
	60.652	0.00	25.26	0.00	0.307	0.00	0.00	6.767	8.061	0.091	101.139
	2.675	0.00	2.675	0.00	0.011	0.00	0.00	0.32	0.689	0.005	5.015
	61.592	0.033	25.542	0.00	0.012	0.00	0.00	6.434	8.214	0.309	102.136
	2.685	0.001	1.313	0.00	0.001	0.00	0.00	0.300	0.694	0.01	5.012
	62.089	0.026	24.949	0.00	0.011	0.089	0.00	5.726	8.299	0.298	101.486
	2.71	0.001	1.257	0.00	0.00	0.003	0.00	0.268	0.704	0.016	4.998
	59.52	0.00	25.714	0.00	0.412	0.066	0.054	6.785	8.138	0.196	100.88
	2.64	0.00	1.345	0.00	0.015	0.002	0.003	0.322	0.70	0.011	5.041
	60.117	0.00	25.86	0.00	0.313	0.032	0.00	7.438	7.841	0.204	101.81
	2.64	0.00	1.34	0.00	0.116	0.001	0.00	0.350	0.668	0.011	5.026
59.567	0.00	25.354	0.102	0.190	0.00	0.00	7.289	7.386	0.135	100.024	
2.657	0.00	1.333	0.003	0.007	0.00	0.00	0.348	0.639	0.008	4.997	
60.55	0.027	24.91	0.097	0.029	0.01	0.00	6.398	7.504	0.237	99.768	
2.697	0.001	1.307	0.003	0.001	0.00	0.00	0.305	0.548	0.013	4.977	
61.117	0.00	25.729	0.008	0.07	0.04	0.00	6.716	7.823	0.329	101.83	
2.674	0.00	1.327	0.00	0.002	0.009	0.00	0.315	0.663	0.018	5.003	

XLII

SLIDE 2210 - : ILMENITE: TABLE E1

Oxide Wt % Formula	Si	Ti	Al	Cr	Fe	Mn	Mg	Cn	Na	K	Total.
0.454	52.228	0.00	0.00	0.00	44.342	2.035	0.00	0.00	0.162	0.033	99.254
0.011	0.995	0.00	0.00	0.00	0.939	0.043	0.00	0.00	0.008	0.001	1.998
0.32	53.898	0.148	0.023	0.023	45.327	1.853	0.291	0.015	0.548	0.00	102.42
0.008	0.993	0.004	0.00	0.00	0.93	0.038	0.010	0.00	0.026	0.00	2.00
2.743	49.47	1.199	0.105	0.105	39.528	2.935	2.308	0.00	0.352	0.06	98.70
0.067	0.918	0.035	0.002	0.002	0.816	0.061	0.085	0.00	0.017	0.002	2.004
0.376	53.177	0.00	0.00	0.00	45.29	1.288	0.00	0.077	0.00	0.00	100.19
0.009	1.001	0.00	0.00	0.00	0.948	0.027	0.00	0.002	0.00	0.00	1.988

## SLIDE 2300 - GARNET:

TABLE E1

Oxide Wt % Formula	Si	Ti	Al	Cr	Fe	Mn	Mg	Ca	Na	K	Total.
<hr/>											
Garnet D:	37.086	0.064	21.403	0.0	35.153	3.617	2.363	1.011	0.180	0.001	100.818
	2.979	0.004	2.027	0.0	2.362	0.246	0.283	0.087	0.028	0.0	8.017
	37.392	0.044	21.399	0.001	35.831	3.775	2.406	0.992	0.061	0.001	101.902
	2.98	0.003	2.01	0.0	2.388	0.255	0.286	0.85	0.009	0.0	8.016
	37.820	0.0	21.309	0.0	36.370	3.867	1.977	0.944	0.126	0.003	102.414
	3.000	0.0	1.995	0.0	2.416	0.260	0.234	0.080	0.019	0.0	8.00
	37.528	0.0	21.711	0.0	35.658	3.783	1.887	1.004	0.189	0.001	101.752
	2.990	0.0	2.04	0.0	2.377	0.255	0.244	0.085	0.029	0.0	8.00
Garnet E:	37.87	0.087	21.839	0.001	35.887	4.036	2.124	0.911	0.354	0.002	103.105
	2.981	0.005	2.027	0.0	2.363	0.269	0.249	0.077	0.054	0.0	8.026
	36.765	0.065	21.174	0.0	35.766	3.424	1.836	1.104	0.0	0.001	100.136
	2.985	0.004	2.026	0.0	2.428	0.235	0.272	0.96	0.0	0.0	7.998
	37.167	0.054	20.970	0.198	36.023	3.663	1.527	1.005	0.200	0.0	100.857
	3.002	0.003	1.996	0.012	2.433	0.250	0.184	0.091	0.031	0.0	8.000
	36.956	0.070	21.338	0.081	34.81	4.116	2.160	1.032	0.179	0.0	100.749
	2.97	0.004	2.026	0.005	2.345	0.281	0.260	0.089	0.028	0.0	8.010



SLIDE 2300 - GARNET continued: TABLE E1

Oxide Wt % Formula	Si	Ti	Al	Cr	Fe	Mn	Mg	Ca	Na	K	Total.
Garnet F:	37.648	0.0	21.46	0.16	36.063	3.686	2.321	1.162	0.615	0.0	103.114
Garnet G:	37.032	0.0	21.029	0.093	35.430	3.697	1.762	1.143	0.0	0.017	100.204
	3.003	0.0	2.010	0.006	2.403	0.254	0.213	0.099	0.0	0.001	7.990
	36.889	0.086	20.966	0.0	34.996	3.528	2.216	1.018	0.149	0.0	99.854
	2.995	0.005	2.007	0.0	2.377	0.242	0.268	0.088	0.024	0.0	8.00
	37.105	0.0	21.097	0.091	35.343	3.428	2.133	0.986	0.119	0.0	100.302
	3.00	0.0	2.01	0.006	2.389	0.234	0.257	0.085	0.018	0.0	8.001
Garnet H: Rim:	37.645	0.114	21.391	0.021	35.519	4.192	1.719	0.988	0.0	0.0	101.588
	3.008	0.007	2.014	0.0	2.373	0.283	0.204	0.084	0.0	0.0	7.990
	37.726	0.101	21.626	0.073	35.852	3.608	2.065	1.035	0.117	0.027	102.230
	2.992	0.006	2.002	0.005	2.378	0.242	0.244	0.088	0.018	0.002	7.997
Core:	37.184	0.0	20.996	0.040	35.357	3.869	1.842	1.038	0.098	0.0	100.423
	3.008	0.0	2.002	0.003	2.392	0.265	0.222	0.09	0.015	0.0	7.997
	37.518	0.083	21.604	0.139	35.217	3.911	2.244	1.012	0.106	0.0	101.834
	2.985	0.005	2.026	0.008	2.343	0.263	0.266	0.086	0.016	0.0	8.000
Rim:	38.228	0.037	22.176	0.0	36.369	4.000	2.123	0.974	0.237	0.0	104.144
	2.979	0.002	2.037	0.0	2.37	0.246	0.246	0.081	0.036	0.0	8.017

SLIDE 2300 - BIOTITE: TABLE E1

Oxide Wt % Formula	Si	Ti	Al	Cr	Fe	Mn	Mg	Ca	Na	K	Total.
34.154 5.831	3.322 0.427	19.077 3.839	0.0 0.0	22.735 3.246	0.026 0.004	5.800 1.476	0.0 0.0	0.085 0.028	9.068 1.975	94.267 16.825	
	35.028 5.730	3.881 0.477	20.571 3.967	0.103 0.013	22.177 3.034	0.0 0.0	6.128 1.494	0.0 0.0	0.580 0.184	9.521 1.987	97.988 16.88
34.622 5.844	3.602 0.457	19.621 3.903	0.0 0.0	22.062 3.114	0.088 0.013	5.635 1.418	0.0 0.0	0.0 0.0	9.274 1.997	94.904 16.746	
	34.277 5.762	4.097 0.518	19.927 3.948	0.127 0.017	22.376 3.146	0.189 0.027	5.057 1.267	0.0 0.0	0.358 0.117	9.289 1.992	95.675 16.792
34.625 5.798	3.425 0.431	20.138 3.975	0.0 0.0	21.734 3.044	0.105 0.015	5.769 1.440	0.0 0.0	0.540 0.175	9.285 1.984	95.622 16.862	
	35.457 5.771	3.665 0.449	20.739 3.978	0.0 0.0	22.194 3.021	0.071 0.010	6.238 1.514	0.0 0.0	0.434 0.137	9.446 1.961	98.245 16.840
34.572 5.777	3.502 0.440	19.530 3.846	0.108 0.014	23.452 3.277	0.088 0.012	5.730 1.427	0.0 0.0	0.429 0.139	9.285 1.979	96.694 16.912	
	34.304 5.731	3.323 0.418	19.853 3.910	0.090 0.012	23.458 3.282	0.0 0.0	6.115 1.523	0.0 0.0	0.265 0.086	9.120 1.944	96.550 16.905
34.372 5.794	3.276 0.415	19.628 3.900	0.0 0.0	23.158 3.265	0.0 0.0	5.693 1.431	0.032 0.000	0.244 0.090	9.210 1.981	95.612 16.87	
	32.677 5.766	3.144 0.417	18.556 3.859	0.057 0.008	22.388 3.304	0.260 0.039	5.496 1.446	0.029 0.005	0.148 0.051	9.97 2.030	91.771 16.924

SLIDE 2300 - CORDIERITE: TABLE E1

Oxide Wt % Formula	Si	Ti	Al	Cr	Fe	Mn	Mg	Ca	Na	K	Total.
47.250 0.0	31.995 0.079	12.008 0.135	5.443 0.012	0.188 0.054	97.165						
5.013 0.0	4.001 0.006	1.065 0.012	0.861 0.002	0.038 0.007	11.00						
47.870 0.0	32.884 0.116	11.884 0.281	5.588 0.046	0.320 0.0	98.969						
4.984 0.0	4.035 0.009	1.032 0.024	0.867 0.005	0.064 0.0	11.025						
47.816 0.002	32.113 0.0	11.959 0.339	5.528 0.130	0.373 0.0	98.260						
5.02 0.0	3.974 0.0	1.05 0.030	0.865 0.014	0.075 0.0	11.030						
48.688 0.0	33.280 0.0	11.943 0.435	5.997 0.0	0.628 0.069	101.041						
4.970 0.0	4.008 0.0	1.020 0.037	0.913 0.0	0.124 0.009	11.088						
46.891 0.039	31.850 0.0	12.045 0.230	5.345 0.0	0.305 0.0	96.704						
5.004 0.003	4.005 0.0	1.074 0.021	0.850 0.0	0.063 0.0	11.022						
48.376 0.027	32.576 0.168	12.156 0.395	5.512 0.064	0.524 0.0	99.799						
5.007 0.002	3.975 0.013	1.052 0.034	0.850 0.006	0.105 0.0	11.04						
47.303 0.013	32.419 0.066	11.868 0.302	5.496 0.116	0.220 0.0	97.800						
4.986 0.0	4.028 0.005	1.046 0.027	0.864 0.013	0.045 0.0	11.017						
47.85 0.090	32.89 0.0	11.986 0.228	5.586 0.024	0.484 0.0	99.143						
4.977 0.006	4.032 0.0	1.042 0.020	0.866 0.003	0.097 0.0	11.04						



SLIDE 2300 - PLAGIOCLASE: TABLE E1

Oxide Wt % Formula	Si	Ti	Al	Cr	Fe	Mn	Mg	Ca	Na	K	Total.
59.795	0.021		26.126	0.0	0.823	0.150	0.0	7.348	7.616	0.134	102.014
2.628	0.0		1.354	0.0	0.03	0.005	0.0	0.346	0.649	0.007	5.318
60.149	0.010		25.741	0.0	0.0	0.056	0.0	6.701	7.615	0.216	100.490
2.66	0.0		1.344	0.0	0.0	0.002	0.0	0.318	0.654	0.012	4.996
61.764	0.0		24.323	0.081	0.0	0.038	0.0	5.869	8.233	0.160	100.468
2.72	0.0		1.26	0.002	0.0	0.001	0.0	0.278	0.705	0.009	4.993

SLIDE 2735 - GARNET: TABLE E1

Oxide Wt % Formula	Si	Ti	Al	Cr	Fe	Mn	Mg	Ca	Na	K	Total.
<hr/>											
Garnet I: Rim:	37.806	0.0	21.478	0.063	29.568	8.919	1.908	1.844	0.226	0.011	101.820
	3.004	0.0	2.012	0.004	1.965	0.600	0.226	0.157	0.035	0.001	8.005
	36.713	0.104	20.715	0.063	29.302	7.917	2.144	2.650	0.106	0.0	99.715
	2.984	0.006	1.984	0.004	1.992	0.545	0.260	0.231	0.016	0.0	8.024
	39.949	0.0	21.642	0.081	27.148	7.424	2.159	2.198	1.530	0.0	102.130
	3.10	0.0	1.984	0.005	1.765	0.489	0.250	0.183	0.230	0.0	8.014
Core:	37.573	0.085	21.345	0.0	29.853	8.066	2.303	2.605	0.042	0.001	101.870
	2.984	0.005	1.998	0.0	1.983	0.542	0.272	0.215	0.007	0.0	8.015
	36.851	0.097	21.043	0.037	29.846	7.544	1.915	2.163	0.098	0.024	99.616
	2.993	0.006	2.014	0.003	2.028	0.519	0.232	0.188	0.015	0.003	8.001
	37.612	0.201	21.579	0.0	30.024	8.037	2.038	2.312	2.132	0.429	102.440
	2.973	0.012	2.010	0.0	1.984	0.538	0.243	0.272	0.180	0.065	8.048
Rim:	37.612	0.097	21.151	0.0	28.923	8.573	2.038	2.062	0.262	0.159	100.851
	3.001	0.006	1.997	0.0	1.983	0.582	0.243	0.177	0.041	0.016	8.012

SLIDE 2735 - GARNET continued: TABLE E1

Oxide Wt % Formula	Si	Ti	Al	Cr	Fe	Mn	Mg	Ca	Na	K	Total.
Garnet J:	37.353 3.006	0.089 0.005	20.937 1.987	0.094 0.006	29.304 1.972	7.664 0.522	1.927 0.231	3.004 0.259	0.0 0.0	0.095 0.001	100.460 7.997
	37.268 2.985	0.0 0.0	21.384 2.019	0.0 0.0	29.550 1.979	8.005 0.543	1.970 0.235	2.737 0.235	0.101 0.015	0.0 0.0	101.467 7.986
	37.653 3.015	0.003 0.0	21.154 1.985	0.036 0.003	30.463 2.039	8.154 0.552	1.974 0.235	1.703 0.146	0.0 0.0	0.0 0.0	101.163 7.986
	37.726 2.957	0.0 0.0	21.569 2.004	0.056 0.004	29.728 1.963	8.034 0.537	2.181 0.256	2.726 0.230	0.520 0.079	0.0 0.0	102.540 8.050
	38.081 2.996	0.159 0.009	21.596 1.932	0.154 0.009	29.360 2.003	8.038 0.535	2.123 0.249	2.800 0.236	0.233 0.035	0.0 0.0	102.551 8.006
	38.364 3.026	0.022 0.002	21.485 1.997	0.026 0.002	29.268 1.931	8.409 0.562	1.790 0.210	2.854 0.241	0.0 0.0	0.033 0.035	102.240 7.974

SLIDE 2735 - BIOTITE: TABLE E1

Oxide Wt % Formula	Si	Ti	Al	Cr	Fe	Mn	Mg	Ca	Na	K	Total.
35.348	3.285	18.892	0.0	22.499	0.391	7.191	0.104	0.738	9.664	98.111	
5.815	0.406	3.663	0.0	3.095	0.054	1.761	0.018	0.235	2.028	17.079	
34.457	2.815	18.114	0.068	21.632	0.519	7.316	0.0	0.0	9.283	94.233	
5.879	0.361	3.649	0.009	3.087	0.075	1.861	0.0	0.0	2.021	6.941	
34.805	3.891	18.315	0.110	22.537	0.343	6.362	0.068	0.015	9.036	95.482	
5.864	0.493	3.637	0.015	3.176	0.049	1.598	0.002	0.005	1.942	16.791	
33.439	2.818	18.387	0.069	23.471	0.321	5.911	0.015	0.0	9.032	93.462	
5.807	0.368	3.764	0.009	3.409	0.047	1.530	0.000	0.0	2.001	16.939	
34.457	2.891	18.529	0.110	23.400	0.505	6.091	0.048	0.242	9.223	95.496	
5.849	0.369	3.707	0.015	3.322	0.073	1.541	0.009	0.080	1.997	16.960	
35.325	2.829	18.542	0.128	23.535	0.558	5.275	0.0	0.284	9.236	95.712	
5.969	0.360	3.693	0.017	3.326	0.080	1.329	0.0	0.093	1.991	16.858	

# APPENDIX F.

## TABLE SHOWING THE POSITIONS OF FIELD LOCALITIES REFERENCED IN THE TEXT AND FIGURES OF THE THESIS.

A.A.= ABERCHALDER ADAMELLITE.  
 C.Q.M.D.= CHLIABHAIN QUARTZ MONZODIORITE.  
 D.G.= DALCRAG GRANODIORITE.  
 D.G.G.= DUNGARBH GRANODIORITE.  
 E.Q.D.= ERROGIE QUARTZ DIORITE  
 E.Q.D.I.= ERROGIE QUARTZ DIORITE INTERMEDIATE.  
 A.D.= APPINITIC DIORITE.  
 M.D.= MICRODIORITE DYKES.  
 M.E.= MICRODIORITE ENCLAVES.  
 M.C.G.= MAOL CHNOC GRANODIORITE.  
 M.C.A.= MAOL CHNOC ADAMELLITE.

### Samples used in granitoid geochemical analyses.

Locality	Lithology	Grid reference.
PX1	A.A.	NH53001841
GP107	C.Q.M.D.	NH54502280
P234	E.Q.D.	NH24602388
GP414	D.G.G.	NH52352184
GP416	D.G.G.	NH52162173
GP592	C.Q.M.D.	NH55672116
GP640	C.Q.M.D.	NH56102046
GP648	C.Q.M.D.	NH56032020
GP654	C.Q.M.D.	NH56202045
P780	A.A.	NH57322012
P835	A.A.	NH55531859
P944	A.A.	NH55451864
P945	A.A.	NH55861845
P948	A.A.	NH55841839
P1093	E.Q.D.	NH53161864

contd..

..contd.

Locality	Lithology	Grid reference.
P1246	D.G.	NH51781557
P1270	D.G.	NH51651650
GP1444A	E.Q.D.I.	NH54562012
GP1444B	E.Q.D.I.	NH54592012
GP1444E	E.Q.D.I.	NH54732015
P1574	C.Q.M.D.	NH57001814
GP1612	E.Q.D.	NH53952262
GP1680	D.G.	NH51731760
GP1702	D.G.	NH51391789

Envelope localities used for quantative structural analyses.

Locality	Grid reference.
233	NH55732397
1244	NH51691541
1253	NH51501538
1945	NH56172355
1962	NH55942493
2093	NH59501915
2095	NH59551920
2136	NH58932050
2139	NH58762010
2192	NH58652263
2205	NH53271715
2212	NH58501720
2216	NH53661717
2361	NH52551715
2362	NH52611722
2396	NH58201579
2826	NH47541555

Slides used in granitoid petrography descriptions.

Locality	Lithology	Grid reference.
PX1	A.A.	NH53001841
P15	E.Q.D.	NH53952285
P109	E.Q.D.	NH54512282
P127	E.Q.D.	NH54432161
P226	E.Q.D.	NH55092465
P186	M.D.	NH54392155
P23811	M.E.	NH55792360
P238111	E.Q.D.	NH55792160
P283	M.E.	NH55452311
P305	M.E.	NH55752297
P640	C.Q.M.D.	NH56102046
P648	C.Q.M.D.	NH56032020
P673	A.D.	NH56252087
P737	A.A.	NH57182045
P749	A.D.	NH57502075
P835	A.A.	NH55531859
P944	A.D.	NH55661780
P1093	E.Q.D.	NH53181864
P1101	C.Q.M.D.	NH52861850
P1154	D.G.	NH52362066
P1214	C.Q.M.D.	NH54051820
P1156	C.Q.M.D.	NH54661846
P1240B	A.A.	NH57431872
P1363	D.G.	NH50901618
P1444E	E.Q.D.I.	NH54732015
P1480	A.A.	NH52422095
P1488	E.Q.D.	NH52582084
P1529	M.D.	NH53802122
P1543	M.D.	NH52982149
P1592	M.D.	NH53552189

contd..



..contd

Locality	Lithology	Grid reference.
P1612	E.Q.D.	NH53952262
P1671	A.D.	NH51201732
P1680	D.G.	NH51731760
P1702	D.G.	NH51391789
P1706B	D.G.	NH51661694
P1785	M.D.	NH50351897
P1858	D.G.	NH52262225
1998A	M.C.G.	NH58082189
1998C	M.C.A.	NH58082189
2001B	M.C.G.	NH58202170
2015	M.C.A.	NH58502141
2134B	M.C.A.	NH58932064
2160A	M.C.G.	NH59402010
P2594	M.D.	NH48051675
P2830	M.D.	NH46541494

Samples of micaceous psammite used in microprobe analyses.

2210	Mic. Psm.	NH53331723
2300	Mic. Psm.	NH52141713
2735	Mic. Psm.	NH46251657.

REFERENCES.

## REFERENCES

- Ahmad, M.U., 1967. Some geophysical observations on the Great Glen Fault. Nature, London., 213, 275-277.
- Aki, K., Chouet, B., Fehler, M. & Zandt, G. 1978. Seismic properties of a shallow magma reservoir in Kilauea Iki by active and passive experiments. Journal of Geophysical Research, 83, B5, 2273-2282.
- Anderson, E.M., 1936. The dynamics of the formation of cone sheets, ring dykes and cauldron subsidences, Proceedings of the Royal Society, Edinburgh., 56, 128-163.
- Anderson, J.G., 1956. The Moinian and Dalradian rocks between Glen Roy and the Monadhliath Mountains, Inverness-shire. Transactions of the Royal Society, Edinburgh, 63, 15-36.
- Arzi, A.A., 1978. Critical phenomena in the rheology of partially melted rocks. Tectonophysics, 44, 173-184.
- Balk, R., 1937. Structural behaviour of igneous rocks. Memoir of the Geological Society of America, 5, 177pp.
- Barr, D., 1985. Migmatites in the Moines. In: Migmatites (ed. Ashworth, J.R.) 180-203. Blackie, Glasgow.

Barriere, M., 1977. Deformation associated with the Ploumanac'h intrusive complex, Brittany. Journal of the Geological Society of London, 134, 311-324.

Barriere, M., 1981. On curved laminae, graded layers, convection currents and dynamic crystal sorting in the Ploumanac'h (Brittany) subalkaline granite. Contributions to Mineralogy and Petrology, 77, 214-224.

Bateman, P.C., Busacca, A.J. & Sawka, W.N., 1983. Cretaceous deformation in the western foothills of the Sierra Nevada, California. Bulletin of the Geological Society of America, 94, 30-42.

Bateman P.C, Kistler, R.W, & DeGraff, J.V., 1988. Part 1, Magmatic and solid state foliations at Courtright Intrusive Zone. In: Criteria for establishing the relative timing of pluton emplacement and regional deformation, Field guide to the Penrose Conference 1988.

Bateman, R., 1984. On the role of diapirism in the segregation, ascent and final emplacement of granitoid magmas. Tectonophysics, 110, 211-231.

Bateman, R., 1985. Aureole deformation by flattening around a diapir during insitu ballooning: the Cannibal Creek granite. Journal of Geology, 93, 293-310.

Barriere, M., 1977. Deformation associated with the Ploumanac'h intrusive complex, Brittany. Journal of the Geological Society of London, 134, 311-324.

Barriere, M., 1981. On curved laminae, graded layers, convection currents and dynamic crystal sorting in the Ploumanac'h (Brittany) subalkaline granite. Contributions to Mineralogy and Petrology, 77, 214-224.

Bateman, P.C., Busacca, A.J. & Sawka, W.N., 1983. Cretaceous deformation in the western foothills of the Sierra Nevada, California. Bulletin of the Geological Society of America, 94, 30-42.

Bateman P.C, Kistler, R.W, & DeGraff, J.V., 1988. Part 1, Magmatic and solid state foliations at Courtright Intrusive Zone. In: Criteria for establishing the relative timing of pluton emplacement and regional deformation, Field guide to the Penrose Conference 1988.

Bateman, R., 1984. On the role of diapirism in the segregation, ascent and final emplacement of granitoid magmas. Tectonophysics, 110, 211-231.

Bateman, R., 1985. Aureole deformation by flattening around a diapir during insitu ballooning: the Cannibal Creek granite. Journal of Geology, 93, 293-310.

page  
included  
to file

- Bateman, R., 1985. Progressive crystallisation of a granitoid diapir and its relationship to stages of emplacement. Journal of Geology, 93, 645-622.
- Bateman, R., 1986. On the role of diapirism in the segregation, ascent and final emplacement of granitoid magmas- Reply. Tectonophysics, 127, 167-169.
- Bateman, R., 1989. Cannibal Creek granite: post tectonic "ballooning" pluton or pre-tectonic piercement diapir?: A discussion. Journal of Geology, 97, 766-768.
- Bell, T.H. & Etheridge, M.A., 1973. Microstructure of mylonites and their descriptive terminology. Lithos, 6, 337-348.
- Berger, A.R. & Pitcher, W.S., 1970. Structures in granitic rocks: a commentary and a critique on granite tectonics. Proceedings of the Geologists Association., 81, 441-461.
- Berner, H., Ramberg, H. & Stephansson, O., 1972. Diapirism in theory and experiment. Tectonophysics, 15, 197-218.
- Blake, D.H., Elwell, R.W.D., Gibson, I.L., Skelhorn, R.R., & Walker, G.P.L., 1965. Relationships resulting from the intimate association of acid and basic magmas. Quarterly Journal of the Geological Society of London, 121, 31-49.

Blake, D.H., 1981. Intrusive felsic-mafic net-veined complexes in North Queensland. B.M.R. Journal of Australian Geology and Geophysics, 6, 95-99.

Bottinga, Y. & Weill, D.F., 1970. Densities of liquid silicate systems calculated from partial molar volumes of oxide components. American Journal of Science, 269, 169-182.

Bottinga, Y. & Weill, D.F., 1972. The viscosity of magmatic silicate liquids: a model for calculation. American Journal of Science, 272, 438-475.

Brown, P.E., Miller, J.A. & Grasty, K.L., 1968. Isotopic ages of late Caledonian granitic intrusions in the British Isles. Proceedings of the Yorkshire Geological Society 36, 251-76.

Brun, J.P. & Pons, J., 1981. Strain patterns of pluton emplacement in a crust undergoing non-coaxial deformation, Sierra Morena, Southern Spain. Journal of Structural Geology, 3, 219-229.

Castro, A., 1986. Structural pattern and ascent model in the Central Extremadura batholith, Hercynian belt, Spain. Journal of Structural Geology, 8, 633-645.



Castro, A., 1987. On granitoid emplacement and related structures. A review. Geologische Rundschau, 76/1, 101-124.

Chappell, B.W. & White, A.J.R., 1974. Two contrasting granite types. Pacific Geology, 8, 173-4.

Chinner, G.A., 1961. The origin of sillimanite in Glen Clova, Angus. Journal of Petrology, 2, 312-323.

Chinner, G.A., 1966. The significance of aluminium silicates in metamorphism. Earth Science Review, 2, 111-126.

Clarke, S.P., Jr., (ed.), 1966. Handbook of Physical constants. Memoir of the Geological Society of America, 97, 587pp.

Coward, M.P., 1981. Diapirism and gravity tectonics: report of the Tectonic Studies Group conference held at Leeds University, 25-26 March 1980. Journal of Structural Geology, 3, 89-95.

Courrioux, G., 1987. Oblique diapirism: the Criffel granodiorite/granite zoned pluton (south west Scotland). Journal of Structural Geology, 9, 313-330.

Dearnley, R., 1967. Metamorphism of minor intrusions associated with the Newer Granites of the Western Highlands of Scotland. Scottish Journal of Geology, 3, 449-457.

Deer, W.A., Howie, R.A. & Zussman, J. 1983. An Introduction to Rock Forming Minerals, 13th impression. Longman. 528pp.

Dixon, J.M., 1975. Finite strain and progressive deformation in models of diapiric structures. Tectonophysics. 28, 89-124.

Ehlers, E.G. & Blatt, H. 1980. Petrology, Igneous, Sedimentary and Metamorphic. Freeman. 732pp.

Emerman, S.H. & Marret R., 1990. Why Dikes?, Geology, 18, 231-233.

Eyles, V.A & MacGregor, A.G. 1972. The Great Glen crush belt. Geological Magazine. 89, 426-436.

Fettes, D.J., Long, C.B., Bevins, R.E., Max, M.D., Oliver, G.J.H., Primmer, T.J., Thomas, L.J., & Yardley, B.W.D., 1985. Grade and time of metamorphism in the Caledonide Orogen of Britain and Ireland. In Harris, A.L. (ed.) The nature and timing of Orogenic activity in the Caledonian rocks of the British Isles. Geological Society of London Memoir No. 9.

French, W.J., 1966. Appinitic intrusions clustered around the Ardara pluton, County Donegal. Proceedings of the Royal Irish Academy 64B, 303-322.

Fyfe, W.S., 1967. The stability of  $Al_2SiO_5$  polymorphs. Chemical Geology, 2, 67-76.

Garson, M.S., Coats, J.S., Rock, N.M.S., & Deans, T., 1984. Fenites, breccia dykes, albites and carbonitic veins near the Great Glen Fault, Inverness, Scotland. Journal of the Geological Society of London, 141, 711-732.

Halliday, A.N., 1984. Coupled Sm-Nd and U-Pb systematics in late Caledonian granites and the basement under northern Britain. Nature, 307, 207-233.

Halliday, A.N., Aftalion, M., van Breemen, O. & Jocelyn, J., 1979. Petrogenetic significance of Rb-Sr and U-Pb isotopic systems in the 400Ma old British Isles granitoids and their hosts. In: Harris, A.L., Holland, C.H. & Leake, B.E. (Eds.), The Caledonides of the British Isles reviewed. Geological Society of London. Special Publication No.8, 653-661.

Harris, A.L., Baldwin, C.T., Bradbury, H.J., Johnson, H.D. & Smith, R.A., 1978. Ensialic basin sedimentation: the Dalradian Supergroup. In Bowes, D.R. and Leake, B.E. (eds.) Crustal evolution in Northwest Britain and adjacent regions. Geological Journal, Special Issue no.10, 115-138.

Harris, A.L., Highton, A.J., Roberts, A.M. & Stoker, M.S., 1983. Discussion on the Glen Kyllachy Granite and its bearing on the nature of the Caledonian Orogeny in Scotland. Journal of the Geological Society of London, 140, 961-963.

Harrison, T.N., 1986. The mode of emplacement of the Cairngorm Granite. Scottish Journal of Geology, 22, 303-314.

Harrison, T.N., Hutchinson, J., 1987. The age and origin of the eastern Grampians Newer Granites. Scottish Journal of Geology, 23, 269-282.

Haselock, P.J. & Winchester, J.A., 1981. A note on the stratigraphic relationship of the Leven Schist and the Monadhliath Schist in the Central Highlands of Scotland. Geological Journal, 16, 237-241.

Haselock, P.J., 1982. The Geology of the Corrieyairack Pass Area, Inverness-shire. PhD thesis, University of Keele, (unpublished).

Haselock, P.J., Winchester, J.A. & Whittles, K.H. 1982. The stratigraphy and structure of the southern Monadhliath Mountains between Loch Killin and Glen Roy. Scottish Journal of Geology, 18, 275-290.

Haselock, P.J., 1984. The systematic geochemical variation between two tectonically separate successions in the Southern Monadhliaths, Inverness-shire. Scottish Journal of Geology, 20, 191-205.

Hatch, F.H., Wells, A.K. & Wells, M.K. 1983. Petrology of Igneous Rocks. Allen and Unwin Ltd.

Hibbard, M.J., 1979. Myrmekite as a marker between preaqueous and postaqueous phase saturation in granitic magmas. Bulletin of the Geological Society of America., 90, 1047-1062.

Hibbard, M.J., 1979. Synneusis stacking of plagioclase and the mantling of alkali feldspar. Geological Society America, Abstract Programme., 11, 84.

Hibbard, M.J. & Watters, R.J., 1985. Fracturing and dyking in incompletely crystallised granitic plutons. Lithos, 18, 1-12.

Hibbard, M.J., 1987. Deformation of incompletely crystallised magma systems: Granitic gneisses and their tectonic implications. Journal of Geology, 95, 543-561.

Highton, A.J., 1986. Caledonian and pre-Caledonian events in the Moines south of the Great Glen. University of Liverpool. (unpubl. Ph.D. thesis.)

Hinxman, L.W. & Anderson, E.M. 1915. The geology of Mid-Strathspey and Strathdean (Explanation of Sheet 74) Memoir of the Geological Survey of Great Britain.

Hobbs, B.E., Means, W.D. & Williams, P.F., 1976. An Outline of Structural Geology, Wiley International. 571pp.

Holdaway, M.J. & Lee, S.M., 1977. Fe-Mg cordierite stability in high grade pelitic rocks based on experimental, theoretical and natural observations. Contributions to Mineralogy and Petrology, 63, 175-198.

Holder, M.T., 1979. An emplacement mechanism for post-tectonic granites and its implications for their geochemical features. In Atherton, M.P. & Tarney, J. (eds.), Origin of granite batholiths. Geochemical evidence. Shiva.

Hossack, J.R., 1967. Pebble deformation and thrusting in the Bygdin area (southern Norway). Tectonophysics, 5, 315-339.

Horne, J., 1923. The geology of the Lower Findhorn and Lower Strath Nairn. (Explanation of Sheet 84 and part of 94) Memoir of the Geological Survey of Great Britain.

Hutchinson, J., 1974. Laboratory Handbook of Petrographic Techniques. Wiley-Interscience.

Hutton, D.W.H., 1982. A Tectonic model for the emplacement of the Main Donegal Granite, N.W. Ireland. Journal of the Geological Society of London, 139, 625-631.

Hutton, D.H.W., 1982b. A method for the determination of the initial shape of deformed xenoliths in granitoids. Tectonophysics, 85, 45-50.

Hutton, D.H.W., 1988. Granite emplacement mechanisms and tectonic controls: inferences from deformation studies. Transactions of the Royal Society, Edinburgh: Earth Sciences, 79, 245-255.



Hutton, D.H.W., 1988. Igneous emplacement in a shear zone termination: The biotite granite at Strontian. Bulletin of the Geological Society of America., 100, 1392-1399.

Jeffrey, G.B., 1922. On the Motion of ellipsoidal particles immersed in a viscous fluid. Proceedings of the Royal Society, London, Series A, 102, 161-179.

Johannes, W., 1985. The significance of experimental studies for the formation of migmatites. In: Ashworth, J.R. (Ed.), Migmatites, 36-85. Blackie, Glasgow.

Johnstone, G.S., 1966. British Regional Geology-The Grampian Highlands, 3rd ed.: London, Institute of Geological Sciences.

Johnstone, G.S., 1975. The Moine Succession. In Harris, A.L., Shackleton, R.M., Watson, J., Downie, C., Harland, W.B. and Moorbath, S. (eds.) A correlation of Precambrian rocks in the British Isles, 30-42. Special Report of the Geological Society of London, 6.

Kafafy, A.M. & Tarling, D.H., 1985. Magnetic fabrics in some granitic aureoles, Southern Uplands. Journal of the Geological Society of London, 142, 1007-1014.

Kamur, C., 1988. Microgranular enclaves in granitoids: agents of magma mixing. Journal of South East Asian Earth Science, 2, 109-121.

Kennedy, W.Q., 1946. The Great Glen Fault. Quarterly Journal of the Geological Society of London, 102, 41-76.

Kerr, P.F., 1977. Optical Mineralogy, 4th Edition. McGraw-Hill Inc.

Lindsay, N.G., Haselock, P.J., & Harris, A.L., 1989. The extent of Grampian orogenic activity in the Scottish Highlands. Journal of the Geological Society of London, 146, 733-735.

Loomis, T.P., 1975. Reaction zoning of garnet. Contributions to Mineralogy and Petrology, 52, 285-305.

Marsh, B.D. 1982. On the mechanics of igneous diapirism, stoping and zone melting. American Journal of Science, 282, 808-855.

Marston, R.J., 1966. The Foyers Granitic Complex. PhD thesis, University of Sheffield, (unpublished).

Marston, R.J., 1967. The Newer Granites of Foyers and Strontian and the Great Glen Fault. Nature, London, 213, 275-277.

Marston, R.J., 1971. The Foyers Granitic Complex, Inverness-shire, Scotland. Quarterly Journal of the Geological Society of London, 126, 331-68.

Mayo, E.B., 1941. Deformation in the interval Mt. Lyell-Mt. Whitney, California. Bulletin of the Geological Society of America, 52, 1001-1084.

Mould, D.D.C.P., 1946. The geology of the Foyers Granite and the surrounding country. Geological Magazine 83, 249-265.

Mykura, W., 1983. The Old Red Sandstone east of Loch Ness, Inverness-shire. Report of the Institute of Geological Sciences. No. 82/13.

Newman, A.C.D., 1987. Chemistry of clays and Clay minerals. Mineralogical Society Monograph No.6. Longman Scientific and Technical, 480pp.

Pankhurst, R.J., 1979. Isotope and trace element evidence for the origin and evolution of Caledonian granites in the Scottish Highlands. In: Atherton M.P. & Tarney, J. (Eds.), Origin of Granite Batholiths- Geochemical Evidence. Shiva Publishing Ltd., 18-43.

Parson, L.M., 1979. The state of strain adjacent to the Great Glen Fault. In: Harris, A.L., Holland, C.H. and Leake, B.E. The Caledonides of the British Isles Reviewed. Geological Society London, Special Publication. No 8.

Parson, L.M., 1982. The Precambrian and Caledonian geology of the ground near Fort Augustus, Inverness-shire. Unpublished Ph.D thesis, University of Liverpool.

Paterson, S.R., 1988. Cannibal Creek granite: post-tectonic "ballooning" pluton or pre-tectonic piercement diapir. Journal of Geology, 96, 730-736.

Paterson, S.R., Vernon, R.H. & Tobisch, O.T., 1989. A review of criteria for the identification of magmatic and tectonic foliations in granitoids. Journal of Structural Geology, 11, 349-363.

Paterson, S.R., Vernon, R.H. & Tobisch, O.T., 1989. Criteria for establishing the timing of pluton emplacement and regional deformation. Geology, 475-476.

Paterson, S.R., 1989. Cannibal Creek granite: post-tectonic "ballooning" pluton or pre-tectonic piercement diapir: a reply. Journal of Geology, 97, 769-771.

Pattison, D.R.M. & Harte, B., 1988. Evolution of structurally contrasting anatectic migmatites in the 3-kbar Ballachulish aureole, Scotland. Journal of Metamorphic Geology, 6, 475-494.

Phillips, W.E.A., Stillman, C.J. & Murphy, T. 1976. A Caledonian plate tectonic model. Journal of the Geological Society of London, 132, 579-609.

Phillips, W.J., 1956. The Criffell-Dalbeattie granodiorite complex. Journal of the Geological Society of London, 112, 221-238.

Phillips, W.J., Fuge, R. & Phillips, N. 1981. Convection and crystallisation in the Criffel-Dalbeattie pluton. Journal of the Geological Society of London, 138, 351-366.

Piasecki, M.A.J., Tectonic and metamorphic history of the upper Findhorn, Inverness-shire, Scotland. Scottish Journal of Geology. 11, 87-115.

Piasecki, M.A.J., 1980. New light on the Moine rocks of the Central Highlands of Scotland. Journal of the Geological Society of London, 137, 41-59.

Piasecki, M.A.J. and Van Breemen, O., 1983. Field and isotopic evidence for a c.750Ma tectonothermal event in the Moine rocks in the Central Highland region of the Scottish Caledonides. Transactions of the Royal Society of Edinburgh, Earth Sciences, 73, 119-34.

Pigeon, R.T., & Aftalion, M., 1978. Cogenetic and inherited zircon U-Pb systems in granites: Palaeozoic granites of Scotland and England. In: Bowes, D.R. and Leake, B.E.(eds.). Crustal Evolution of north west Britain and adjacent regions. Geological Journal, Special Issue. 10, 183-220.

Pitcher, W.S & Berger, A.R., 1972. The Geology of Donegal: A Study of Granite Emplacement and Unroofing. Wiley-Interscience. 435pp.

Pitcher, W.S., 1979. The nature, ascent and emplacement of granitic magmas. Journal of the Geological Society of London, 136, 627-622.

Pitcher, W.S., 1982. Granite Type and Tectonic Environment. In Hsu, K.J. (Ed.), Mountain Building Processes, 19-24. Academic Press, London,

Pwinski, A.J., 1968. Experimental studies of igneous rock series central Sierra Nevada Batholith, California. Journal of Geology, 79, 548-570.

Pwinski, A.J. & Wyllie P.J., 1967. Experimental studies of igneous rock series: a zoned pluton in the Wallowa Batholith, Oregon. Journal of Geology, 76, 205-234.

Pwinski, A.J., 1973. Tsch. Min. Petr. Mitt., 20, 107-130.

Ramberg, H.B.H., 1967. Model experimentation of the effects of gravity on tectonic processes. Geophysical Journal of the Royal Astronomical Society, 13.

Ramberg, H.B.H., 1981. Gravity, Deformation and the Earth's Crust. Academic Press London, 452pp.



Ramsay, J.G. 1967. Folding and Fracturing of Rocks.  
McGraw-Hill Inc., 568pp.

Ramsay, J.G. 1975. The structure of the Chindamora batholith. 19th Ann. Rep., Research Institute of African Geology, Univ. Leeds, 81.

Ramsay, J.G. 1981. Emplacement mechanics of the Chindamora batholith, Zimbabwe, In: Coward M.P, Diapirism and granite tectonics: report of the Tectonic Studies Group Conference held at Leeds University. 25-26 March, 1980. Journal of Structural Geology, 3, 89-95.

Ramsay, J.G. and Huber, M.I., 1983. The techniques of modern structural geology, vol. 1: Strain analysis. Academic Press.

Ramsay, J.G. and Huber, M.I., 1987. The techniques of modern structural geology, Vol. 2: Folds and Fractures. Academic Press.

Ramsay, J.G., 1989. Emplacement kinematics of a granite diapir: the Chindamora batholith, Zimbabwe. Journal of Structural Geology, 11, 191-209.

Rast, N., 1956. The origin and significance of Boudinage. Geological Magazine, 93, 401-408.

Read, H.H., 1961. Aspects of Caledonian magmatism in Britain. Manchester and Liverpool Geological Journal, 2, 653-683.

Rock, N.M.S., Jeffereys, L.A. & MacDonald, R., 1984. The problem of anomolous local limestone-pelite successions within the Moine outcrop. I: metamorphic limestones of the Great Glen area, from Ardgour to Nigg. Scottish Journal of Geology, 20, 383-406.

Rock, N.M.S., MacDonald, R., Drewery, S.E., Penkhurst, R.J. & Brook, M., 1986. Pelites of the Glen Urquart serpentinite-metamorphic complex, west of Loch Ness (Anomalous local limestone-pelite successions within Moine outcrop: III). Scottish Journal of Geology 22, 179-202.

Rogers, G., Dempster, T.J., Bluck, B.J. & Tanner, P.W.G., 1989. A high precision U-Pb age for the Ben Vuirich granite: implications for the evolution of the Scottish Dalradian Supergroup. Journal of the Geological Society of London, 146, 789-798.

Roscoe, R., 1952. The viscosity of suspensions of rigid spheres, Br. Journal of Applied Physics, 3, 267-269.

Sabine, D.A. 1963. The Strotian Granite Complex, Argyllshire. Bulletin of the Geological Survey of Great Britain. No:20, 6-42.

Sengupta, S., 1983. Folding in boudinaged layers. Journal of Structural Geology, 5, 197-210.

Shand, S.J., 1952. Mylonite, slickensides, and the Great Glen Fault. Geological Magazine, 88, 423-428.

Shaw, H.R., 1980. The fracture mechanisms of magma transport from the mantle. In: Hargreaves, R.B., (Ed.), Physics of magmatic processes. Princeton University Press, 201-232.

Shelly, D., 1968. A note on the relationship of sillimanite to biotite. Geological Magazine, 105, 543-545.

Simpson P.R., Brown, G.C., Plant, J. & Ostle, D. 1979. Uranium mineralisation and granite magmatism in the British Isles. Philosophical Transactions of the Royal Society, London, A291, 385-412.

Smith, D.I., Caledonian minor intrusions of the N. Highlands of Scotland. In: The Caledonides of the British Isles-reviewed., (eds. Harris, A.L., Holland, C.H. & Leake, B.E.) Geological Society of London, Special Publication. No.8, 1979.

Smith, D.I. North of Scotland Hydro-electric Board. Foyers project. Geological report on the Loch Mhor-Loch Ness section. Geological Survey report No. HE70/R13., Institute of Geological Science.

Spera, F.J., 1980. Aspects of magma transport. In: Hargreaves, R.B., (Ed.), Physics of magmatic processes. Princeton University Press, 265-314.

Soper N.J., 1986. The Newer Granite problem: a geotectonic view. Geological Magazine, 123, 227-236.

Soula, J., 1982. Characteristics and mode of emplacement of gneiss domes and plutonic domes in central-eastern Pyrenees. Journal of Structural Geology, 4, 313-342.

Stephens, W.E. and Halliday A.N., 1984. Geochemical contrasts between late Caledonian granitoid plutons of northern, central and southern Scotland. Transactions of the Royal Society of Edinburgh: Earth Science., 75, 259-273.

Stone, M. & Austin, W.G.C., 1961. The metasomatic origin of the potash feldspar megacrysts in the granites of south west England. Journal of Geology, 69, 464-472.

Streckeisen, A.L., 1976. To each plutonic rock its proper name. Earth Science Review., 12, 1-34.

Schwerdtner, W.M., 1981. In Coward, M.P., (auth.), Diapirism and gravity tectonics: report of a Tectonic Studies Group conference held at Leeds University, 25-26 March 1980. Journal of Structural Geology, 3, 89-95.

Thirwall, M.S., 1988. Geochronology of late Caledonian magmatism in northern Britain. Journal of the Geological Society of London, 145, 951-976.

Thompson, A.B., 1976. Mineral reactions in pelitic rocks: II. Calculation of some P-T-X(Fe-Mg) phase relations. American Journal of Science, 276, 425-454.

Thompson, M. & Walsh, J.N., 1983. A handbook of inductively coupled plasma spectrometry. Blackie, Glasgow.

Tobisch, O.T., Paterson, S.R., Saleeby, J.B. & Geary, E.E., 1989. Bulletin of the Geological Society of America, 101, 401-413.

Turner, F.J., 1968. Metamorphic Petrology. New York. (McGraw Hill).

Tyler, I.M. & Ashworth, J.R. 1981. Garnet zoning and re-equilibration in the Strontian area, Scotland. Mineralogical Magazine, 44, 293-300.

Tyler, I.M. & Ashworth, J.R., 1983. The metamorphic environment of the Foyers Granitic Complex. Scottish Journal of Geology, 19, 275-285.

Van Breemen, O. and Bluck, B.J., 1981. Episodic granite plutonism in the Scottish Caledonides. Nature, 291, 113-117.

Van Breemen, O. & Piasecki, M.A.J., 1983. The Glen Kyllachy Granite and its bearing on the nature of the Caledonian Orogeny in Scotland. Journal of the Geological Society of London, 140, 47-62.

Van Den Eeckhout, B., Grocott, J. & Vissers, R., 1986. On the role of diapirism in the segregation, ascent and final emplacement of granitoid magmas- discussion. Tectonophysics, 127, 161-166.

Van der Molen, I. & Paterson, M.S., 1979. Experimental deformation of partially melted granite. Contributions to Mineralogy and Petrology, 70, 299-318.

Vance, J.A., 1969. On synneusis. Contributions to Mineralogy and Petrology, 24, 7-29.

Vernon, R.H. & Flood, R.H., 1982. Some problems in the interpretation of microstructures in granitoid rocks. In: Runnegar, B. & Flood, P. (eds.). New England Geology, Univ. New England and AHV Club, Armidale, N.S.W., 201-210.

Vernon, R.H., 1983. Restite, xenoliths and microgranitoid enclaves in granites. Journal and proceedings, Royal Society of New South Wales. 116, 77-103.

Vernon, R.H., Williams, V.A. & D'Arcy, W.F., 1983. Grain size reduction and foliation development in a deformed granitoid batholith. Tectonophysics, 92, 123-145.

Vernon, R.H., 1984. Microgranitoid enclaves in granites-globules of hybrid magma quenched in a plutonic environment. Nature, 309, 438-439.

Vernon, R.H., Etheridge, M.A. & Wall, V.J., 1988. Shape and microstructure of microgranitoid enclaves: indicators of magma mingling and flow. Lithos, 22, 1-11.

Vernon, R.H., 1989. Criteria for establishing the relative timing of pluton emplacement and regional deformation. Geology, 17, 5, 475-476.

Vernon, R.H., Paterson, S.R. & Greary, E.E., 1989. Evidence for syntectonic intrusion of plutons in the Bear Mountains fault zone, California. Geology, 17, 723-726.

Walker, G.P.L. & Skelhorn, R.R., 1966. Some associations of acid and basic igneous rocks. Earth Science. Review, 2, 93-109.



Walker, G.P.L., 1969. The breaking of magma. Geological Magazine, 106, 166-173.

Watson, J. 1984. The ending of the Caledonian orogeny in Scotland. Journal of the Geological Society of London, 141, 193-214.

Wells, P.R.A., 1979. P-T. Conditions in the Moines of the Central Highlands. Journal of the Geological Society of London, 139, 71-84.

Wells, P.R.A., 1981. Discussion on P-T conditions in the Moines of the Central Highlands, Scotland. Journal of the Geological Society of London, 138, 205-209.

Wikstrom, A., 1987. Magmatic diapirism of granites in south-eastern Sweden. Revista Brasileira de Geociencias, 17, 456-458.

Williams, H., Turner, F.J. & Gilbert, C.M. 1958. Petrography. San Francisco. (Freeman)

Winchester, J.A., 1974. The zonal pattern of regional metamorphism in the Scottish Caledonides. Journal of the Geological Society of London, 130, 509-525.

Winchester, J.A., 1981. Discussion on P-T conditions in the Moines of the Central Highlands, Scotland. Journal of the Geological Society of London, 138, 205-209.

Winkler, H.G.F., 1976. Petrogenesis of Metamorphic rocks,  
fourth edition. Springer-Verlag. 334pp.

Yoder, H.S. 1968. Carnegie Institute Year Book 66, 477-478.

THE BRITISH LIBRARY DOCUMENT SUPPLY CENTRE

**TITLE** THE FOYERS GRANITIC COMPLEX AND ITS AUREOLE.  
.....

.....  
**AUTHOR** Philip Thomas Hood.  
.....

City of London Polytechnic.  
1990

UNIVERSITY \_\_\_\_\_

Attention is drawn to the fact that the copyright of this thesis rests with its author.

This copy of the thesis has been supplied on condition that anyone who consults it is understood to recognise that its copyright rests with its author and that no information derived from it may be published without the author's prior written consent.

1	2	3	4	5	6
cms.					

THE BRITISH LIBRARY  
DOCUMENT SUPPLY CENTRE  
Boston Spa, Wetherby  
West Yorkshire  
United Kingdom

REDUCTION X .....

12

MEERA. 7

**MAPS/CHARTS  
RELATING TO THIS THESIS  
HAVE NOT BEEN FILMED**

**PLEASE APPLY DIRECT  
TO ISSUING UNIVERSITY**

**A**

THE BRITISH LIBRARY DOCUMENT SUPPLY CENTRE

TITLE

THE FOYERS GRANITIC COMPLEX AND ITS AUREOLE.

AUTHOR

Philip Thomas Hood.

City of London Polytechnic.  
1990

UNIVERSITY

Attention is drawn to the fact that the copyright of this thesis rests with its author.

This copy of the thesis has been supplied on condition that anyone who consults it is understood to recognise that its copyright rests with its author and that no information derived from it may be published without the author's prior written consent.

1	2	3	4	5	6
cms.					

THE BRITISH LIBRARY  
DOCUMENT SUPPLY CENTRE  
Boston Spa, Wetherby  
West Yorkshire  
United Kingdom

REDUCTION X .....

12

IMERA. 7

THE FOYERS GRANITIC COMPLEX AND ITS AUREOLE.

Volume 2. Plates, Figures and Enclosures.

Philip Thomas Hood.

August 1990.

Degree of Doctor of Philosophy.

City of London Polytechnic.

This thesis is submitted to the Council for National Academic Awards in partial fulfilment of the requirements for the degree of Doctor of Philosophy.

**THE BRITISH LIBRARY DOCUMENT SUPPLY CENTRE**

# **BRITISH THESES NOTICE**

The quality of this reproduction is heavily dependent upon the quality of the original thesis submitted for microfilming. Every effort has been made to ensure the highest quality of reproduction possible.

If pages are missing, contact the university which granted the degree.

Some pages may have indistinct print, especially if the original pages were poorly produced or if the university sent us an inferior copy.

Previously copyrighted materials (journal articles, published texts, etc.) are not filmed.

Reproduction of this thesis, other than as permitted under the United Kingdom Copyright Designs and Patents Act 1988, or under specific agreement with the copyright holder, is prohibited.

**THIS THESIS HAS BEEN MICROFILMED EXACTLY AS RECEIVED**

**THE BRITISH LIBRARY  
DOCUMENT SUPPLY CENTRE  
Boston Spa, Wetherby  
West Yorkshire, LS23 7BQ  
United Kingdom**



**MAPS/CHARTS  
RELATING TO THIS THESIS  
HAVE NOT BEEN FILMED**

**PLEASE APPLY DIRECT  
TO ISSUING UNIVERSITY**

**A**

CONTENTS.

VOLUME 2.

CHAPTER 1. GEOLOGICAL RESEARCH IN THE FOYERS AREA.

Figures 1.1-1.5 Pg.2

CHAPTER 2. PETROGRAPHY AND FIELD RELATIONSHIPS  
OF IGNEOUS UNITS IN THE FOYERS COMPLEX.

Figures 2.1-2.15, Tables 2.1-2.7 Pg.9  
Plates 2.1-2.33 Pg.39

CHAPTER 3. GRANITOID VEINING AND STOPING IN  
THE FOYERS COMPLEX.

Figures 3.1-3.4, Tables 3.1-3.2 Pg.58  
Plates 3.1-3.6 Pg.64

CHAPTER 4. FABRICS AND FOLIATIONS IN  
THE FOYERS GRANITIC COMPLEX.

Figures 4.1-4.16 Pg.69  
Plates 4.1-4.14 Pg.85

CHAPTER 5. THE MAOL CHNOC COMPLEX.

Figure 5.1, Table 5.1 Pg.94  
Plates 5.1-5.15 Pg.96

CHAPTER 6. INNER AUREOLE PSAMMITE  
MOBILISATION IN THE ENVELOPE OF THE  
FOYERS COMPLEX.

Figure 6.1 Pg.106  
Plates 6.1-6.8 Pg.107

CHAPTER 7. RELATIONSHIP BETWEEN THE FOYERS  
COMPLEX AND REGIONAL STRUCTURES.

Figures 7.1-7.22, Tables 7.1-7.3 Pg.112  
Plates 7.1-7.19 Pg.131

CHAPTER 8. PETROLOGY AND CONTACT METAMORPHISM  
OF THE ENVELOPE ROCKS.

Figures 8.1-8.4B, Table 8.1 Pg.143  
Plates 8.1-8.13 Pg.151

CHAPTER 9. THE EFFECTS OF DENSITY ON THE  
EMPLACEMENT OF THE FOYERS ENVELOPE.

Figures 9.1-9.3, Tables 9.1-9.6

Pg.160

CHAPTER 10. THE INTRUSION OF THE FOYERS COMPLEX;  
SUMMARY AND CONCLUSIONS.

Figures 10.1-10.2

Pg.168

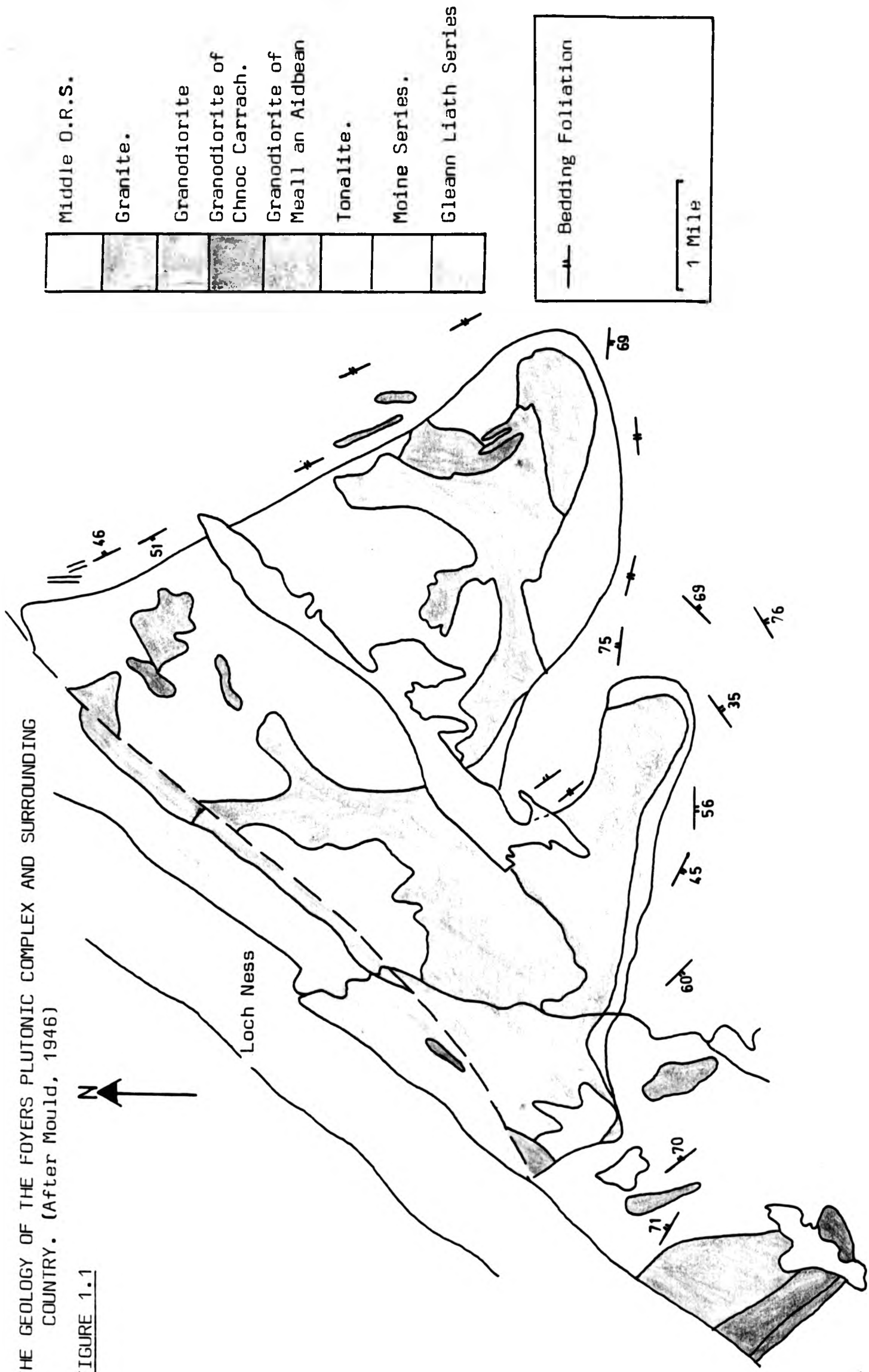
ENCLOSURES.

Enclosure 1-Enclosure 5, located in pocket on the back  
board.

CHAPTER 1. GEOLOGICAL RESEARCH IN THE FOYERS AREA.

THE GEOLOGY OF THE FOYERS PLUTONIC COMPLEX AND SURROUNDING COUNTRY. (After Mould, 1946)

FIGURE 1.1



THE FOYERS GRANITIC COMPLEX. (After Marston, 1967)

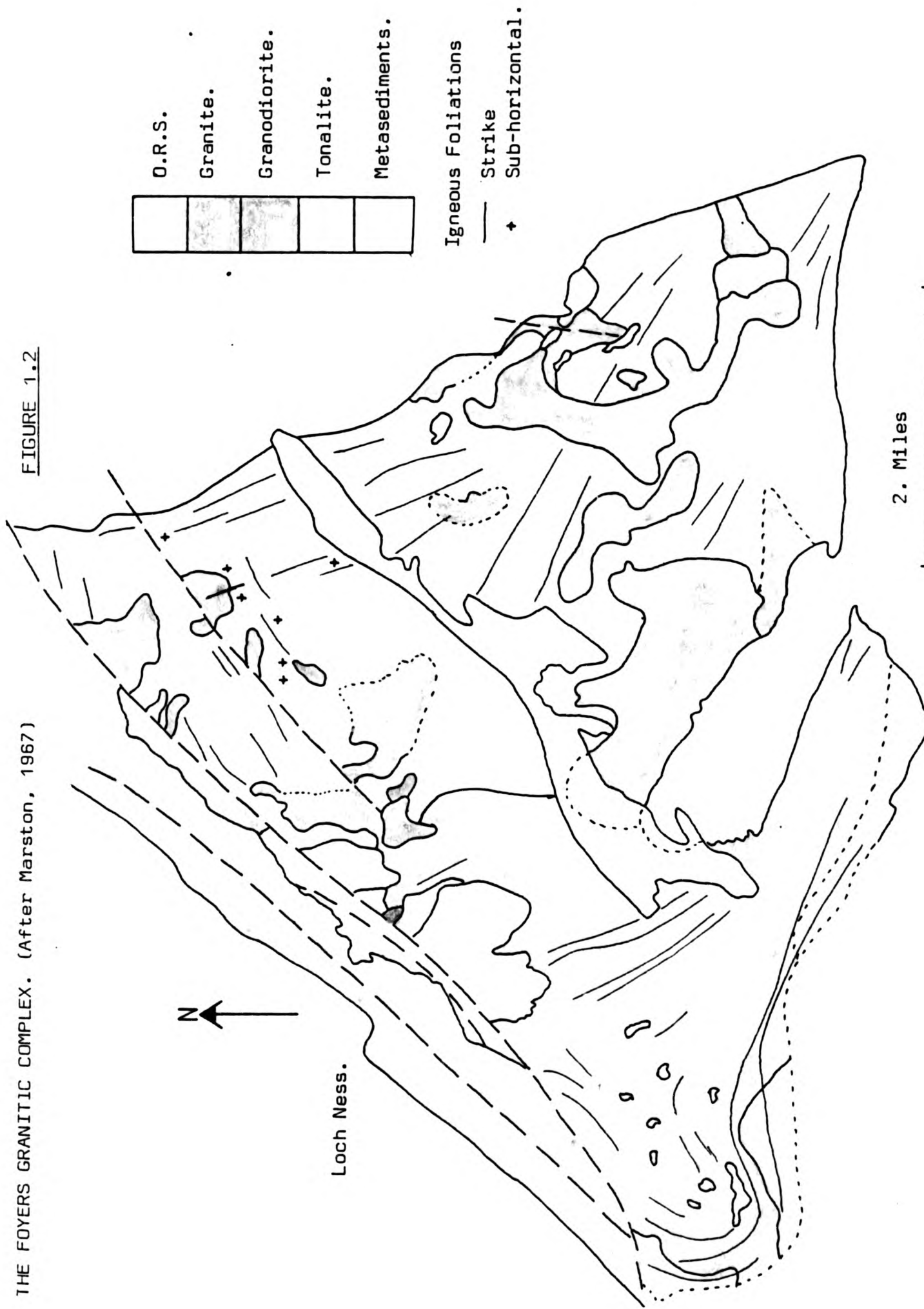
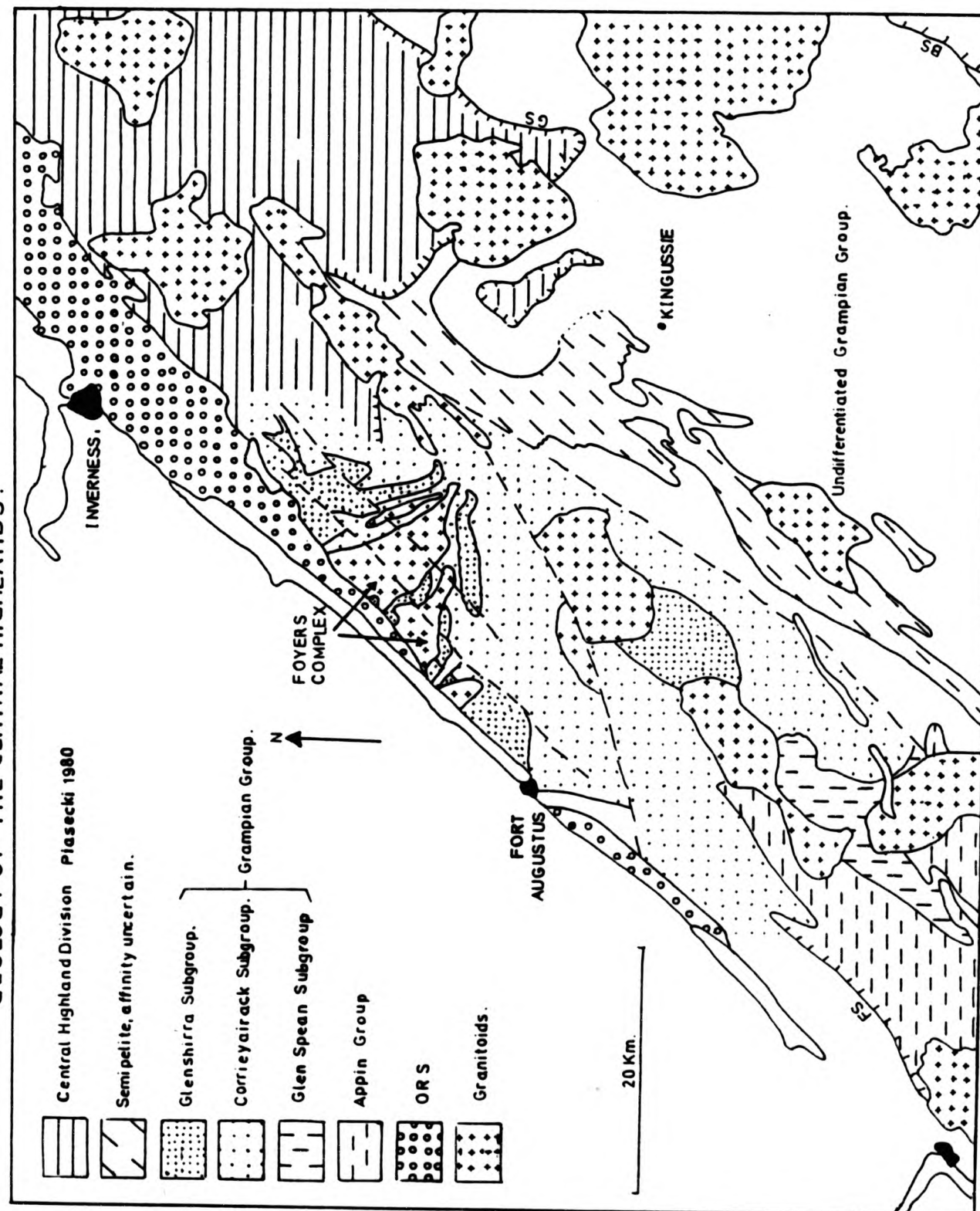




FIGURE 1.3

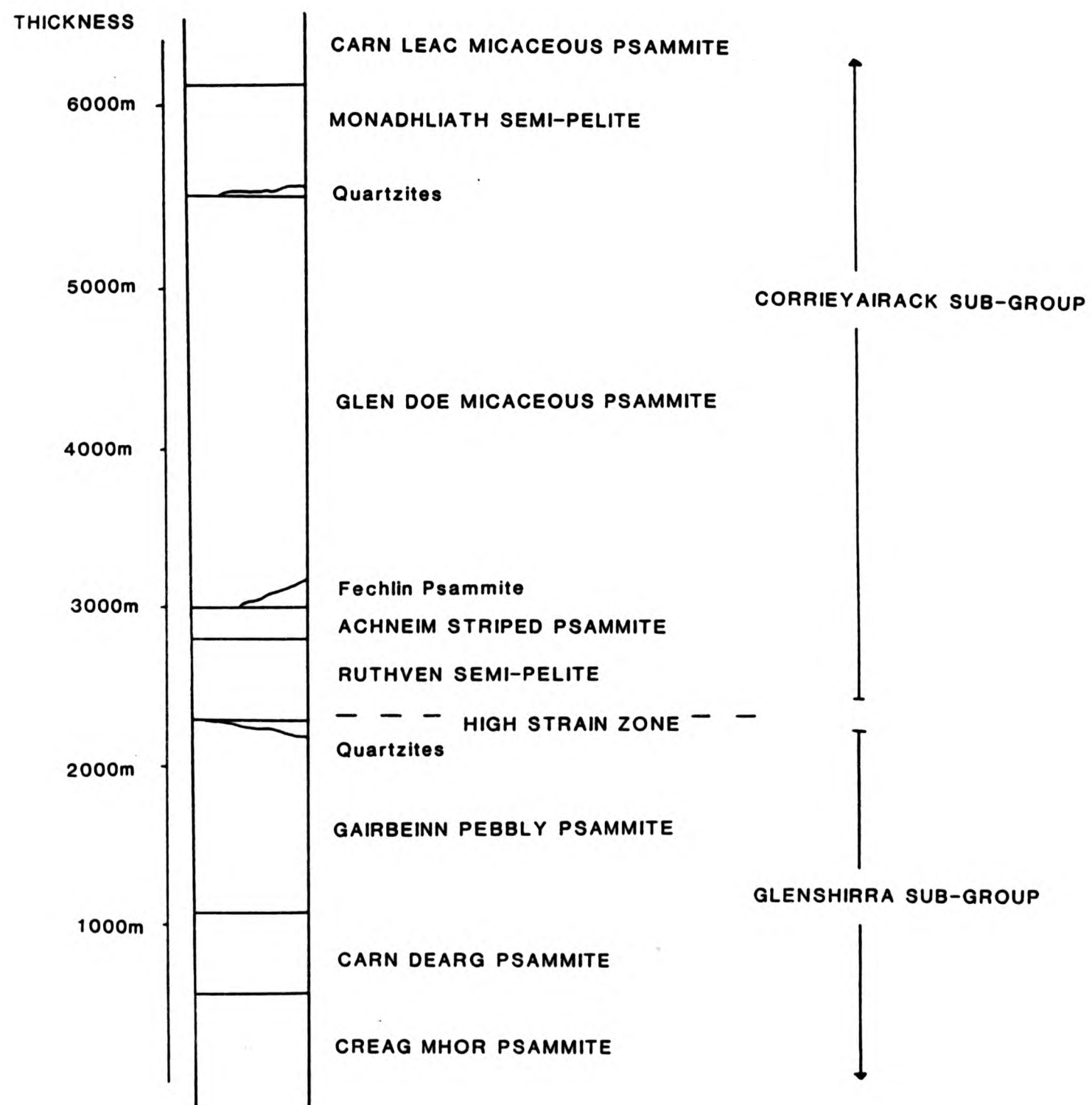
# GEOLOGY OF THE CENTRAL HIGHLANDS.





GRAMPIAN GROUP STRATIGRAPHY IN THE SOUTH WEST  
AND NORTH WEST MONADHLIATHS. Haselock 1990.

FIGURE 1.4



MAJOR CALEDONIAN GRANITIC PLUTONS OF NORTHERN BRITAIN.

FIGURE 1.5

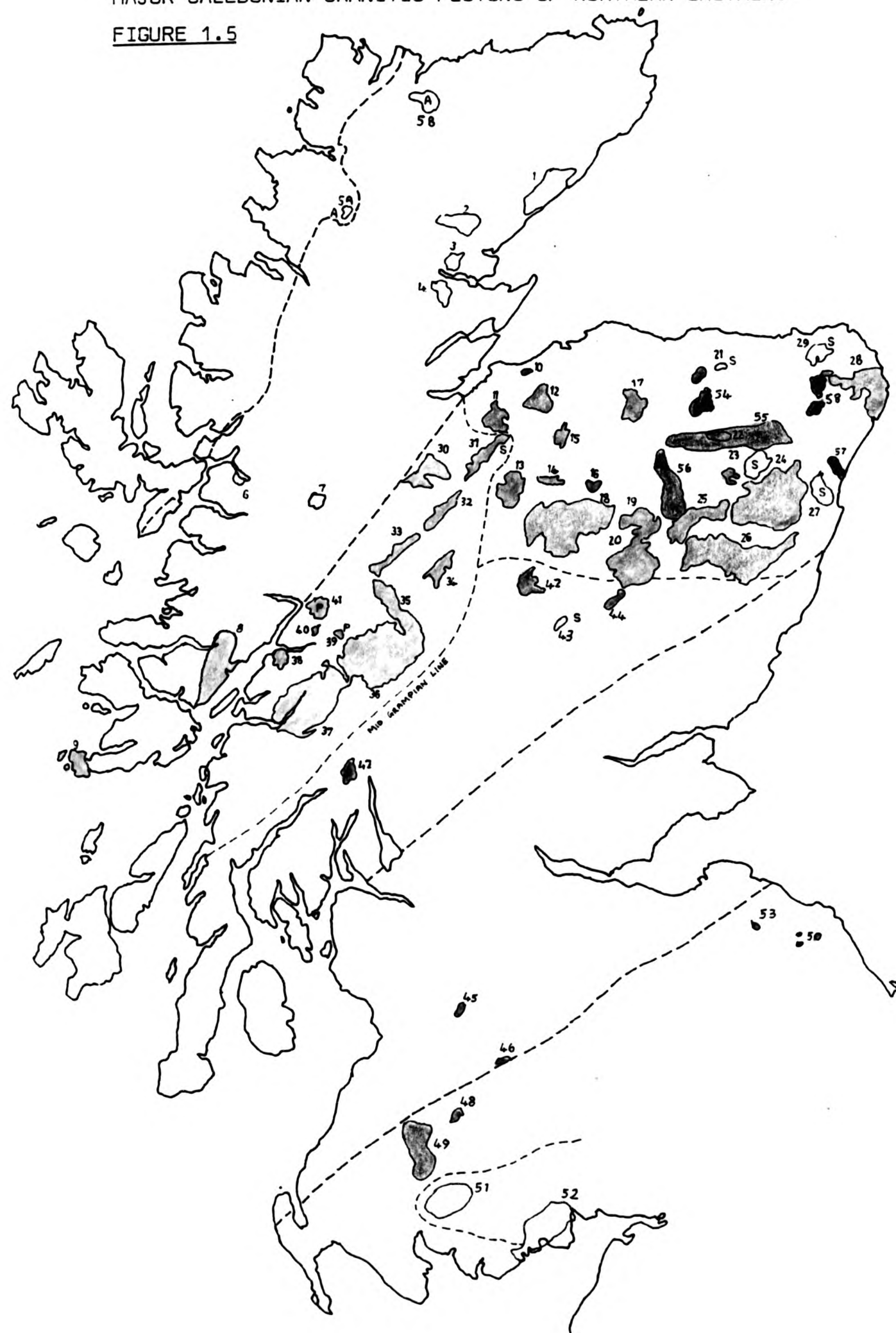


FIGURE 1.5

MAJOR CALEDONIAN GRANITIC PLUTONS OF NORTHERN BRITAIN.

1- Helmsdale, 2- Rogart, 3- Migdale, 4- Fearn, 5- Loch Borrlan,  
5A- Ben Loyal, 6- Ratagan, 7- Cluanie, 8- Strontian,  
9- Ross of Mull, 10- Auldearn, 11- Moy, 12- Ardclach, 13- Monadliath,  
14- Boat of Garten, 15- Grantown, 16- Dorback, 17- Ben Rinnes,  
18- Cairngorm, 19- Glen Gairn, 20- Lochnagar, 21- Aberchirder,  
22- Kennethmont, 23- Bennachie, 24- Hill of Fare, 25- Torphins?,  
26- Battock, 27- Aberdeen, 28- Peterhead, 29- Strichen, 30- FOYERS  
31- Findhorn & Glen Kyllachy, 32- Allt Crom, 33- Corrieyairack,  
34- Loch Caoldair, 35- Strath Ossian, 36- Rannoch Moor, 37- Etive,  
38- Ballachulish, 39- Glencoe, 40- Mullach nan Coirean,  
41- Ben Nevis, 42- Glen Tilt, 43- Ben Vuirich, 44- Glen Doll,  
45- Distinkhorn, 46- Spango, 47- Glen Fyne, 48- Carsphain,  
49- Loch Doon, 50- Cockburnlaw, 51- Cairnsmore of Fleet, 52- Criffel  
53- Priestlaw, 54- Huntly Gabbro, 55- Inch gabbro, 56 -Morven Gabbro  
57- Belhelvie Gabbro, 58- Mahd and Haddo Gabbro.

P- Permitted Newer Granite (Read, 1961)

S- S-Type Ordovician granites (van Breemen & Bluck, 1981,  
Stephens & Halliday, 1984).

C- Pre-Caledonian granites.

A- Alkaline suite of the north west Highlands.



Argyll Suite



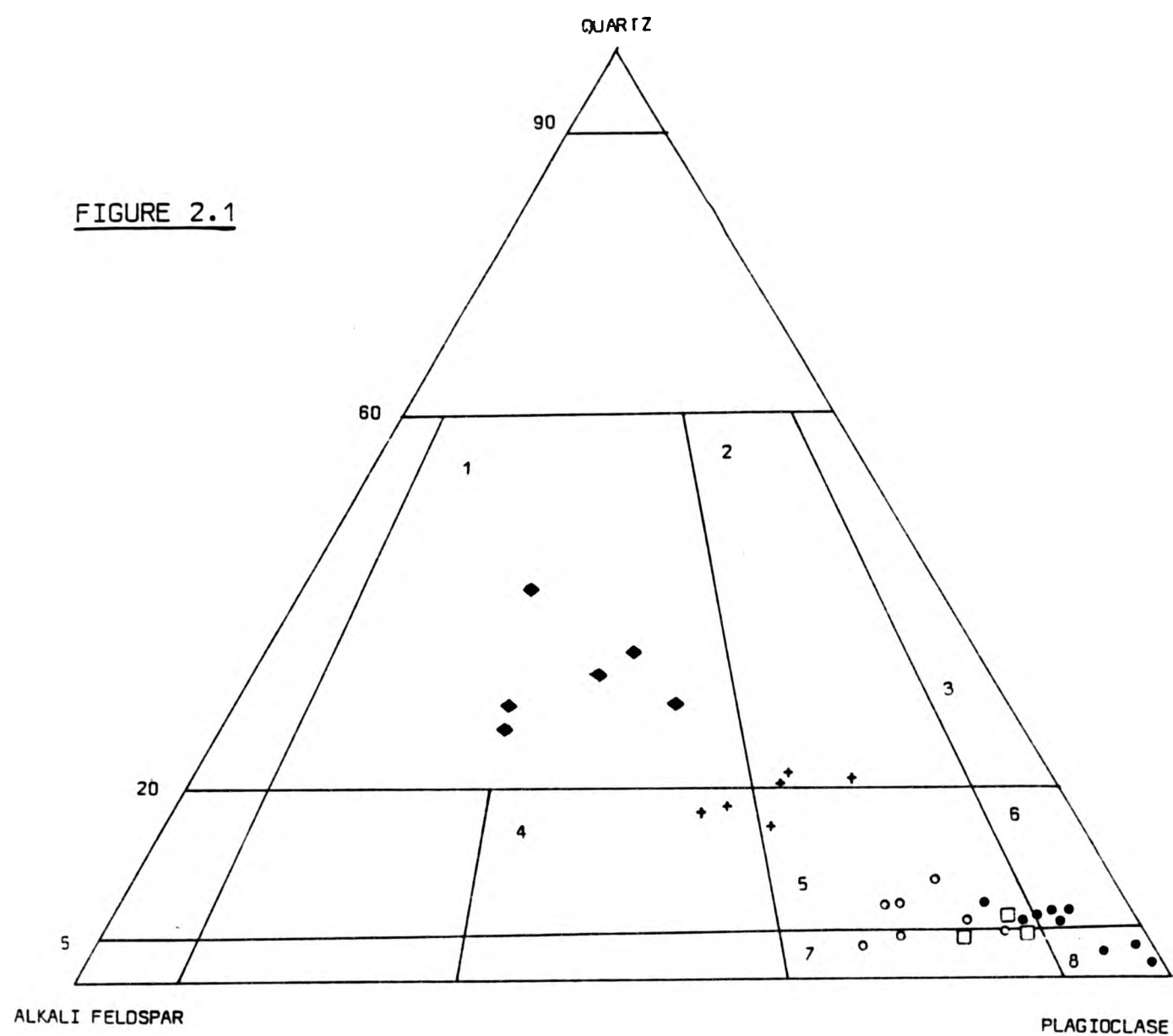
Cairngorm Suite



South of Scotland Suite.

CHAPTER 2. PETROGRAPHY AND FIELD RELATIONSHIPS OF  
IGNEOUS UNITS IN THE FOYERS COMPLEX.

FIGURE 2.1



1. GRANITE 2. GRANODIORITE 3. TONALITE 4. QUARTZ MONZONITE 5. QUARTZ MONZODIORITE  
6. QUARTZ DIORITE 7. MONZODIORITE 8. DIORITE

KEY.

- ERROGIE QUARTZ DIORITE.
- QUARTZ DIORITE/QUARTZ MONZODIORITE INTERMEDIATE.
- CHLIABHAIN QUARTZ MONZODIORITE INTERMEDIATE.
- ✦ JALCRAG GRANODIORITE.
- ◆ APERCHALDER ADAMELLITE

IGNEOUS ROCK UNITS FROM THE FOYERS COMPLEX PLOTTED ON A Q.A.P. PLOT.  
(STRECKEISEN, 1976).

FIGURE 2.2

KEY AS FOR FIG.2.1

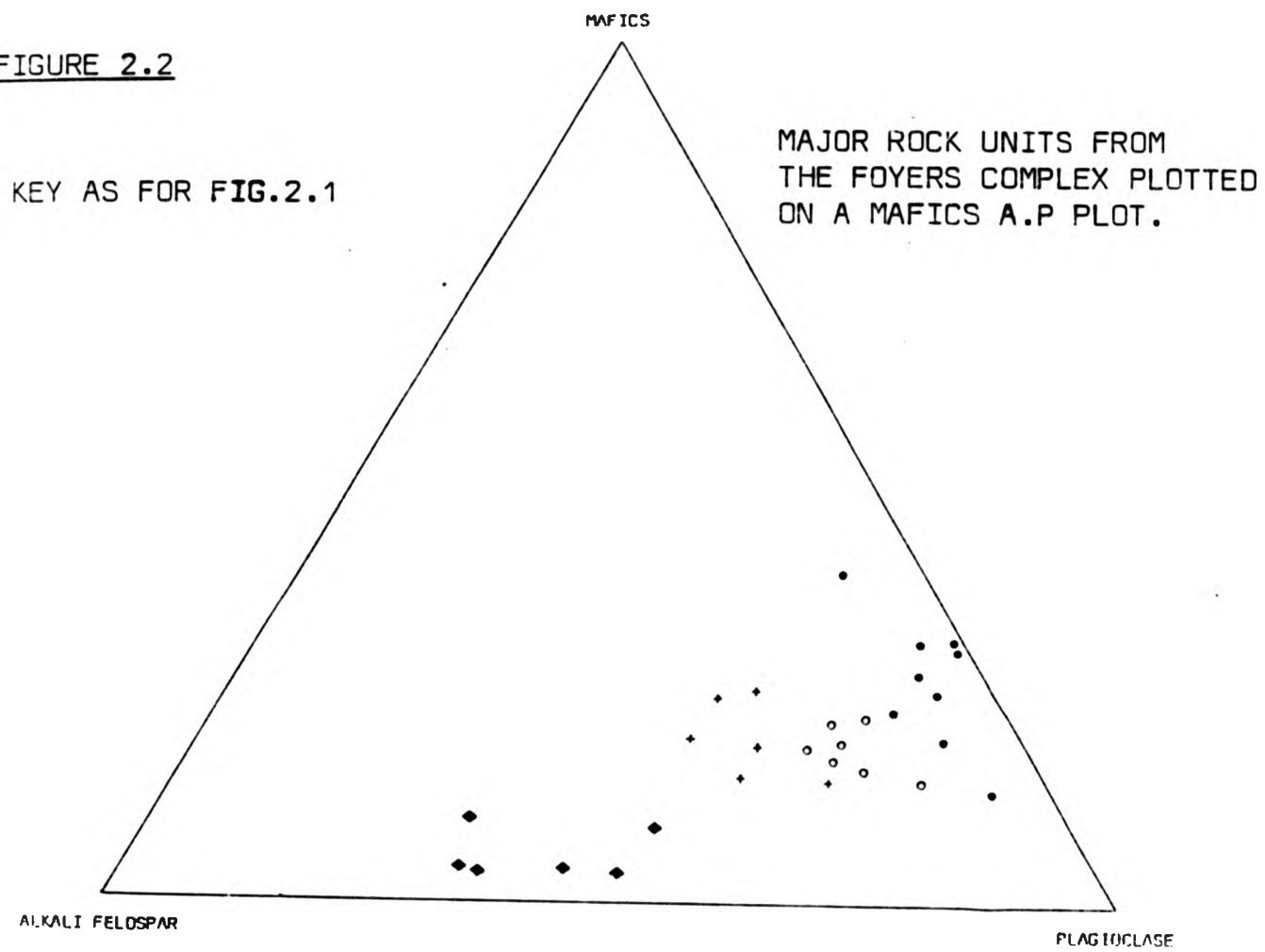
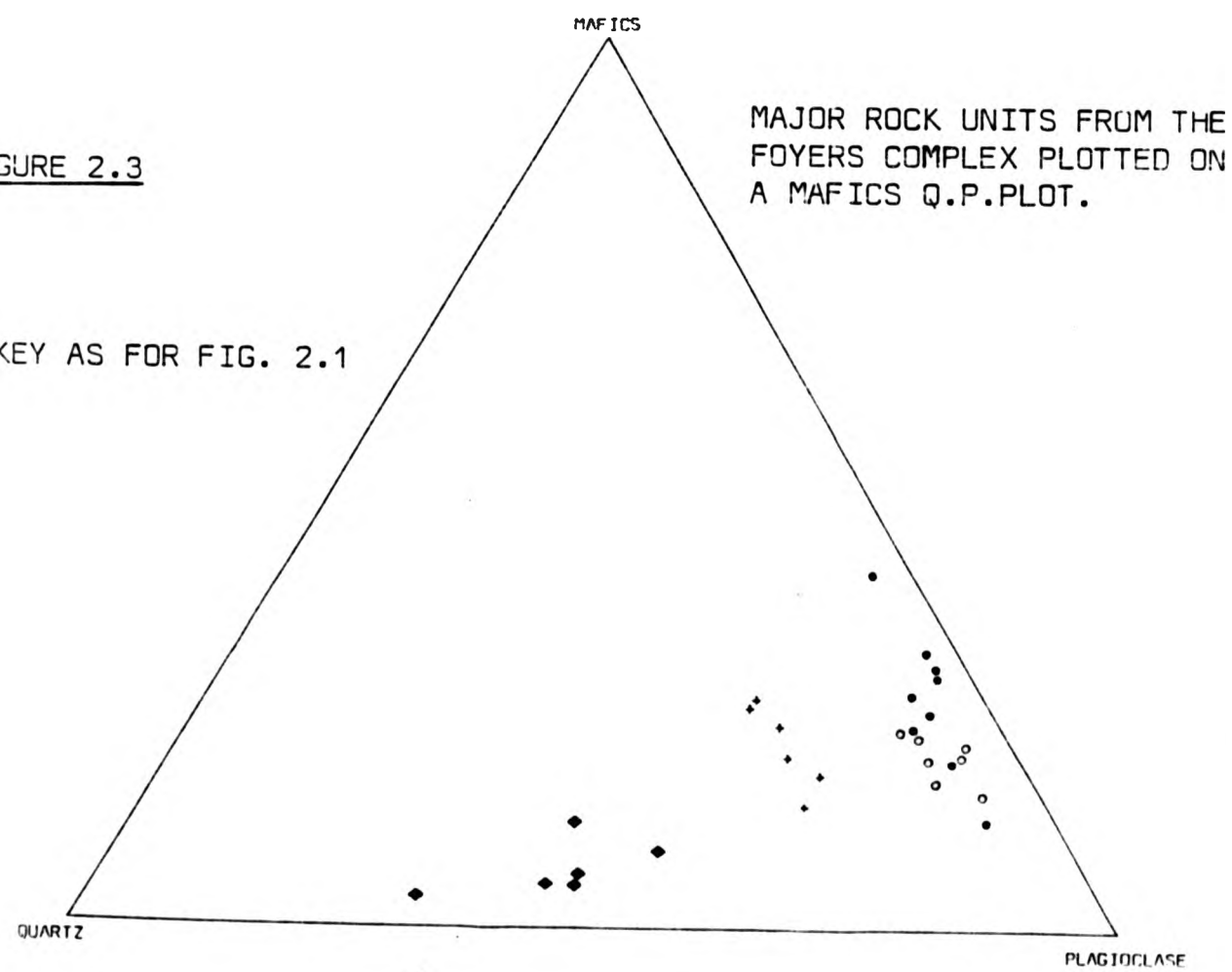


FIGURE 2.3

KEY AS FOR FIG. 2.1





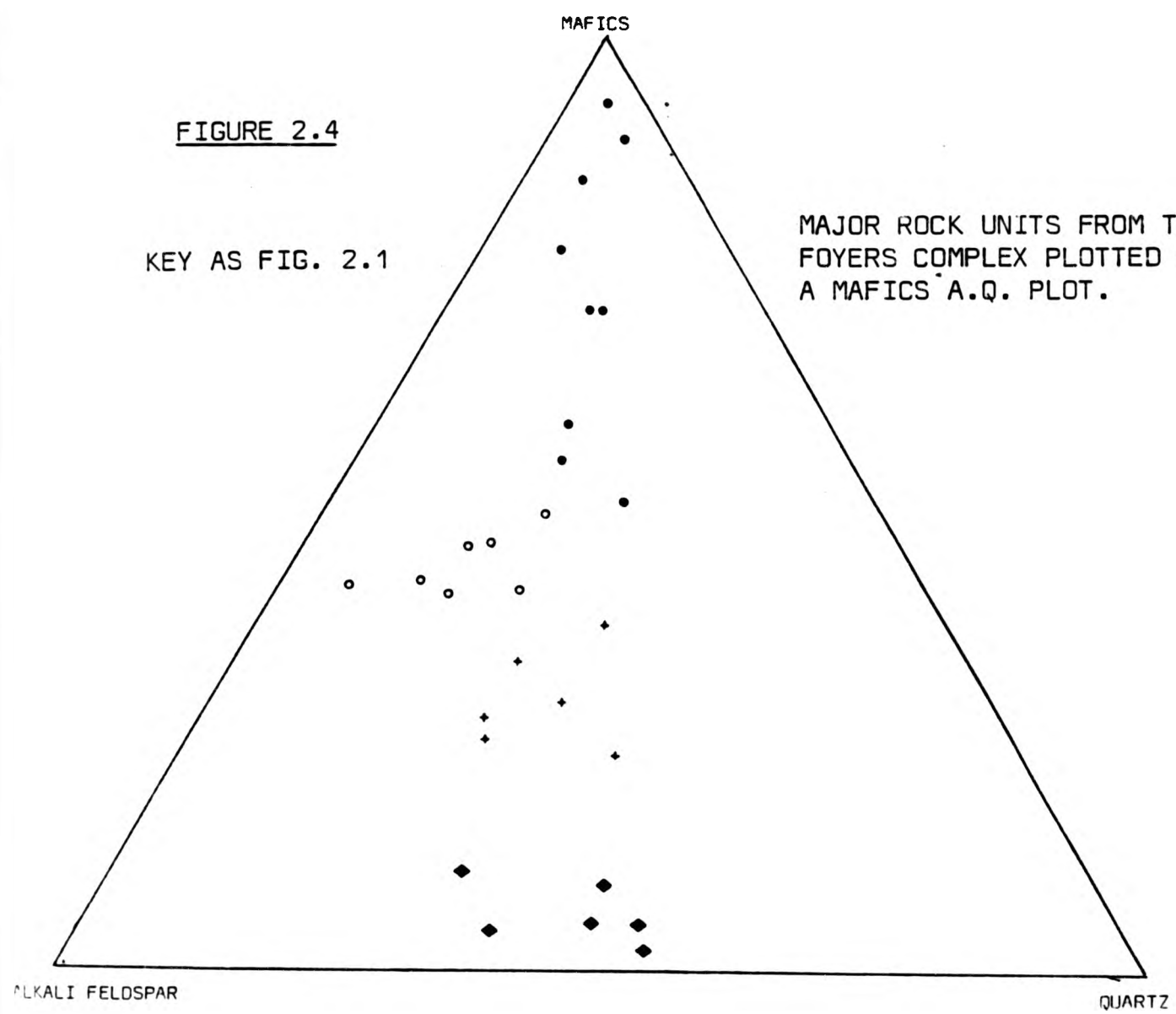
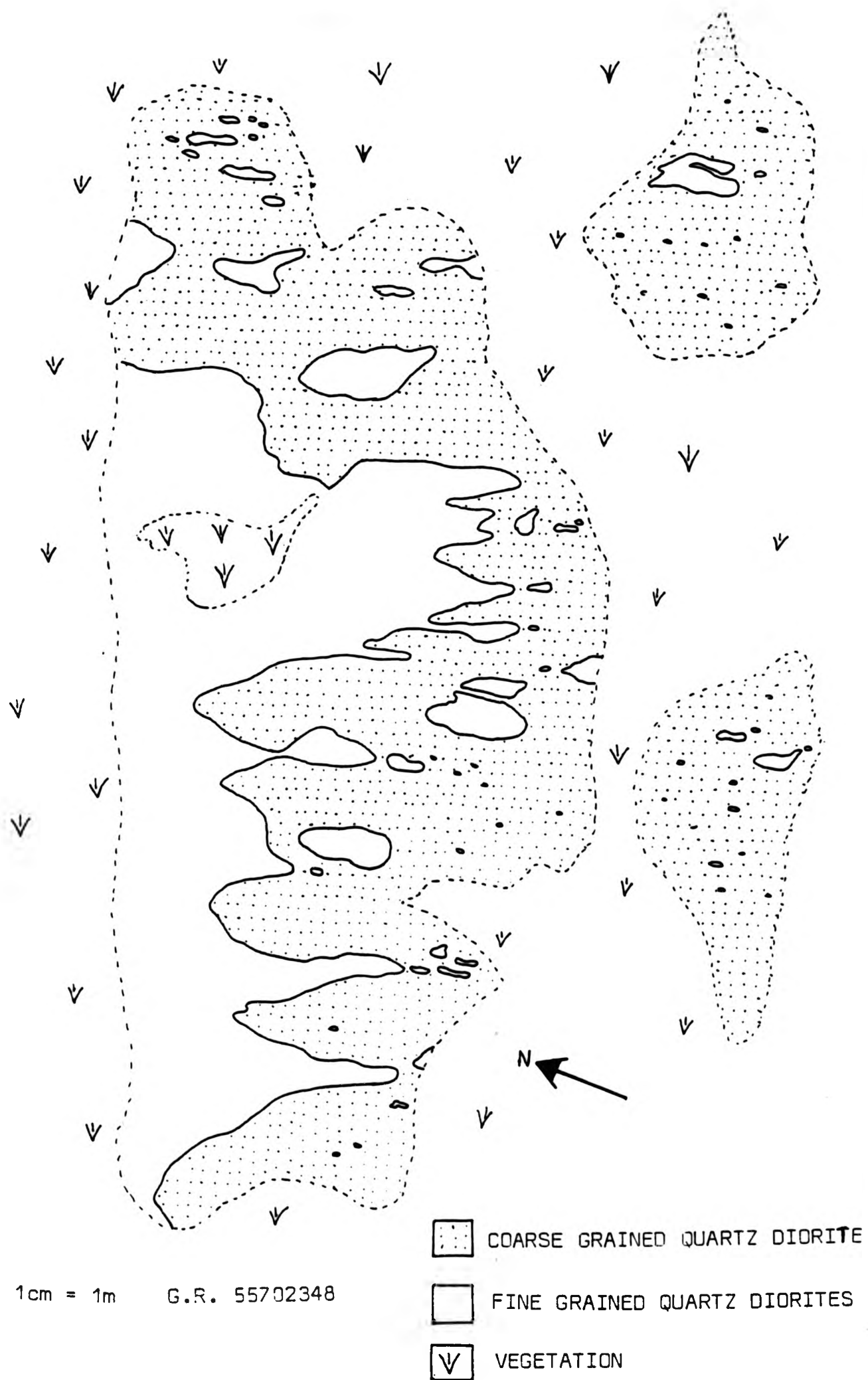




TABLE 2.1		Modal Analyses of Errogie Quartz Diorite.									
SAMPLE No.	P1612	P15	P1093	P226	P109	P234	P1488	P127	P238111		
Plagioclase	67.2	66.0	63.7	62.2	63.5	51.6	76.0	67.1	68.6		
Alkali feldspar	0.8	5.1	3.3	9.97	5.49	7.4	5.4	1.0	7.7		
Quartz	1.5	5.09	2.0	6.8	5.3	3.3	6.3	2.6	5.66		
Biotite	25.6	16.5	20.8	18.0	21.9	16.7	9.7	20.8	10.46		
Hornblende	2.3	1.8	7.8	0.5	0.58	18.9	1.12	6.6	5.66		
Sphene	1.0	2.7	1.0	1.6	2.13	1.9	0.56	0.37	1.3		
Accessories	1.58	2.66	1.2	0.7	0.96	0.1	0.74	1.5	0.54		
TOTAL	98.49	99.85	99.8	99.77	99.86	99.9	99.82	99.97	99.92		

FIGURE 2.5

MAP SHOWING THE CONTACT RELATIONSHIPS OF FINE AND COARSE GRAINED  
ERROGIE QUARTZ DIORITE.



SCALE: 1cm = 1m G.R. 55702348

TABLE 2.2

Modal Analyses of Chliabhain Quartz Monzodiorite.

SAMPLE NO.	P1101	P648	P1156	P640	P280	P1214	P1444E
Plagioclase	70.3	61.0	58.6	64.2	58.5	59.0	57.0
Alkali feldspar	11.2	18.2	21.2	13.2	12.6	17.8	16.6
Quartz	4.4	4.07	2.9	4.6	8.3	6.8	6.44
Biotite	12.5	15.0	13.9	12.2	13.2	14.1	16.3
Hornblende	0.4	trace	2.49	1.07	1.1	0.77	1.25
Sphene	trace	1.06	0.6	1.0	1.1	0.75	1.1
Accessories	1.0	0.53	0.2	1.53	0.6	0.9	0.7
TOTAL	99.8	99.86	99.89	98.0	99.8	100.27	99.89

FIGURE 2.6

FORM OF CONTACT BETWEEN DIFFERENT GRANITOID UNITS.

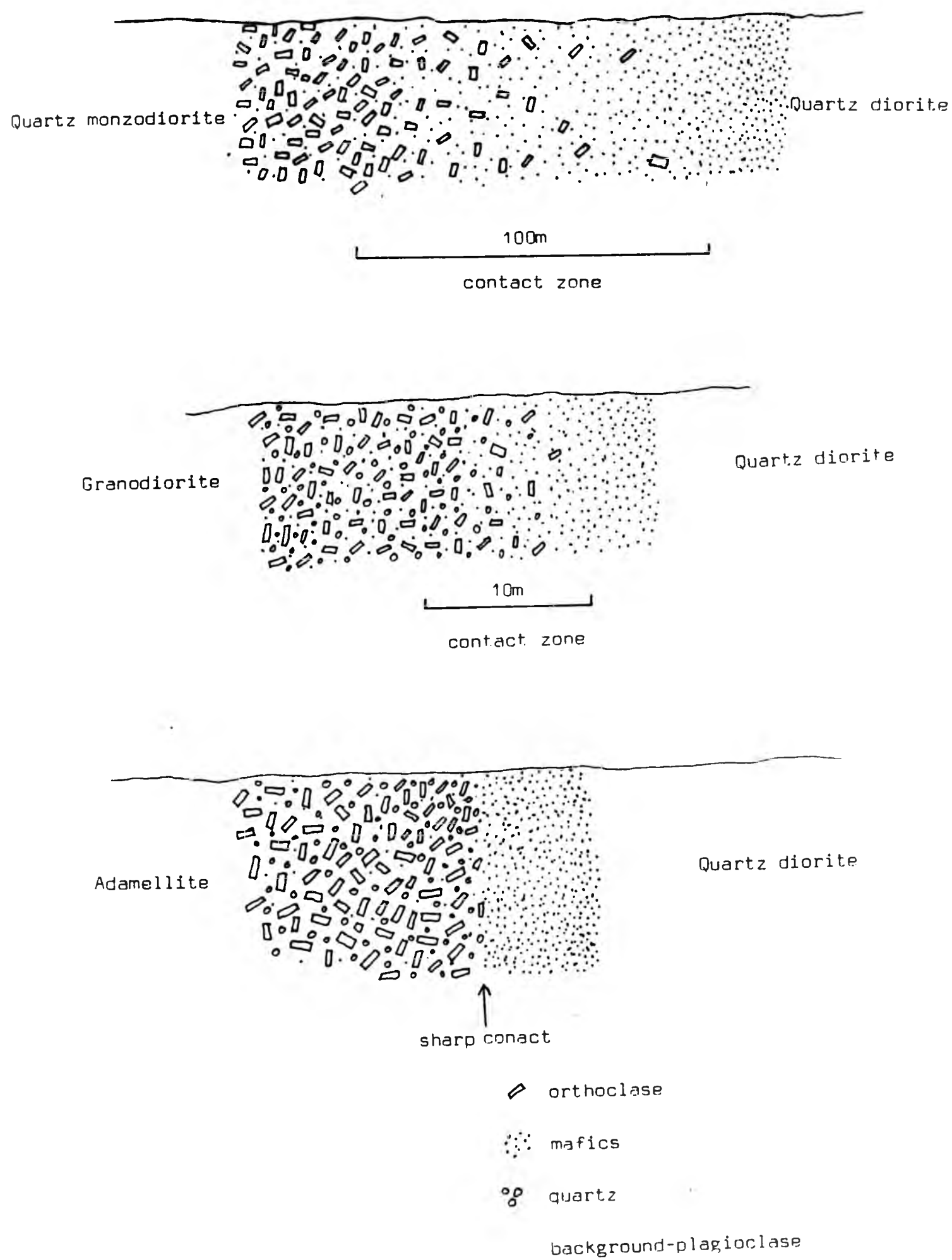


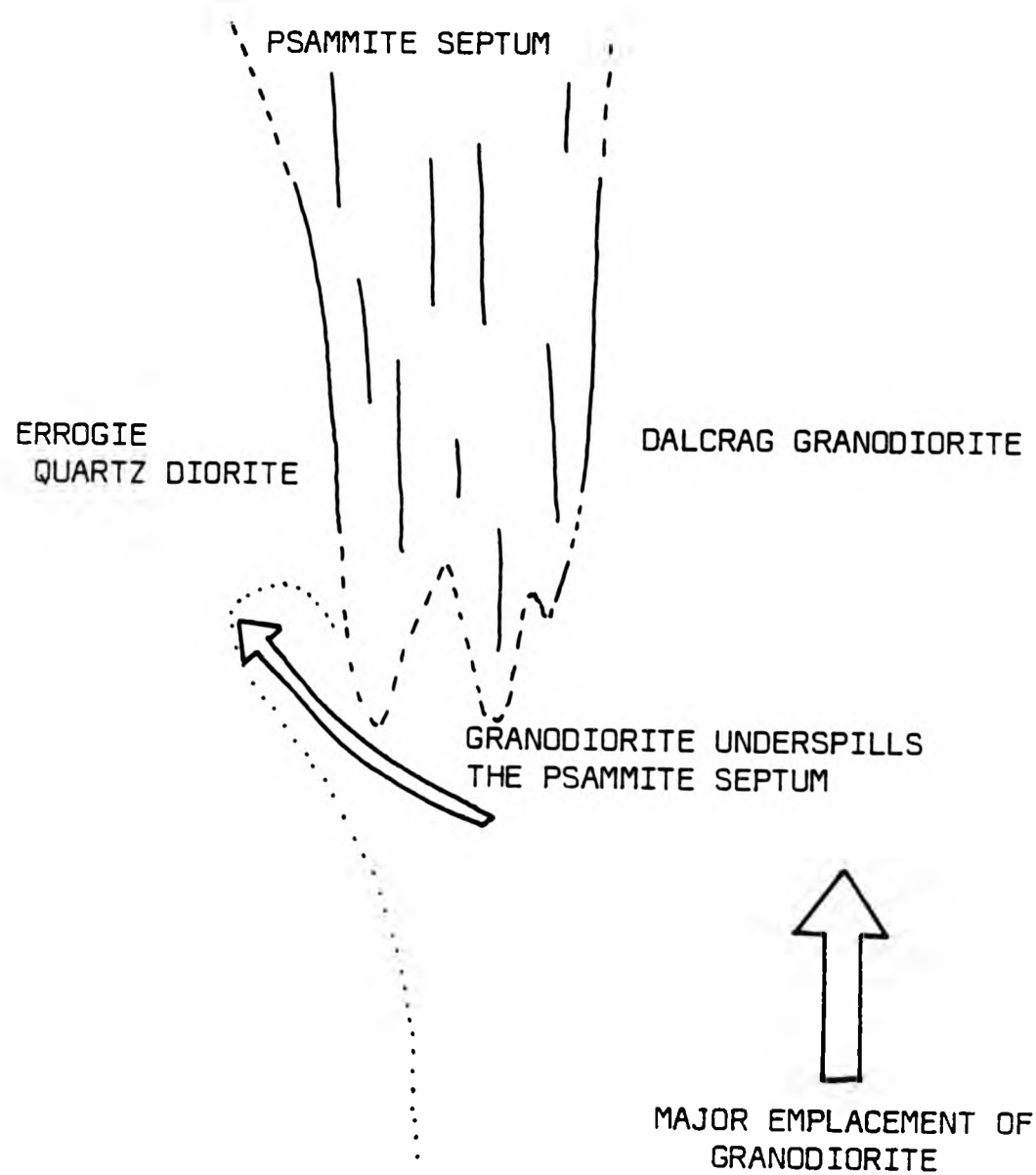
TABLE 2.3      Modal Analyses of Dalcrag Granodiorite

SAMPLE No.	P1363	P1680	P1154	P1706B	P1702	P1858
Plagioclase	42.8	47.4	45.8	40.5	40.1	52.3
Alkali feldspar	18.2	25.5	21.5	28.15	24.1	17.6
Quartz	17.4	14.0	17.2	14.7	15.0	18.6
Biotite	15.3	7.7	13.5	12.0	17.1	9.0
Hornblende	5.2	3.9	1.1	4.0	2.2	0.6
Sphene	0.38	0.23	0.62	trace	0.5	0.7
Accessories	0.4	0.93	0.09	0.5	0.9	1.2
TOTAL	99.68	99.66	99.81	99.85	99.9	100



FIGURE 2.7

DIAGRAM TO ILLUSTRATE DALCRAG GRANODIORITE UNDERSPELLING THE CENTRAL PSAMMITE SEPTUM.



SCHEMATIC VERTICAL CROSS SECTION.

TABLE 2.4 Modal Analyses of Aberchalder Adamellite.

SAMPLE NO.	P737	P1108	P835	P1413	PX1	P1240B
Plagioclase	23.5	23.5	20.5	30.39	31.88	37.3
Alkali feldspar	44.5	46.3	35.5	33.8	30.43	28.0
Quartz	28.9	25.0	41.7	31.4	33.9	27.0
Biotite	2.0	6.9	2.1	3.9	3.4	7.0
Hornblende	trace	0.6	trace	trace	0.28	trace
Sphene	0.67	0.2	trace	trace	trace	0.1
Accessories	0.2	trace	trace	0.2	trace	trace
TOTAL	99.77	99.8	99.8	99.49	99.89	99.4
Plagioclase Total feldspar	0.34	0.35	0.36	0.47	0.51	0.57



FIGURE 2.8

DIAGRAMS ILLUSTRATING THE DEVELOPMENT OF ABERCHALDER ADAMELLITE STOCKS

AT DEPTH

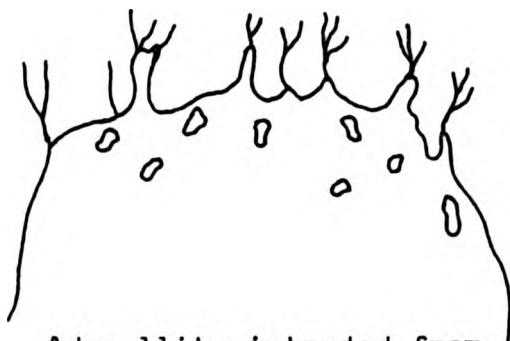
1.



The Aberchalder adamellite rises as a narrow intrusion by veining and stoping its roof of solid Foyers granitoids.

AT PRESENT LEVEL OF EXPOSURE.

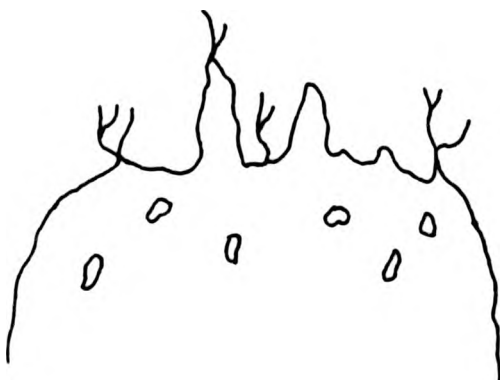
2.



Adamellite intruded from below.

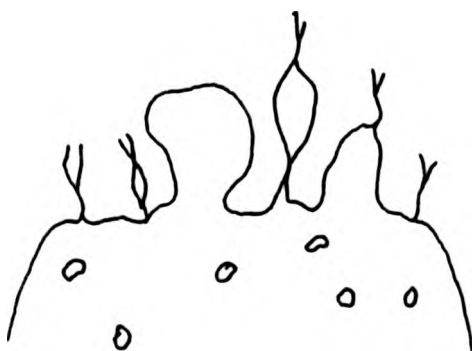
Stoping and ascent slow, and the pluton expands by lateral stoping and perhaps dilation of the host.

3.



Some adamellite veins receive an increased magma flow and expand.

4.



Further magma intrusion leads to the development of stocks above the major adamellite body.

# SCHEMATIC SECTION THROUGH BANDING WITHIN THE CARN BHREABAIG GRANITE

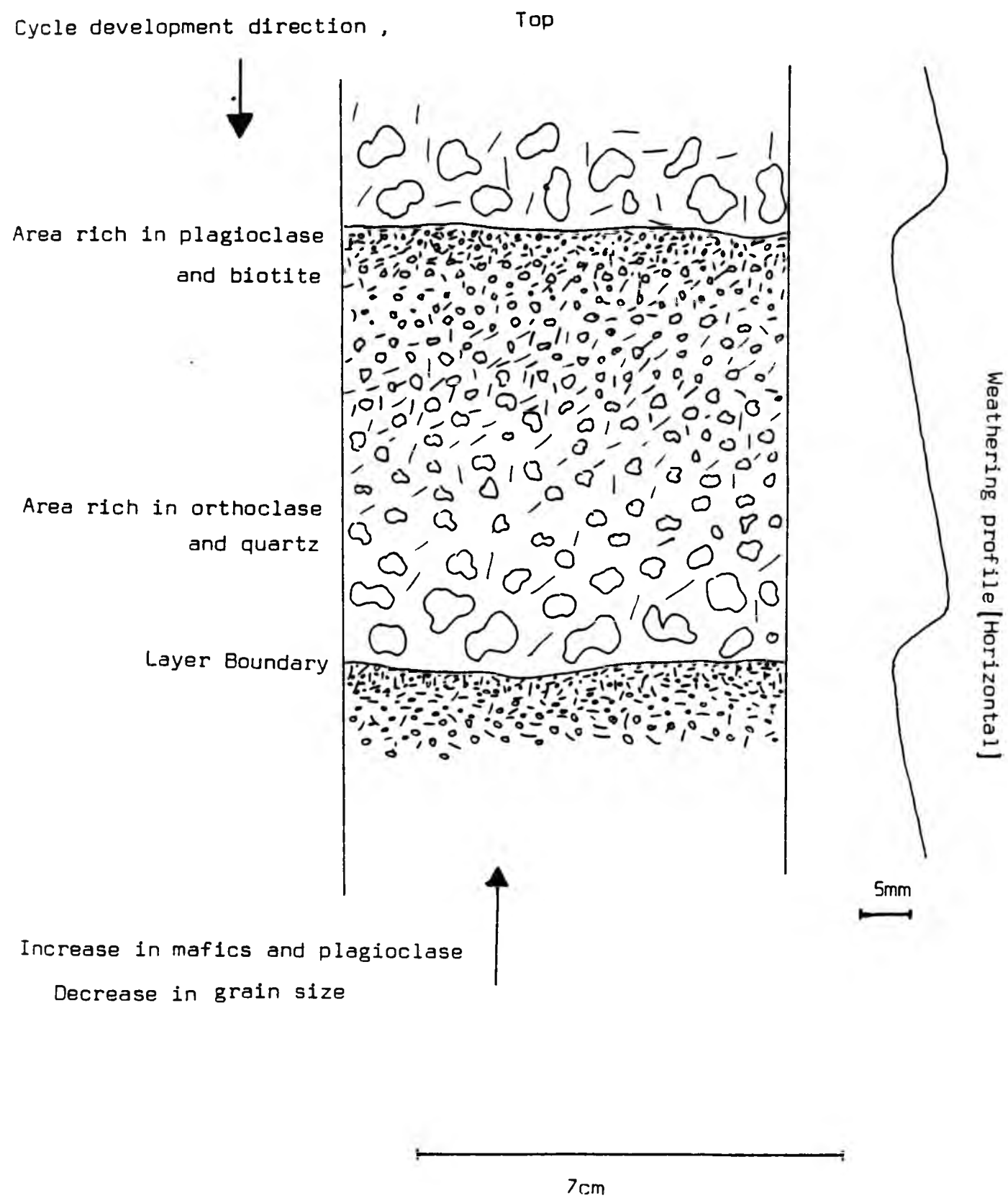


FIGURE 2.9

FIGURE 2.10

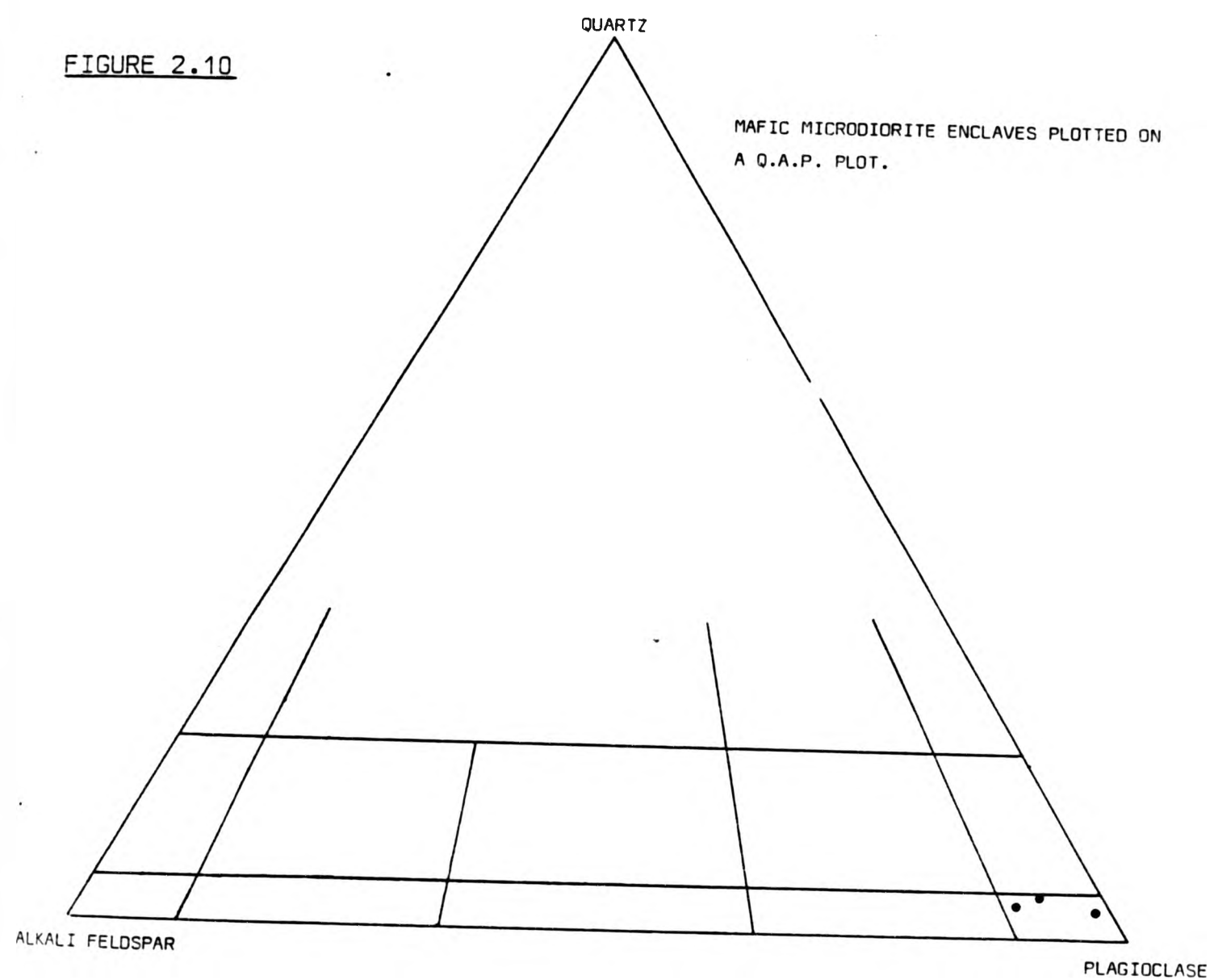


TABLE 2.5

Modal Analyses of Microdiorite Enclaves.

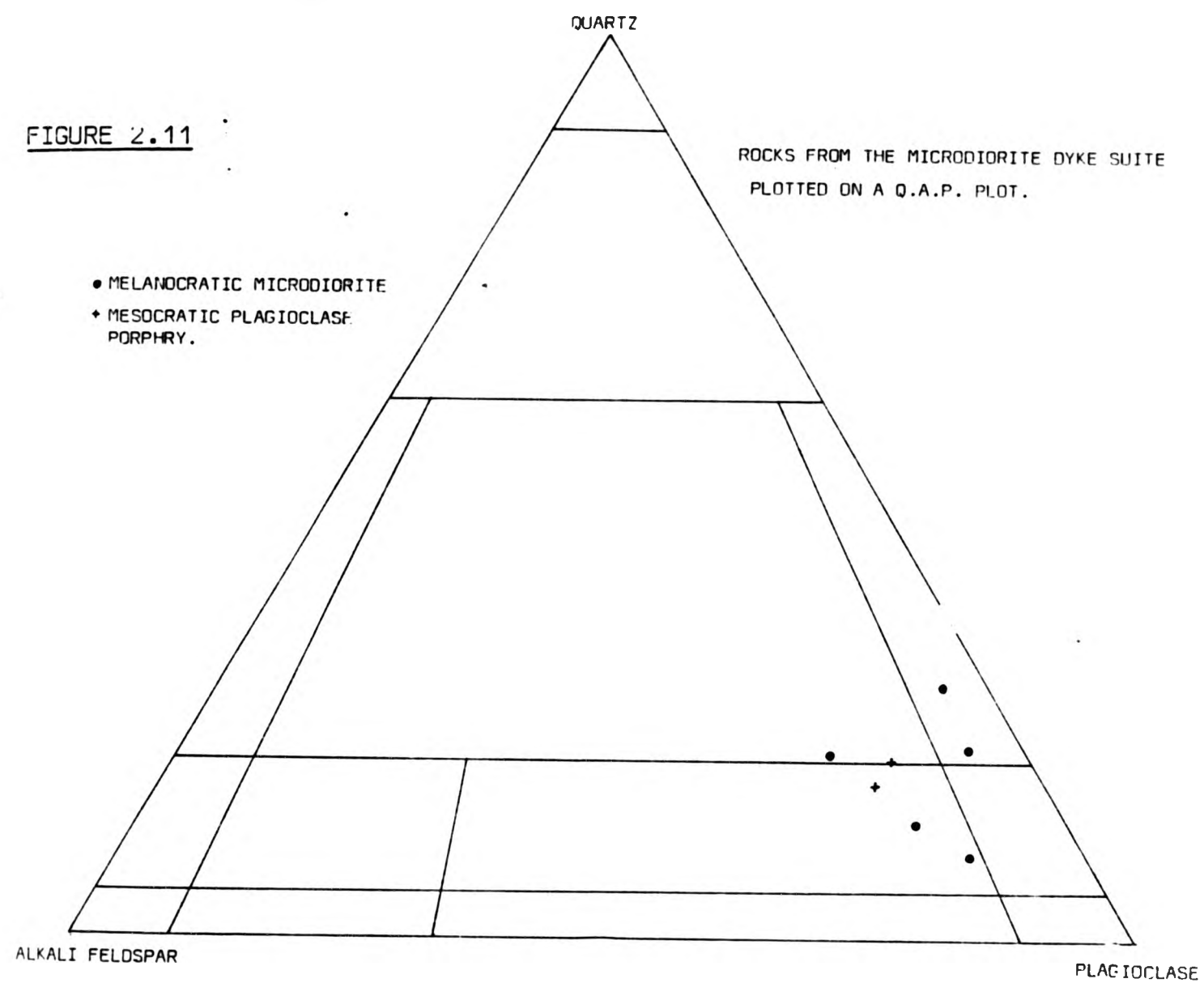
SAMPLE NO.	P23811	P305	P283
Plagioclase	57.4	63.2	57.6
Alkali feldspar	1.46	6.3	4.2
Quartz	1.75	2.6	2.9
Biotite	19.0	13.2	17.2
Hornblende	18.1	8.46	14.3
Sphene	1.75	4.3	2.5
Accessories	0.43	1.85	0.98
TOTAL	99.89	99.91	99.68

TABLE 2.6 Modal Analyses of Rocks from the Microdiorite Suite.

SAMPLE No.	P1529*	P1785*	P1592*	P1543*	P184*	P2830*	P2597*
Plagioclase	54.3	59.1	64.1	50.5	58.5	58.0	57.0
Alkali feldspar	3.35	4.14	7.6	15.4	11.66	12.2	11.6
Quartz	21.3	16.5	6.8	16.8	9.9	15.1	16.5
Biotite	7.3	4.77	4.0	6.1	10.3	13.4	12.8
Hornblende	12.5	13.9	16.3	10.7	7.6	0.85	1.02
Sphene	0.47	0.62	0.33	0.3	1.3	0.28	0.3
Accessories	0.6	0.82	0.66	0.2	0.57	0.14	0.25
TOTAL	99.82	99.85	99.79	100	99.83	99.97	99.47

\* = Melanocratic Microdiorite, + = Mesocratic Microdiorite.

FIGURE 2.11





POSITION OF MINOR INTRUSIVES IN THE ENVELOPE  
AND BODY OF THE FOYERS GRANITIC COMPLEX.

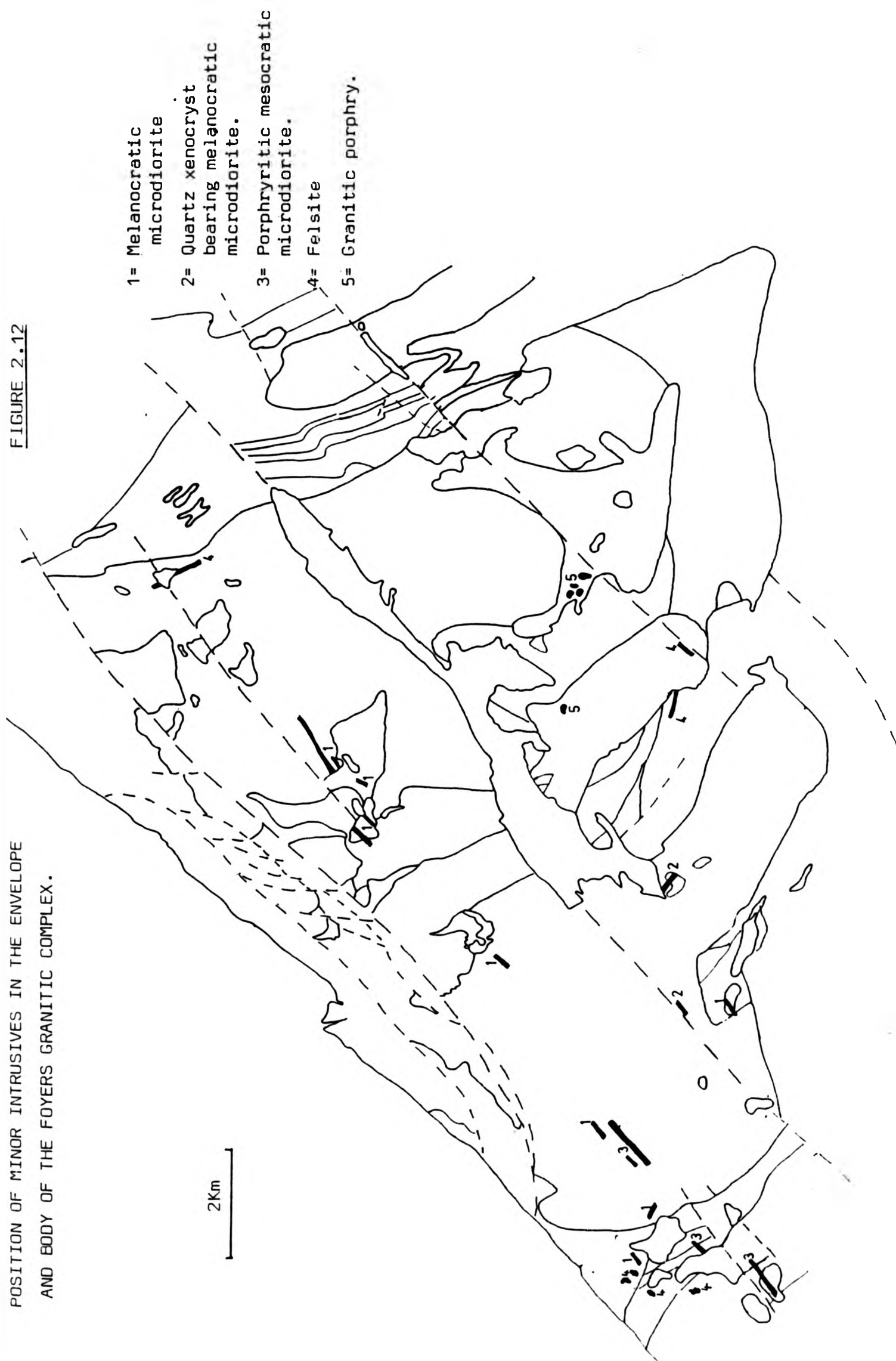




TABLE 2.7 Modal Analyses of Rocks from the Appinite Suite.

SAMPLE No.	P673	P994	P749	P1671
Plagioclase	49.0	26.0	20.0	38.23
Alkali feldspar	0.54	0.65	16.4	7 "
Quartz	trace	11.08	0.73	1
Biotite	trace	17.6	21.8	12.7
Hornblende	49.3	43.4	20.5	37.9
Pyroxene	0.0	0.0	15.4	0.0
Sphene	0.07	0.5	2.2	1.3
Accessories	1.0	0.58	2.7	1.0
TOTAL	99.91	99.81	99.73	99.3

FIGURE 2.13

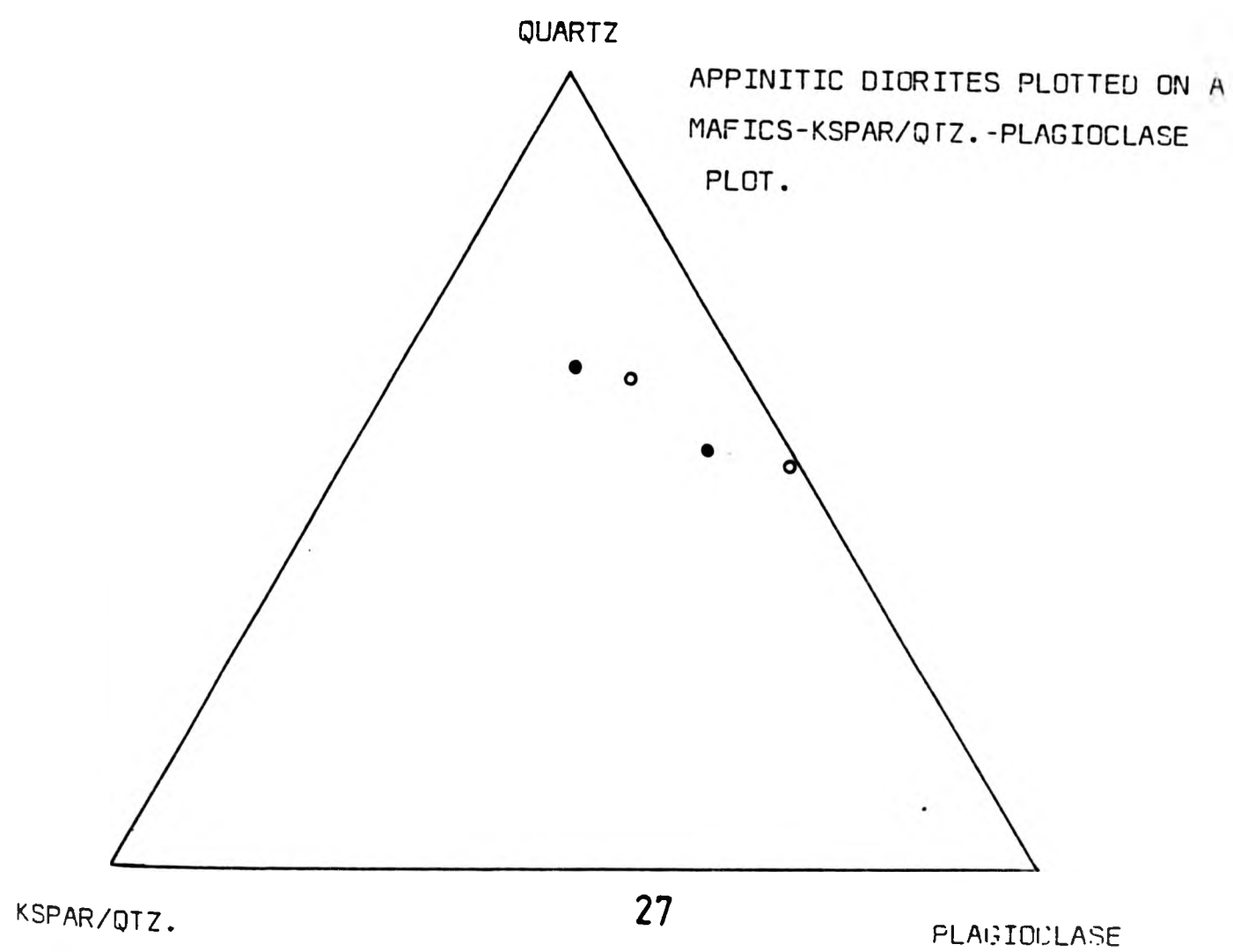
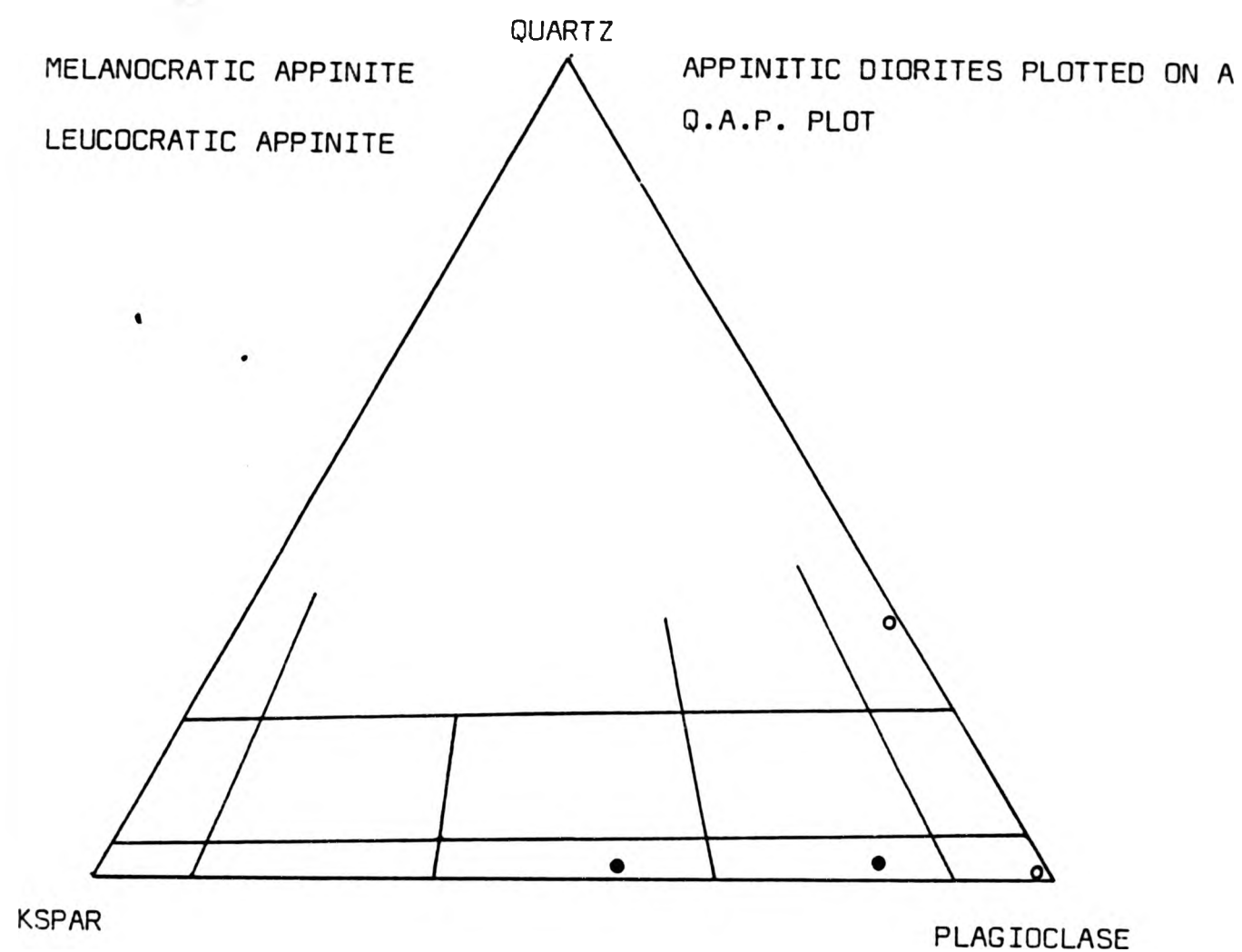


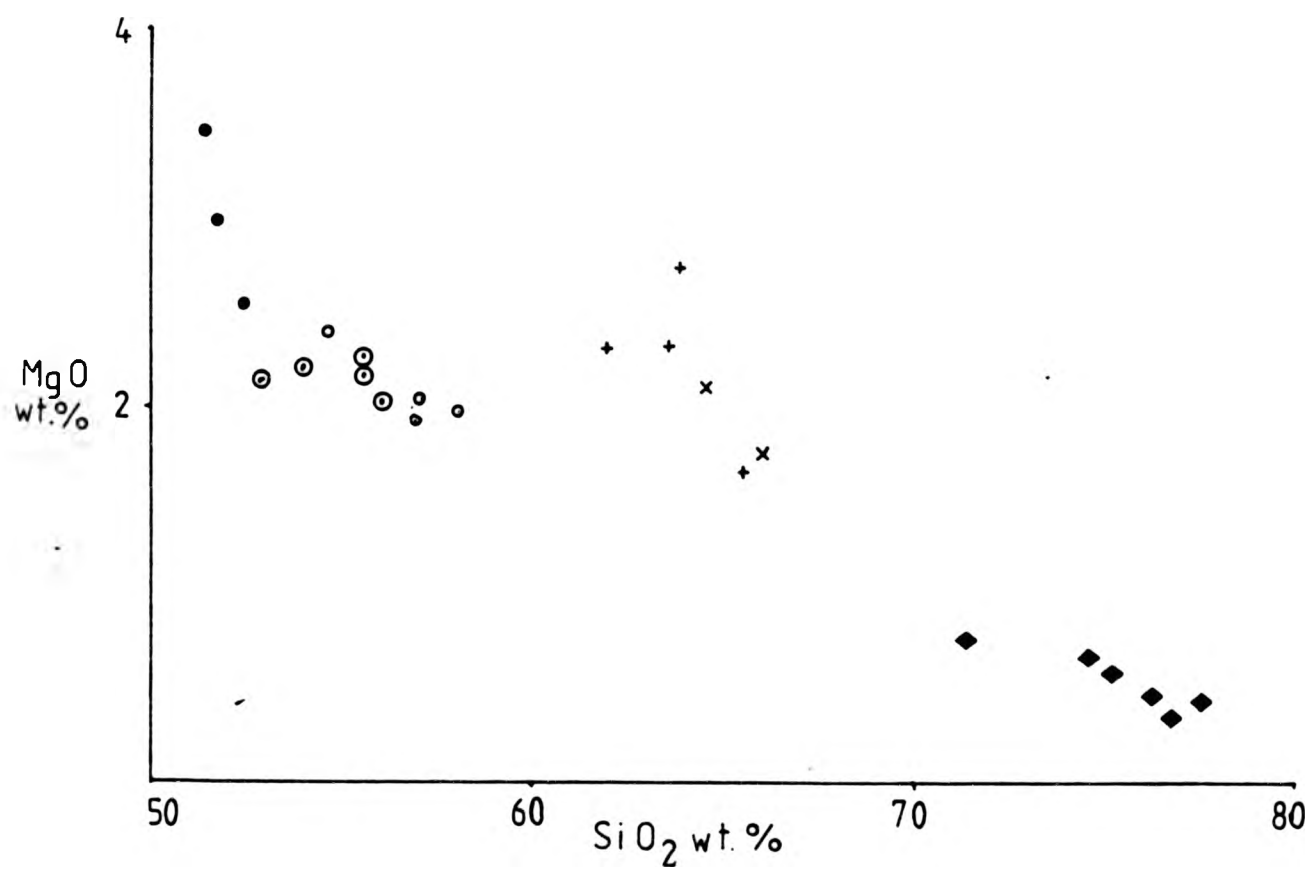
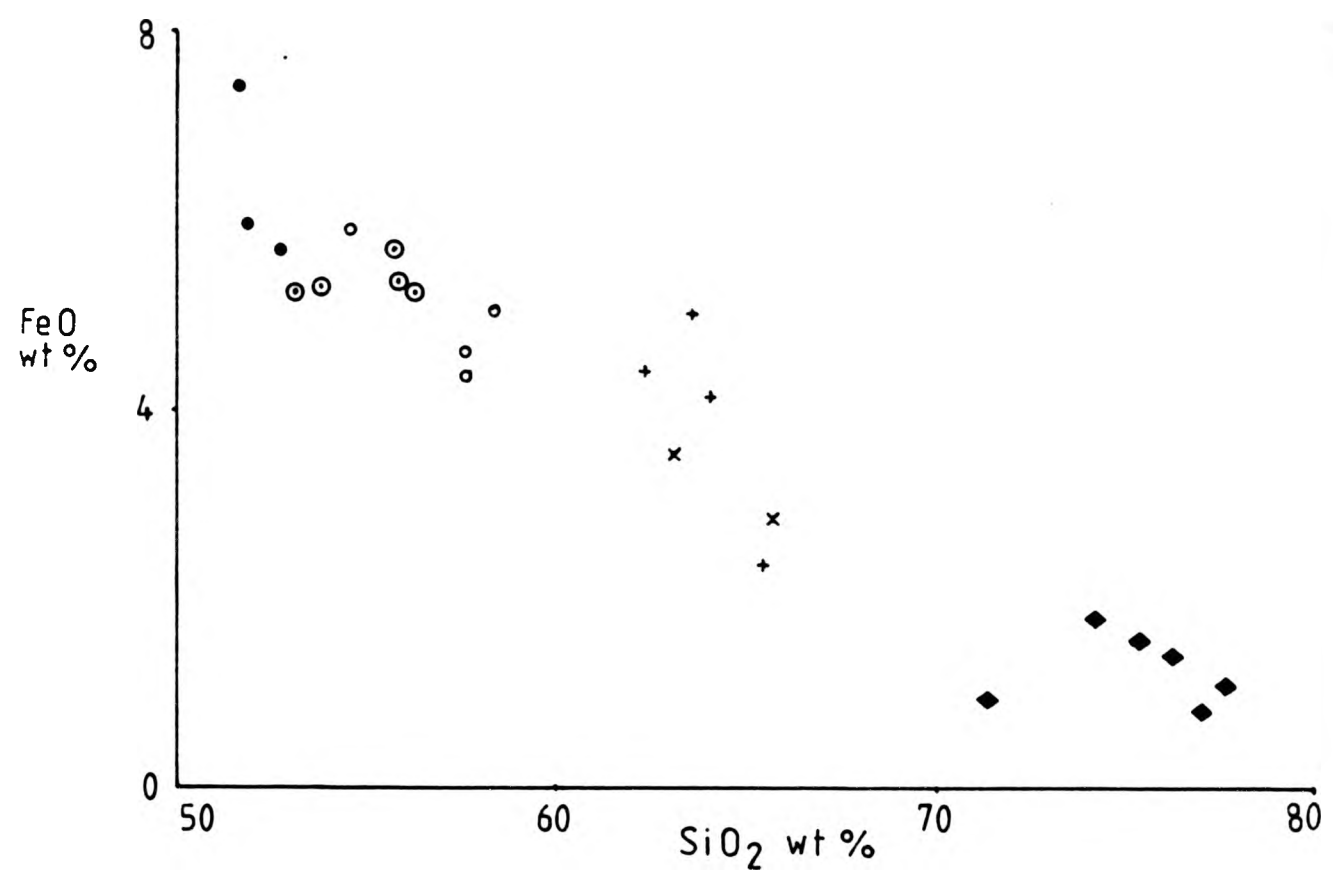
FIGURE 2.14

THE FOLLOWING SEQUENCE OF GRAPHS SHOW THE MAJOR AND TRACE ELEMENT GEOCHEMISTRIES OF THE MAJOR GRANITOID UNITS FROM THE FOYERS COMPLEX. THE GEOCHEMICAL DATA IS PRESENTED AS A SERIES OF HARKER PLOTS.

- Erroglie Quartz Diorite.
- Chliabhain Quartz Monzodiorite.
- + Dalcrag Granodiorite.
- ◆ Aberchalder Adamellite.
- ⊙ Quartz diorite/Quartz Monzodiorite Intermediate.
- × Dun Garbh Granodiorite.

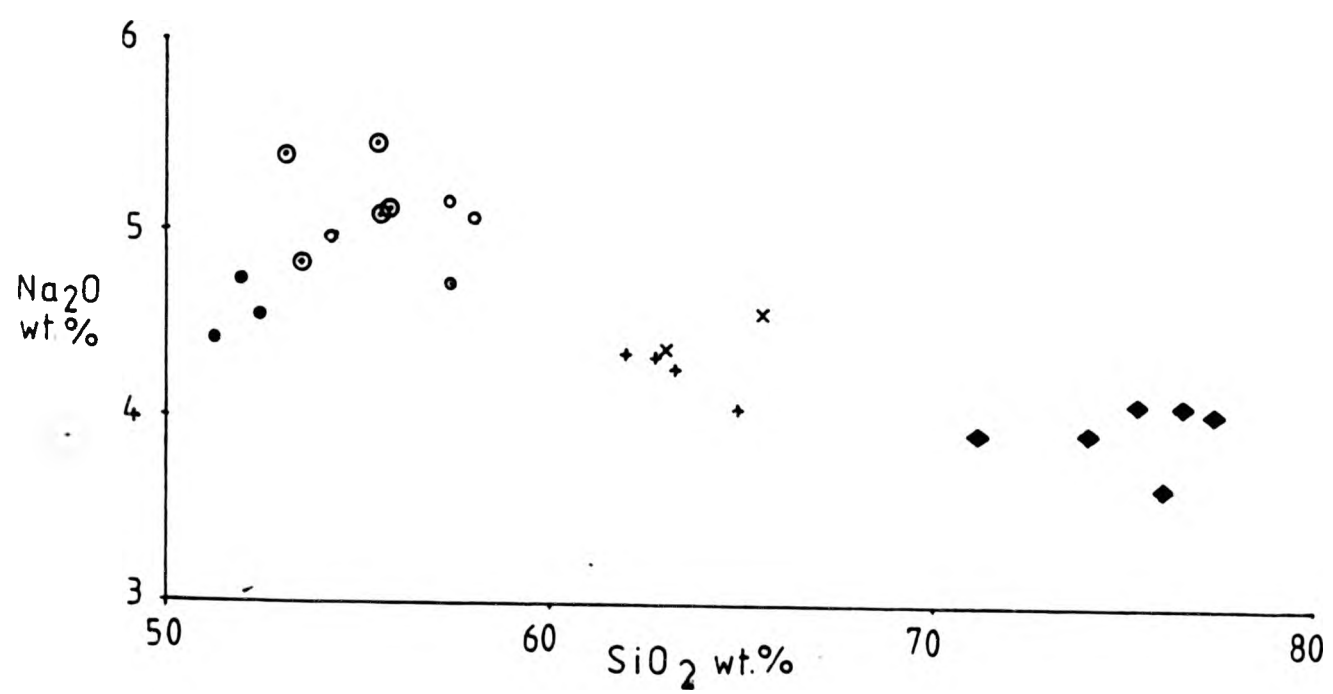
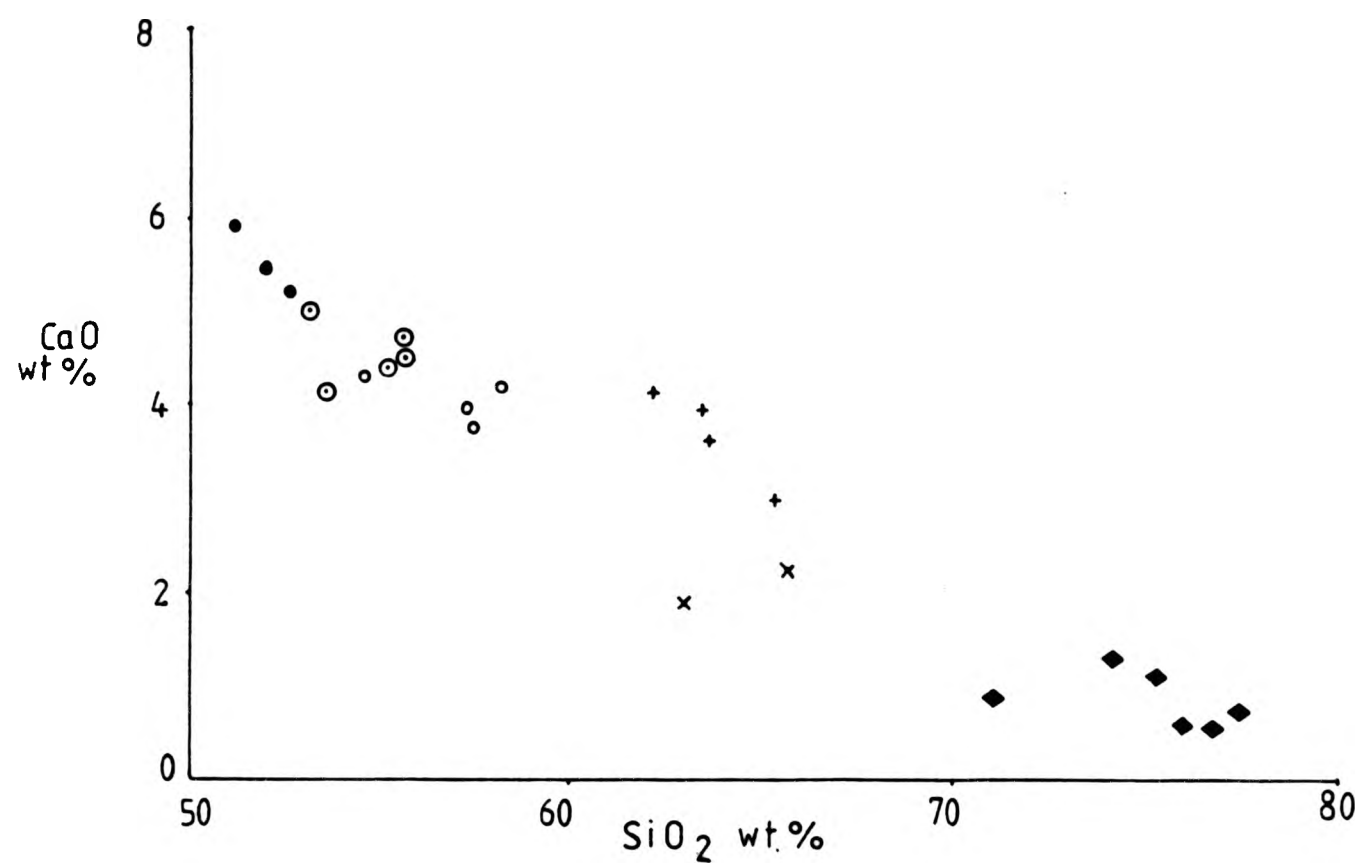
Contd...

FIGURE 2.14



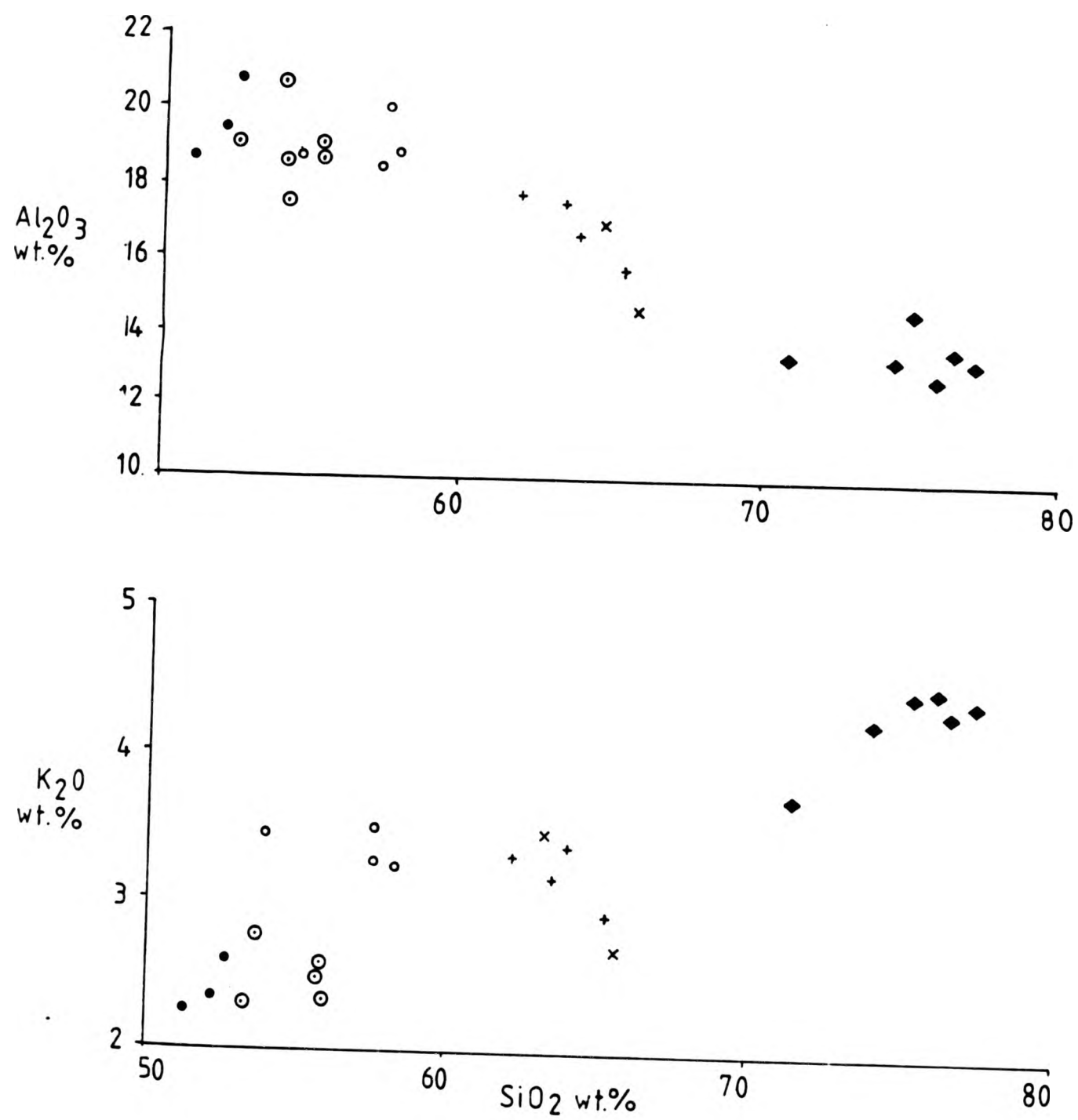
Contd...

FIGURE 2.14



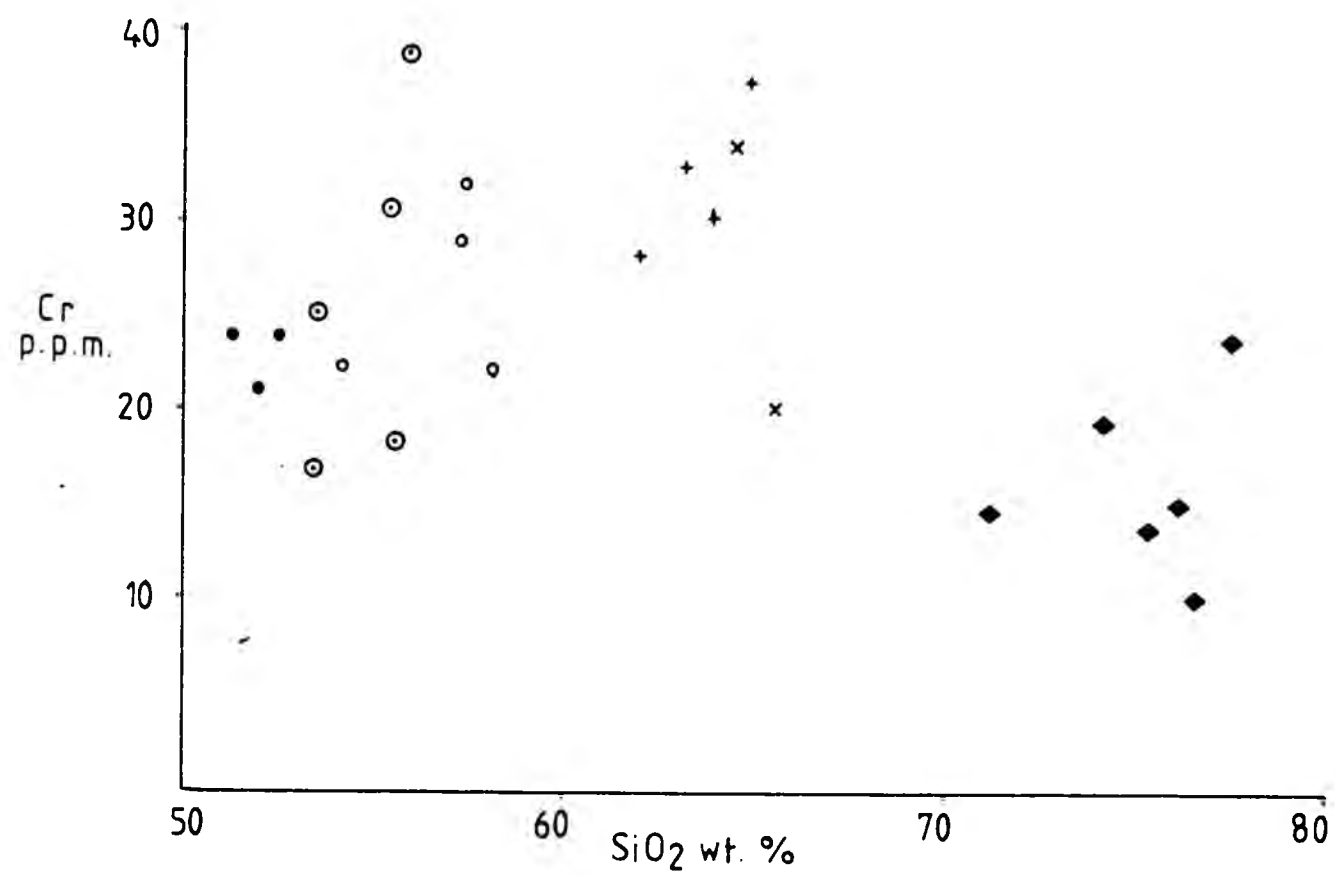
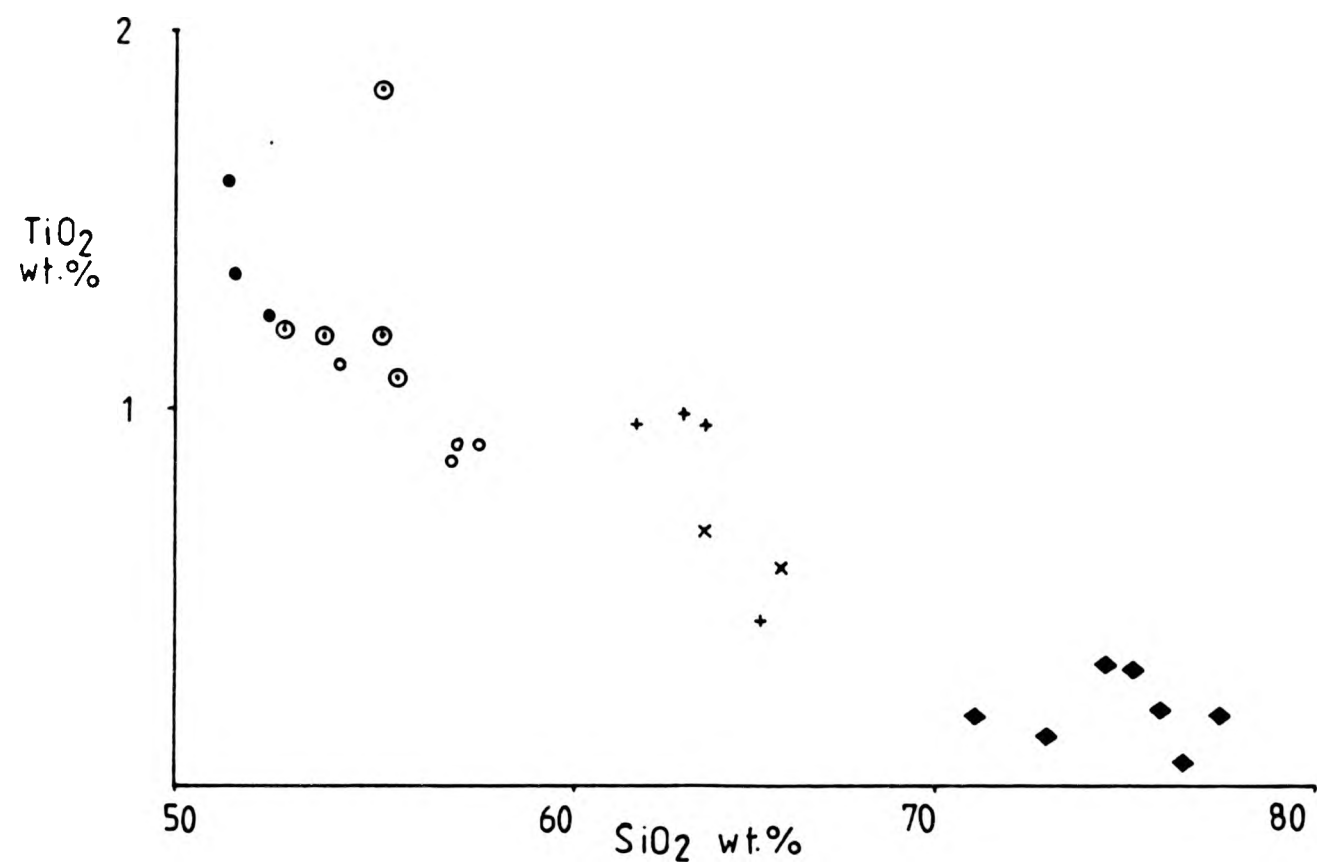
Contd...

FIGURE 2.14



Contd...

FIGURE 2.14



Contd...



FIGURE 2.14

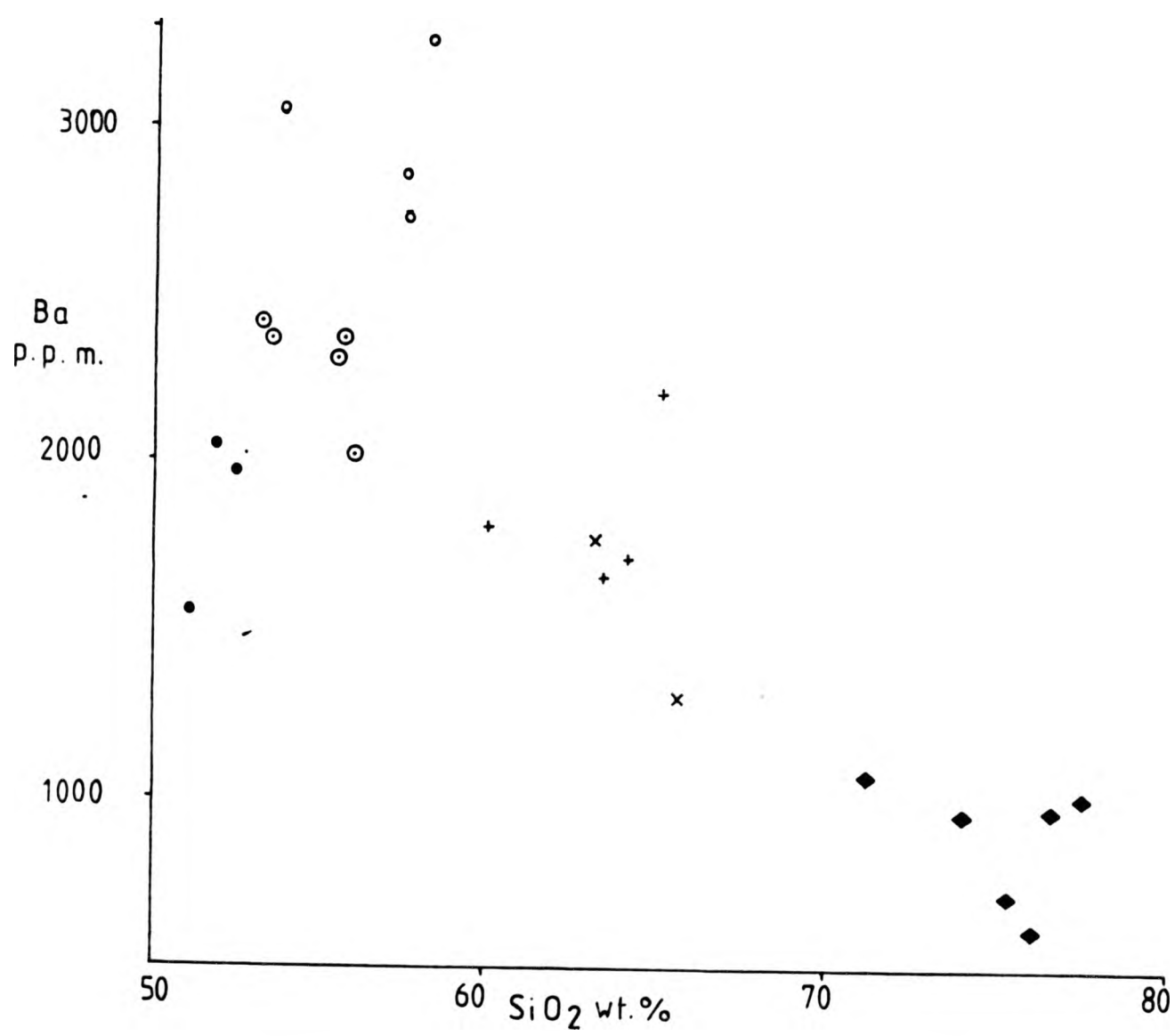
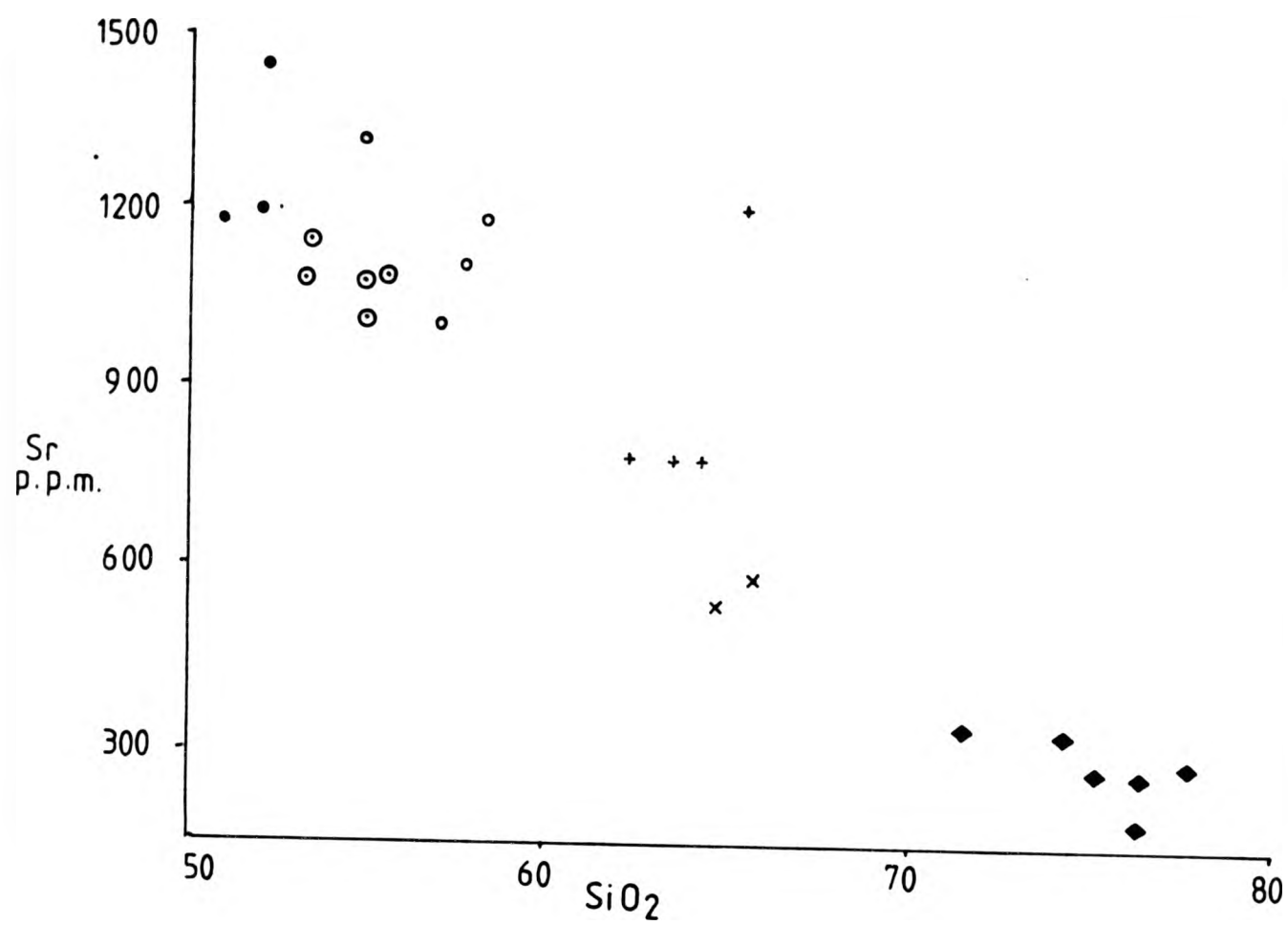
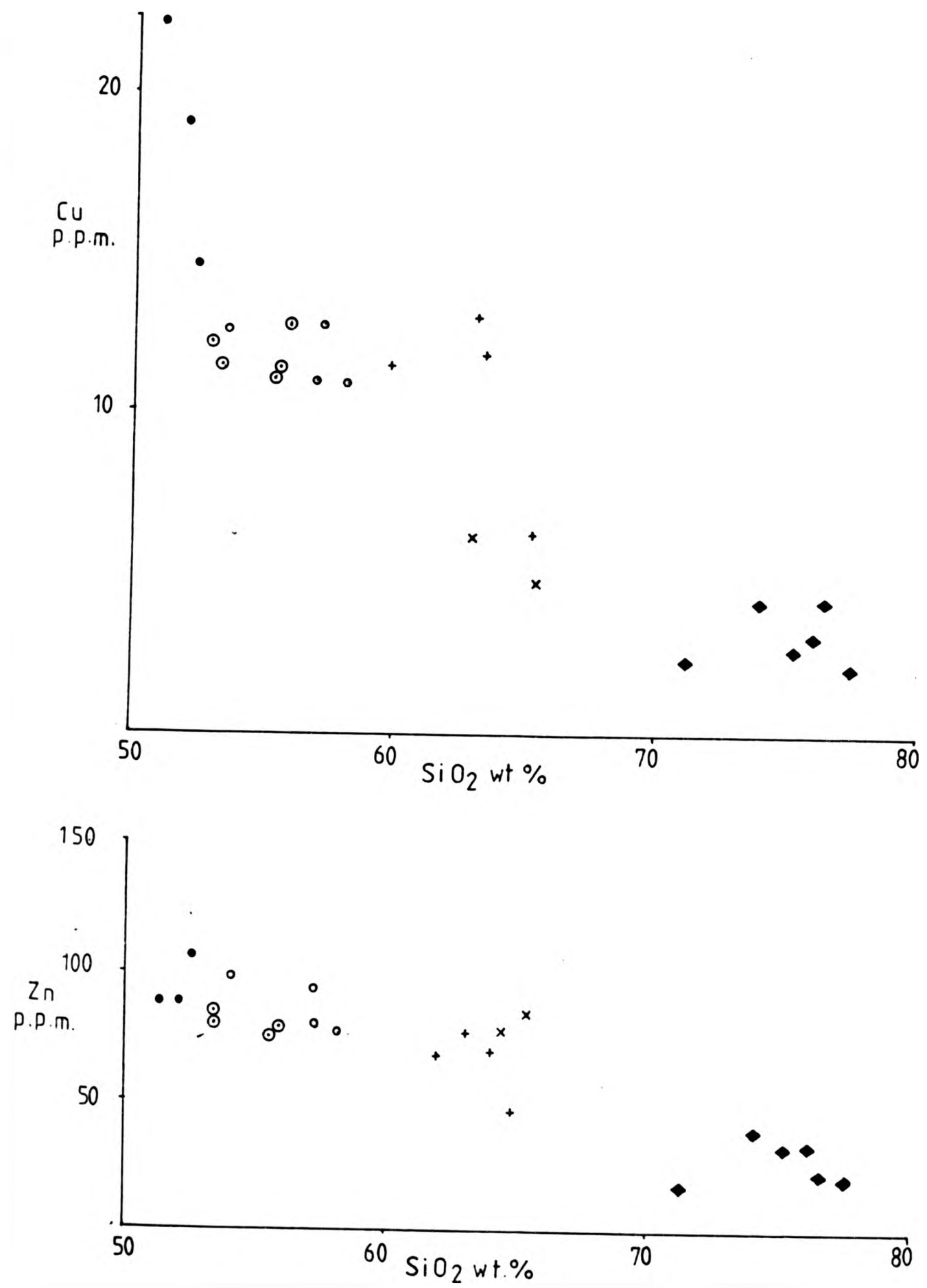
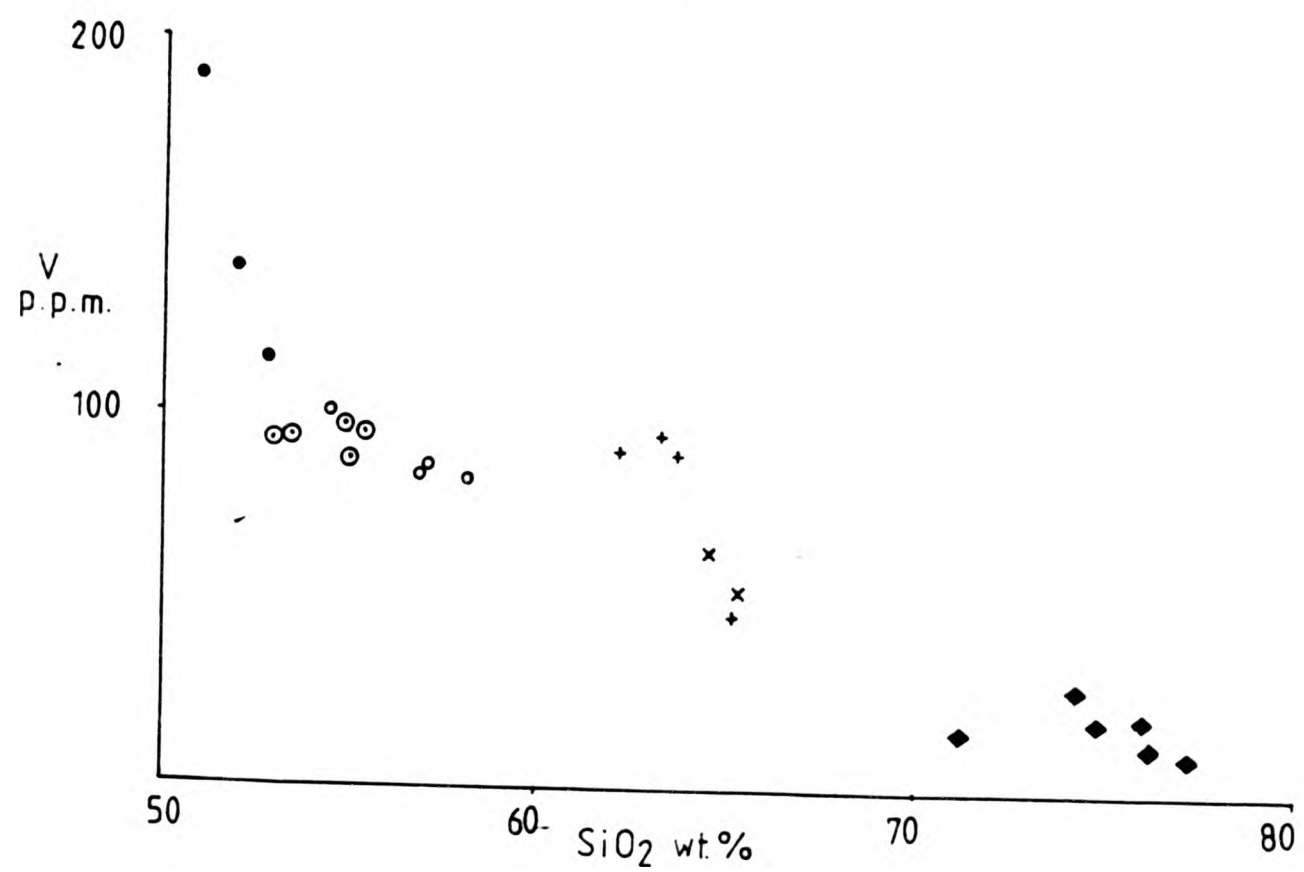
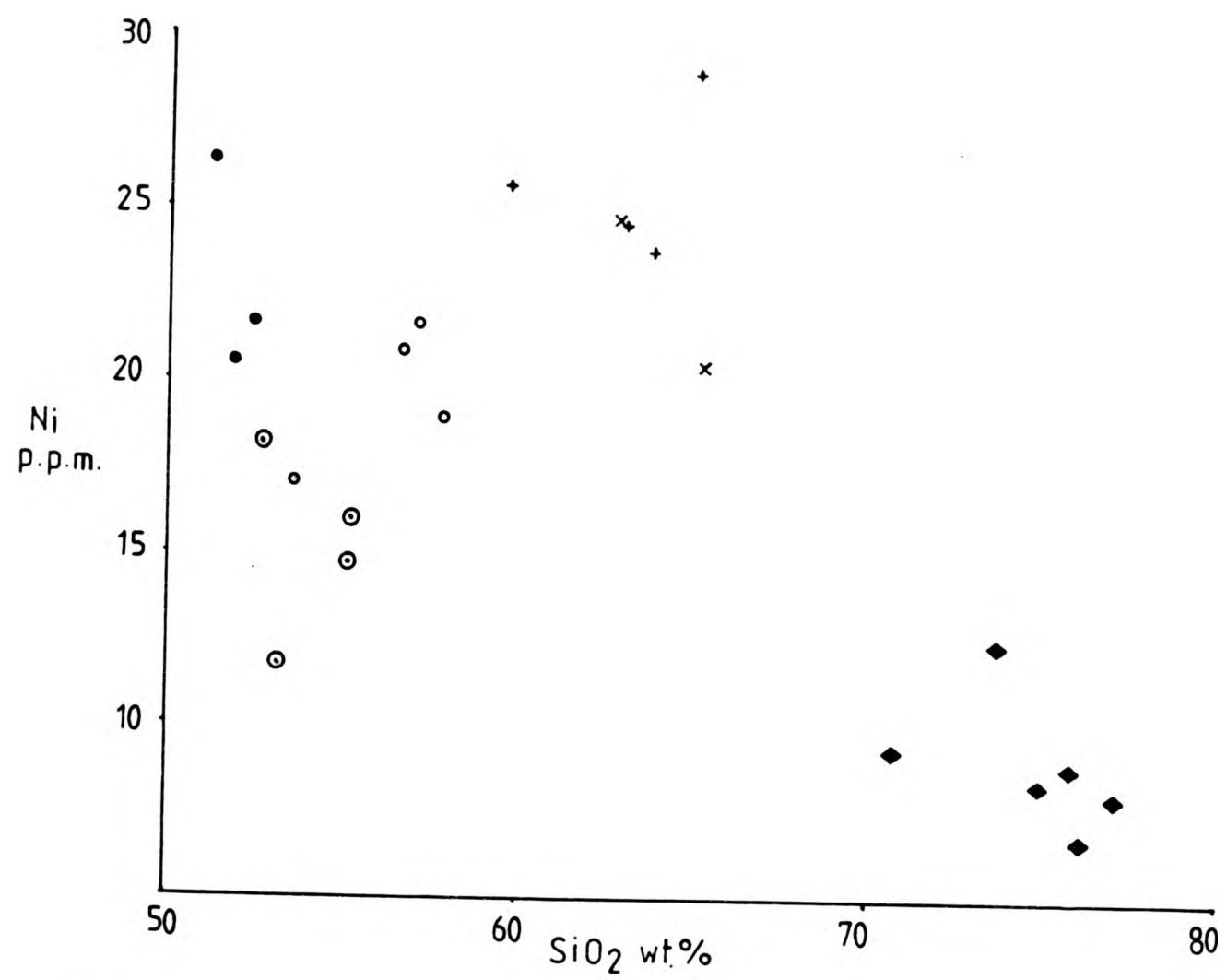


FIGURE 2.14

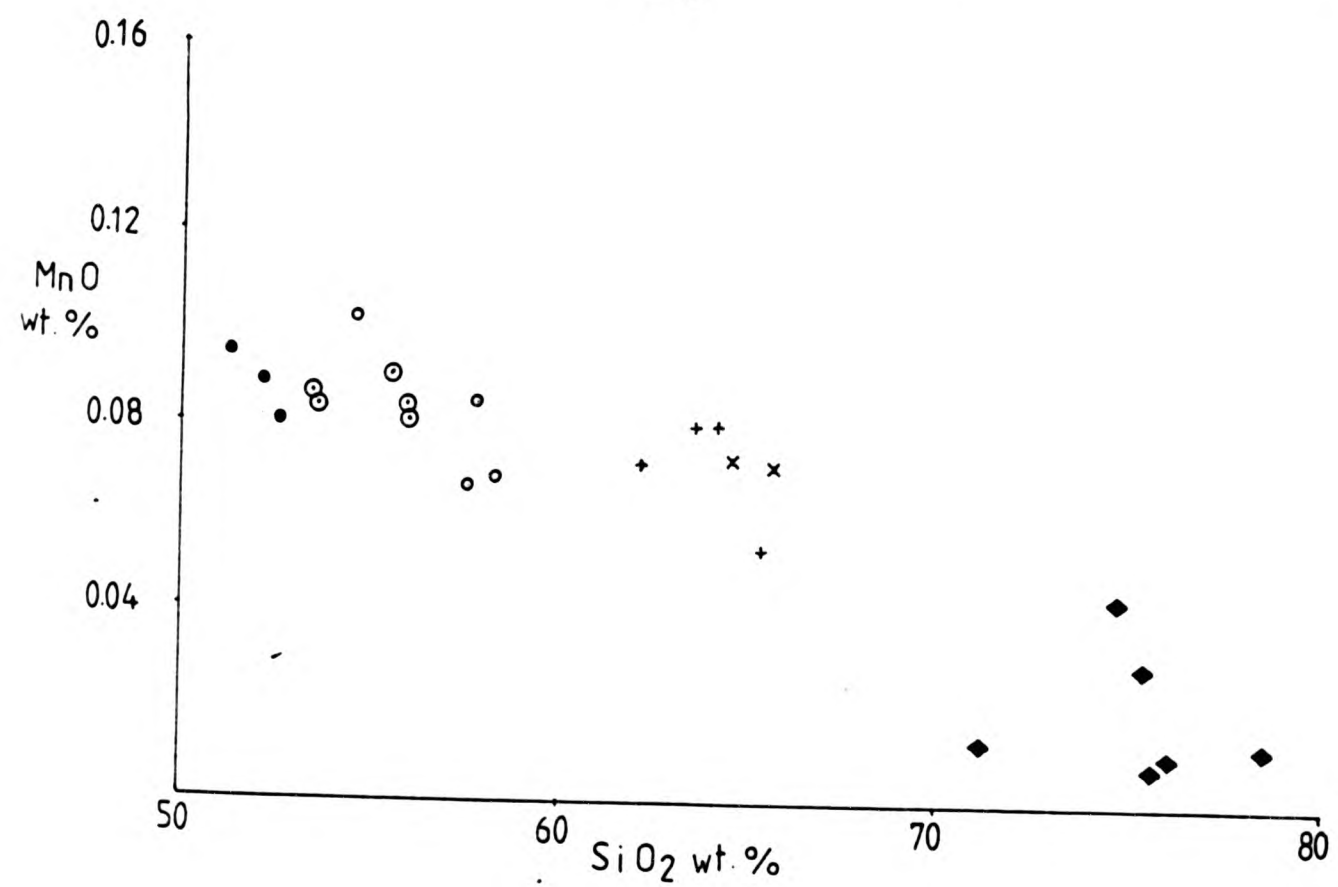
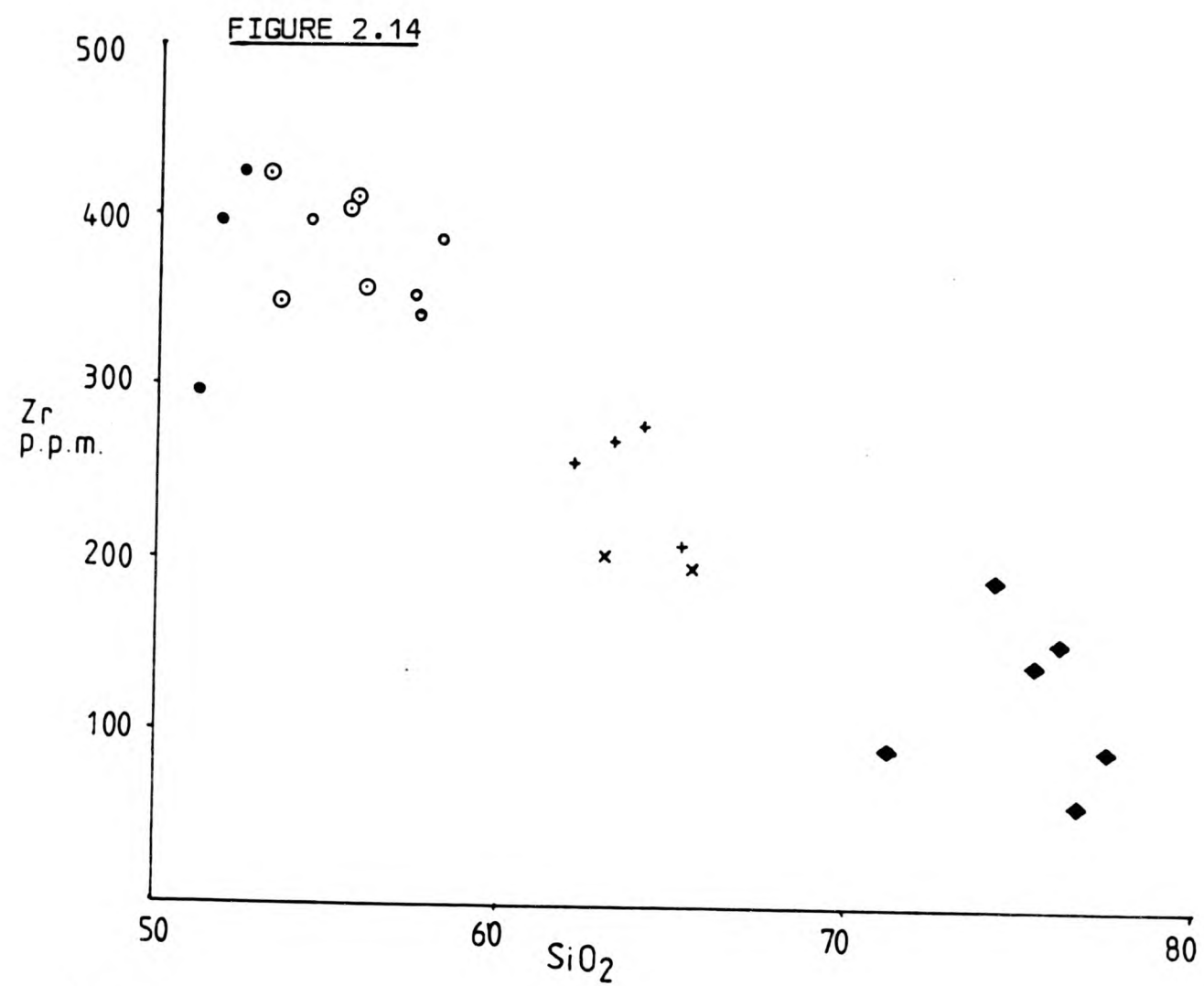


Contd...

FIGURE 2,14



Contd...



Contd...

FIGURE 2.14

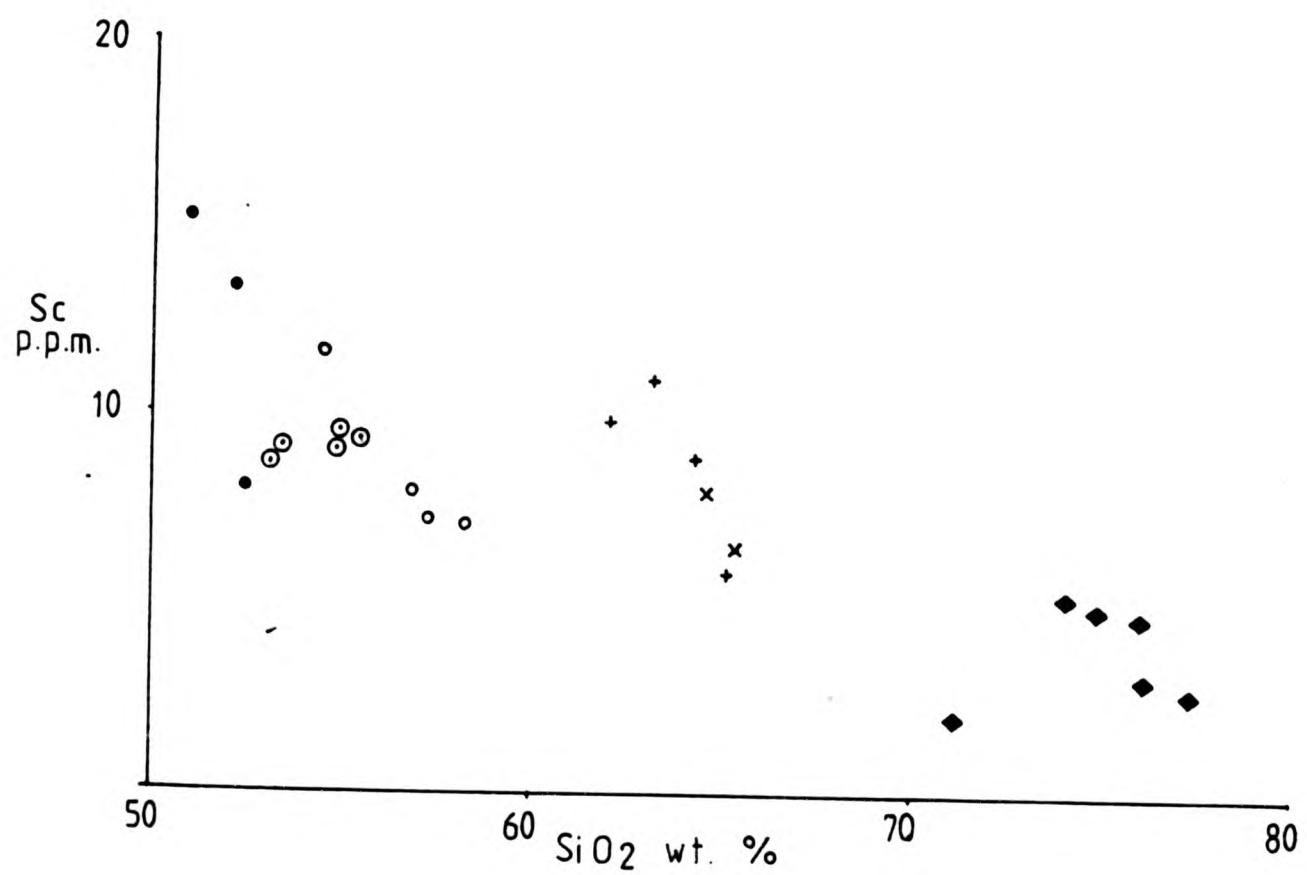
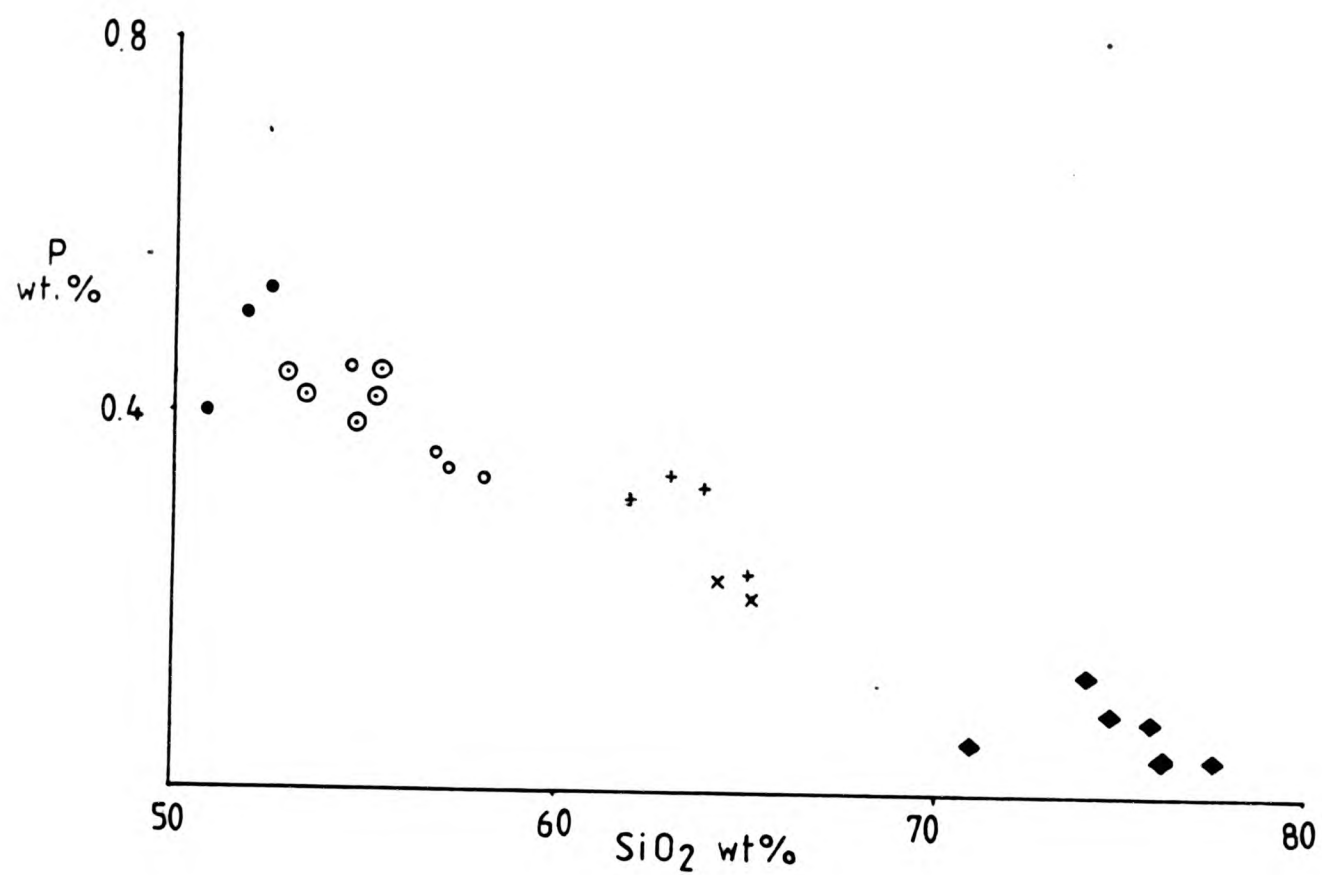
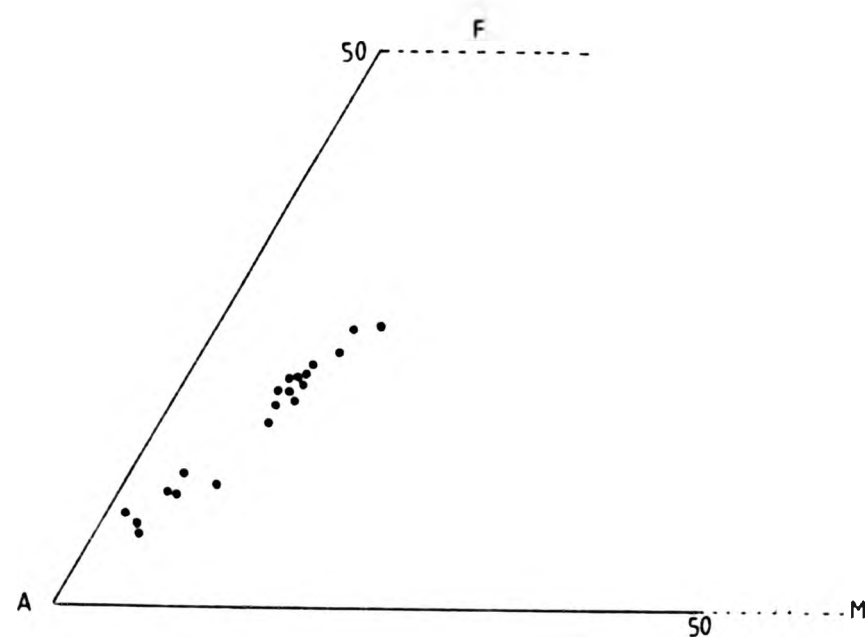
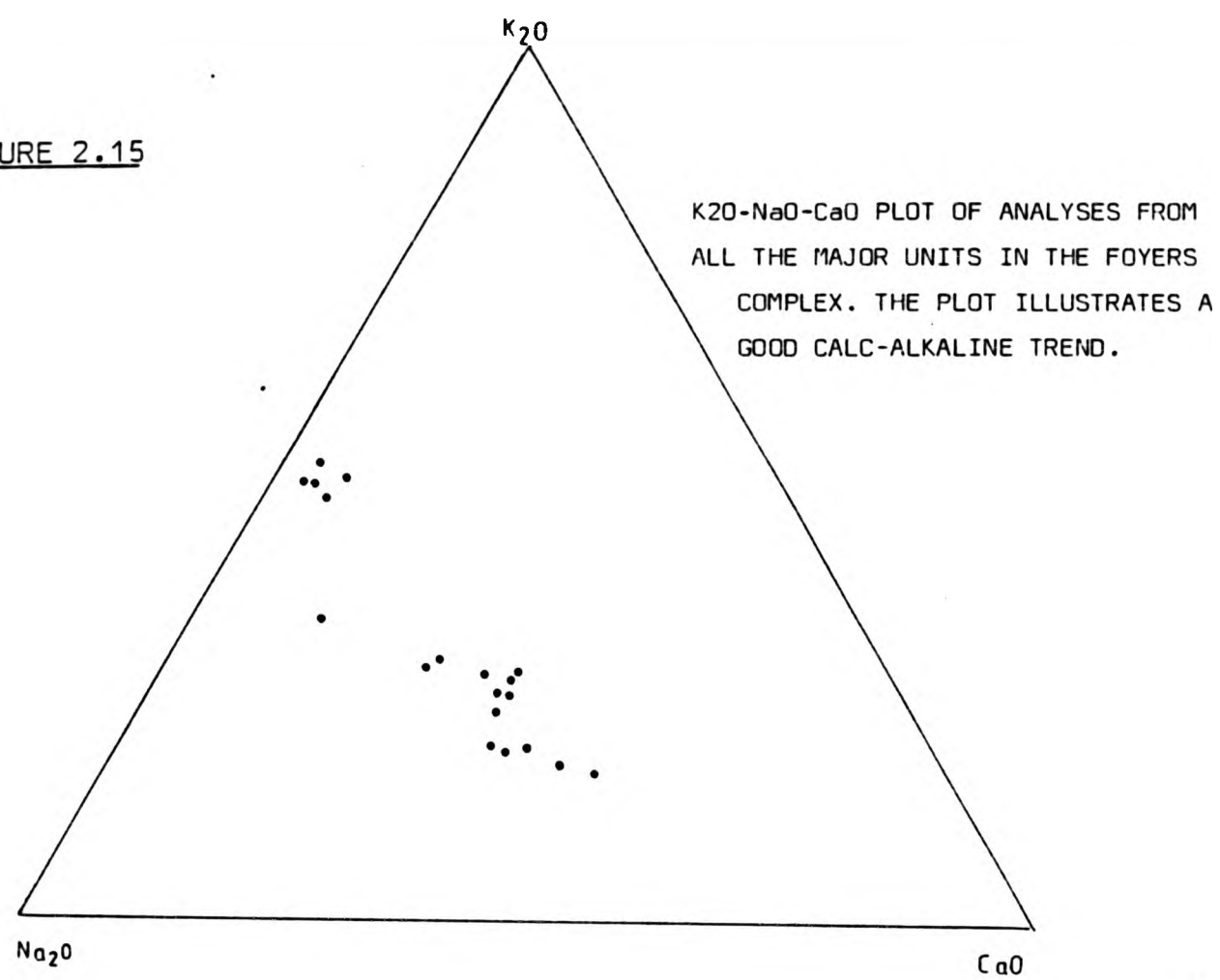


FIGURE 2.15



PLATES  
Chapter 2



Plate 2.1

Field view of Errogie Quartz Diorite, showing a weak alignment of plagioclase and mafics. (Stratherrick War Memorial).

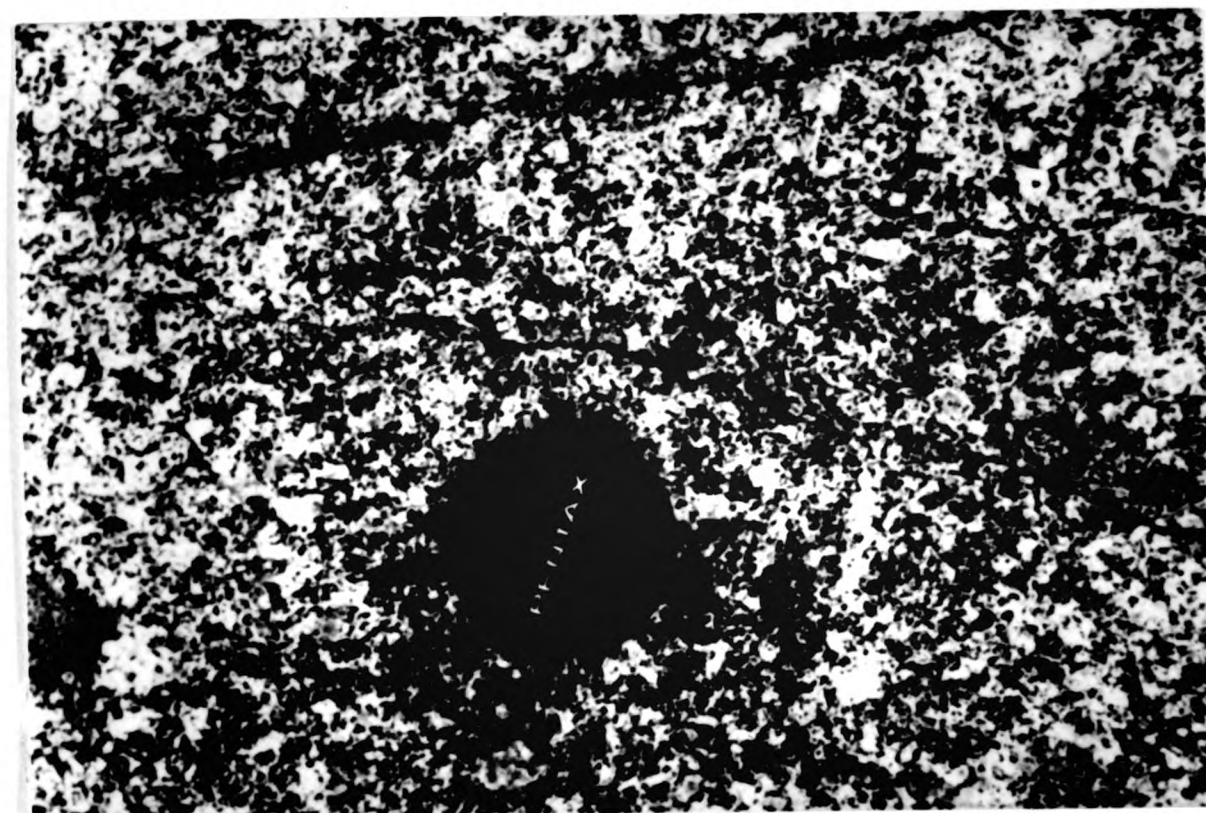


Plate 2.2

Subhedral hornblende(H), and plagioclase(P) chadocrysts, enclosed by a large orthoclase oikocryst (O). Errogie Quartz Diorite. (Crossed polars, x47).

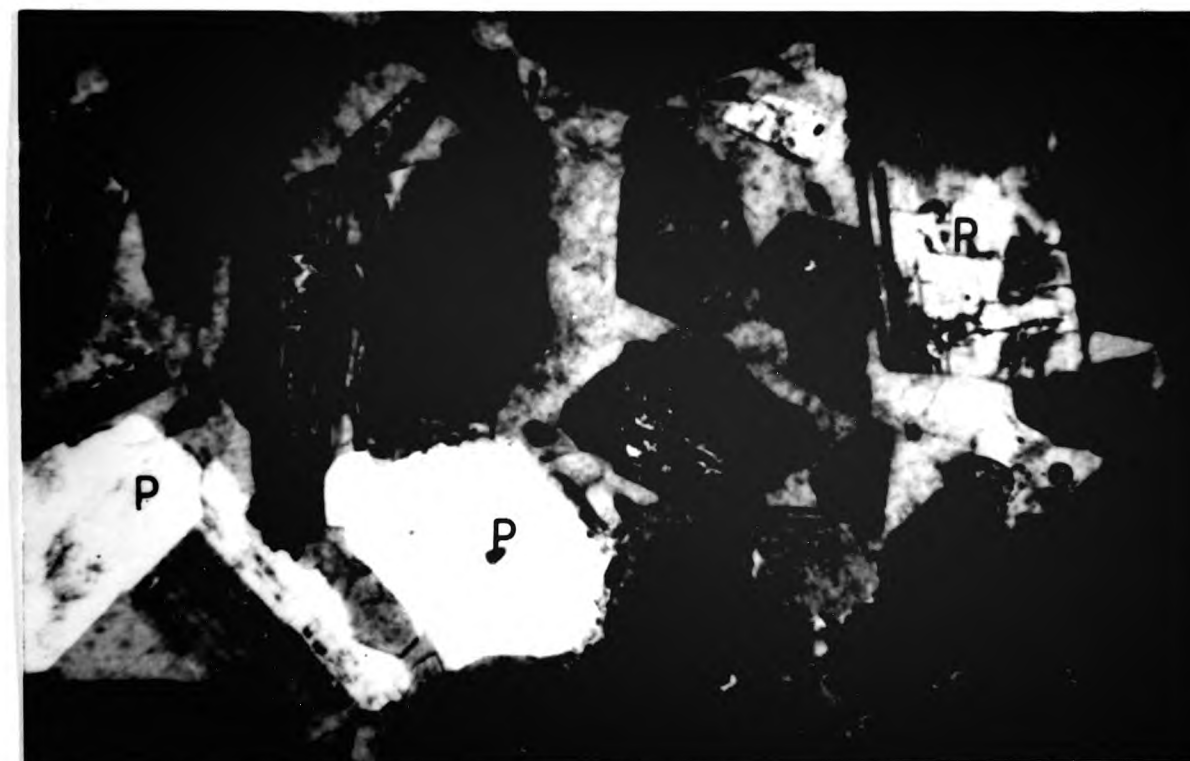


Plate 2.3  
General view of Chliabhain Quartz Monzodiorite,  
containing large plagioclase laths (P), carlsbad  
twinned orthoclase (O), and abundant biotite. Note the  
absence of hornblende. (Crossed polars, x47)

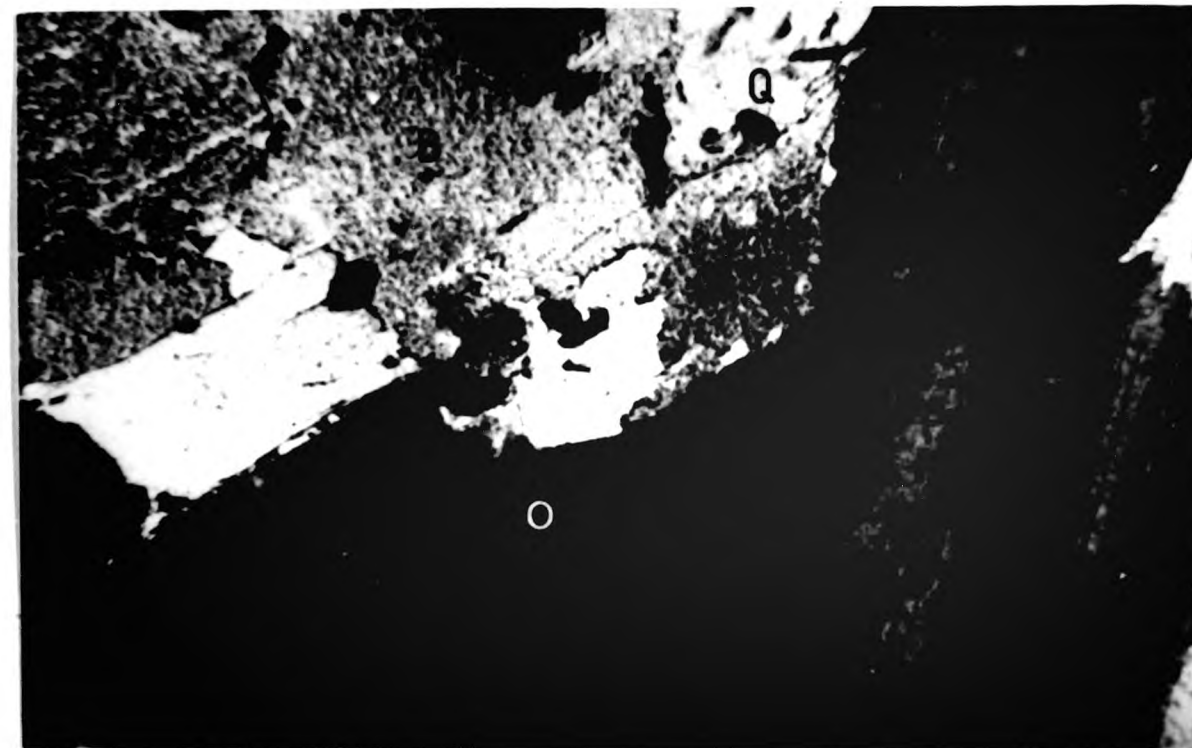


Plate 2.4  
Large plagioclase phenocryst, displaying oscillatory  
zoning. Chliabhain Quartz Monzodiorite. (Crossed  
polars, x47)





Plate 2.5

Euhedral plagioclase lath, cut and replaced by orthoclase. Chliabhain Quartz Monzodiorite. (Crossed polars, x47)

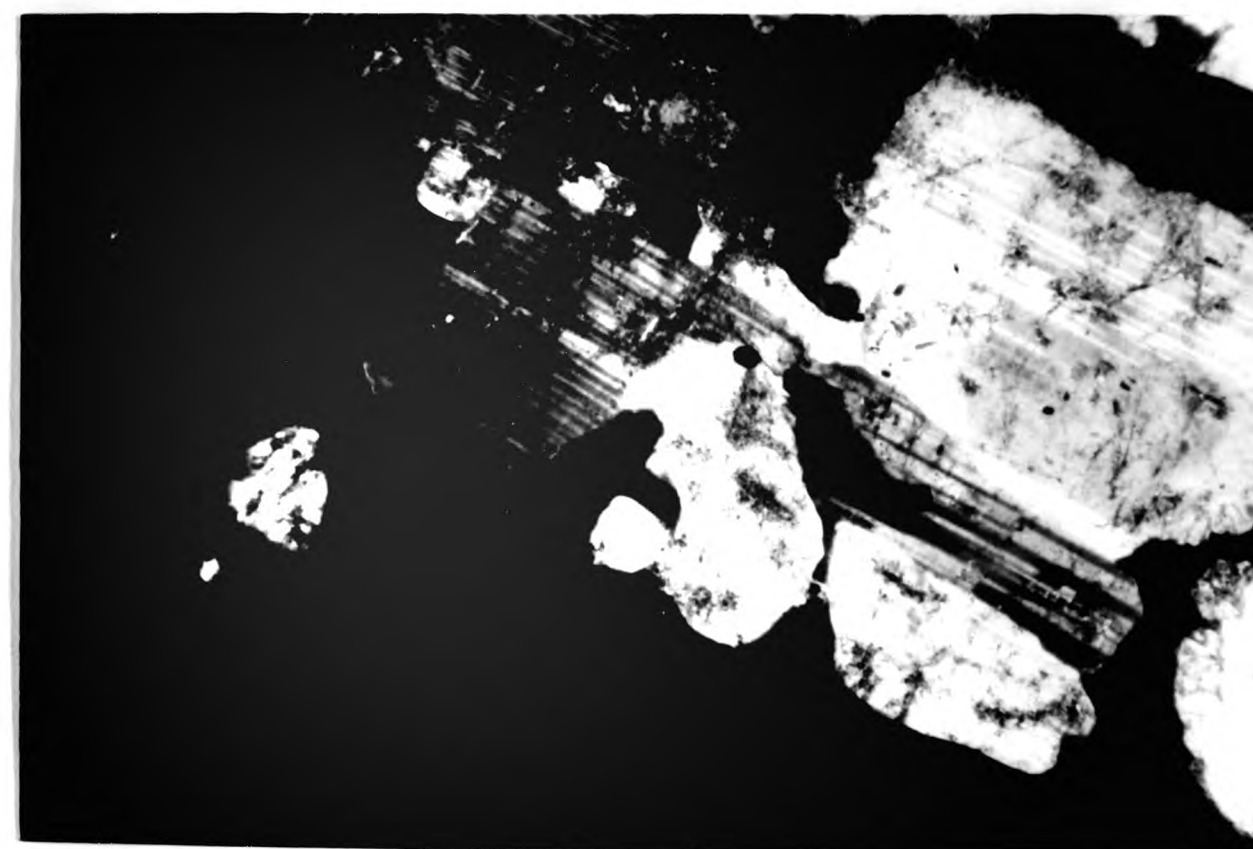


Plate 2.6

Field view of Dalcrag Granodiorite. (Trinloist).

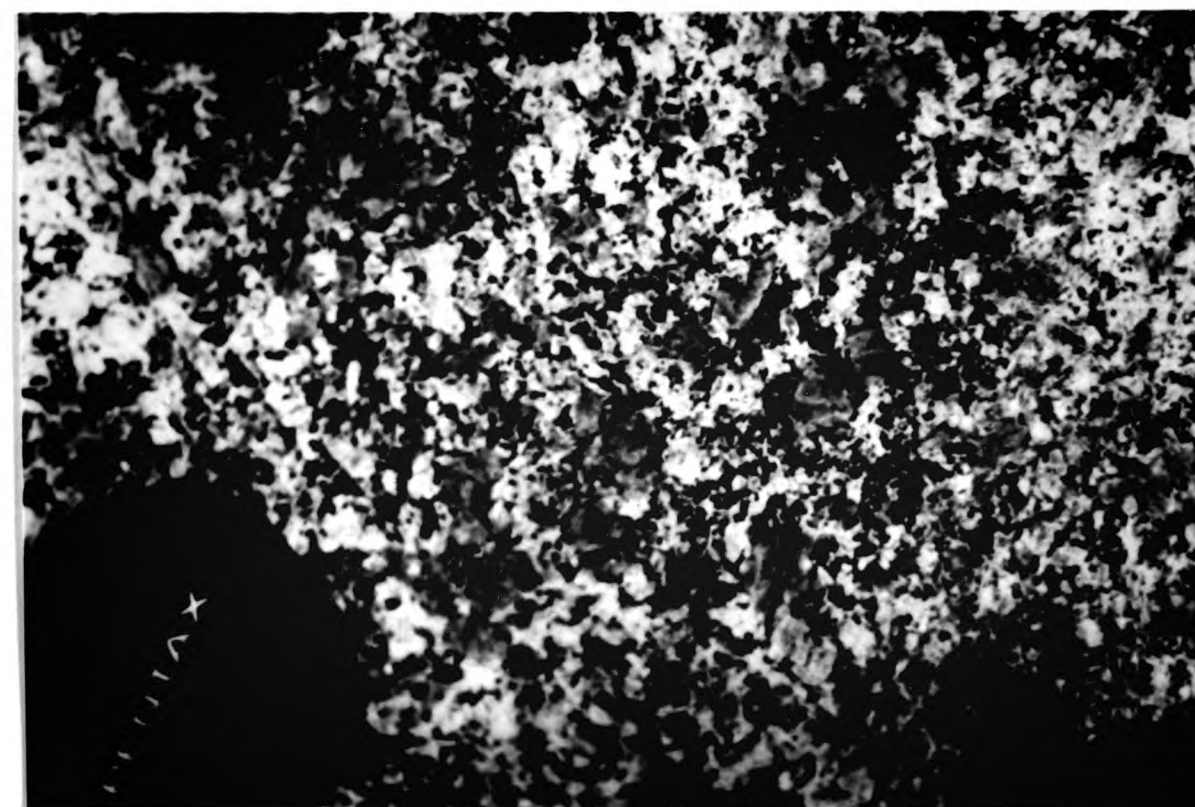


Plate 2.7  
General view of Dalcrag Granodiorite, displaying  
plagioclase, quartz and large orthoclase phenocrysts.  
(Crossed polars, x5)

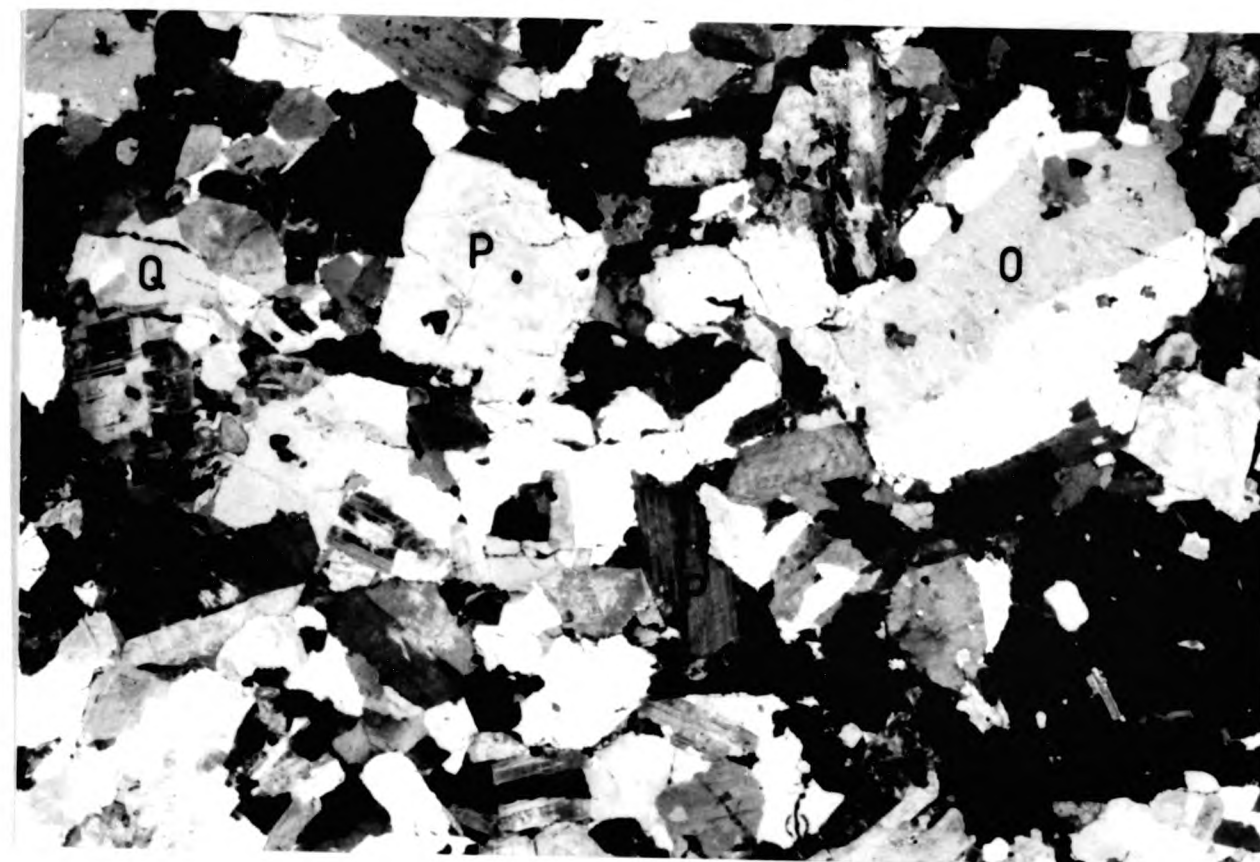


Plate 2.8  
Field view of Aberchalder Adamellite. (Trinloist).

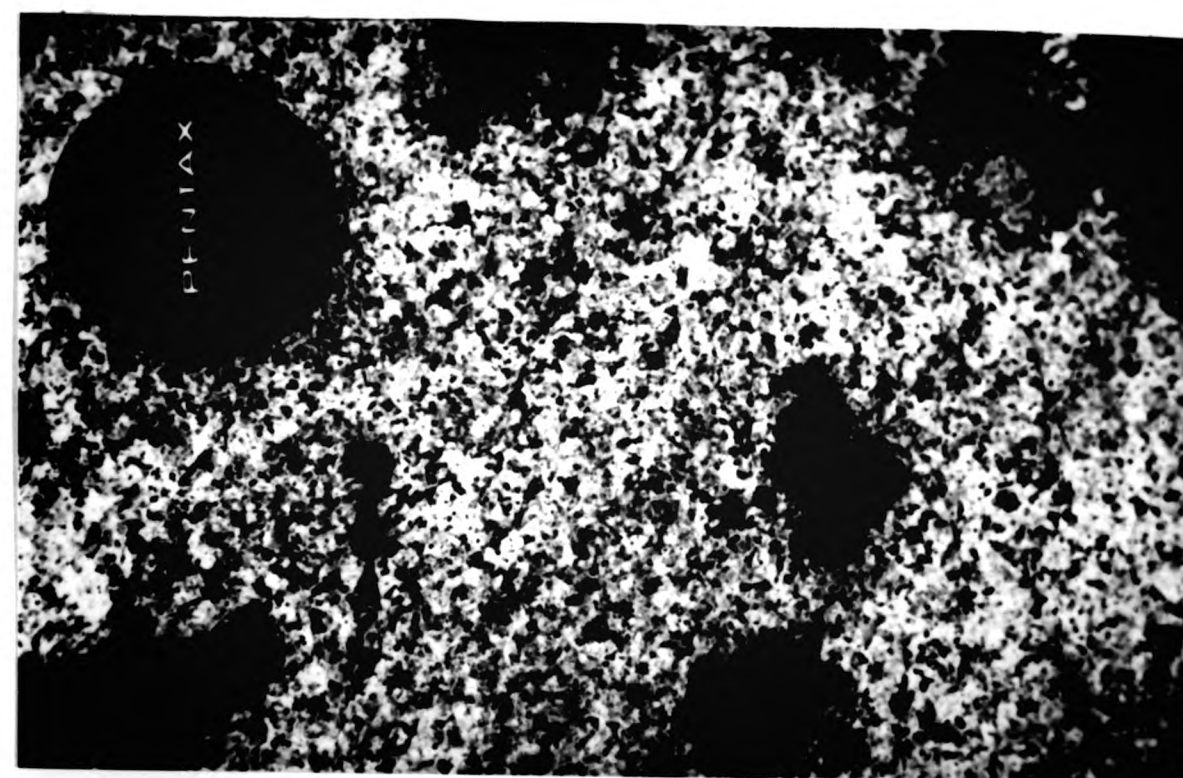




Plate 2.9

General view of Aberchalder Adamellite, dominated by quartz and orthoclase feldspar. The quartz shows a strong consertal texture and the twinned orthoclase is perthitic. Note the irregular patches of finer grained crystals. (Crossed polars, x5)

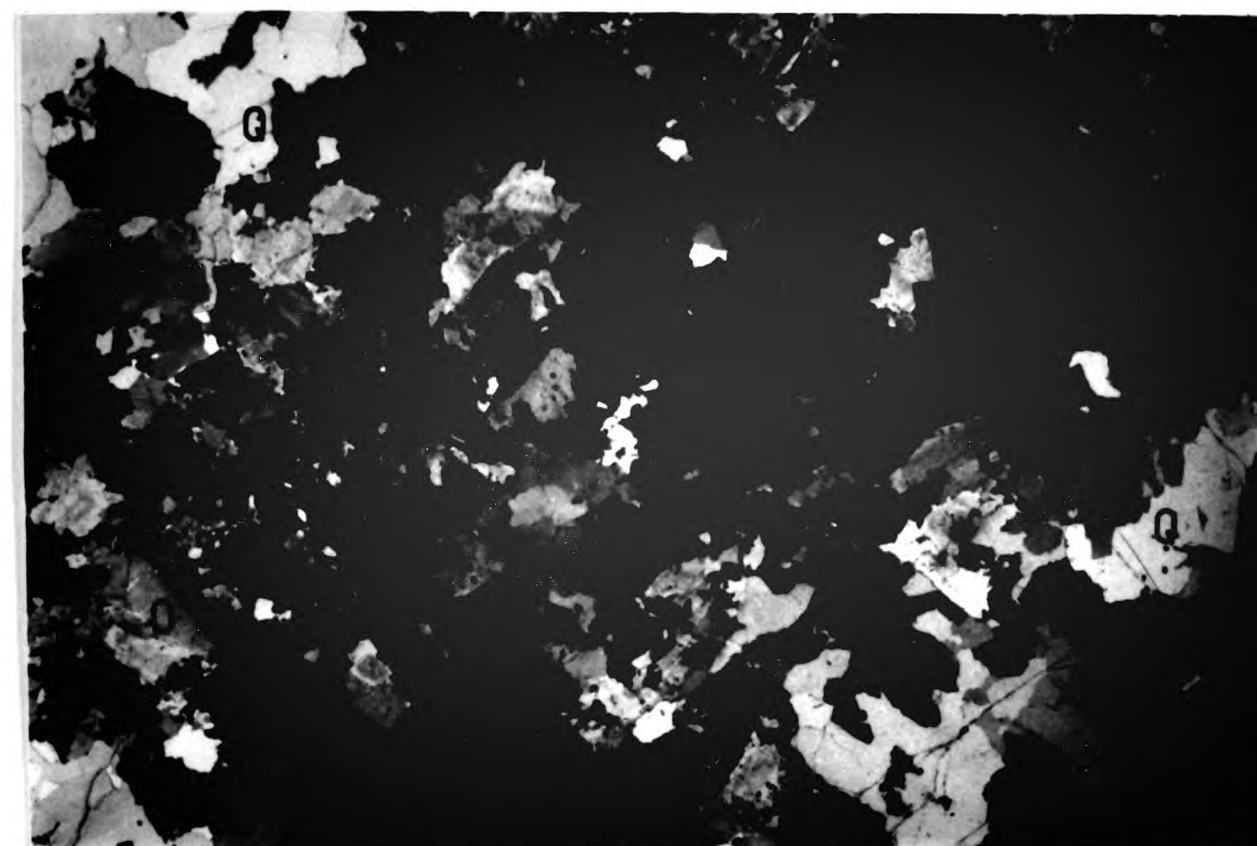
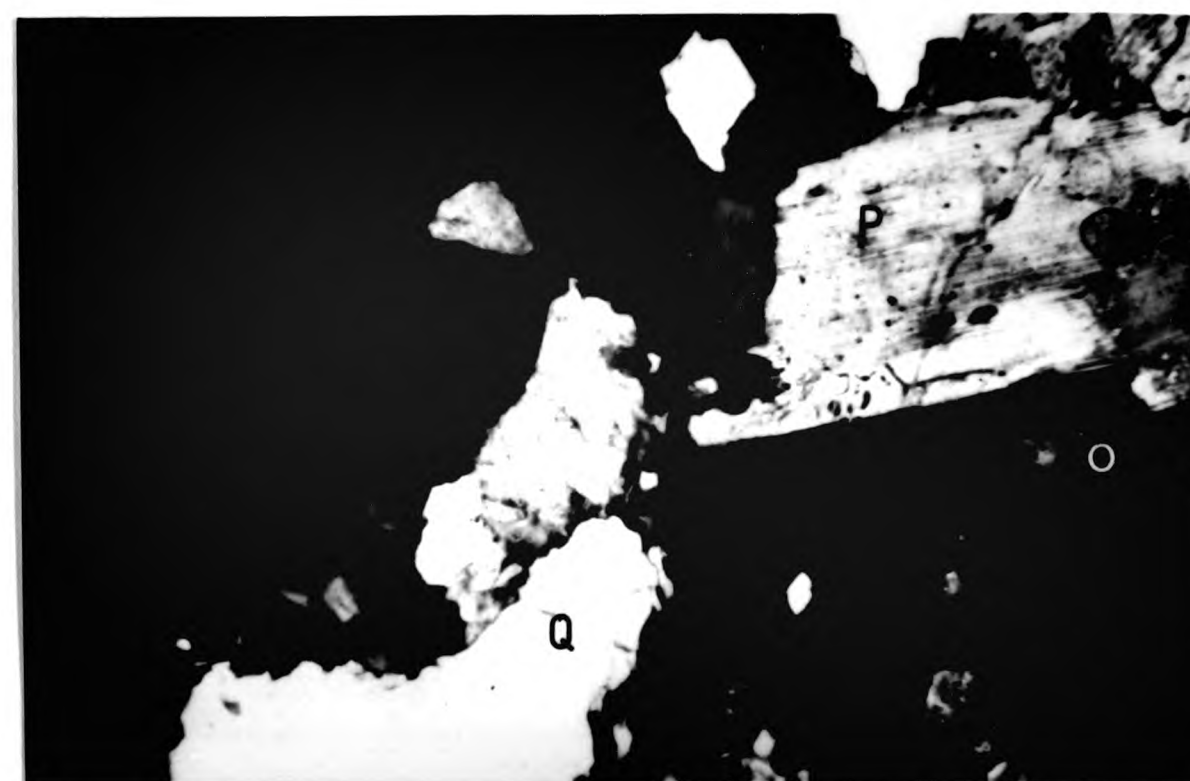


Plate 2.10

General view of Aberchalder Adamellite, showing coarse anhedral quartz (Q), twinned orthoclase (O), and euhedral plagioclase (P). No microcline is visible in this section. (Crossed polars, x47).



**Plate 2.11**

Biotite and quartz phenocrysts within a fine groundmass of, granular quartz and irregular, weakly enclosing, orthoclase (O). Granitic Porphyry. (Crossed polars, x47)

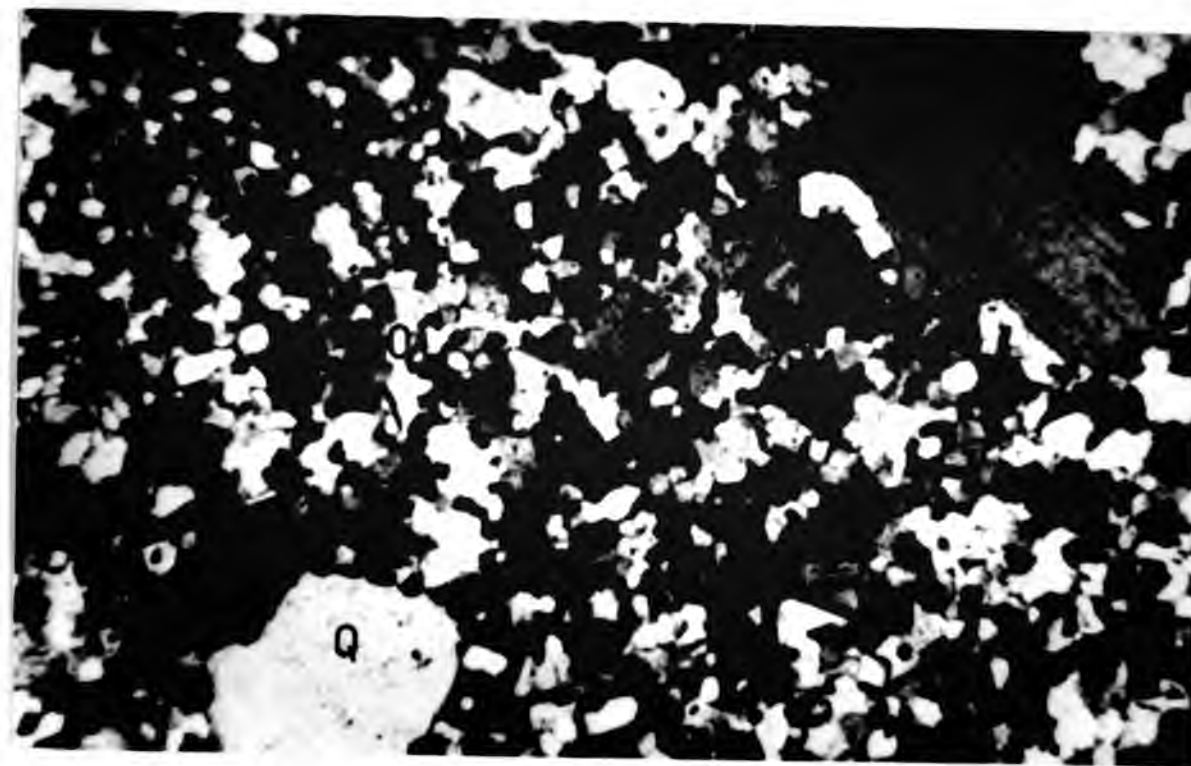


**Plate 2.12**

General view of a granitic porphyry, containing quartz, plagioclase, biotite and orthoclase phenocrysts. (Crossed polars, x5)

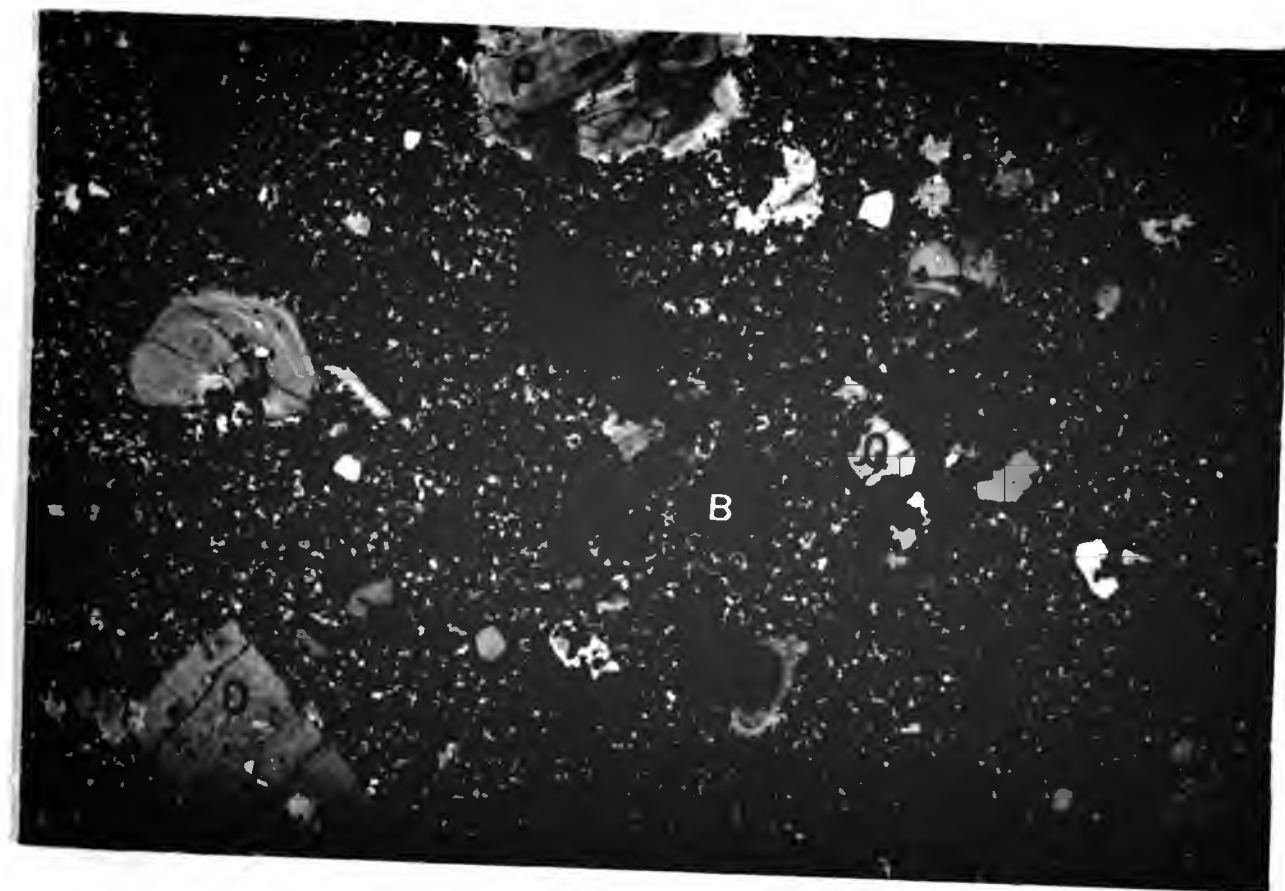




Plate 2.13

Parallel lithological banding, exposed on a flat outcrop surface of the Carn Bhreabaig granite stock.



Plate 2.14

Single lithological band within the Carn Bhreabaig granitic stock. A sharp contact is visible between relatively coarse grained, orthoclase rich granite (C), and finer grained biotite rich granite (B). The biotite rich granite (moving towards the right of the photograph) becomes increasingly leucocratic and coarse grained as it grades into granite more typical of that found within unlayered parts of the stock.





Plate 2.15

Elliptical melanocratic microdiorite enclave, in the Dalcrag Granodiorite. The microdiorite shows a fabric defined by plagioclase phenocrysts, and is parallel to the fabric in the host and to the long axis of the ellipse. (length of enclave is 8cm.)

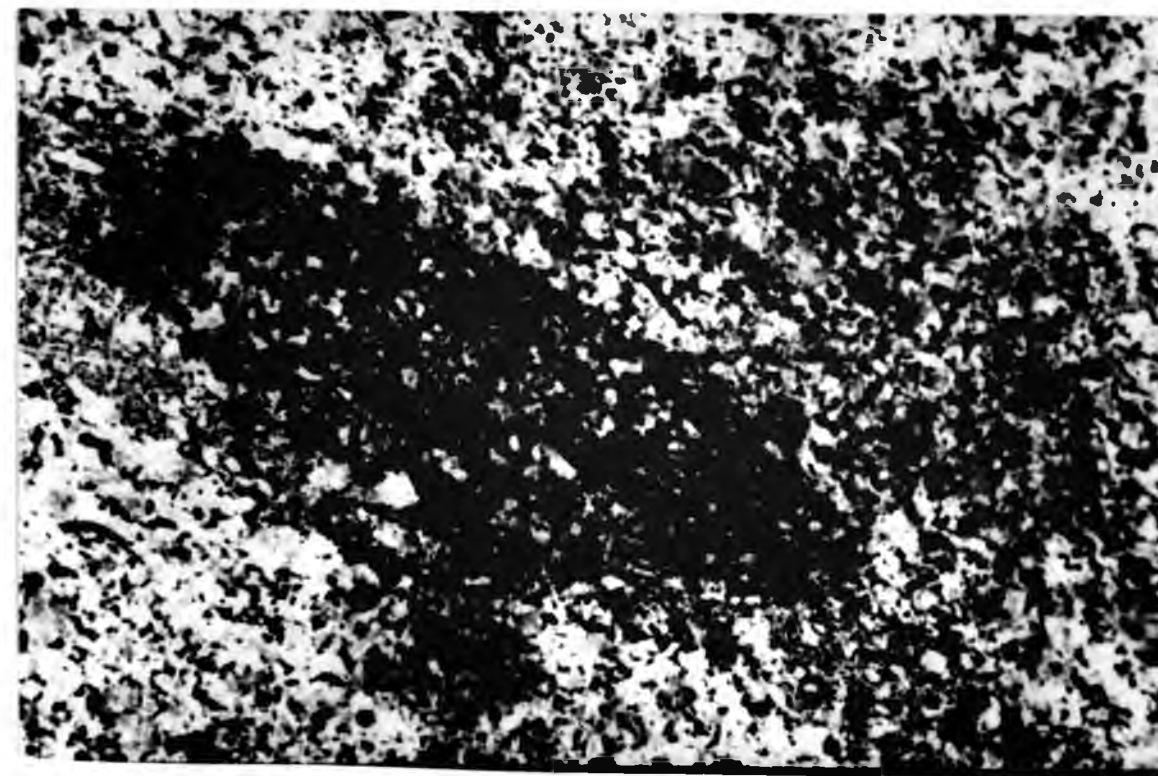
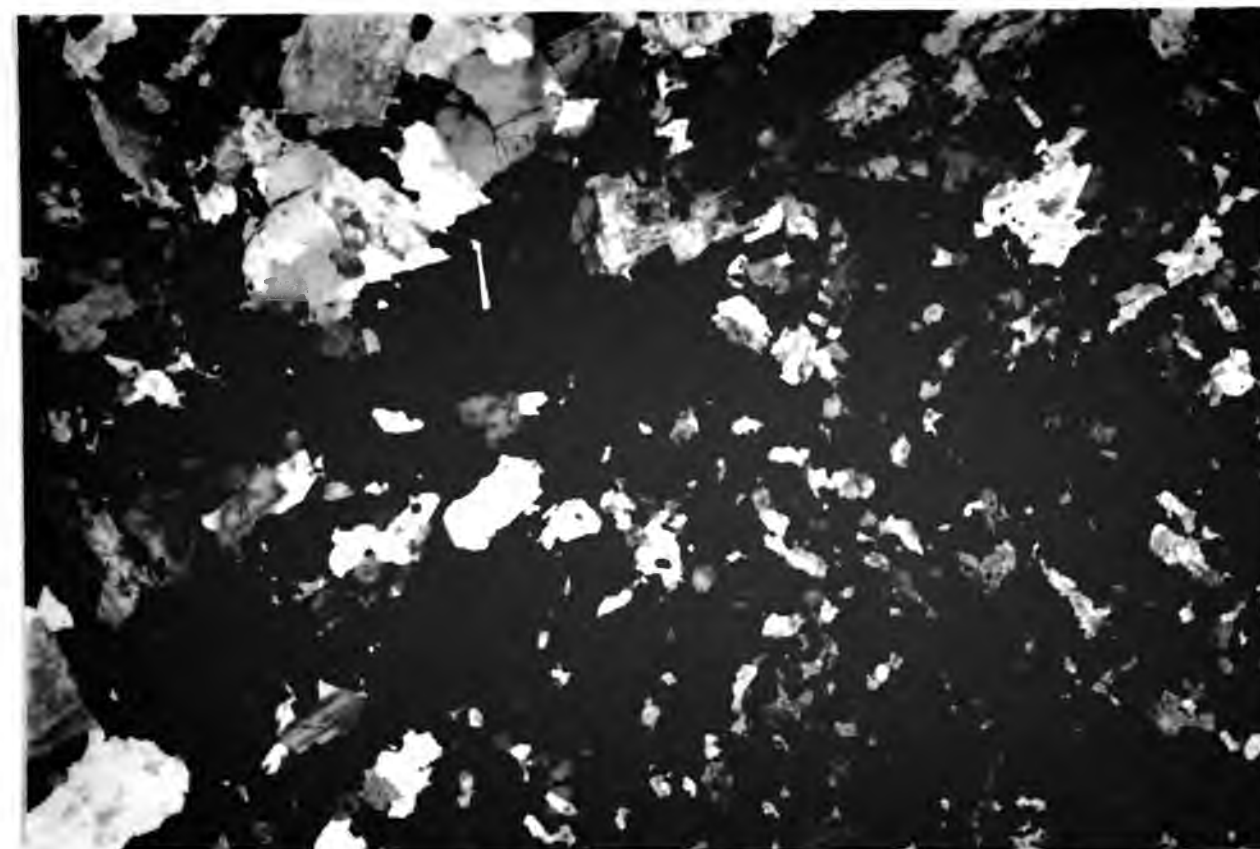


Plate 2.16

Dalcrag Granodiorite, with part of a microdiorite enclave in the bottom right hand corner of the photograph. The enclave shows no parallel mineral fabric and no chill. The enclave/host contact is formed from interlocking crystals. (Crossed polars, x5).



**Plate 2.17**

Irregular microdiorite enclaves in an Errogie Quartz Diorite/Chliabhlain Quartz Monzodiorite intermediate host. The enclaves are joined by small microdiorite necks and the host/enclave contact is straddled by plagioclase laths. (Note the parallel fabric defined by the plagioclase in the enclave).

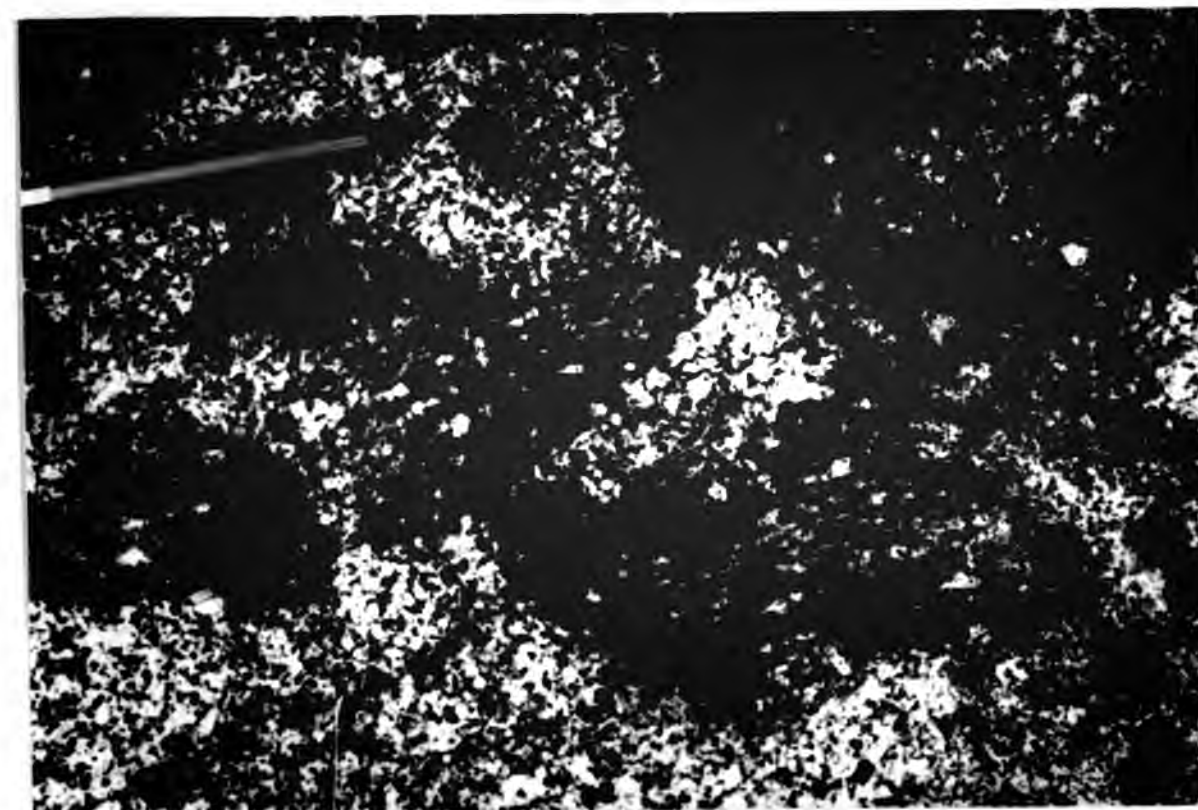


**Plate 2.18**

Swarm of micaceous psammite and appinitic diorite xenoliths, and microdiorite enclaves, within Dalcrag Granodiorite. The microdiorite enclaves have a morphology from blocky to ribbon-like, the psammite xenoliths are small and tabular, and the dark coloured appinitic diorite xenoliths are blocky.

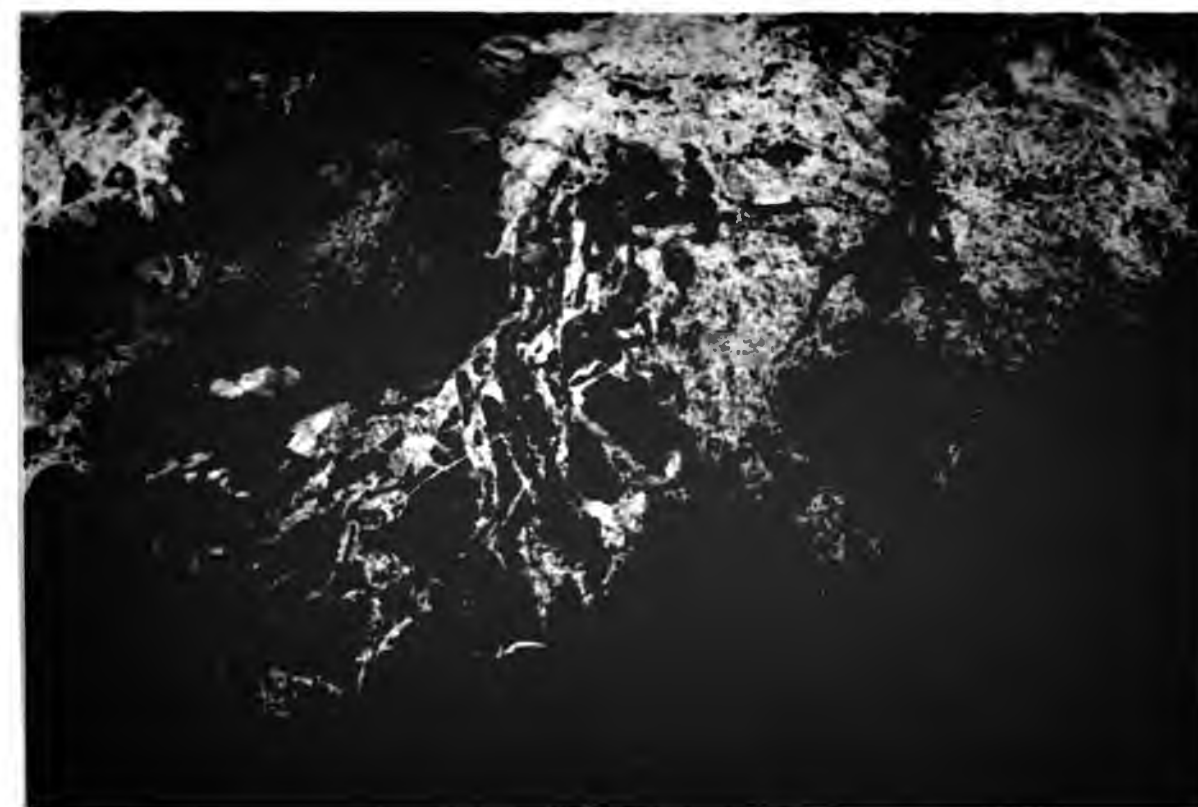




**Plate 2.19**

Well formed flow fabric, defined by undeformed plagioclase laths. Melanocratic microdiorite dyke. (Crossed polars, x47)



**Plate 2.20**

Melanocratic microdiorite dyke displaying hollow acicular hornblendes. The background dust is due to sericitisation of the plagioclase dominated matrix. (Plane polarised light, x5)

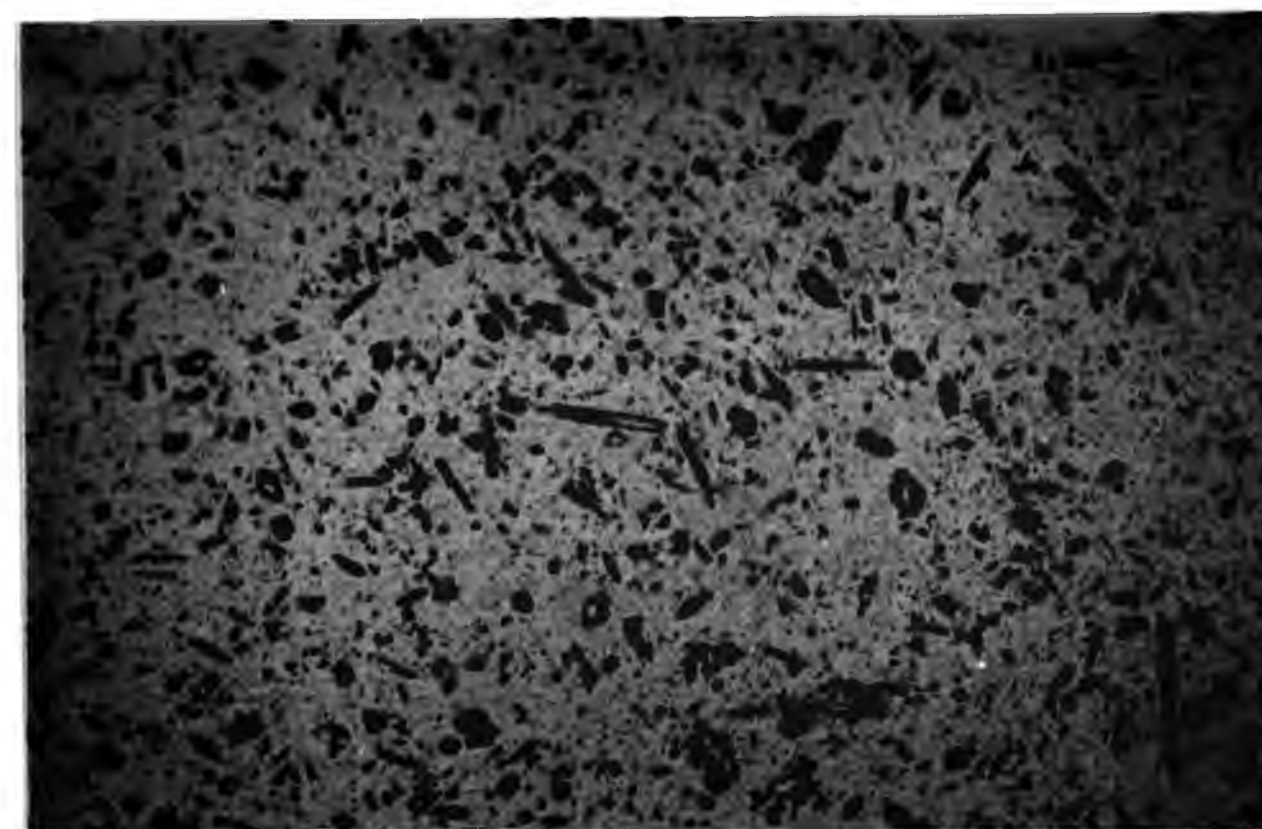


Plate 2.21

Elongate, hornblende phenocryst, with a plagioclase filled core and well developed exsolution lamellae of dusty opaques. The groundmass is dominated by euhedral plagioclase laths with distinctive highly sericitised cores. Melanocratic microdiorite dyke. (Crossed polars, x47)

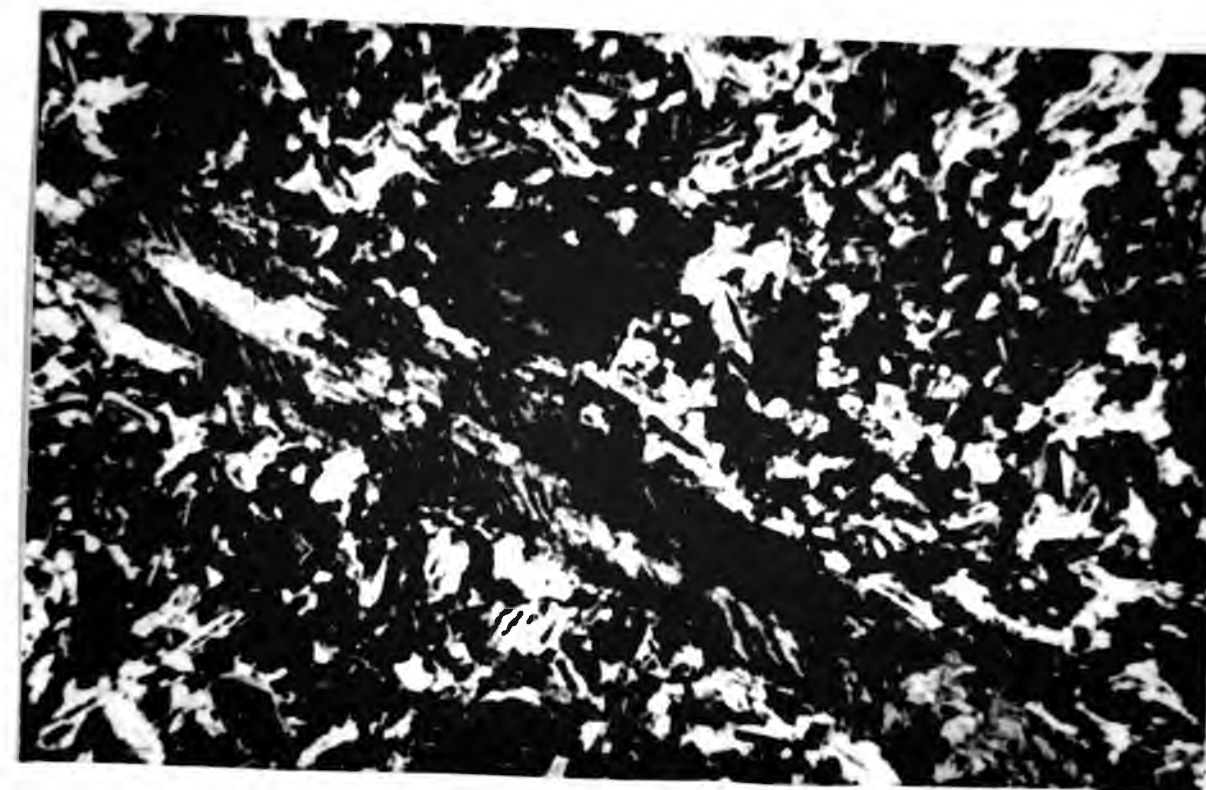


Plate 2.22

Field view of a quartz xenocrystic microdiorite dyke, showing large pink plagioclase phenocrysts and rounded quartz xenocrysts within a fine melanocratic groundmass.





Plate 2.23

General view of a fine grained microdiorite dyke, containing large embayed quartz xenocrysts and plagioclase phenocrysts. Note the rims around the quartz grains. (Crossed polars, x5)



Plate 2.24

Corroded and embayed quartz xenocrysts, surrounded by a reaction rim of actinolite. The groundmass is fine grained and dominated by plagioclase. Quartz xenocrystic microdiorite dyke. (Crossed polars, x47)

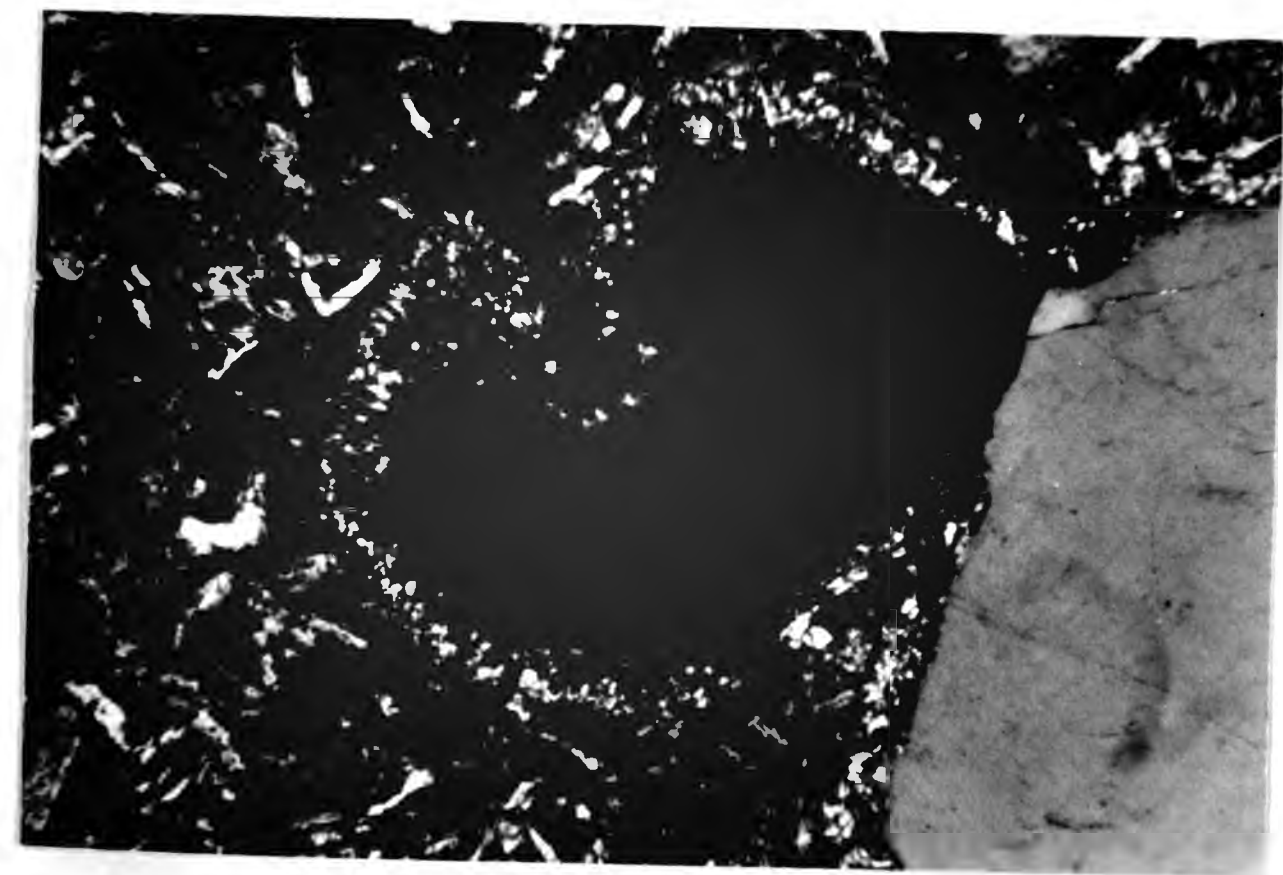


Plate 2.25

Mesocratic microdiorite dyke containing a large  
glomerocryst of three synneused plagioclase laths.  
(Crossed polars, x5)

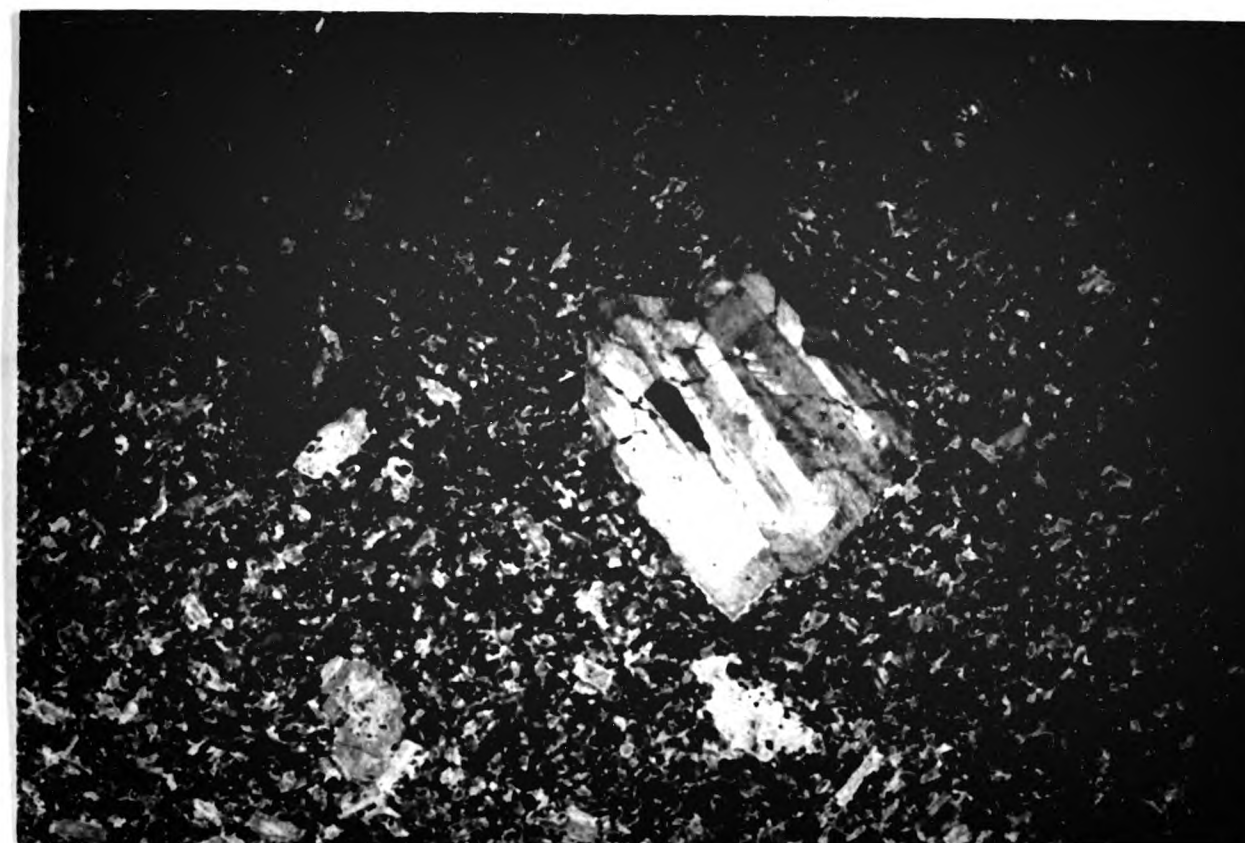


Plate 2.26

Synneusis cluster of zoned plagioclase phenocrysts.  
The outer zone contains numerous melt inclusions and  
encloses the synneusis cluster. Mesocratic microdiorite  
dyke. (Crossed polars, x47)





**Plate 2.27**

Section of a narrow apophysis connected, (off picture), to a large melanocratic microdiorite dyke. The contacts with the Dalcrag Granodiorite are sharp, irregular and often straddled by plagioclase laths from the host Dalcrag Granodiorite.



**Plate 2.28**

Melanocratic microdiorite dyke showing a parallel flow fabric, defined by acicular hornblendes adjacent to a large orthoclase pegmatite crystal. (plane polarised light, x5)





Plate 2.29

Granular augite (A), enclosed by hornblende. The hornblende, augite, and the large apatite crystals are all enclosed within a perthitic orthoclase oikocryst. Appinitic diorite. (Crossed polars, x47)



Plate 2.30

Large, euhedral, olive green hornblende (H), rimming pale green augite (A). Note the large elongate sphene prisms (Sp). Appinitic diorite. (Crossed polars, x47)



**Plate 2.31**

Elongate, hornblende chadocrysts (H), enclosed by a plagioclase oikocryst. Note the large apatite prisms. Appinitic diorite. (Crossed polars, x47)



**Plate 2.32**

One of the many lithologies within the appinitic diorite suite of rocks showing granular and stubby hornblende prisms (H). (Crossed polars, x47).

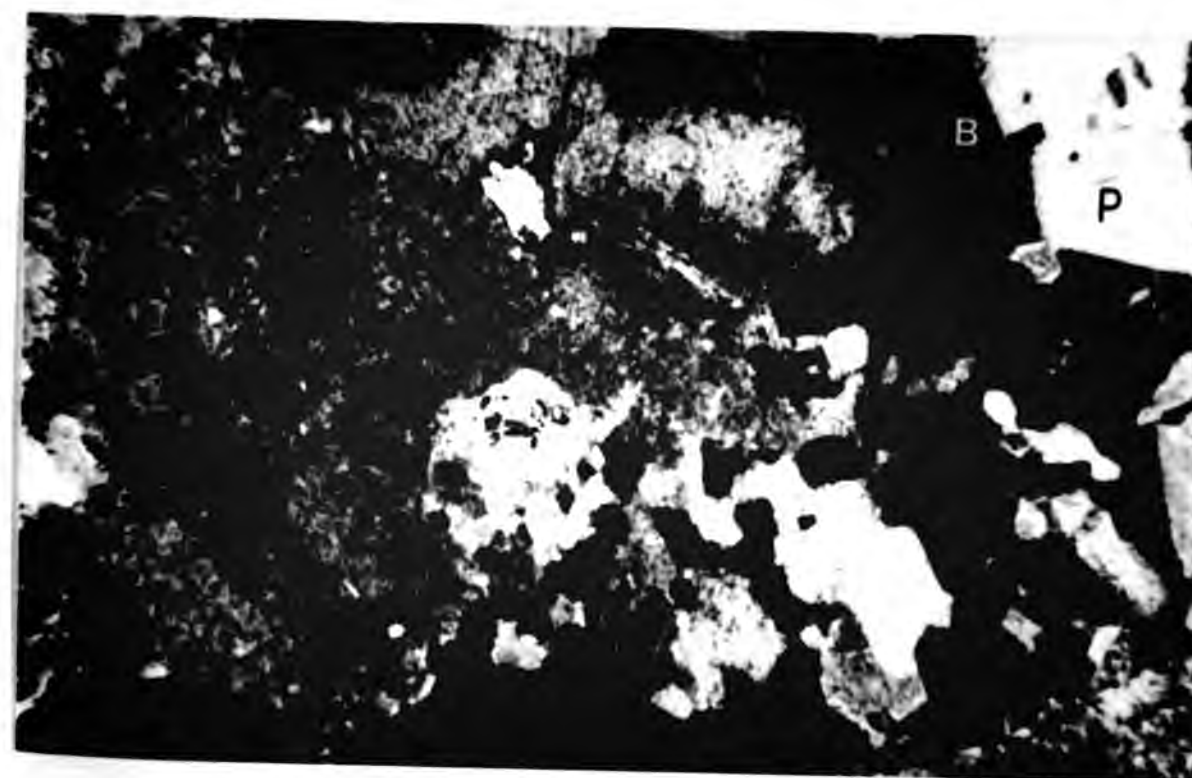
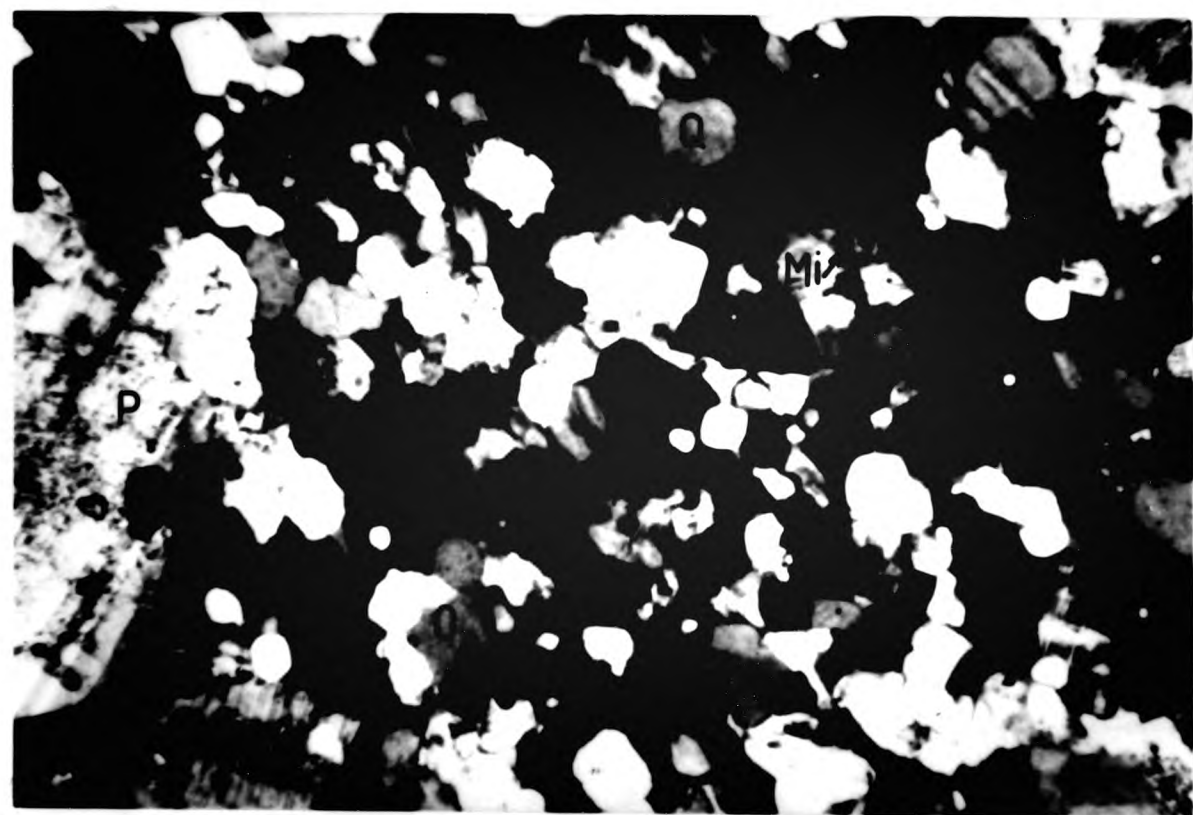


Plate 2.33

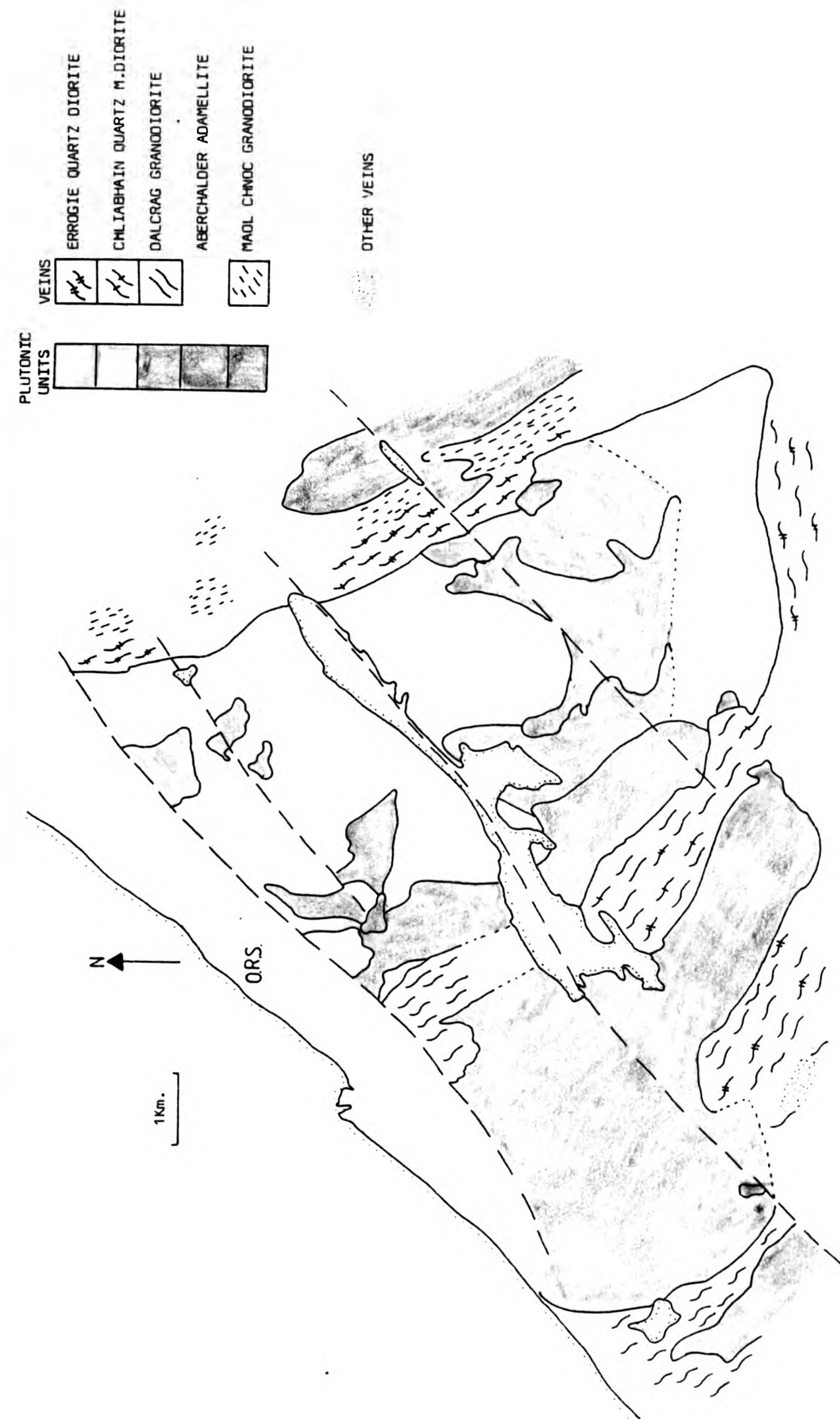
Equant, granular quartz (Q), equant microcline (Mi), and slightly coarser anhedral orthoclase (O). Large phenocrysts of plagioclase (P) are also present. Aplite dyke. (Crossed polars, x47).



CHAPTER 3. GRANITOID VEINING AND STOPING IN THE  
FOYERS COMPLEX.



DISTRIBUTION OF GRANITOID VEINS IN THE ENVELOPE OF THE FOYERS COMPLEX. FIGURE 3.1



A- Bedding separated by dilational vein      B- Bedding cross cut and replaced by granitoid

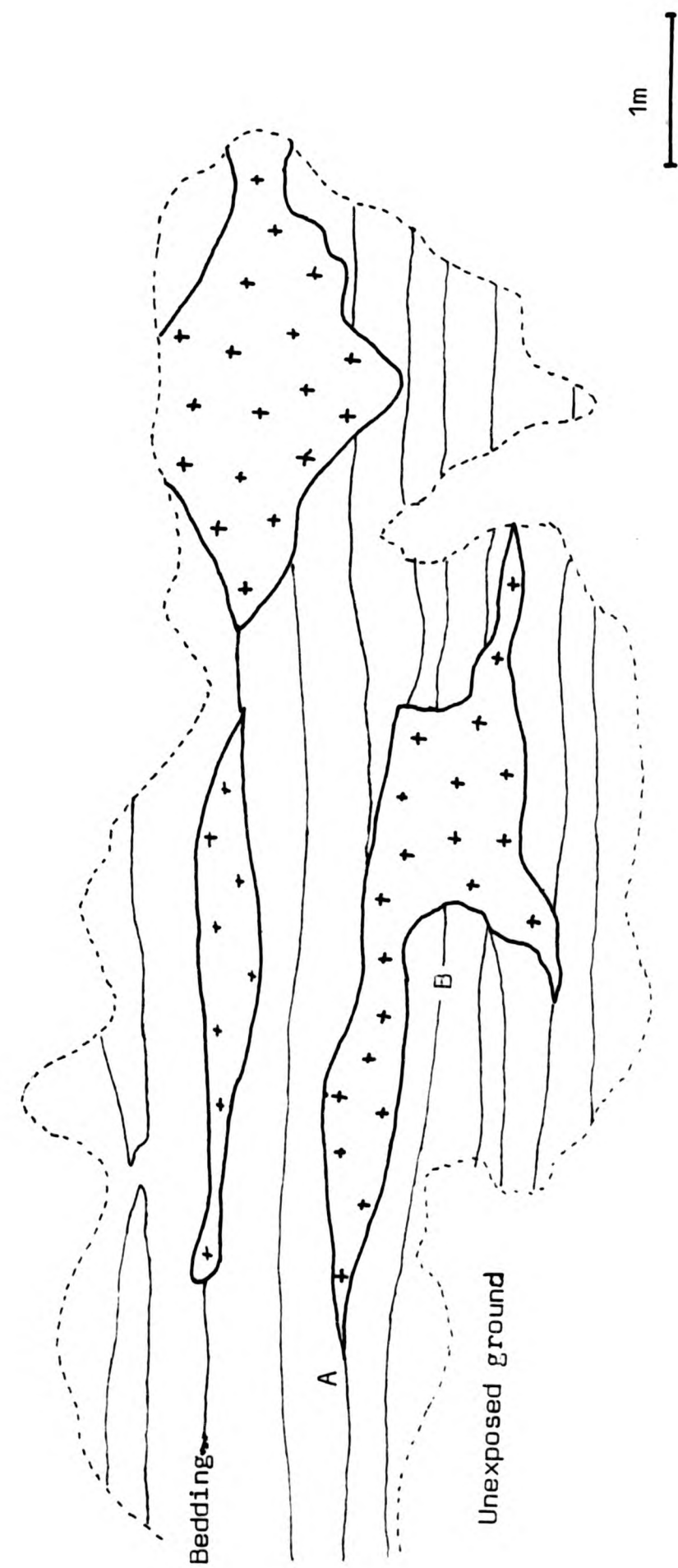


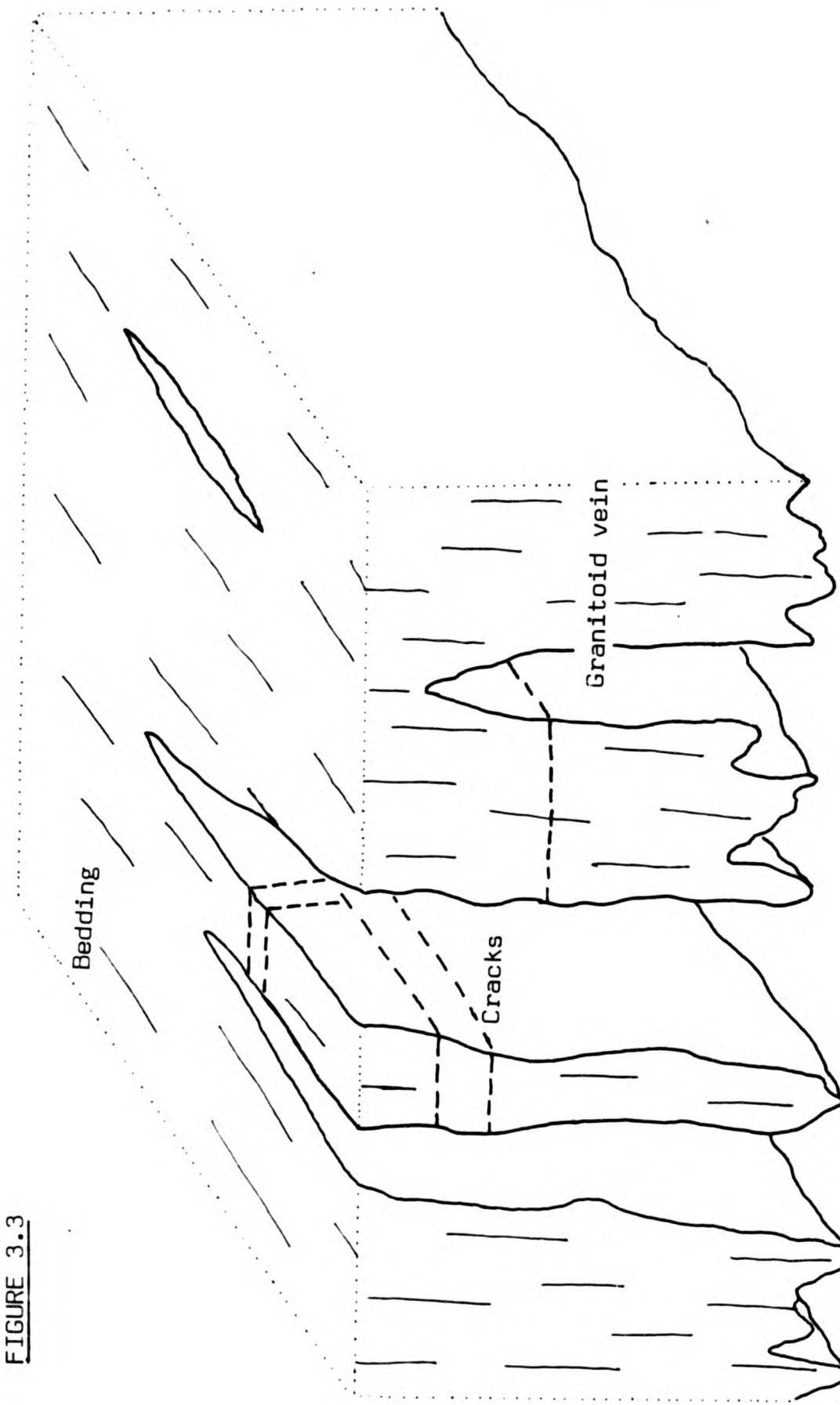
FIGURE 3.2

FIELD SKETCH SHOWING GRANITOID BODIES FORMED BY DILATION AND REPLACEMENT (STOPING) OF BEDDING.

	Weakly veined area	Strongly veined area	Increase due to veining	Expected increase if veining is dilational	Dilation component	Replacement component
LOCALITY 1.						
Distance between marker beds	31m	35m	4m	9m	44%	56%
Total thickness of granitoid veins	3m	12m	9m	9m		
LOCALITY 2.						
Distance between marker beds	27m	30m	3m	7.89m	38%	62%
Total thickness of granitoid veins	0.81m	8.7m	7.89m	7.89m		

TABLE 3.1 TABLE SHOWING THE DILATIONAL AND REPLACIVE COMPONENTS DURING THE FORMATION OF ENVELOPE VEINS IN THE CENTRAL PSAMMITE SEPTUM.

FIGURE 3.3



BLOCK DIAGRAM ILLUSTRATING THE TWO FRACTURE SETS NEEDED TO ISOLATE A PSAMMITE SEPTUM LOCATED BETWEEN TWO GRANITOID VEINS.



TABLE 3.2

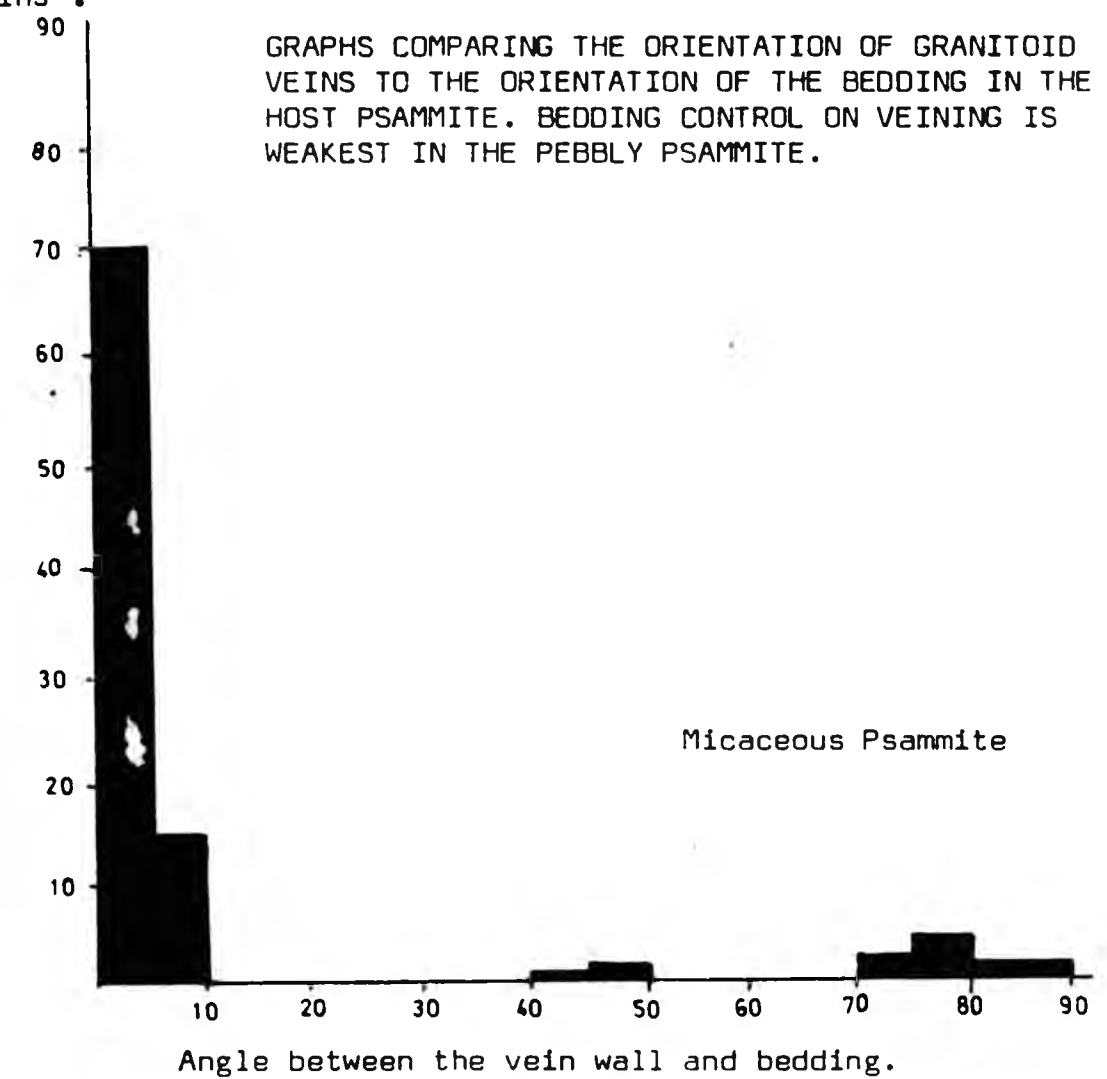
Micaceous psammite		Pebbly psammite		Quartzite	
Length (m)	Width (m)	Length (m)	Width (m)	Length (m)	Width (m)
300	170	180	100	120	50
350	20	200	140	250	60
500	120	230	105		
280	85	190	150		
400	50	150	60		
700	80	280	250		
65	50	100	90		
		280	200		
		400	210		
		250	120		
		120	100		
6.4 : 1		1.64 : 1		3.25 : 1	Mean axial ratio

TABLE SHOWING DIMENSIONS OF VARIOUS PSAMMITE RAFTS WITHIN  
THE FOYERS GRANITIC COMPLEX

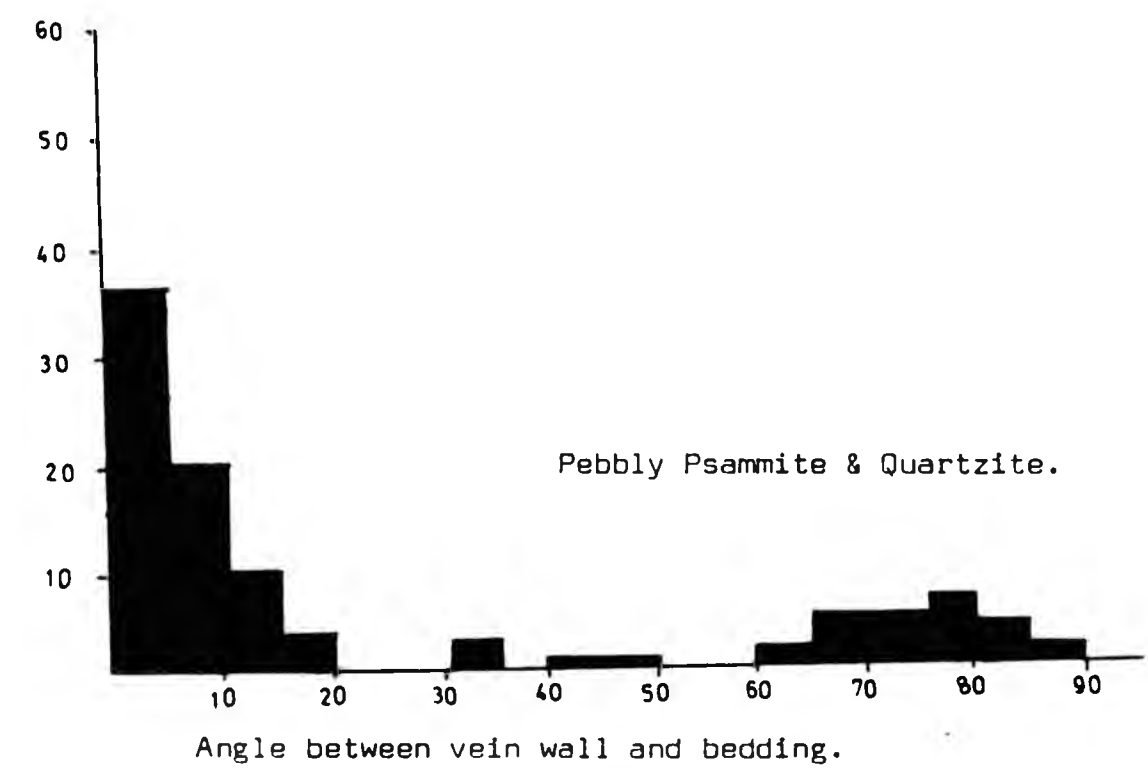
Number of veins %

FIGURE 3.4

GRAPHS COMPARING THE ORIENTATION OF GRANITOID VEINS TO THE ORIENTATION OF THE BEDDING IN THE HOST PSAMMITE. BEDDING CONTROL ON VEINING IS WEAKEST IN THE PEBBLY PSAMMITE.



Number of veins %



PLATES  
Chapter 3

Plate 3.1

Chliabhain Quartz Monzodiorite vein, occupying a shear zone in micaceous psammite. (Meall Donn).



Plate 3.2

Irregular distribution of Dalcrag Granodiorite veins within an area of mobilisation. (Central Psammite Septum).

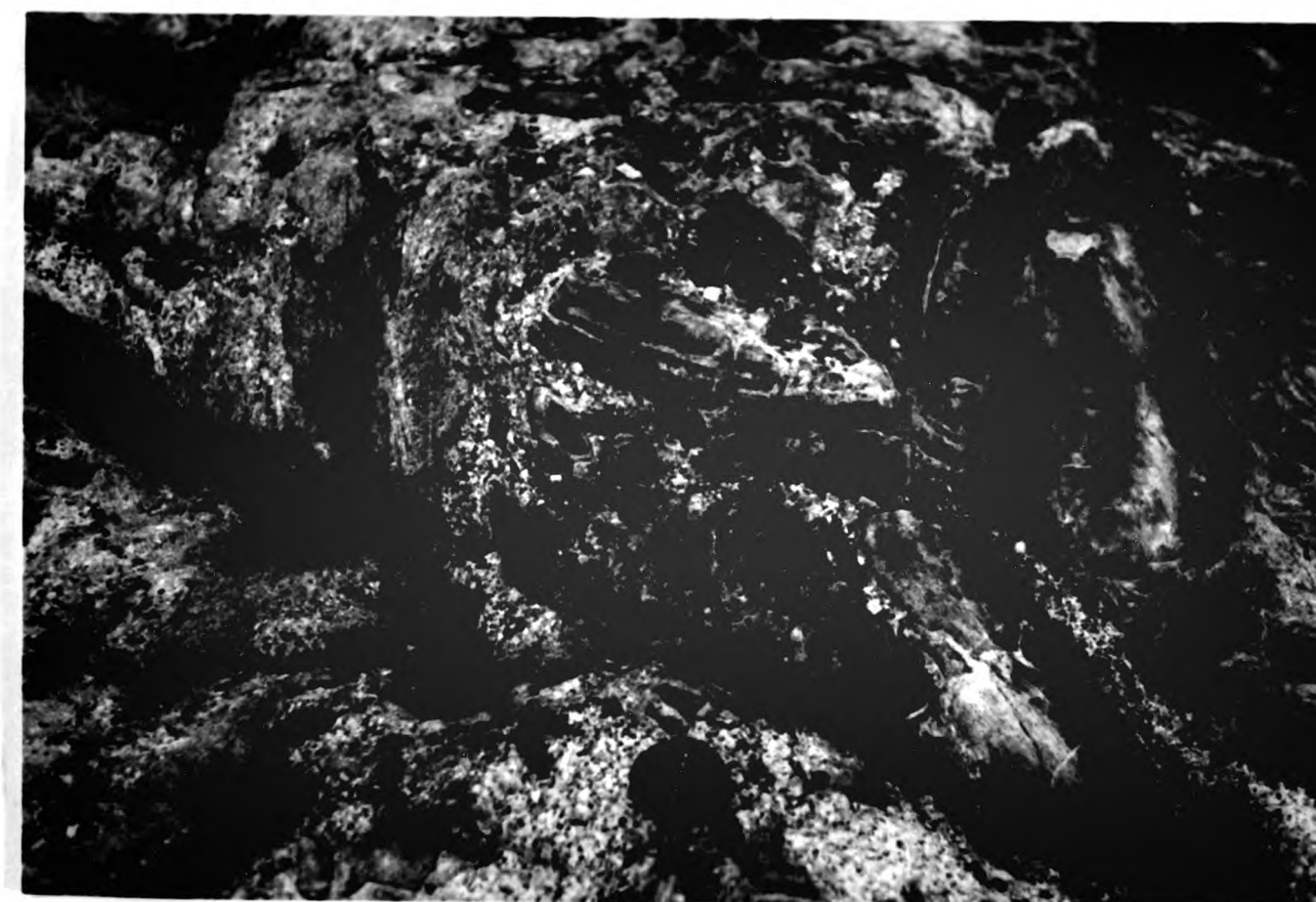




**Plate 3.3**

Dalcrag Granodiorite veins lying obliquely to bedding in a psammite host. One vein shows a well developed biotite shlieren, which lies parallel to the vein wall. (Central Psammite Septum).

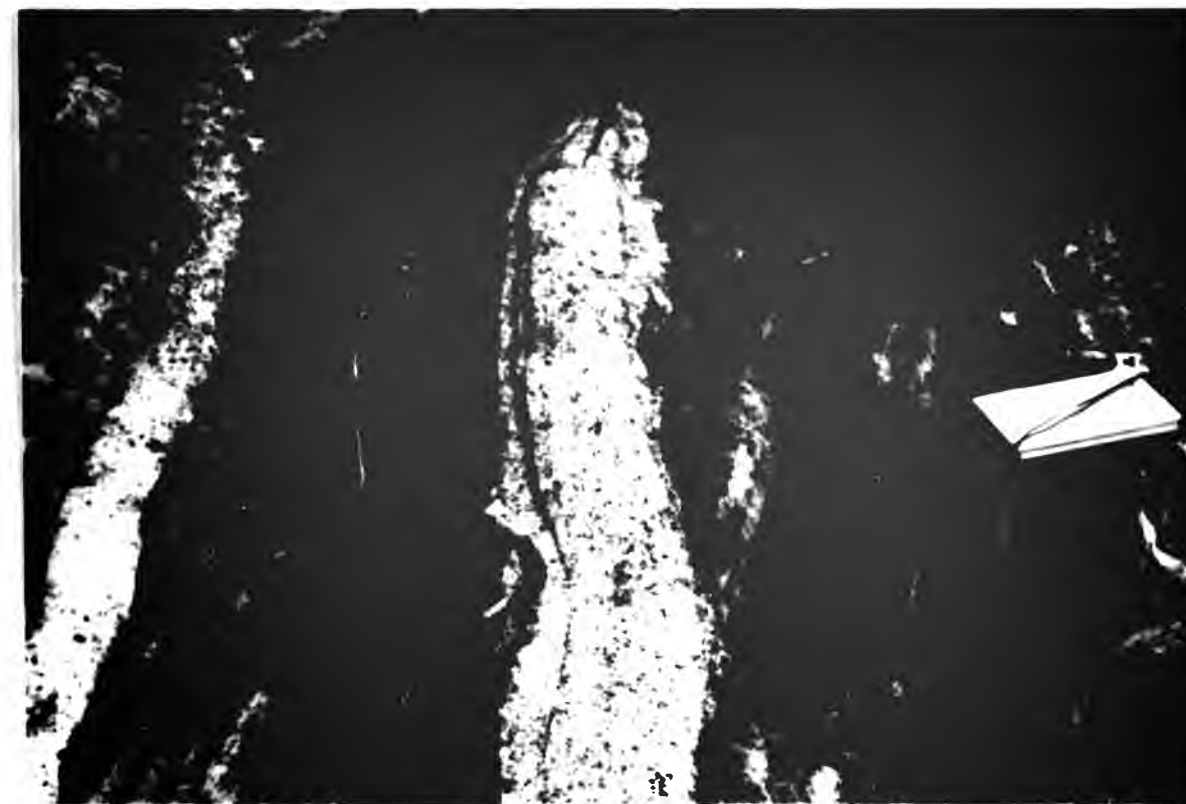


**Plate 3.4**

Large Dalcrag Granodiorite vein parallel to bedding. In the foreground, the vein terminates against an area of mobilised psammite, which is intruded by irregular patches of granodiorite. (Central Psammite Septum).



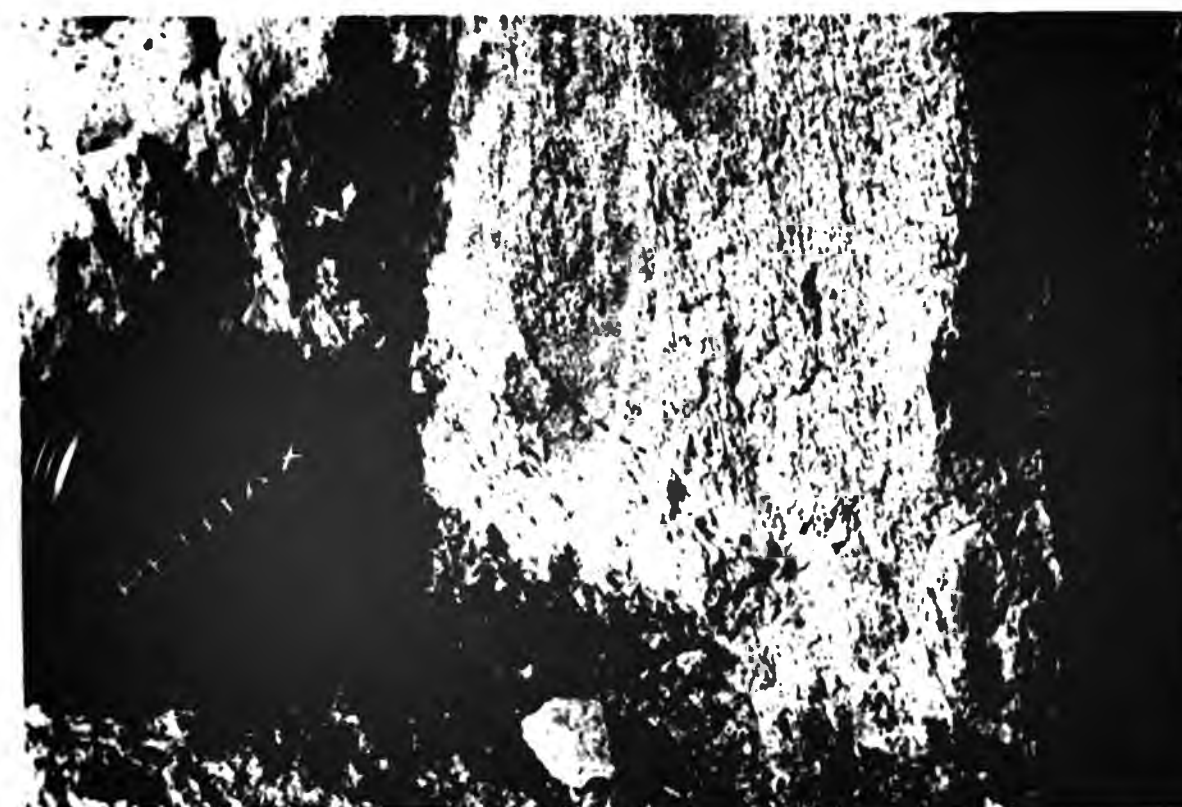
**Plate 3.5**

Granite vein cross cutting micaceous psammite bedding. The vein contains numerous psammite xenoliths orientated parallel to the vein wall. The vein also contains a large psammite block, which is rotated away from the vein wall, with granite intruding the space created during rotation. (Beinn Sgurrach)



**Plate 3.6**

Strong, penetrative, D1 bedding parallel fabric, cutting the contact between micaceous psammite, (top), and the pre-Grampian granite vein. The cleavage defracts as it crosses the contact. (Beinn Sgurrach).



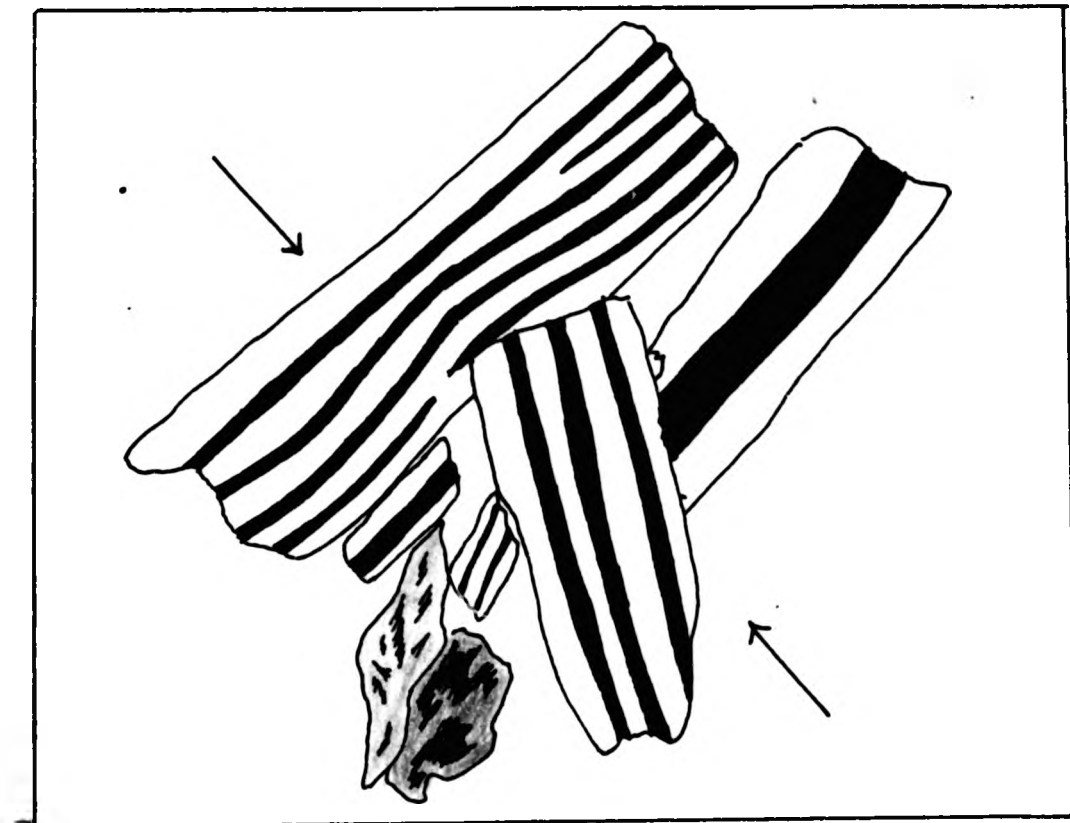


CHAPTER 4. FABRICS AND FOLIATIONS IN THE FOYERS GRANITIC  
COMPLEX.

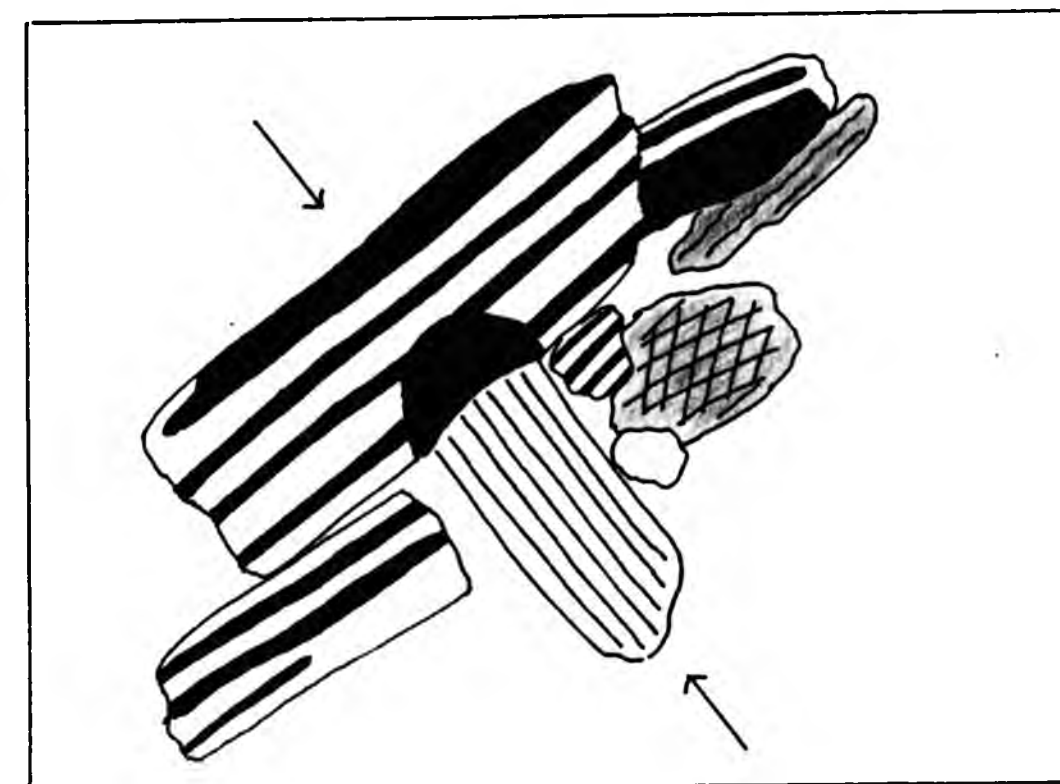
FIGURE 4.1

INTERNAL DEFORMATION DISPLAYED BY PLAGIOCLASE LATHS FROM THE  
ERROGIE QUARTZ DIORITE.

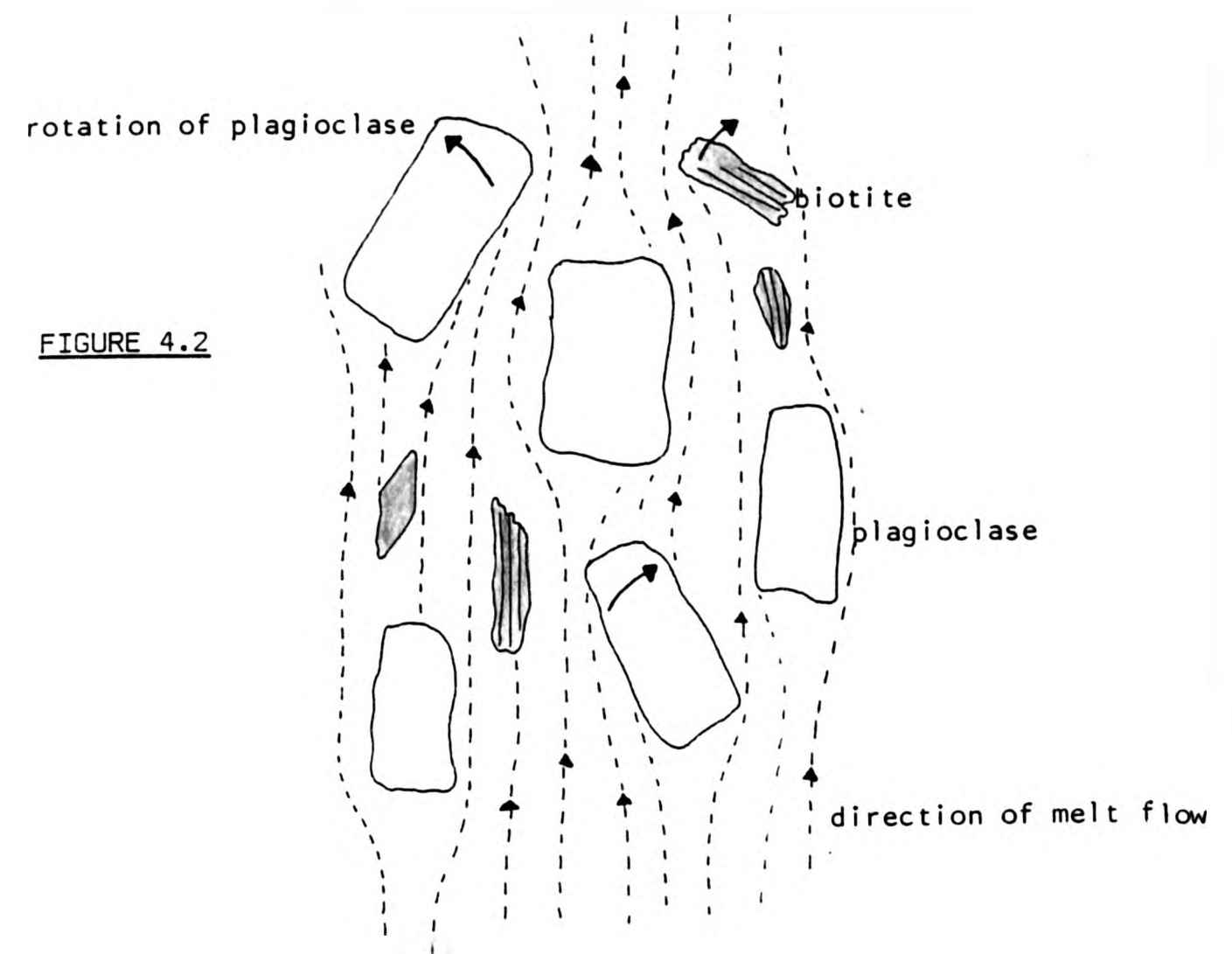
Field of view, (width=1cm). Arrows= maximum stress direction



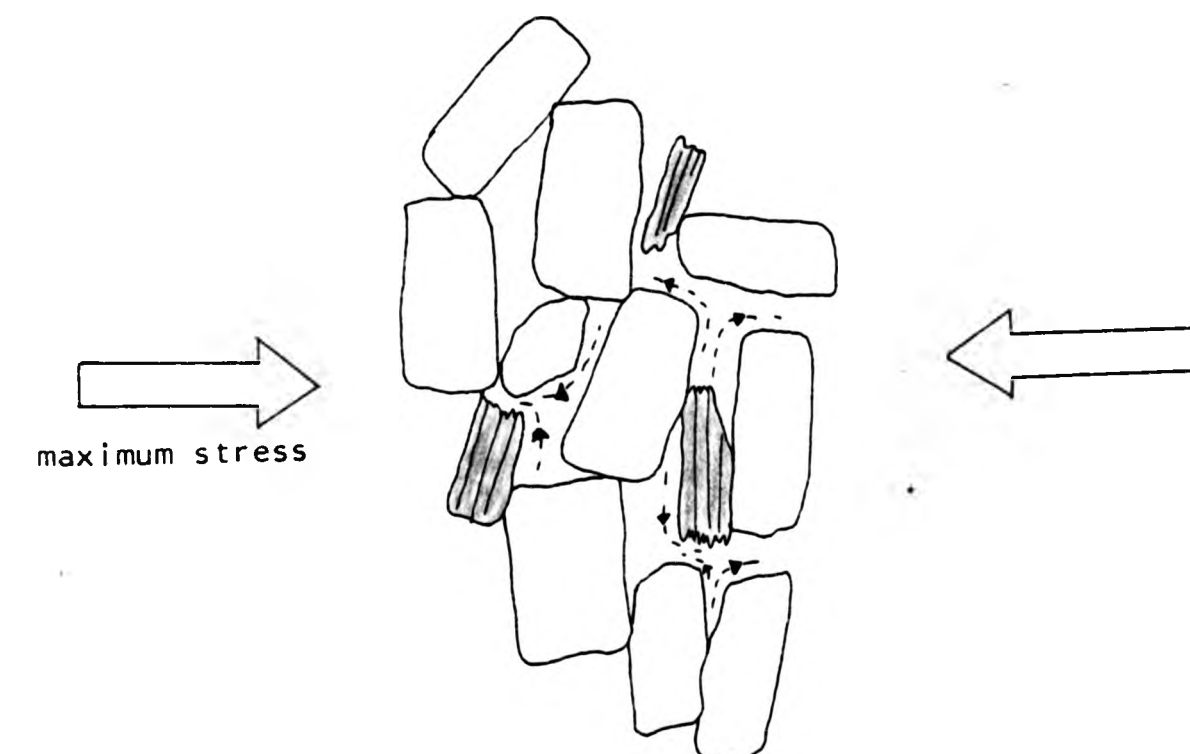
Albite twins displaying plastic deformation where  
two plagioclase laths contact



Dislocation of the crystal lattice in one of the  
plagioclase laths, giving rise to a lack of optical  
continuity, (extinction). The dislocation occurs at the  
contact between two plagioclase laths.



Rotation of crystals by flowing melt creates a magmatic parallel mineral fabric.



Deformation of the crystalline framework forces residual melt into pressure shadow positions.

The crystals will show solid state deformation.

FIGURE 4.3

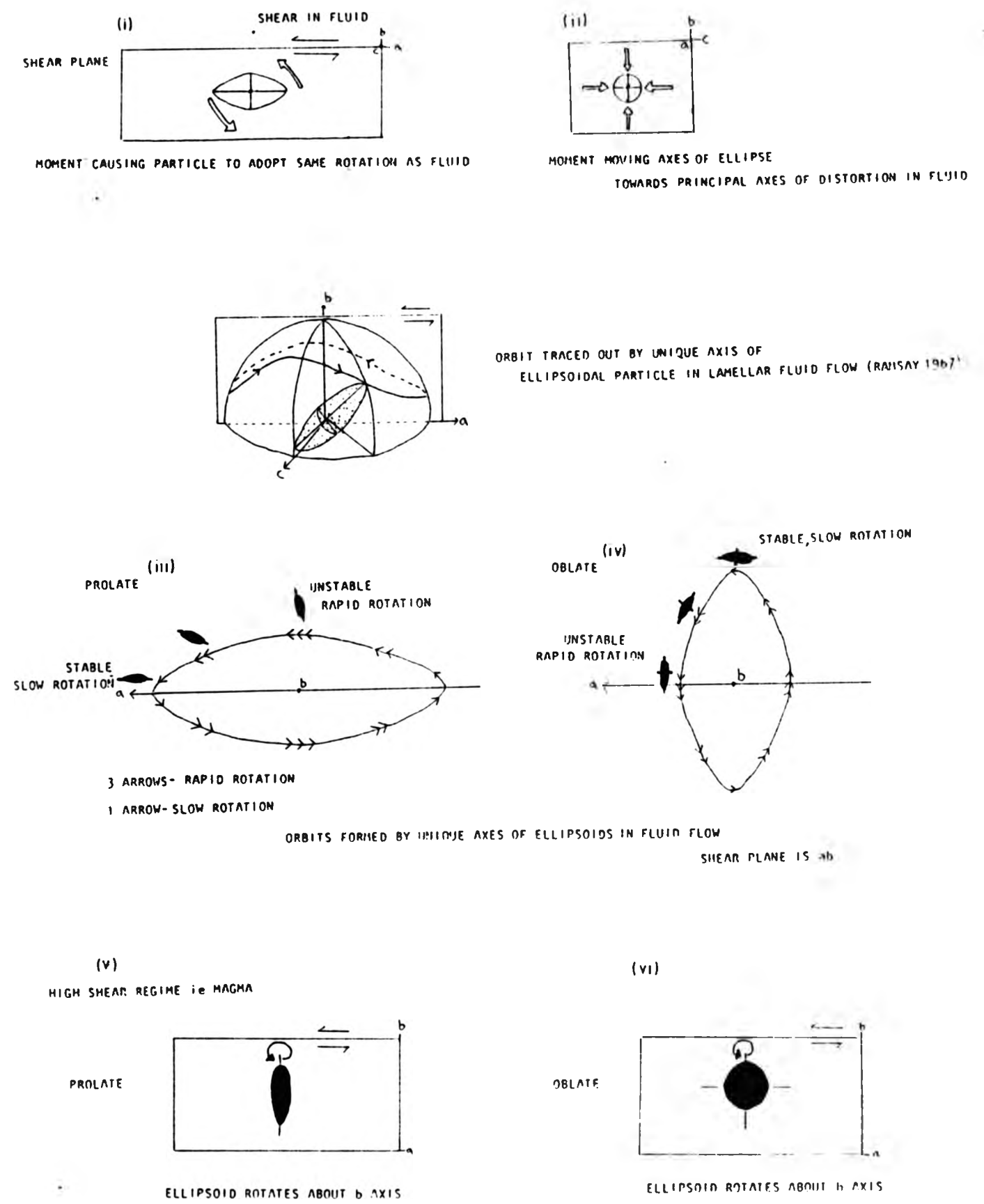
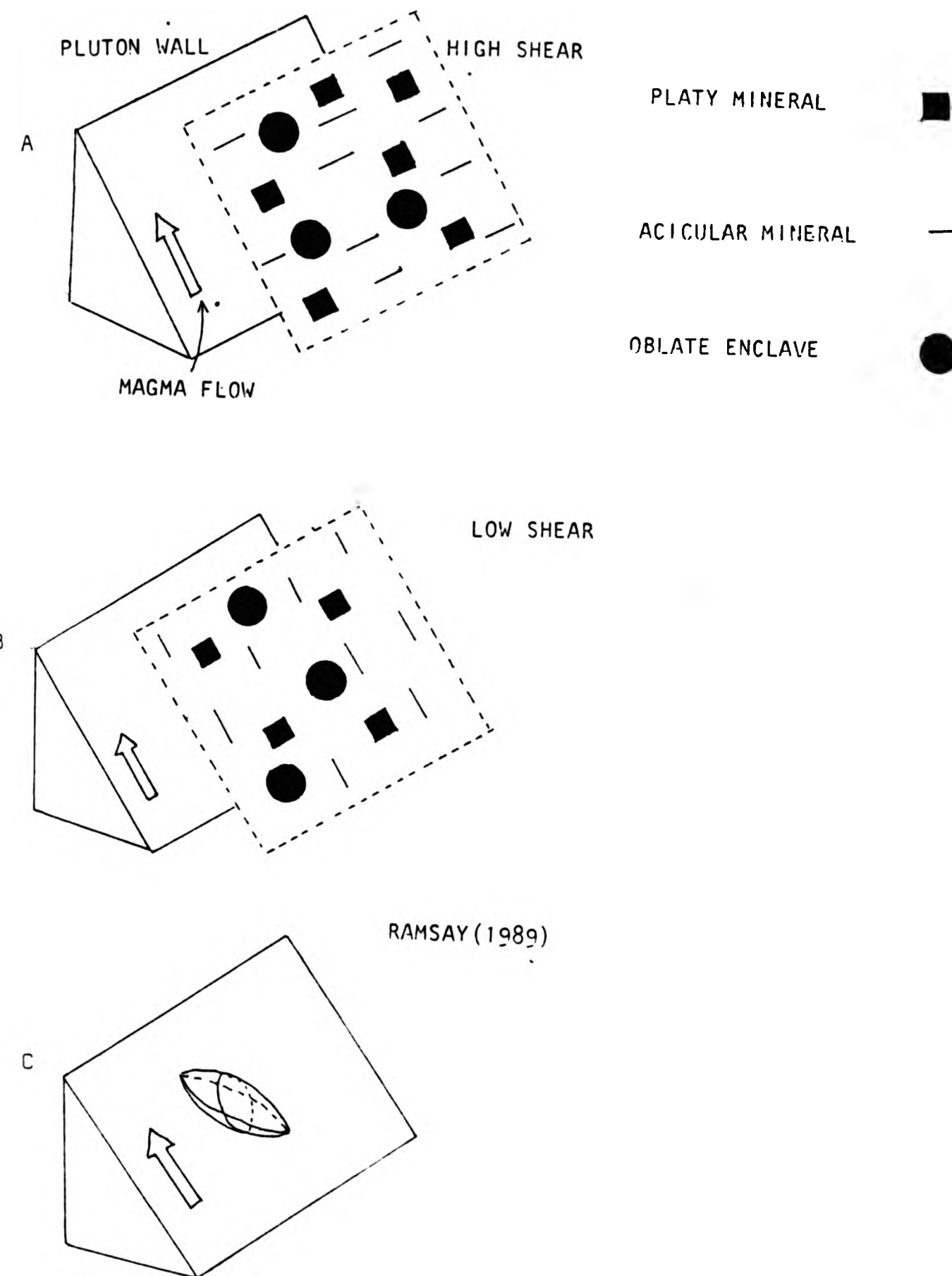


FIGURE 4.4

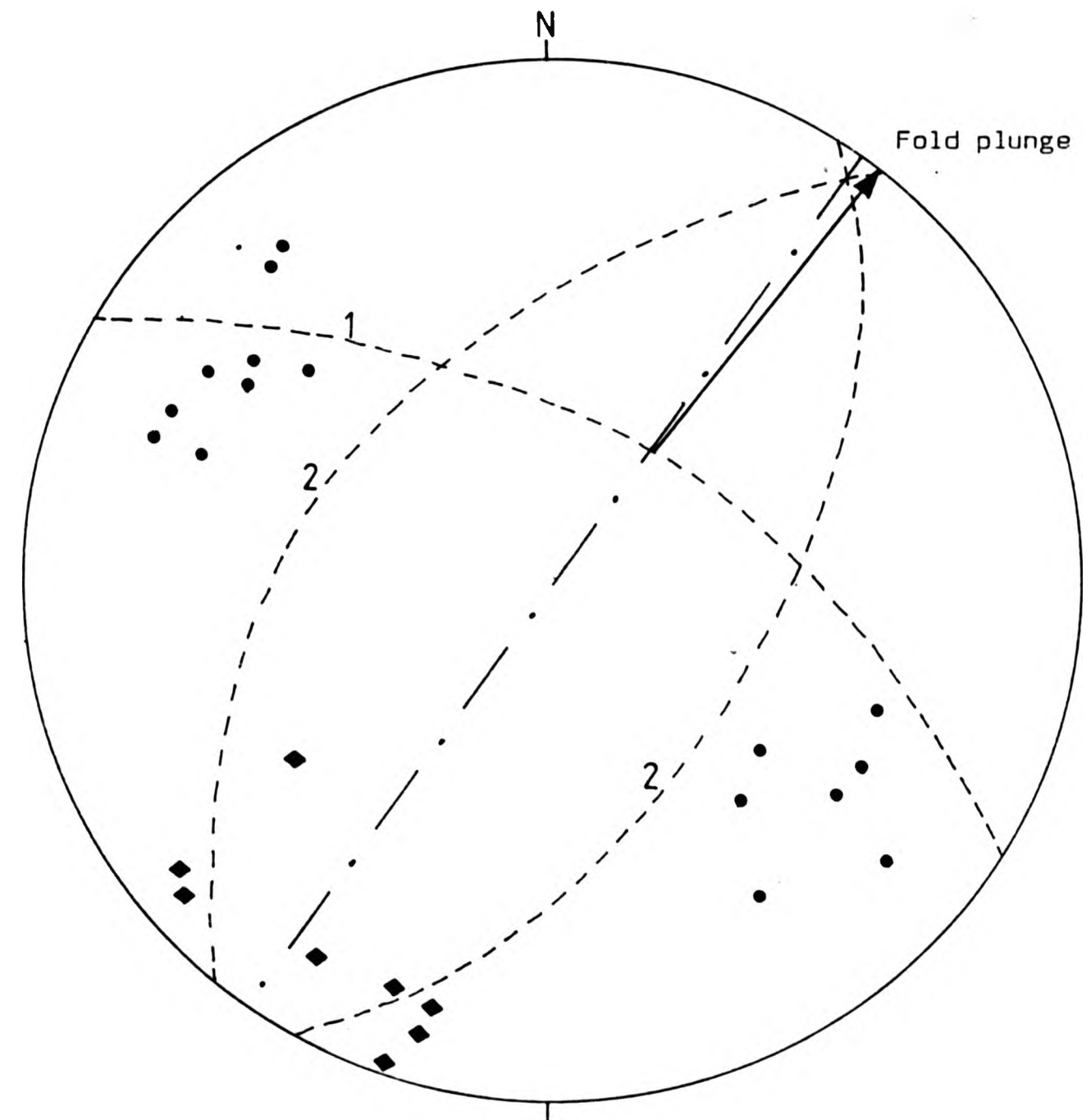


DIAGRAMS SHOWING THE ATTITUDES OF ACICULAR MINERALS, PLATY MINERALS AND OBLATE ENCLAVES DUE TO MAGMA FLOWING UP THE PLUTON WALL. THE ATTITUDES OF THE MINERALS IN THE TOP TWO DIAGRAMS ARE PREDICTED BY RAMSAY (1967).



FIGURE 4.5

STEREOGRAPHIC PLOT OF BEDDING FOLIATIONS WITHIN METASEDIMENTARY  
RAFTS WITHIN DALCRAG GRANODIORITE, NORTH EAST OF LOCH KEMP.

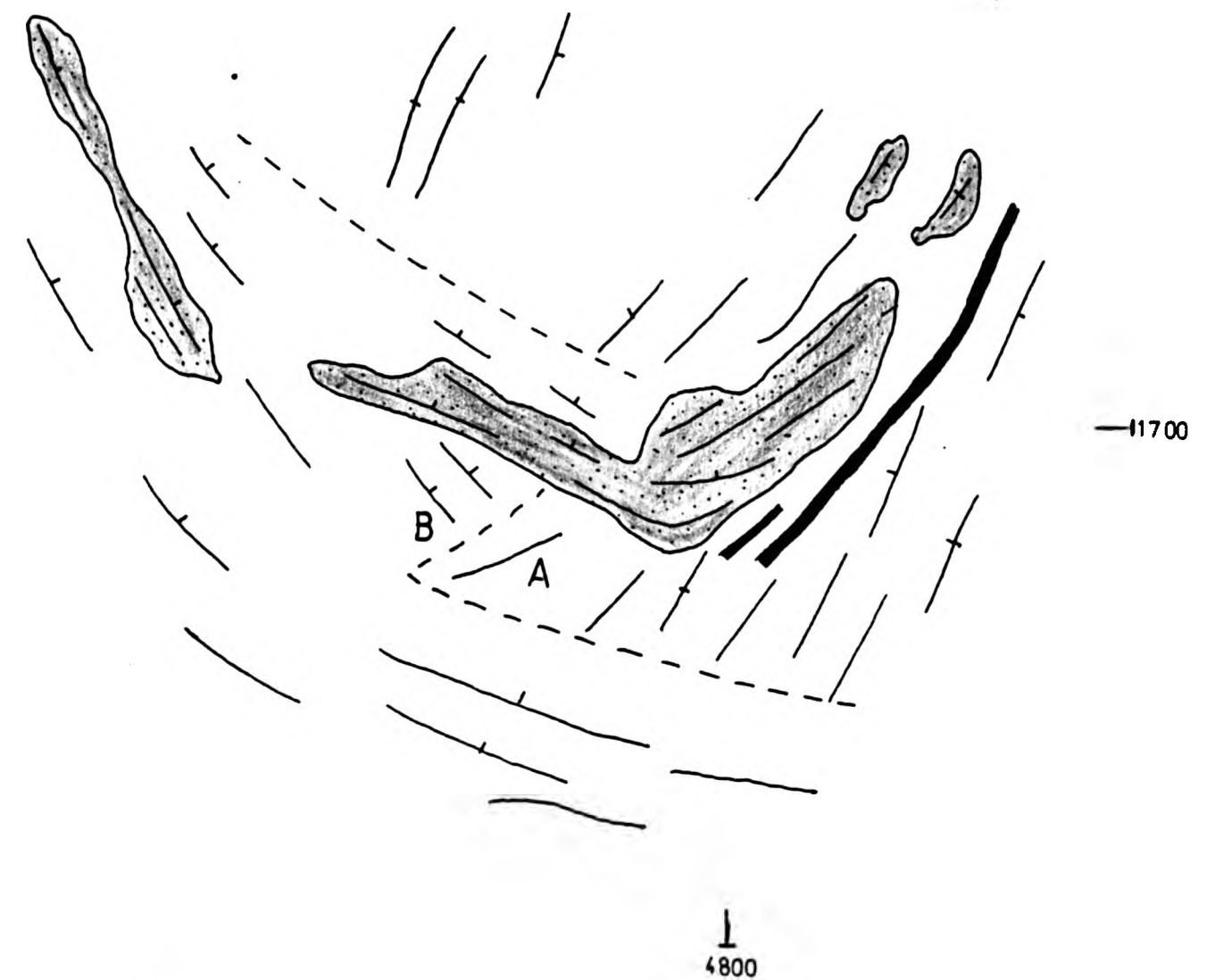


- POLES TO N.E. TRENDING BEDDING FOLIATIONS.
- ◆ POLES TO N.W. TRENDING BEDDING FOLIATIONS.
- 1 - - - - MEAN ORIENTATION OF N.W. TRENDING BEDDING FOLIATIONS.
- 2 - - - - MEAN ORIENTATION OF N.E. TRENDING BEDDING FOLIATIONS.
- • MEAN ORIENTATION OF N.E. TRENDING BEDDING FOLIATIONS  
IF N.W. AND S.E. DIPS OF THE BEDDING ARE CAUSED BY  
ROTATION DURING GRANODIORITE INTRUSION. (ESTIMATE ONLY).



FIGURE 4.6

MAP ILLUSTRATING THE RELATIONSHIP BETWEEN A LARGE GENICULATE PSAMMITE RAFT AND THE POSITION OF THE FABRIC ORIENTATION BOUNDARY, NORTH WEST OF LOCH KEMP.



Orientation of bedding foliations and mineral foliations in psammite rafts and Dalcrag granodiorite respectively.

Psammite raft.

Microdiorite Dyke.

Zone where mineral fabrics in the Dalcrag granodiorite lie at high angles to each other.

SCALE= 1:50,000.

FIGURE 4.7

GRAPH SHOWING HOW THE X:Z HORIZONTAL AXIAL RATIOS OF ELLIPSOIDAL MICRODIORITE ENCLAVES VARY WITH DISTANCE FROM THE WALL OF THE FOYERS COMPLEX.

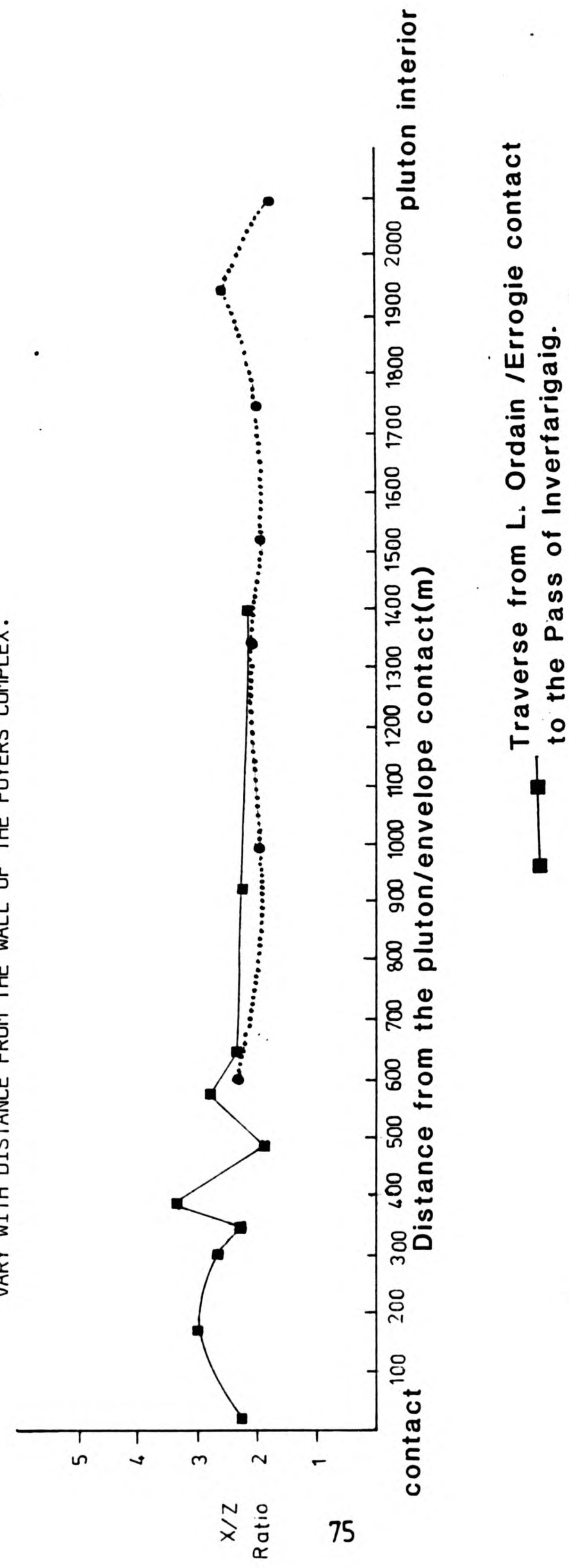


FIGURE 4.8

SHAPE OF MICRODIORITE ENCLAVES (HORIZONTAL SECTION)  
IN TRAVERSE 1

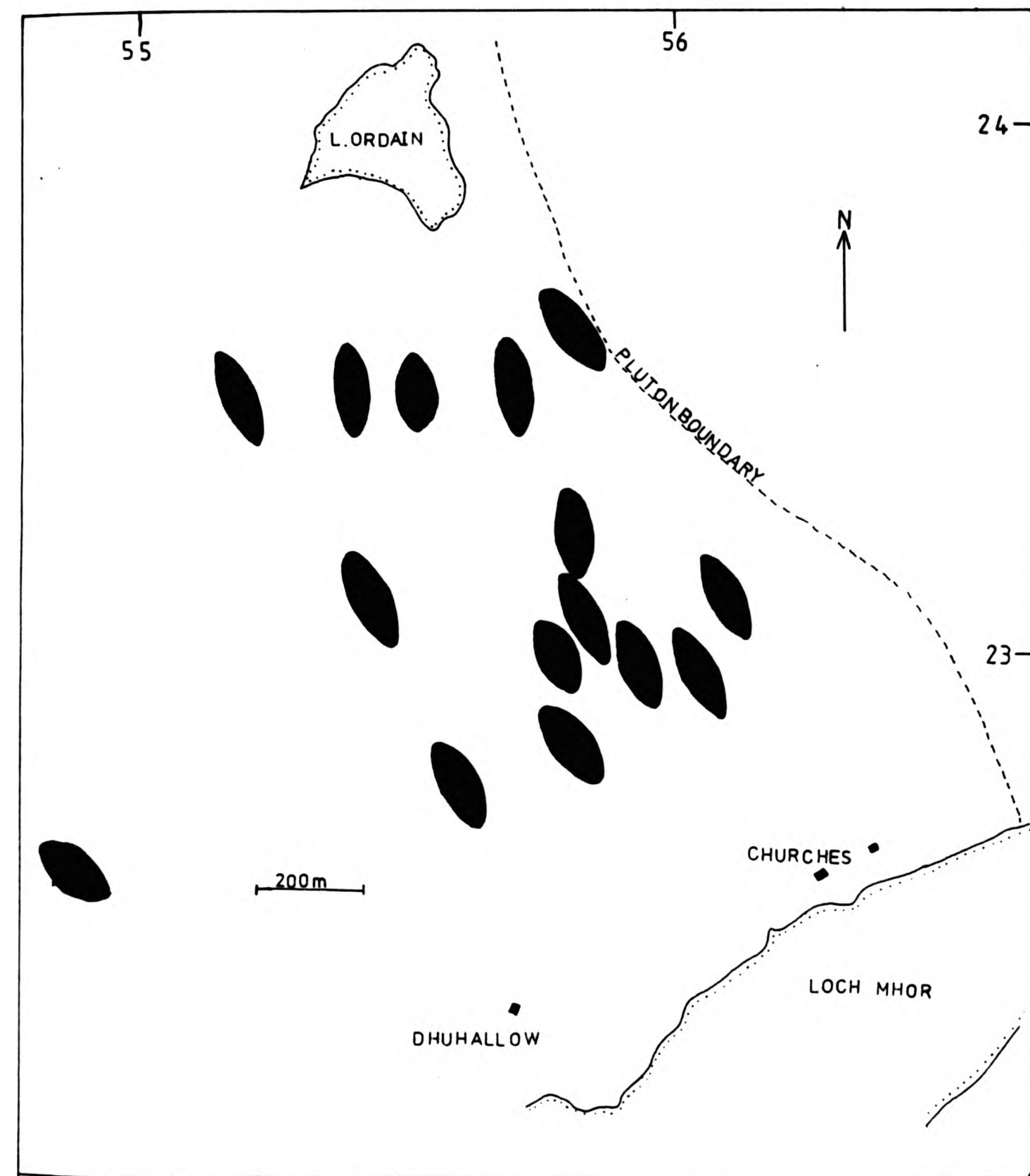


FIGURE 4.9

GRAPH SHOWING THE RELATIONSHIP BETWEEN THE ELLIPTICITY AND SIZE (HORIZONTAL AREA) OF MICRODIORITE ENCLAVES IN TRAVERSE 1

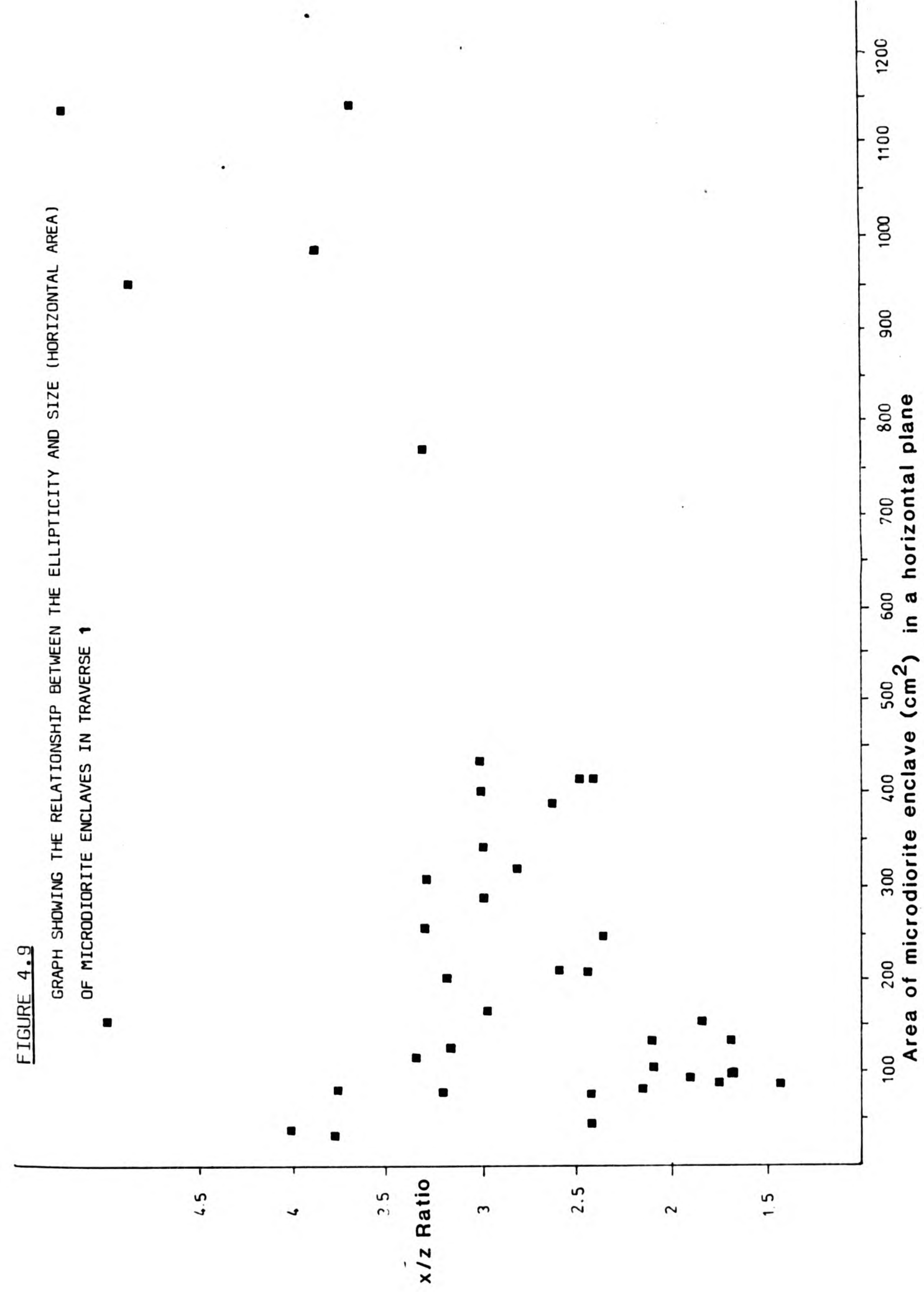


FIGURE 4.10  
 GRAPH SHOWING THE RELATIONSHIP BETWEEN THE ELLIPTICITY AND SIZE (HORIZONTAL AREA)  
 OF MICRODIORITE ENCLAVES IN TRAVERSE 2.

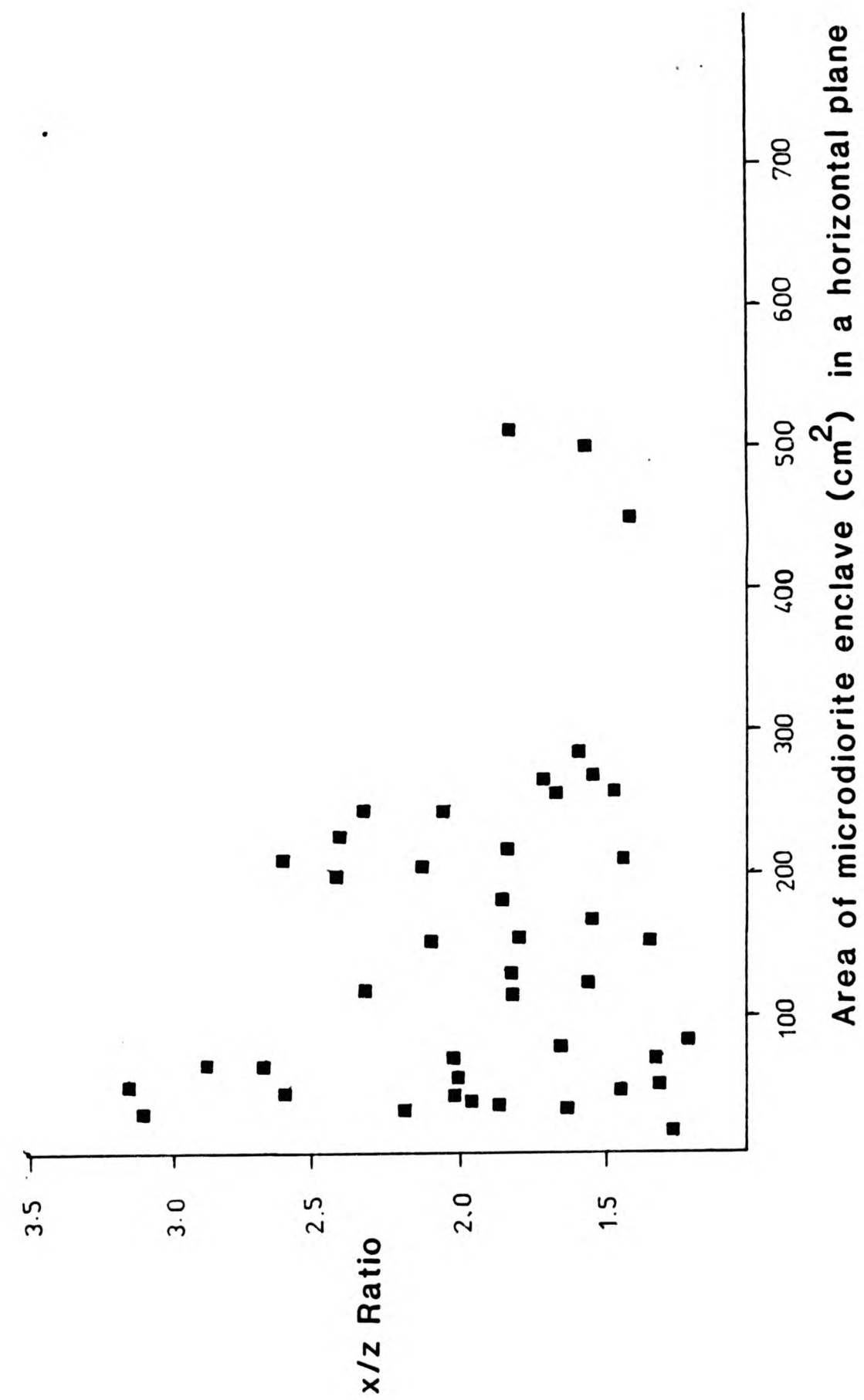




FIGURE 4.11

GRAPH SHOWING THE RELATIONSHIP BETWEEN THE ELLIPTICITY AND SIZE  
(HORIZONTAL AREA) OF MICRODIORITE ENCLAVES IN TRAVERSE 3.

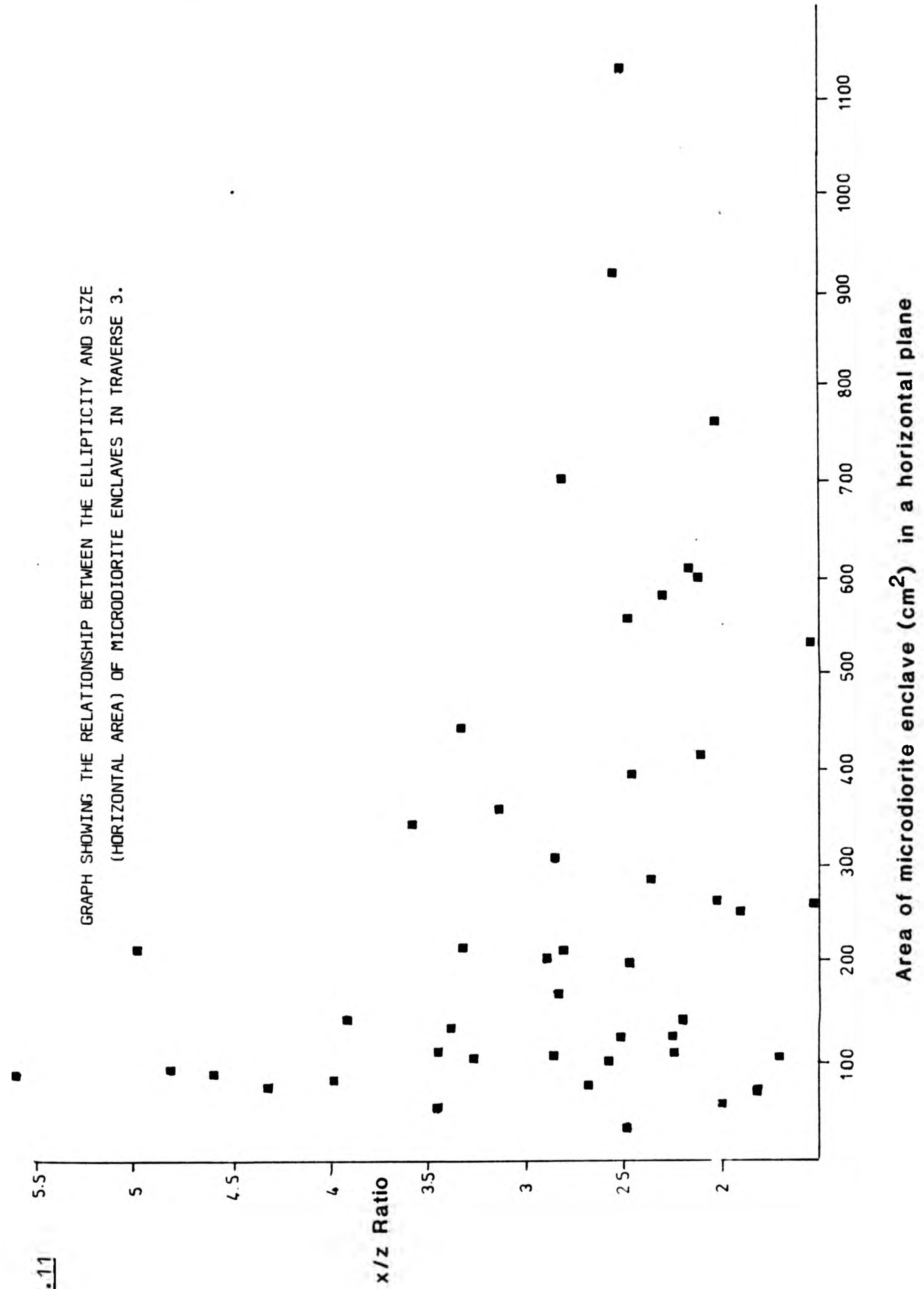
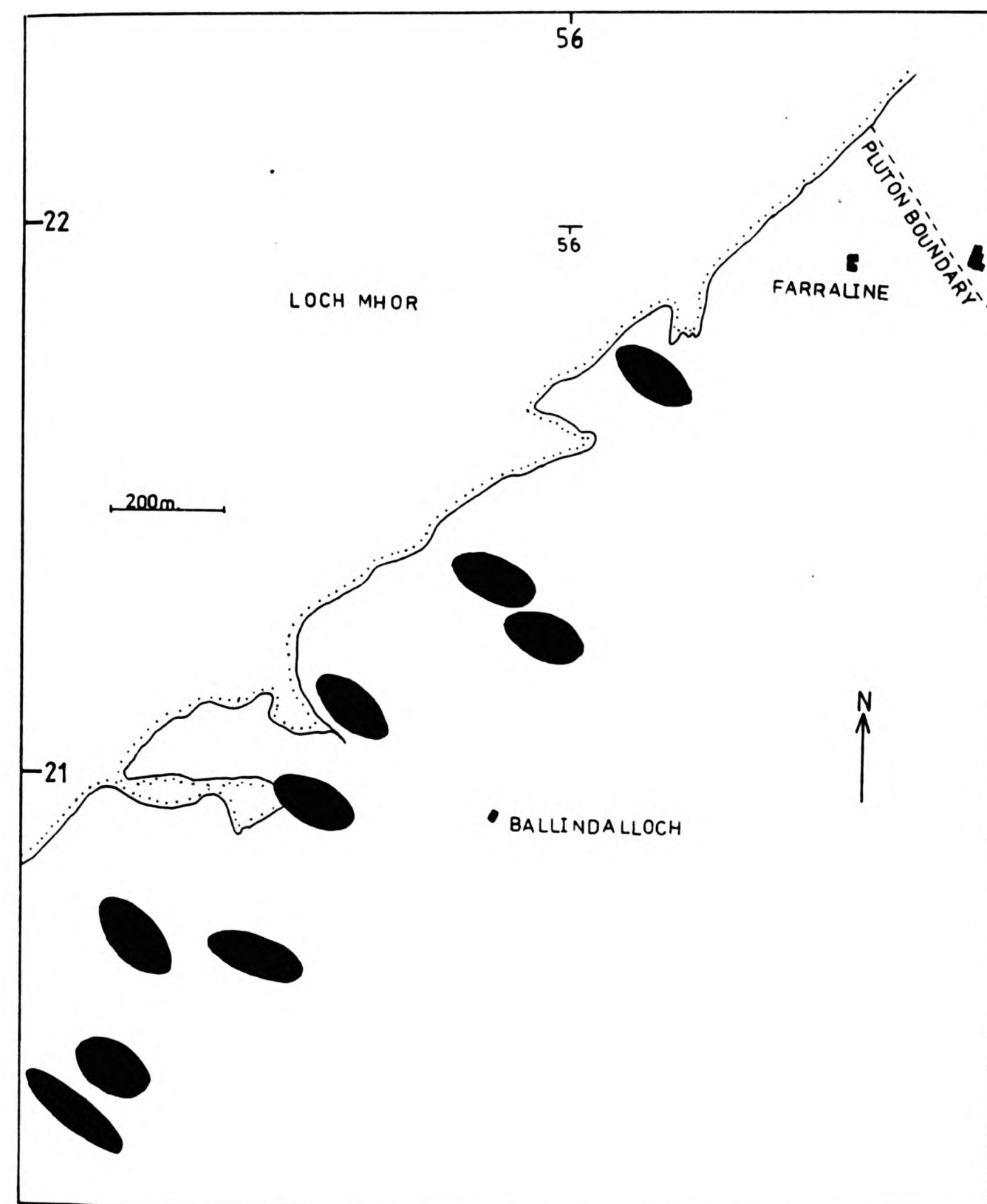




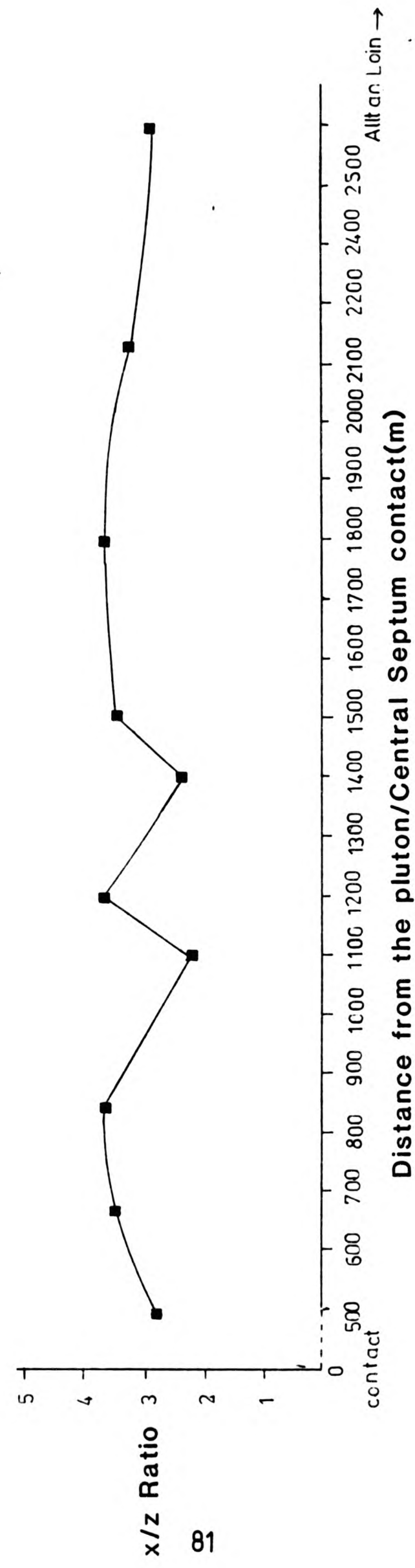
FIGURE 4.12



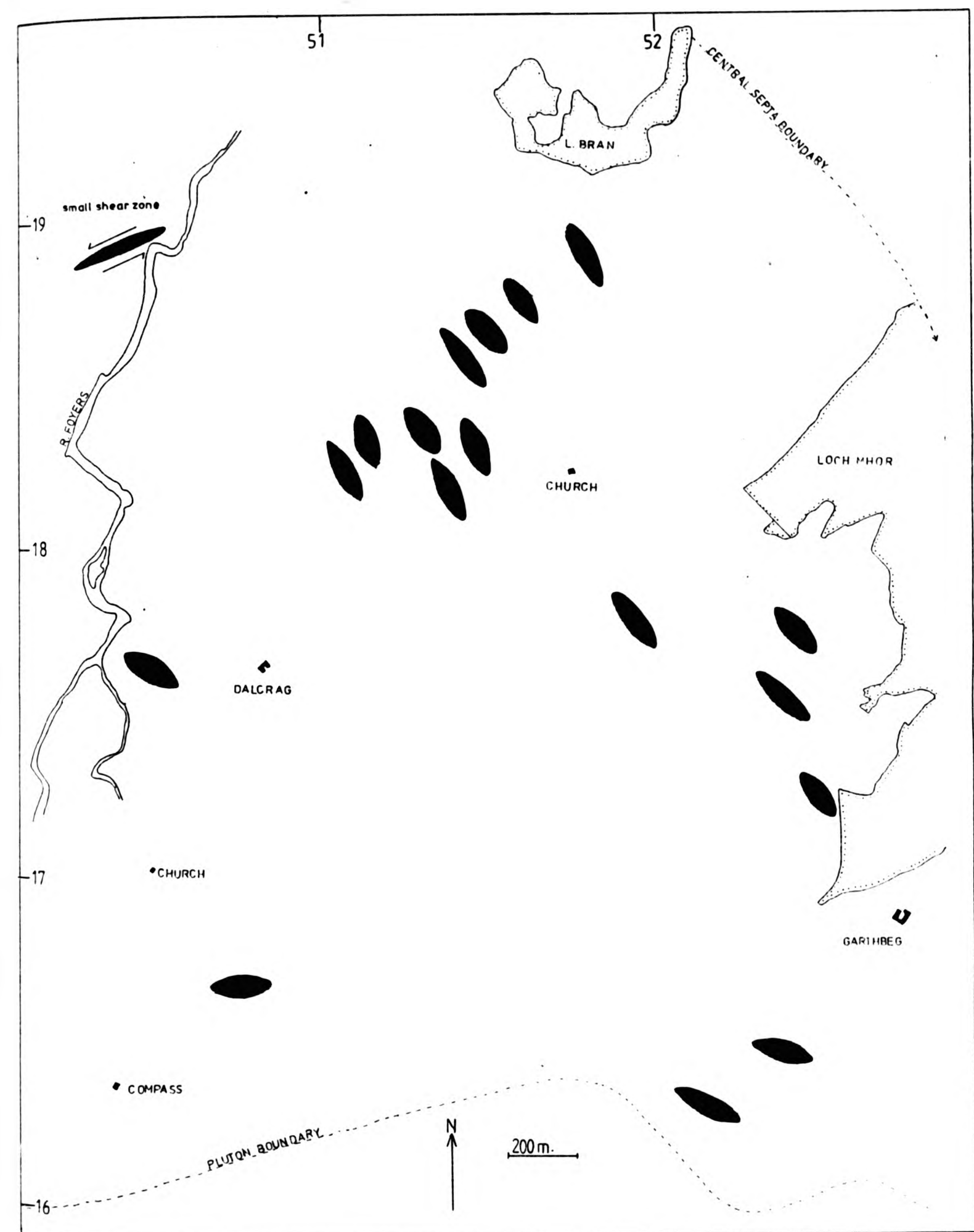
SHAPE OF MICRODIORITE ENCLAVES (HORIZONTAL SECTION)  
IN TRAVERSE 2.

FIGURE 4.13

GRAPH SHOWING HOW THE X:Z HORIZONTAL AXIAL RATIOS OF ELLIPSOIDAL MICRODIORITE ENCLAVES VARY WITH THE DISTANCE FROM THE CENTRAL PSAMMITE SEPTUM. THE ENCLAVES ARE SOUTH WEST OF THE SEPTUM IN A DALCRAG GRANODIORITE HOST.



—■— Traverse from L. Bran to the junction of the Foyers and Gorthleck roads.



SHAPE OF MICRODIORITE ENCLAVES (HORIZONTAL SECTION) IN TRAVERSE 3

FIGURE 4.14

FIGURE 4.15  
MAP DISPLAYING ENCLAVE SHAPE DISTRIBUTION  
THROUGHOUT THE FOYERS COMPLEX.

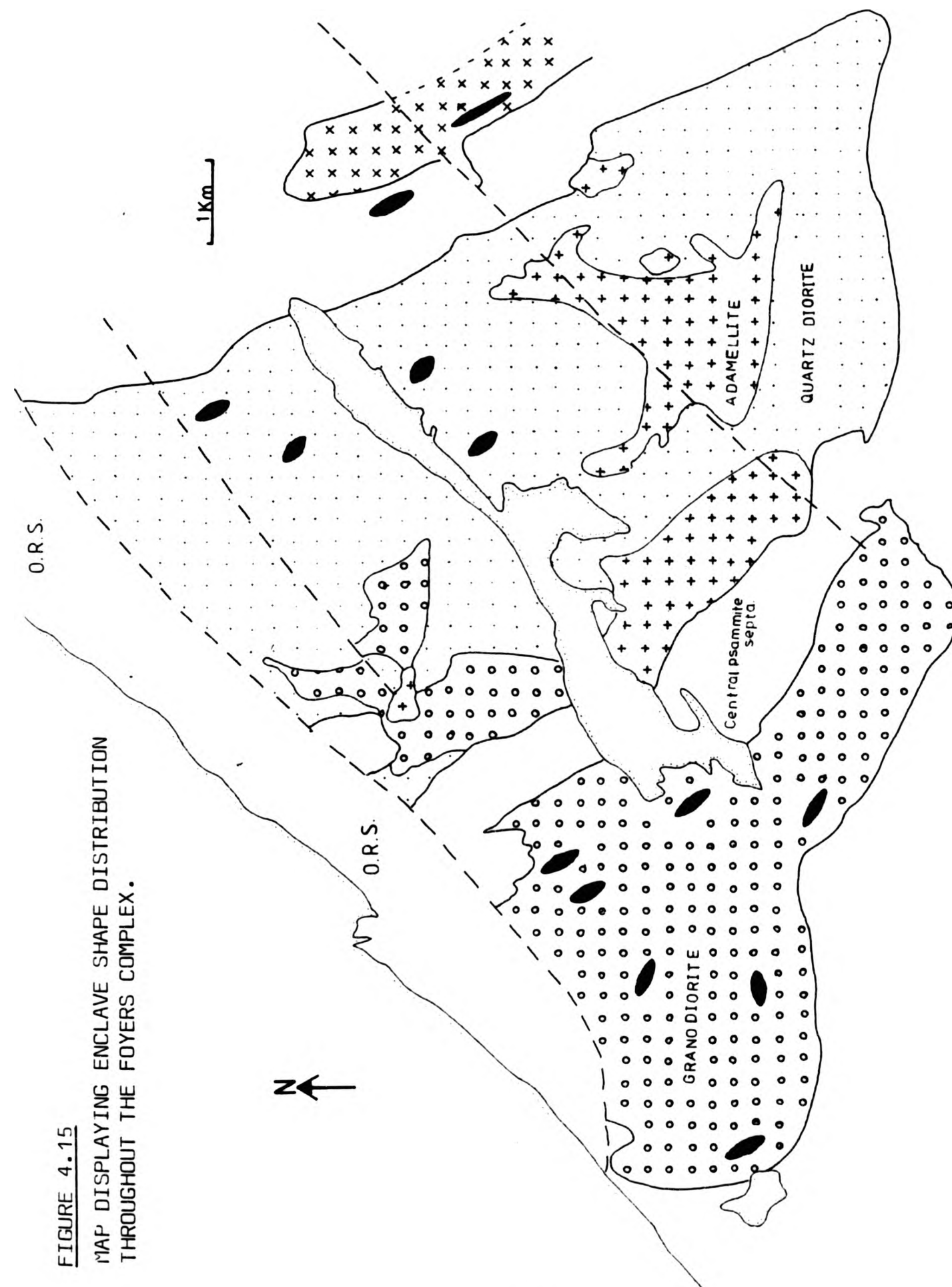
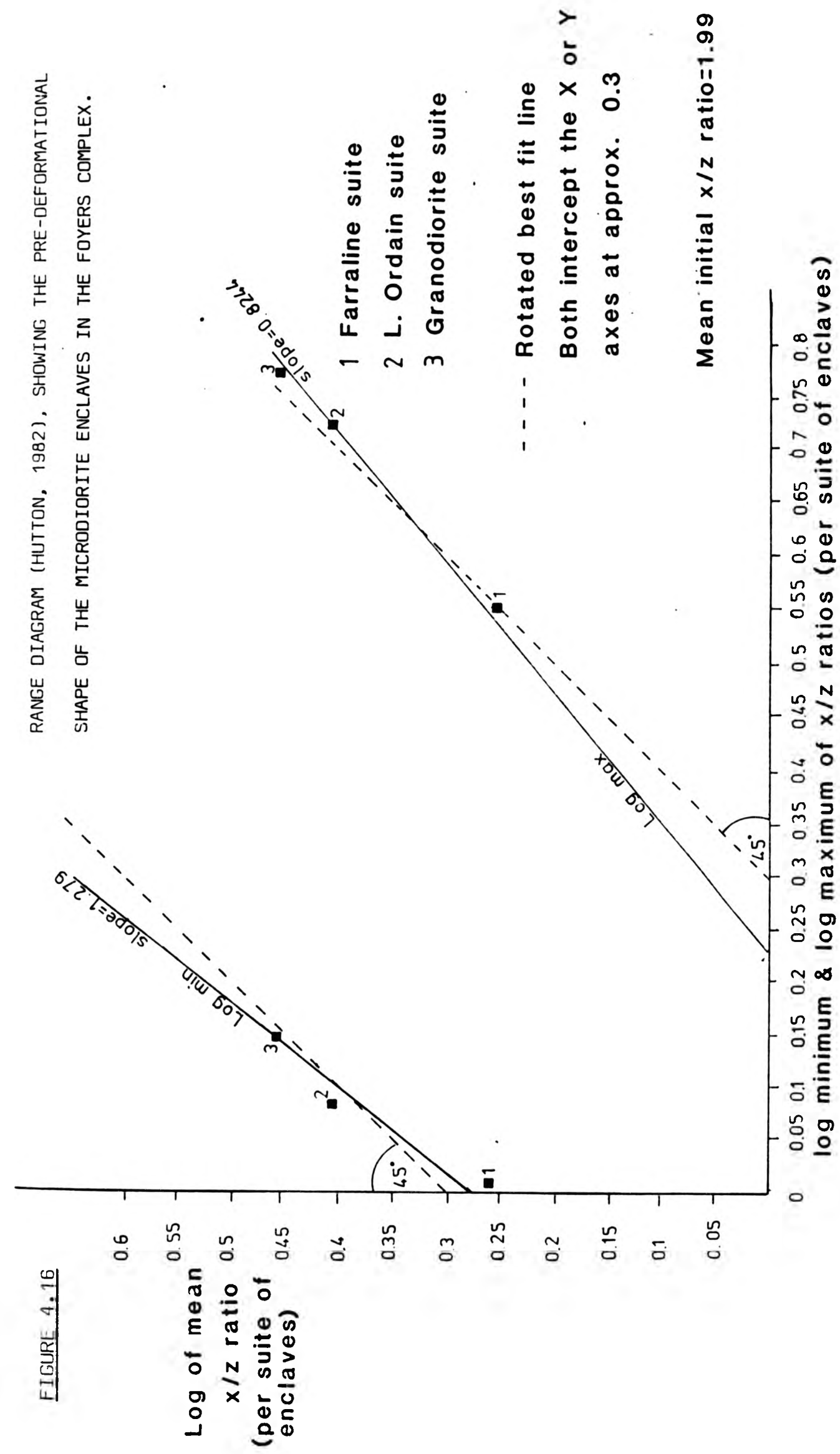




FIGURE 4.16



PLATES  
Chapter 4



Plate 4.1

Steeply inclined foliations, defined by the preferred orientation of plagioclase laths and mafic minerals in the Errogie Quartz Diorite.

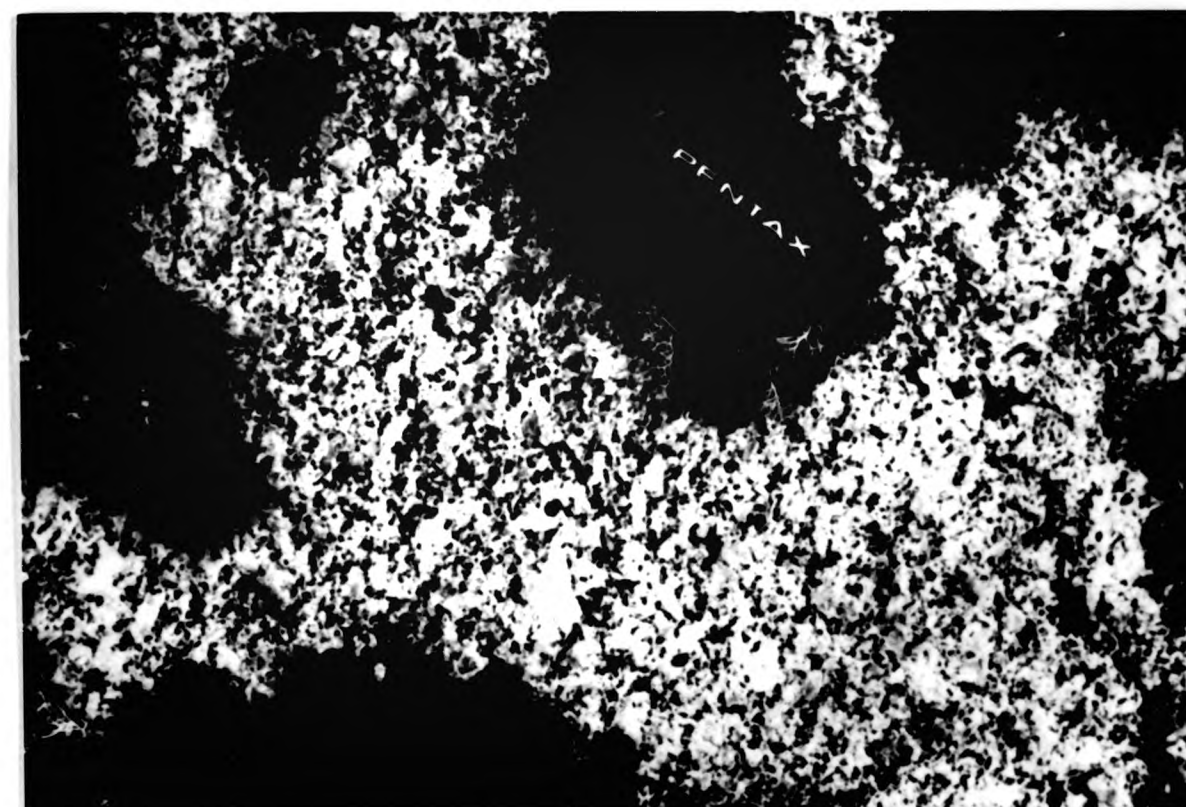


Plate 4.2

Elliptical microdiorite enclave containing an internal mineral fabric parallel to the long axis of the enclave, and the foliation within the host Errogie Quartz Diorite.

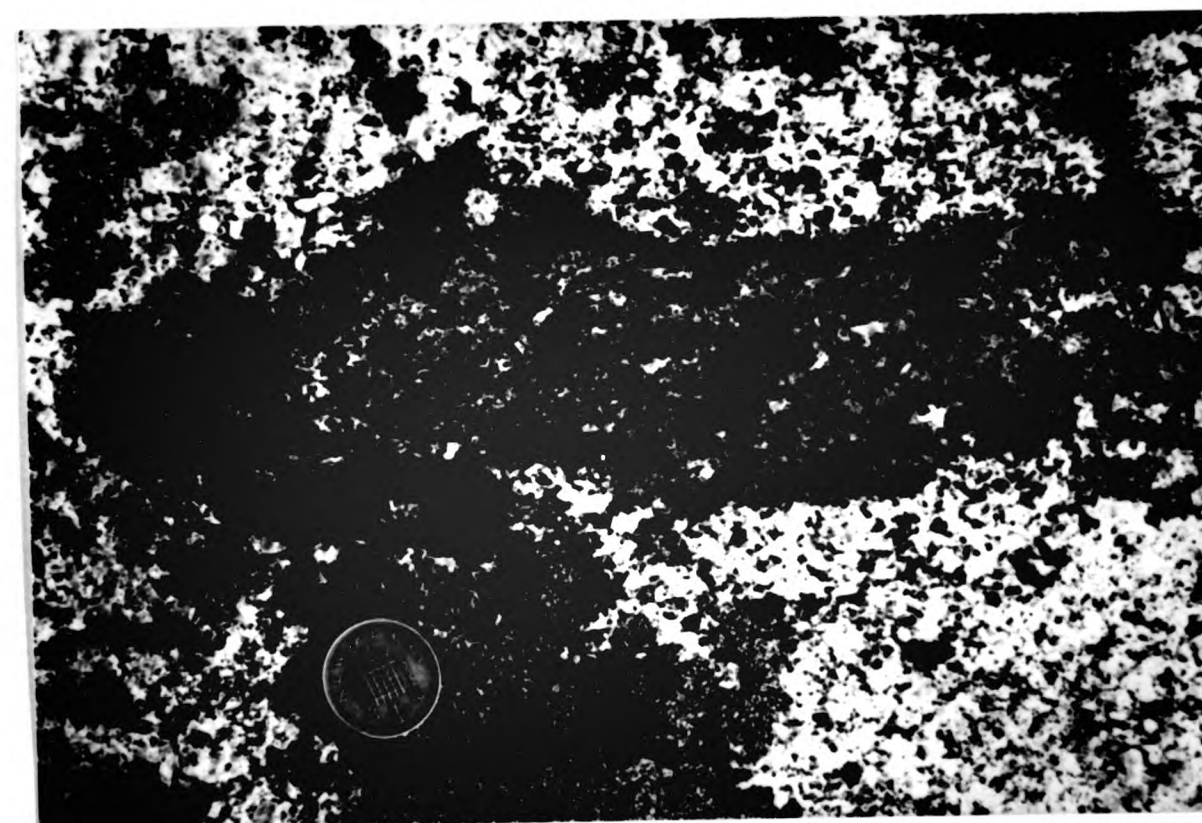


Plate 4.3

Microdiorite enclave with no internal parallel mineral fabric. The surrounding Dalcrag Granodiorite shows a preferred alignment of plagioclase laths and mafics, which are parallel to the long axis of the pen.

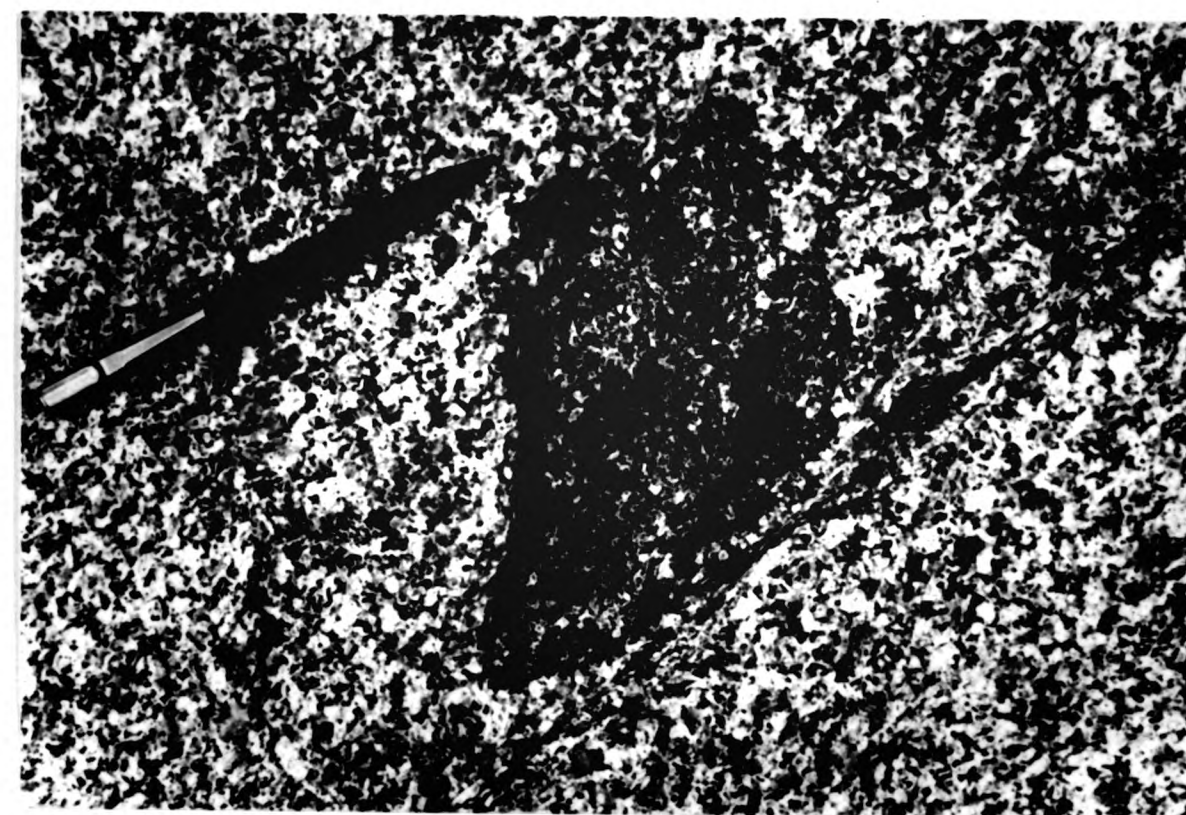
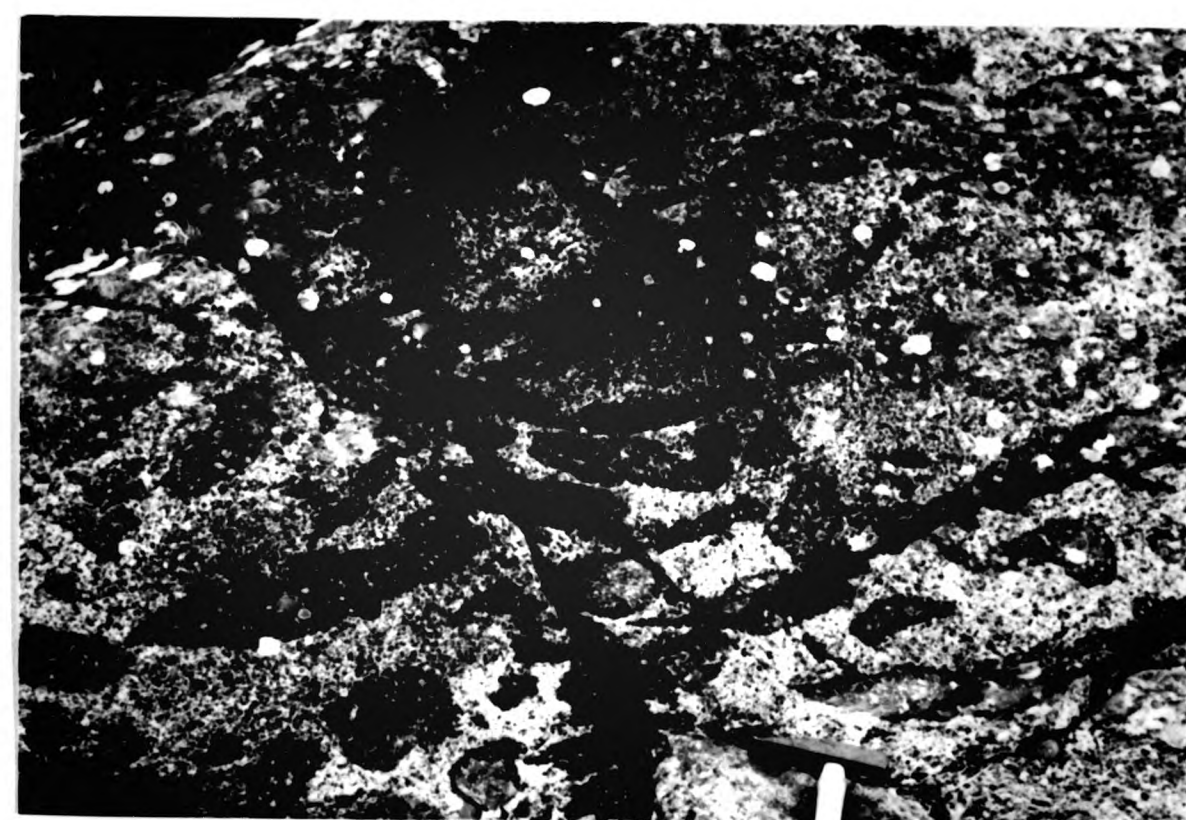


Plate 4.4

Swarm of microdiorite enclaves in the Errogie Quartz Diorite, with long axes lying in a sub-horizontal attitude.





**Plate 4.5**

Elongate microdiorite enclave, showing a mineral fabric defined by plagioclase phenocrysts lying at a high angle to the long axis of the ellipse.

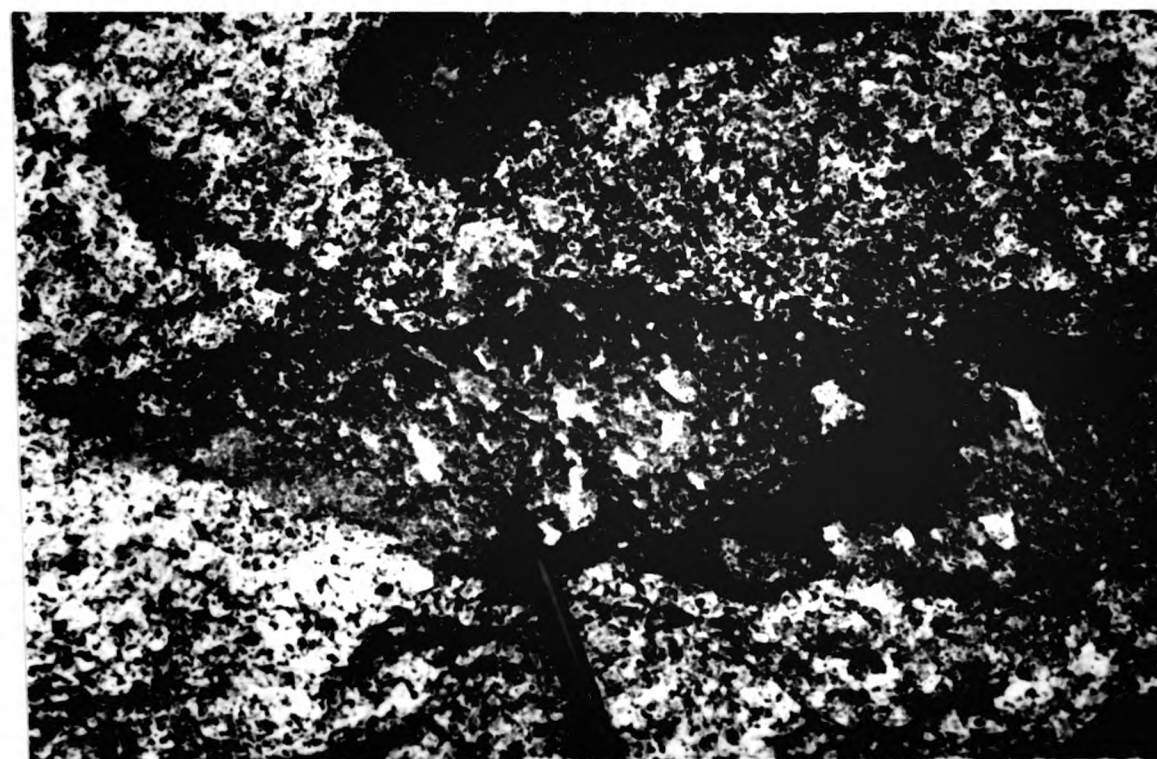


**Plate 4.6**

Appinitic diorite from the Central Psammite Septum, viewed in plane polarised light. It displays aligned ribbons (R) of recrystallised hornblende and aligned aggregates of plagioclase laths (P). (x5)

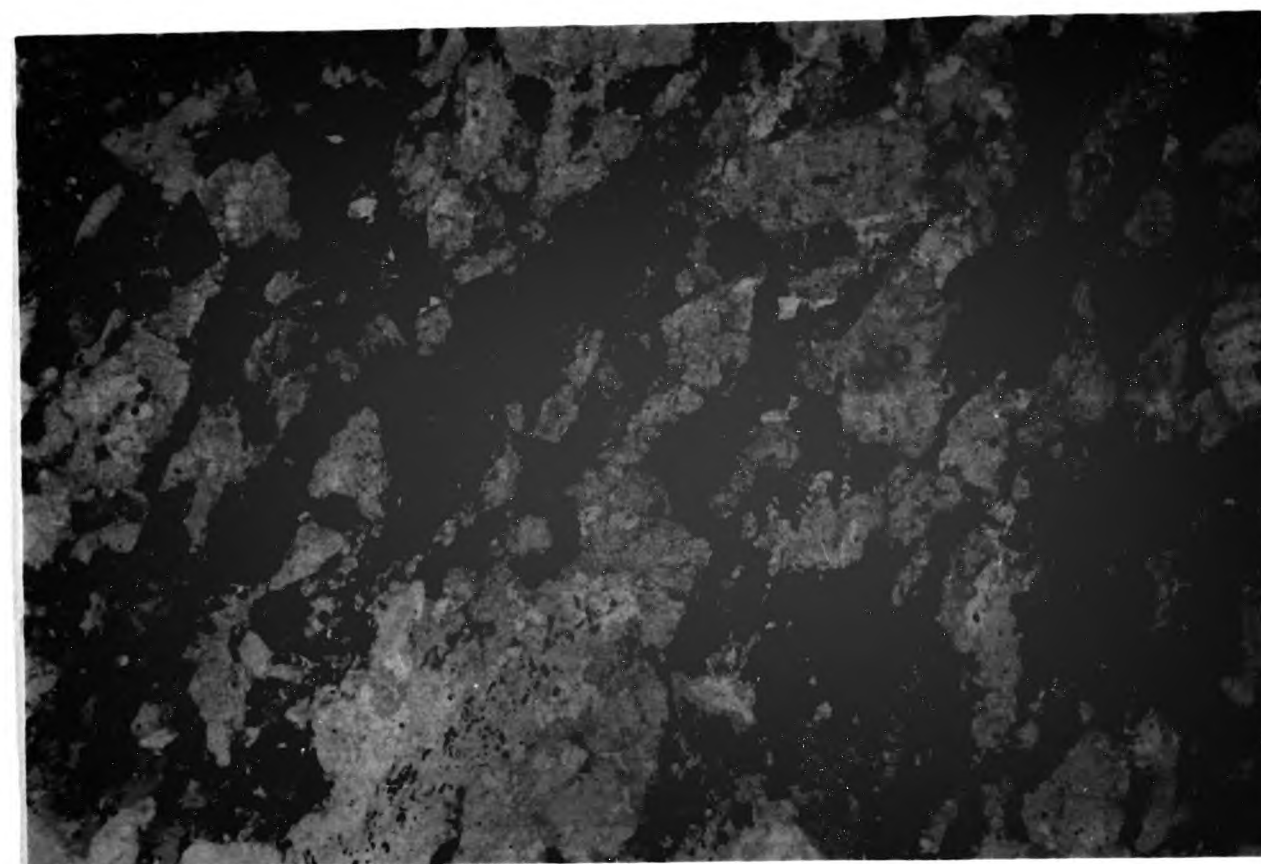


**Plate 4.7**

Plate 4.6 viewed under cross polars, showing that the internal structure of the ribbons (R), is composed of equant recrystallised hornblende. (x5)

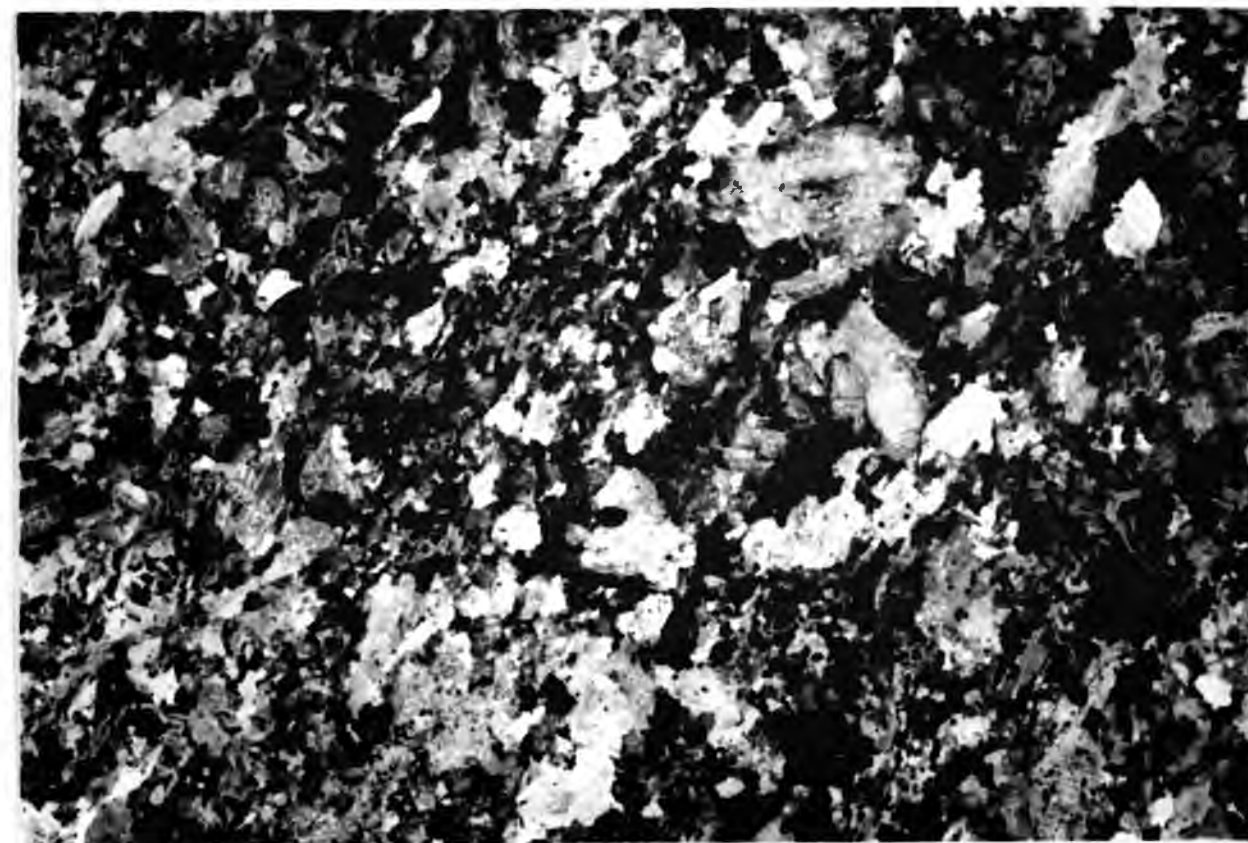


**Plate 4.8**

Unique type of margin between medium grained, and coarse grained, rather acidic granodiorite. The margin is sharp, and the coarse grained granodiorite develops a strong margin parallel fabric whose intensity dies quickly away from the margin. The contact also shows 2-3, margin parallel, biotite schlieren, with the concentration of biotite decreasing away from the contact. These contact structures developed during margin parallel magma flow.

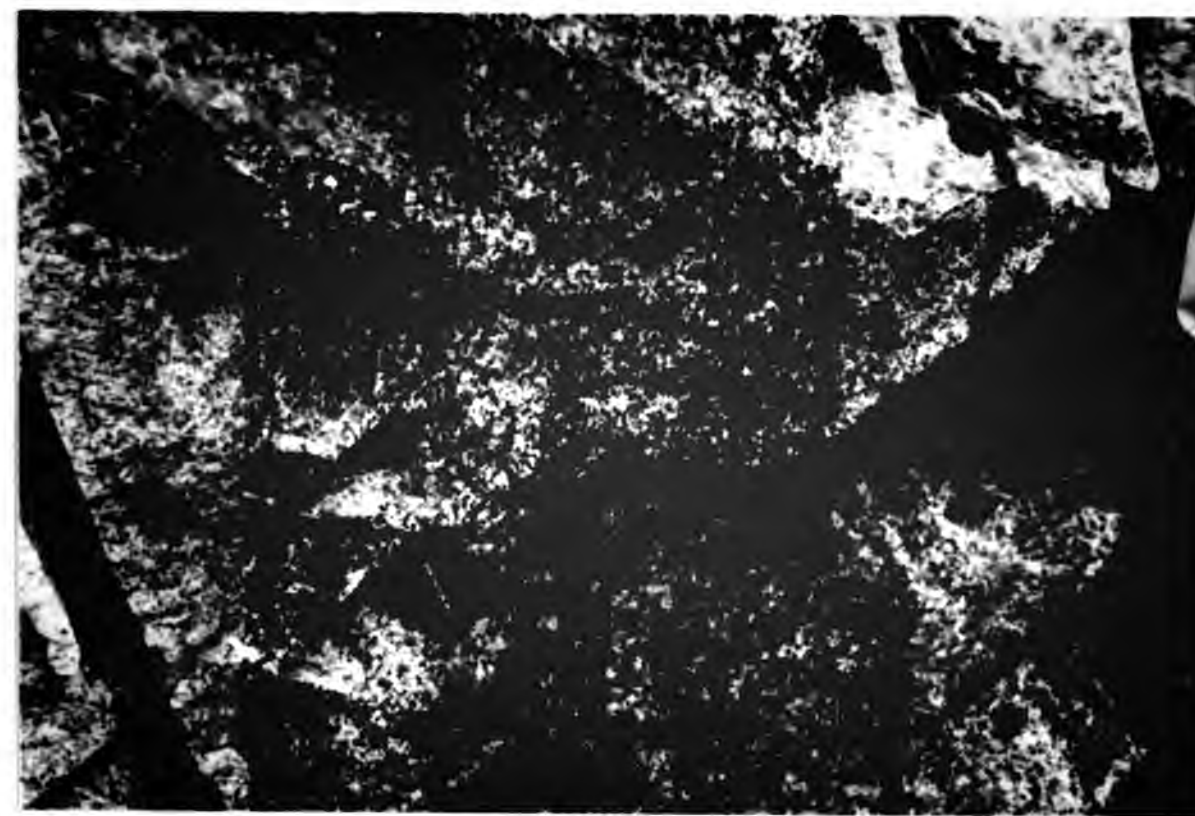




Plate 4.9

Large anhedral quartz grain, showing undulatory extinction. Dalcrag Granodiorite. (Crossed polars, x47).

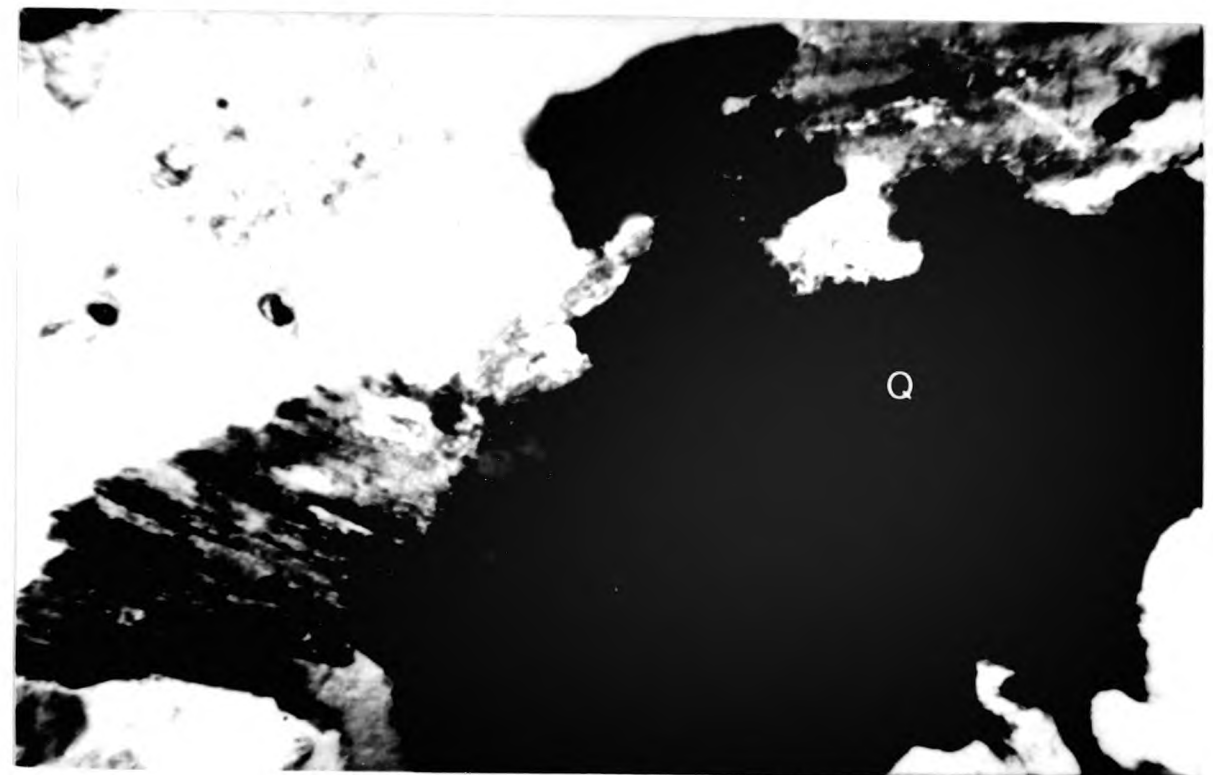


Plate 4.10

Errogie Quartz Diorite containing a well defined flow alignment of undeformed plagioclase laths. Note the occasional lath at a high angle to the mineral fabric. (Crossed polars, x5).

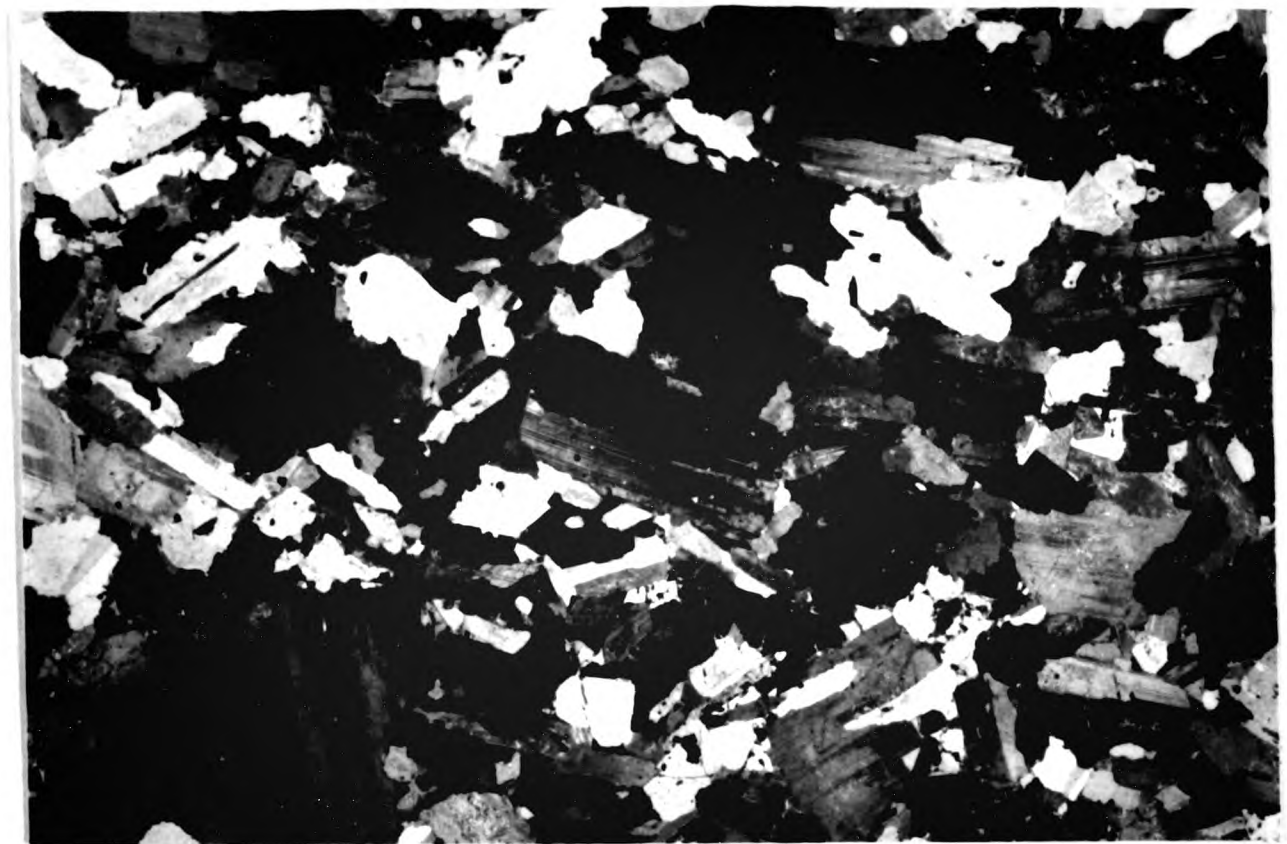


Plate 4.11

Errogie Quartz Diorite displaying a weak alignment of plagioclase laths. Note the well defined oscillatory zoning in the large plagioclase phenocryst. (Crossed polars, x5).

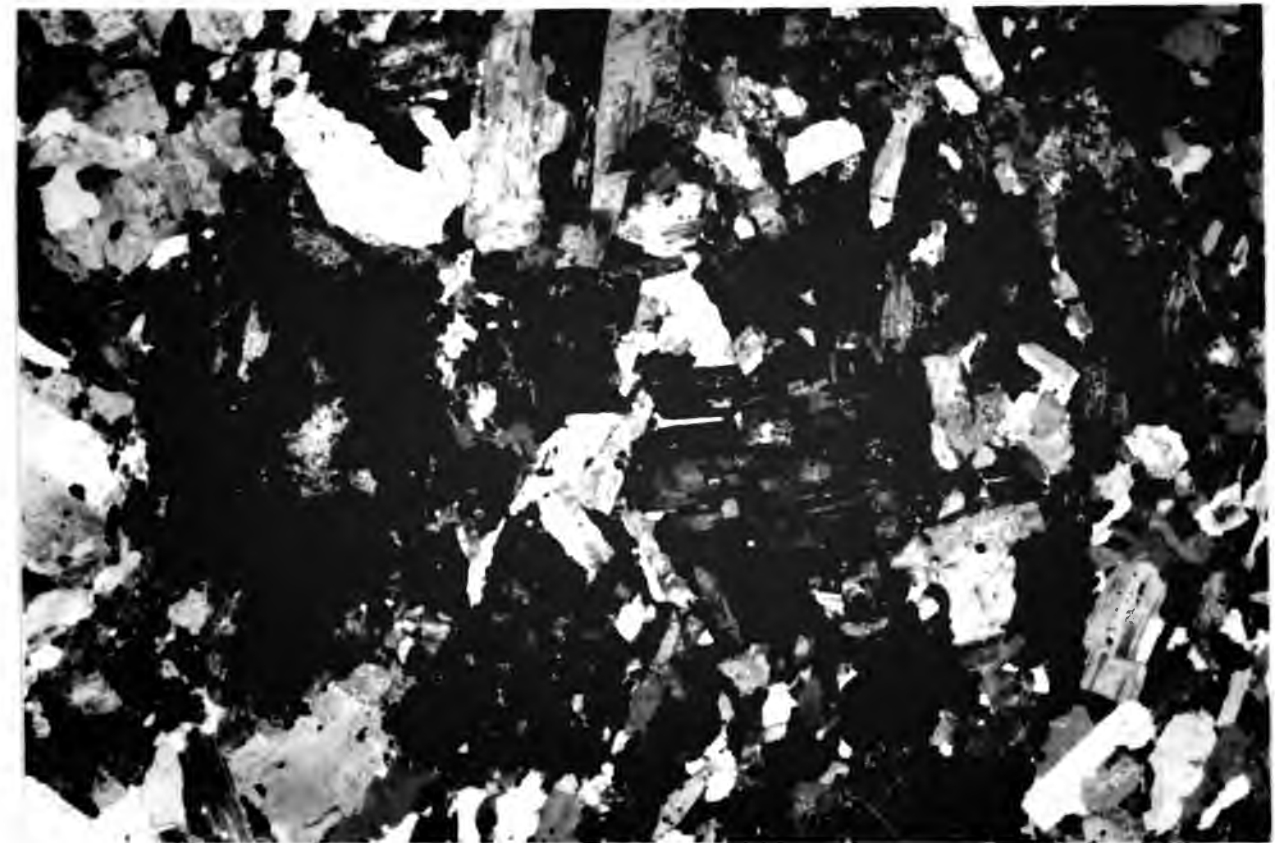


Plate 4.12

Large plagioclase lath showing undulatory extinction, providing good evidence of solid state strain. Errogie Quartz Diorite. (Crossed polars, x47).

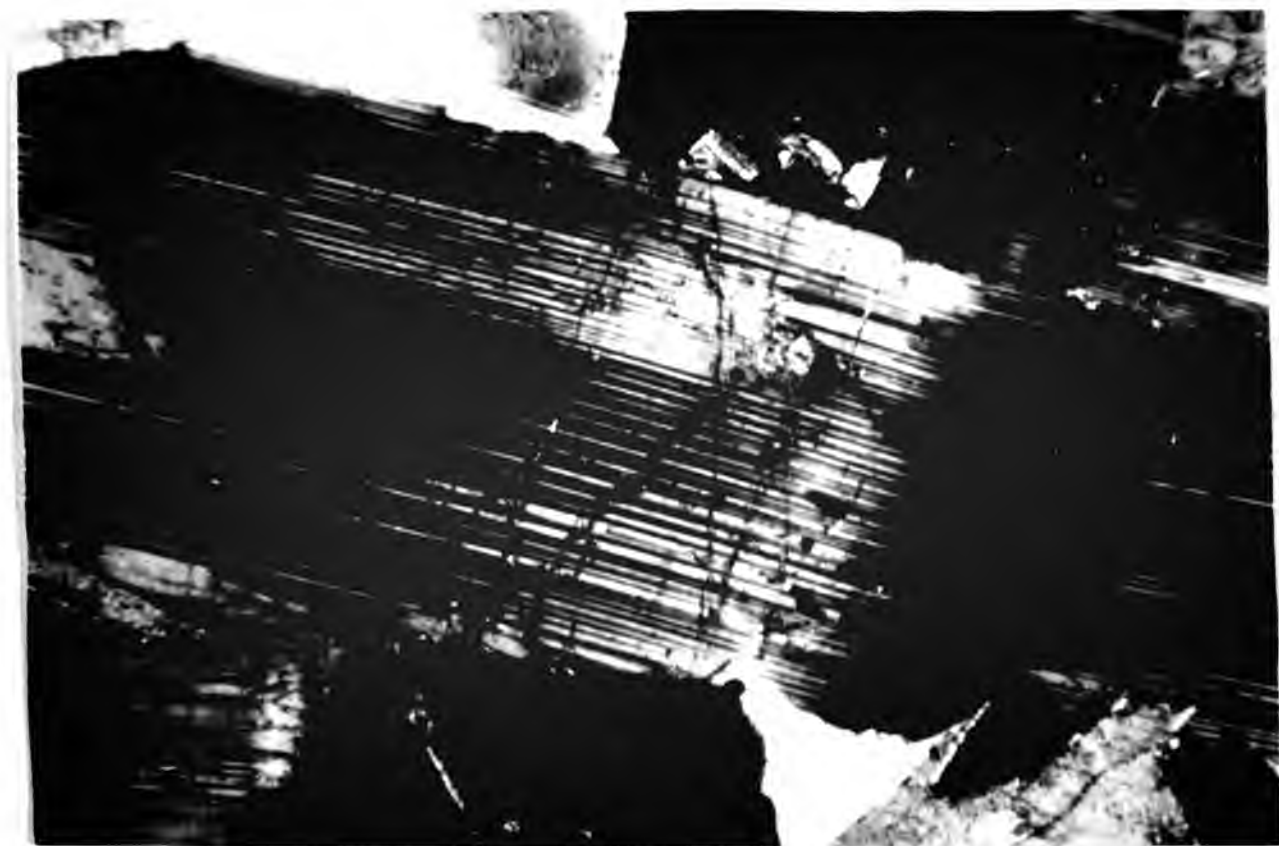




Plate 4.13

Deformation of albite twins, where one plagioclase lath impinges on another. Chliabhain Quartz Monzodiorite. (Crossed polars, x47).

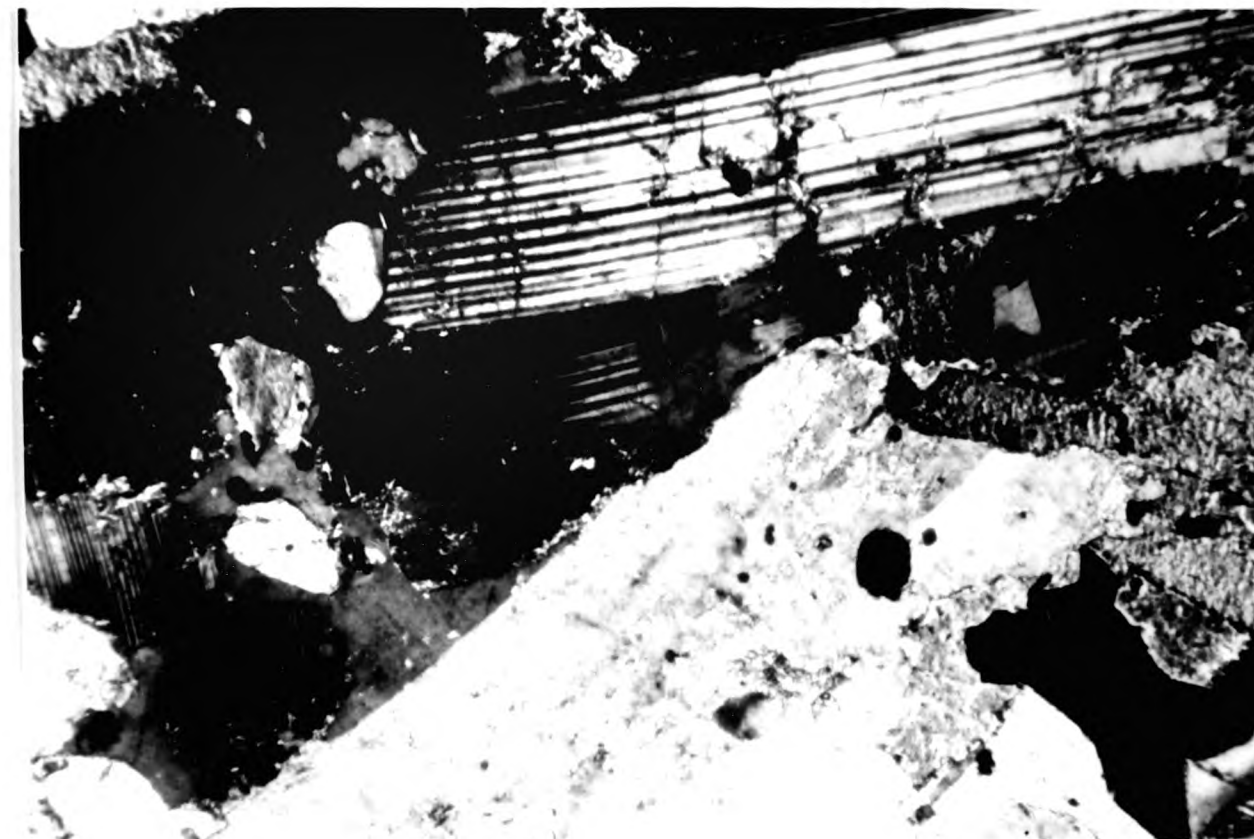
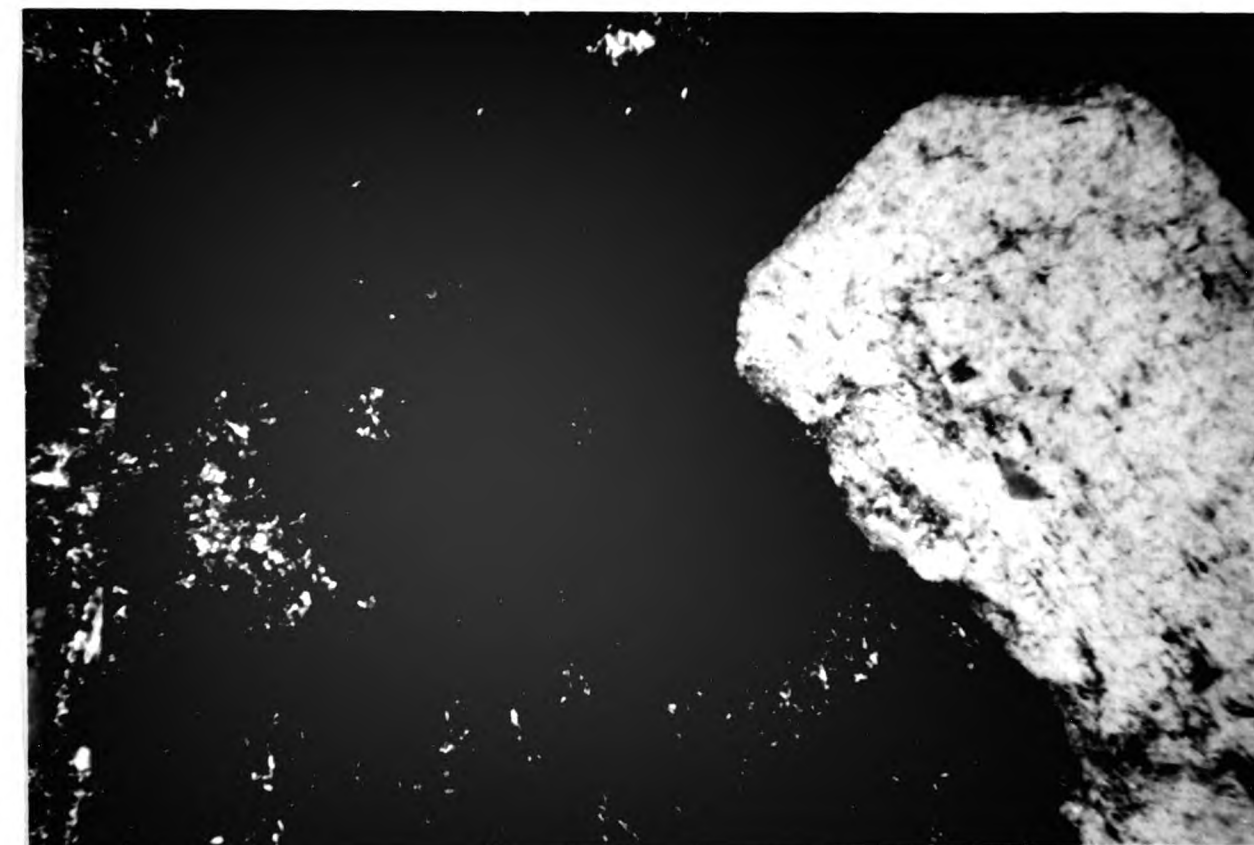


Plate 4.14

One plagioclase lath impinging on another. At the contact, dislocation of the lattice has occurred causing part of the plagioclase lath to lie out of optical continuity with the remainder of the crystal. Chliabhain Quartz Monzodiorite. (Crossed polars, x47).



CHAPTER 5. THE MAOL CHNOC COMPLEX.

FIGURE 5.1

GRANODIORITE AND ADAMELLITE FROM THE MAOL CHNOC COMPLEX PLOTTED  
ON A Q.A.P. PLOT.

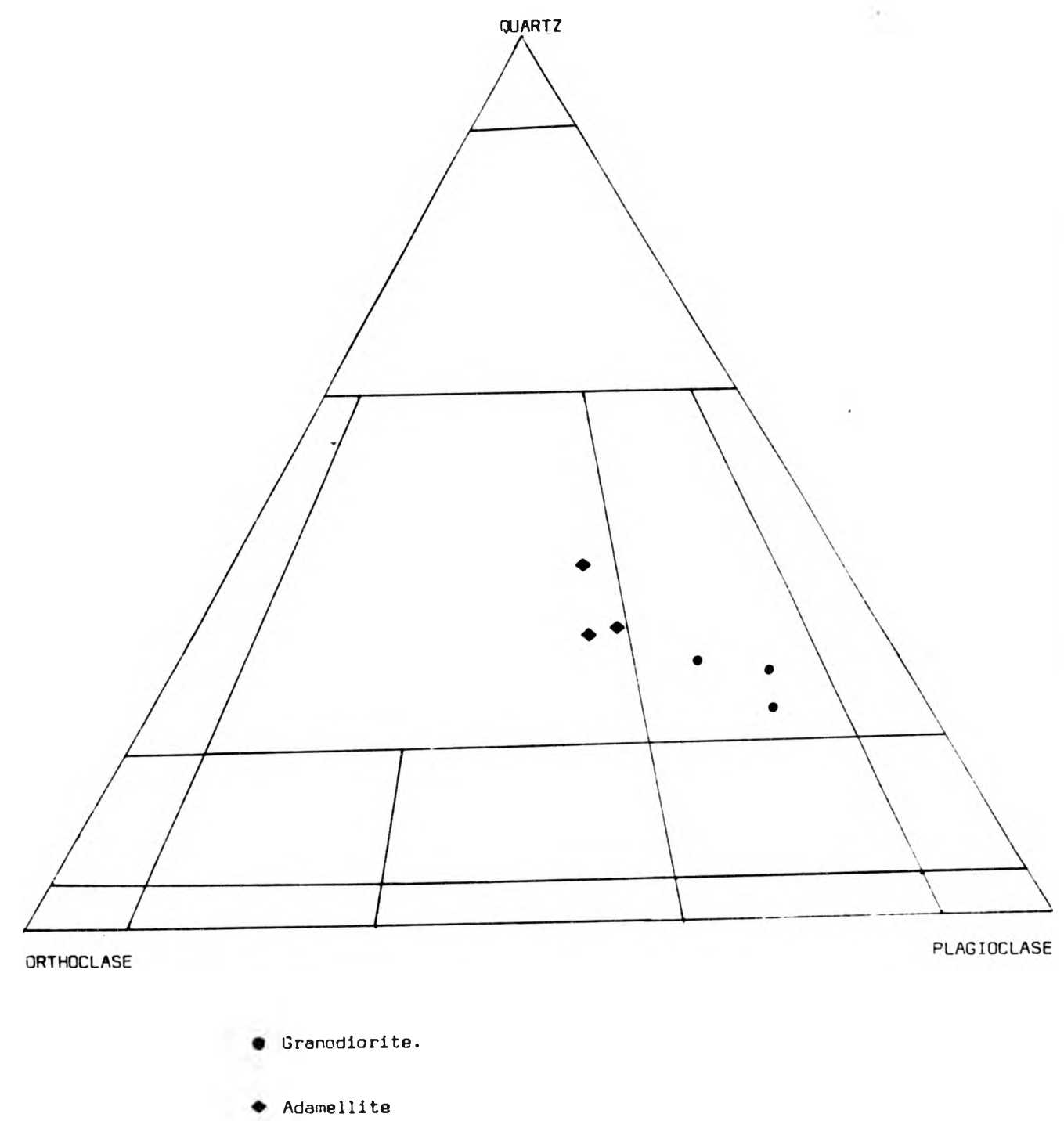


TABLE 5.1 Modal Analyses of Maol Chnoc Granodiorite and Adamellite\*.

SAMPLE No.	2134B*	1998C*	2190*	216DA	1966A	2002B
Plagioclase	30.1	38.5	36.5	52.0	46.0	51.1
Orthoclase	23.0	23.5	26.4	12.3	18.0	12.8
Quartz	35.5	30.5	30.1	24.7	26.8	20.1
Biotite	9.5	6.5	7.3	8.86	9.4	15.5
Hornblende	0.6	0.3	trace	2.31	trace	0.1
Sphene	0.3	0.2	0.2	0.3	0.5A	n.2
Accessories	0.6	0.3	0.2	0.15	0.58	0.2
TOTAL	99.6	99.8	100.7	100.62	100.86	100.0

PLATES  
Chapter 5



Plate 5.1

Orthite grain displaying a metamict texture. Surrounding the grain is a narrow, dark pleochroic haloe, well developed within the biotite. Maol Chnoc Granodiorite. (Plane polarized light, x47).

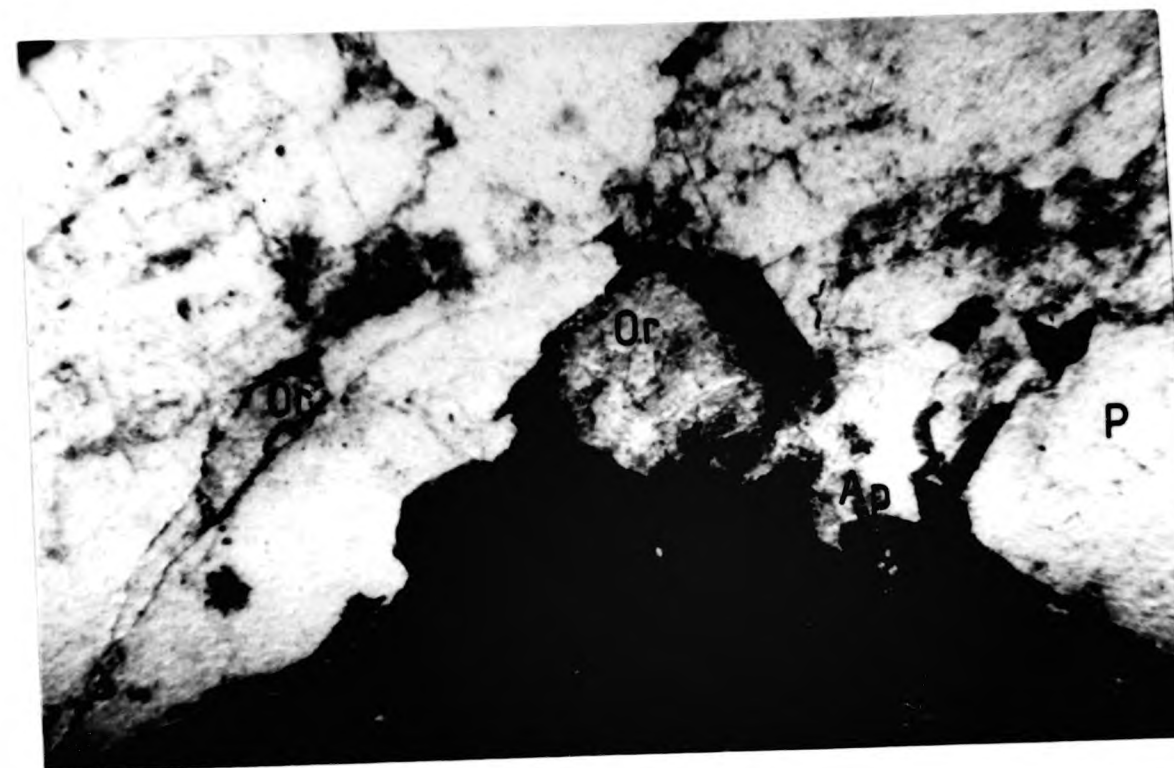


Plate 5.2

Porphyritic Maol Chnoc Micro-adamellite containing, irregular quartz aggregates, euhedral plagioclase phenocrysts, and subhedral orthoclase phenocrysts, in a fine grained groundmass. Observed under cross polars there is little evidence of a parallel mineral fabric. (Crossed polars, x5).

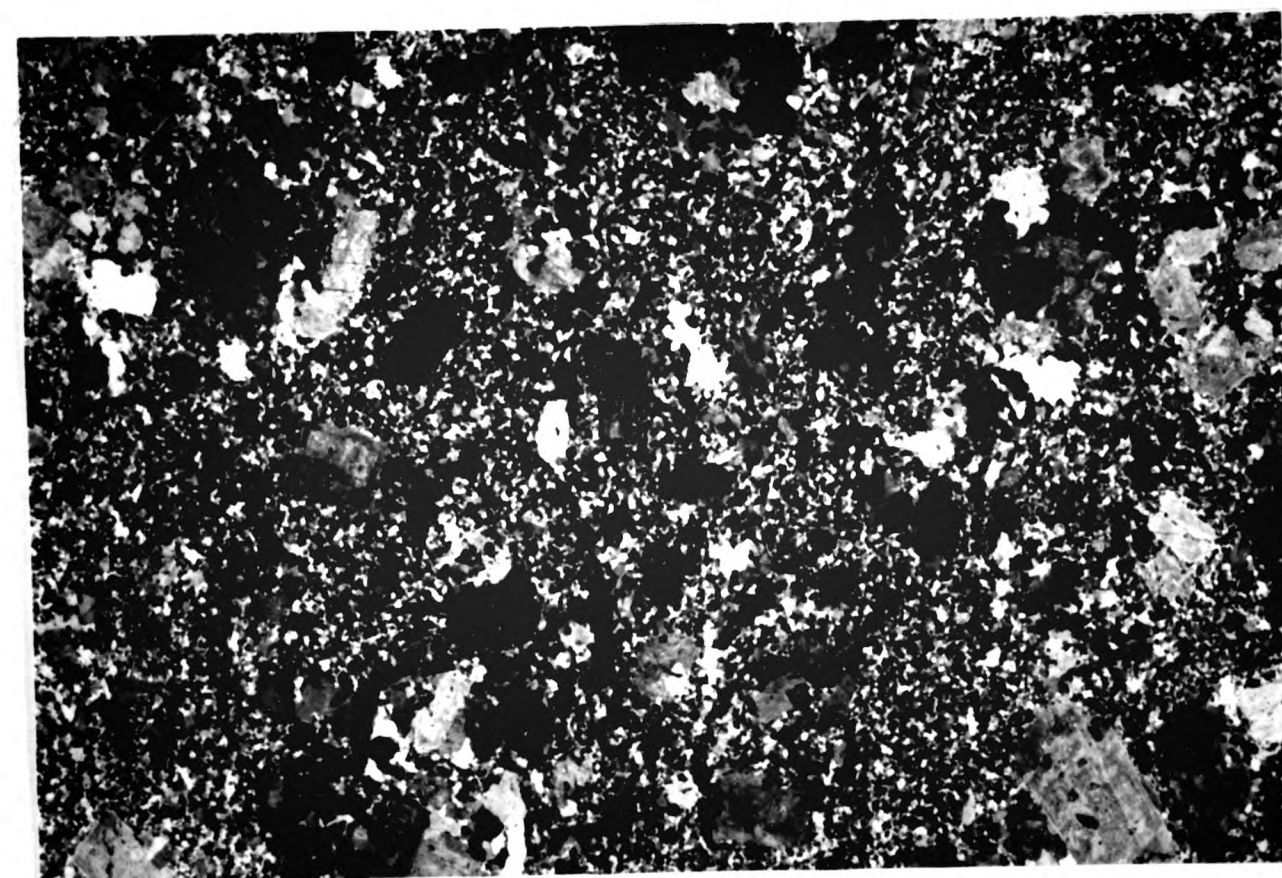




Plate 5.3

Strong mineral foliation, within Maol Chnoc Granodiorite. The fabric becomes more intense towards the foliated aplite vein. The increase in intensity is marked by a decrease in grain size, mainly through the loss of orthoclase phenocrysts. To the left of the aplite, the fabric in the granodiorite becomes exceptionally strong, as a mylonitic texture develops.



Plate 5.4

Strong, parallel, mineral fabric, defined by mica flakes, augened plagioclase phenocrysts and fine grained lenticular quartz/feldspar aggregates. Maol Chnoc Micro-adamellite.

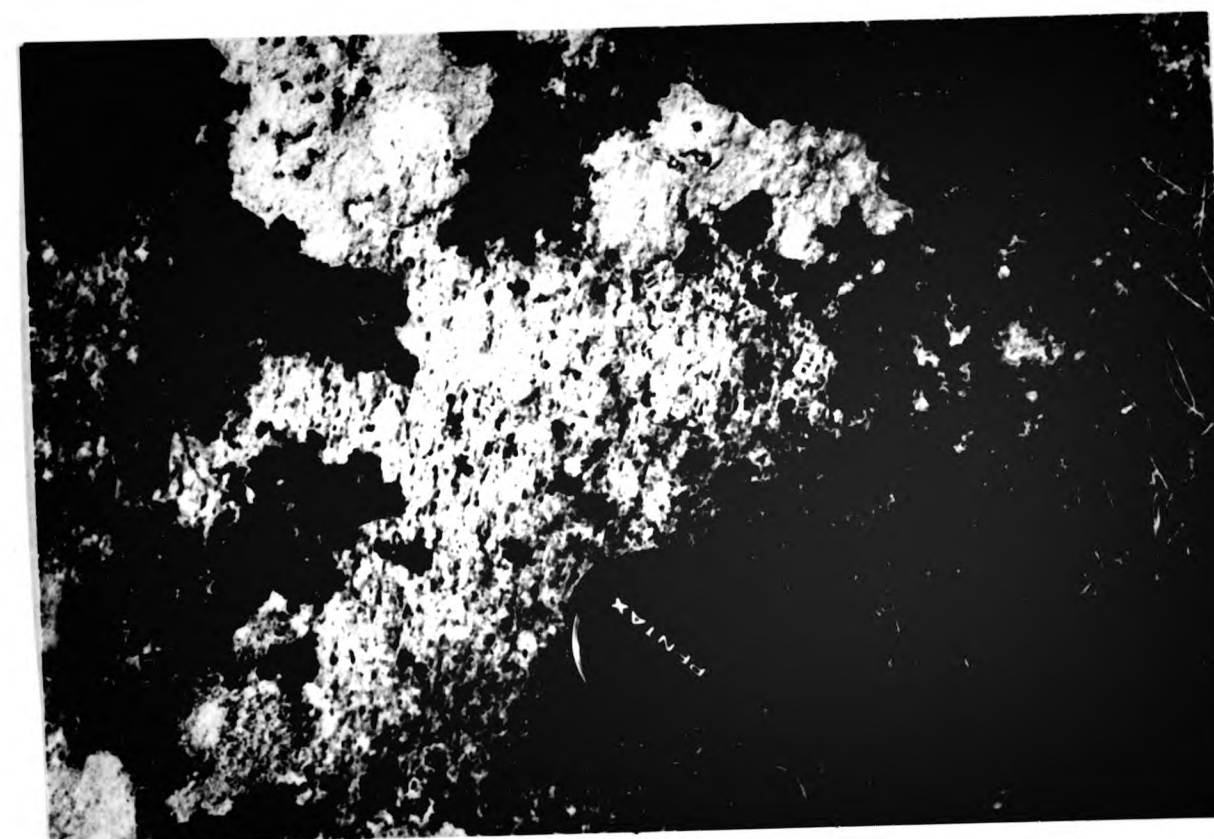


Plate 5.5

Strong fabric, defined by the parallel alignment of mafics and plagioclase laths within diorite veins. (Beinn Dubhcharaidh).



Plate 5.6

Strong mineral fabric, cutting across a sharp contact between Maol Chnoc Granodiorite and Maol Chnoc Micro-adamellite. Width of view is 10cm.





Plate 5.7

Wispy, elongate, microdiorite enclaves lying parallel to the foliation within the Maol Chnoc Granodiorite. Towards the centre of the photograph is a weakly deformed, micaceous psammite xenolith.

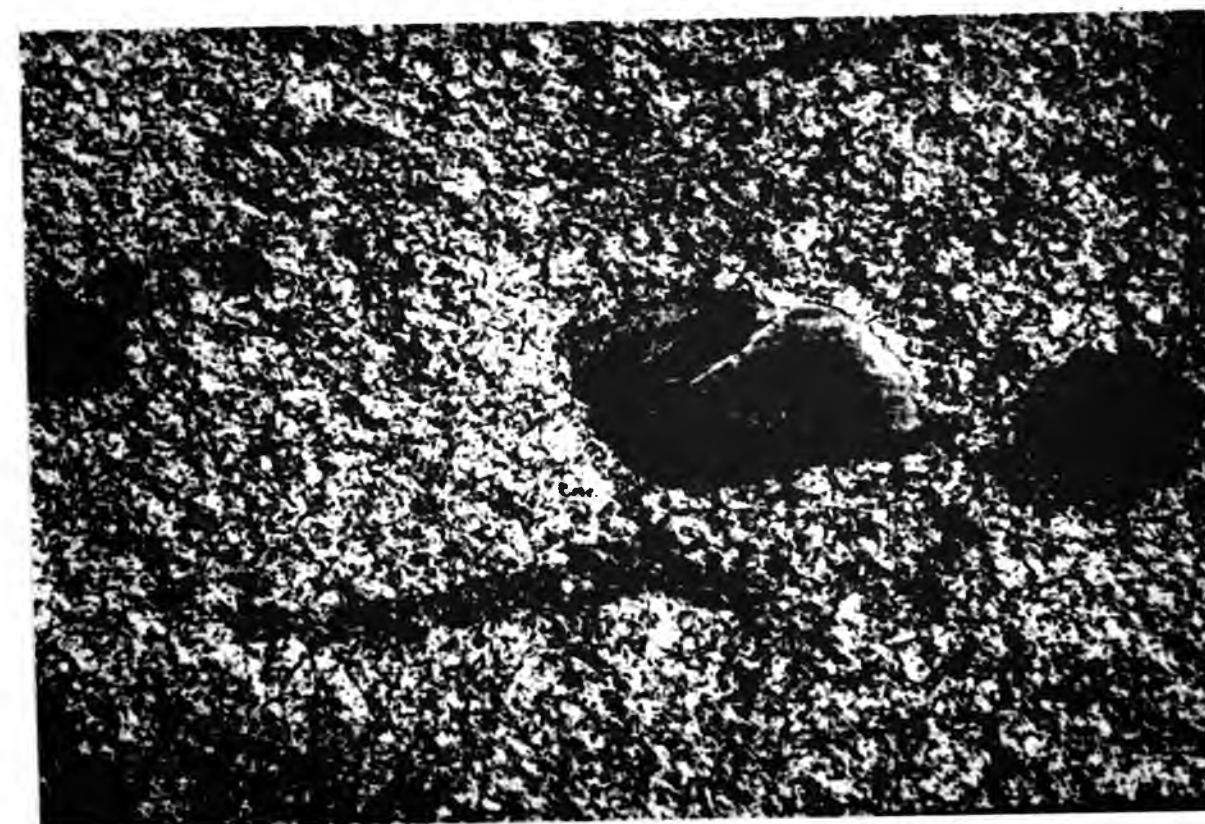


Plate 5.8

Strong flow fabric in Maol Chnoc Granodiorite, defined by parallel plagioclase and orthoclase laths. The fine oscillatory zoning, in the top left hand corner of the photograph, indicates the laths are internally undeformed. (Crossed polars, x5).

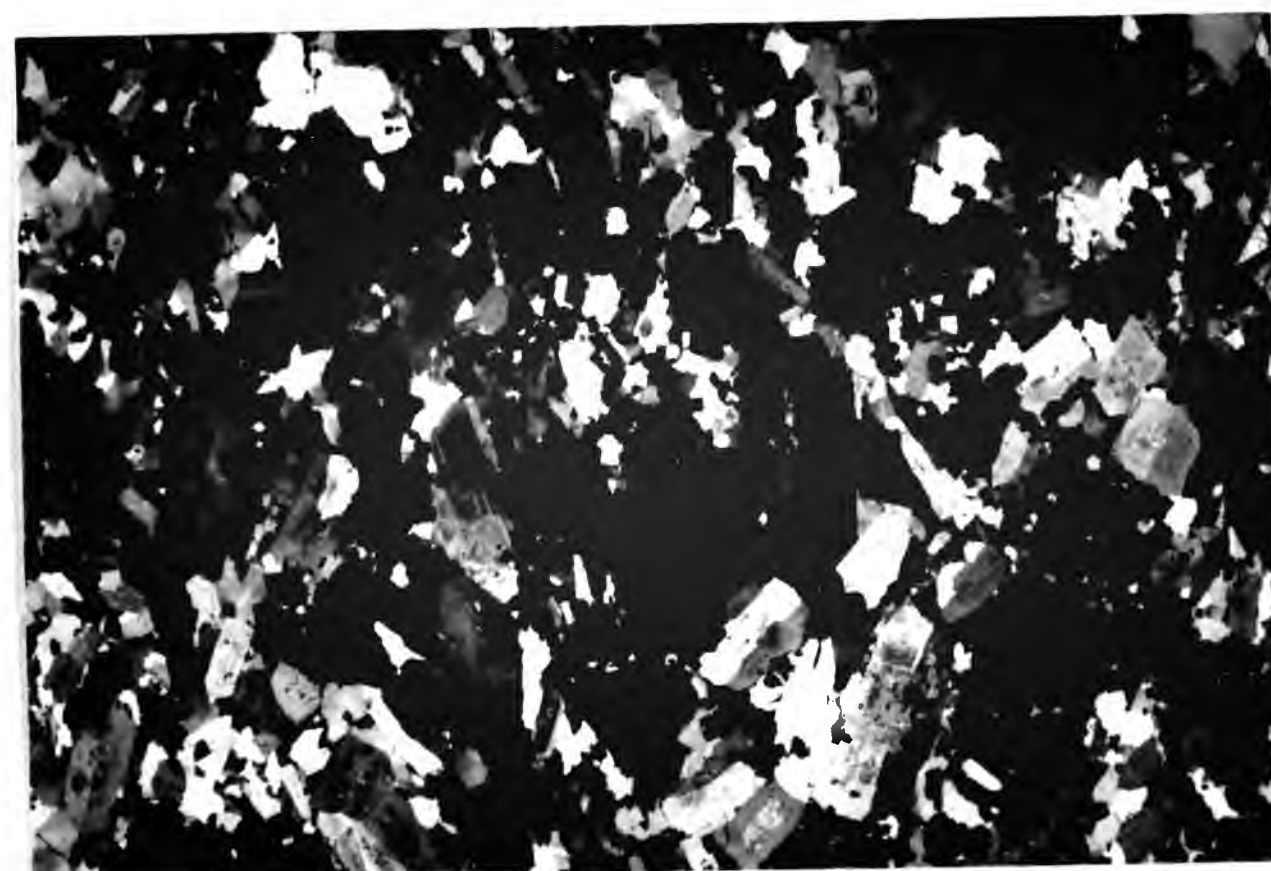


Plate 5.9

Plate 5. in plane polarised light. The biotite defines a good fabric, but the tendency of some biotites to form poorly defined aggregates, which are weakly shaped around the plagioclase laths (P), hints at minor plastic deformation. (x5).

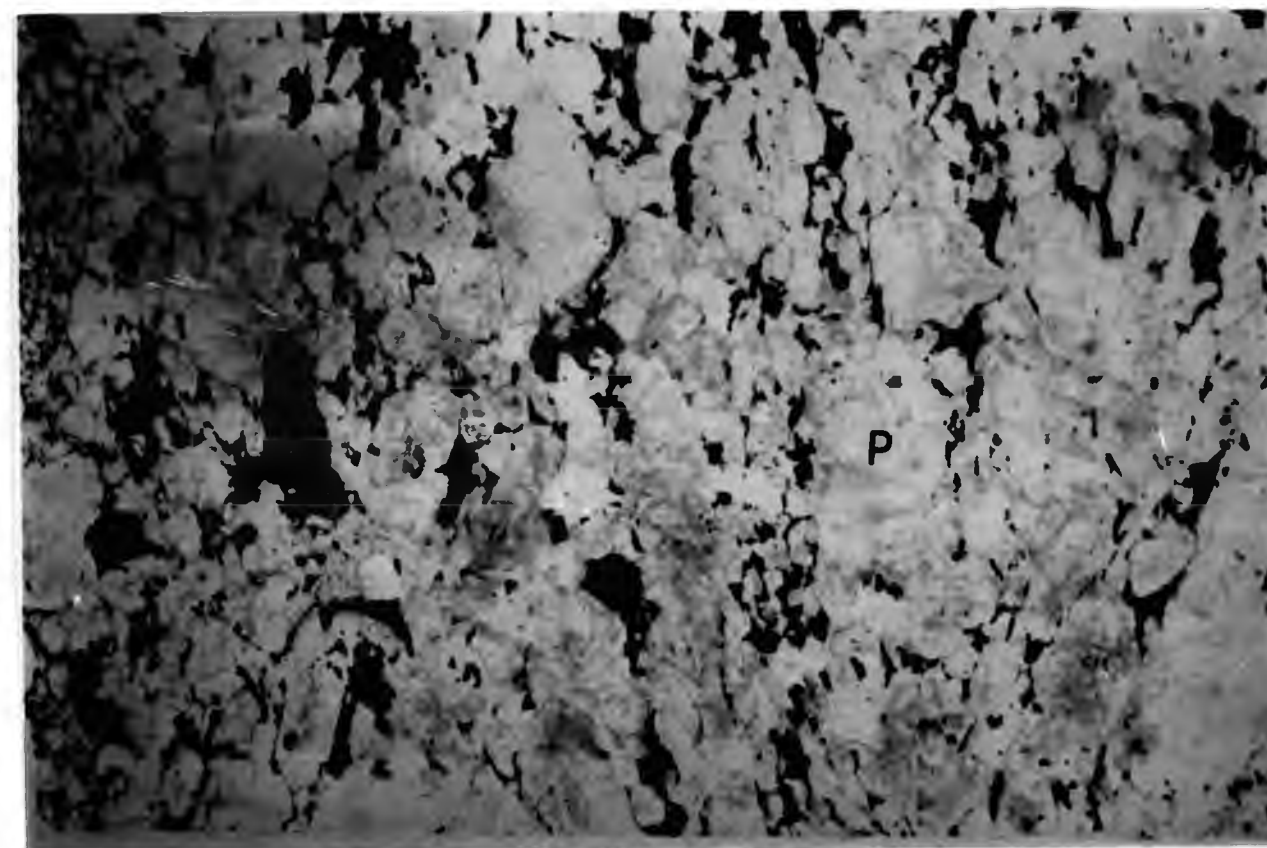


Plate 5.10

Dislocation of the lattice in a plagioclase lath, expressed as an irregular patch out of optical continuity with the remainder of the lath. Maol Chnoc Adamellite. (Crossed polars, x47).





**Plate 5.11**

Plate 5.2 in plane polarised light, displaying a strong, parallel, mineral fabric defined by biotite. The tips of the biotite ribbons are beginning to break down into finer biotite grains. Such features may be indicative of plastic strain, deforming biotites that were initially co-axially aligned. (x5).

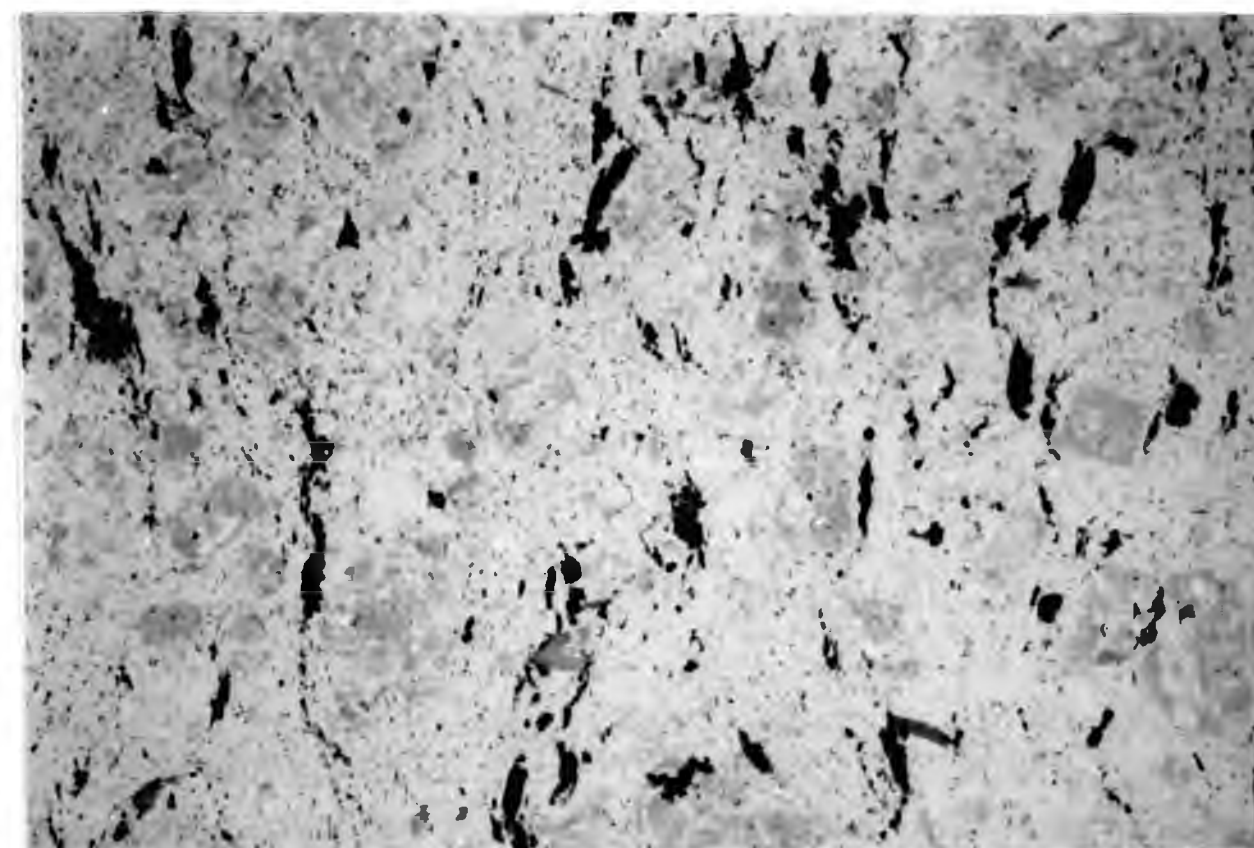


**Plate 5.12**

Parallel, biotite fabric in mylonitised Maol Chnoc Granodiorite. The biotite ribbons define weak augening, implying solid state fabric is not intense enough to create a truly parallel foliation. (Plane polarised light, x5).



**Plate 5.13**

Plate 5.12 viewed in cross polars. Grainsize reduction of the Maol Chnoc granodiorite is intense, although a few larger protoclasts are preserved towards the bottom of the photograph. (x5).

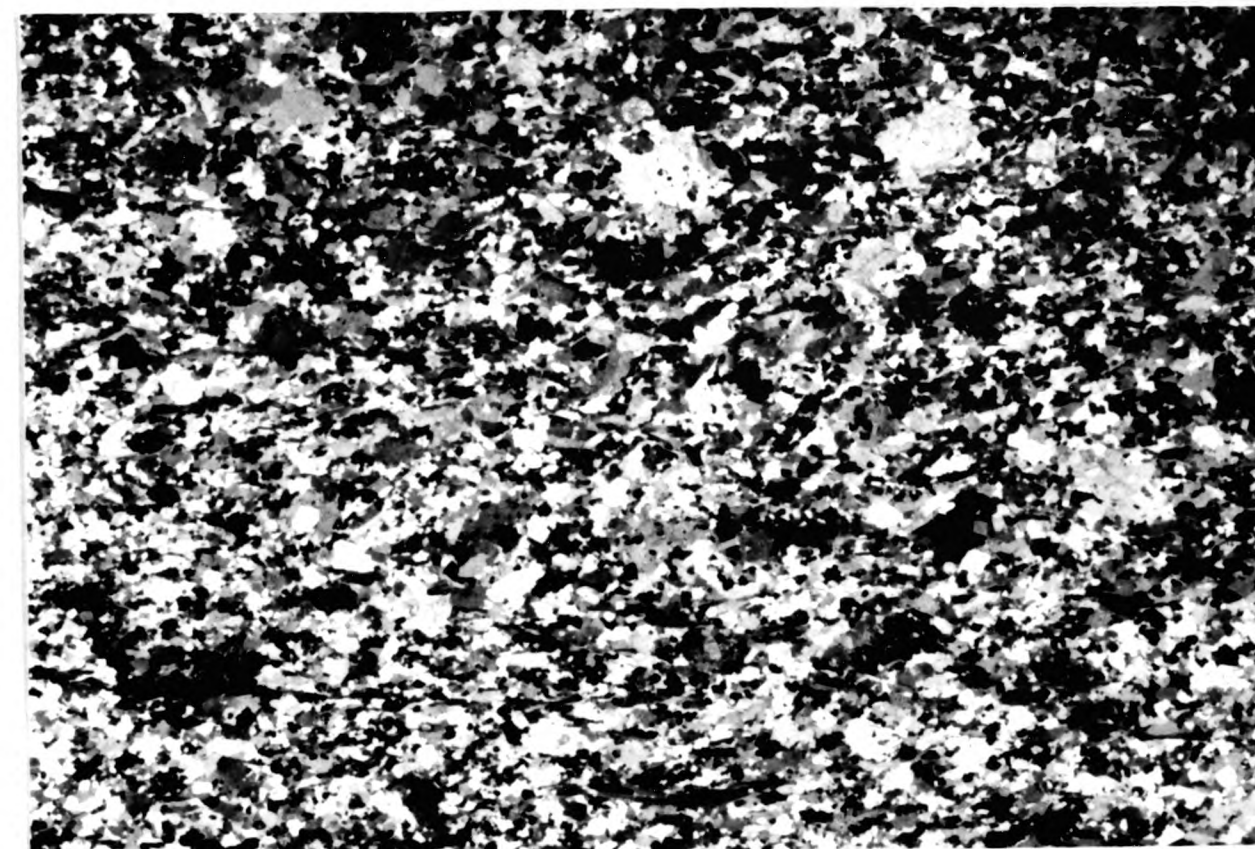


**Plate 5.14**

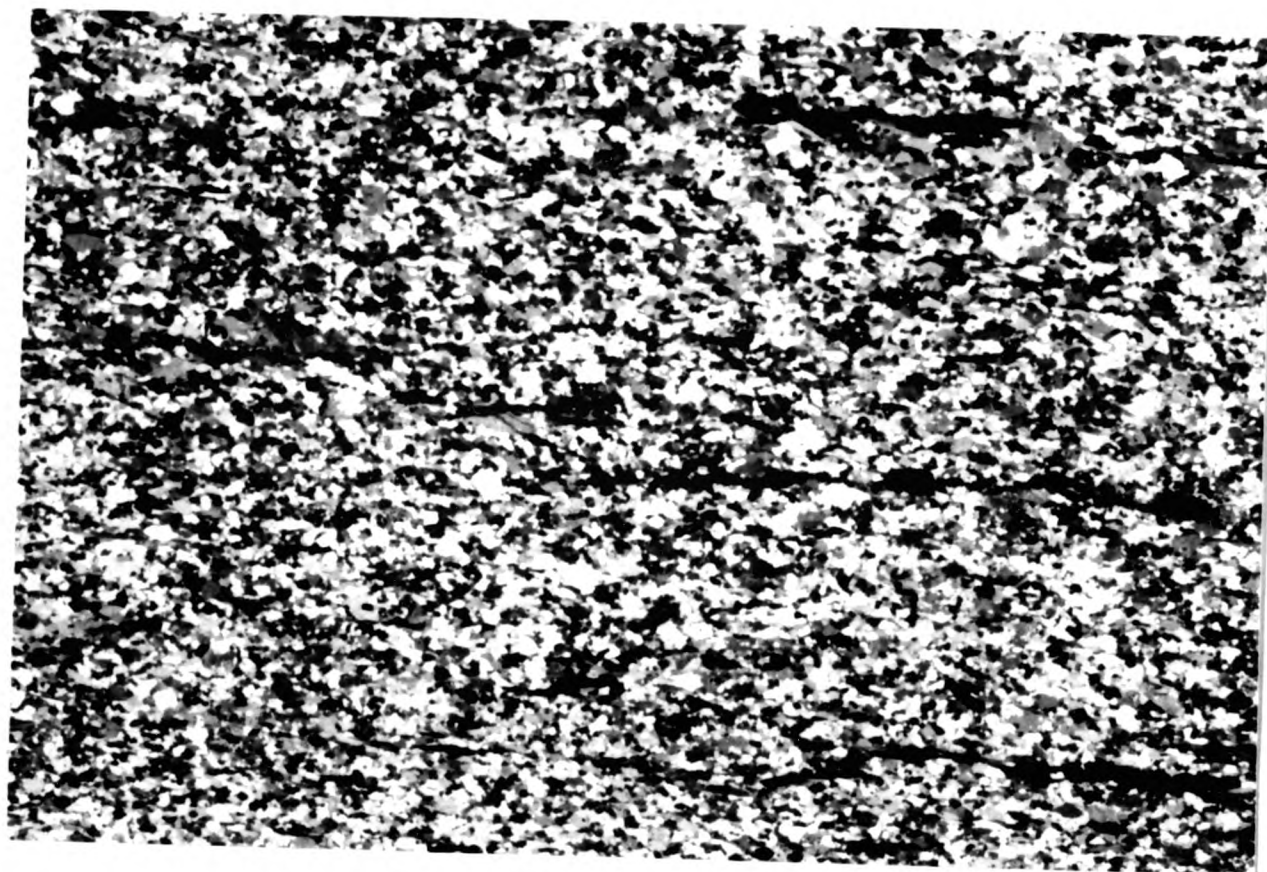
Very intense mylonitisation of Maol Chnoc Granodiorite produces a parallel biotite fabric, and felsic material lacking augens. (Plane polarised light, x5)





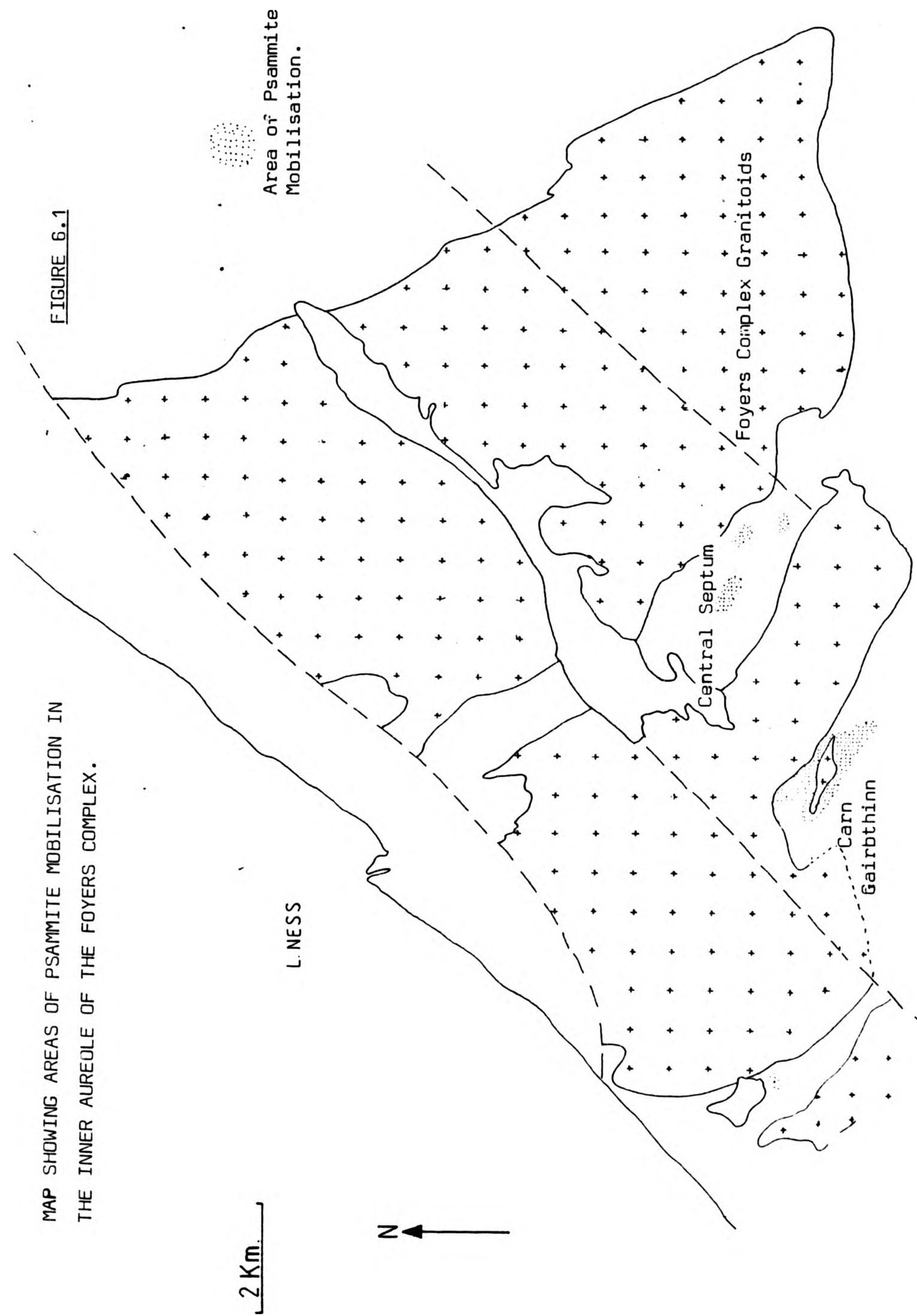
Plate 5.15

Photograph 5.15 showing intense grainsize reduction,  
with no protoclasts remaining. (Crossed polars, x5)



CHAPTER 6. INNER AUREOLE PSAMMITE MOBILISATION IN THE  
ENVELOPE OF THE FOYERS COMPLEX.

MAP SHOWING AREAS OF PSAMMITE MOBILISATION IN  
THE INNER AUREOLE OF THE FOYERS COMPLEX.



PLATES  
Chapter 6



**Plate 6.1**

Small patch of mobilised psammite, veined by Dalrag Granodiorite. One vein completely wraps one of the boudins. The calc-silicate boudins show large angular rotations. The external morphology of the mobilised area is controlled by the bedding in the adjacent psammites. (Central Psammite Septum).



**Plate 6.2**

Calc-silicate boudins, edged by psammite, enclosed within the mobilised psammite matrix, within an area of mobilised psammite. (Carn Gairbthinn).



Plate 6.3

Mobilised psammite exposed on a bedding parallel surface. The blocky pelitic boudins form traceable trains, whilst the rounded siliceous psammite boudins are exotic. (Central Psammite Septum).



Plate 6.4

Flow fabric in mobilised psammite matrix, defined by single biotite laths in a granoblastic quartz and plagioclase matrix. (Crossed polars, x47).

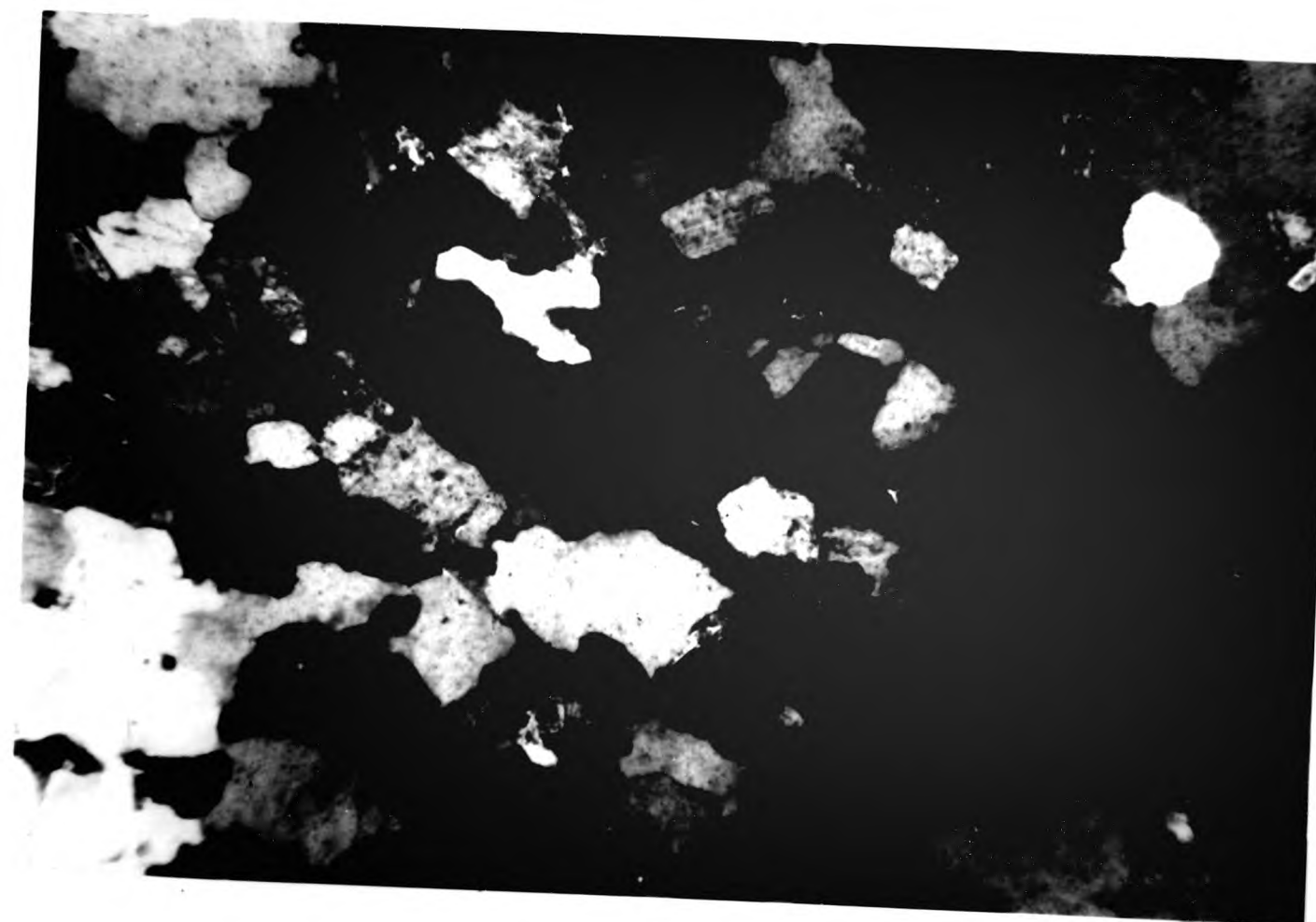




Plate 6.5

Boudinaged pelite bed within an area of mobilised psammite. The biotite schlieren within the mobilised psammite impart a streaky texture on the psammitic matrix. Note the rather diffuse veins of Dalcrag Granodiorite cutting the matrix. (Carn Gairbthinn).



Plate 6.6

Calc-silicate boudins, rotated into a attitude perpendicular to the main fabric in the adjacent psammite. The boudins are enclosed within rather streaky mobilised psammitic material.

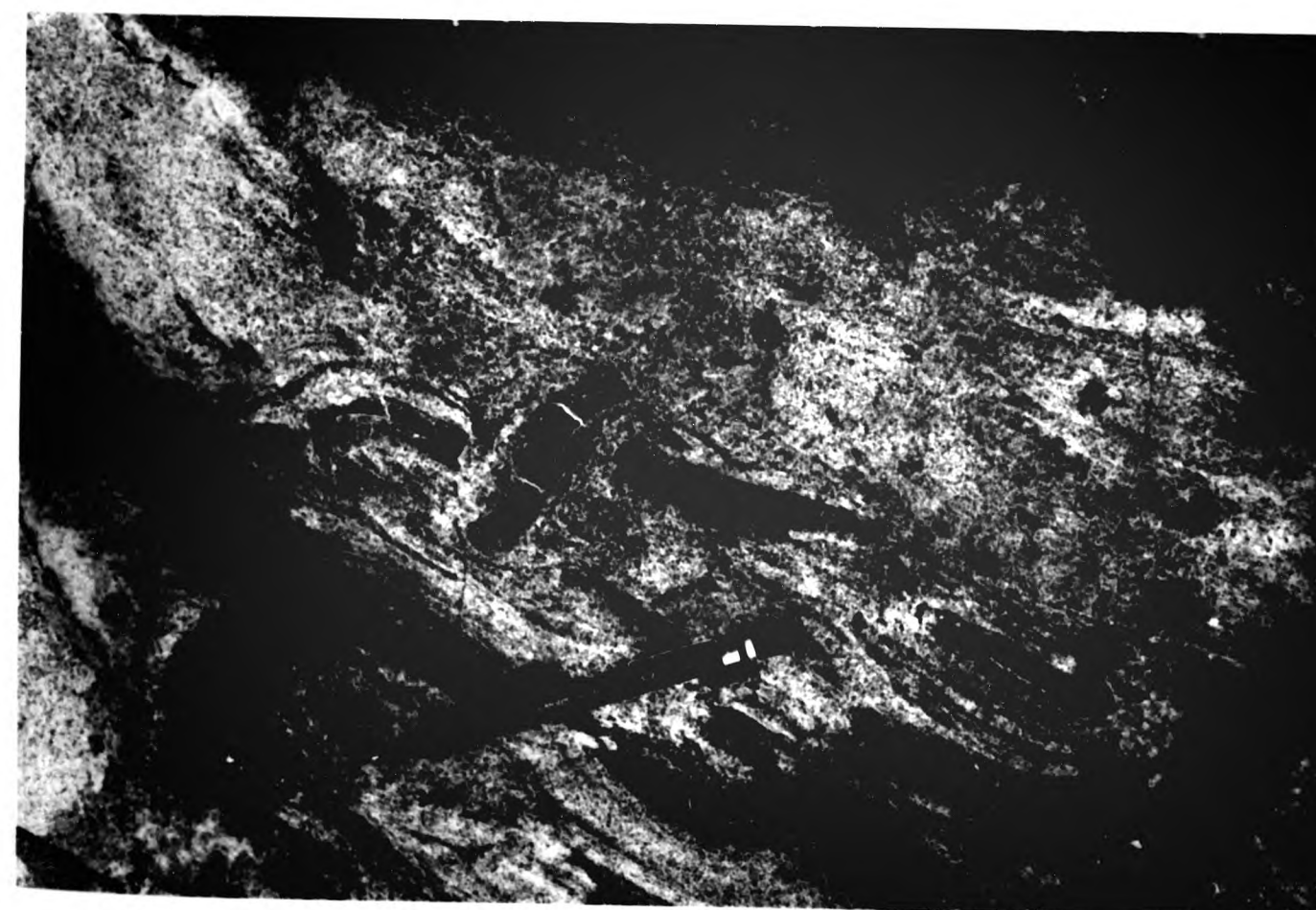




Plate 6.7

Mobilised psammite containing a large psammite clast, which is injected by diatexite material from the enclosing matrix. (Central Psammite Septum).

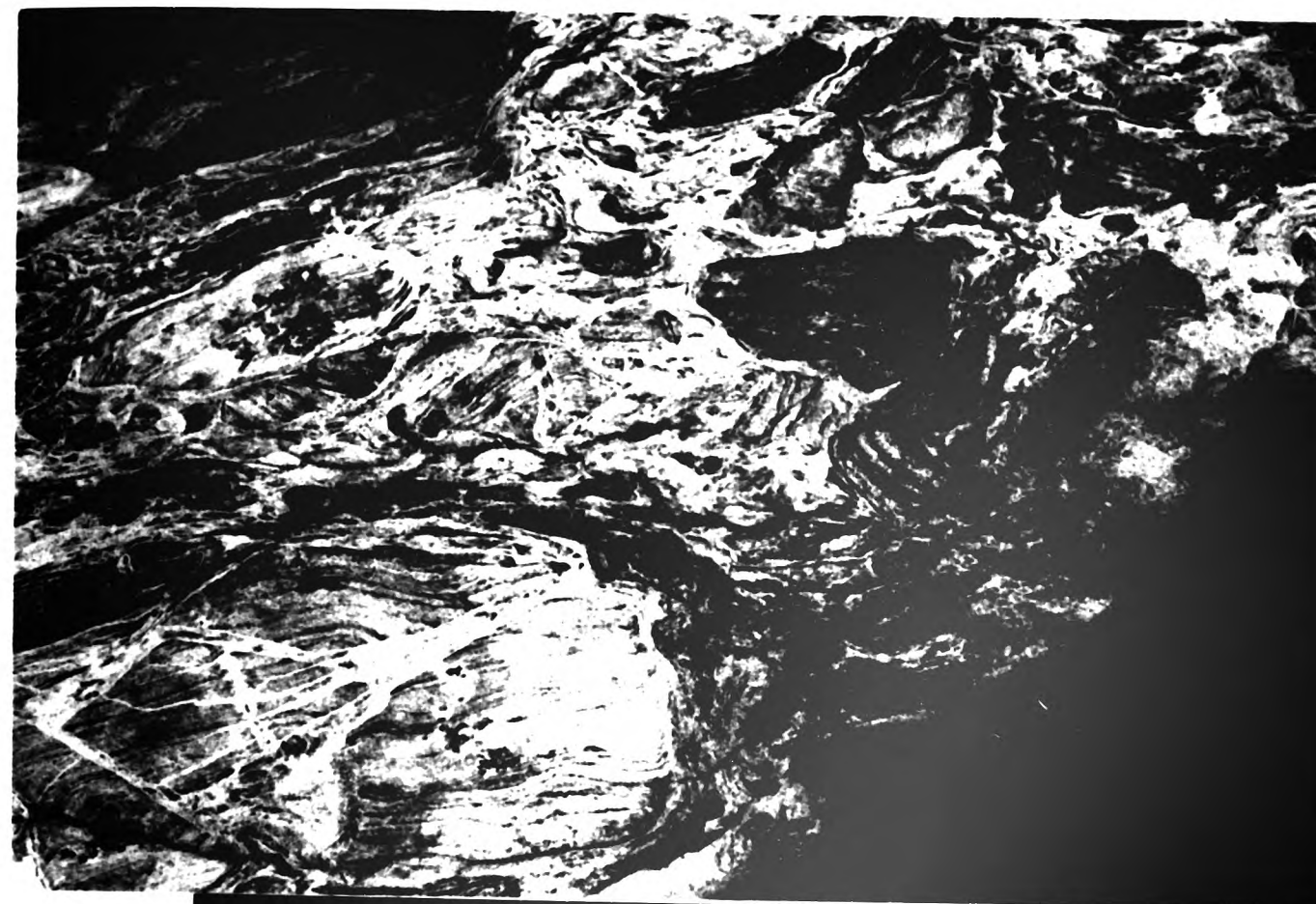


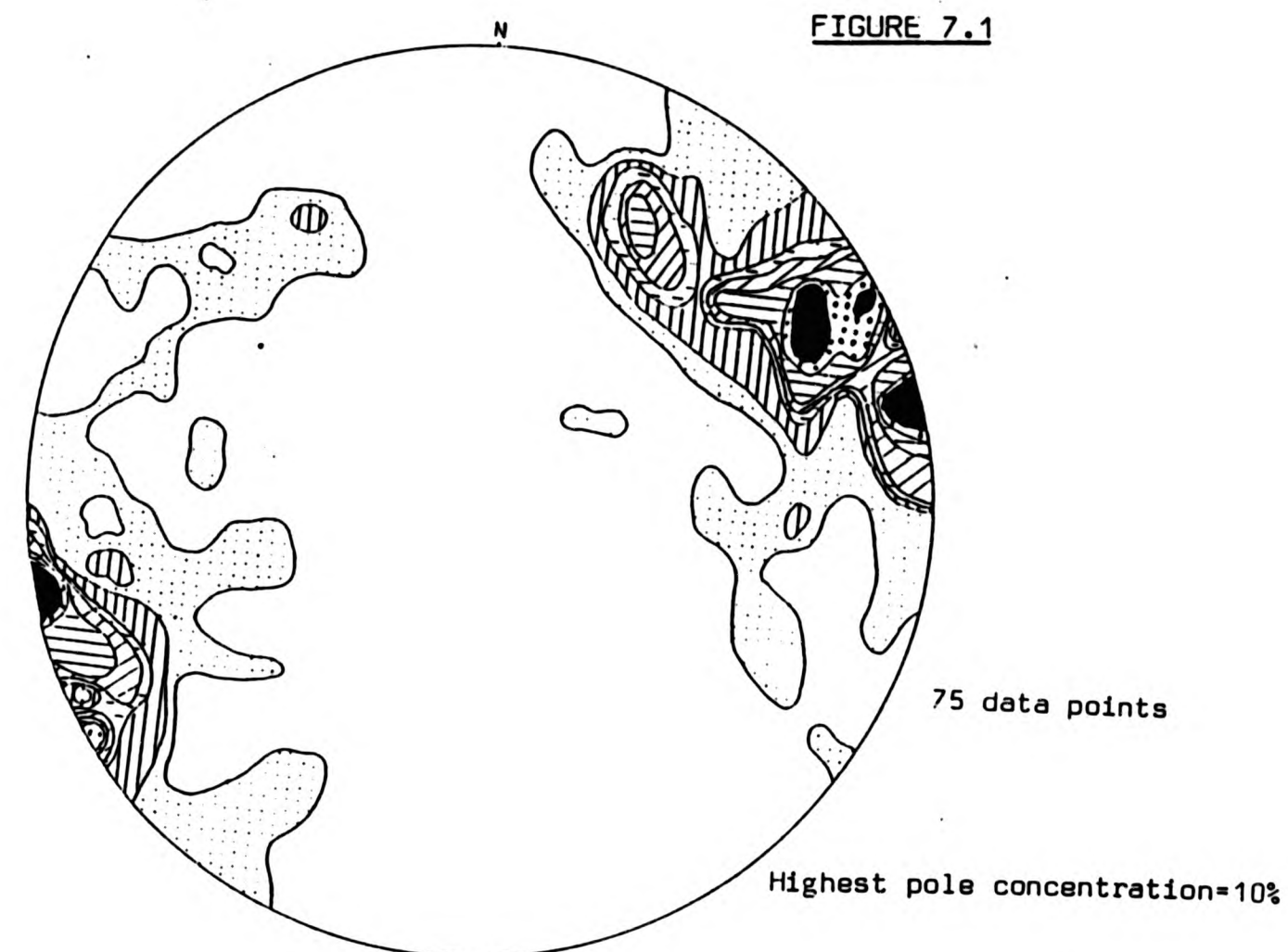
Plate 6.8

Boudinaged micaceous psammite, cut by a network of quartz and plagioclase diatexite veins. (Central Psammite Septum).



CHAPTER 7. RELATIONSHIP BETWEEN THE FOYERS COMPLEX AND THE  
REGIONAL STRUCTURES.

FIGURE 7.1



CONTOURED POLES TO BEDDING PLOTTED IN AN EQUAL AREA PROJECTION.  
NORTHERN MARGIN OF THE FOYERS GRANITIC COMPLEX

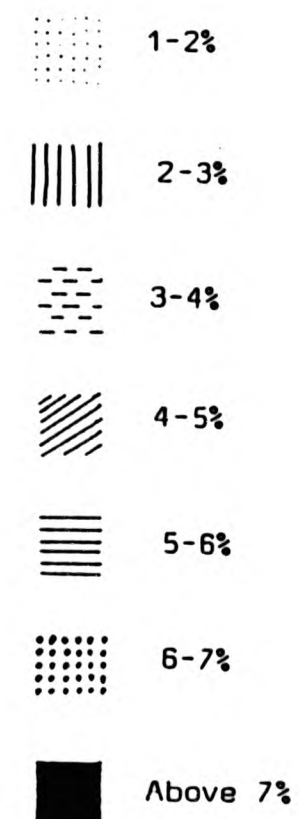
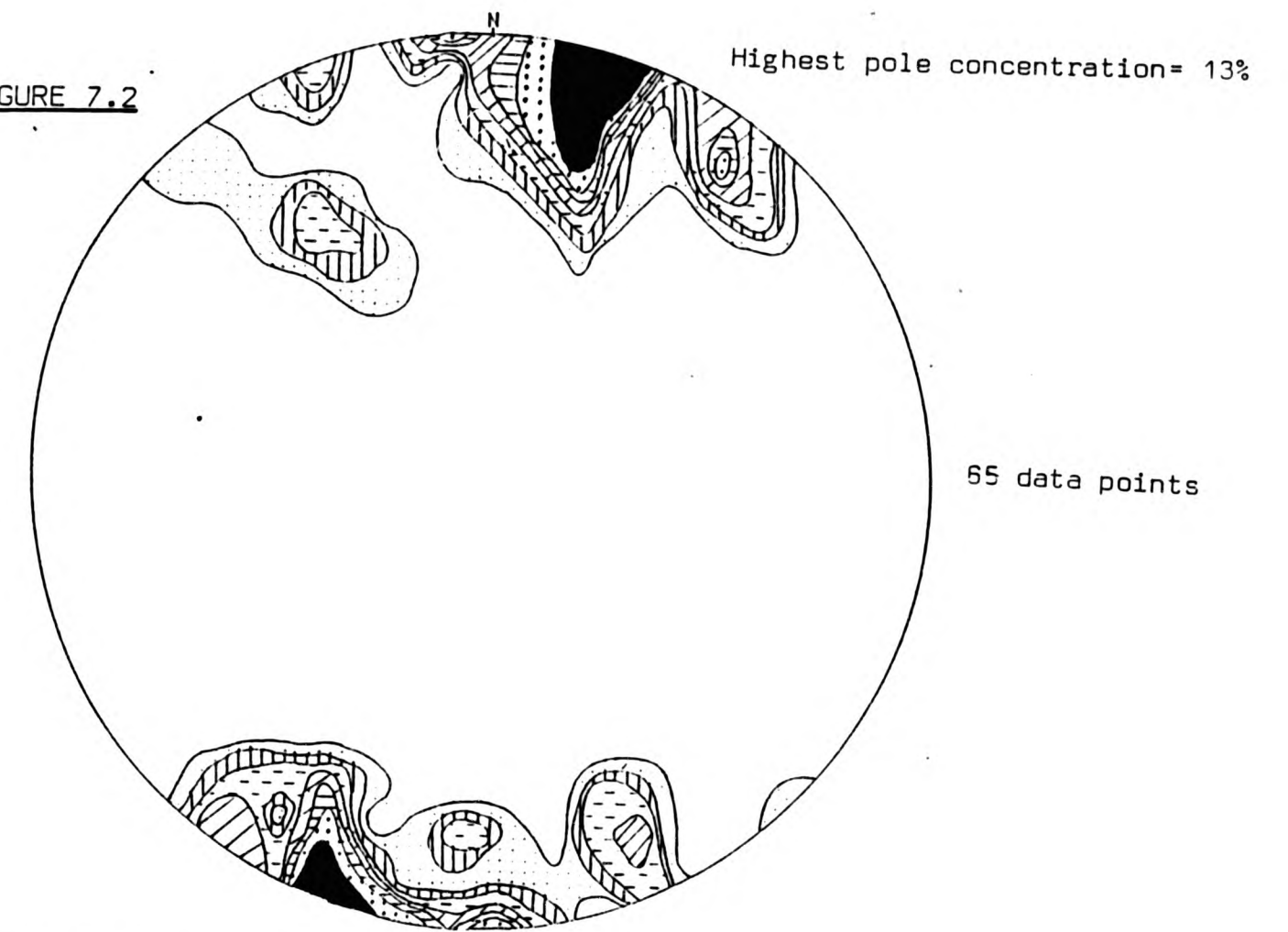


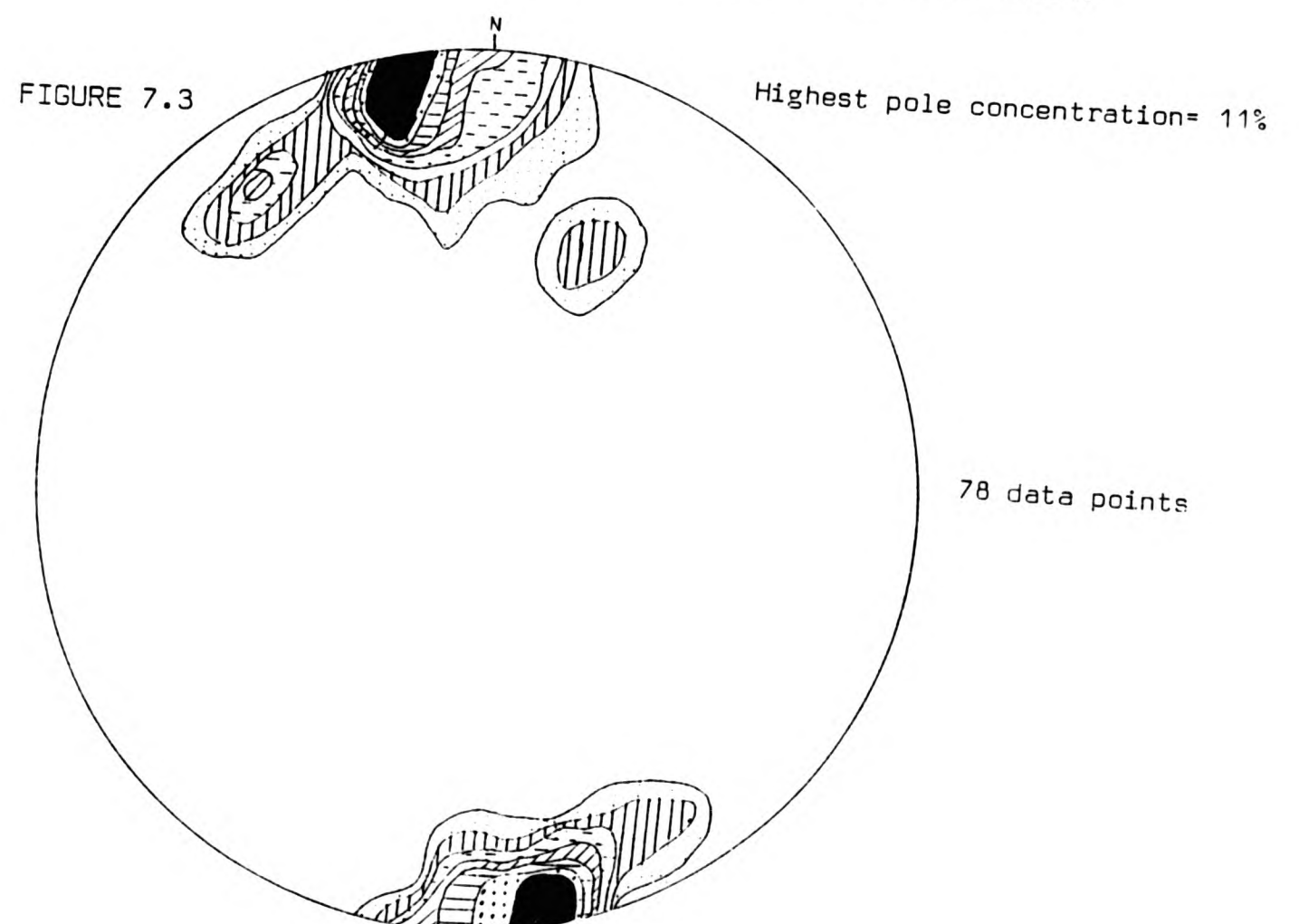
FIGURE 7.2



CONTOURED POLES TO BEDDING PLOTTED IN AN EQUAL AREA PROJECTION.  
CENTRAL PSAMMITE SEPTUM

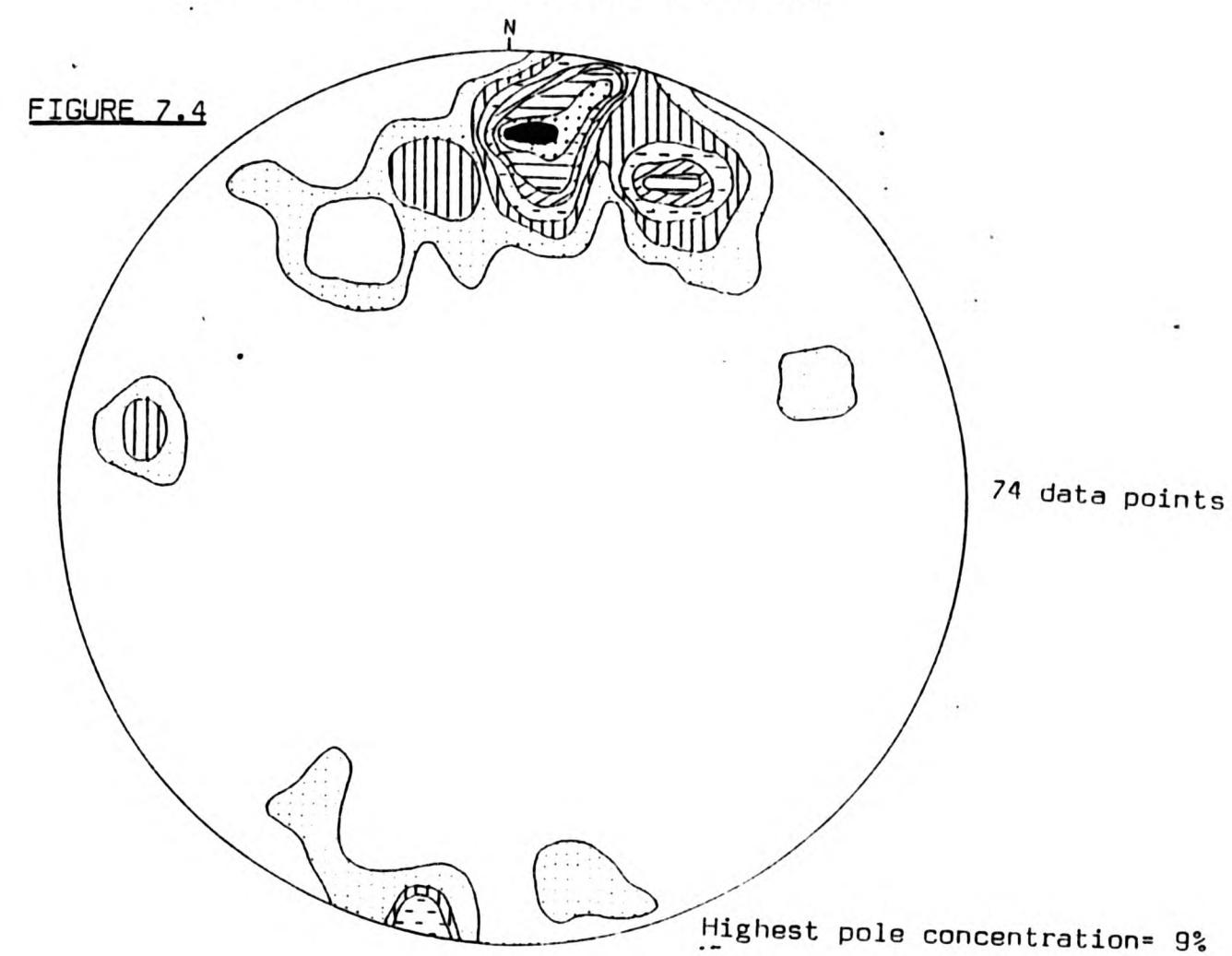
CONTOURED POLES TO BEDDING PLOTTED IN AN EQUAL AREA PROJECTION.  
EASTERN SLOPES OF CAIRN GAIRBTHINN TO BEINN BHURAICH (SOUTHERN MARGIN)

FIGURE 7.3

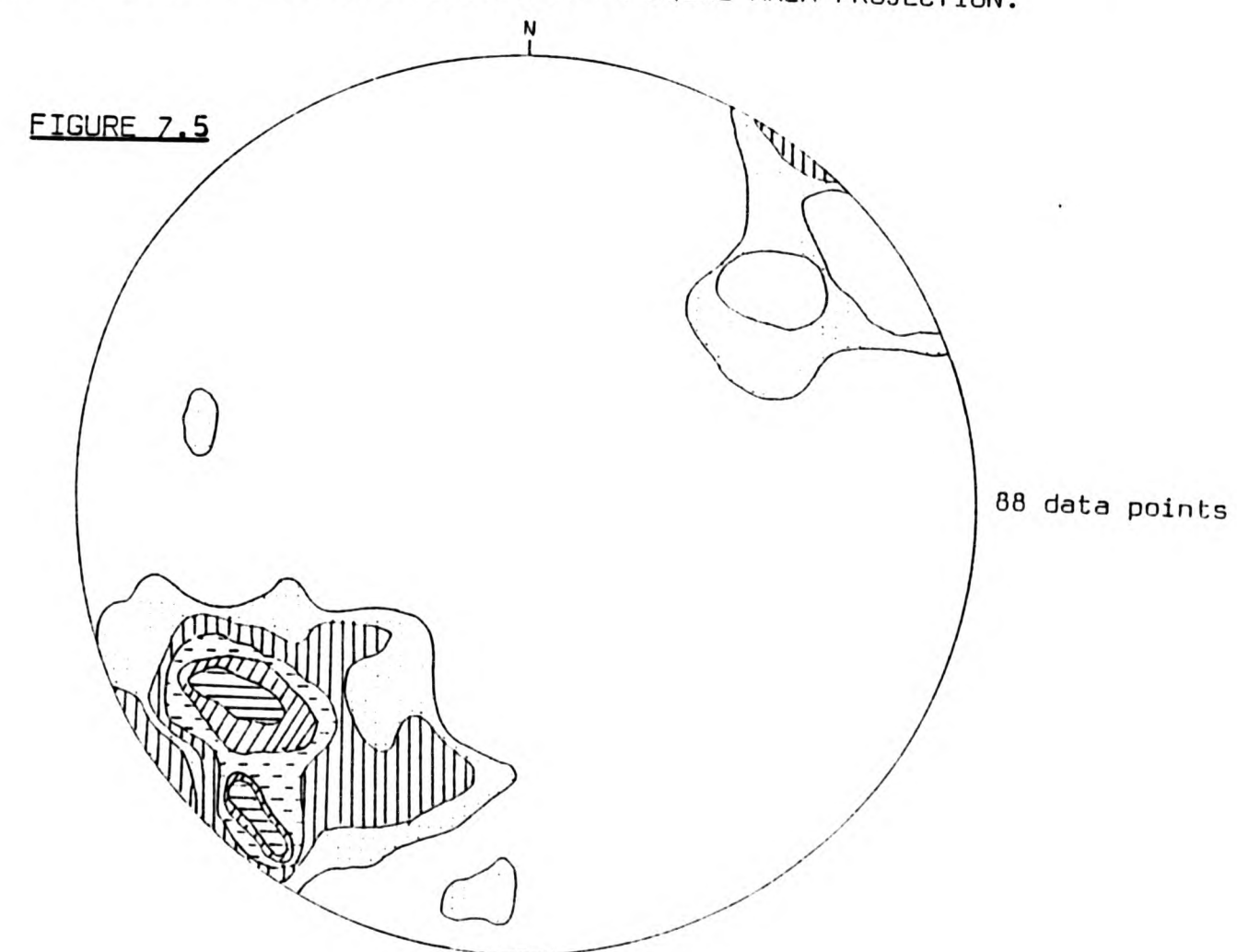




CONTOURED POLES TO BEDDING PLOTTED IN AN EQUAL AREA PROJECTION.  
BEINN SGURRACH RIDGE (SOUTHERN MARGIN)



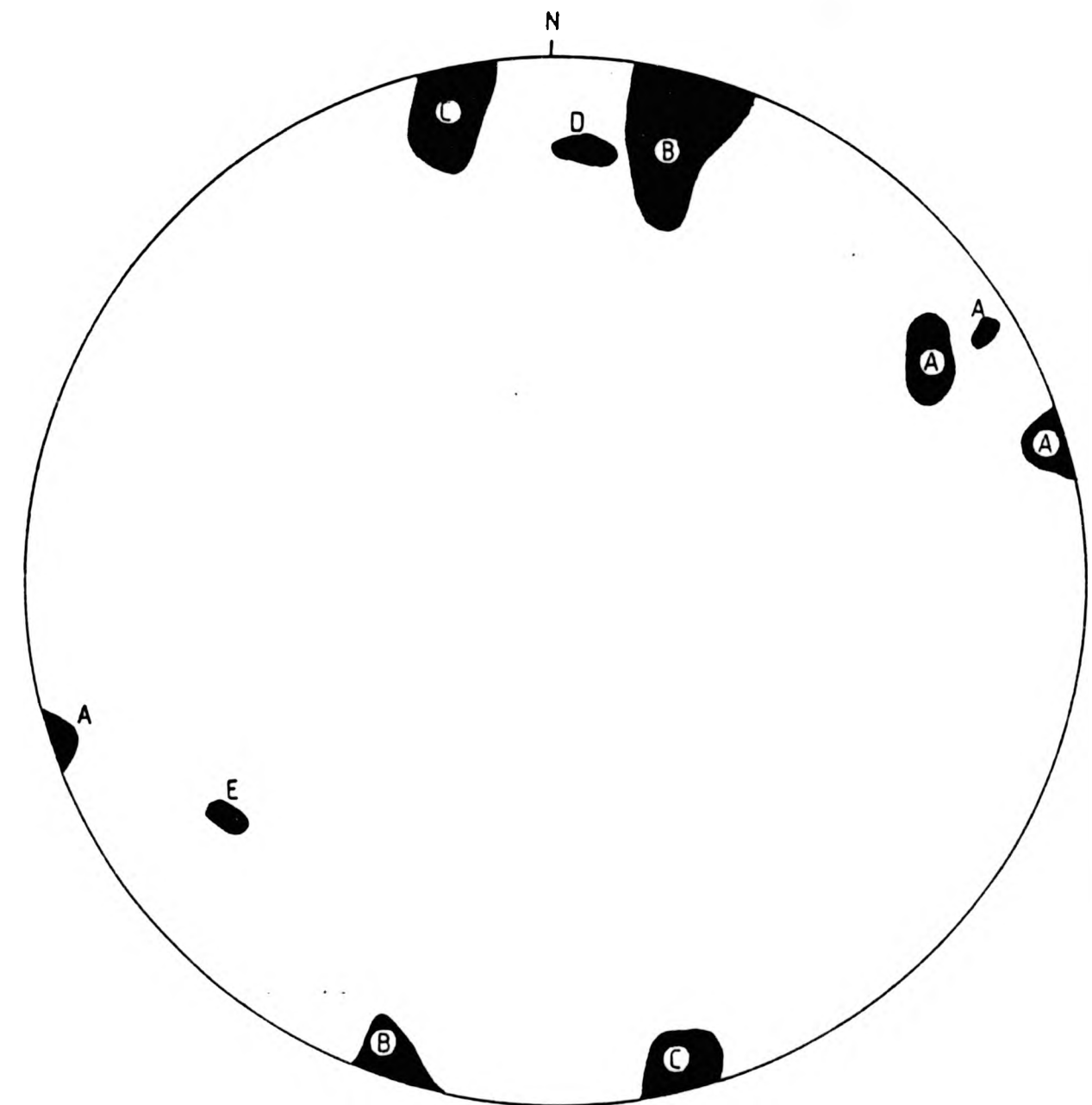
SOUTH WEST OF LOCH KEMP TO THE LOCH MHOR FAULT ZONE (SOUTHERN MARGIN)  
CONTOURED POLES TO BEDDING PLOTTED IN AN EQUAL AREA PROJECTION.



**FIGURE 7.6**

STEREOGRAPHIC PROJECTION SHOWING THE HIGHEST CONCENTRATIONS OF POLES TO BEDDING FROM VARIOUS AREAS OF ENVELOPE AROUND THE FOYERS GRANITIC COMPLEX.

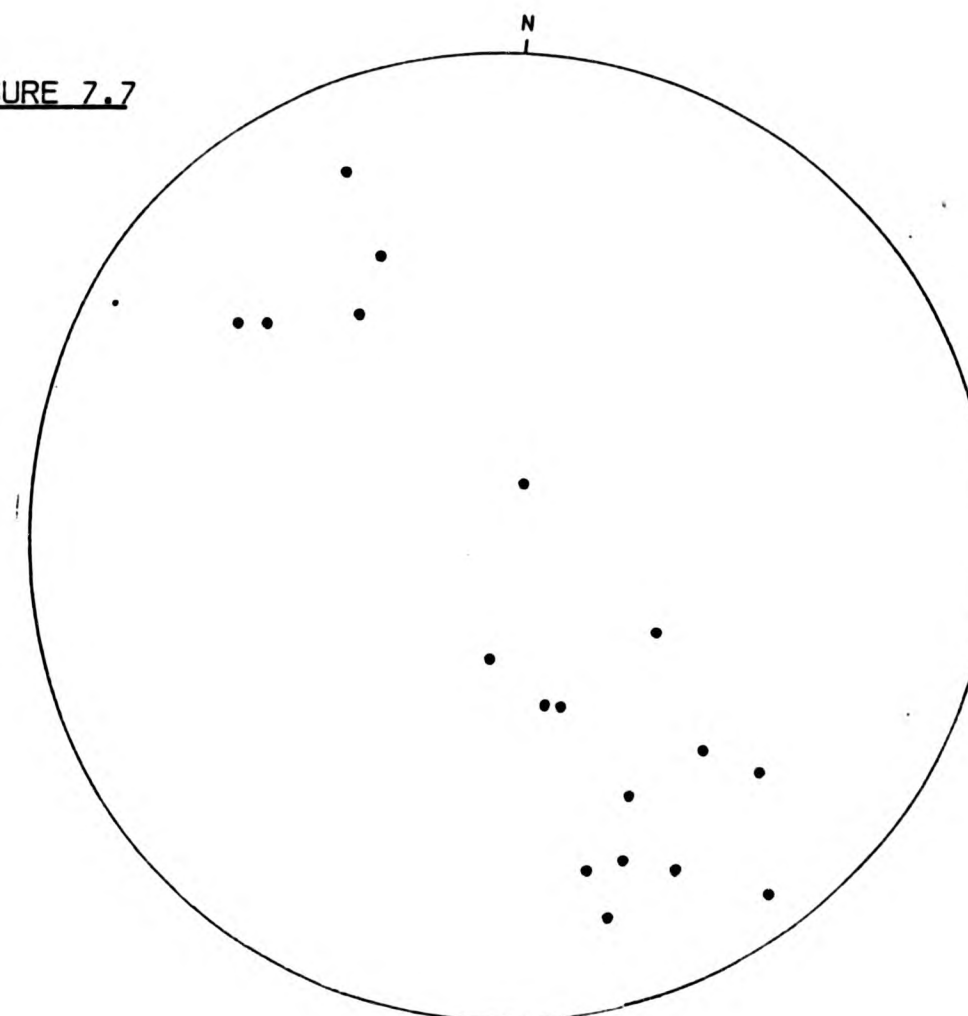
- A- NORTHERN MARGIN OF THE FOYERS COMPLEX
- B- CENTRAL PSAMMITE SEPTUM
- C- CAIRN GAIRBTHINN TO BEINN BHURAICH
- D- BEINN SGURRACH RIDGE
- E- SOUTH WEST OF LOCH KEMP TO THE LOCH MHOR FAULT ZONE





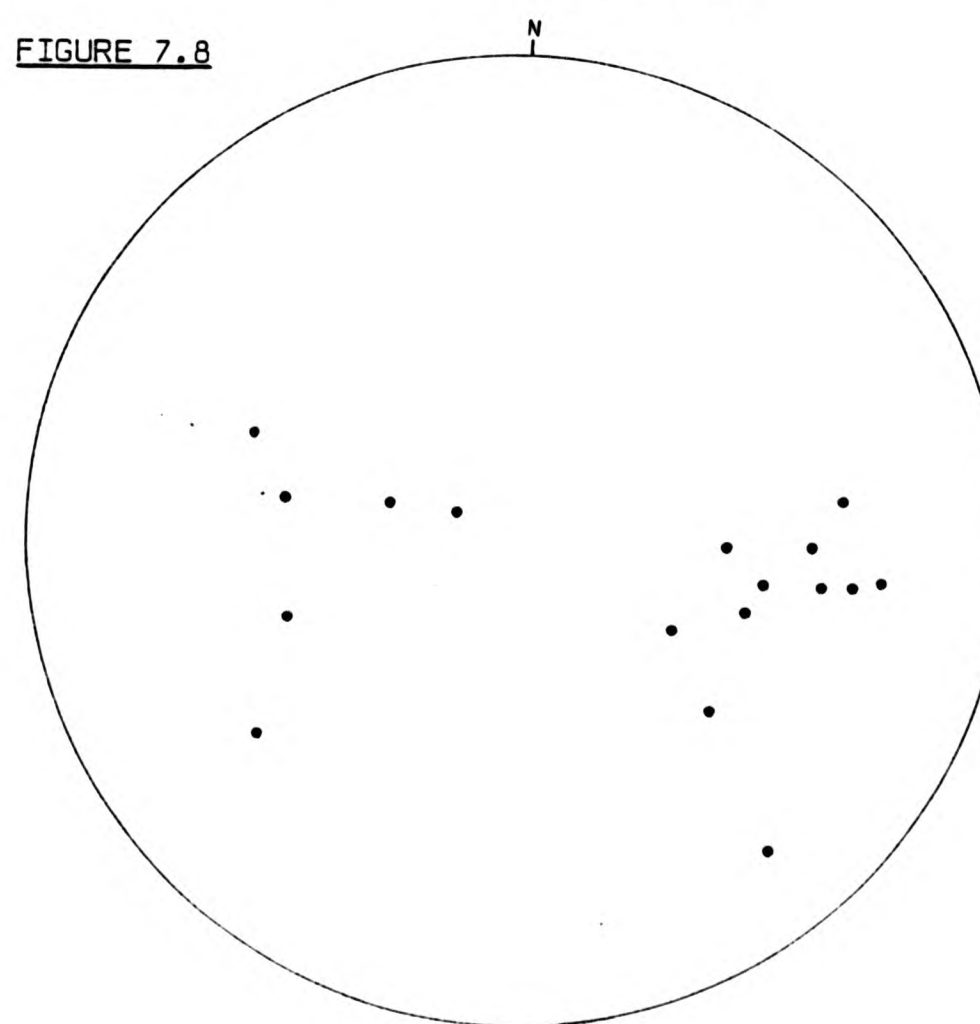
PLUNGE OF ASYMMETRICAL MINOR FOLDS (F2) AXES, PLOTTED ON AN EQUAL AREA PROJECTION  
NORTHERN MARGIN OF THE FOYERS GRANITIC COMPLEX

FIGURE 7.7



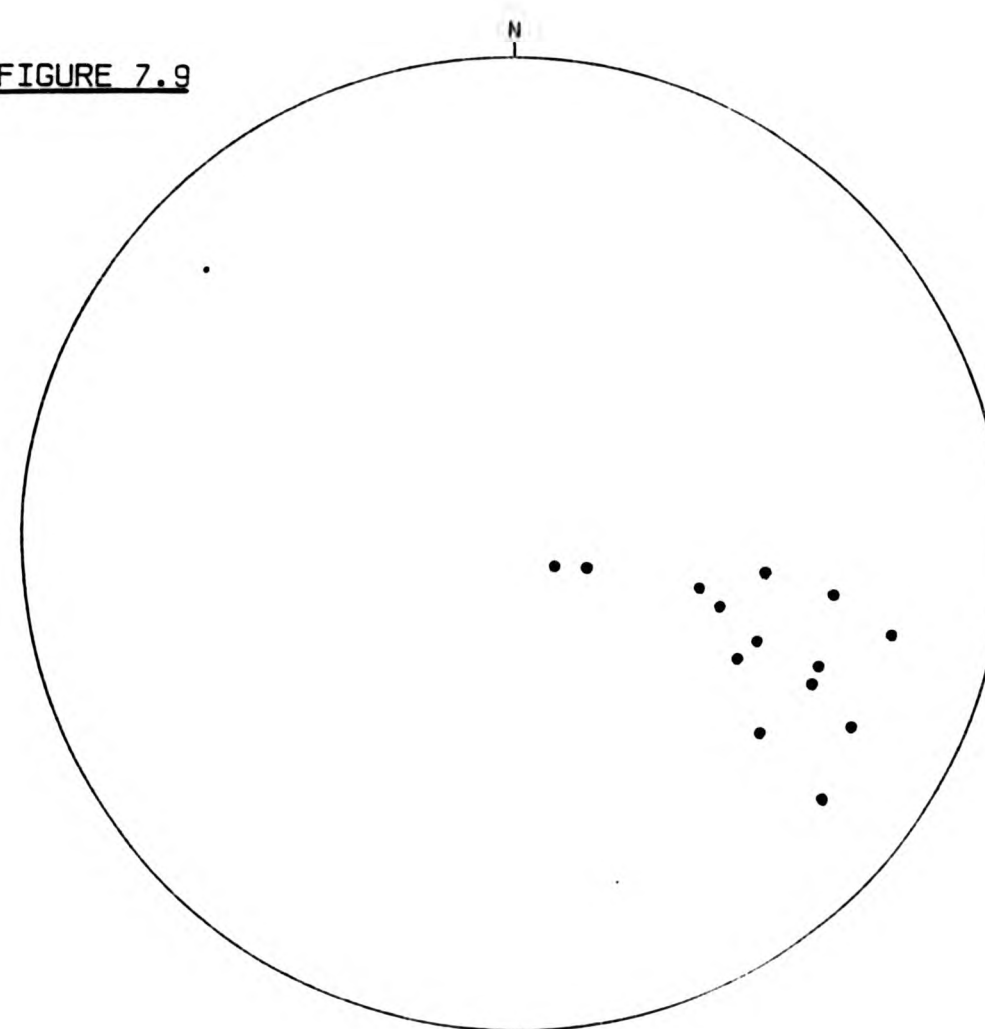
CENTRAL PSAMMITE SEPTUM

FIGURE 7.8



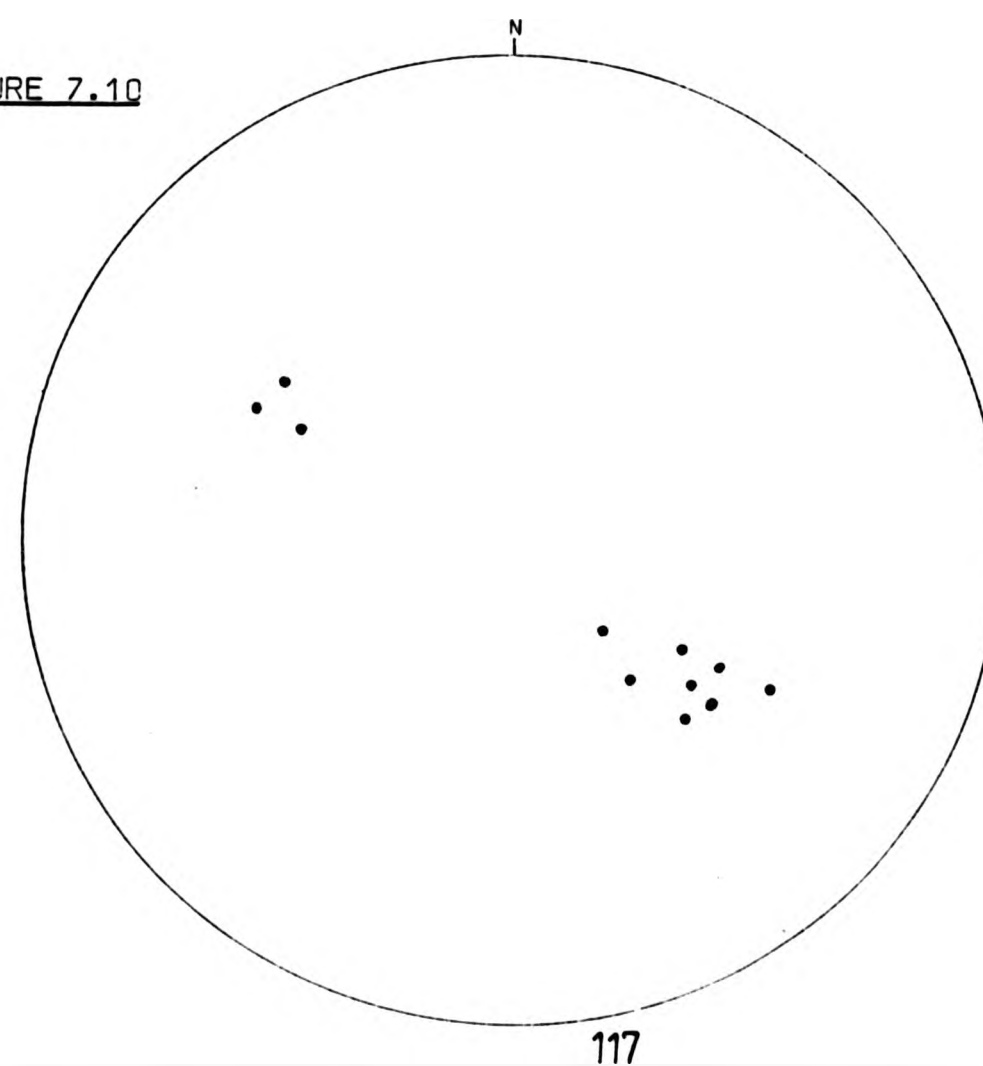
PLUNGE OF ASYMMETRICAL MINOR FOLDS (F2) AXES, PLOTTED ON AN EQUAL AREA PROJECTION  
BEINN SGURRACH TO BEINN BHURAICH

FIGURE 7.9



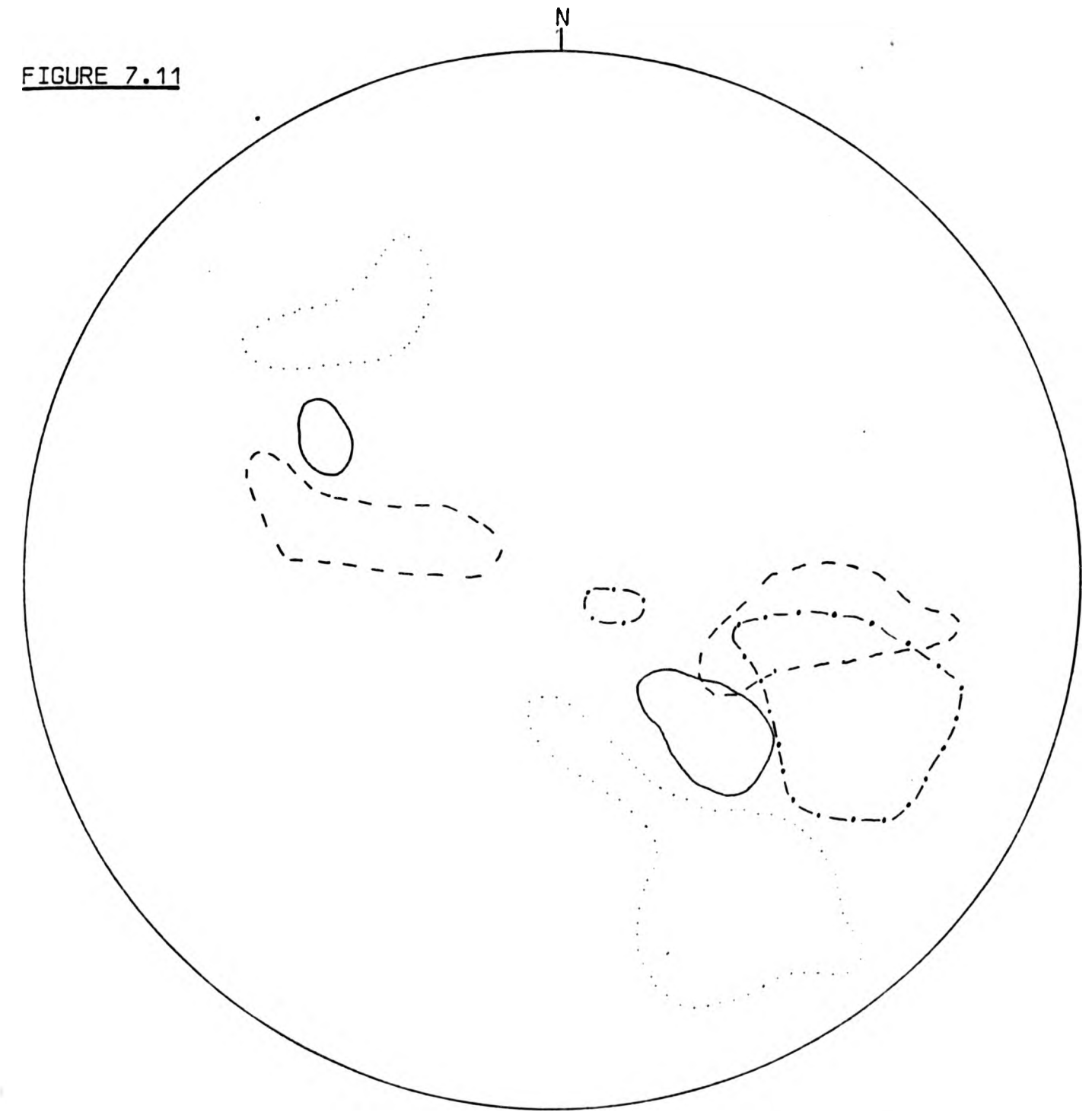
SOUTH WEST OF LOCH KEMP TO THE LOCH MHOR FAULT ZONE (SOUTHERN MARGIN)

FIGURE 7.10



FIELDS SHOWING PLUNGES OF F2 ASYMMETRICAL MINOR FOLDS FROM VARIOUS ENVELOPE AREAS  
AROUND THE FOYERS GRANITIC COMPLEX

FIGURE 7.11

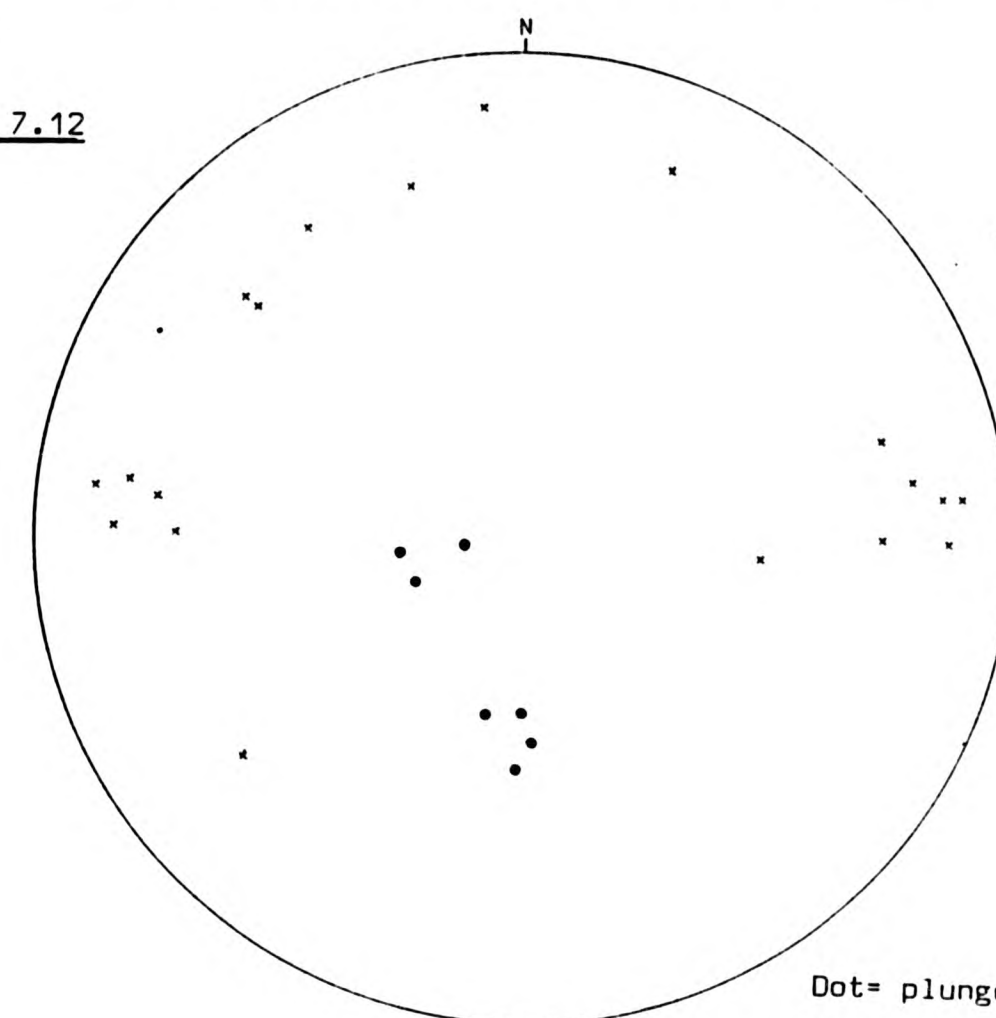


Dotted line- northern margin of the Foyers complex  
Dashed line- Central Psammite Septum  
Dashed and dotted line- Beinn Sgurrach to Beinn Bhuraich  
Solid line- south west of Loch Kemp.

PLUNGE OF FOLD AXES AND POLES TO THE FOLD AXIAL PLANES SHOWN BY CRENULATIONS (F3),  
PLOTTED IN AN EQUAL AREA PROJECTION

NORTHERN MARGIN OF THE FOYERS GRANITIC COMPLEX

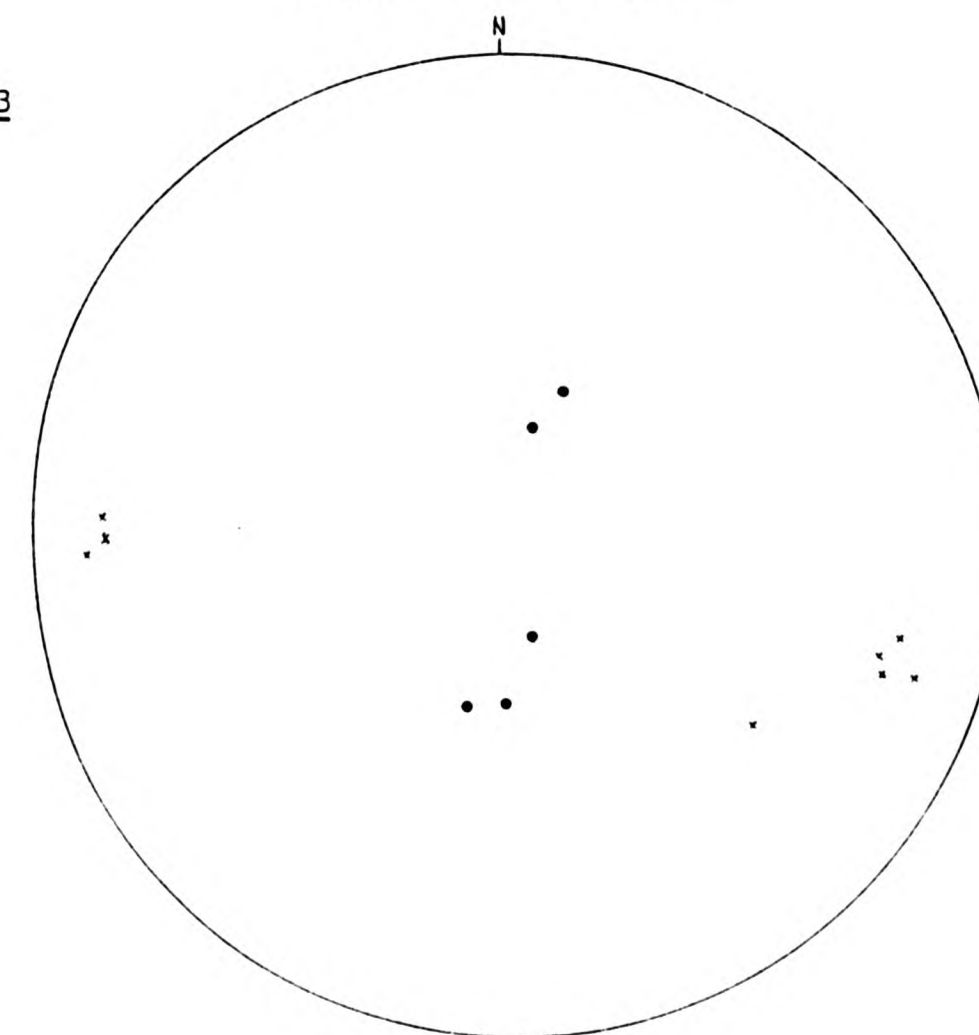
FIGURE 7.12



Dot= plunge  
Cross= pole to fold axial  
plane

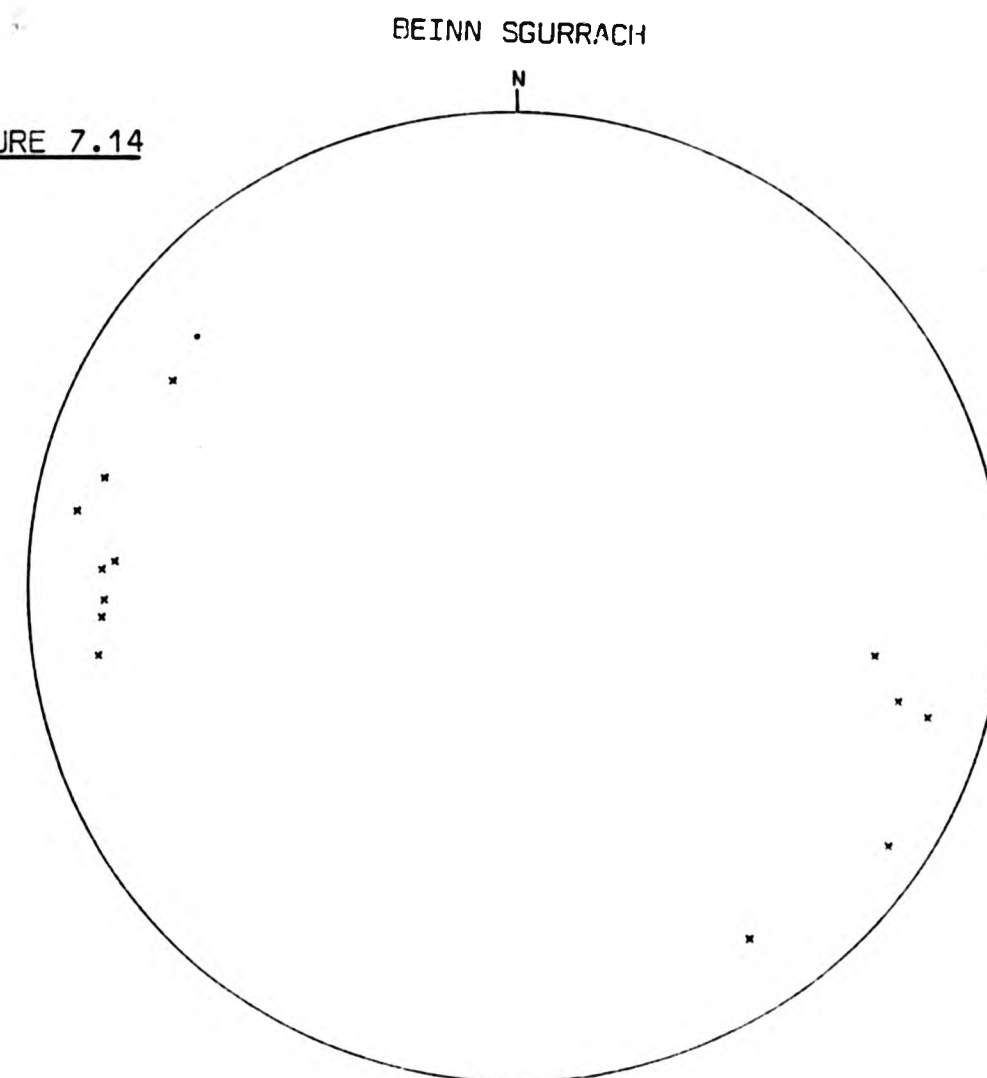
CENTRAL PSAMMITE SEPTUM

FIGURE 7.13



PLUNGE OF FOLD AXES AND POLES TO THE FOLD AXIAL PLANES SHOWN BY CRENULATIONS (F3),  
PLOTTED IN AN EQUAL AREA PROJECTION

FIGURE 7.14



SOUTH WEST OF LOCH KEMP TO THE LOCH MHOR FAULT ZONE (SOUTHERN MARGIN)

FIGURE 7.15

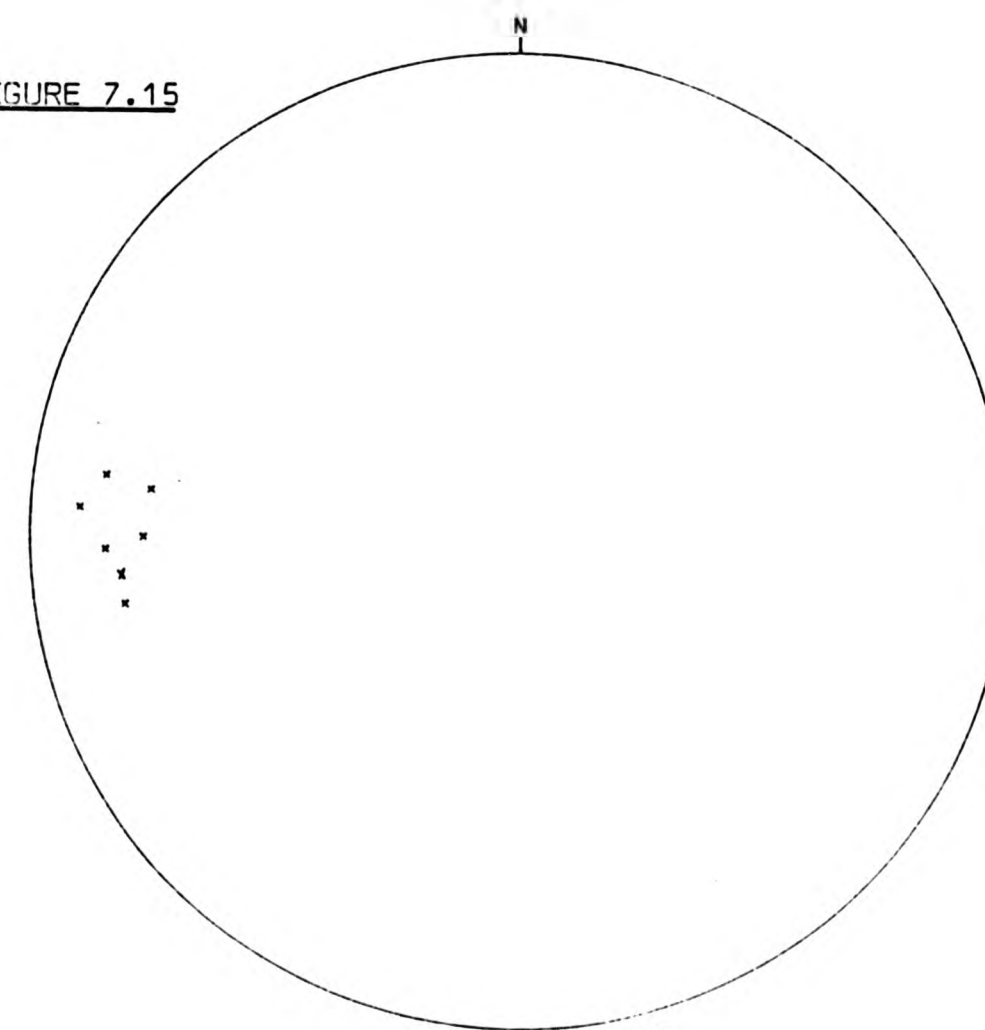
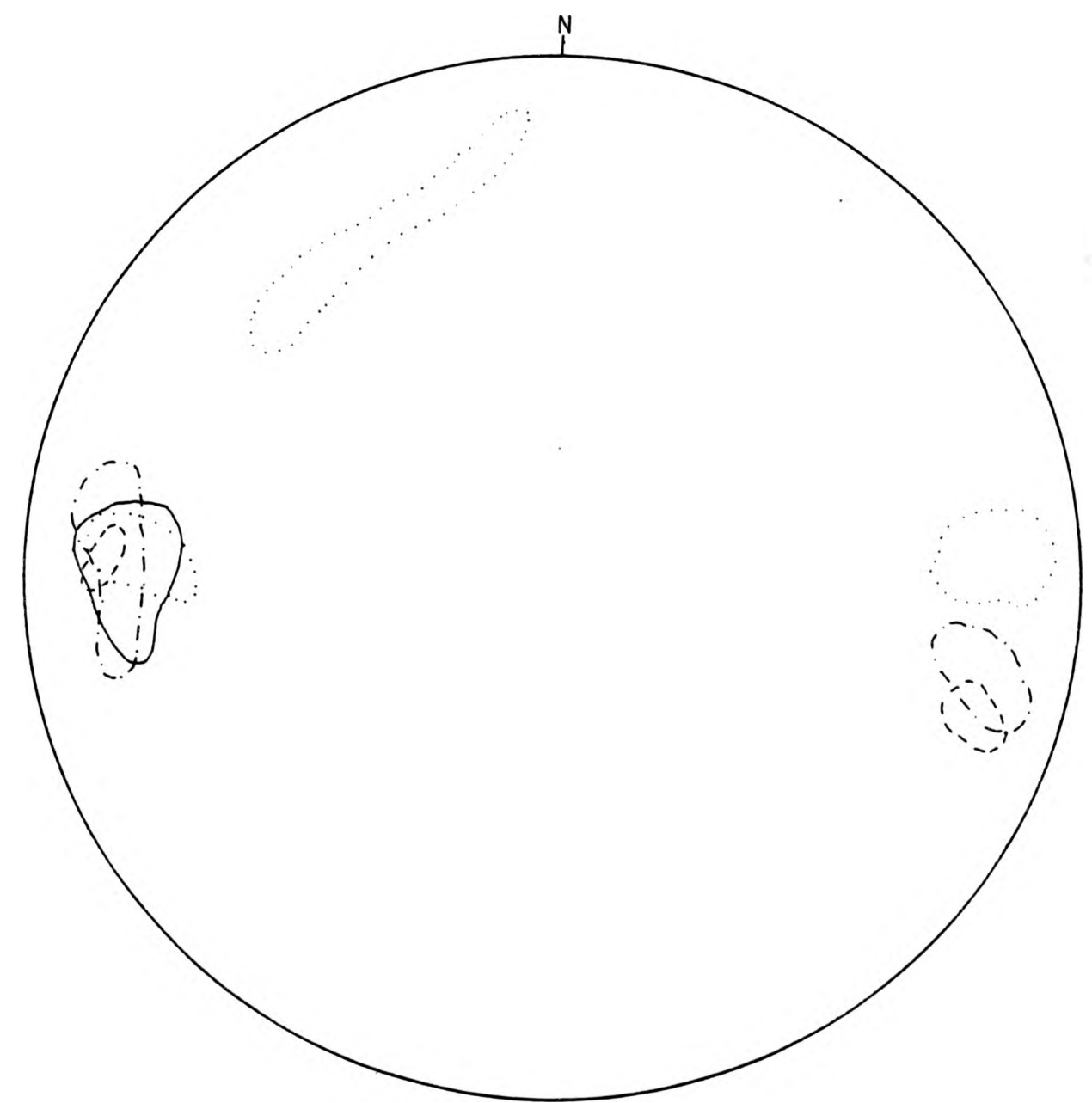


FIGURE 7.16

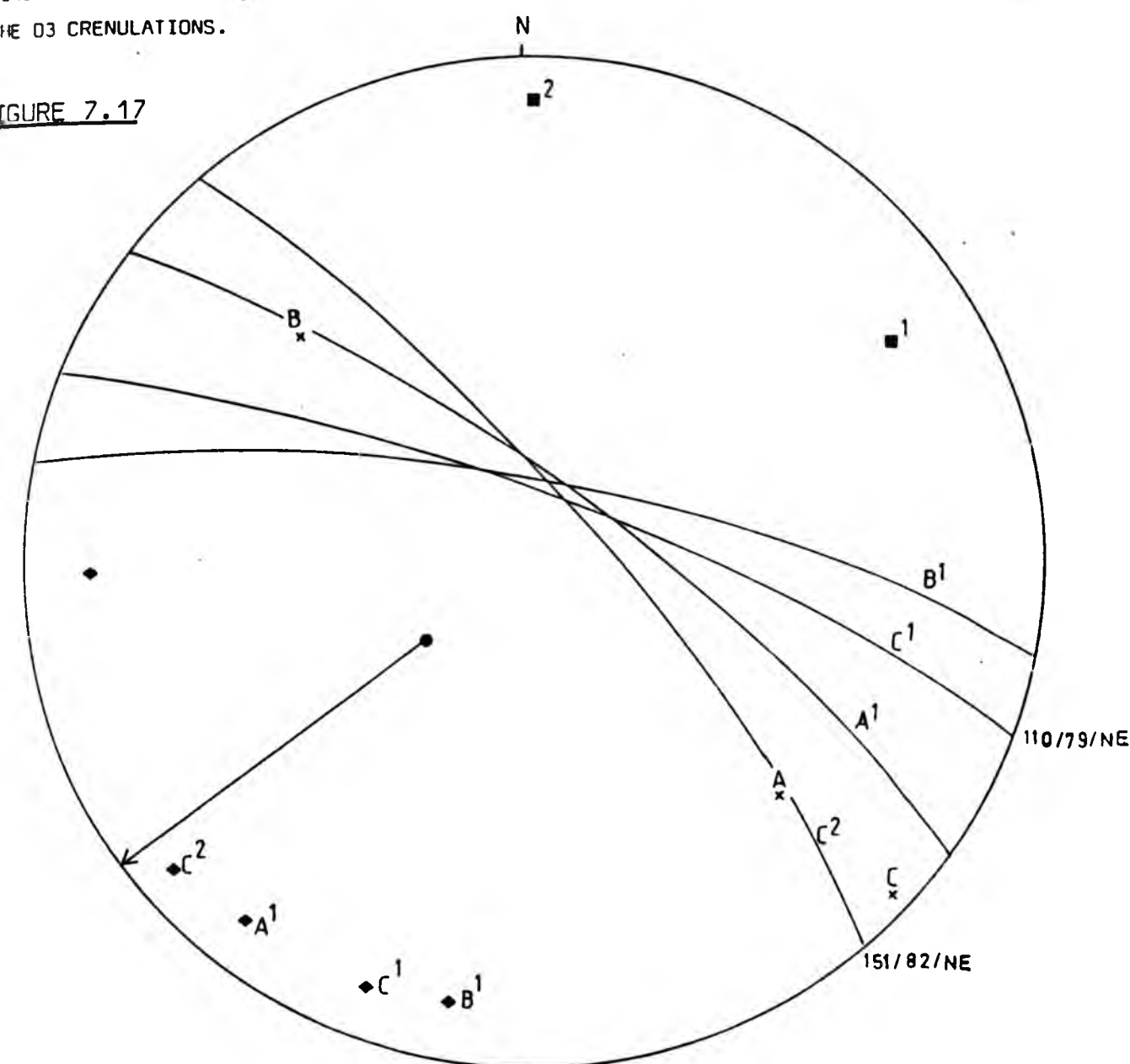
FIELDS SHOWING POLES TO F3 CRENULATION FOLD AXIAL PLANES, FROM VARIOUS ENVELOPE AREAS  
AROUND THE FOYERS GRANITIC COMPLEX.





PROJECTED ORIENTATION OF D3 CRENULATION FOLD AXIAL PLANES, PRESUMING THE FOYERS FOLD IS A LATE FOLD WHICH POST DATES THE FORMATION OF THE D3 CRENULATIONS. ROTATION OF NORTH WEST TRENDING BEDDING AROUND THE FOYERS FOLD PROVIDES THE AMOUNT AND DIRECTION OF ROTATION APPLIED TO THE D3 CRENULATIONS.

FIGURE 7.17



- <sup>1</sup> PRESENT ORIENTATION OF BEDDING ON BEINN SGURRACH
- <sup>2</sup> PRESENT ORIENTATION OF BEDDING ON THE NORTHERN MARGIN OF THE FOYERS COMPLEX

×A, ×B, ×C VARIOUS ORIENTATIONS OF BEDDING FROM SOUTH OF THE FOYERS COMPLEX IN THE GLEN BRETN SECTION OF THE CORRIEYAIRACK SYNCLINE (HASELOCK et al., 1982)

● PLUNGE OF THE FOYERS FOLD

◆ POLE TO FOLD AXIAL PLANES OF D3 CRENULATION CLEAVAGES IN THE FOYERS ENVELOPE

◆A<sup>1</sup>→◆C<sup>1</sup> POLES TO D3 CLEAVAGE AFTER ROTATION AROUND THE FOLD AXIS OF THE FOYERS FOLD, SO BEDDING FROM THE CORRIEYAIRACK SYNCLINE LIES IN THE SAME ORIENTATION AS THE BEDDING ON THE NORTHERN MARGIN OF THE FOYERS COMPLEX. BEDDING ORIENTATION C2 PRODUCED THE MOST ACCURATE ROTATION AROUND THE FOLD AXIS.

◆C<sup>2</sup> POLE TO D3 CLEAVAGE AFTER ROTATION AROUND THE FOLD AXIS OF THE FOYERS FOLD, SO BEDDING FROM THE CORRIEYAIRACK SYNCLINE LIES IN THE SAME ORIENTATION AS THE BEDDING ON BEINN SGURRACH. CORRIEYAIRACK BEDDING ORIENTATION C WAS USED.

TABLE 7.1

TABLE SHOWING THE EXTENSION DISPLAYED BY CALC-SILICATE BOUDIN  
TRAINS IN THE ENVELOPE OF THE FOYERS COMPLEX.

Area	Locality	l	lf	extension
Maol Chnoc	2192	0.8	0.98	0.23
Beinn Dubhcharaidh	2093	7	12	0.78
		9.5	21.5	1.26
		2.9	5.9	1.03
	2095	4.3	9.2	1.14
		3.2	8.6	1.68
Central septum	2205	1.47	1.82	0.24
		1.6	2.57	0.6
		1.11	1.31	0.18
	2216	1.44	1.84	0.3
		0.91	1.23	0.35
	2361	0.78	1.2	0.54
		0.74	1.18	0.59
		1.98	2.7	0.36
	2212	1.12	1.54	0.38
Croftdhu	233	0.66	0.74	0.12
	1945	0.55	0.62	0.13
Carn Gairbthinn	1870	0.46	1.12	1.43
	1253	0.53	1.1	1.07
Whitebridge Plantation	2826	0.57	0.80	0.40
		1.9	2.9	0.52

FIGURE 7.18

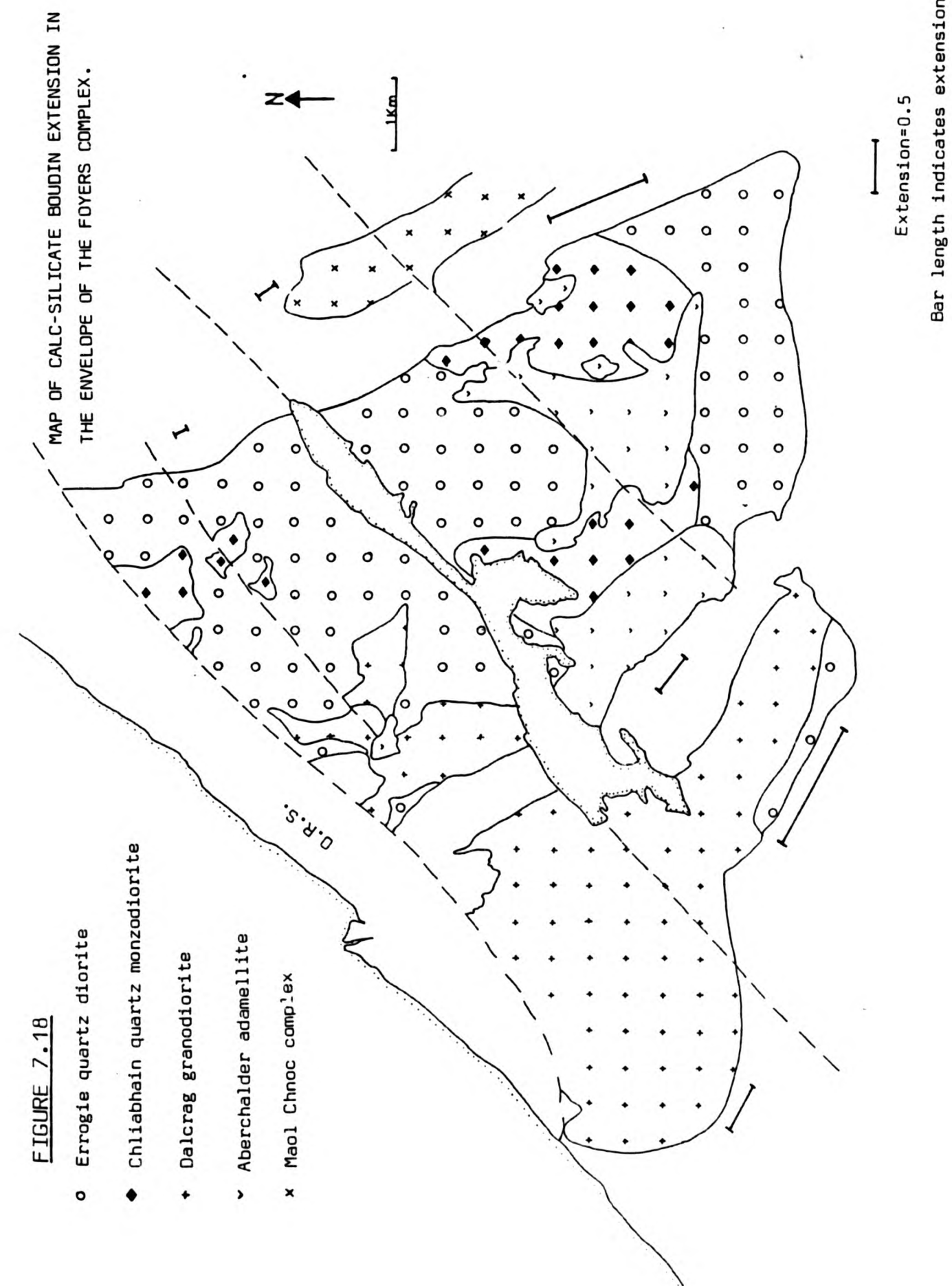
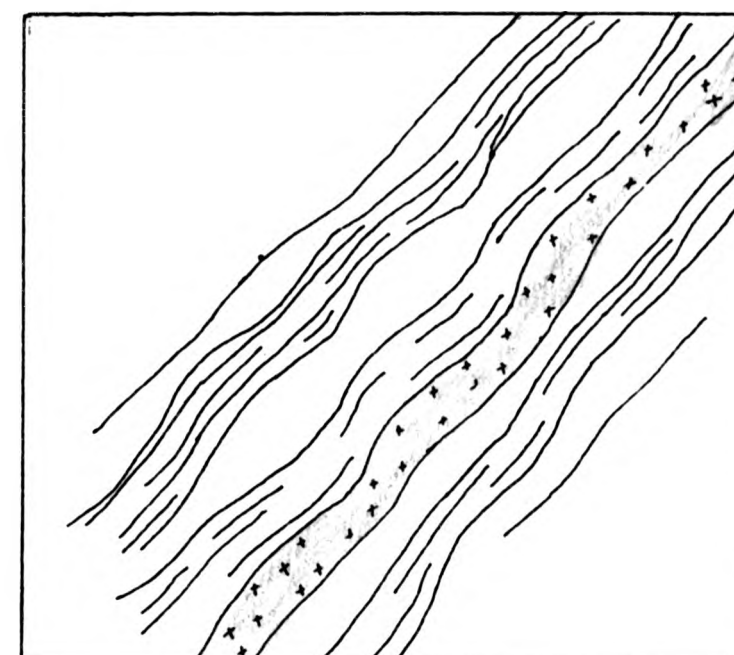


FIGURE 7.19

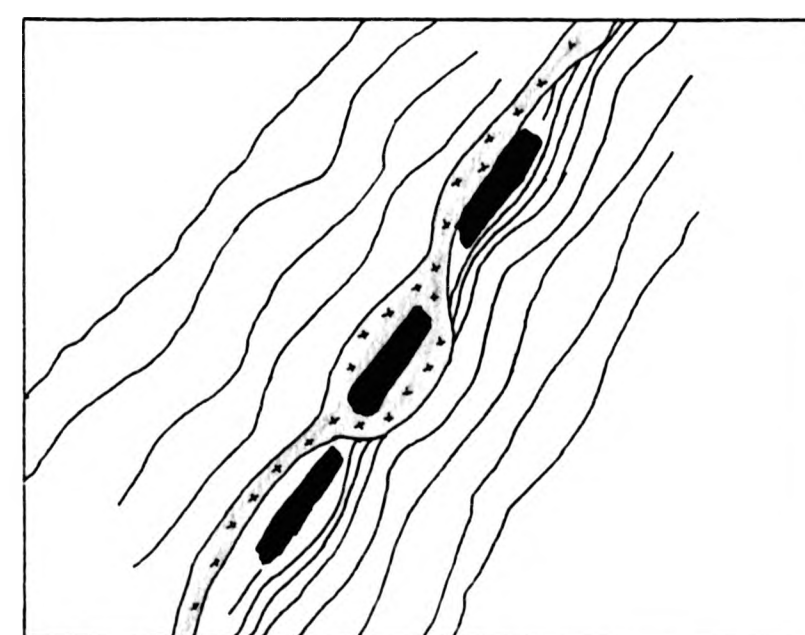
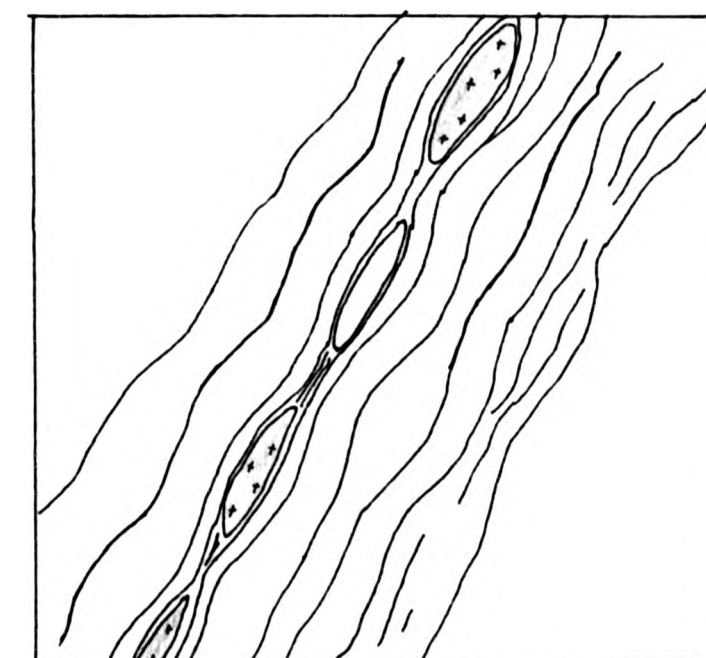


Morphology of the granitoid vein influenced by the pinch and swell structures in the adjacent psammities.

1m

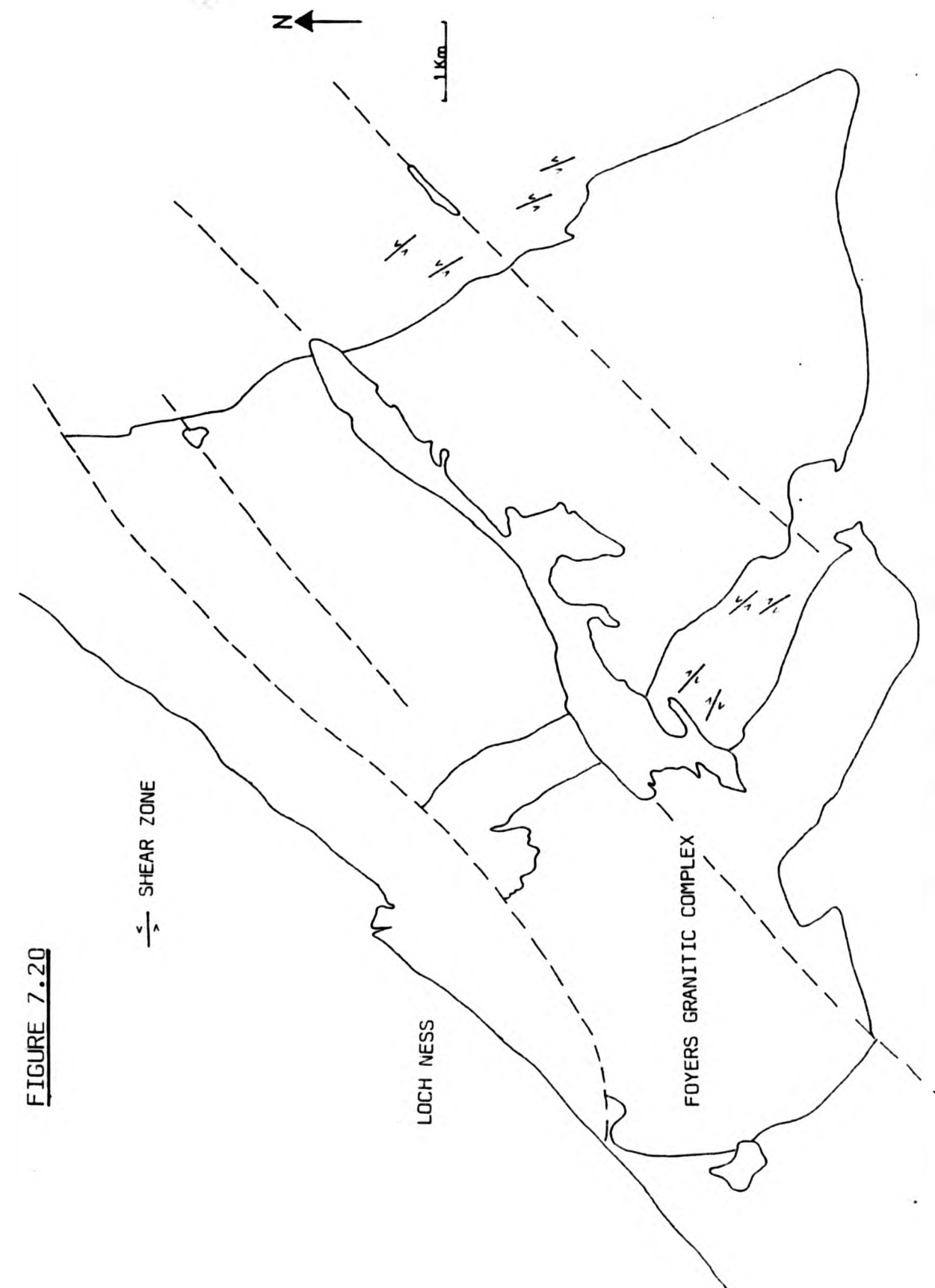
THREE DIAGRAMS SHOWING THE  
RELATIONSHIP BETWEEN BOUDINAGE &  
GRANITOID VEINING

Granitoid material preferentially  
intruding into the boudin position  
of weakly boudinaged psammities.



Granitoid vein enclosing  
a calc silicate boudin.

FIGURE 7.20



MAP SHOWING THE STRIKE AND SHEAR SENSE OF MINOR SHEAR STRUCTURES IN THE ENVELOPE OF THE FOYERS GRANITIC COMPLEX.



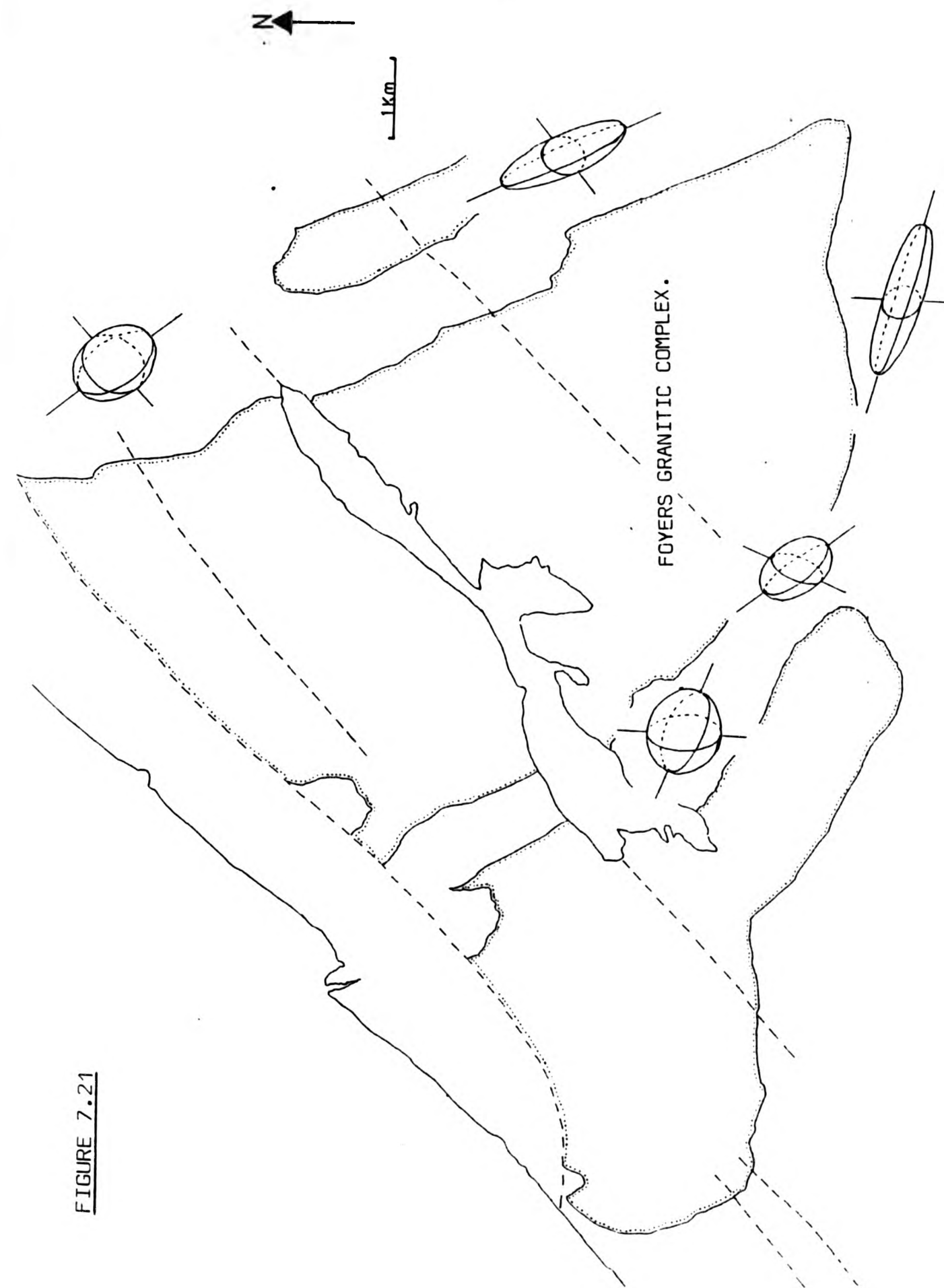
TABLE 7.2

AREA	LOCALITY	LENGTH & ORIENTATION OF MAJOR AXES		
		X	Y	Z
Beinn Dubhcharaidh	2136	2.9 10/142	1 78/310	0.81
Beinn Dubhcharaidh	2139	2.77 12/130	1 75/309	0.91
Beinn Bhuraich	2396	4.04 18/276	1 70/110	0.76
Tom Mor	1988	1.23 2/140	1 vert.	0.97
Central Septum	2341	1.25 10/120	1 72/304	0.90
Central Septum	2212	1.15 0/120	1 vert.	0.48

DIMENSIONS OF METAMORPHIC SPOTS WITHIN AMPHIBOLITES IN THE  
ENVELOPE OF THE FOYERS COMPLEX.



FIGURE 7.21



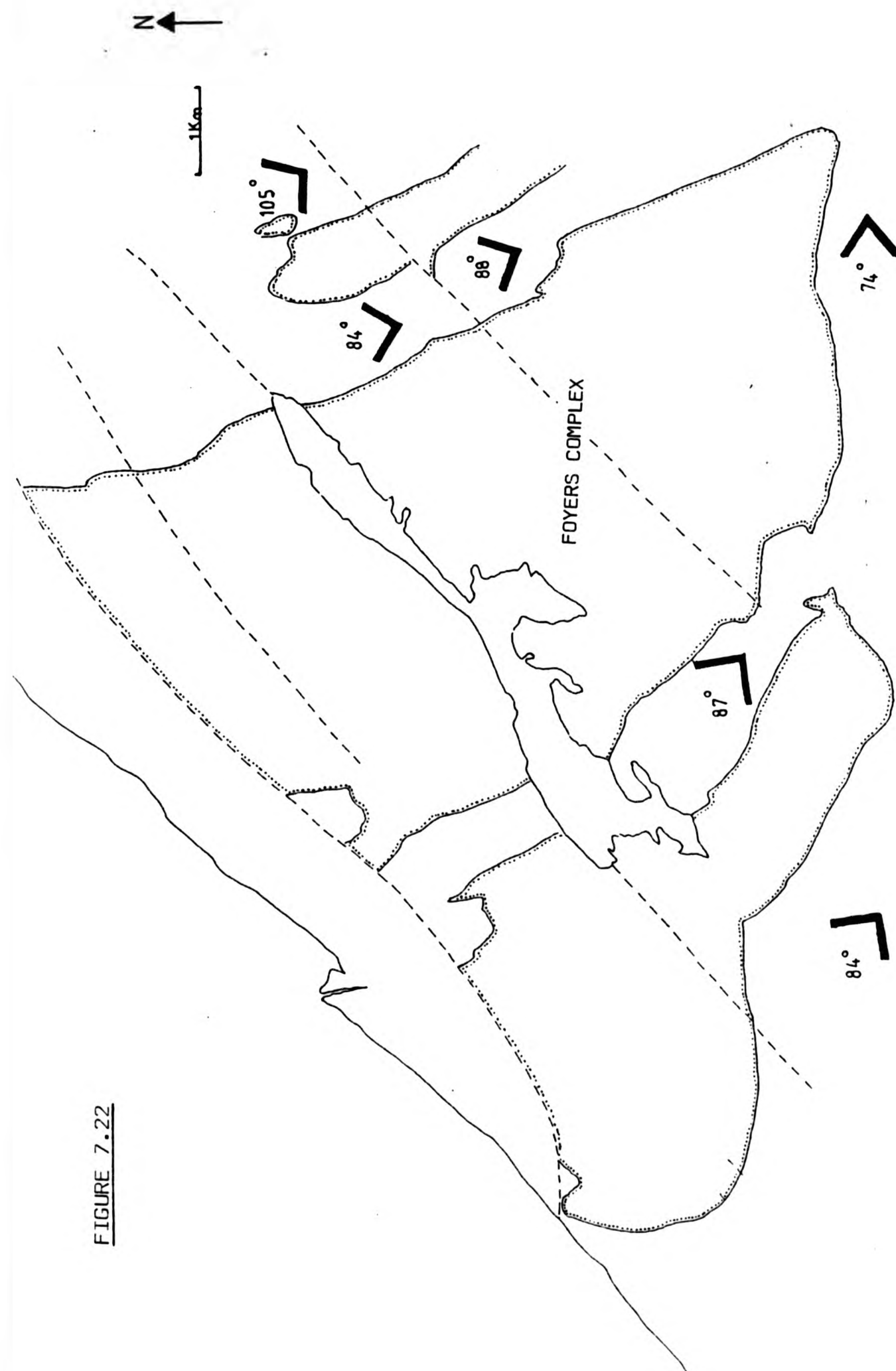
MORPHOLOGY OF METAMORPHIC SPOTS (RETROGRESSED GARNETS) IN AMPHIBOLITE BODIES WITHIN DIFFERENT REGIONS OF THE FOYERS COMPLEX ENVELOPE

TABLE 7.3

PLACE	No. FOLDS MEASURED	INTER LIMB ANGLE (MEAN)
Meall Donn	11	114
Beinn Dubcharaidh	18	105
Carn Bad Earbaig	12	116
Central Septum	30	87
Beinn Bhuraich	5	74
Beinn Sgurrach	12	84

MEAN INTER LIMB ANGLES DISPLAYED BY D2 CALEDONIAN FOLDS WITHIN THE  
FOYERS ENVELOPE.

FIGURE 7.22



MORPHOLOGY AND INTERLIMB ANGLE OF CALEDONIAN "D2" FOLDS AT SELECTED SITES IN THE FOYERS COMPLEX ENVELOPE.

PLATES  
Chapter 7



Plate 7.1  
Bedding in the pebbly psammite, defined by well  
preserved cross beds. (Central Psammite Septum).

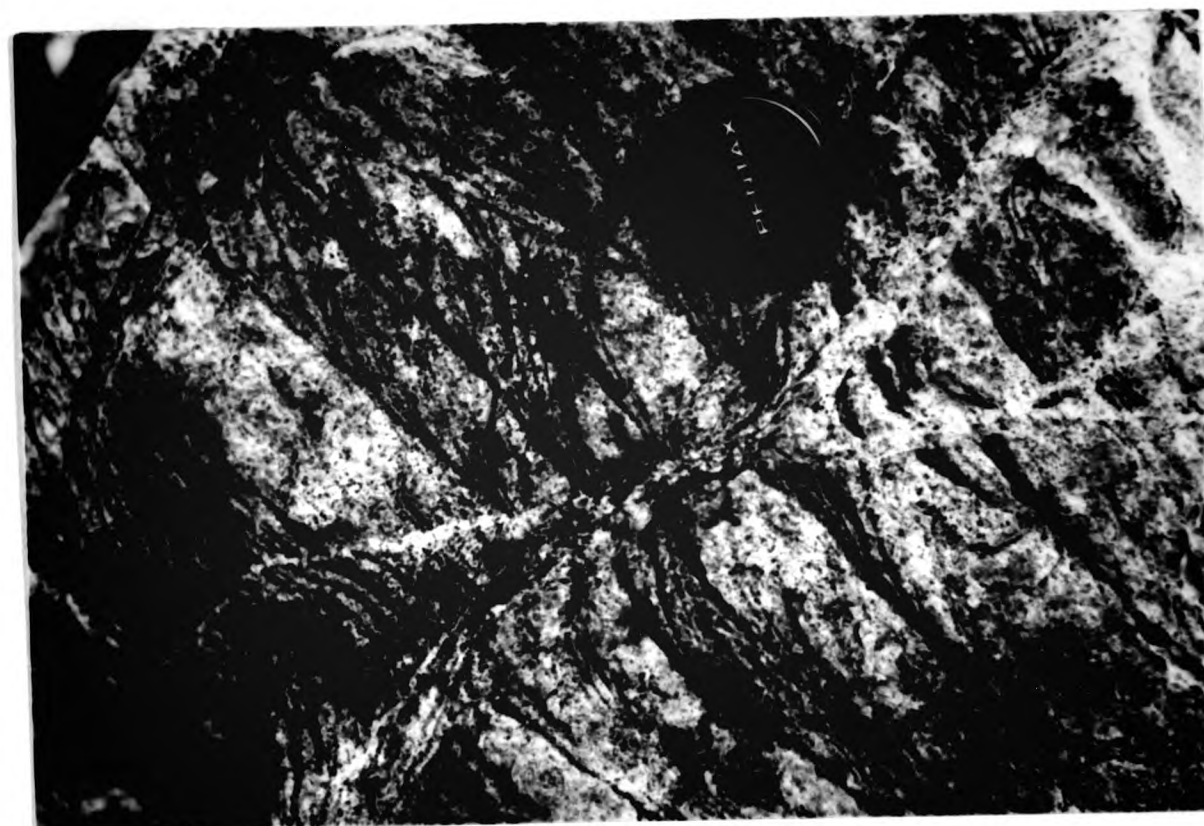


Plate 7.2  
D2 minor folds, within the micaceous psammite.  
(Central Psammite Septum).

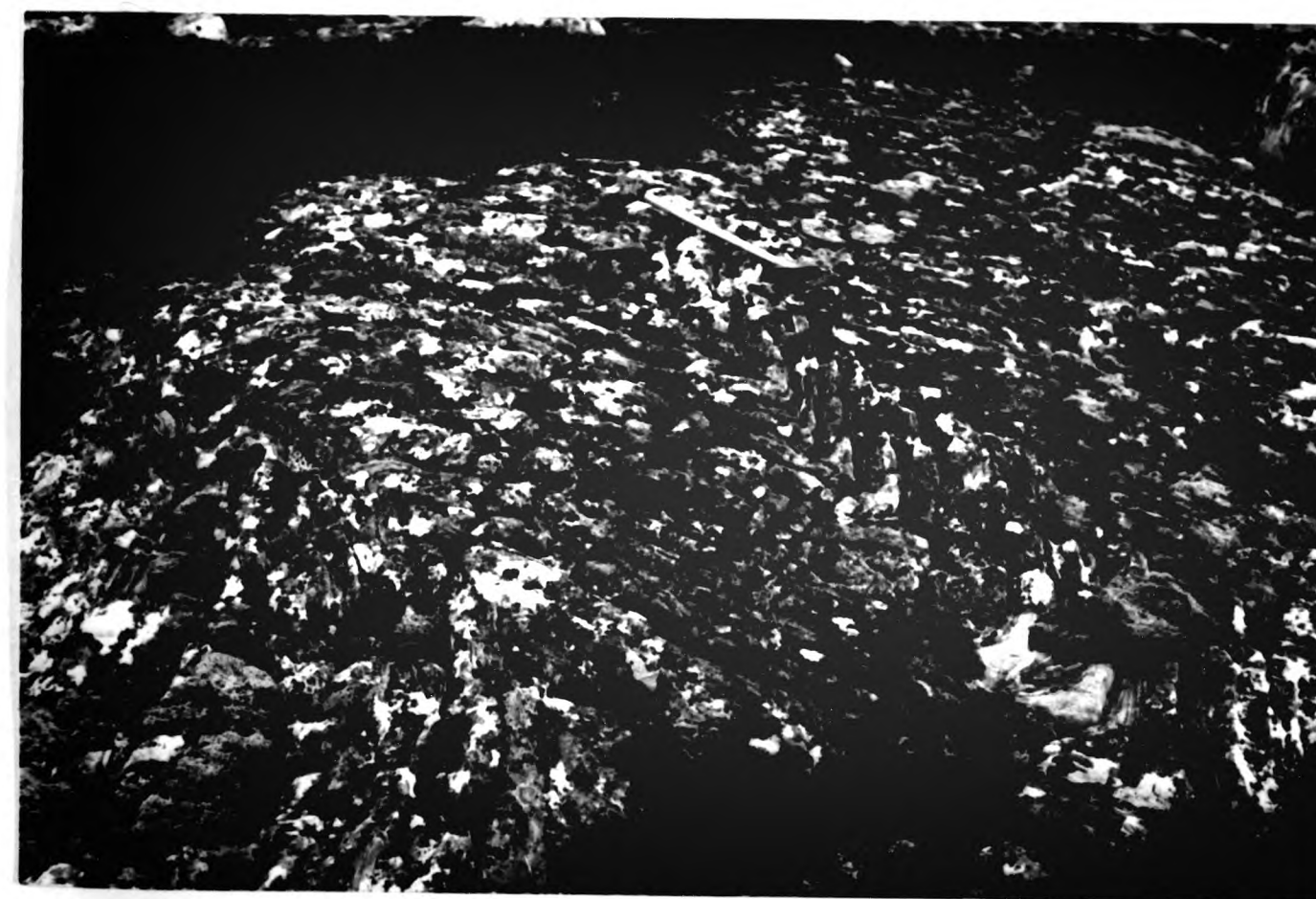


Plate 7.3  
Axial planar crenulations, developed in the core of a  
D2 minor fold. (Central Psammite Septum).

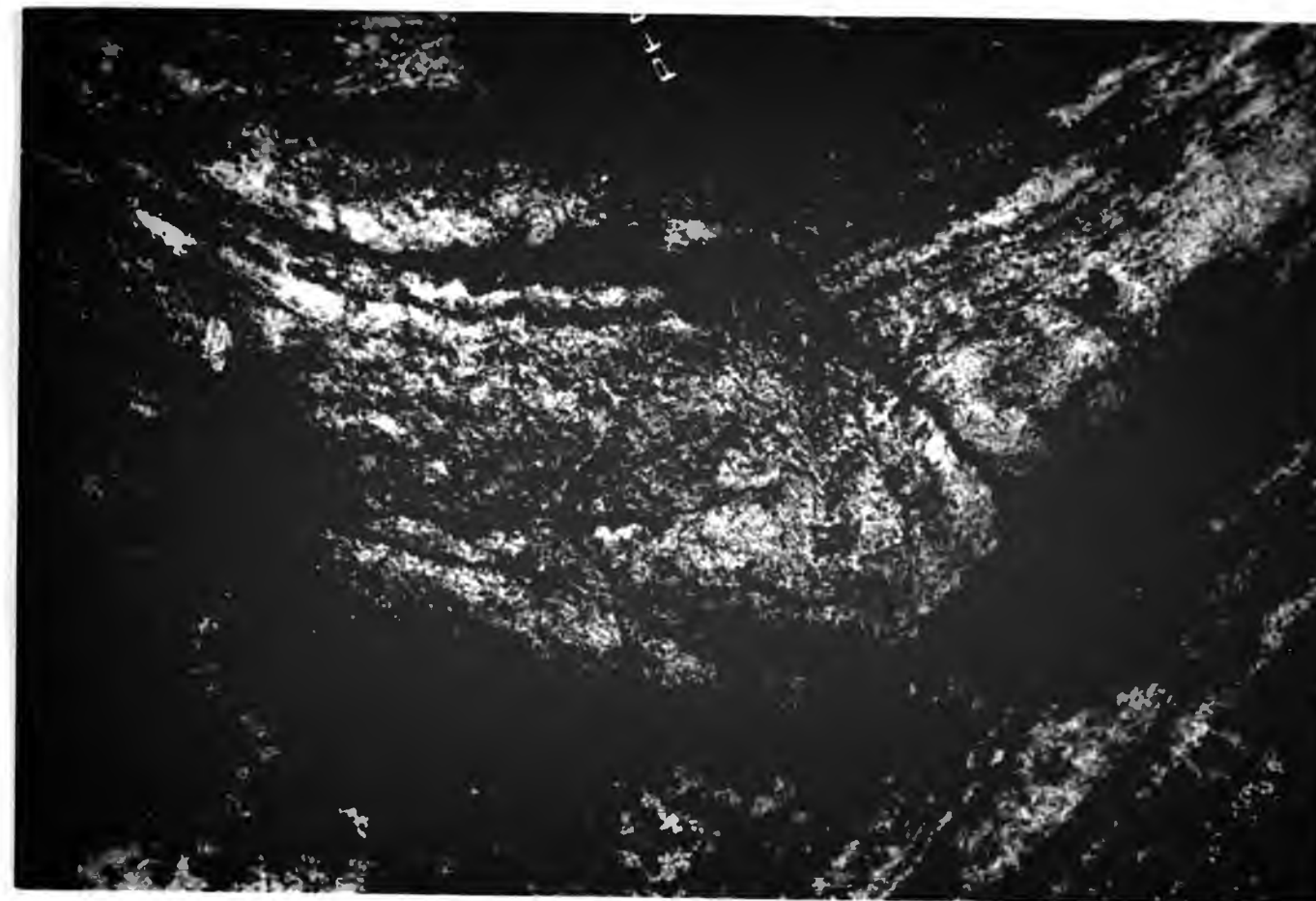


Plate 7.4  
Steeply plunging D3 fold in the Micaceous Psammite.  
(Central Psammite Septum).

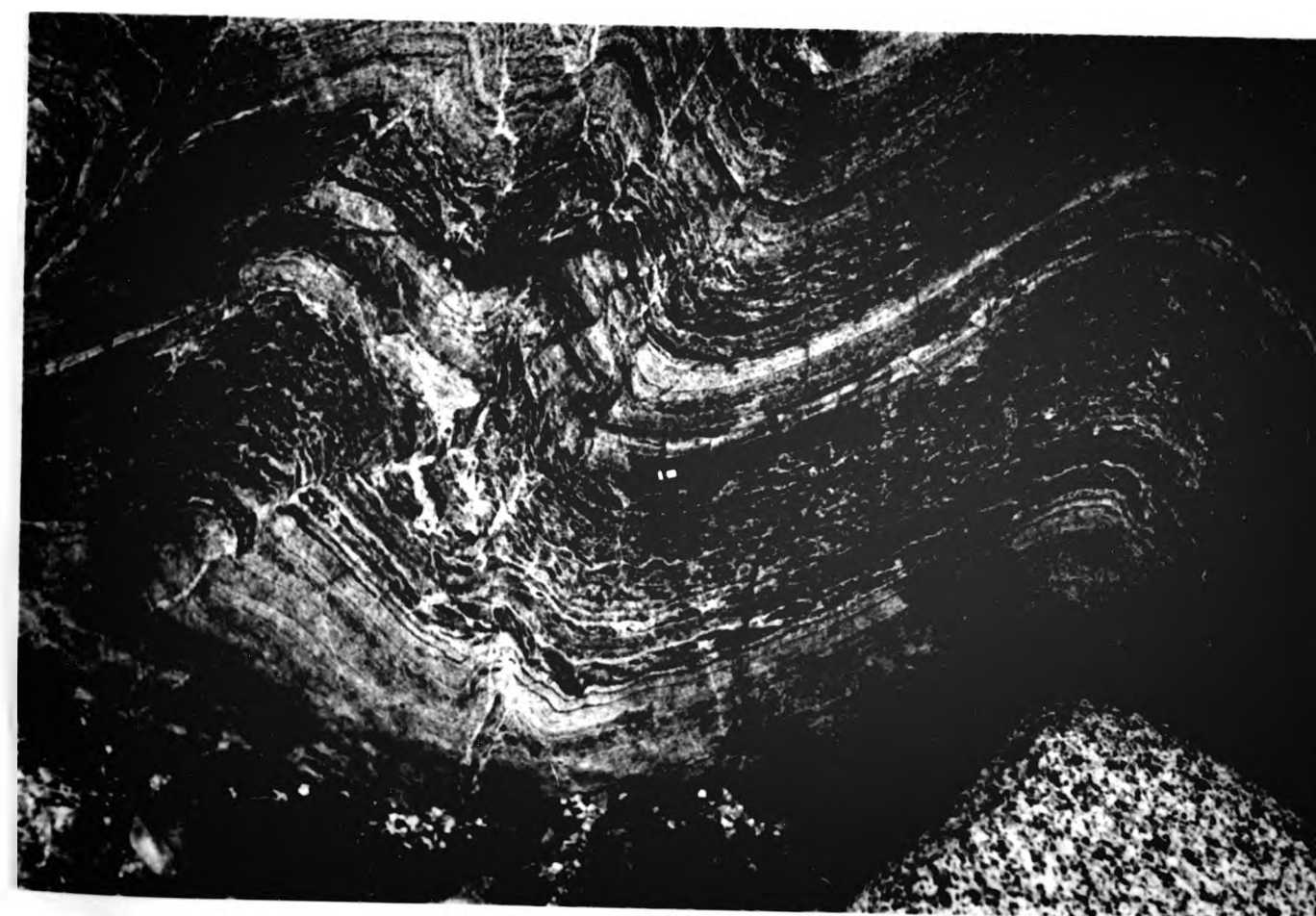




Plate 7.5

D2 fold in micaceous psammite, showing one limb  
refolded by later D3 folds. (Beinn Sgurrach).



Plate 7.6

Boudinaged calc-silicate layer, within a loose block.  
(Carn Gairbthinn).

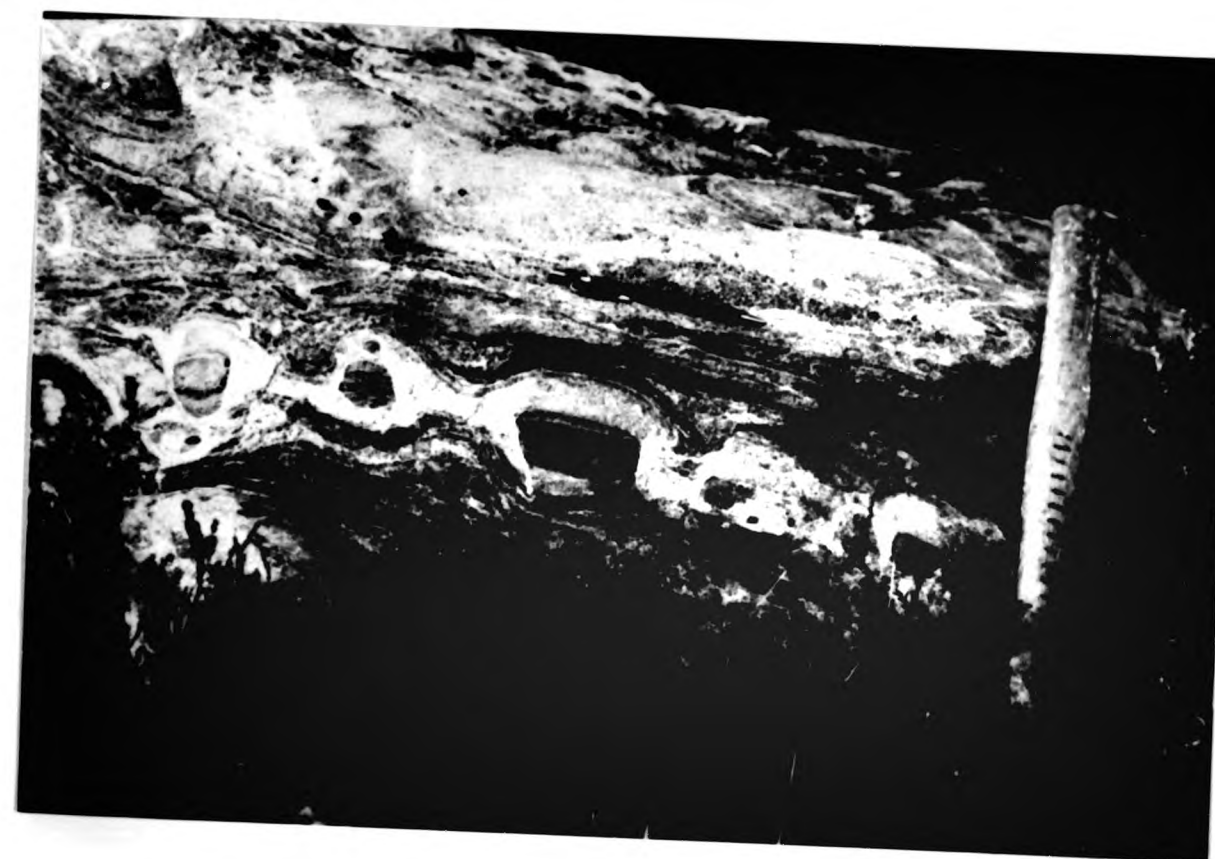


Plate 7.7

Boudinaged bed, within micaceous psammite. The break between the boudins is filled by the infolding of adjacent psammite beds. (Carnoch).



Plate 7.8

En echelon boudins. Each boudin shows slight rotation, which is accommodated by shearing between the boudins. (Central Psammite Septum).





Plate 7.9

External morphology of a granitoid vein, controlled by the pinch and swell structure in the adjacent micaceous psammite. (Beinn Dubhcharaidh).

Plate 7.10

Late, wave-like, open folds within the micaceous psammite. (Beinn Dubhcharaidh).

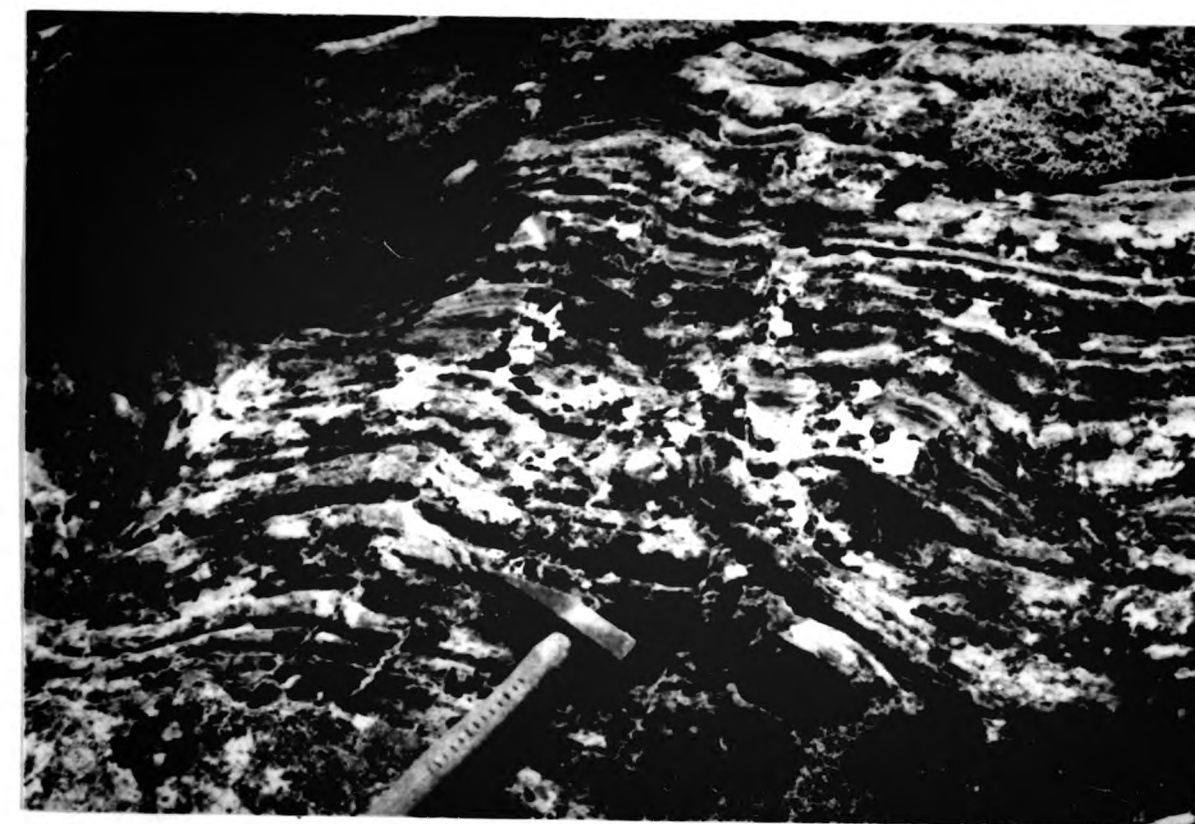
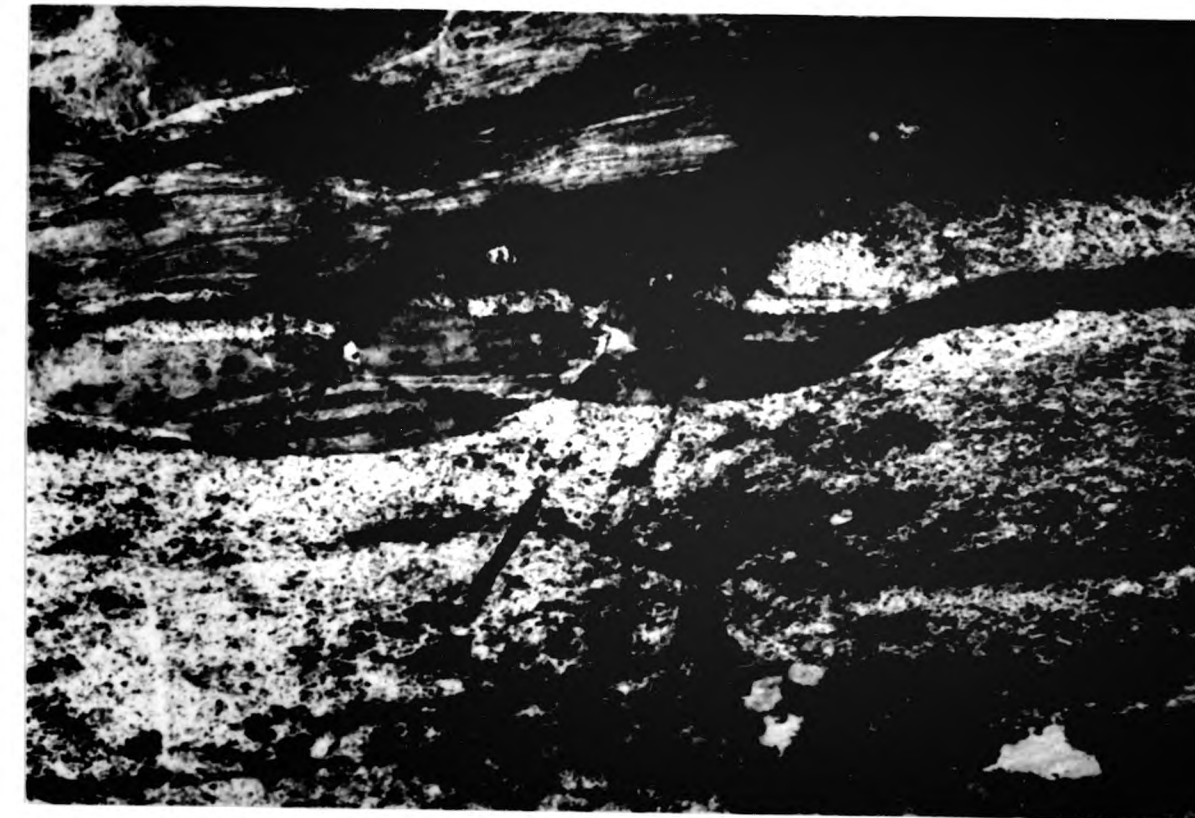


Plate 7.11

Possible weak zig-zag arrangement of calc-silicate boudins, due to folding around the hinge of a late open fold. (Central Psammite Septum).

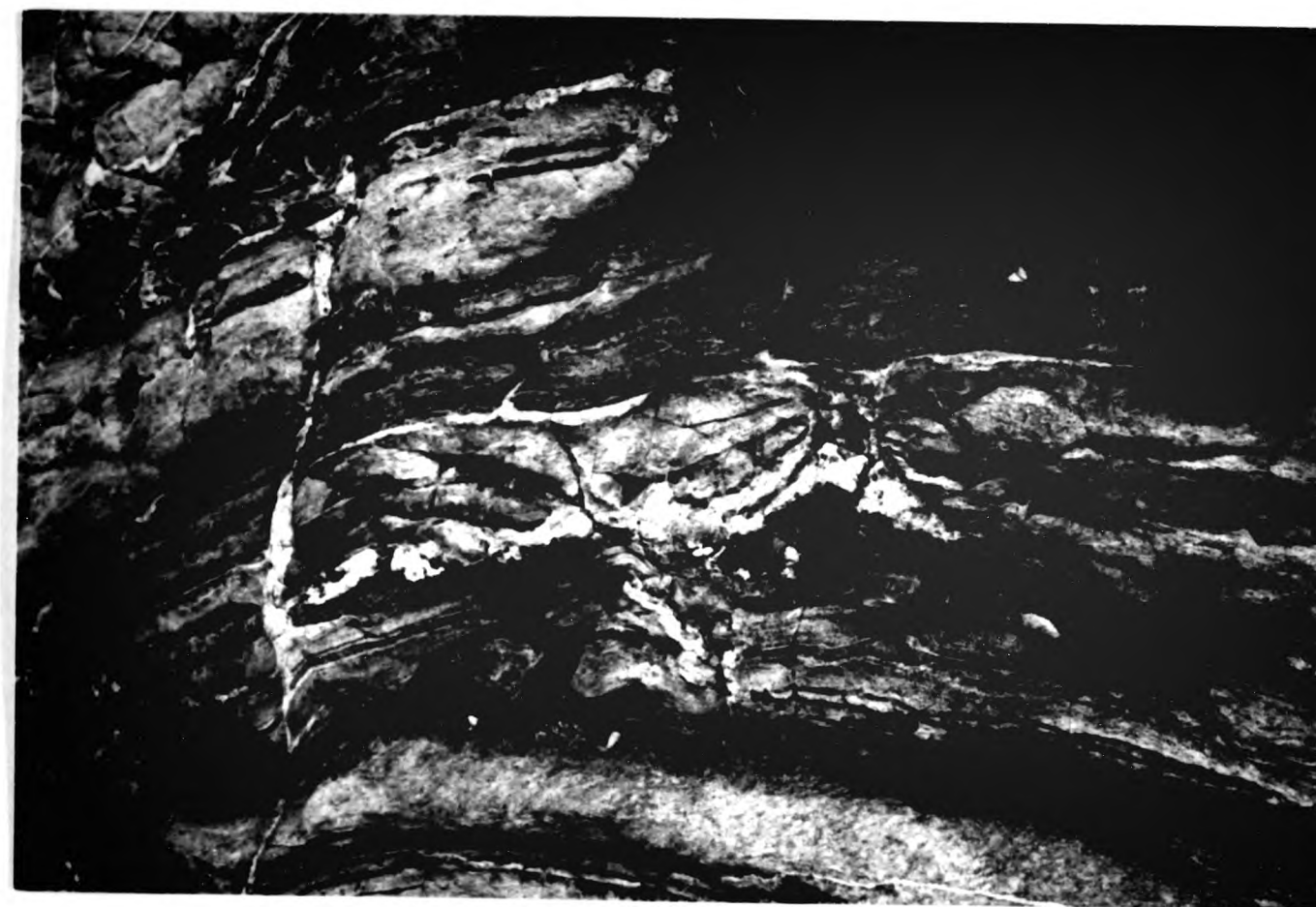
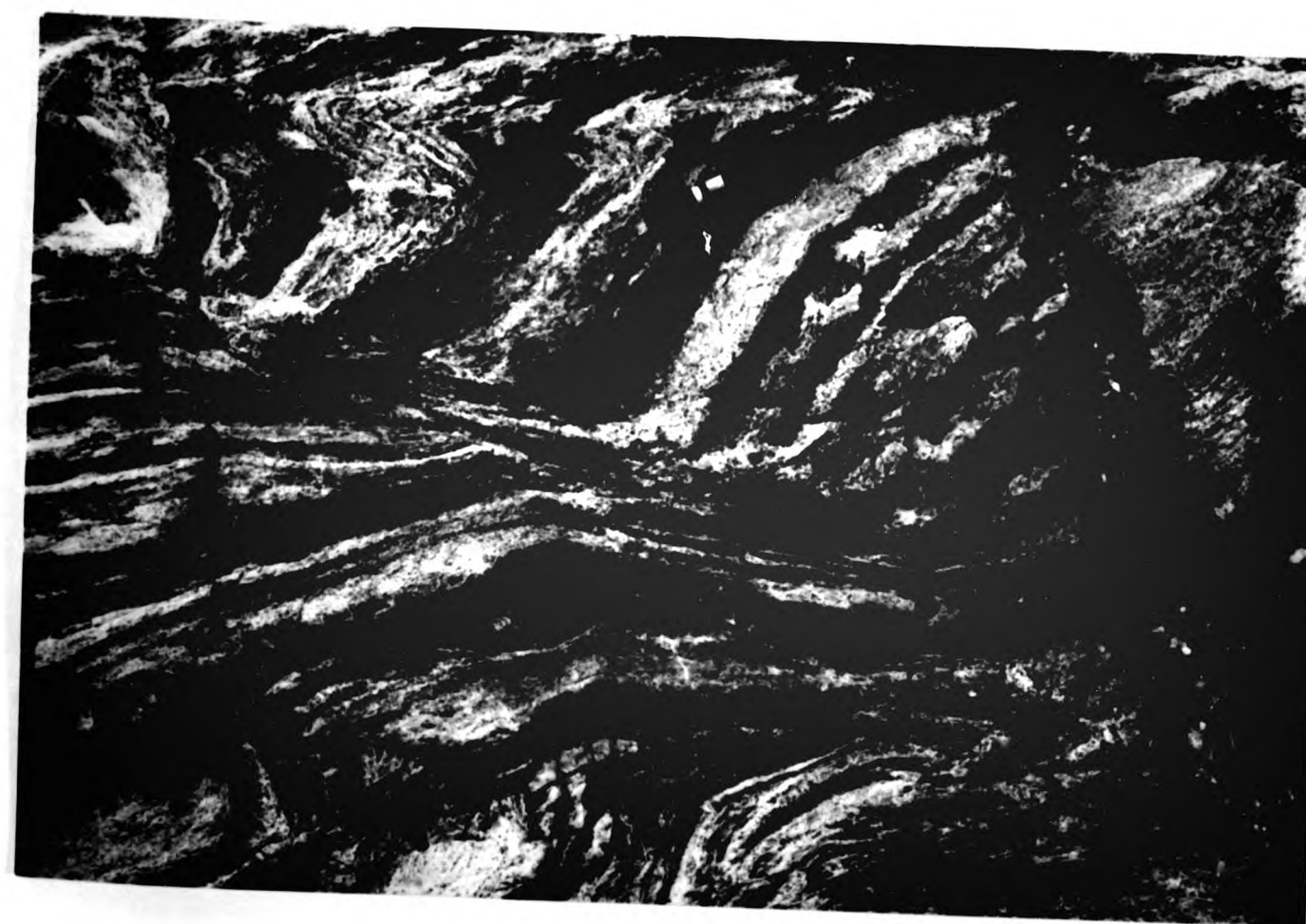


Plate 7.12

Small dextral shear, cutting micaceous psammite. (Central Psammite Septum).





**Plate 7.13**

Shear zone within siliceous psammites, showing bedding rotated into parallelism with the shear zone wall. Note the boudinaged quartz vein towards the top of the photograph. (Central Psammite Septum).

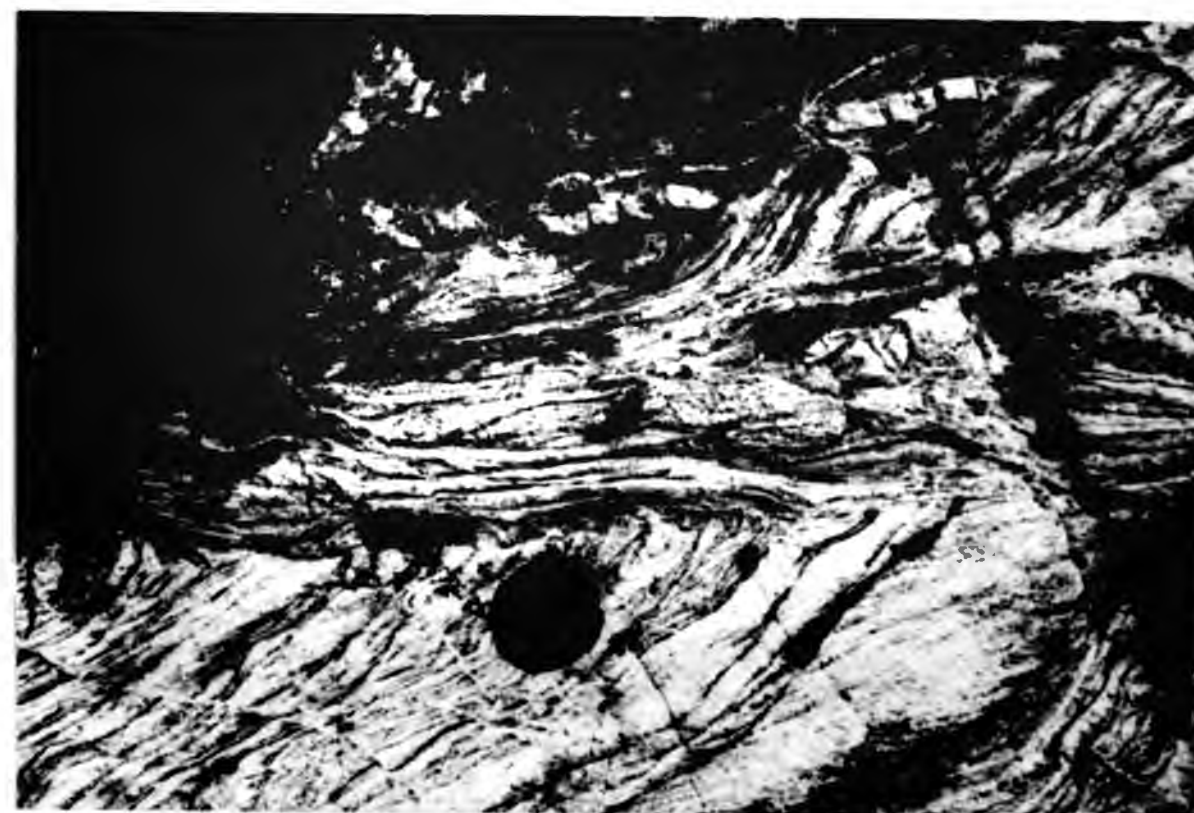


**Plate 7.14**

Rotated block of boudins, the rotation is accommodated by shearing within the micaceous psammites adjacent to the block. (Beinn Dubhcharaidh).

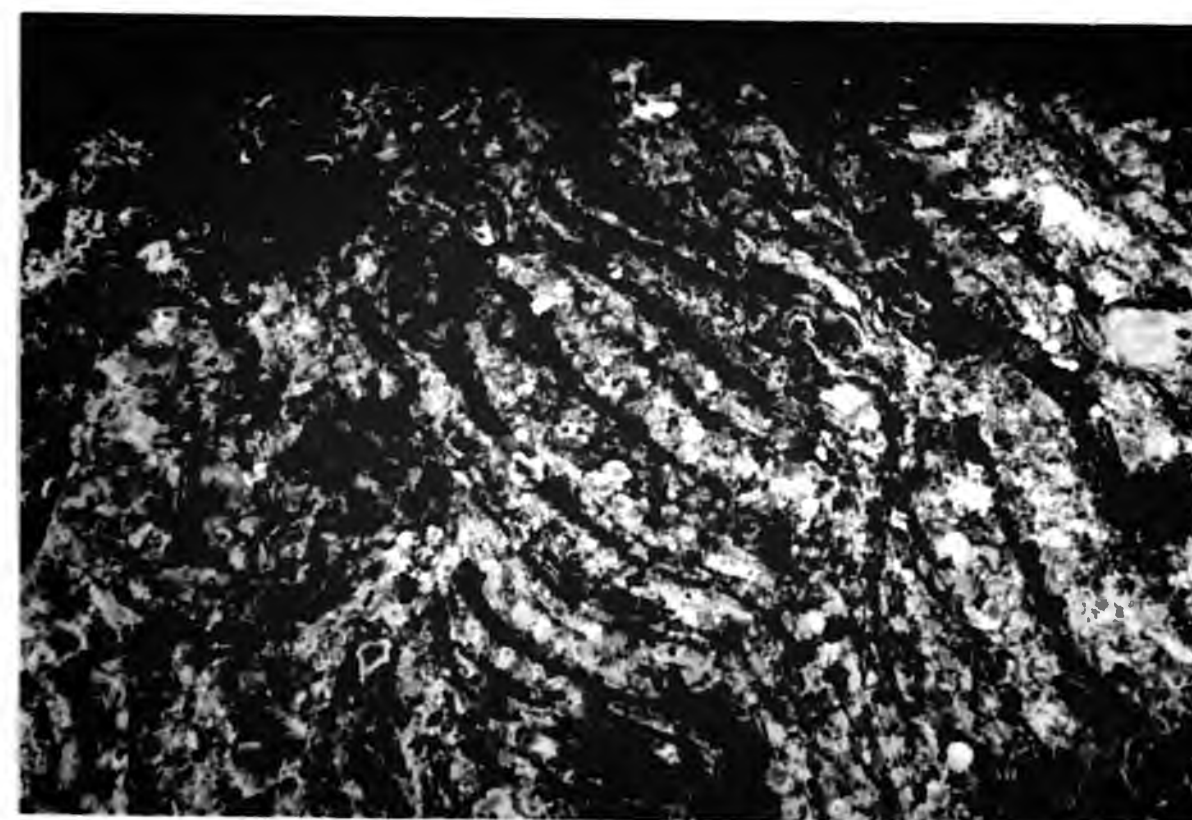


Plate 7.15

Elliptical, contact metamorphic spots (after garnet), within a foliated amphibolite body. (Tom Mor).



Plate 7.16

Tightened D2 fold, containing a calc-silicate layer, which is boudinaged in the limbs of the fold. Note the D3 crenulations deforming the thickened hinge zone of the fold. The fold axial planes of the D2 and D3 structures are approximately perpendicular to each other. (Central Psammite Septum).





Plate 7.17

North easterly view of the broad valley of Stratherrick and Loch Mhor, both topographical expressions of the Loch Mhor fault zone. In the mid-distance, on the right, is the ridge of hills formed by the Central psammite septum. The photograph is taken from the summit of Cairn Gairbthinn.



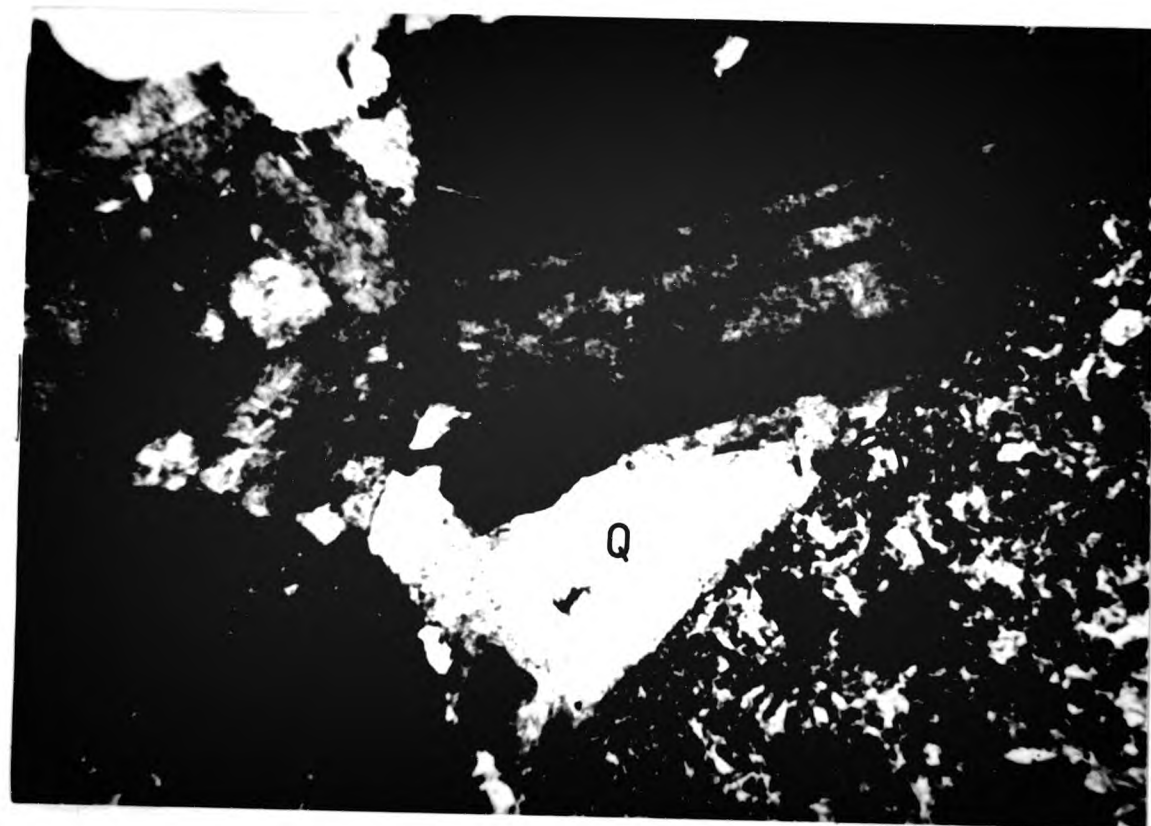
Plate 7.18

North easterly view of the north eastern margin of the Foyers Complex, with the deep fault valley of Conagleann incising the psammite envelope. The margin of the complex runs along the top of the south western slopes of Creag a Chliabhain on the range of hills to the left of Conagleann. In the mid-ground, to the left of the photograph, is the drift terraced valley of Allt an Ruthain Ruaidh, an expression of the Conagleann fault as it cuts the Foyers complex. The photograph is taken from the summit of Beinn Meadhoin.



**Plate 7.19**

Edge of a microbreccia vein (bottom left corner of photograph), sharply truncating plagioclase and quartz crystals in Chliabhain Quartz Monzodiorite. Note the epidote (Ep), pseudomorphing biotite in the host granitoid. (Crossed polars, x47).



**CHAPTER 8. PETROLOGY AND CONTACT METAMORPHISM OF THE  
ENVELOPE ROCKS.**

DISTRIBUTION OF CONTACT METAMORPHIC MINERALS IN THE AUREOLE OF THE FOYERS COMPLEX.  
Isograds after Highton, 1987.

FIGURE 8.1

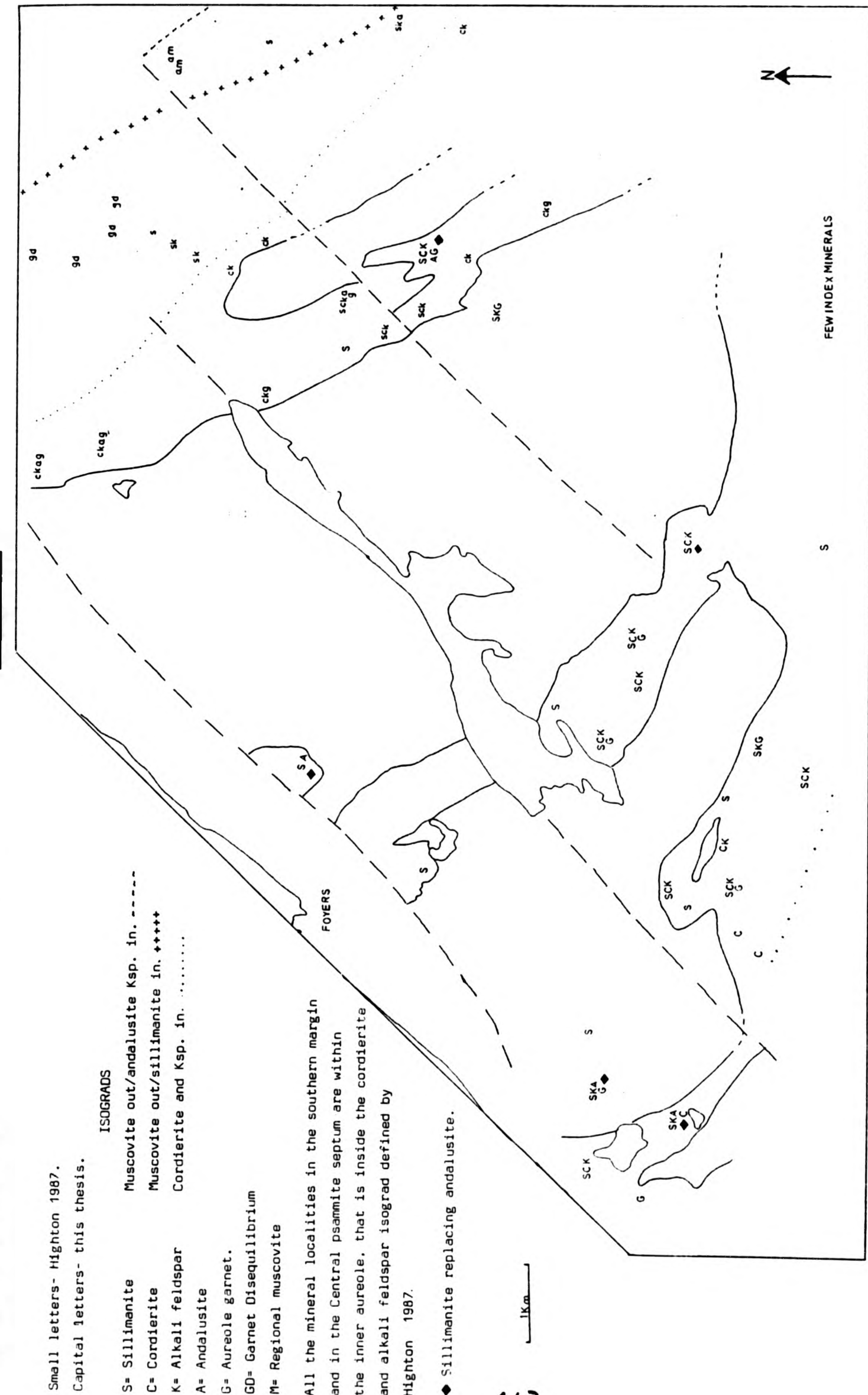


TABLE B.1

AVERAGE COMPOSITION OF A NUMBER OF GARNETS FOUND WITHIN 3 SAMPLES FROM THE INNER AUREOLE

SLIDE NO.	Si	Ti	Al	Cr	Fe	Mn	Mg	Ca	Na	K	
2110											
Garnet A	37.83	0.057	21.61	0.044	36.14	3.711	2.134	0.998	0.252	0.023	Oxide Weight %
	2.988	0.003	2.012	0.003	2.386	0.248	0.249	0.084	0.038	0.002	Formula
Garnet B	37.88	0.033	21.74	0.027	35.22	4.115	2.156	1.015	0.274	0.028	
	2.995	0.000	2.025	0.000	2.328	0.275	0.253	0.086	0.025	0.003	Slides 2110 & 2300 are micaceous
Garnet C	37.588	0.037	21.51	0.009	35.78	3.748	1.998	1.00	0.114	0.022	psammites from the Central psammite
	2.998	0.002	2.019	0.000	2.383	0.264	0.237	0.11	0.066	0.000	septum.
2300											
Garnet D	37.454	0.027	21.45	0.000	35.75	3.76	2.158	0.987	0.139	0.001	Slide 2735 is taken from a micaceous
	2.987	0.002	2.018	0.000	2.385	0.254	0.262	0.084	0.021	0.000	band within the pebbly psammites
											south west of Loch Kemp.
Garnet E	37.33	0.069	21.33	0.07	35.621	3.81	1.911	1.025	0.183	0.000	
	2.945	0.004	2.018	0.004	2.392	0.258	0.228	0.088	0.028	0.000	
Garnet F	37.00	0.027	21.03	0.161	35.25	3.551	2.037	1.049	0.089	0.000	
	2.999	0.000	2.009	0.004	2.389	0.243	0.246	0.09	0.014	0.000	
Garnet G	37.66	0.070	21.557	0.054	35.662	3.916	1.998	1.009	0.112	0.001	
	2.994	0.004	2.02	0.003	2.371	0.263	0.236	0.085	0.017	0.000	
2735											
Garnet H	37.74	0.045	21.354	0.062	29.61	8.050	1.994	2.637	0.142	0.021	
	2.997	0.002	1.998	0.004	1.969	0.542	0.236	0.225	0.021	0.002	
Garnet I	37.72	0.083	21.27	0.026	29.23	8.068	2.111	2.236	0.384	0.054	
	3.00	0.005	1.999	0.000	1.95	0.545	0.25	0.164	0.004	0.004	Contd...



TABLE B.1

AVERAGE COMPOSITION OF BIOTITE FROM THREE SAMPLES WITHIN THE INNER AUREOLE OF THE FOYERS GRANITIC COMPLEX

SLIDE No.	Si	Ti	Al	Cr	Fe	Mn	Mg	Ca	Na	K
2110	34.65	3.897	20.09	0.083	22.47	0.117	5.655	0.063	0.375	9.198
	5.757	0.483	3.935	0.011	3.123	0.016	1.405	0.011	0.132	1.950
2300	34.40	3.524	19.78	0.048	22.57	0.083	5.766	0.006	0.308	9.346
	5.780	0.445	3.912	0.006	3.173	0.021	1.443	0.00	0.099	1.983
2735	34.64	3.088	18.47	0.081	22.84	0.439	6.614	0.039	0.213	9.245
	5.863	0.392	3.685	0.011	3.236	0.043	1.603	0.007	0.068	1.996

AVERAGE COMPOSITION OF CORDIERITE FROM TWO SAMPLES WITHIN THE INNER AUREOLE OF THE FOYERS GRANITIC COMPLEX.

2110	48.22	0.027	32.89	0.027	11.61	0.400	5.500	0.035	0.533	0.300
	4.984	0.002	4.026	0.002	1.046	0.034	0.851	0.007	0.108	0.092
2300	47.75	0.021	32.50	0.053	11.98	0.293	5.561	0.049	0.380	0.015
	4.995	0.004	4.007	0.004	1.047	0.025	0.867	0.005	0.076	0.00

Contd...

TABLE 8.1

AVERAGE COMPOSITION OF ILMENITE AND PLAGIOCLASE WITHIN SLIDE 2110

	Si	Ti	Al	Cr	Fe	Mn	Mg	Ca	Na	K
ILMENITE	0.383	53.10	0.049	0.007	44.98	1.725	0.097	0.03	0.236	0.011
	0.029	0.996	0.00	0.00	0.938	0.036	0.003	0.00	0.011	0.00
PLAGIOCLASE	60.30	0.012	25.265	0.02	0.313	0.048	0.000	6.6/3	7.7	0.223
	2.672	0.00	1.468	0.00	0.023	0.003	0.00	0.316	0.667	0.016



FIGURE 8.2 ZONING PROFILES OF 3 AUREOLE GARNETS

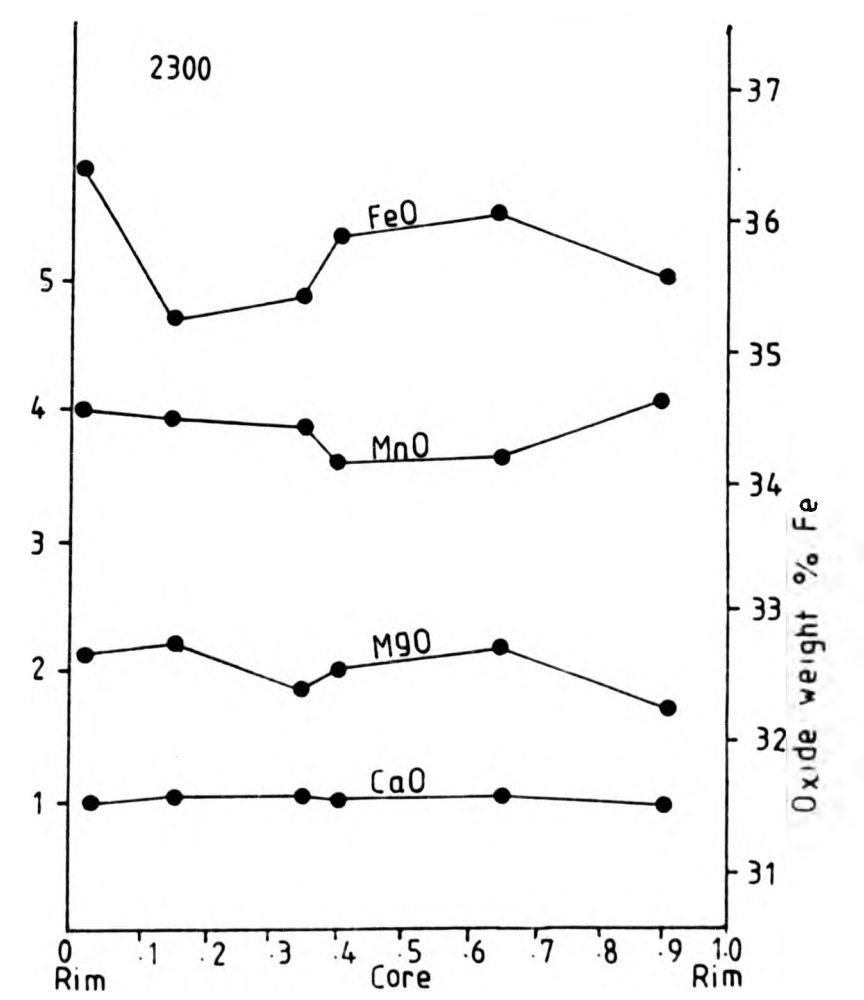
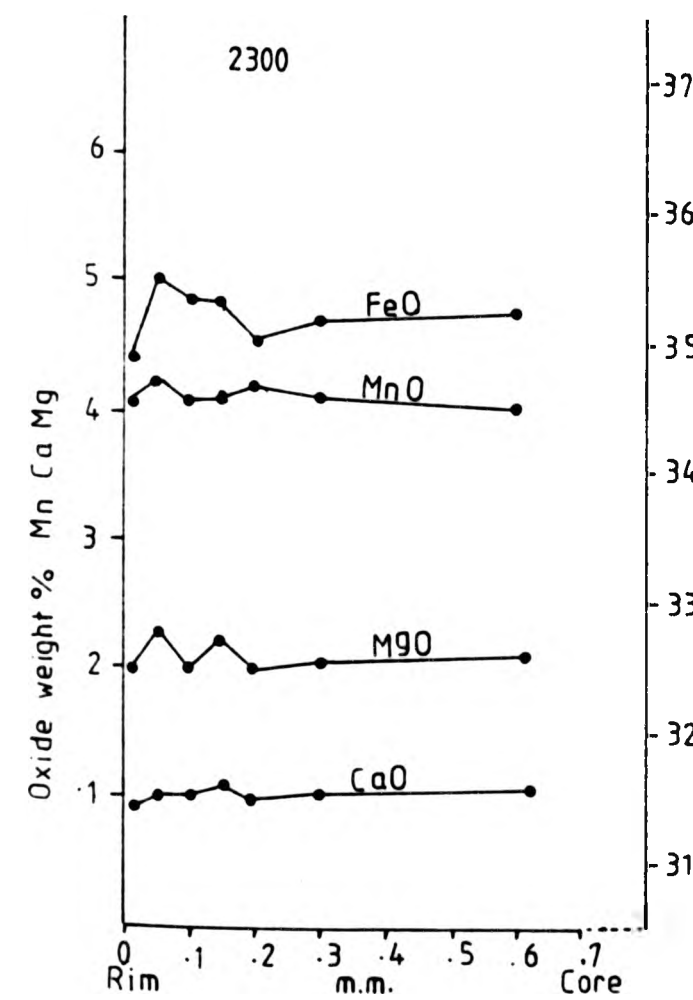
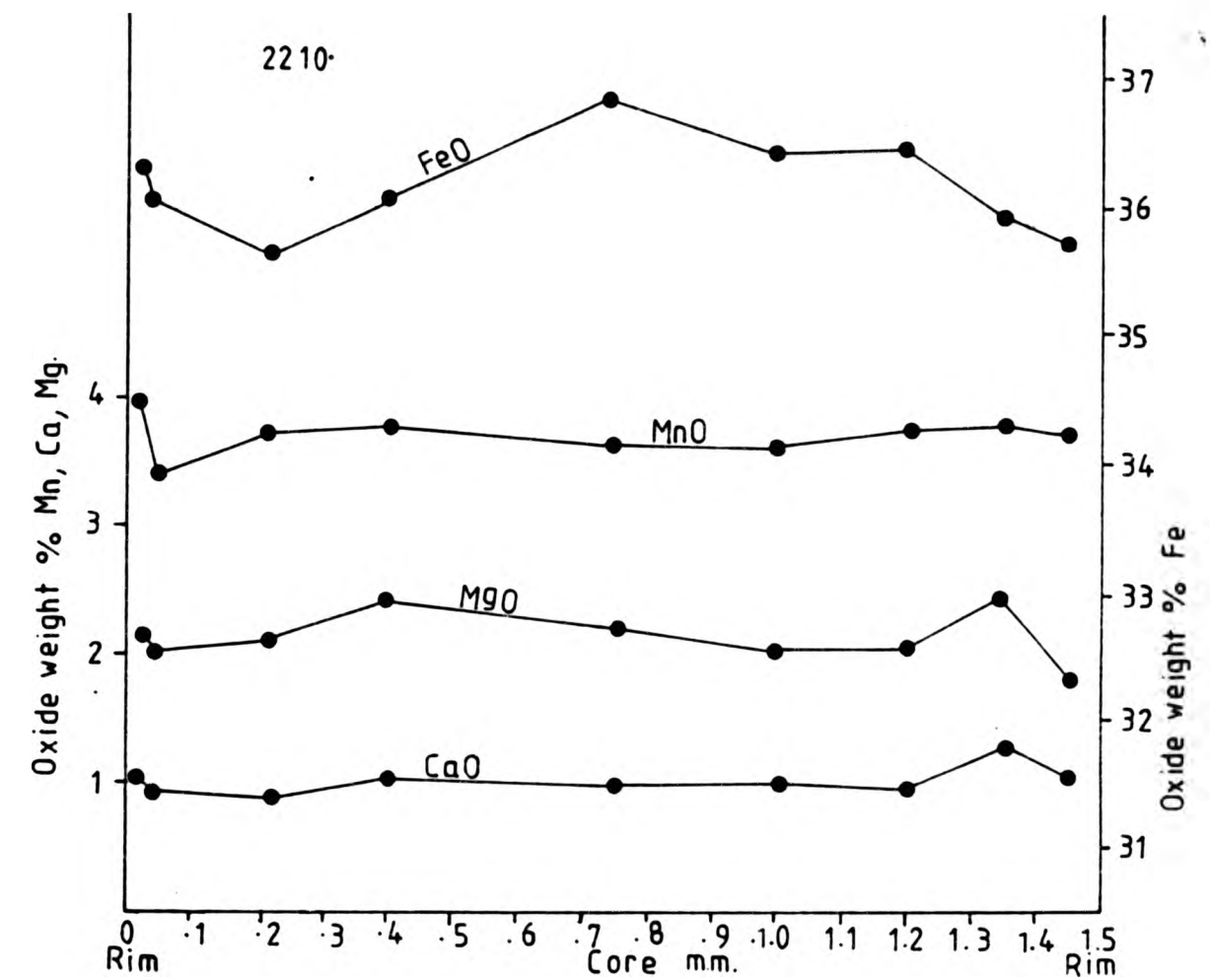


FIGURE 8.3

ZONING PROFILE OF AN AUREOLE GARNET

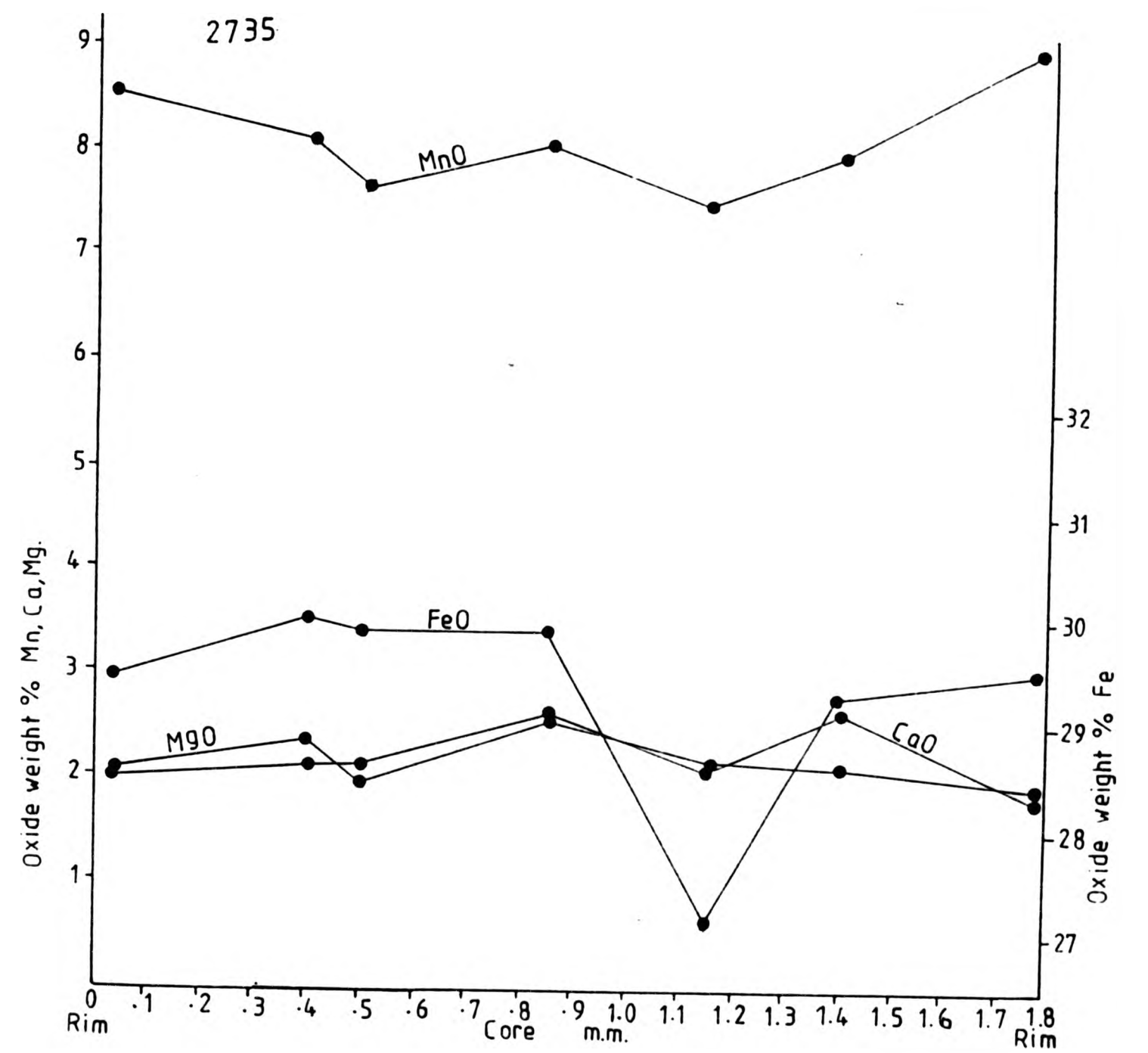
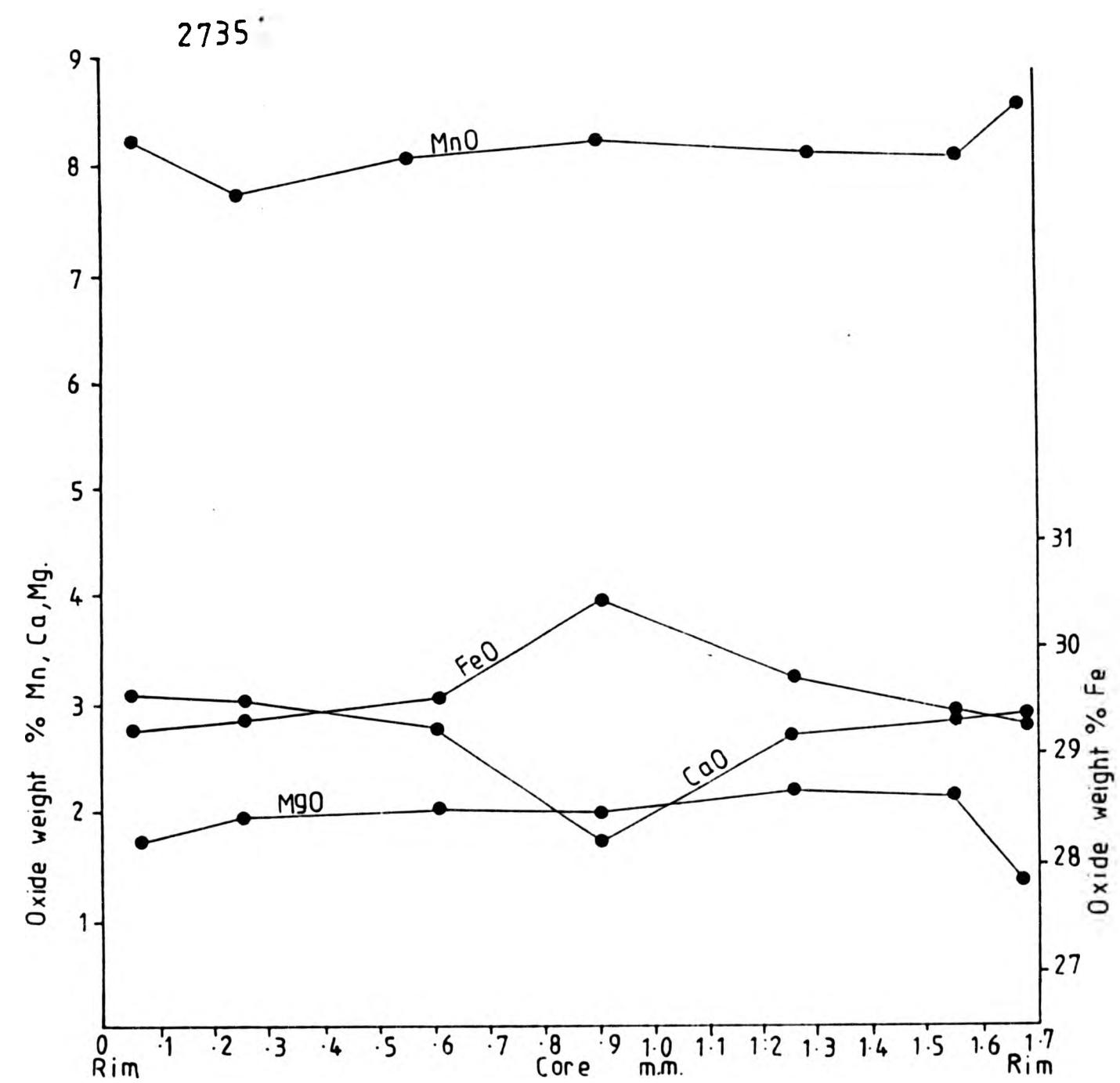


FIGURE 8.3

ZONING PROFILE OF AUREOLE GARNET



Contd...

FIGURE 8.4A

AFM projection of biotite, garnet, and cordierite from slides 2210 and 2308, from the Central psammite septum.

$$A = 100(A1203-K2O-Na2O-CaO) \\ (A1203-K2O-Na2O-CaO+FeO+MgO) \\ M = 100-MgO/(MgO+FeO) \\ F = 100-M$$

Projection through alkali feldspar.

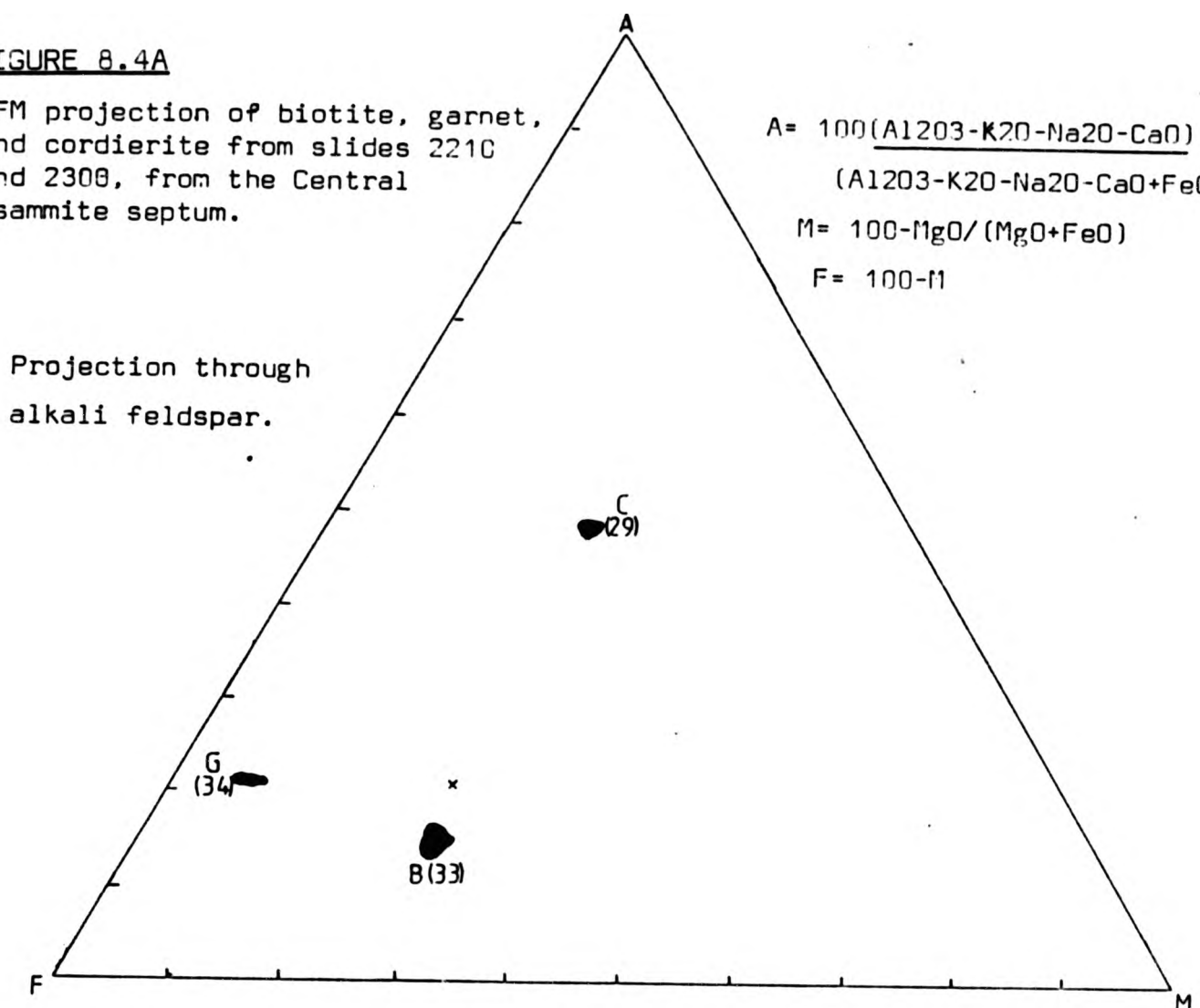
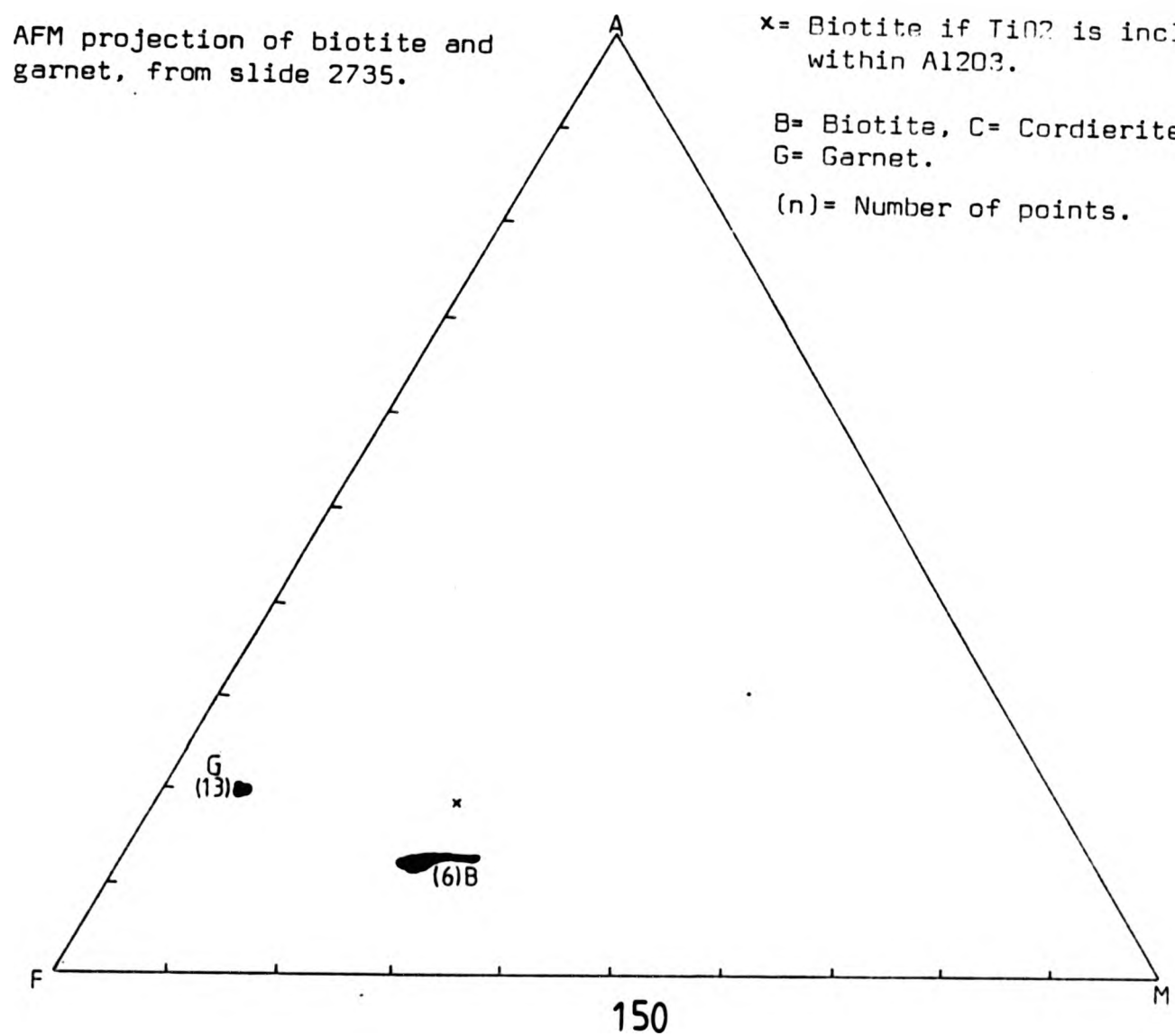


FIGURE 8.4B

AFM projection of biotite and garnet, from slide 2735.

x = Biotite if  $TiO_2$  is included within A1203.  
B = Biotite, C = Cordierite  
G = Garnet.  
(n) = Number of points.



PLATES  
Chapter 8



Plate 8.1

Large porphyroblast of unstrained quartz, enclosing numerous grains of biotite and plagioclase, illustrating the loss of quartz grain boundaries during extensive annealing. Micaceous Psammite. (Crossed polars, x47)

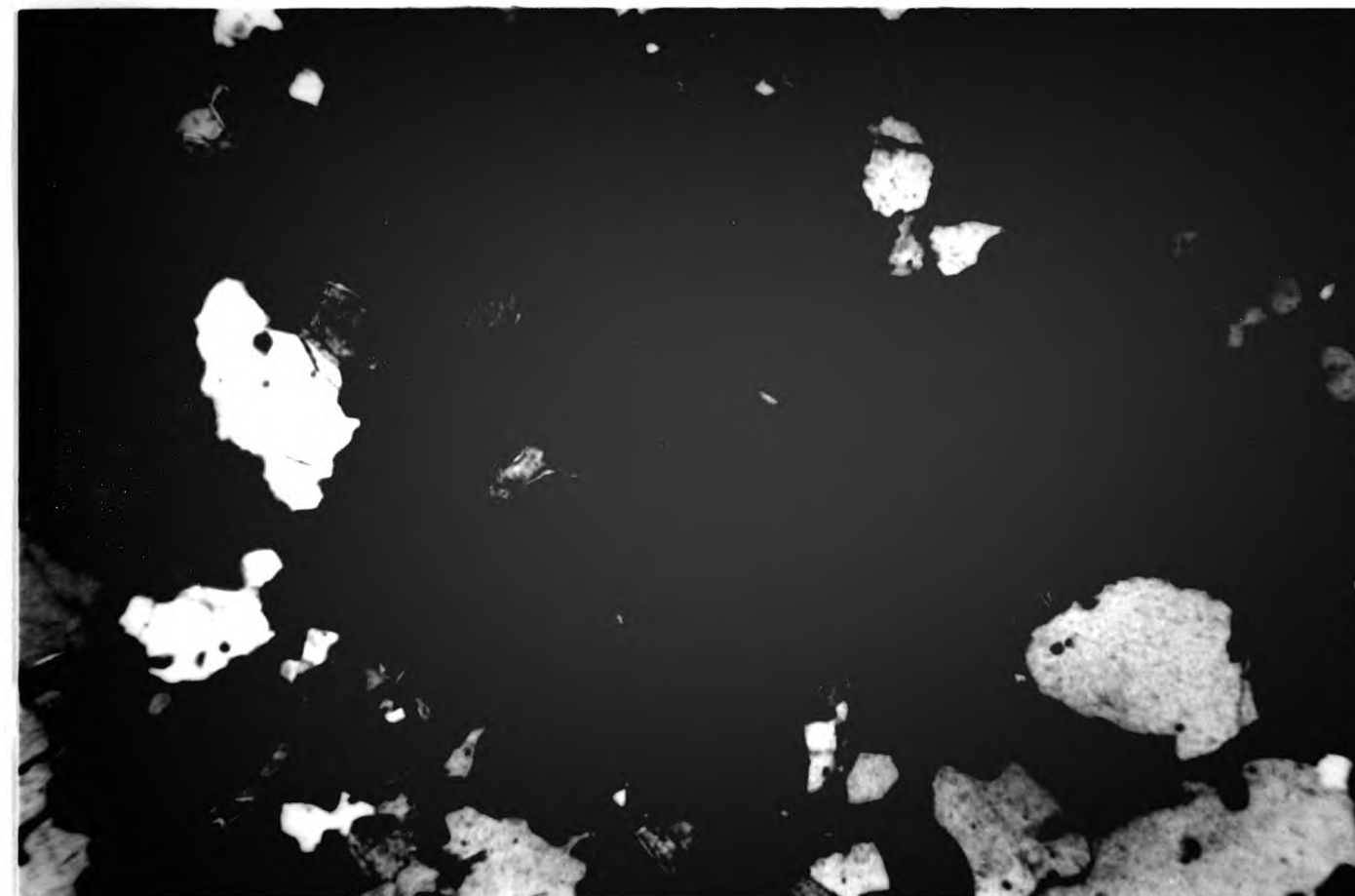


Plate 8.2

Epitaxial relationship between biotite, defining the F1 regional foliation, and sillimanite needles. The sillimanite may be replacing, or simply nucleating on, the biotite. Micaceous Psammite. (Plane polarised light, x47).





**Plate 8.3**

Sillimanite needles, either replacing or intergrowing with, a biotite lath. Micaceous Psammite. (Plane polarised light, x47).



**Plate 8.4**

Regional F3 crenulation overprinted by large sillimanite needles either growing epitaxially alongside the biotite, (Chinner, 1961), or possibly replacing the biotite. Growth orientation of the sillimanite is controlled by orientation of the biotite. Micaceous Psammite. (Plane polarised light, x47).



Plate 8.5

Mesh of randomly orientated fascicular sillimanite, containing numerous irregular grains of ilmenite and the occasional scrap of biotite. This texture possibly reflects the breakdown of biotite during the formation of sillimanite. Micaceous Psammite. (Plane polarised light, x47).



Plate 8.6

Incomplete replacement of a large andalusite porphyroblast (A), by sillimanite needles (S). The andalusite and sillimanite share a common c-axis, and the whole crystal develops a corona of muscovite. A trace of the early F1 regional fabric is enclosed within the porphyroblast. Micaceous Psammite. (Crossed polars, x47).





**Plate 8.7**

Xenoblastic and subidioblastic grains of andalusite (A), partially replaced by sillimanite needles (S).  
Micaceous Psammite. (Crossed polars, x47).

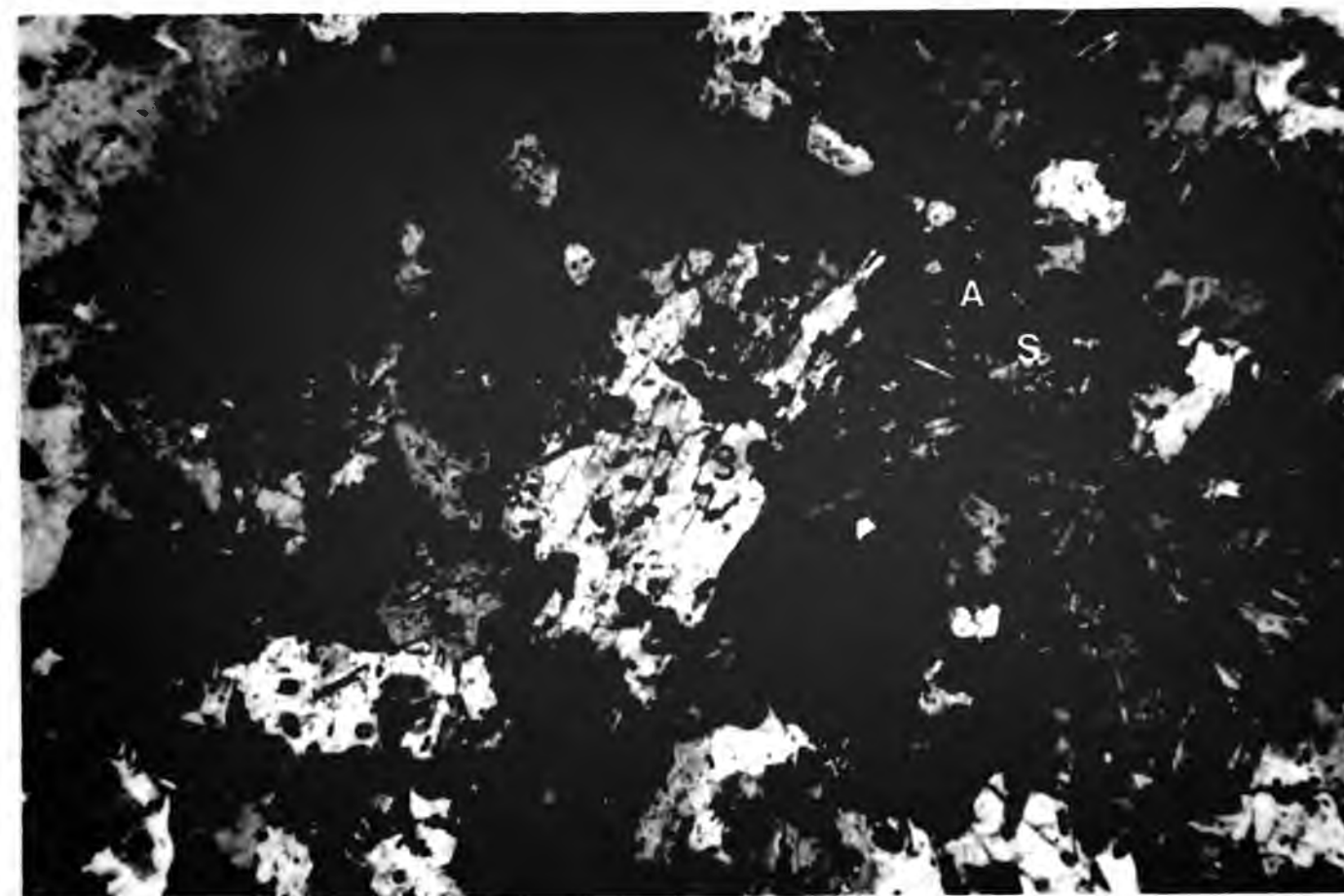


**Plate 8.8**

Pinnitised cordierite, replacing large grains of biotite, which are now preserved as biotite scraps.  
Micaceous Psammite. (Plane polarised light, x47).

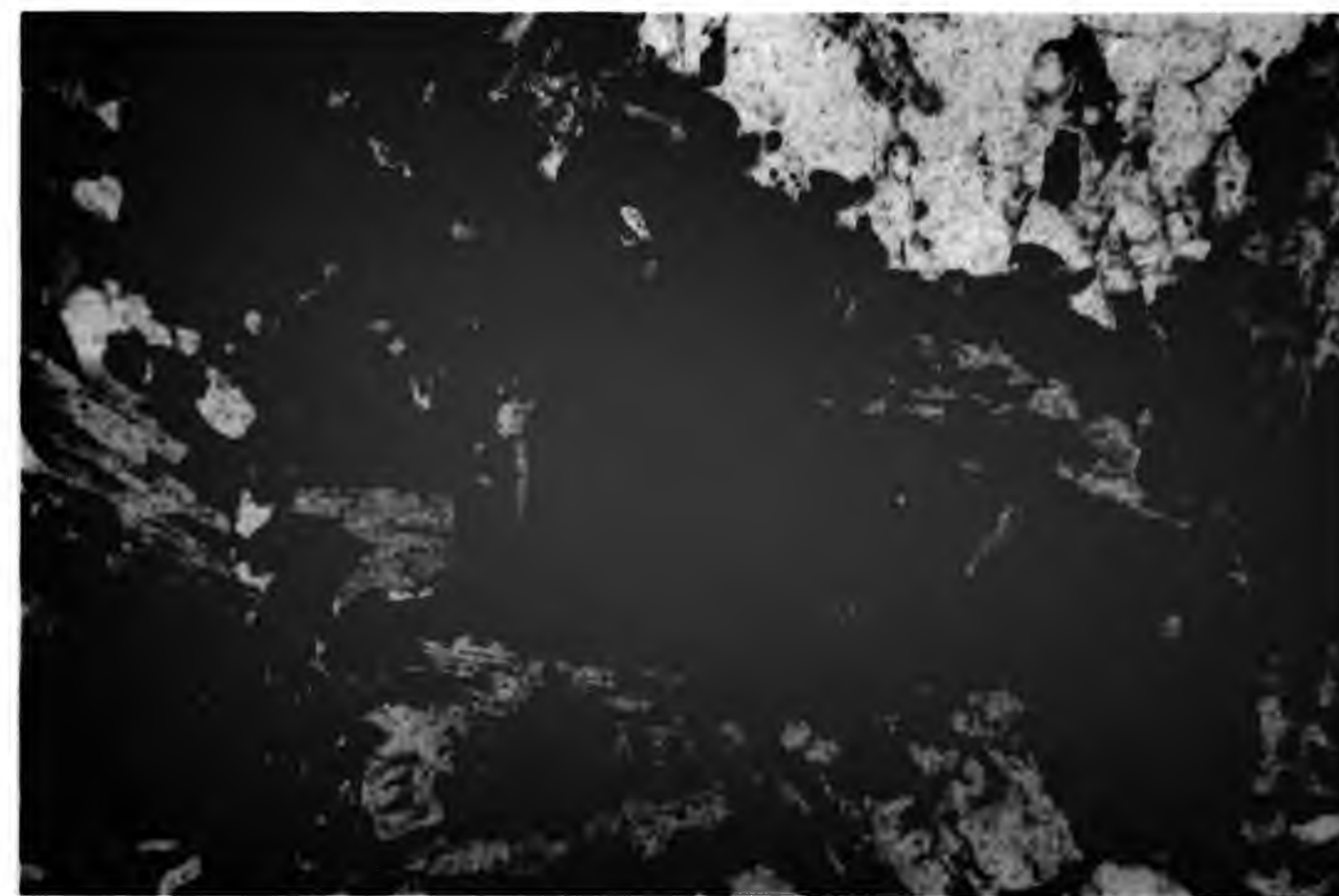


Plate 8.9

Pinnitised cordierite (C), concentrated along, and replacing biotite (B), F1 foliations. Micaceous Psammite. (Plane polarised light, x47).

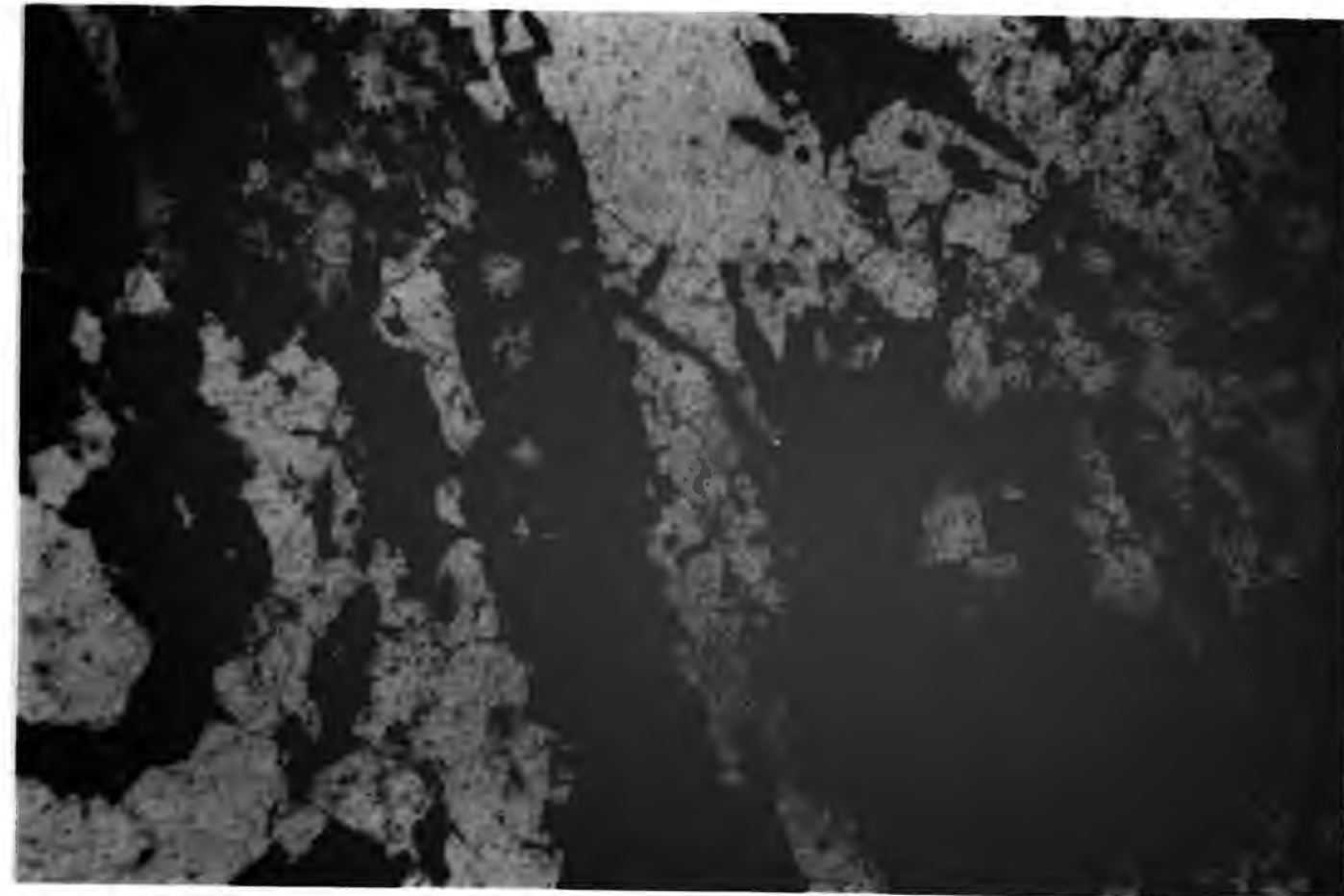


Plate 8.10

Skeletal aureole garnet, within whose boundary is abundant granoblastic pinnitised cordierite (C). The aureole garnet and cordierite are pseudomorphing regional garnet, with the cordierite perhaps replacing aureole biotite. Micaceous Psammite. (Plane polarised light, x47).





Plate 8.11

Aureole garnet, intimately associated with biotite. Both minerals are probably pseudomorphing regional garnet. Micaceous Psammite. (Plane polarised light, x47).

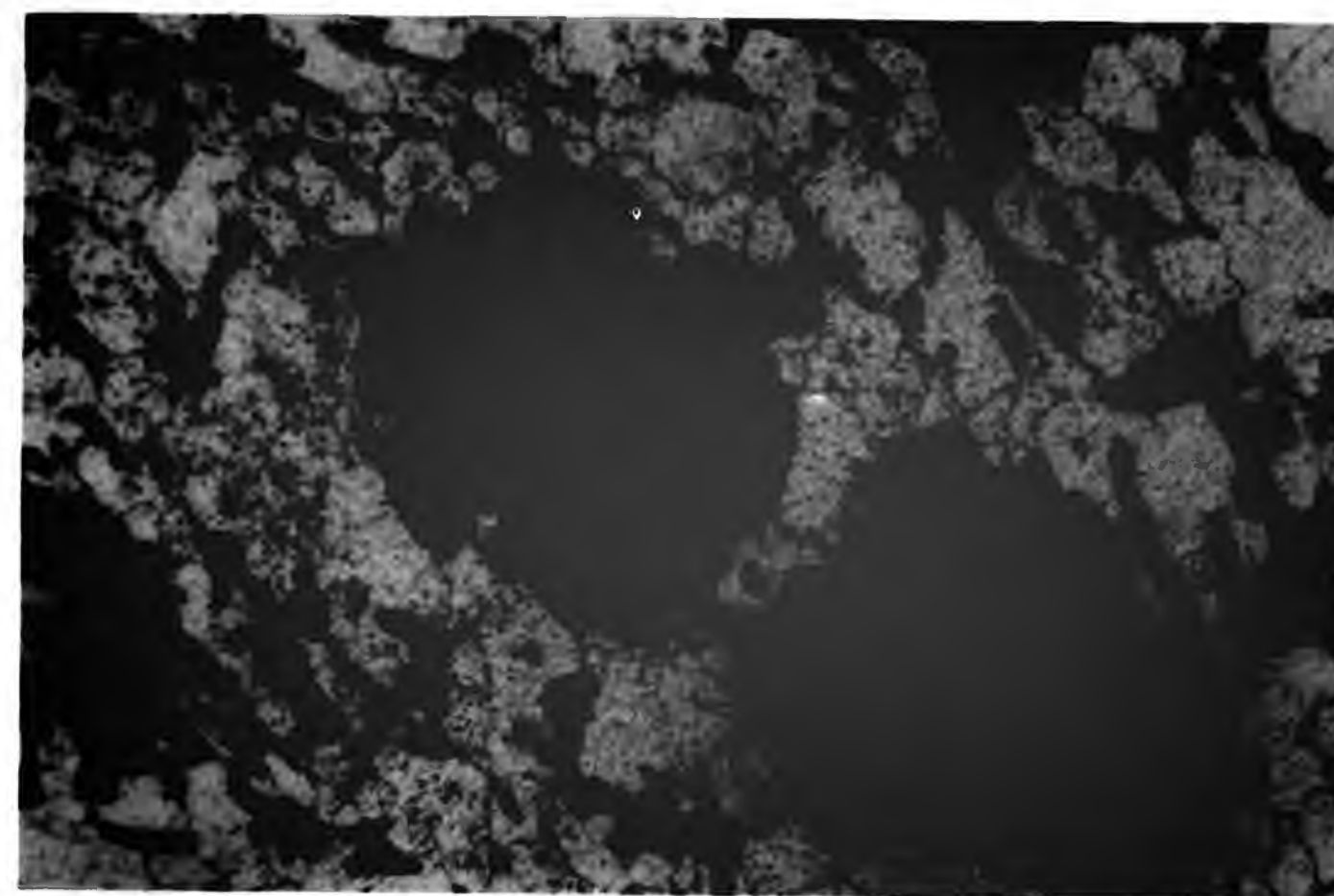


Plate 8.12

Pebbly psammite hornfels, showing the development of a polygonal granoblastic texture. Located within a small raft in the Dalcrag Granodiorite. (Crossed polars, x47).

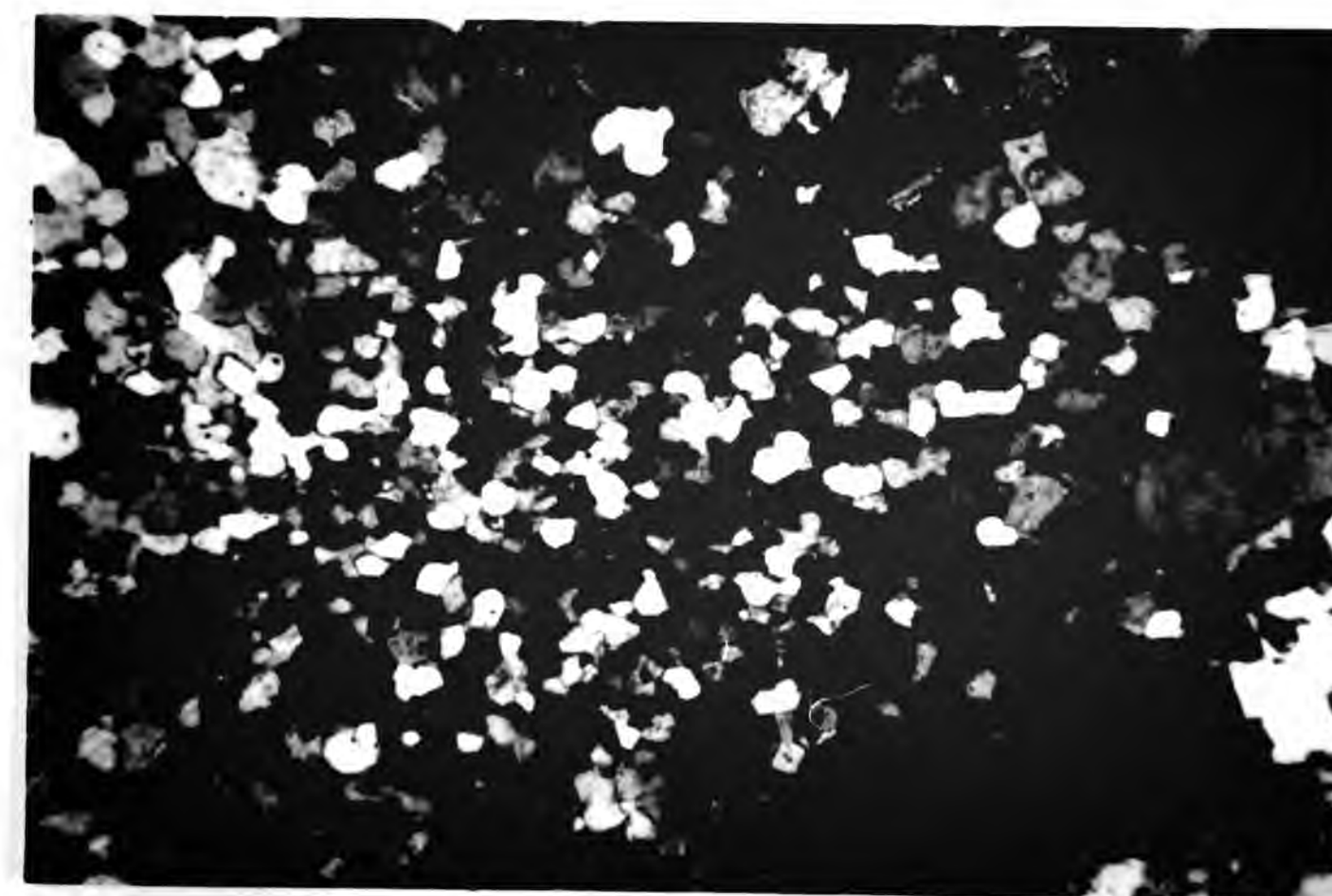
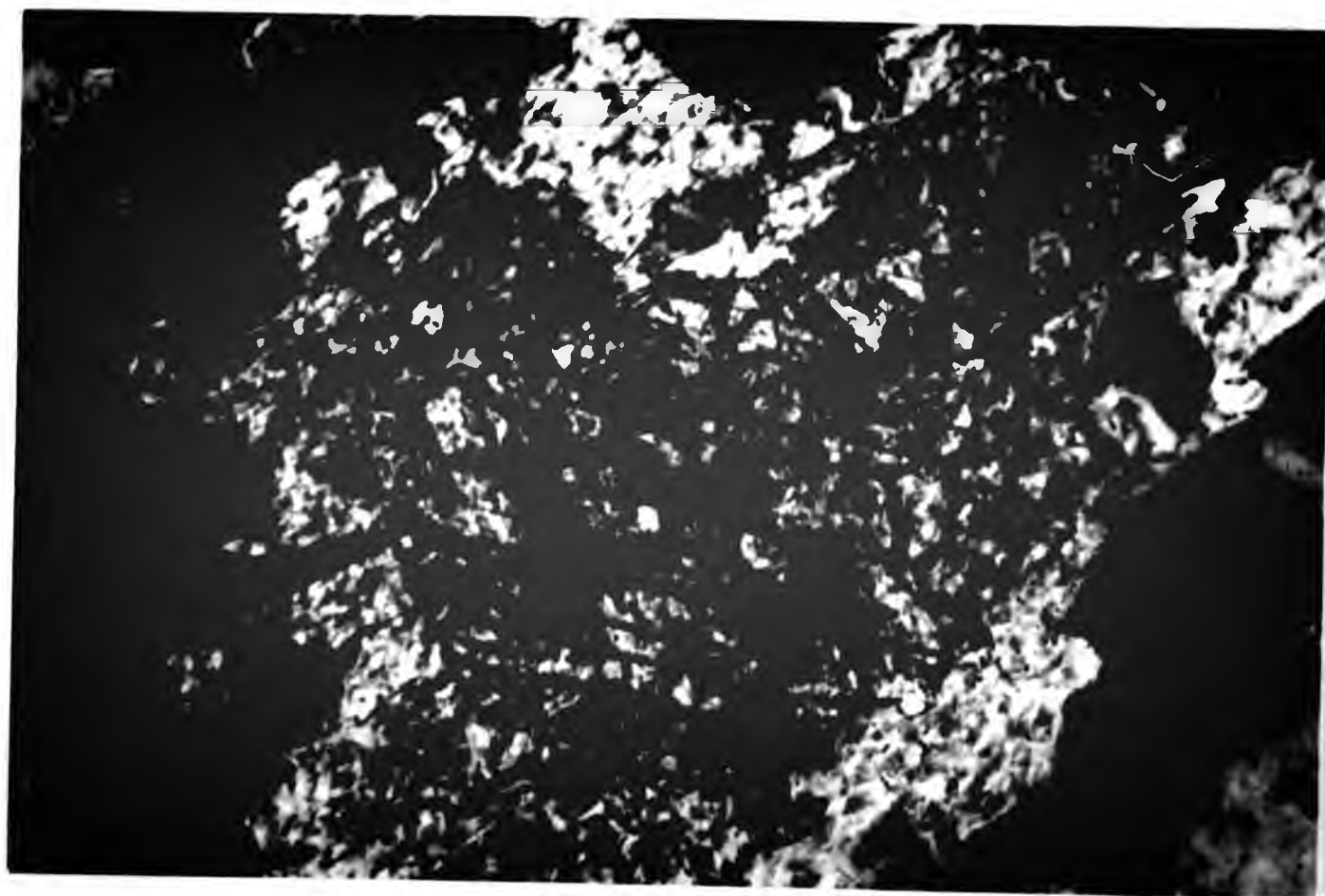


Plate 8.13

Sillimanite porphyroblast, with a corona of retrogressive muscovite. Micaceous Psammite. (Crossed polars, x140).



CHAPTER 9. THE EFFECTS OF DENSITY ON THE EMPLACEMENT OF THE FOYERS COMPLEX.



TABLE 9.1

TABLE ILLUSTRATING THE DENSITIES OF DIFFERENT ROCK LITHOLOGIES FROM THE FOYERS COMPLEX AND ENVELOPE. (MEASURED AT 15C & ATMOSPHERIC PRESSURE).

LITHOLOGY	NUMBER OF SAMPLES	DENSITY (g/cm <sup>3</sup> )
Erroglie quartz diorite.	13	2.775
Chliabhain quartz- monzodiorite.	8	2.675
Dalcrag granodiorite	8	2.68
Aberchalder adamellite	6	2.57
Appinitic diorite	2	2.7
Microdiorite enclave	2	2.78
Micaceous psammite	9	2.69
Pebbly psammite	5	2.65
Migmatitic semi-pelite	5	2.72
Quartzite	3	2.52

TABLE 9.2 MINERAL COMPOSITION OF THE MAJOR LITHOLOGIES IN THE ENVELOPE OF THE FOYERS GRANITIC COMPLEX

	Pebbly psammite	Micaceous psammite	Semi-pelite	Quartzite
Plagioclase	32	20	30	5
Quartz	37	50	30	80
Biotite	9	30	40	5
Orthoclase	22	Trace	Trace	10

Data sources: Haselock (1982), Highton (1986) & Hood.

FIGURE 9.1

KEY TO GRAPHS IN FIG. 9.1

- 1- Density of Errogle quartz diorite magma
  - 2- Density of Errogle quartz diorite magma including the effects of fractional crystallisation.
  - 3- Volume percent of solids in the Errogle quartz diorite magma.
  - 4- Density of Dalcrag granodiorite magma.
  - 5- Density of Dalcrag granodiorite magma including the effects of fractional crystallisation.
  - 6- Mean of the densities presented by lines 4 and 5.
  - 7- Volume percent of solids in the Dalcrag granodiorite magma.
- Start of crystal formation in the magma.
- Complete solidification of the magma.

FIGURE 9.1

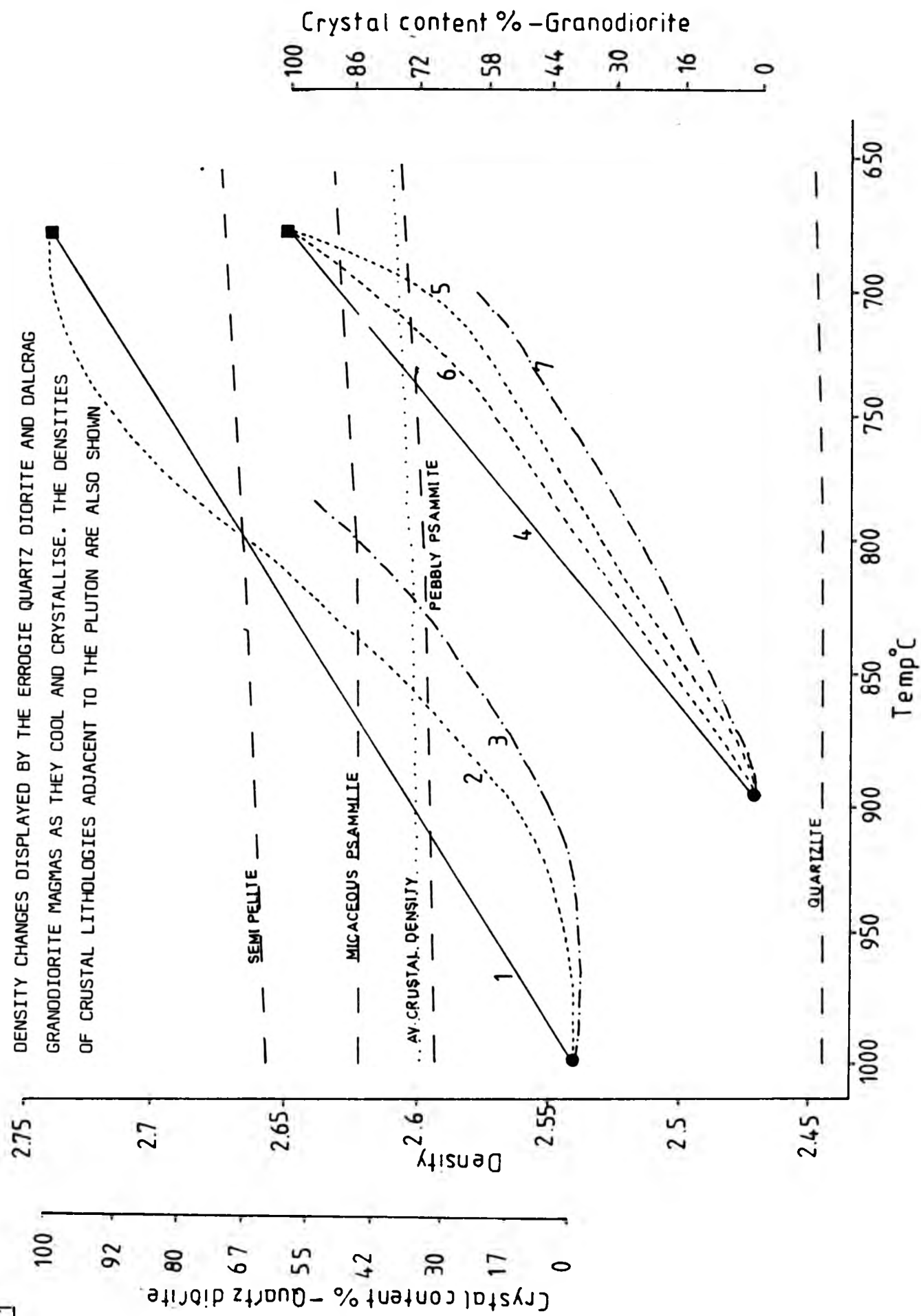


FIGURE 9.2

CRYSTALLISATION SEQUENCE IN THE ERROGIE QUARTZ DIORITE.

A.

HORNBLENDE	_____
PLAGIOCLASE	_____
BIOTITE	_____
QUARTZ	_____
KSPAR	_____

Crystallisation →

APPROXIMATION OF THE CRYSTALLISATION SEQUENCE IN THE  
DALCRAG GRANODIORITE.

B.

HORNBLENDE	_____
PLAGIOCLASE	_____
BIOTITE	_____
QUARTZ	_____
KSPAR	_____

Crystallisation →

TABLE 9.3 . TABLE SHOWING THE VOLUME PERCENT OF CRYSTALS IN ERROGIE QUARTZ DIORITE MAGMA AT VARYING TEMPERATURES

T°C	Mineral starting to crystallise from the magma	Percentage of crystals in magma			
		Total	Hb.	Plg.	Bio.
970	Hornblende	0	0	-	-
915	Plagioclase	2.4	2.4	-	-
850	Biotite	20.58	5.33	15.25	-
790	Quartz	44.9	8.0	30.5	-

TABLE 9.4

Mineral	Density of molten mineral	Density of solid mineral at room T & P	Density of solid mineral at 3.9Kb and-		
			915 C	850 C	790 C
Hornblende	2.606	3.21	3.143	3.149	3.154
Plagioclase	2.385	2.63	-	2.612	2.615
Biotite	2.748	3.01	-	-	2.954

TABLE SHOWING THE DENSITIES OF VARIOUS MINERALS AT TEMPERATURES WHICH MARK THE START OF CRYSTALLISATION OF A NEW MINERAL SPECIES FROM THE ERROGIE QUARTZ DIORITE MELT.



Temperature C	Increase of magma density (%) Minerals responsible for increase increase in (%)	Density of magma
915	0.4944 (Hornblende)	2.555
850	1.11 (Hornblende) 1.457 (Plagioclase)	2.608
790	1.6824 (Hornblende) 2.94 (Plagioclase) 0.479 (Biotite)	2.672

TABLE 9.5

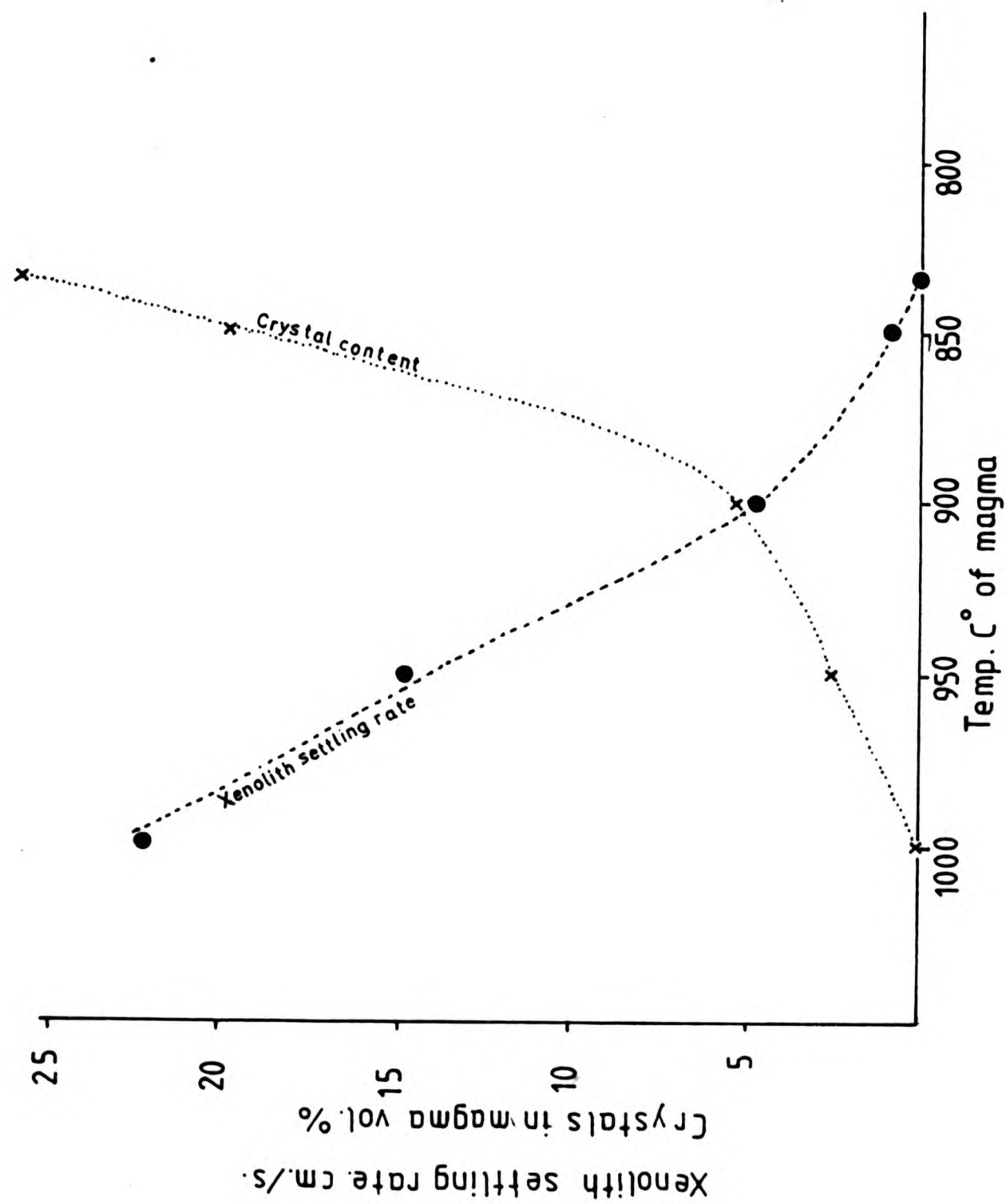
TABLE SHOWING THE DENSITY OF ERROGIE QUARTZ DIORITE MELT  
AT VARIOUS TEMPERATURES

TABLE 9.6

TABLE SHOWING SETTLING VELOCITIES OF A MICACEOUS PSAMMITE RAFT  
(DIAMETER 100m) IN ERROGIE QUARTZ DIORITE MAGMA AT VARYING  
TEMPERATURES.

TEMPERATURE C	SOLIDS IN MAGMA VOL. %	SETTLING VELOCITY cm/s.
1000	0 0	22.4
950	2.5	14.5
900	5.2	4.5
850	20	0.8
830	26	0.0

FIGURE 9.3 GRAPH SHOWING CHANGES IN THE SETTLING RATE OF A MICACEOUS PSAMMITE RAFT (DIAMETER 100m.) AS ERROGIE QUARTZ DIORITE MAGMA COOLS.



CHAPTER 10. THE INTRUSION OF THE FOYERS COMPLEX;  
SUMMARY AND CONCLUSIONS.

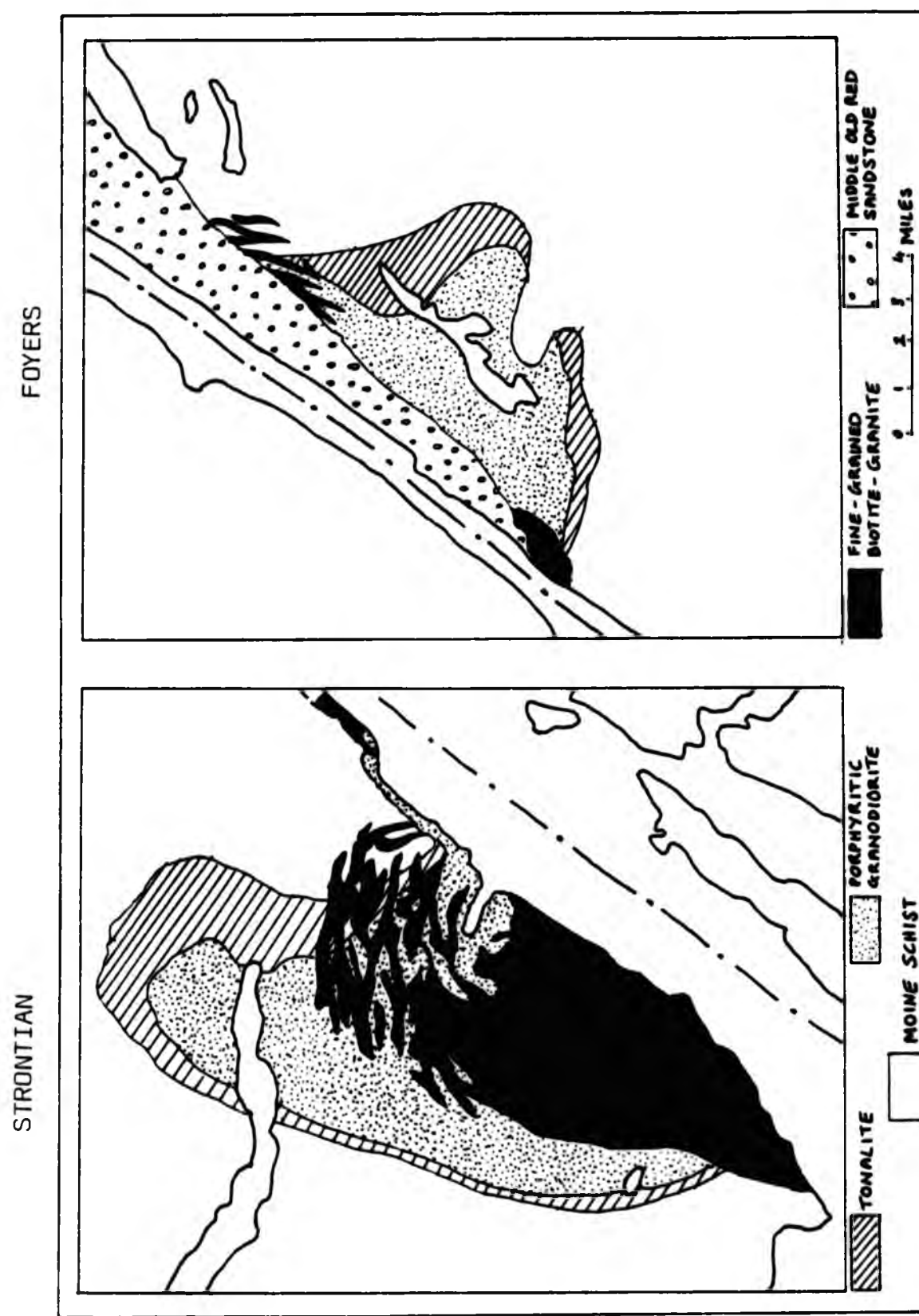
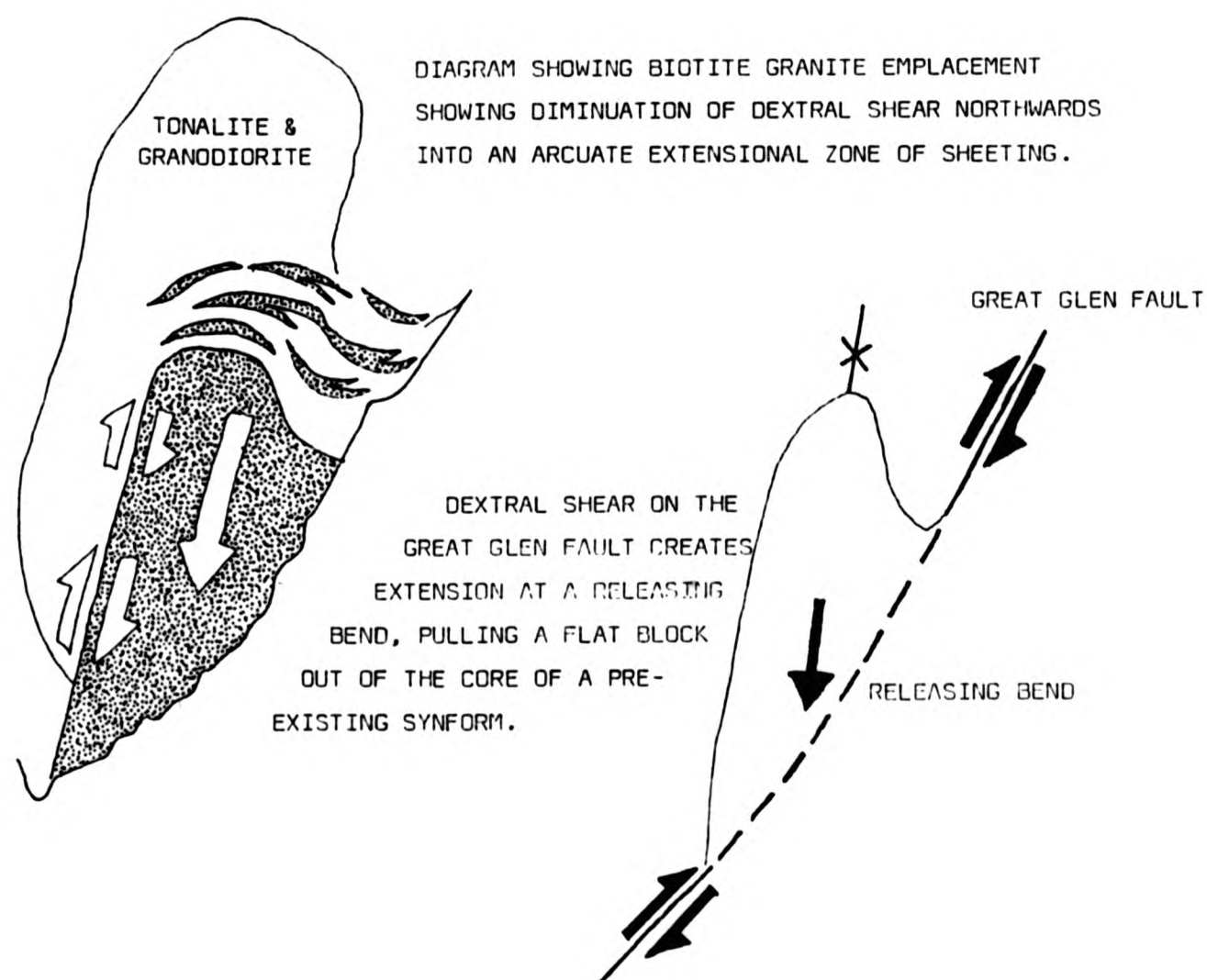
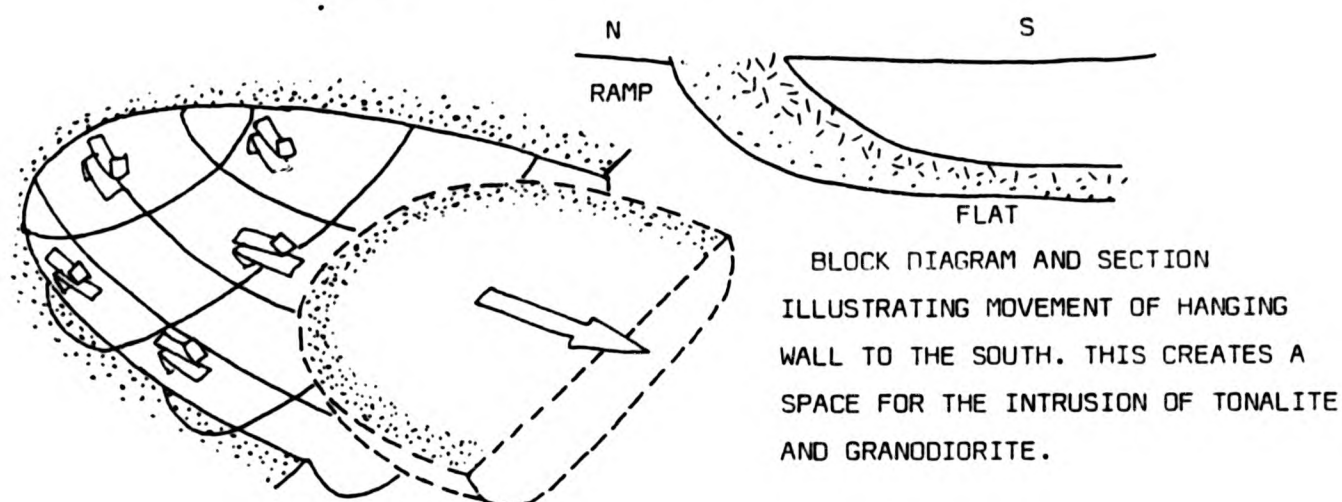


FIGURE 10.1  
MAPS OF THE STRONTIAN AND FOYERS GRANITIC PLUTONS, COPIED FROM KENNEDY, (1946), SHOWING AN OUTER TONALITE, AN INNER GRANODIORITE AND A CROSS CUTTING BIOTITE GRANITE IN BOTH COMPLEXES. NOTE THE BIOTITE GRANITE VEINS IN THE NORTH EAST OF BOTH PLUTONS.

FIGURE 10.2

SERIES OF DIAGRAMS ILLUSTRATING THE EMPLACEMENT OF THE STRONTIAN GRANITE. TAKEN FROM HUTTON, (1988).





THE BRITISH LIBRARY DOCUMENT SUPPLY CENTRE

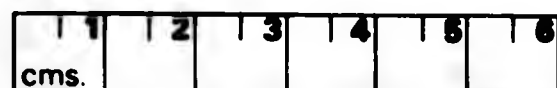
TITLE THE FOYERS GRANITIC COMPLEX AND ITS AUREOLE.  
.....

.....  
AUTHOR Philip Thomas Hood.  
.....

City of London Polytechnic.  
UNIVERSITY 1990

Attention is drawn to the fact that the copyright of this thesis rests with its author.

This copy of the thesis has been supplied on condition that anyone who consults it is understood to recognise that its copyright rests with its author and that no information derived from it may be published without the author's prior written consent.



THE BRITISH LIBRARY  
DOCUMENT SUPPLY CENTRE  
Boston Spa, Wetherby  
West Yorkshire  
United Kingdom

REDUCTION X .....

12

CAMERA 7

**MAPS/CHARTS  
RELATING TO THIS THESIS  
HAVE NOT BEEN FILMED**

**PLEASE APPLY DIRECT  
TO ISSUING UNIVERSITY**

**A**

**DX79 249**

**VOL 2**